



**HAL**  
open science

# Investigation of aggregates size effect on the stiffness of lime and/or cement treated soils: from laboratory to field conditions

Jucaï Dong

► **To cite this version:**

Jucaï Dong. Investigation of aggregates size effect on the stiffness of lime and/or cement treated soils: from laboratory to field conditions. Other. Université Paris-Est, 2013. English. NNT : 2013PEST1063 . pastel-00966315

**HAL Id: pastel-00966315**

**<https://pastel.hal.science/pastel-00966315v1>**

Submitted on 26 Mar 2014

**HAL** is a multi-disciplinary open access archive for the deposit and dissemination of scientific research documents, whether they are published or not. The documents may come from teaching and research institutions in France or abroad, or from public or private research centers.

L'archive ouverte pluridisciplinaire **HAL**, est destinée au dépôt et à la diffusion de documents scientifiques de niveau recherche, publiés ou non, émanant des établissements d'enseignement et de recherche français ou étrangers, des laboratoires publics ou privés.

THÈSE

Pour obtenir le grade de

**Docteur de l'Université Paris - Est**

**Discipline : Géotechnique**

Présentée et soutenue publiquement par

**Jucal DONG**

Le 26 juin 2013

Titre

**Investigation of aggregates size effect on the stiffness  
of lime and/or cement treated soils: from laboratory  
to field conditions**

*Directeur de thèse :*

**Yu-Jun CUI**

**JURY**

Farimah MASROURI	ENSG de Nancy	Rapporteur/Président
Jean-Marie FLEUREAU	École Centrale Paris	Rapporteur
Yasmina BOUSSAFIR	IFSTTAR	Examineur
Valéry FERBER	Entreprise Charier	Examineur
Anh-Minh TANG	École des Ponts ParisTech	Examineur
Yu-Jun CUI	École des Ponts ParisTech	Directeur de thèse



# Résumé

**Titre :** Étude de l'effet de la taille d'agrégats sur la raideur des sols fins traités à la chaux et/ou au ciment : des conditions de laboratoire aux conditions *in situ*

Le traitement des sols est une technique connue qui a largement été utilisée dans les constructions ferroviaires et routières. Il améliore la maniabilité des sols en réduisant la teneur en eau et en améliorant les performances hydromécaniques par renforcement et lien des agrégats du sol. Cependant, la durabilité des sols traités reste une question ouverte, elle constitue l'objectif principal du projet ANR TerDOUEST (Terrassements Durables – Ouvrages en Sols Traités, 2008-2012).

La présente étude fait partie des travaux réalisés dans le cadre du projet TerDOUEST, et traite de l'effet de la taille des agrégats sur l'évolution de la raideur ( $G_{\max}$ ) des sols fins provenant d'Héricourt (70) et traités à la chaux et/ou au ciment, à l'aide de la technique piézo-électrique (bender element). Dans les conditions de laboratoire, quatre tailles d'agrégats ont été étudiées ( $D_{\max} = 0.4, 1, 2 \text{ et } 5 \text{ mm}$ ). Afin d'obtenir des tailles d'agrégats souhaitées, les sols ont d'abord été séchés, broyés puis tamisés à une taille désirée. Les sols ont ensuite été ramenés à la teneur en eau souhaitée, mélangés au liant hydraulique (chaux et/ou ciment) puis compactés du côté sec et du côté humide de l'optimum du Proctor normal, tout en conservant la même densité sèche. Les mesures de  $G_{\max}$  des sols traités ont été réalisées pendant la cure et pendant l'application de cycles humidification/séchage. Dans les conditions du terrain, qui correspondent au remblai expérimental d'Héricourt, les tailles des agrégats sont nettement plus élevées :  $D_{\max} = 20 \text{ et } 31.5 \text{ mm}$  pour le limon et l'argile, respectivement.

Les résultats montrent que le comportement hydromécanique des sols traités est fortement influencé par la taille des agrégats, que les sols soient argileux ou limoneux, préparés en laboratoire ou bien dans les conditions du terrain : plus la taille des agrégats est élevée, plus la raideur diminue avec le temps de cure et moins les sols résistent à la succession de cycles humidification/séchage. Une forte hétérogénéité des sols *in-situ* a aussi été identifiée clairement.

Un modèle hyperbolique a été développé afin de permettre l'application des résultats obtenus en laboratoire à ceux obtenus dans des conditions de terrain, étant donné l'effet de la taille des agrégats. La comparaison entre le modèle de prédictions et les mesures expérimentales démontre la performance du modèle proposé, à condition d'utiliser les valeurs moyennes des données expérimentales afin de minimiser l'effet de l'hétérogénéité du sol.

**Mots clés :** traitement des sols ; taille maximale des agrégats ; raideur ( $G_{\max}$ ) ; limon ; argile ; temps de cure ; cycles humidification / séchage ; hétérogénéité ; remblai d'Héricourt ; modèle hyperbolique.



# Abstract

**Title:** Investigation of aggregates size effect on the stiffness of lime and/or cement treated soils: from laboratory to field conditions

Soil treatment is a well-known earthwork technique, which has been widely used in the construction of railway and highway substructures. It can improve the workability of soils by lowering their water content and ameliorate hydro-mechanical performance by reinforcing and binding the soil grains/aggregates. However, the durability of treated soils is still an open question. It constitutes the main objective of the ANR project TerDOUEST (Terrassements Durables - Ouvrages en Sols Traités, 2008 - 2012).

The present study is part of the work carried out in the TerDOUEST project, and deals with the aggregates size effect on the evolution of the stiffness ( $G_{\max}$ ) of lime and/or cement treated fine-grained soils from Héricourt using the Bender element technique. In laboratory conditions, four aggregates sizes were accounted for ( $D_{\max} = 0.4, 1, 2$  and  $5 \text{ mm}$ ). To prepare an aggregates size, the soils were first air-dried, crushed and sieved through a target sieve. The soils were then brought to a desired water content, mixed with an additive (lime and/or cement) and compacted on both the dry and wet sides to the optimum of the normal Proctor while maintaining the same dry density. The  $G_{\max}$  measurements were performed during curing and during the application of the wetting/drying cycles. In field conditions that refer to the experimental embankment in Héricourt, the aggregate size is significantly larger:  $D_{\max} = 20 \text{ mm}$  and  $31.5 \text{ mm}$  for silt and clay, respectively. Core samples were taken from the embankment at two different times and the  $G_{\max}$  measurements on core specimens were performed.

The results show that the hydromechanical behaviour of the cementitious treated soils is strongly influenced by the aggregate size for the treated silt and clay prepared in both laboratory and field conditions: the larger the aggregates after treatment, the lower the  $G_{\max}$  and the resistance to wetting/drying cycles. The high heterogeneity of the *in-situ* soils was also clearly identified.

A hyperbolic model was developed enabling the up-scaling of the laboratory conditions results to those in field conditions by considering the effect of aggregate size. Comparison between the model predictions and experimental measurements shows the performance of the model proposed, provided that the mean values of experimental data are used to minimize the effect of soil heterogeneity.

**Keywords:** soil treatment; maximum soil aggregate size; stiffness ( $G_{\max}$ ); silt; clay; curing time; wetting/drying cycles, heterogeneity, embankment in Héricourt; hyperbolic model.

# Acknowledgements

The work presented in this thesis would not have been possible without the help of many people who were always there when I needed them. I take this opportunity to acknowledge them and express my sincere gratitude.

First and foremost, I would like to extend my deepest gratitude to my supervisor Yu-Jun CUI, Professor at Ecole des Ponts ParisTech. His guidance, patience and encouragement were constant during the preparation of my thesis. Besides his profound scientific vision, his extraordinary passion in research and good methodologies in many aspects were invaluable. It is my great fortune to have had the opportunity to work with him.

I am equally thankful to Dr Anh Minh TANG, who provided me with extended discussion and valuable suggestions. This contributed greatly to this thesis. His deep understanding and great experience in laboratory testing and in the elaboration of the best figures enabled me to present my results clearly. He was always there to discuss my research and answer my questions. Again, I feel that I am lucky to have enjoyed this collaboration along my PhD study.

I would like to especially thank the reviewers of my thesis, Professor Farimah MASROURI at Ecole Nationale Supérieure de Géologie (Nancy), who also presided over the jury, and Professor Jean-Marie Fleureau at Ecole Central Paris and CNRS, for agreeing to take the time to read the manuscript carefully and to inspire a discussion on my thesis, even just before the summer vacation. The same gratitude goes to the examiners: Yasmina BOUSSAFIR of IFSTTAR (Institut français des sciences et technologies des transports, de l'aménagement et des réseaux) and Dr Valéry FERBER of Entreprise Charier.

The experimental work would not have been possible without the constant assistance of the technical team of the CERMES. I especially thank them for their incredible help: Emmanuel De Laure, Xavier Boulay, Hocine Delmi, Baptiste Chabot, etc. They assisted me during the long experimental work. I address my deep thanks to the China Scholarship Council (CSC) and the French National Research Agency for funding this thesis. Note that this thesis is part of the TerDOUEST project for "Sustainable earthworks involving treated soils".

I also give deep thanks to the teachers Tianhua DAI, Xiaotao ZHANG, Yaping QIANG, Jingmei ZHAO, Ruimin ZHOU, from the Education Office of Embassy of the

People's Republic of China in France, who organised several activities enriching my doctoral life (ex. Activities for Spring Festivals).

My gratitude also goes out to everyone of CERMES for their encouragement, support and all the nice times I had with them (Valerie VALLIN, Solenn LE PENSE, Van-Cuong LE, Thi Thanh Hang NGUYEN, Pengyun HONG, Qiong WANG, Weikang SONG, etc.). Special gratitude goes to the secretary of the CERMES Armelle FAYOL, to my English teacher, Stacey BENOIT, to the people in charge of the doctoral students at the ENPC (Cécile BLANCHEMANCHE ; Claude TU ; Marine DANIEL, etc.).

Finally, I would like to thank my family, both in China and in France, and especially my wife. She gave me great help and courage to complete this thesis and for the everyday life in France. My deepest gratitude goes to my parents who will not read this thesis, but I could not accomplish the special stage of my life without their love and support. I am also thankful to all my friends who helped me directly or indirectly during the successful completion of my thesis. It is worth noting that the Chinese family also includes some of my previous teachers, such as Professors Renshu YANG and Zhongwen YUE from China University of Mining and Technology in Beijing (CUMTB), Professor Xuechao NIU from Beijing Polytechnic College, etc. They also advised and encouraged me a lot in the scientific field and in my personal life.

So, I dedicate this dissertation to my French and Chinese close relatives, as this work would not have been possible without their love, affection and encouragement.



# Contents

<b>Introduction.....</b>	<b>1</b>
<b>Chapter 1. Literature review.....</b>	<b>5</b>
1.1. Practice: use of soil treatment in geotechnical engineering.....	5
1.1.1. Treatment goals.....	5
1.1.2. Cementitious stabilization methods.....	6
1.1.3. Treatment design in laboratory.....	7
1.1.3.1. Suitability of treatment methods.....	7
1.1.3.2. Determination of optimum additive percentage.....	8
1.1.3.3. Determination of moisture-density relationship.....	10
1.1.4. Compaction in field.....	13
1.1.5. Quality control in earthwork engineering.....	15
1.2. Fundamental mechanisms about the cementitious treatments of soils.....	16
1.2.1. Physical/chemical characteristics changes.....	16
1.2.1.1. Chemical characteristics changes of lime-treated soils.....	16
1.2.1.2. Chemical characteristics changes of cement-treated soils.....	20
1.2.1.3. Chemical characteristics changes of mix lime/cement-treated soils.....	22
1.2.1.4. Physical characteristics changes by cementitious treatment.....	23
1.2.1.5. Conclusion.....	25
1.2.2. Microstructure models for cementitiously-treated fine-grained soils.....	26
1.2.2.1. Microstructure models for lime-treated soils.....	26
1.2.2.2. Microstructure models for cement-treated soils.....	28
1.2.2.3. Microstructure models for lime/cement-treated soils.....	29
1.2.2.4. Conclusion.....	30
1.2.3. Factors influencing the physical/chemical changes for cementitiously treated fine-grained soils.....	30
1.2.3.1. Additives and quantity.....	30
1.2.3.2. Soil nature and clay mineral composition.....	31
1.2.3.3. Compaction condition.....	32
1.2.3.4. Curing conditions.....	32
1.3. Experimental techniques.....	33
1.3.1. Evaluation on strength and stability of the treated soils.....	34
1.3.2. Evaluation of soils' modulus.....	34
1.3.2.1. Strain range and modulus measurements.....	36
1.3.2.2. Small strain shear modulus measurement.....	37
1.3.2.3. Bender element measurement.....	38
1.3.3. Durability tests for treated soils.....	41
1.3.3.1. Resistance to wetting/drying cycles.....	42
1.3.3.2. Resistance to frost-thaw cycles.....	42
1.3.3.3. Resistance to soaking.....	43
1.3.3.4. Resistance to leaching.....	43
1.3.4. Microstructure investigation on treated soils.....	44
1.3.4.1. Scanning Electron Microscope.....	44
1.3.4.2. Computer Tomography scanning and X-/γ-ray method.....	44
1.3.4.3. Mercury Intrusion Porosimetry.....	45
1.4. Hydro-mechanical behaviour of treated soils.....	45
1.4.1. Factors affecting the strength development.....	45

1.4.1.1. Methods and dosages .....	45
1.4.1.2. Water content .....	46
1.4.1.3. Curing time.....	47
1.4.1.4. Curing temperature.....	49
1.4.2. Factors affecting the small strain shear modulus .....	49
1.4.2.1. Soil properties .....	51
1.4.2.2. Density .....	54
1.4.2.3. Hydric state .....	54
1.4.2.4. Curing time.....	57
1.4.2.5. Cementation .....	61
1.4.3. Climate change effect on the hydro-mechanical behaviour of treated soils .....	63
1.4.3.1. Wetting/drying cycles .....	63
1.4.3.2. Freezing/thawing cycles.....	66
1.4.3.3. Long term leaching and soaking effect .....	67
1.4.4. Microstructure investigation .....	68
1.4.4.1. Microstructure change during curing time .....	68
1.4.4.2. Microstructure analysis by durability tests .....	76
1.5. Correlation between laboratory and field conditions .....	78
1.6. Conclusions .....	81
<b>Chapter 2. Materials and methods.....</b>	<b>83</b>
2.1. Materials.....	83
2.1.1. Soils.....	83
2.1.2. Lime for treatment .....	84
2.1.3. Cement .....	84
2.2. Sample preparation in the laboratory.....	86
2.2.1. Soils preparation .....	86
2.2.2. Compaction of specimens .....	90
2.2.3. Test program .....	100
2.3. Preparation of samples taken from the experimental embankment.....	102
2.3.1. Experimental embankment at Héricourt .....	102
2.3.2. Cores taken from the embankment .....	105
2.3.3. Preparation of specimens from core samples.....	108
2.3.4. Test program .....	109
2.4. Experimental methods.....	111
2.4.1. Experimental setup.....	111
2.4.2. Travel time identification methods .....	113
2.4.3. Signals received at various frequencies .....	113
2.4.4. Effects of frequency on the determination of soil stiffness .....	120
2.5. Conclusions .....	123
<b>Chapter 3. Aggregates size effect during curing time.....</b>	<b>125</b>
3.1. Silty soil treated with lime .....	125
3.1.1. Samples obtained by sieving method 1 .....	125
3.1.2. Samples obtained by sieving method 2 .....	127
3.2. Results on silty soil treated with cement.....	128
3.2.1. Samples obtained by sieving method 1 .....	128
3.2.2. Samples obtained by sieving method 2 .....	130
3.3. Results for the clay treated with lime.....	132
3.3.1. Samples obtained by mixing method A .....	132
3.3.2. Samples obtained by mixing method B .....	134

3.4. Results on the clay treated with mixture .....	136
3.4.1. Samples obtained by mixing method A .....	136
3.4.2. Samples obtained by mixing method B .....	138
3.5. Aggregate size effect on shear modulus.....	139
3.5.1. For the silty soil.....	139
3.5.2. For the clayey soil .....	145
3.6. Discussion .....	150
3.6.1. For the silt .....	150
3.6.1.1. Treatment mechanisms for $G_{max}$ -time curves .....	150
3.6.1.2. Aggregate size effect.....	152
3.6.2. For the clay.....	154
3.6.2.1. Treatment mechanisms for $G_{max}$ -time curves .....	154
3.6.2.2. Aggregate size effect.....	156
3.7. Conclusions.....	157
<b>Chapter 4. Aggregates size effect during drying/wetting cycles.....</b>	<b>159</b>
4.1. Wetting/drying process .....	159
4.2. Results of silt treated with lime.....	162
4.2.1. Results for dry side.....	162
4.2.2. Results for wet side .....	165
4.2.3. Matric suction change .....	168
4.2.4. Results with intensive drying .....	170
4.3. Results on cement treated silt.....	171
4.3.1. Results for dry side.....	171
4.3.2. Results for wet side .....	174
4.3.3. Matric suction change .....	177
4.3.4. Results with intensive drying .....	178
4.4. Results on the lime treated clay .....	180
4.4.1. Mixing method A .....	180
4.4.1.1. Results for dry side.....	180
4.4.1.2. Results for wet side .....	183
4.4.2. Mixing method B .....	186
4.4.2.1. Results for dry side.....	186
4.4.2.2. Results for wet side .....	186
4.4.3. Matric suction change .....	188
4.5. Results of the mixture treated clay.....	190
4.5.1. Mixing method A .....	190
4.5.1.1. Results for dry side.....	190
4.5.1.2. Results for wet side .....	192
4.5.2. Mixing method B .....	194
4.5.2.1. Results for wet side .....	194
4.5.3. Matric suction change .....	196
4.6. Aggregates size effect through the failure number of cycles .....	198
4.7. Aggregates size effect on shear modulus .....	202
4.7.1. Results for silt treated with lime .....	202
4.7.2. Results for silt treated with cement.....	205
4.7.3. Results for the lime treated clay.....	206
4.7.4. Results for the mixture treated clay .....	207
4.8. Aggregates size effect on the saturation degree change.....	209
4.9. Aggregates size effect on volume change .....	210
4.10. Aggregates size effect on the drying period.....	212

4.11. Discussion .....	213
4.12. Conclusions .....	215
<b>Chapter 5. <i>In-situ</i> specimens from the experimental embankment in Héricourt.....</b>	<b>217</b>
5.1. Results of silt side .....	217
5.2. Results on the silt treated with cement.....	219
5.2.1. First batch of core sample SC31-1 .....	219
5.2.2. Core SC49-1 of the second batch.....	221
5.2.3. Time effect .....	223
5.2.4. Climate effect .....	224
5.3. Results of clay side.....	225
5.3.1. Cores dominantly treated by lime .....	225
5.3.1.1. SC5-1.....	225
5.3.1.2. SC14-1.....	227
5.3.1.3. SC14-2.....	229
5.3.1.4. SC46-1.....	232
5.3.1.5. SC46-2.....	233
5.3.2. Time effect .....	234
5.3.3. Climate effect .....	235
5.3.3.1. The surface layers of clay side (SC14-1, SC46-1) .....	235
5.3.3.2. Central layers of the embankment (SC14-2 and SC46-2).....	237
5.4. Cores dominantly treated by mixture .....	238
5.4.1.1. SC20-1.....	238
5.4.1.2. SC20-2.....	241
5.4.1.3. SC20-3.....	242
5.4.1.4. SC20-4.....	243
5.4.1.5. SC47-1.....	245
5.4.1.6. SC47-2.....	247
5.4.2. Time effect .....	248
5.4.3. Climate effect .....	250
5.4.3.1. Comparison between SC20-1 and SC47-1 .....	250
5.4.3.2. Comparison between SC20-2 and SC47-2 .....	251
5.5. Discussion .....	252
5.5.1. Heterogeneity of <i>in-situ</i> soils .....	252
5.5.1.1. Additive distribution effect .....	252
5.5.1.2. Aggregates size effect .....	253
5.5.1.3. Effect of stone presence .....	254
5.5.1.4. Water content effect .....	255
5.5.1.5. Dry density effect.....	256
5.5.1.6. Compaction process effect .....	259
5.5.2. Time effect .....	260
5.5.3. Climate effect .....	261
5.5.3.1. Water content-stiffness change .....	261
5.5.3.2. Dry density change.....	265
5.5.3.3. Fissures development.....	267
5.5.4. Treatment effect.....	267
5.5.4.1. Water content change.....	267
5.5.4.2. Stiffness change.....	268
5.6. Conclusions.....	270

<b>Chapter 6. Modelling of curing behaviour in both laboratory and field conditions.....</b>	<b>271</b>
6.1. Model proposed.....	271
6.2. Modelling of the curing behaviour of lime treated silt.....	275
6.2.1. Curing behaviour.....	275
6.2.2. Aggregates size effect for the parameters.....	277
6.3. Modelling of the curing behaviour of the cement treated silt.....	281
6.3.1. Curing behaviour.....	281
6.3.2. Aggregates size effect.....	283
6.4. Modelling of the curing behaviour of lime treated clay.....	286
6.4.1. Curing behaviour.....	286
6.4.2. Model parameters for different aggregates sizes.....	288
6.5. Modelling of the curing behaviour of mixture treated clay.....	291
6.5.1. Curing behaviour.....	291
6.5.2. Model parameters for different aggregates sizes.....	293
6.6. Synthesis of the aggregates size effect.....	297
6.7. Application of the hyperbolic model to the field aggregates size level.....	300
6.8. Comparisons between laboratory and field conditions.....	303
6.9. Discussion.....	306
6.9.1. Modelling and aggregates size effect in laboratory size level.....	306
6.9.2. Comparison of the results between laboratory and field conditions.....	309
6.10. Conclusions.....	310
<b>General conclusion.....</b>	<b>311</b>
Aggregates size effect during curing.....	311
Aggregates size effect during wetting/drying cycles.....	314
Perspectives.....	316
<b>Appendix.....</b>	<b>317</b>
1. Description of the core samples on the silt side of the experimental embankment.....	317
2. Description of the core samples on the clay side of the experimental embankment.....	318
<b>Reference.....</b>	<b>325</b>



## Introduction

Cementitious treated soils are widely used in road and railway construction, embankments, dams, slab foundations, piles, etc. because it can not only improve the workability of soils by lowering water content, but also improve their hydro-mechanical performance by reinforcing and binding the soil grains/aggregates.

Even though the efficiency of soil treatment is proved in practice, the good hydro-mechanical performance of treated soils in long term is still an open question. Indeed, we know that all pavement layers suffer from the effects of the environment changes and can be damaged over time. This is of course the case of pavement with treated soils. Previous studies show that well-designed stabilized layers can effectively resist to the environment changes and present good behaviour for many years. However, there is no consensus on the long-terms hydro-mechanical behaviour of treated soils; some studies show that the soil performance still improve, even after several decades (Kelley, 1977; Ali *et al.*, 2011), while some others show a serious degradation only a few years after the compaction. For instance, the lime treated very plastic clay - A3/A4, used in the construction of the highway between Rethel and Charleville-Mézières in France, lost its mechanical performance 6 years after the construction of highway (Cuisinier *et al.*, 2009). This shows the importance of the question about the durability of treated soils.

In this context, the TerDOUEST project (Terrassements Durables - Ouvrages en Sols Traités) (2008 - 2012) was set-up, aiming at advancing the knowledge on the reusability of unsuitable materials (very clayey soils, swelling soils, etc.) and their durability in earthworks after treatment, under climatic changes (flood, evaporation/infiltration, wetting/drying cycles, etc.). This project contains four parts:

- physico-chemical behaviours of treated soils (Module A);
- durability of treated soils in both laboratory and field conditions (Module B);
- experimental embankment behaviour (earthwork in field) in a flooding area (Héricourt (70), France) (Module C) ;
- environmental impact of soil treatment operations (Module D).

The work carried out in the present PhD thesis is part of Module B and Module C of TerDOUEST project, focusing on the effects of three different factors on the mechanical behaviour of treated soils:

- the curing time (curing effect);
- the size of aggregates (aggregates size effect);
- the wetting / drying cycles (climate effect).

This work is defined based on the consideration as follows:

Several studies reported that the cementitious treatment products are usually located on the surface of aggregates (Locat *et al.*, 1990; Ingles *et al.*, 1970; Le Roux *et al.*, 1969). Moreover, some attempts were done to correlate the laboratory results to field ones; but divergent conclusions are often obtained (Bryhn, 1984; Locat *et al.*, 1990; Hopkins, 1996; Puppala *et al.*, 2005; Horpibulsuk *et al.*, 2006; Bozbey and Guler, 2006; Kavak and Akyarh, 2007; Cuisinier and Deneele, 2008a; Snethen *et al.*, 2008). Most studies reported that the soils mixed in the laboratory usually show better mechanical performance than those mixed in field.

Examination of the laboratory mixing conditions and the field ones shows that the most notable difference between them may be the aggregates sizes. This difference might be the main factor causing the divergence between the laboratory and field conditions. Obviously, the soils mixed in field have large aggregates, while the soils mixed in the laboratory often have much smaller aggregates. Based on this idea, Tang *et al.* (2011) studied the aggregate size effect on the stiffness of lime treated Tours silt compacted at a very low water content in the laboratory. The results evidence the significant aggregates size effect. This suggests the laboratory results cannot be used to design and guide field operations. This phenomenon leads us to be interested in the aggregate size effect on the mechanical behaviour of treated soils.

For this purpose, we investigate the effects of aggregates size on the small strain shear modulus,  $G_{\max}$ , of lime and/or cement treated soils at both laboratory size scale and field size scale. For the specimens prepared in the laboratory, we study the stiffness of the soils of different initial aggregates sizes (sub-series), by different treatments and compacted at different moulding water contents. The evolution of  $G_{\max}$  was studied during curing and during application of drying/wetting cycles. For the specimens prepared in field for the construction of the experimental embankment, we investigate the stiffness of the *in-situ* core



samples. Comparison between the results obtained from tests on different specimens enables the aggregates size effect to be investigated.

$G_{max}$  was chosen in this study mainly because fundamentally it is closely related to changes in soil cohesion, and moreover it can be easily measured using the wave propagation technique by bender element. This is a non-destructive technique, allowing the performance of the same soils to be investigated at different states and at different times.

The dissertation contains six chapters.

Chapter one provides an overview of the current knowledge on the lime and/or cement treated soils. Firstly, we recall the soil treatment techniques in geotechnical engineering, involving both laboratory design and field application. Then, we introduce the fundamental mechanisms of the cementitious treated soils, including the physical/chemical changes within the soil/additive system and microstructure changes due to the cementitious treatment. Some factors influencing the efficiency of treatments are also presented. Thereafter, we present the common experimental techniques used to evaluate the performance of the treated soils, involving the strength, stiffness, durability and microstructure changes. Finally, we introduce the hydro-mechanical behaviour of treated soils, involving changes in strength and stiffness due to the effects of treatments and cyclic climate changes. Emphasis is put on the microstructure changes due to curing and climate effects, and on the difficulties of correlating the results between laboratory and field conditions.

The second chapter is devoted to the presentation of materials (lime, cement, water, and silt/clay powders), different compaction conditions of specimens (ex. dry and wet sides in the laboratory, different aggregates size levels between laboratory and field), test program and experimental techniques employed. For the specimens prepared in the laboratory, we present the preparation of the powders of different initial maximum aggregates size ( $D_{max} = 0.4 \text{ mm}, 1 \text{ mm}, 2 \text{ mm}, 5 \text{ mm}$ ) by two sieving methods (method 1 and method 2), for both the silt and the clay taken in Héricourt. Then, we present how to mix and compact the soils/additives (two soils: silt/clay; four treatments; two mixing methods). Thereafter, we present the test program allowing investigation of the effects of curing time, climatic change and aggregates size on the stiffness. For the specimens compacted *in-situ*, two batches of cores of silt and clay with several treatments were taken at different times. Note that the aggregates size are controlled during compaction:  $D_{max} = 31.5 \text{ mm}$  for the clay and  $D_{max} = 20 \text{ mm}$  for the silt. After the core samples are transported to the laboratory, they are firstly

described visually and a protocol of preparation of core specimens is then defined. Finally, the test program on these core specimens is specified (ex.  $G_{\max}$ , density, water content measurements). In addition, we illustrate how to determine  $G_{\max}$  using the technique of bender element. An identification method of the travel time of shear waves is defined for this purpose. The relationship between the frequency chosen and the stiffness of the soils is established, allowing the accuracy of measurement to be improved.

The third chapter presents the effect of aggregates size on the stiffness of the treated soils during curing time. The specimens involved are the ones prepared in laboratory, with the initial maximum aggregates size scales 0.4 ~ 5 mm. The  $G_{\max}$  change with time was recorded for several thousands of hours, allowing the curing effect, water effect (dry and wet sides) and aggregates size effect being identified.

The fourth chapter investigates the sensitivity of the treated soils to water content changes at the laboratory aggregates size scale. The aggregates size effect during wetting/drying cycles is identified on the specimens after the curing time.

The fifth chapter presents the results of the specimens compacted in field for the construction of the experimental embankment in Héricourt. The profiles of  $G_{\max}$ , dry density and water content are depicted for the two batches of cores taken. The effects of soil heterogeneity (including the aggregates size effect in the field aggregates size levels for the silt and the clay), curing time and climate are investigated.

The sixth chapter is devoted to building the relationship between the laboratory and field based on the aggregates size effects identified at the laboratory aggregates size scale. Firstly,  $G_{\max}$  evolution curves obtained in laboratory are modelled by a hyperbolic model. The parameters of the model are determined for each  $D_{\max}$  and then analysed as a function of  $D_{\max}$ . Then, by considering the field aggregate sizes, the  $G_{\max}$  of *in situ* specimens can be obtained. Comparison between the model predictions and experimental measurements shows the performance of the model proposed, provided that the mean values of experimental data are used to minimize the effect of soil heterogeneity related to the presence of stones, distributions of additives and water content.

## Chapter 1. Literature review

In this chapter, a description of the current practice of soil treatment is firstly presented, followed by the presentation of the fundamental mechanisms involved in treated soils as well as the presentation of the experimental techniques and of hydraulic and mechanical behaviours identified.

### 1.1. Practice: use of soil treatment in geotechnical engineering

#### 1.1.1. Treatment goals

Earthworks are widely used in civil engineering practice, such as road and railway construction, embankments, dams, canals, airstrips or air fields, slab foundations and piles, etc. In order to make the earthwork meet all the requirements in terms of safety and efficiency, the soil needs to satisfy the physical and mechanical characteristics defined in the design. Commonly, earthworks are carried out based on an organised sequence of operations such as: 1) excavation of adequate soils from appropriate sites; 2) transportation; 3) placing to the construction site. Considering the economical and environmental factors, the earthworks are usually conducted using the soil in place. Therefore, soil treatment becomes a necessity when meeting problematic soils such as clayey soils (Bell, 1993). The treatment aims at improving the soils’:

- ◆ Strength – the ability to resist stresses that develop as a result of traffic loading;
- ◆ Stiffness (modulus) – the ability to respond elastically and thereby minimize permanent deformation when subjected to traffic loading;
- ◆ Stability – the ability to maintain its physical volume and mass when subjected to loading or moisture changes;
- ◆ Durability – the ability to maintain material and its engineering properties when exposed to environmental conditions (moisture and temperature changes for example).

### 1.1.2. Cementitious stabilization methods

Cementitious stabilization or modification of soils is the most common method in earthworks, especially in pavement, where lime and cement additive together with the by-product of the lime/cement manufacturing process (Ex. fly ash and lime kiln dust), are traditionally used (Croft, 1967 and 1968; Little *et al.*, 2000). The cementitious stabilization for high plastic soils using calcium-based stabilizers, such as lime and ordinary Portland cement, has been widely practiced over the last six decades. It should be noted that other chemical materials used in soil stabilization also exhibit cementitious properties, such as rice husk ash (Basha *et al.*, 2005; Yin *et al.*, 2006; Alhassan *et al.*, 2008; Okafor *et al.*, 2009), silica fume (Kalkan *et al.*, 2011), slag (Yuan *et al.*, 2010), fly ash (Amadi, 2010) and natural pozzolans (Hossain *et al.*, 2011). In practice, these materials are combined with lime and/or cement, such as lime-fly ash (Ferrell *et al.*, 1988; Lim *et al.*, 2002; Barstis *et al.*, 2003; Beeghly, 2003), lime-fly ash, cement kiln dust (Solanki *et al.*, 2010), cement-ash (Kolias *et al.*, 2005; Altun *et al.*, 2009) and lime-cement (Puppala *et al.*, 2005; Joel and Agbede 2010; Okyay and Dias 2010; Jauberthie *et al.*, 2010; Azadegan *et al.*, 2011; Sirivitmaitrie *et al.*, 2011).

Lime stabilization is well known to chemically transform unstable soils into relatively stable subgrade soils, subbase materials and base materials, either alone or in combination with other materials (Highways Agency, 2000). However, lime may be used also for short-term soil modification by reducing the plasticity of soil, and thereby rendering unsuitable materials workable for bulk fill and other earthworks applications. Lime stabilization or modification can be applied to a large range of soils (Boardman *et al.*, 2001; Little and Nair, 2009). Lime in the form of quicklime (calcium oxide–CaO), hydrated lime (calcium hydroxide–Ca (OH) <sub>2</sub>), or lime slurry can be used for this purpose (National Lime Association, 2004). Based on ASTM D5102-04, lime is generally classified as calcitic or dolomitic. Usually in soil stabilization, high-calcium hydrated lime [Ca(OH)<sub>2</sub>] or monohydrated dolomitic lime [Ca(OH)<sub>2</sub>+MgO] are used.

Soil cement stabilization technique has also been employed since early 30s (Christensen, 1969; Das, 1990). Cement treatment causes chemical reaction similarly to lime and can be also used for both modification and stabilization purposes. Cement-stabilized materials generally fall into two classes: cement-modified and soil-cement (soil stabilized) (Little *et al.*, 2000; European standard 14227-10). Soil-cement is usually used to make a hard

surface as a base course for roads. Compared to soil-cement material, the cement-modified soil is a soil treated with a relatively small proportion of Portland cement. Cement-modified soil is typically used to improve subgrade or to amend local aggregates for use as base instead of more costly transported aggregates. Alternative terms include cement-treated or cement-stabilized soil or subgrade.

### **1.1.3. Treatment design in laboratory**

A well designed soil treatment can support the deleterious effects of environment and thus ensure the earthwork to be reliable and durable. The current treatment design includes: 1) Suitability study for treatment; 2) Determination of optimum additive percentage; 3) Determination of moisture/density relationship by compaction test (Little and Nair, 2009).

#### **1.1.3.1. Suitability of treatment methods**

A credible design should include an additive which is mineralogically reactive with a given soil or aggregate and uses minimum additive content to meet the requirements in terms of strength, stiffness and durability. Currently, the suitability of treatments is mostly evaluated by the soils' swelling properties, plasticity, grain sizes distribution and organic contents etc. (Currin *et al.*, 1976; Little *et al.*, 1995a; McNally, 1998). Although both lime and cement are the calcium-based additives, the suitability of lime and cement treatment is different due to their different compositions and modification mechanisms.

Lime works well for clayey soils, especially those with moderate to high plasticity index ( $PI > 15$ ) (Little *et al.*, 1995b; Thagesen, 1996; handbook GTR, 2000; Muhunthan and Sariosseiri, 2008). Many works show that very substantial and structurally significant changes are expected as lime substantially improves the physical properties of fine-grained soils (McCallister and Petry, 1990; Locat *et al.*, 1990; Bell, 1996; Locat *et al.*, 1996; Rogers and Glendinning 1997; Rajasekaran and Rao 1997; Rao *et al.*, 2001; Boardman *et al.*, 2001; Tono *et al.*, 2004; Cai *et al.*, 2006; Khattab *et al.*, 2007; Sakr *et al.*, 2009; Maubec, 2010; Mleza and Hajjaji, 2011; Tang *et al.*, 2011), especially expansive soils (McCallister and Petry, 1990; Rao *et al.*, 2001; Tono *et al.*, 2004; Puppala *et al.*, 2005; Bozbey *et al.*, 2010). However, lime does not work well for silts and granular materials, due to lack of aluminates and silicates in these materials, which does not allow the pozzolanic reactions to take place. Further, the soil-lime reactions and the stabilization process are not only affected by

mineralogy but also by other compounds within the soil, including organic matters and salts. Little (1999) reported that the soils with organic contents in excess of 1% may be difficult to stabilize with lime. High sulfate concentrations can lead to loss of stability and heaving of soils (Harris *et al.*, 2006).

In case of cement treatment, any type of soil may be concerned. The method is especially suitable for the granular soils (Thagesen, 1996) and the clayey materials with low plasticity index (Currin *et al.*, 1976; Engineering manual 1110-3-137, 1984; Little *et al.*, 1995c; Prusinski and Bhattacharja, 1999; Texas Department of Transportation, 2005), with the exception of highly organic soils or some clay with high plasticity (Bell, 1993). Granular soils are preferred since they pulverize and mix more easily than fine-grained soils and so result in more economical soil-cement as they require less cement. Typically, soils containing between 5 and 35% fines yield the most economical soil cement. The American Concrete Institute (Anon, 1990) reported that the soils with organic content greater than 2% or having pH lower than 5.3 are not suitable for cement treatment.

#### **1.1.3.2. Determination of optimum additive percentage**

Prior to earthwork construction, laboratory tests of soils shall be carried out to determine the quantity of addition required in the mix, aimed at soil modification or stabilization. The most famous method is the determination of the minimum lime content (or lime-fixation point) by Eades and Grim pH test (Hilt and Davidson 1960; Eades and Grim 1966; McCallister and Petry 1992; Locat *et al.*, 1996; Little *et al.*, 1995, Rogers and Glendinning, 1997; 2000; ASTM D6276-99a). This point indicates the percentage of lime required to produce a saturated solution of lime in a suspension of clay in water and thereby to satisfy fully ion exchange. ASTM D6276 was established to determine the proper amount of lime that a particular soil needs to obtain a mixture pH of 12.4 (Figure 1-1). Later, Rogers and Glendinning (1997; 2000) improves the Eades and Grim pH test by proposing the Method for Determining Stabilization Ability of Lime (ASTM C977-95).

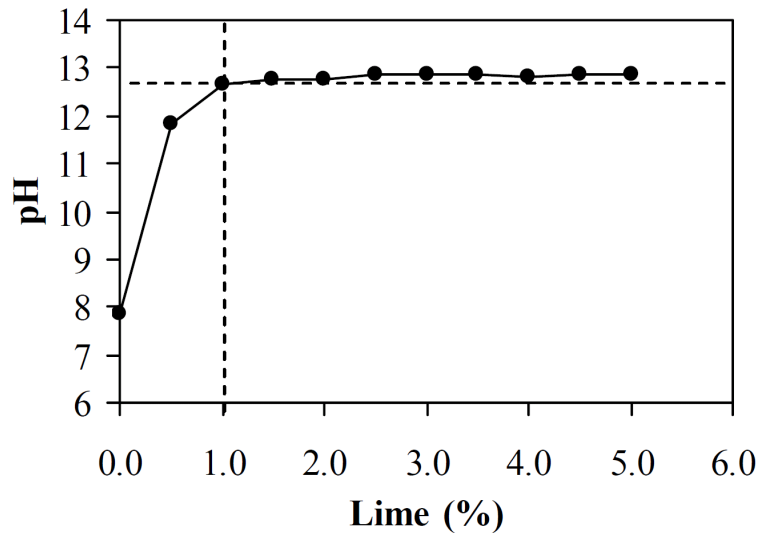


Figure 1-1 Cation exchange capacity tests (Le Runigo, 2008; Akbulut and Arsan2010)

After knowing the lime-fixation point, the required amount of lime can be determined for the desired degree of stabilization or modification. Since the clay content is one of the important factors controlling the chemical and physical properties of soils, some researchers give the empirical equation for different treatment purposes based on the clay percentage or soil's PI value. Some studies (Hilt and Davidson, 1960; Bergado *et al.*, 1996) suggested a semi-empirical formula (1-1) to calculate the optimum lime content; note that the percentage of treatment is usually calculated using the weight of dry soil (see in 1-2). For the modification purposes, normally 2% to 3% by dry weight of soil is sufficient (Das, 1990; Maher *et al.*, 2005). Larger quantities are required for the stabilization induced by pozzolanic reactions, increasing the soil strength. Typically, 5% to 10% by weight of dry soil are used (Das, 1990). However, this clay fraction content-based optimum lime content has its shortcoming because it omits the cation exchange capacity nature determined by considering the clay mineral composition (Christensen, 1969), which may be also decisive in controlling the chemical and physical properties of soils.

$$\text{Optimum Lime Content} = \frac{\% \text{ of clay}}{35} + 1.25 \quad (1-1)$$

$$\text{Additive percentage} = \frac{m_{\text{additive}}}{m_{\text{dry soil}} + m_{\text{additive}}} \times 100\% \quad (1-2)$$

The Eades and Grim's procedure (through pH measurement) is not applicable for cement treatment because of the presence of alkali ions (K<sup>+</sup> and Na<sup>+</sup>) in cement (Prunsinski and Bhattacharja, 1999). Currently, the principle of determining the cement dosage for soil

treatment is simple: we firstly determine the relationship of dry density/water content for different cement contents; then investigate the strength of cement stabilized soil respective to the cement content, water-cement ratio and the related conditions. The dosage can then be determined according to the requirements in terms of designed strength. Many studies recommended considering water-cement ratio and the strength characteristics when determining cement content (Fitzmaurice, 1958; Aderibigbe *et al.*, 1985; Kamang, 1998; Guthrie *et al.*, 2002; Horpibulsuk *et al.*, 2003; Pathivada, 2007; Olugbenga *et al.*, 2007; Kang *et al.*, 2008; Zhang and Tao, 2008; Ayangade *et al.*, 2009). According to the European standard 14227-10, the cement stabilized soil is designed to attain the stability measured by California Bear Ratio (CBR) capacity testing and to attain a structural integrity directly measured by unconfined compressive strength or tensile strength and elastic modulus (E) testing. Some American standards (ASTM C150, ASTM C595), together with the standards ASTM D806, ASTM D2901 and ASTM D5982, are elaborated to determine the required amount of cement or minimum amount of cement required for cement stabilization. In addition, Prunsinski and Bhattacharja (1999) proposed to use PI reduction measurements by performing the Atterberg limits tests to determine the dosage requirements for both cement and lime treatment. Nevertheless, it is still unknown if the solidification reactions (pozzolanic reaction) really happen when meeting these aforementioned requirements. It is also necessary to evaluate the quality of cement-soil by durability tests in the laboratory prior to field application.

### **1.1.3.3. Determination of moisture-density relationship**

Water content-density relationship is important in determining the soil suitability for stabilization (NF P 94-093; ASTM D698).

In the laboratory, compaction usually employs the tamping or impact compaction method using the equipment and methodology developed by R. R. Proctor in 1933, known as the Proctor test. Either Normal Standard Proctor or Modified Proctor Test is performed to determine the water content-density relationship of a soil, where the optimum water content results in the greatest density. Figure 1-2 presents a normal proctor curve with different compaction methods (Seed and Chan, 1960). The dry side, the wet side and the optimum water content can be identified on this curve. In order to obtain effective compaction, the engineering behaviours among optimum water content (OWC), dry of optimum and wet of optimum on the proctor curve should be investigated prior to compaction in field.



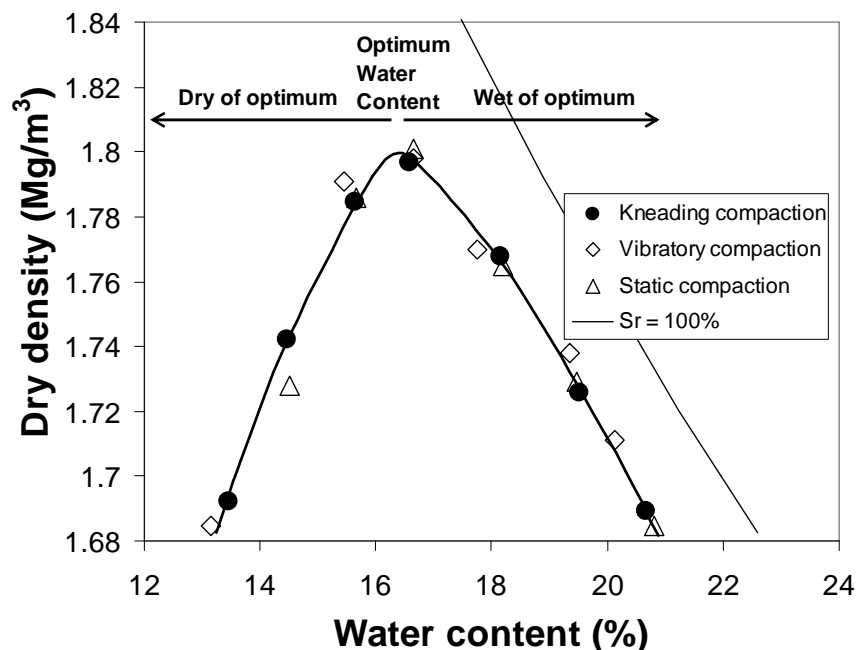


Figure 1-2 Normal proctor curves by several compaction methods (according to Seed and Chan 1960)

Several studies (Seed and Chan 1960; Lambe and Whitman 1969; Barden and Fice, 1974; Holtz and Kovacs, 1981; Daniel and Benson, 1990; Daita *et al.*, 2005; Russo *et al.*, 2006) show the different engineering properties of the cementitious treated soils compacted on wet side, on dry side and at optimum. These studies also show the good engineering properties when soil-additive mixture are compacted at or near the optimum water content. Thus, this compacted soil-additive mixture is recommended for embankment or other earthworks (Barden and Fice 1974; Locat, 1990).

Several factors may modify the proctor curve of soils, such as soil type, cementitious treatment method and compaction delay.

Firstly, soil parameters such as texture, grain size distribution, particle shape, plasticity, and moulding water content are important material properties in controlling how well the soil can be compacted (Holtz and Kovacs, 1981; Forssblad, 1981; Rollings M. P. and Rollings R. R., 1996).

Secondly, the cementitious treatment of soil can also modify the compaction curves under the same proctor energy conditions. For lime treatment of soils, numerous studies (Lee *et al.*, 1982; Petry and Lee, 1988; Bell, 1989; Bell, 1996; Mallela *et al.*, 2004; Russo *et al.*, 2006; Le Runigo, 2008; Cuisinier and Deneele, 2008a; Hachum *et al.*, 2011; Cuisinier *et al.*, 2011) indicate that the addition of lime to clayey materials increases their optimum moisture

content and reduces their maximum dry density for the same compaction effort. Several studies (Christensen, 1969; Tabatabai, 1997; Sariosseiri, 2008; Bahador and Pak, 2011) reported the similar observation for cement treated soils. However, the modification effect on the compaction curves is rather controversial for treated clays, especially for heavy clays (defined as soils with a clay fraction larger than 60%, by the Canadian System of Soil Classification) (Croft, 1967; Bell, 1996; ACI committee 230, 1990; Sariosseiri, 2008).

Thirdly, the compaction delay or mellowing (the period, after mixing, but prior to compaction) can also significantly modify the compaction curves due to the immediate hydration reaction. Mellowing and remixing allows achieving a homogeneous mixture and improving workability (Little and Nair, 2009). In the literature, the mellowing periods are variable for both lime and cement treated soils. For lime treated soils, the specified amount of time for mellowing varies greatly throughout the literature. Some researchers have used 1 hour (Dempsey 1967; Sauer and Weimer, 1978; EN 14227-11:2006; Kavak and Akyarh, 2007; Le Runigo, 2008; Parker, 2008; Harichane *et al.*, 2010; Stoltz and Cuisinier, 2010; Stoltz *et al.*, 2010; Harichane *et al.*, 2010; Tang *et al.*, 2011; Al-kiki *et al.*, 2011; Stoltz *et al.*, 2012), 3 hours (Oflaherty and Andrews, 1968; Esmer *et al.*, 1969), or several hours (Osinubi, 1998; Osinubi *et al.*, 2006; Hachum *et al.*, 2011); some others have used 12 hours (Pedarla, 2009), 24 hours (Townsend and Klym, 1966; Walker *et al.*, 1967; Christensen, 1969; Russo *et al.*, 2006), 24 ~ 72 hours (Rogers and Glendinning, 2000; United Kingdom Manual of Contract Documents for Highway Works cited by Rogers *et al.*, 2006), 48 hours and even 72 hours (Dempsey and Thompson, 1967). For cement treated soils, the mellowing period also varies in different studies and generally is shorter than lime treated soils: less than 40 minutes (Horpibulsuk *et al.*, 2010); 30 ~ 60 min (EN 14227-10:2006); 1 hour (Sariosseiri, 2008; Pedarla, 2009; ASTM D 698); 1/2/3 hours by Osula (1996); variable periods 0~5 hours by Ingles and Metcalf (1973); 0/24 hours by Christensen (1969). For both lime treated and cement treated soils, the European standard (EN 14227-11 and EN 14227 -10) specifies that the specimen shall be manufactured immediately or no later than 90 min after mixing when measuring the immediate bear index test. In general, a mellowing period of 1 hour is the most commonly specified. The suitable mellowing or compaction delay is commonly thought to be helpful for the strength development of lime treated soils. However, long term delay compaction of cement treatment is revealed to be adverse for cement-soil stabilization (Christensen, 1969; Ingles and Metcalf, 1973; Charman, 1988; Osula, 1996; Osinubi *et al.*, 2006).

#### 1.1.4. Compaction in field

An extremely important task for geotechnical engineers is to ensure that compacted fills meet the prescribed design specifications. Several different methods are used to compact soil in the field, such as tamping, kneading, vibration, and static load compaction. Cementitious modification/stabilization materials can be variable as mentioned previously, while the process is similar. Here we take lime treatment for example to explain the treatment process in field. The construction steps involved in lime stabilization or lime modification are similar, although the stabilization requires more lime and more thorough processing control than the modification. The application is a little different between central mixing and in-place mixing method (National Lime Association, 2004):

- For central mixing which means the mixing working is off site in stead of in-place mixing, the process is: 1) spreading the lime–aggregate-water mixture; 2) compacting; 3) curing.
- For in-place mixing, it is used in most earthworks: 1) scarifying or partially pulverizing soil (Bozbey and Garaisayev, 2010); 2) spreading lime; 3) adding water and mixing; 4) mellowing; 5) compacting to the maximum density; 6) curing prior to placing the next layer or wearing course (ex. base of roads), and 7) scarifying for the next compaction layer (see Figure 1-3).

Compaction should begin immediately after the final mixing. If this is not possible, delays of up to four days should not be a problem for lime treatment if the mixture is lightly rolled and water content permits. To ensure adequate compaction, the equipment should be matched to the depth of the lift and the final surface compaction is completed using a steel wheel roller.

The mellowing requirement is usually different between cement and lime treated soils in field compaction. Firstly, for lime treatment, mellowing is gainful for modification, typically 1 to 7 days is common used (National Lime Association, 2004). For low Plasticity soils, or when drying or modification is the goal, mellowing is often not necessary (National Lime Association, 2004). Secondly, for cement treated soils, the solidification induced by hydration process begins as soon as it contacts the soil. Normally, any delay can be harmful for cement-soil stabilization. However, as it is difficult to mix dry cement with very clayey soils (ex. heavy clays according to the Canadian System of Soil Classification or A4 according to NF 300 - 11) and large amount of cement have to be added to make appreciable

changes in their properties. The Heavy clays may often be pre-treated with 2~3% cement or more frequently with hydrated lime, which reduces the plasticity, thereby rendering the clay more workable. After curing for 1~3 days (mellowing), the pre-treated clay is stabilized with cement (Bell, 1993).



(a) Scarifying/pulverizing



(b) Spreading lime



(c) Scarification after spreading



(d) Adding water



(e) Mixing



(f) Compaction with vibratory padfoot rollers

**Figure 1-3 In-place earthwork process (National Lime Association, 2004)**

Comparison between laboratory and field compaction conditions shows that the aggregates size distribution is different between two conditions. In the laboratory, soils' aggregates are usually of several millimetres or micrometers; By contrast, the largest grain/aggregate size can reach several centimetres in field. Moreover, the compaction effort applied is also different due to the development of much heavier earth moving and vibratory roller compaction equipment in field, which leads to non attainable densities by laboratory compaction using the current "water content-density" standards. Higher compaction efforts, routinely applied in field, not only result in higher unit weight but also lower optimum moisture contents than those found in the laboratory. Finally, the mellowing conditions are often different: 1) mellowing time is often longer in field than in the laboratory; 2) the temperature, moisture may also be different.

### **1.1.5. Quality control in earthwork engineering**

Soil water content and dry density are the properties generally used for controlling compaction in earthwork engineering. In France, a quality control guide was elaborated for pavement (GTR, 1992, 2000). In this classification system, the quality is classified into four grades, namely q1, q2, q3 and q4, respectively. For an embankment/sub-grade of road (see the work of Boussafir and Froumentin., 2010 in TerDOUEST project: Module C; NF P98 331: 2005; CORREZE, 2009), the centre of embankment is classified q4 which means the mean density  $\rho_{dm} \geq 95\% \rho_{dOPN}$  and the density of the bottom part (8 cm)  $\rho_{dfc} \geq 92\% \rho_{dOPN}$ ; for the subgrade part (CDF) and the top of earthwork (PST), it requests higher quality than for the embankment: with q3 - the mean density  $\rho_{dm} \geq 98.5\% \rho_{dOPN}$  and the density of the bottom part  $\rho_{dfc} \geq 96\% \rho_{dOPN}$ ; for the base (Assise), q2 is needed - the mean density  $\rho_{dm} \geq 97\% \rho_{dOPM}$  and the density of the bottom part (8 cm)  $\rho_{dfc} \geq 95\% \rho_{dOPM}$ .

Because of lack of the modified proctor data, only the normal proctor data will be presented in the following sections when it comes to the quality control of the density in field. For the embankment, the water content control is usually controlled in the zone near the optimum water content.

## **1.2. Fundamental mechanisms about the cementitious treatments of soils**

### **1.2.1. Physical/chemical characteristics changes**

From a physical/chemical point of view, the calcium-based reactions in lime and/cement treatment is similar to the reactions in the soil-water system. The additives modify the soil properties through their hydration and ionization, the flocculation and agglomeration caused by cation exchange and the cementation products induced by pozzolanic actions (Bell *et al.*, 1996; Boardman *et al.*, 2001). Additionally, these reactions results in different products due to the additive nature and the interaction in the soil-water-additive system. Of course, these additives require water or water plus silica/alumina present in clays to perform these reactions. Prunsinski and Bhattacharja (1999) stated that Portland cement provides the compounds (cementitious hydration) and chemistry necessary to achieve all the processes while lime can accomplish all the processes except cementitious hydration. The mineralogy, quantity, and particle size of fines in the soil can also greatly impact the performance of additives.

#### **1.2.1.1. Chemical characteristics changes of lime-treated soils**

Many studies reported that when adding an agent to a wet soil, complex reactions occur among clay fraction, water and agent systems. Boardman *et al.* (2001) stated that adding lime to a soil system containing water results in several chemical reactions that cause a profound alteration of the physico-chemical properties of clayey soils, depending on factors such as soil gradation, types of clay minerals, organic matter, pH, sulphate and etc. which significantly influence the ability of clay to react with lime and cement (Sherwood, 1958 and 1962; Moh, 1962; Mateos, 1964; Eades and Grim, 1966; Thompson, 1966; Croft, 1967; Currin *et al.*, 1976; Hunter, 1988; Anon, 1990; Bell, 1993; Prunsinski and Bhattacharja, 1999). Furthermore, the reaction mechanism can be different between short term modification and long term solidification or stabilization. Long term solidification reactions need high pH pore water produced by the addition of lime or cement which promotes the dissolution of silicon and aluminium from the edge sites of the clay plates (Sherwood, 1993). In this section, the short term modification and long term solidification mechanisms are termed as first and second mechanism, respectively. The corresponding reactions will be

introduced too, for lime treatment, cement treatment and mix treatment with both cement and lime.

Lime stabilization develops due to base-exchange (modification or first mechanism) and cementation processes (stabilization or second mechanism) between clay particle and lime. Another mechanism caused by carbonation in lime treatment is still controversial. The primary effect of small lime additions is to decrease significantly the liquid limit (Hilt and Davidson, 1960; Brandl, 1981; Rogers and Glendinning, 1997), plasticity index, maximum dry density and swelling pressure, as well as to increase the optimum water content, strength, and durability of clays (Rogers and Glendinning, 1996).

Changes of these parameters are time dependent and governed by different chemical reactions processes. In general, stabilization of soil by lime is achieved through cation exchange, flocculation, agglomeration, lime carbonation and pozzolanic reaction. Cation exchange, flocculation and agglomeration reactions take place rapidly and bring immediate changes to soil properties such as strength, plasticity and workability (Bell, 1988). Guney *et al.* (2007) states that the cation exchange of lime stabilized soil usually takes place within a few hours. When adding lime to a wet soil, a series of chemico-physical changes in soils can happen, giving rise to the immediate or short term effects: a reduction in moisture content that occurs as the quicklime is hydrated; changes in soil properties due to physico-chemical reactions; an immediate reduction in the plasticity of clays and renders the soil more friable and workable with an increased bearing capacity. In the case of long term improvement in strength, the 'stabilisation' reaction, generally caused by pozzolanic reactions, involves interactions between soil silica and/or alumina and lime to form various cementitious products that contribute to enhancing the strength. These pozzolanic reactions can last several years (Little, 1999). Normally, when quicklime is added to a wet soil (especially clayey soil), the chemical reactions occur almost immediately, giving rise to soil drying by lime hydration (National Lime Association, 2004). The chemical interaction plays an important role in the lime stabilization of soils. Umesha *et al.* (2009) listed these basic reactions in details when lime is added to soil and Le Runigo (2008) introduced also these similar reactions occurring between kaolinite-lime treatments, as follows:

### (1) Hydration and ionization of quicklime

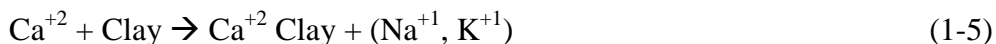
When the quicklime, water, soil are mixed together, hydration reaction of the quicklime firstly takes place as:



The calcium hydroxide ( $\text{Ca}(\text{OH})_2$ ) can be dissolved by the reaction of ionization, as follows:



(2) Cation exchange



(3) Flocculation/Agglomeration

(4) Carbonation (possible reaction)



(5) Pozzolanic reactions



Hydration of quicklime leads to soil drying, providing immediate hydrate (i.e., chemically combines with water) and heat (see formula 1-3). Soils are dried because water present in the soil participates in this reaction and the heat generated can evaporate additional water. The hydrated lime through these initial reactions will subsequently react with clay particles. These subsequent reactions will slowly produce additional drying because they reduce the soil's moisture retention capacity. If hydrated lime or hydrated lime slurry is used instead of quicklime, drying occurs only through the chemical changes in the soil that reduce its capacity to hold water and increase its stability, therefore, normally less efficient in this drying process (National Lime Association, 2004).

Modification of soil caused by lime treatment is controlled by cation exchange and flocculation/agglomeration processes: after initial mixing, the calcium ions ( $\text{Ca}^{2+}$ ) from the hydrated lime migrate to the surface of the clay particles and displace water and other ions. The cation exchange starts to occur between the metallic ions associated with the surface of clay particles. These clay particles are surrounded by a diffuse hydrous double layer, which is modified by the ion exchange of calcium. The alteration of the electrical charge density around the clay particles by exchange of ions leads to flocculation of particles (Umesha *et al.*,



2009). This process is mainly responsible for the modification of the engineering properties of clay soils treated with lime (Boardman *et al.*, 2001). Prunsinski and Bhattacharja (1999) proposed a schema to explain the cation exchange or ion-exchange process for the calcium-based soil stabilizer that will provide sufficient calcium ions so that the monovalent cations are exchanged. Upon ion exchange, the higher charge density of di- or tri-valent ions results in a significant reduction of the double-layer thickness. This ion-exchange process is generally quite rapid (usually within a few hours), followed by flocculation and agglomeration process. Agglomeration is forming from weak bonds at the edge surface interfaces of the clay particles because of the deposition of cementitious material at the clay particle interface (Figure 1-4). Then, the soil becomes friable and granular, which makes it easier to work and compact (National Lime Association, 2004). The process, which is often called flocculation and agglomeration, generally occurs in a several hours or days. The flocculation and agglomeration decrease the Plasticity Index of the soil dramatically and provide an immediate reduction in swell and shrinkage.

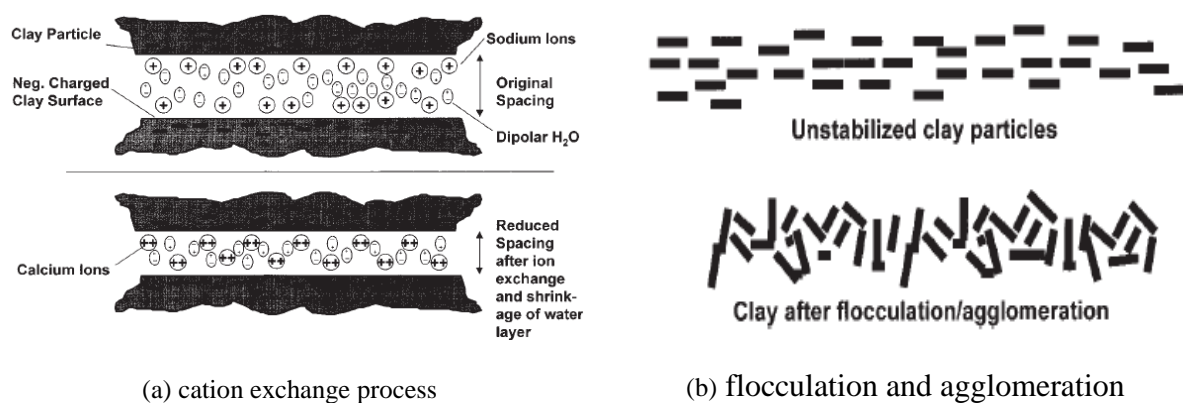


**Figure 1-4 Cation exchange, flocculation and agglomeration (Prunsinski and Bhattacharja, 1999)**

Stabilization of lime treatment caused by pozzolanic takes place as follows: when adequate quantities of lime and water are added, as mentioned before, the pH of the soil quickly increases to above 10.5, which enables the clay particles to break down. Silica and alumina are released and react with calcium from lime to form calcium-silicate-hydrates (CSH), calcium-aluminate-hydrates (CAH) and calcium-aluminosilicate-hydrates (C-A-S-H), which are the cementitious products similar to those formed in Portland cement. Numerous studies have evidenced this formation of hydration compounds by lime treatment (Eades and Grim, 1960; Diamond *et al.*, 1964; Rossi *et al.*, 1983; Locat *et al.*, 1990; 1996; Wild *et al.*, 1993; Bell, 1996; Rajasekaran and Rao, 1997; Onitsuka *et al.*, 2001; Khattab, 2002; Cai

*et al.*, 2006 ; Le Runigo, 2008 ; Millogo *et al.*, 2008 ; Rios *et al.*, 2009 ; Deneele *et al.*, 2010). These compounds form the matrix that contributes to the strength of lime-stabilized soils. As this matrix forms, the soil transform from a sandy, granular material to a stiffer with significant higher load bearing capacity. The process begins within hours and can continue for years in a properly designed system.

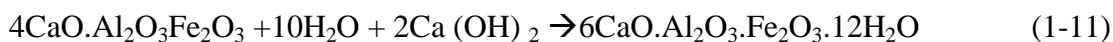
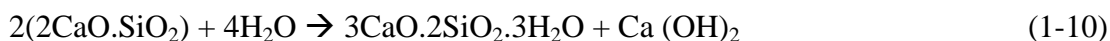
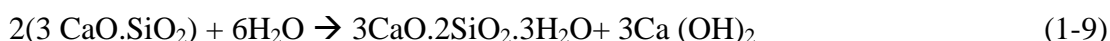
The carbonation reaction mechanism within lime treatment is still an open question. Numerous studies show the carbonation process induced by lime treatment (Goldberg and Klein, 1952; Glenn and Handy, 1963; Diamond and Kinter1965; Bell, 1996; De Bel *et al.*, 2005). Carbonation (see formula 1-6) is partial or complete destruction of magnesium hydroxide or soil-lime reaction products or all of them due to reaction with carbon dioxide (ASTM D5102-04). Further, several studies (Rossi *et al.*, 1983; Bell, 1996 ; Le Runigo, 2008; Millogo *et al.*, 2008; Deneele *et al.*, 2010) showed this carbonation in lime treatment. Carbonation may take place during manufacturing and storage of lime, laboratory mixing, curing and testing of soil-lime mixtures, construction, and in service. Carbonation is detrimental (Thompson, 1966; Bagonza *et al.*, 1987; ASTM D5102-04) because the formation of calcium and magnesium carbonates ( $\text{CaCO}_3$  and  $\text{MgCO}_3$ ) are weak cements (Joel and Agbede, 2010). However, the work by Graves *et al.* (1987) and Little *et al.* (1996) has demonstrated the long-term benefits from the carbonation reaction in the stabilization of calcareous aggregates. In calcareous materials, lime has found to enhance the growth of carbonate cement which bonds carbonate particles together resulting in a substantial strength and a substantial stiffness increase (Grave *et al.*, 1987; Little *et al.*, 1996).

#### **1.2.1.2. Chemical characteristics changes of cement-treated soils**

The mechanisms of cement stabilization involve also two basic reactions: hydration reactions and pozzolanic reactions (Little and Nair, 2009). When cement is mixed with soil, hydration of cement-water system and a series of primary and secondary cementitious reactions in the soil cement matrix will happen, generally which will gives rise to a decrease in liquid limit, plastic limit the potential for volume change of soils and an increase in the shrinkage limit and shear strength.

Hydration of cement is also an exothermic reaction, which occurs immediately when in contact with water. According to Prunsinski and Bhattacharja (1999), hydration of cement results in not only the cation exchange, flocculation and agglomeration, but also the formation of a variety of compounds and gels. These compounds and gels include the

formation of hydrated calcium silicates (C-S-H), hydrated calcium aluminates (C-A-H). In addition, the hydration of cement provides also excess of hydrated lime-calcium hydroxide (Prunsinski and Bhattacharja, 1999), which is necessary product to initiate the subsequent pozzolanic reactions. Additionally, Portland cement is a heterogeneous substance containing tricalcium silicate ( $C_3S$ ), dicalcium silicate ( $C_2S$ ), tricalcium aluminate ( $C_3A$ ) and tetra calcium alumino-ferrite ( $C_4AF$ ). In order to better understand these hydration reactions, Umesha *et al.* (2009) listed all the hydration compounds into which the Portland cement are transformed upon addition of water, and their reactions are described by the following equations (1-9 ~ 1-13):



Compared to the hydration reactions, the subsequent pozzolanic reactions or secondary cementitious reactions are much slower processes, because the initiation of pozzolanic reactions depends on the availability of the hydrated lime-calcium hydroxide from the hydration reaction, and the silica or alumina released from clay. Moreover, the secondary cementitious reactions by cement treatment also result in the formation of additional C-S-H, C-A-H or C-A-S-H, respectively, which is similar to the pozzolanic reaction products in lime treatment.

In addition, the pozzolanic reaction increases the pH of pore water further and makes silica and alumina be released from clay minerals. The hydrous silica and alumina slowly react with calcium ions liberated from hydrolysis of cement to form insoluble compounds that stabilize the soil (Umesha *et al.*, 2009). Since these cementitious products are also responsible for the strength gain of cement-treated materials, both the hydration and pozzolanic reactions contribute to the overall strength of soils. Several studies have evidenced these formations of hydration and pozzolanic reaction compounds by cement treatment (Croft, 1967; Onitsuka *et al.*, 2001; Tremblay *et al.*, 2002; Chew *et al.*, 2004; Solanki *et al.*, 2007; Horpibulsuk *et al.*, 2010).

### 1.2.1.3. Chemical characteristics changes of mix lime/cement-treated soils

Although the application of mix treatment of lime plus cement is often done in current earthwork engineering, no adequate chemical explanation of the long-term changes in physical properties has been put forward in this mix treatment. Application of the lime and cement together as the stabilization agent could be a solution for the problems in some special conditions. This kind of application has been still an open question. Recent years, several studies (Puppala *et al.*, 2005; Rogers *et al.*, 2006; Joel and Agbede 2010; Okyay and Dias, 2010; Jauberthie *et al.*, 2010; Azadegan *et al.*, 2011; Sirivitmaitrie *et al.*, 2011) have been devoted to the mixture lime /cement stabilization of soils. Joel M. and Agbede I.O. (2010) worked on stabilization of Igumale shale lime admixture for use as a flexible pavement construction material; Okyay U.S. and Dias D. (2010) used lime and cement treated soils as pile supported load transfer platform; Azadegan *et al.* (2011) studied the effects of geogrids on the geotechnical behaviour of lime/cement treated soils used as base, sub-base or structural foundation materials. All these applications show that if appropriate mix design (lime/cement) is applied, the soils' mechanical properties can be well improved. Sirivitmaitrie *et al.* (2011) presented a study of stabilizing road subsoils with a combined lime and cement stabilizer in both laboratory and field conditions, aiming at enhancing the service life of the low-volume roads. In the laboratory, Puppala *et al.* (2005) and Jauberthie *et al.* (2010) studied the same percentage of lime, cement, lime plus cement treatments, showing different 28-day strength values.

However, as mentioned before, the chemical explanation of the long-term changes is seldomly reported in the physical properties of mix treatment (lime plus cement) of soils. Prunsinski and Bhattacharja (1999) stated that as both cement and lime provide calcium ions when mixed in a soil-water system, both have the ability to accomplish cation exchange. Then, the pozzolanic reaction also exists (Figure 1-5), which is a secondary process of soil stabilization in both the lime- and cement-soil systems. The cementitious materials from cement hydration (similar to cement alone reactions) occur more quickly than the second process products (C-A-H and C-S-H) by pozzolanic reaction due to the high-pH environment of a calcium-stabilized system which increases the solubility and reactivity of the silica and alumina present in clay particles. These pozzolanic reactions are shown in equations (1-14 and 1-15) (Eades, 1962; Herzog and Mitchell, 1963; Diamond *et al.*, 1964; Harty, 1971; Prunsinski and Bhattacharja, 1999). Indeed, several studies (Onitsuka *et al.*, 2001; Borgne, 2010; Jauberthie *et al.*, 2010) have evidenced these cementing products due to the mix

treatment by lime and cement. Onitsuka *et al.* (2001) studied a high plastic clayey soil (PI = 89, LI = 142; PI = 71, LI = 133) treated by lime plus cement, and the formation of these cementing products due to pozzolanic reactions was evidenced by the micrograph method.

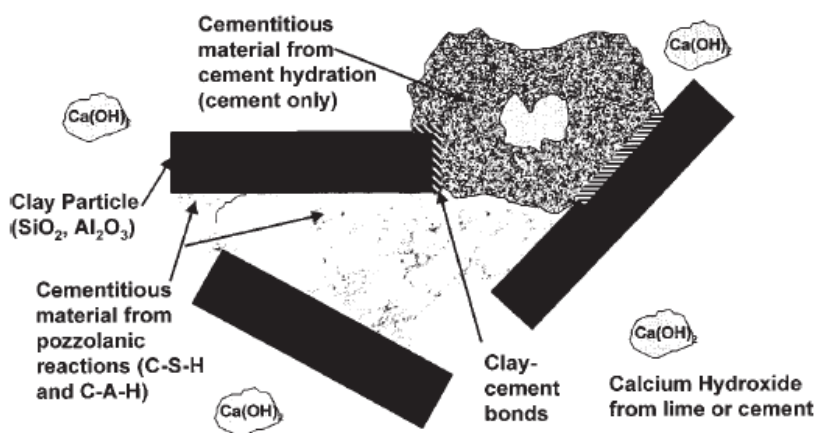
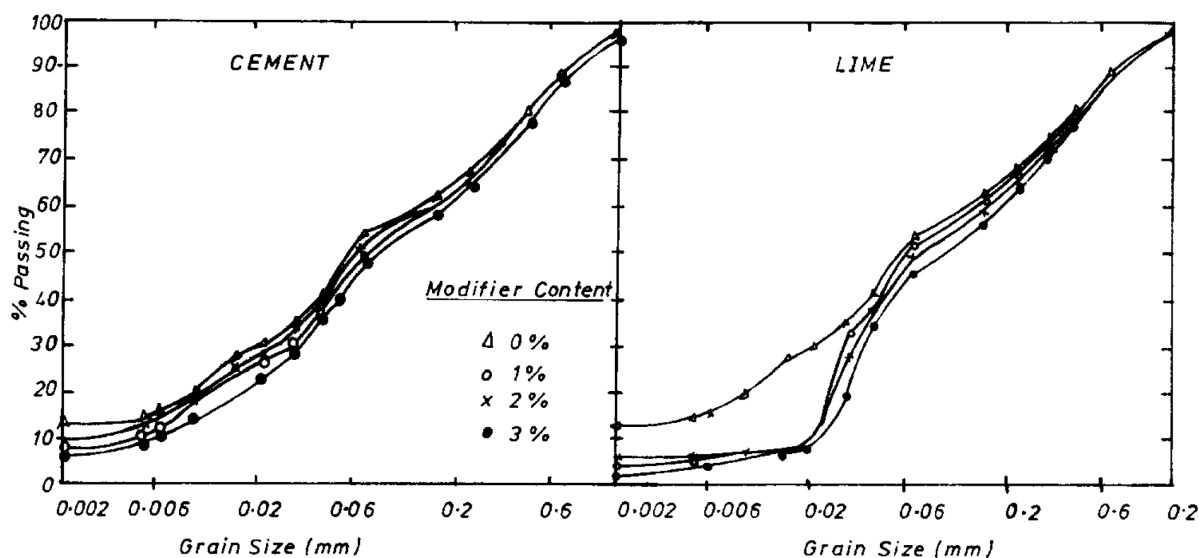


Figure 1-5 Cement plus lime treatment - pozzolanic reaction (Prunsinski and Bhattacharja 1999)

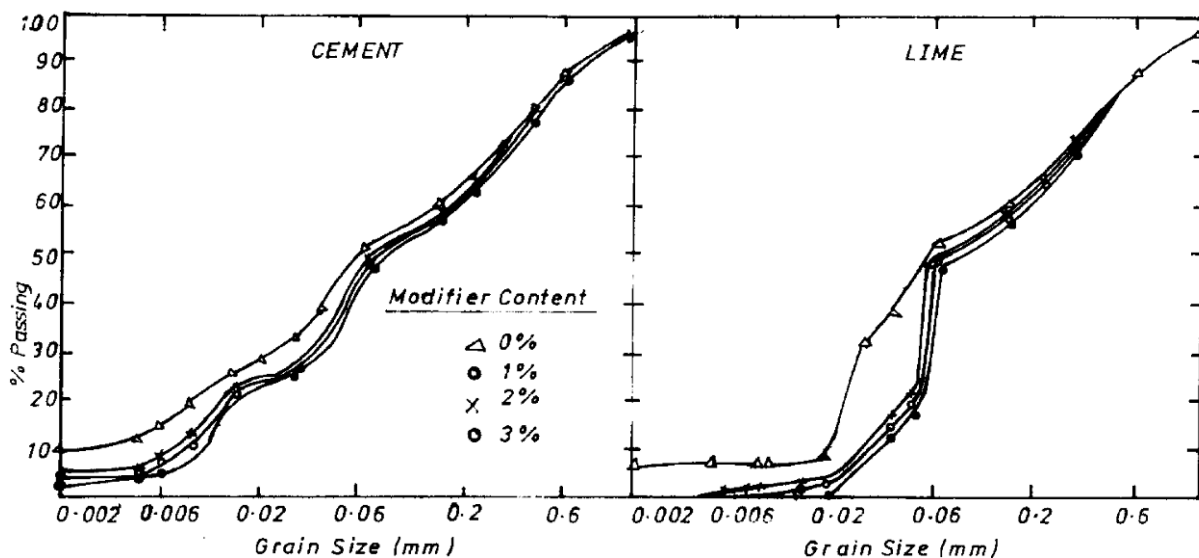
#### 1.2.1.4. Physical characteristics changes by cementitious treatment

As mentioned before, these calcium-based reactions by lime and/or cement treatment has similar complex reactions to those in the soil-water system, which also gives rise to complicated physical changes of soils due to base-exchange and cementation processes between clay particles and agents. Indeed, many studies show that lime treatment modifies the Atterberg limits (Hilt and Davidson, 1960; Croft, 1967; Brandl, 1981; Rogers and Glendinning, 1996, 1997; Bell, 1996), the granulometric composition by flocculation and agglomeration caused by cation exchange (Tuncer and Basma, 1991 ; Sherwood, 1993; Osula, 1996), the moisture-density relationship mentioned before (Croft, 1967; Ormsby, 1973; Brandl, 1981; Osula, 1996; Rogers and Glendinning, 1996) and the water content by either hydration or long term pozzolanic reactions (see formula 1-3 and 1-7). Similarly, cement treatment normally reduces the liquid limit, plasticity index and swelling potential etc. In addition, the water content decreases immediately due to the hydration of lime or cement and long-term pozzolanic reactions as water is absorbed and transformed to cementitious products (Bergado *et al.*, 1996; Bennert *et al.* 2000; Chew *et al.*, 2004). Cement treatment tends to decrease the permeability of soil (Bergado *et al.*, 1996) due to accumulation of the cementitious products caused by pozzolanic reactions (mix treatment)

and hydration reactions (cement only). However, for lime treatment, numerous studies (Brandl, 1981; McCallister, 1990, McCallister & Petry 1992; Nalbantoglu & Tuncer, 2001) show that modification of permeability is lime-content dependent: when lime content is less than the lime-fixation point, it seems to increase the permeability, and when it is more than the lime-fixation point, it decreases the permeability. Note that the reduction in plasticity index is due to the increase of plastic limit, strongly depending on the cement content and curing time (Bergado *et al.*, 1996).



(a) Effect of modification on grain size distribution just after mixing



(b) Effect of modification on grain size distribution 1 hour after mixing

Figure 1-6 Effect of modification on grain size distribution of cement and lime treatment of laterite at different elapsed times after mixing (Osula 1996)

Because soils are made of mineral grains, their behaviour is governed by the forces between particles (Santamarina, 2003). Soil grains are connected by these forces between them and the cementitious products can transform the grains to clods or aggregates therefore increasing the forces. Grain size distribution can play an important role in the soil shear strength, soil compaction, bearing capacity, and stiffness, etc. Therefore, for lime and/or cement treated fine-grained soils, the grain size modification by flocculation (causing clay particles to become closer to each other, forming flocs) as well as the glue effect induced by pozzolanic reaction may be fundamental. Indeed, Sherwood (1993) stated that flocculation is primarily responsible for the modification of the engineering properties of lime treated clayey soils. Osula (1996) performed lime and cement treatment on laterite soil, and the results show that lime treatment is more efficient than cement treatment for the short term modification of soils, because the grain size distribution is more significantly modified by lime treatment than cement treatment in a few hours (see Figure 1-6).

### **1.2.1.5. Conclusion**

For lime and/or cement treatment fine-grained soils, it is well known that short term and long term reactions can occur, responsible for modification and stabilization respectively. However, the exact duration for each term is difficult to determine.

In short term, the hydration reactions, for either lime or cement, occur very quickly but the products are quite different. For lime treatment, this stage leads to ionization of lime and cation exchange (typically calcium or magnesium) with clay fractions, giving rise to flocculation/agglomeration of fine soils. The high pH environment created can dissolve clay minerals and produce silica and alumina products in the subsequent pozzolanic reaction (primary solidification process). The hydration of lime does not make contribution to the soil solidification, as no cementitious products are formed. However for cement treatment, the hydration provides a large quantity of cementitious products. Cement hydration also creates a favourable environment for further pozzolanic reactions.

From a physical point of view, short term reactions of both lime and cement treatment can improve physical properties, such as reduction of plasticity, moisture-holding capacity, shrink-swell response. In long term, the pozzolanic reactions are responsible for the increase of soil's strength and the improvement of the structure, for both treatments, while it is a primary solidification process for the lime treatment and secondary one for the cement treatment.

## 1.2.2. Microstructure models for cementitiously-treated fine-grained soils

Soil microstructure refers to the arrangement of solid and void space. The grain size distribution of a soil determines the governing particle-level forces, inter-particle packing and the ensuing macroscale behaviour (Santamarina and Cho, 2004). The microstructure evolution of cementitiously-treated fine-grained soils can be described by the change of grain size, shape, the arrangement of the primary particles, as well as the voids change in aggregate materials, over curing time.

From the angle of aggregate development, the treatment effect is through changes of the force between contacts or along chains of grains or aggregates. Coating, binding particles together and forming of new compounds can be the main mechanisms that occur when using an additive. Since 1953, when the Lamé model was first elaborated by considering clay particles as single platelets (Horpibulsuk *et al.*, 2010), several conceptual models of microstructure for fine-grained soils have been developed and then significantly improved based on the development of microstructure observation techniques.

### 1.2.2.1. Microstructure models for lime-treated soils

When lime is combined with water and the soluble silica and alumina present in clay, a chemical reaction occurs, resulting in the formation of new compounds. The first function is to lessen water and modify the particle structure. That is why mellowing time, resulting in a homogeneous and friable mixture, is necessary for lime treatment before compaction. A secondary function is particles' binding and strength gain. Indeed, some studies have evidenced these mechanisms. Rajasekaran and Rao (1997) examined the reaction products of CSH (gel) in a reticulated network (well-knit framework) in a marine clay due to soil-lime reactions and observed that these products bind the individual clay particles together to form aggregates. Locat *et al.* (1990) observed the formation of platy CASH and reticular CSH cementitious compounds in lime-treated soils, etc.

As shown in Figure 1-7, a schematic model describing the physicochemical process of lime treatment soils was proposed by Ingles and Metcalf (1973). This model illustrates how the reaction product (C-S-H) is formed in the pore water, disseminated in the soil particles and composed between soil particles and pores under unsaturated state. Some necessary condition is presented also to initiate the pozzolanic reactions: the presence of water, enough  $\text{Ca}^{2+}$ ,  $\text{OH}^-$ , and the diffusion of  $\text{SiO}_2$  in the liquid, etc. Furthermore, it seems that



solidification products appear on the surface of clay grains (C-S-H like a gel between soil grains).

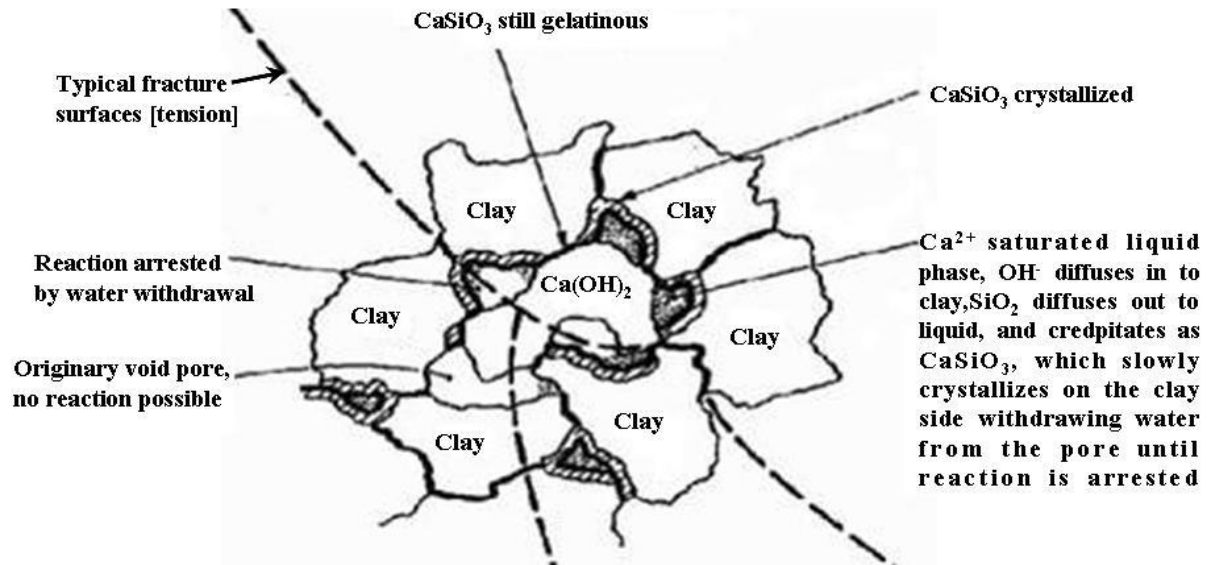
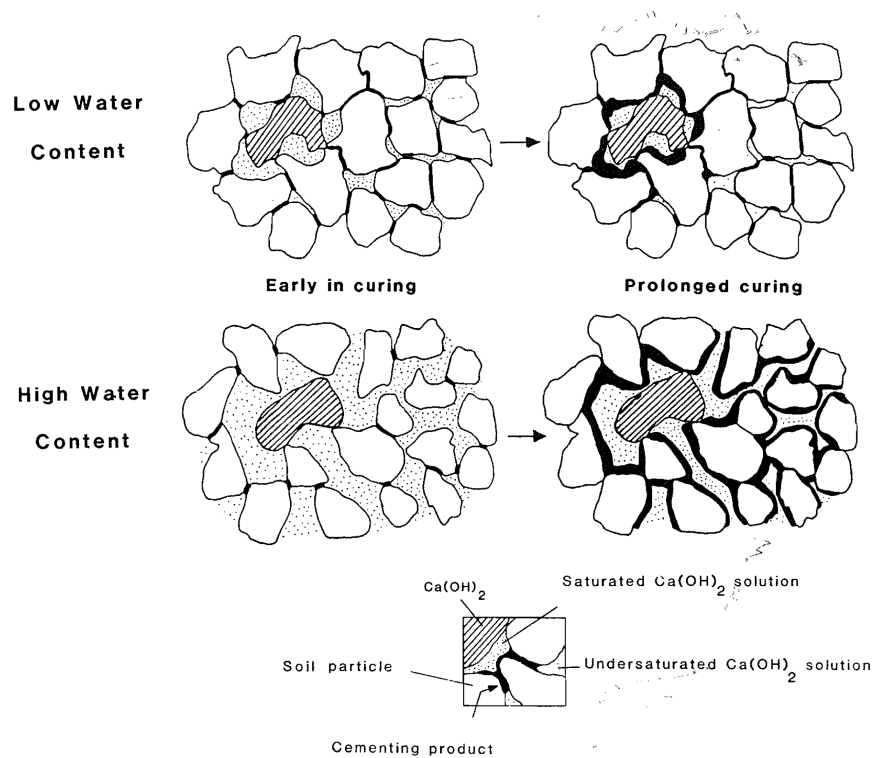


Figure 1-7 Schema of a physical conceptual model for lime treatment clays (Ingles and Metcalf, 1973)

As shown in Figure 1-8, this schematic physical model was later modified by Choquette (1989) to take into account the results for saturated soils, and by Locat *et al.* (1990) to illustrate the difference of lime treated soils' microstructure and cementation process between low and high water content conditions during the curing time. This model of Locat *et al.* (1990) illustrates how the reaction products are disseminated within the soil matrix, creating bridges or coating between or on soil particles. Note that the cementation process is responsible for the improvement of mechanical performance, especially in terms of cohesion developments.



**Figure 1-8** Schema of a physical conceptual model proposed for lime stabilization of sensitive clays (Locat *et al.*, 1990)

### 1.2.2.2. Microstructure models for cement-treated soils

Similarly, when cement is combined with water, hydration occurs, resulting in the formation of new compounds, most of which have strength-producing properties. When mixed with soil or base, soil particles are bound together and the mixture increase in strength. Depending on the composition of cement and the soil mineralogy, chemical reaction can occur between calcium hydroxide and soluble silica and alumina present in clay, resulting in alteration of soil microstructure and increase of resistance against shrink-swell. Approximately two hours after the soil-cement mixture is exposed to moisture, the soil particles are bound together and compaction must be complete (Osula, 1996). Additional handling of the treated material will break the bonds that have been created. Strength gain can continue for several days or longer term. Particle alteration at this stage is inhibited because of the bound state.

Figure 1-9 shows how the cement treated clay works (Prunsinski and Bhattacharja, 1999). Similar to lime treatment, cement stabilization improves soil properties by the cementitious bonds between the calcium silicate and aluminate hydration products of cement (CSH and CAH) and the soil particles. Major cementitious products are induced by hydration

of cement and secondary cementitious products come from the subsequent pozzolanic reactions. A hardened skeleton matrix is formed when these cement particles bind the adjacent cement grains together and encloses the unaltered particles. The silicate and aluminate phases are internally mixed and may not be completely crystalline.

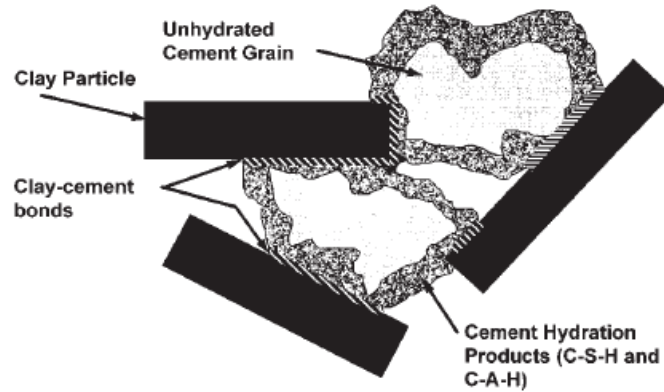


Figure 1-9 Schema of hydration process for cement treatment (Prunsinski and Bhattacharja, 1999)

### 1.2.2.3. Microstructure models for lime/cement-treated soils

Figure 1-10 shows how the mix-treatment clay works (Le Roux, 1969). This model explains the reaction processes among cement, lime and wet soil. It also shows that the cementitious compounds are placed on the surface of clay grains and bond the grains together. Furthermore, the specific positions of cementitious products reflect the order of their solidification. Normally, hydration of cement occurs much faster than the following pozzolanic reactions because the latter needs a high pH environment and the presence of sufficient silica and alumina coming from clay.

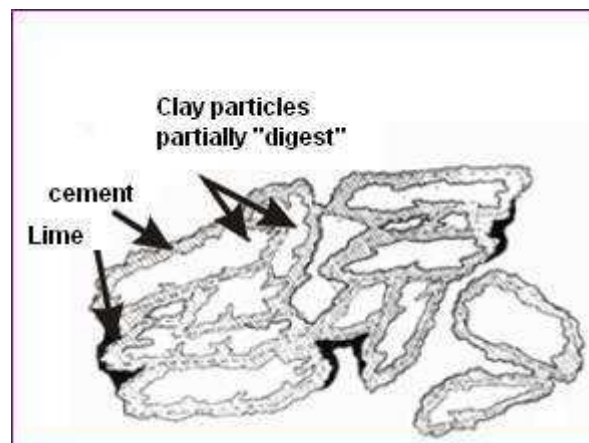


Figure 1-10 Schema of physical conceptual model for mix-treatment clays (Le Roux, 1969)

#### **1.2.2.4. Conclusion**

All these conceptual models reflect a common point: the grains are not treated completely and the cementitious products are coating on the surface of grains. Therefore, the reaction process depends much on the grain or aggregate size and mixing method in application. Indeed, Bin *et al.*, (2007) reported that lime is usually concentrated in pores or on the surface of aggregates and has few effects on the inner of aggregates with size ranging from 5 to 10 mm. This surface treatment effect may affect significantly the soil hydro-mechanical behaviour.

#### **1.2.3. Factors influencing the physical/chemical changes for cementitiously treated fine-grained soils**

Several factors can affect the physical/ chemical changes during the cementitious treatment of soils, therefore the cementitious stabilization effectiveness. They are: 1) soil nature (ex. chemical composition of soil particles, sand, silt, lean clay, heavy clay; expansive or non expansive, etc.); 2) stabilizer's nature, test procedure, dosage (pH of mixture), mixing, compaction, gradation and pulverization (Prunsinski and Bhattacharja, 1999); 3) curing conditions in terms of temperature and humidity.

##### **1.2.3.1. Additives and quantity**

Normally, as the strength gain with curing time is induced by the presence of cementitious gel, it is strongly related to the type of additive and the quantity of additive consumed. In fact, the amount of lime added should be related to the clay mineral content (Bell, 1996), which is correlated with the cation exchange capacity. Indeed, Ingles (1987) stated that a good rule of thumb in practice is to allow 1% lime for 10% clay in a soil. However, according to Bell (1996), this rule is not suitable for soils of very high clay content, in excess of 80% clay content for example, because normally it is not necessary to add more than 8% lime in earthwork engineering. In turn, lime treatment can also affect soil cation exchange capacity. Mathew and Rao (1997) reported the lime effect on cation exchange capacity of marine clay and showed that lime stabilization increases the pH as well as the cation exchange capacity of the soil.

### 1.2.3.2. Soil nature and clay mineral composition

Cation exchange capacity, pH, carbonate content, organic matter, clay minerals, size and shape of grain are the main properties of a soil, which can play an important role in the physical/chemical reactions with lime and /or cement.

Clay mineral composition is one of these important factors controlling the chemical and physical properties of soils. Kaolinite is quite reactive in pozzolanic reactions, thus shows a highly pozzolanic behaviour (Eades and Grim, 1960; Chew *et al.*, 2004). Illite, on the other hand, is less reactive in the pozzolanic reaction and is considered to require a higher lime content to initiate the pozzolanic reactions (Eades and Grim, 1960). Montmorillonite, usually with high cation exchange capacity, even in small quantities, may exert a great influence on the physical properties of soils. According to Christensen (1969), a clay soil containing a large amount of montmorillonite usually has a cation exchange capacity ranging from 80 to 150 milliequivalents per 100 g compared with 3 to 15 meq per 100 g for kaolinite and 10 to 40 meq per 100 g for illite, and the quartz or calcite should be much smaller (Figure 1-11). This work showed that high clay content often results in a high cation exchange capacity (with an exception shown in Figure 1-11 for No. 10).

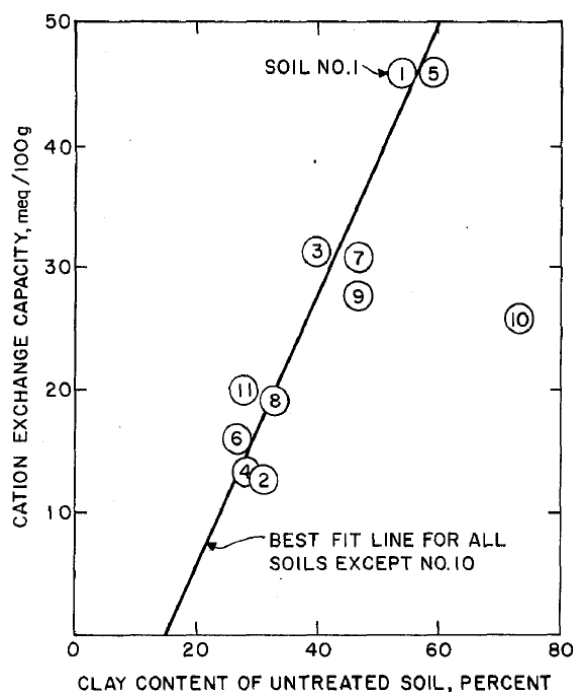


Figure 1-11 Relationship between cation exchange capacity and clay content (Christensen, 1969)

Christensen (1969) pointed out also that as the particle size decreases, the surface area of a given amount of soil increases greatly. As cation exchange is essentially an interface activity, especially for kaolinite and illite, smaller particle size will result in greater cation exchange capacities. Prunsinski and Bhattacharja (1999) claimed that the rate of dissolution of lime depends principally on particle size: finer gradations go into solution faster because of the higher exposed surface area. Indeed, some studies (Santamarina and Cho, 2004; Santamarina, 2003) on the effect of particle shape and particle size on the particle force and soil behaviour support this idea well.

### **1.2.3.3. Compaction condition**

Many studies investigated the compaction effects on soil engineer properties, including compaction energy (Attom, 1997; Osinubi *et al.*, 1998; Tascon, 2011), compaction delay (see section 1.1.3.3), compaction moisture control, density, compaction method (Hu *et al.*, 2001), etc. Recently, the compaction effect, especially the initial moisture control on the hydro-mechanical behaviour has been widely discussed: the modulus-suction-moisture relationship for compacted soil in postcompaction state was reported by Sawangsuriya *et al.* (2009); the compaction effect on aging characteristics of soft soil's microstructure by Ye (2010); the wet compaction effect on the volume change behaviour of lime treated swelling soils by Kasangaki and Towhata (2009), etc. As mentioned before, the water/cement ratio is an important parameter in controlling the cement treated soil's strength and stiffness development after compaction (Fitzmaurice, 1958; Aderibigbe *et al.*, 1985; Kamang, 1998; Pathivada, 2007; Olugbenga *et al.*, 2007; Kang *et al.*, 2008; Zhang and Tao, 2008; Ayangade *et al.*, 2009). Furthermore, Consoli *et al.* (2009; 2011; 2012) suggested using the porosity/cement ratio and void/lime ratio parameter to assess both the initial stiffness and the unconfined compressive strength of soil-cement or soil-lime mixtures. As a conclusion, the compaction conditions can modify the void volume, pore distribution and the contact state in the additive-water-soil grain system and thus change the pore chemistry environment of soils and affect the treatment effectiveness.

### **1.2.3.4. Curing conditions**

Curing condition is also a decisive factor for the strength gain, because the reactions are often influenced by the curing moisture condition, the curing period and the curing temperature.

The effect of curing moisture condition on the chemical reactions is obvious, as water takes part in either hydration or cementitious reactions.

According to the reaction mechanisms of cementitious treatment, the curing time can be a positive impact with the shear strength gain and stiffness gain. And many studies showed that the pozzolanic reaction is a long time process for the strength gain (Kelley, 1977; Locat *et al.*, 1990; 1996; Bell, 1996; Little, 1999; Ali *et al.*, 2011). Bell (1996) reported that strength increases most notably within the first 7 days. The curing duration can vary depending on the objective of the research; however, 7, 28, and 90 days are most common according to ASTM D 5102 (Standard Test Method for Unconfined Compressive Strength of Compacted Soil-Lime Mixtures).

Curing temperature is also an important factor. Usually, elevated curing temperature can promote pozzolanic reactions. This is the basic principle of designing the accelerated tests for cementitious treated soils. On the contrary, if the temperature falls below 4 °C, pozzolanic reactions are delayed and may cease at lower temperatures (Bell, 1996). However, elevated curing temperatures should be applied with caution since temperatures above 120 °F (48.89 °C) have been shown to produce uncommon pozzolanic reactions in field curing conditions (Parker, 2008; Chou, 1987).

### **1.3. Experimental techniques**

As mentioned before, the quality control and quality assurance (generally referred to as QC/QA), usually based on the soils' density and water content (French practice guides for subgrade GTR, 1992), are commonly used in earthwork engineering. However, water content and unit weight requirements are indirect indicators of complex characteristics of a subgrade and are not sufficient for quality control of a stabilized subgrade. In order to evaluate the cementitious treatment effect and to study their hydro-mechanical behaviour, many tests in both laboratory and field have been carried out to investigate the treated soils' strength stiffness (modulus) and durability behaviour. Further, microstructure investigation is also essential because it allows a deep insight into the reactions taking place in the treated soils (cementitious product and its distribution, etc.).

### 1.3.1. Evaluation on strength and stability of the treated soils

In the laboratory, according to several standards, several parameters are required for evaluating the strength and stability of treated soils, involving the unconfined compressive strength (UCS or  $R_c$ ) (EN 13286-40; EN 13286-41; EN 13286-42; ASTM D1633; ASTM D5102), California bearing ratio (CBR) and immersion CBR (iCBR) (EN 14227 -10 and EN 14227 -11), tensile strength  $R_t$  (NF EN 13286-40 and NF EN 13286-42), elastic modulus  $E$  (NF EN 13286-43), the strength after immersion in water  $R_i$  (by  $R_i/R$  ratio for cement treatment in EN 14227 -10), the linear swelling  $G_l$  (EN 13286 - 47) and volumetric swelling  $G_v$  (EN 13286-49), etc. In field, dynamic cone penetrometer (Snethen *et al.*, 2008), in situ CBR, nuclear  $w$ - $\gamma$ , stiffness gauge, portable FWD (falling weight deflectometer) (Fernando *et al.*, 2001) and PANDA penetrometer (Snethen *et al.*, 2008) are often employed. Strength investigation by UCS is most often used. Compared to lime treatment soils, Portland cement-treatment soils often have more completed specification standards. Specimens are usually cured for 7 days at room temperature and 100% relative humidity. Other common curing times include 28 and 56 days. Tests that have been used to quantify the strength of cement-treated materials include UCS and California bearing ratio (Kennedy *et al.*, 1987; Portland cement association, 1992; Dempsey, 1973). Specimens tested for UCS are usually soaked for 4 hours prior to testing (Kennedy *et al.*, 1987; Shihata and Baghdadi, 2001; Portland cement association, 1992). Volume Change is prevalent in areas where subgrade soils undergo significant volume changes with changes in water content (ASTM D4609-01; Fleureau *et al.*, 1993). If the treatment achieves the desired control in terms of volume changes, the material may be judged effective. This is an important test for treated fine-grained soils, especially for soils containing expansive clays (ASTM D4609-01, D3877; Ferber, 2005).

### 1.3.2. Evaluation of soils' modulus

Lime and/or cement treatment can improve soil's stiffness, which can be expressed or evaluated by different moduli, such as shear modulus ( $G$ ) and Young's modulus ( $E$ ), P-wave modulus ( $M$ ) and resilient modulus ( $M_R$ ), etc. The relationship between stiffness and modulus is simple, as stated by Briaud (2001), "if the modulus is a soil property; the stiffness is not a soil property and depends on the size of the loaded area." Therefore, for a given elastic material, the stiffness measured with one test may be different from that by another test if the loading is different. Yet, for the same elastic material, the modulus obtained from both tests



would be the same. Thereby, the use of the modulus is preferred to characterize the soils' engineering properties (Briaud, 2001).

G is related to the shear wave velocity  $V_s$  as follows:

$$G = \rho V_s^2 . \quad (1-16)$$

where  $\rho$  is the bulk density.

G is linked with E by:

$$G = \frac{E}{2(1+\nu)} \quad (1-17)$$

where  $\nu$  is the Poisson coefficient.

P-Wave modulus (M) is calculated using the following expression:

$$M = \rho V_p^2 \quad (1-18)$$

where  $V_p$  is the compression wave velocity.

$M_R$  is a stiffness parameter under cyclic loading. The strain amplitudes commonly observed in  $M_R$  determination are usually much higher than the pure elastic zone (0.001%). The resilient modulus is commonly used to characterise the base or subgrade materials under the traffic effect. Generally, the resilient modulus test is measured by triaxial test (AASHTO T292) and quite time consuming. Recently, the  $M_R$  measurement has been much improved using the wave propagation technique (Nazarian *et al.*, 1999; Yuan and Nazarian, 2003) that is employed in triaxial test as a wave measurement device. From triaxial tests,  $M_r$  is calculated as follows:

$$M_R \text{ (or } E_R) = \frac{\sigma_d}{\varepsilon_r} \quad (1-19)$$

where  $\sigma_d$  is the deviator stress and  $\varepsilon_r$  is the axial strain.

As a conclusion,  $M_R$  is usually used in relatively large strain conditions to study the cyclic traffic loading effect, while other moduli are often used in the small strain range (Pezo and Hudson, 1994).

### 1.3.2.1. Strain range and modulus measurements

Several factors can influence soil's modulus. The strains level associated with the loading process is one of the most important factors. Figure 1-12 shows the relationship of shear modulus and shear strain, together with the typical tests for determining different strains. The shear modulus has almost a constant value at very small strains range ( $\gamma_s < 10^{-6}$ ), and then it decreases gradually with increase of the shear strain ( $\gamma_s > 10^{-6}$ ).

In very small strains range ( $\gamma_s < 10^{-6}$ ), dynamic methods are often used, such as bender element and surface seismic wave methods (Atkinson, 2000; Szczepanski, 2008).

In small strain range ( $10^{-6} < \gamma_s < 10^{-3}$ ), the modulus measurements are usually based on the dynamic methods and local strain gauges, such as resonant column device and local strain measurements by triaxial apparatus (Atkinson, 2000; Szczepanski, 2008).

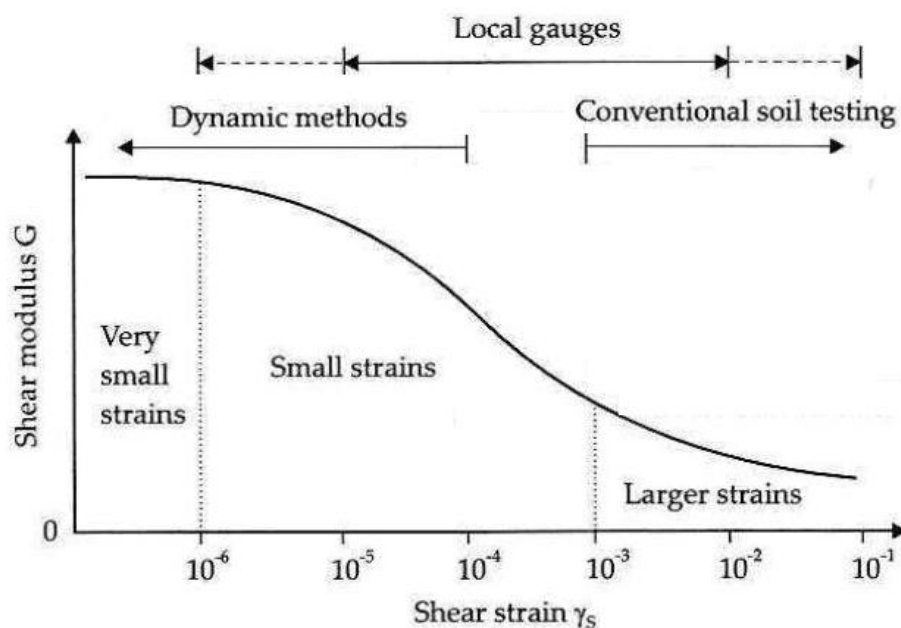


**Figure 1-12 Typical strain ranges and their corresponding determination methods (Atkinson and Sallförs, 1991, modified)**

In large strain range ( $\gamma_s > 10^{-3}$ ), conventional triaxial tests become appropriate methods (Atkinson, 2000; Szczepanski, 2008), but these methods are usually time consuming and involve material destructive tests.

The moduli observed at high strain levels are smaller than those observed at low strain levels. Therefore, making material comparison based on the modulus values is difficult. However, in very small strains range (usually strain  $\gamma_s < 10^{-6}$ ), the shear modulus has a constant value for a given material.

Seed and Idriss (1970) for the first time proposed a different method of presenting the stress-strain behaviour of soils: the normalized moduli  $G_0$ , ( $G_0 = G/G_{\max}$ ). This method presents the shear modulus,  $G$ , normalized with respect to initial shear modulus  $G_{\max}$ , versus the log of shear strains. The usefulness of this type of plot is that once the maximum modulus of the material is obtained, any modulus at any strain amplitude can be easily estimated. Further, the modulus over the linear portion of the curve in the stress-strain diagram corresponds to material's maximum modulus, commonly denoted  $E_{\max}$ , maximum Young's modulus,  $M_{\max}$ , maximum constrained modulus, or  $G_{\max}$ , maximum shear modulus, which can be measured and calculated by wave propagation methods, by unconstrained compression wave, constrained compressive wave and shear wave, respectively (Brignoli *et al.*, 1996). These maximum moduli allow for the direct comparison of stiffness because they are constant in small strain range.

Resilient modulus tests are expensive and cannot be applied to materials containing large particles ( $D_{\max} > 25$  mm for example) (Schuettpeitz *et al.*, 2010). On the contrary, the small strain shear modulus measurement by wave propagation technique is a non-destructive and economic method, thus widely used recently in both laboratory and field.

### 1.3.2.2. Small strain shear modulus measurement

Small strain shear modulus ( $G_{\max}$ ) is a fundamental parameter in many static and dynamic analyses involving design of foundation and soil dynamics problems (Brignoli *et al.*, 1996, Youn *et al.*, 2008). It can be measured in both laboratory and field by wave propagation technique. Figure 1-13 shows some examples of methods allowing obtaining small strain parameters of soils (Szczepański, 2008). In the laboratory, bender element and resonant column tests are commonly employed, together with the shear modulus traditional measurement in conventional triaxial tests. In situ, thanks to the development of wave propagation technique, many wave measurements have been greatly improved, such as down-hole and cross-hole method (Hoar and Stokoe, 1978); wave propagation methods such as SASW (Spectral-Analysis-of-Surface-Wave) used by Gabriels *et al.*, (1987), CSWS (continuous Surface Wave System), Seismic CPT (Cone-Penetration Tests) (Axtell and Stark, 2008) and Seismic DMT (Szczepański, 2008), etc. This allows the comparison between laboratory field results either in a much easier fashion than before. The comparisons made include: bender element in the laboratory with SASW and CSWS in field (Szczepański, 2008), resonant column in the laboratory with cross-hole method in situ (Axtell and Stark,

2008). A bender element device can also be installed in a cyclic triaxial test device to determine the shear modulus at small strain levels (Sahaphol and Miura, 2005; Asonuma *et al.*, 2002).

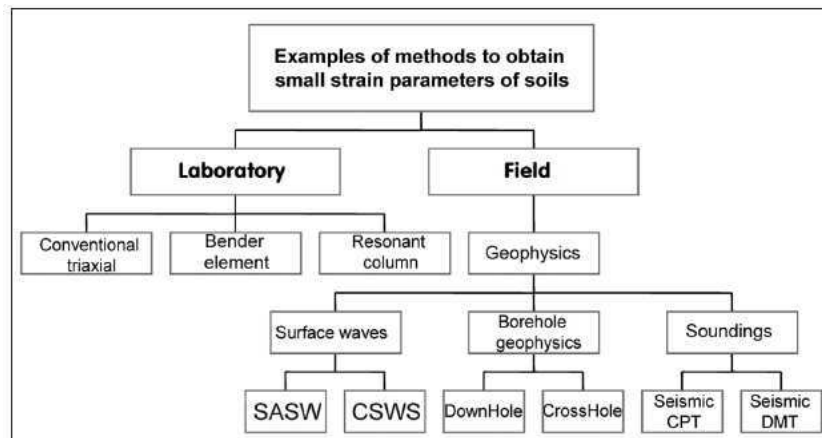


Figure 1-13 Methods for measurement of soil small strain modulus (Szczepanski, 2008)

Although the  $G_{\max}$  measurements are various, the testing principle by wave propagation technique is simple and common: usually two transducers are used in these devices, one is an emitter which will give input wave signals and the other is a receptor. The wave travelling time is recorded by these transducers and the distance between them are determined before test, then the wave travelling velocity can be measured. Note that the travelling distance of shear wave is determined by the current tip-to-tip distance between the transmitter and receiver of bender elements (Dyvik and Madshus, 1985; Viggiani and Atkinson, 1995a). Finally, using the formula (1-16), the  $G_{\max}$  can be calculated.

### 1.3.2.3. Bender element measurement

Bender element (BE) is usually used to determine the shear wave velocity (Shirley, 1978), and hence the  $G_{\max}$ . Note that several other techniques have also been used to evaluate  $G_{\max}$  in the laboratory, such as resonant column (Lo Presti *et al.*, 1997) and torsional shear device (Brignoli *et al.*, 1996; Youn *et al.*, 2008). Compared to these methods, the bender element (BE) method is more popular and widely used in determining shear wave velocity in the laboratory because of its simplicity, low cost and non-destructive nature (Yamashita *et al.*, 2005).

Usually, there are three different approaches of identifying the arrival time: (i) first start-to-start method, (ii) first peak-to-peak method and (iii) cross-correlation method or

frequency domain technique method. All these three methods belong to the time domain method. The former two methods are used more commonly than the 3<sup>rd</sup> method, and the cross-relation method is based on the first and second arrival events to provide accurate travel times.

No matter using the first start-to-start method or the first peak-to-peak method, the first task is to identify the arrival time of the received shear wave. Although the principle of determining the shear wave velocity is simple, the subjectivity of determining the arrival time represents a critical difficulty in BE test (Sawangsuriya *et al.*, 2006; Youn *et al.*, 2008). Figure 1-14 depicts a typical shear wave shape in several studies (Kawaguchi *et al.*, 2001; Lee *et al.*, 2005; Yamashita *et al.*, 2005; Bonal *et al.*, 2012). The transmitted shear wave is a typical sinusoidal signal. Yet, the received one is tortured from “A” to “C” due to the near field effect and thus it is difficult to identify the arrival point. We can see that the received wave experiences a first deflection (point ‘A’), then comes to the first bump maximum (point ‘B’), thereafter arrives to zero (point ‘C’) and finally comes to the major first peak (point ‘D’). Of course, choosing arrival points in different parts of the received wave will give different shear velocities, because the transmitted shear wave starts at a common point. In the literature, “A”, “B” and “C” points were all used to be identified as arrival time, and “D” was commonly considered as the first peak of this arrival shear wave. This subjectivity of identifying the arrival time makes the comparison of results difficult, especially for soils with high stiffness. Kawaguchi *et al.* (2001) adopted point “C” as the arrival time. Later in 2005, the international parallel test was applied on the same sand (organised by the Technical Committee TC29), showing a large scatter in shear modulus data. Finally, it was confirmed that the scattered data are mainly caused by the different determination methods of arrival time. Due to the near field effect, for high stiffness soils, the error induced by the determination of first arrival points can reach far from acceptable. As stated by Yamashita *et al.* (2005), when using the unique zero crossing method for the international parallel test (point C in Figure 1-14, proposed by Kawaguchi *et al.*, 2001), the error is significantly reduced and the result is thus comparable. Thereafter, in order to eliminate the error and facilitate the comparison of the results, more and more researchers define point ‘C’ as arrival time (Kawaguchi *et al.*, 2001; Lee *et al.*, 2005; Yamashita *et al.*, 2005; Bartake and Singh, 2007; Youn *et al.*, 2008; Kumar *et al.*, 2010).

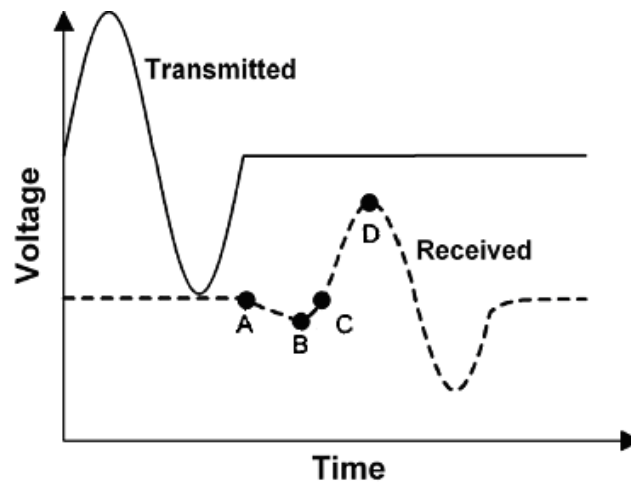


**Figure 1-14 Classic shear wave through a sand sample and determination method of the arrival time (Kawaguchi *et al.*, 2001; Lee, *et al.*, 2005; Yamashita *et al.*, 2005; Bonal *et al.*, 2012 among others)**

However, this typical received shear wave in Figure 1-14 can only represent the signals through sand or a sandy soil, as identified in other studies (Salgado *et al.*, 1999; Blewett *et al.*, 1999; Dano *et al.*, 2003; Leong *et al.*, 2005; Yamashita *et al.*, 2005; Ferreira and Fonseca, 2005; Sharifipour, 2006; Cho *et al.*, 2006; Youn *et al.*, 2008; Leong *et al.*, 2009; Kumar *et al.*, 2010). If the “B” point does not appear in the received shear waves, the arrival identification by “C” would lose its efficiency. Unfortunately, the waveforms can be affected by many factors: such as soil types (Brignoli *et al.*, 1996; Leong *et al.*, 2005), soil state (Brignoli *et al.*, 1996; Yamashita *et al.*, 2005), grain size distribution (Wichtmann and Triantafyllidis, 2009; 2010) and damping ratio (Lo Presti *et al.*, 1997; Teachavorasinskun *et al.*, 2001, 2008). Brignoli *et al.* (1996) defined six classic waveforms to explain how to choose the time arrival points for soft saturated clay soils. Leong *et al.* (2005) also observed the different received wave types for sand, mudstone residual soil and kaolin. Therefore, the complexity of the waveforms at near field often makes the first arrival point identification difficult, especially for stiff soils (ex. cemented soils). Sometimes, it is difficult to determine the arrival time by the first start-to-start method, as the arrival zone of shear wave is usually masked or disturbed by noisy signals, namely near field effect.

The first peak-to-peak method means that the time lag between the peak of an input wave and the first peak of the received wave is for the wave travelling time. At the time of identification, the direction of the initial motion of BE is considered similarly as that in the start-to-start method. Considering the influence of the near field effect or noisy waves in the arrival zone, the first peak-to-peak method successfully avoids the problem related to

identification of the arrival time, and therefore is normally more objective than the first start-start method. Indeed, a comparison between the start-start (first break) and peak-to-peak travel times by Clayton (2011) shows that it is easier to obtain consistent peak-to-peak travel time, and the data obtained by start-start method by different operators are much more scattered than that by the first peak-to-peak method. Thereby, more and more researchers choose the first peak-to-peak method for determining the travel time (Viggiani and Atkinson, 1995; Lee *et al.*, 2005; Ng and Leung, 2007; Chan, 2006; Yamashita *et al.*, 2005).

The first peak-to-peak method should be used with caution as the travelling time may be influenced by the triggering frequencies. In other words, the shear wave responses (especially their periods) for a same soil may be different if different triggering frequencies are used. Youn *et al.* (2008) pointed out that the frequency effect on  $G_{\max}$  is related to soil types, and that this effect is negligible for clean sand, but significant for cohesive soils. This is consistent with the statements of Mitchell (1976), Iwasaki *et al.* (1977) and Kim (1991): for cohesive soils,  $G_{\max}$  increases with increasing frequency. The period of the output signal changes regularly with the increase of input signals. Whenever the frequency of the input and the receiving wave differs, the error on the travelling time identification by the first peak-to-peak occurs. As reported by Yamashita *et al.* (2009), when the peak-to-peak method is used, the frequency of input and output waves shall be almost equal. In a word, the resonant frequency between soil and BE system needs to be determined prior to the shear wave velocity measurement.

### 1.3.3. Durability tests for treated soils

In long term, the expected performance of cementious treated soils can be degraded due to various outside loadings (wetting/drying, freeze/thaw cycles etc), by either loss of stabilizer over time or ineffectiveness of stabilizer (Little *et al.*, 2000). Several parameters such as soil type, treatment method, compaction procedure and the curing conditions can influence the soil durability (Allam and Sridharan 1981; Dif and Bluemel, 1991; Lin and Benson, 2000; Rao *et al.*, 2001; Guney *et al.*, 2007; Chittoori, 2008; Pedarla, 2009; Charlier *et al.*, 2009; Pedarla *et al.*, 2010; Harichane *et al.*, 2010; Al-kiki *et al.*, 2011; Akcanca and Aytakin, 2011). Of course, the behaviour of treated soils depends on the type of loadings. For example, Thompson and Dempsey (1967; 1969) and Little *et al.* (1995c) have demonstrated that the rate of strength loss due to wetting/drying cycles and freezing-thawing cycles is substantially improved by lime stabilization.

### **1.3.3.1. Resistance to wetting/drying cycles**

Wetting/drying-induced failure is a crucial climatic factor for the durability of treated soils, especially for the treated expansive soils. The impact of first wetting or drying path may be different. For lime treatment soils, the process is different from one study to another and it is short of standard. For cement treatment soils, the first cycle of wetting followed by drying (namely wetting/drying cycle) is most often seen in the literature and is also specified in standard ASTM D559. ASTM D560 provides procedures of determining the soil-cement losses, moisture changes, and volume changes (swell and shrinkage) produced by repeated wetting/drying cycles.

The test procedure defined in ASTM D559 is as follows: after mixing the cement/soil thoroughly, the specimens are firstly compacted at maximum density at the optimum water content (ASTM D558). Then the specimens are cured for 7 days and immersed in water for 5 hours. Afterwards, they are oven-dried at 160 °F (71 °C) for 42 hours to complete one wetting/drying cycle. The procedure above is repeated until the specimens undergo 12 cycles. For each cycle, some specimen is weighed and measured only for the volume and moisture change purpose and others are weighed and abraded with two firm strokes on all areas with a wire scratch brush for soil-cement loss purpose. Finally, the specimens are dried at 110 °C to evaluate their weight loss.

Although ASTM D559 specifies that specimen durability should be measured in terms of percentage of mass loss, some studies omit the brushing portion of the test due to the variability associated with the brushing process and replace it with UCS testing or modulus testing after completion of all 12 cycles (Pedarla, 2009; Al-kiki *et al.*, 2011).

### **1.3.3.2. Resistance to frost-thaw cycles**

Freezing-thawing cycling is also an important deleterious climatic factor for soils. Some parameters are important in analysing the effect of freezing-thawing cycles: cooling rate, freezing temperature, duration of freezing period, warming rate, thawing temperature, duration of thawing period and number of freezing-thawing cycles (Dempsey and Thompson, 1973). However, there has been insufficient experience in defining a method for resistance to frost, that can be used everywhere over the world, even though a standard exists in Europe (NF EN 14227-11: 2006). ASTM D560 specifies the methods to determine the soil-cement losses, moisture changes and volume changes (swell and shrinkage) produced by repeated



freezing-thawing cycles of cement stabilized specimens. Yet, there is still no standard for lime-soil mix in terms of resistance to frost.

The test procedure in ASTM D560 follows several steps: 1) the specimen preparation (same as wetting/drying cycles test according to ASTM D559); 2) curing for 7 days preventing from any water contact; 3) undergoing freezing/thawing cycles in a fog room (12 cycles). For each cycle, the specimen is weighed and abraded with two firm strokes on all areas with a wire scratch brush for soil-cement loss purpose. This procedure requires freezing for 24 hours at a temperature not warmer than  $-10^{\circ}\text{F}$  ( $-23.3^{\circ}\text{C}$ ) and thawing for 23 hours at  $70^{\circ}\text{F}$  ( $21.1^{\circ}\text{C}$ ) and 100% relative humidity.

Probably due to the similar reasons as for wetting/drying cycles in ASTM D559, many studies also replace the weight loss with UCS testing or modulus testing after completion of all 12 freezing-thawing cycles (Shihata and Baghdadi, 2001; Bandara *et al.*, 2002; Parsons and Milburn, 2003; Guthrie *et al.*, 2008; Altun *et al.*, 2009; Al-kiki *et al.*, 2011).

#### **1.3.3.3. Resistance to soaking**

There are usually two saturation methods: vacuum saturation method (ASTM C593) and capillary saturation method. The vacuum saturation test requires 2 hours and is the durability test specified for lime-fly ash- and Class C fly ash-stabilized soils. Its shortcoming is that vacuum saturating disturbs the air-water interface, causing substantial strength reduction and hence making the curing regime unrealistic (Rogers *et al.* (2006). The capillary saturation is by receiving water from the base and top via capillary action. For the capillary soaking method, the Tube Suction Test (TST) by the Finnish National Road Administration in cooperation with the Texas Transportation Institute (TTI) for assessing the moisture susceptibility of granular base materials (Guthrie *et al.*, 2001; Guthrie and Scullion, 2003; Puppala *et al.*, 1999; 2003).

#### **1.3.3.4. Resistance to leaching**

Leaching test is a classic method to evaluate the soils' resistance to the circular fluent water with specific chemicals, and over certain periods (ex. saturated  $\text{Ca}(\text{OH})_2$  solution in Deneele *et al.*, 2010). The analysis of chemical composition of the lechate liquid shows a loss

of stabilizer over time and allows knowing the dissolvable potential of the formed cementitious product in certain solution environment (Le Runigo, 2008; McCallister, 1990).

### **1.3.4. Microstructure investigation on treated soils**

#### **1.3.4.1. Scanning Electron Microscope**

The scanning electron microscope (SEM) uses a focused beam of high-energy electrons to generate a variety of signals at the surface of solid specimens. There are many advantages of using the SEM. The signals reveal information about the sample including the external morphology (texture), chemical composition, and crystalline structure and orientation of materials making up of the sample. SEM analysis is considered to be ‘non-destructive’; that is, x-rays generated by electron interactions do not lead to volume loss of the sample; thus, it is possible to analyze the same materials repeatedly. The strength gain of treated soils is attributed to formation of the products such as CAH and CSH, and these products can be observed at the scanning electron microscope. The grain-pores can also be well seen, thus the pore distribution can also be visualized for the treated soils. Due to the non-destructive nature of this technique, the soil specimens can be investigated in long term. Thus, the evolution of the chemical treatment process can also be followed.

#### **1.3.4.2. Computer Tomography scanning and X-/ $\gamma$ -ray method**

Computer Tomography (CT) is also a powerful non-destructive evaluation (NDE) technique for producing 2-D and 3-D cross-sectional images of an object from flat X-ray images. Characteristics of the internal structure such as dimensions, shape, internal defects and density are available from CT images. Compared to nanometres of spatial resolution in SEM, CT is much larger in the range of micrometers. By CT technique we can also analyze the homogeneity of treated fine-grained soils. Similarly, single-crystal X-ray diffraction is also a non-destructive analytical technique which provides detailed information about the internal lattice of crystalline substances, including unit cell dimensions, bond-lengths, bond-angles, and details of site-ordering. In the mineralogy analysis, X-ray diffraction is used in an attempt to identify the reaction products formed when lime is added to the clay material (Bell, 1996).

### **1.3.4.3. Mercury Intrusion Porosimetry**

Mercury Intrusion porosimetry (MIP) is a widely used analytical technique for the determination of pore size distributions in the mesopore and macropore ranges. The technique also gives information on the total pore volume and therefore on the soil porosity. Usually two types of curves are plotted to analyse pore size distribution: cumulative pore size distribution and incremental volume as a function of entrance diameter. By the MIP tests, we can evaluate the homogeneity of a cementitious treated fine-grained soil.

For lime treated soils, MIP test is widely used to evaluate the pore-size distribution. For the cement treated soils, however, it has been sometimes recognised that the MIP method is rather controversial. For example, Diamond (2000) and Chatterji (2001) reported that the MIP method is inappropriate for cement-based materials, because, in cement-based system: 1) nearly all mercury intrusion is held up until the pressure corresponding to the threshold diameter is reached, 2) subsequently, the large and small pores are filled indiscriminately (Diamond, 2000).

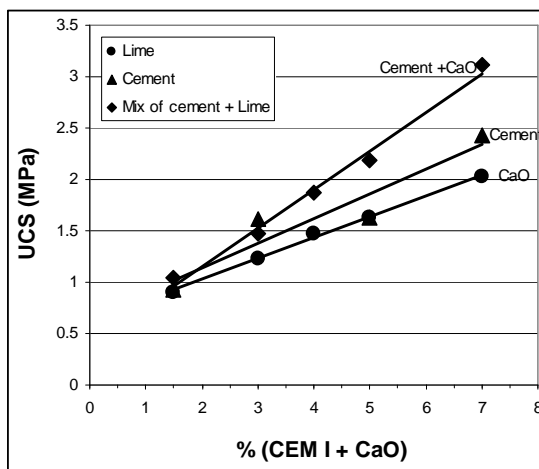
## **1.4. Hydro-mechanical behaviour of treated soils**

### **1.4.1. Factors affecting the strength development**

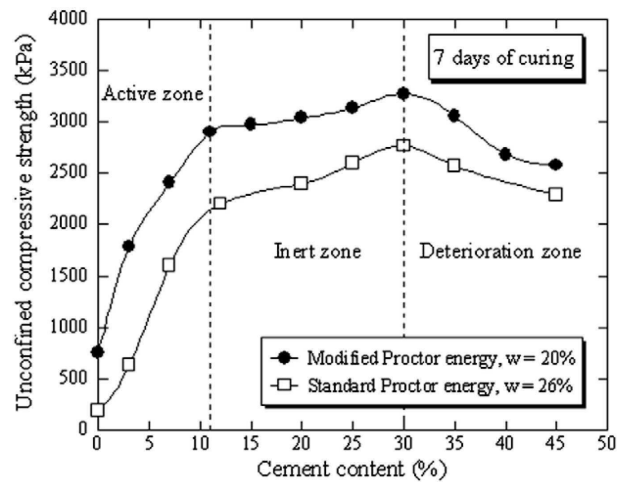
#### **1.4.1.1. Methods and dosages**

At the same percentage of treatment, different additives often give different strength. Puppala *et al.* (2005) studied expansive soils treated with different lime/cement ratios (1:0, 1:3, 3:1 and 0:1) and the results show that the cement predominant specimens have larger shear modulus ( $G_{max}$ ) and strength. Furthermore, the results obtained by Rogers *et al.* (2006) on the English china clay (a relatively pure kaolinite clay) treated by mix (2.5% cement + 2.5% lime), 2.5% lime and 2.5% cement alone show that the pozzolanic reactions only take place in the treatment with lime alone after 14-day curing time. Jauberthie *et al.* (2010) studied the stabilization of an estuarine silt with lime and/or cement and the results show that the UCS with mix treatment (ratio of cement/lime =1) is higher than that with lime or cement treatment alone, indicating that more formation of pozzolanic reaction products is expected (Figure 1-15a). Figure 1-15b shows the effect of cement content on the strength development

at a specific water content (Horpibulsuk *et al.* 2010), showing that there is an optimum dosage for a specific treatment and water content.



(a) Same dosage of 28-day curing  
(Jaubertie *et al.*, 2010)



(b) Cement content on the 7-day strength  
(Horpibulsuk *et al.* 2010)

Figure 1-15 Treatment method and dosage effect on the strength development

#### 1.4.1.2. Water content

For treated soils, the strength gain is also affected by the molding water content (Locat *et al.*, 1990), and the effect of molding water content on strength development is quite complicated due to complex reactions. The mechanical model based on the short term hydration of agents and long term cementitious reactions for lime-stabilized clayey soils both at high water content (HWC) and low water content (LWC) was first elaborated by Pirret (1977) (identified by letter P), and later developed by Locat *et al.* (1990) (Figure 1-16). This model assumes that strength increase results chiefly from the particle bridging by the pozzolanic reaction products (CASH and CSH minerals), as long as reactants are available. Strength development can be subdivided into three phases over time. Phase I corresponds to the initial period when bridging is not mechanically initiated, even if the chemical reactions take place. Phase II is a period of efficient bridging development where the pozzolanic reactions are the main mechanism. Phase III is characterized by a decrease in the rate of shear strength gain.

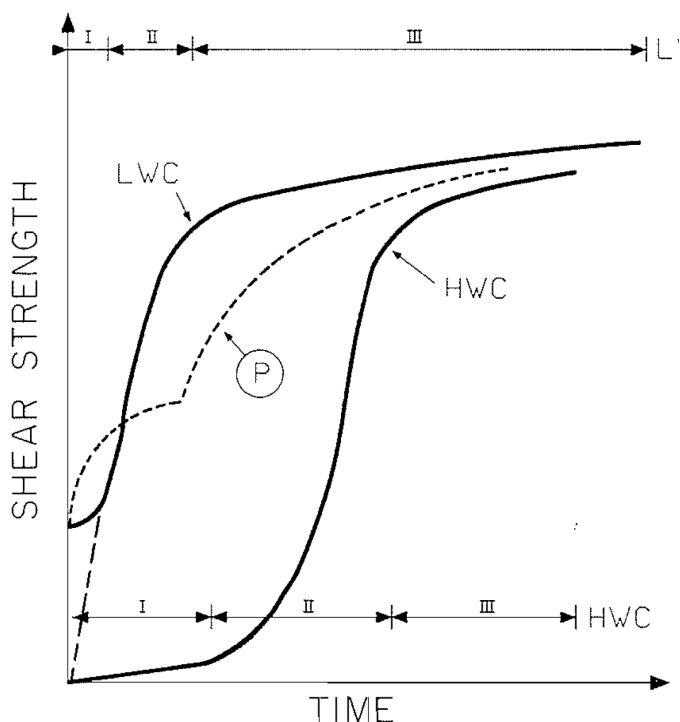


**Figure 1-16 Shear strength development model of lime stabilized clayey soils at both high water content (HWC) and low water content (LWC) (Locat *et al.*, 1990)**

#### 1.4.1.3. Curing time

Cementitious treatment gives rise to a significant increase of both compressive and shear strength, mainly due to the cementitious products formation by either cementitious hydration (cement treatment) or pozzolanic reactions (lime and/or cement treatment), as evidenced by many authors (Perret, 1979; Brandl, 1981; Christensen, 1969, Bell, 1996; Little *et al.*, 1995; Locat *et al.*, 1990). The strength gain is time dependent and can develop gradually over a long period (Christensen, 1969; Brandl, 1981; Locat *et al.*, 1990; Bell, 1996; Little, 1999; Brandl, 1981; Osinubi and Nwaiwu, 2006; Sivapullaiah *et al.*, 2006; Consoli *et al.*, 2009). Figure 1-17 presents the curing time effect on the shear strength parameters of lime treated silt/clay (Brandl, 1981). Firstly, for the cohesion of both clay and silt, the value observed at 270 days is much higher than at 7 days, under different dosages of lime treatments. This significant increase after 270-day curing reflects the continuous cementing or pozzolanic reactions in long term. For the friction angle, depending on the soil nature and treatment, it may be related to the effect of flocculation and agglomeration due to cation exchange in short term, as it is unchanged from 7 to 270 days. In some field conditions, it was identified that lime stabilized soils show good mechanical performance over 40 years

(Kelley, 1977). Ali *et al.*, (2011) also reported strength gains of treated subgrade soils, even 40 years after the construction.

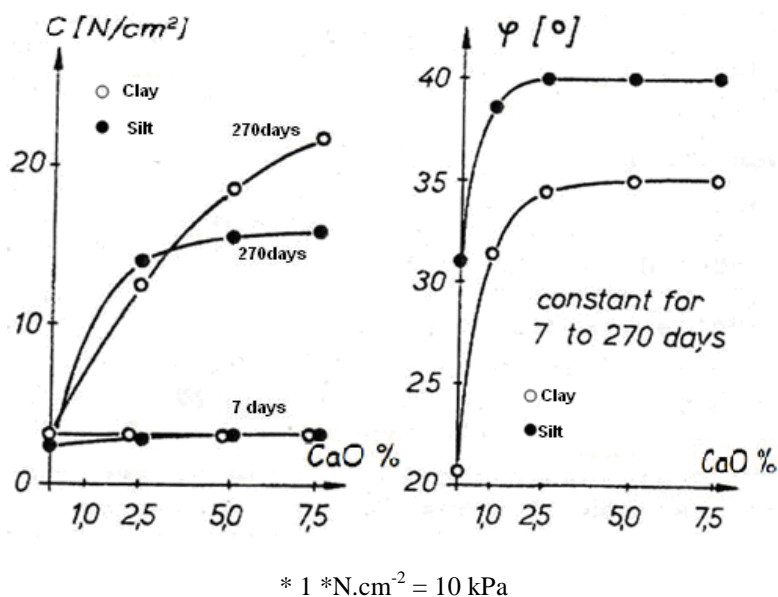


**Figure 1-17 Curing time effect (7 and 270 days) on the shear strength parameters of silt/clay treated by different percentages of lime (Brandl, 1981).**

Although the three phases of strength development with time was proposed by Locat *et al.* (1990), the term length determination and starting time for each phrase is still unknown and under discussion. They may be much related to the soil type, the treatment method and the homogeneity of the mix. For lime treatment, Bell (1996) indicated the two quite different time scales between the two mechanisms, Little (1999) stated that the 2<sup>nd</sup> phrase (pozzolanic reactions) can last 10 years under constant water content and temperature, and several other studies (Osinubi, 1998; Osinubi *et al.*, 2006; Rogers *et al.*, 2006; Little and Nair, 2009; Maubec, 2010) also reported that the hydration process of lime treatment is much slower than that of cement treatment. Further, the starting time of the 2<sup>nd</sup> phrase is different from one study to another (Chew *et al.*, 2004; Rogers *et al.*, 2006; Little and Nair, 2009), varying from several hours to several days even weeks: about 7 days for Little and Nair (2009), over 14 days for Rogers *et al.* (2006), after 10 days for Locat *et al.* (1990) and 21 days for Wild *et al.* (1993). For cement treatment, the starting time of the 2<sup>nd</sup> phrase is usually much quicker (often in several hours). Sabry and Parcher (1979) reported that, in general, the most notable increase in strength occurs within the first 7 days for cement treatment if enough water is available. Chew *et al.* (2004) reported that water loss induced by pozzolanic reaction probably occurs in the period from 7 and 28 days.

#### 1.4.1.4. Curing temperature

As elevated curing temperature can promote pozzolanic reactions, curing temperature plays also an important role in strength development (Bell, 1996) (Figure 1-18). As the strength gain depends on curing time, while the test of strength design is often expected to be applied in short term, elevating the curing temperature is a conventional method to accelerate curing in the laboratory (Baghdadi, 1982; Ferrell *et al.*, 1988; Mooney *et al.*, 2010; Daniels *et al.*, 2010; Gnanendran *et al.*, 2011). ASTM D 5102-96 also proposes to allow elevated temperatures in the accelerated tests (Mooney *et al.*, 2010).

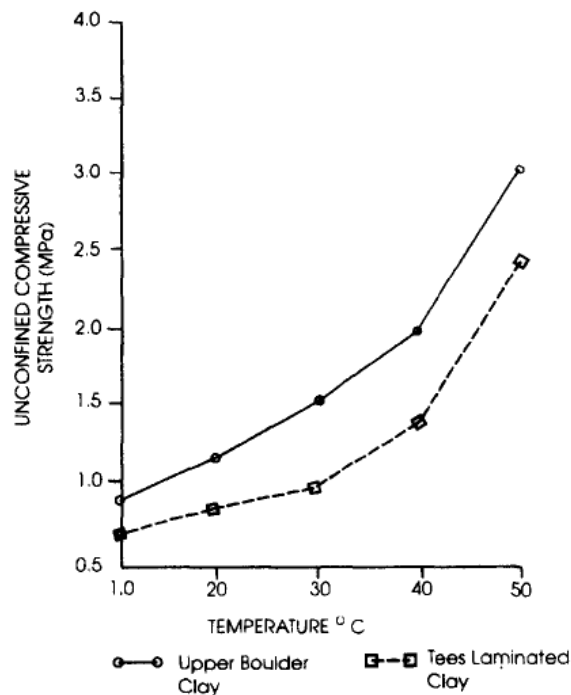


Figure 1-18 Influence of curing temperature on the development of unconfined compressive strength (sample cured for 7 days) (Bell, 1996)

#### 1.4.2. Factors affecting the small strain shear modulus

The impact of stress state on the small strain shear modulus ( $G_{max}$ ) of soils have been widely discussed (Hardin1978; Dobry and Vucetic, 1987; Alarcon-Guzman1989; Viggiani & Atkinson,1995; Lo Presti *et al.*, 1996, 2002; Santamarina and Aloufi, 1999; Yamashita2003; Ortiz, 2004; Piriyaikul, 2006), in terms of stress history or over consolidation ratio (Hardin1978; Alarcon-Guzman *et al.*1989; Houlsby & Wroth1991; Viggiani & Atkinson,1995; Ng and Yung, 2008; Katarzyna, 2008; Ng *et al.*, 2009), loading rate (Dobry and Vucetic, 1987 and Lo Presti et alo., 1996; Matešić and Vucetic, 2003), loading paths (Hardin and Drnevich, 1972; Houlsby & Wroth1989; Santamarina and Aloufi, 1999; Ortiz,

2004; Khosravi *et al.*, 2010; Jesmani *et al.*, 2010), stress anisotropy (Hight *et al.*, 1997; Piriyaikul *et al.*, 2006; Vassallo *et al.*, 2007; Ng *et al.*, 2009), creep (Lo Presti *et al.*, 1996; Lo Presti and Pallara, 2002), effective confining stress (Santamarina and Aloufi, 1999; Ortiz, 2004), etc. Ortiz (2004) reported that  $G_{max}$  increases with increasing confinement for fine-grained silt. Ng *et al.* (2009) performed suction controlled tests with wetting/drying cycles on a non-expansive clayey silt and observed that the stress path or loading history has a significant effect on the soil stiffness. In short, previous studies show that the stiffness behaviour of soil is complex, depending on the stress states.

In addition to the stress state, some other factors can also play a role in soil's  $G_{max}$ , such as soil properties, water content, density, curing conditions and cementation degree (see Table 1-1).

**Table 1-1 Factors affecting the  $G_{max}$**

Type	Factor	Reference
Soil basic properties	Soil plasticity for silts and clays	Nordlund and Deere (1970); Vucetic and Dobry (1991); Schnaid <i>et al.</i> (1993); Vucetic (1994); Lo Presti <i>et al.</i> (1996); Powell and Butcher (2002); Jesmani <i>et al.</i> (2010)
	Fine content	Sahaphol and Miura (2005)
	Grain/aggregate size effect (coarse/ fine-grained soil)	Viggiani and Atkinson (1995); Jovicic and Coop (1997); Santamarina (2003); Wichtmann and Triantafyllidis (2009); Tang <i>et al.</i> (2011)
	Grain shape	Holubec and D'Appolonia (1972); Santamarina <i>et al.</i> (1998); Meidani <i>et al.</i> (2008)
	Plastic index	Lima <i>et al.</i> (2011)
	Void ratio	Nordlund and Deere (1970); Hardin (1978); Hardin and Drnevich (1972); Schnaid (1993)
Compaction	Water content (dry/wet side)	Snachez-Salinerio <i>et al.</i> (1986); Mancuso <i>et al.</i> (2002); Schuettpelez <i>et al.</i> (2009); Lima <i>et al.</i> (2011); Tascon (2011)
	Density	Al-Hussaini (1973); Holubec and D'Appolonia (1972); Hight <i>et al.</i> (1997); Briaud (2001); Elhakim and Mayne (2003); Sun <i>et al.</i> (2007); Pokhrel (2009)
Treated soils	Cementation degree	Clough <i>et al.</i> (1981); Lade and Overton (1989); Airey and Fahey (1991); Reddy and Saxena (1993); Cuccovillo and Coop (1998); Fernandez and Santamarina (2001); Fernandez and Santamarina (2001); Axtell and Stark (2008); Flores <i>et al.</i> (2010); Bahador and Pak (2011)
	Void/lime ratio; Porosity/cement ratio	Consoli <i>et al.</i> (2009, 2011); Consoli <i>et al.</i> (2007, 2010, 2012)
	Treatment methods and dosage	Puppala <i>et al.</i> (2005); Bahador and Pak (2011)
Cure condition	Curing time	Anderson and Stokoe (1978); Holm (1979); Flores <i>et al.</i> (2010); Ali <i>et al.</i> (2011)
	Cyclic drying and wetting	Liao (2007); Ng and Yung (2008); Ng <i>et al.</i> (2009); Vaunat <i>et al.</i> (2009); Vaunat <i>et al.</i> (2009, 2010); Tang <i>et al.</i> (2011)
	Drying	Pokhrel <i>et al.</i> (2009); Vaunat <i>et al.</i> (2009); Ng and Xu (2012); Stoltz <i>et al.</i> (2012) (stability)
	Wetting	Ng and Xu (2012); Stoltz <i>et al.</i> (2012); Stoltz <i>et al.</i> (2012) (stability)



### 1.4.2.1. Soil properties

As shown in Table 1-1, attempts have been made to correlate  $G_{\max}$  to soil plasticity properties (Nordlund and Deere, 1970; Schnaid, *et al.*, 1993; Vucetic, 1994; Lo Presti *et al.*, 1996; Powell and Butcher, 2002), in particular to soil plasticity index. Figure 1-19 indicates that the plasticity index of fine-grained soils does not correlate clearly with  $G_{\max}$  in the small strain range, while it plays an important role in the range of large strains. The results of Nordlund and Deere (1970) also indicate that the modulus change is not sensible to the plasticity index in the range of small strains. Some other studies (Nordlund and Deere 1970; Schnaid, *et al.* 1993) reported that the  $G_{\max}$  increases with the void ratio decrease, and Hardin (1978) further elaborated a generalized empirical relation between  $G_{\max}$ , void ratio, stress and over-consolidation ratio.

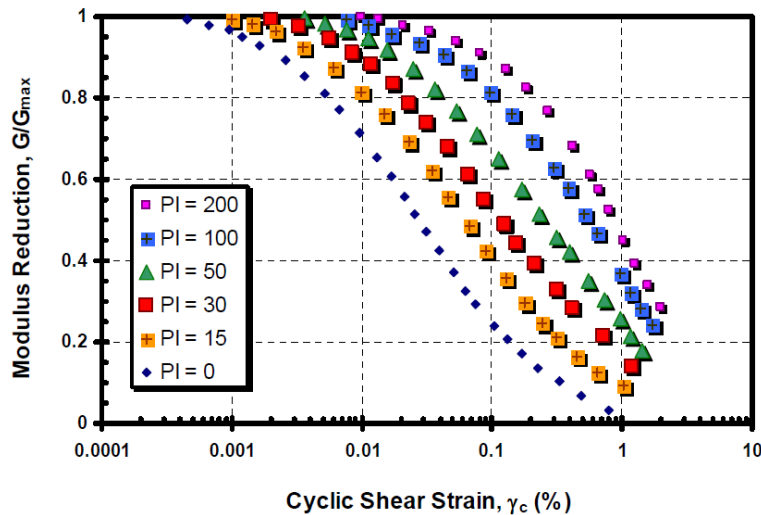


**Figure 1-19 Plastic index impact on soils' modulus decrease with increasing cyclic shear strain (Elhakim, 2005)**

Recently, more and more attention has been paid to the effect of the grains properties on the  $G_{\max}$ . For example, Jovicic (1995; 1997) compared the shear modulus behaviour of fine-grained and coarse-grained soils at very small strains; Cascante (1996) established the relationship between the interparticle contact behaviour and the wave propagation; Santamarina *et al.* (1998) studied the effect of surface roughness on the stiffness. Santamarina (2003) reported that the degradation threshold strain for coarse-grained soils increases with the applied load and decreases with the stiffness of particles. For fine-grained soils, this threshold strain increases with decreasing particle size; hence, the higher the plastic index the higher the degradation threshold strain. Further, based on the fine content after

consolidation of Touhoro volcanic soil, Sahaphol and Miura (2005) established a relationship between the  $G_{\max}$  and fine content, greatly advancing the knowledge regarding the effect of grain properties on soil stiffness. They observed that a significant decrease in shear modulus occurs when the fine content increases, showing the impact of the lower stiffness of fines on the global one. Figure 1-20 shows that the shear wave generally has a tendency to propagate faster through the stiff parts (coarse grains) than through the weak parts (fines with low stiffness). Therefore, the shear wave velocity, and hence the shear modulus of a soil with a small fine content are usually higher than that of a soil with a larger fine content.

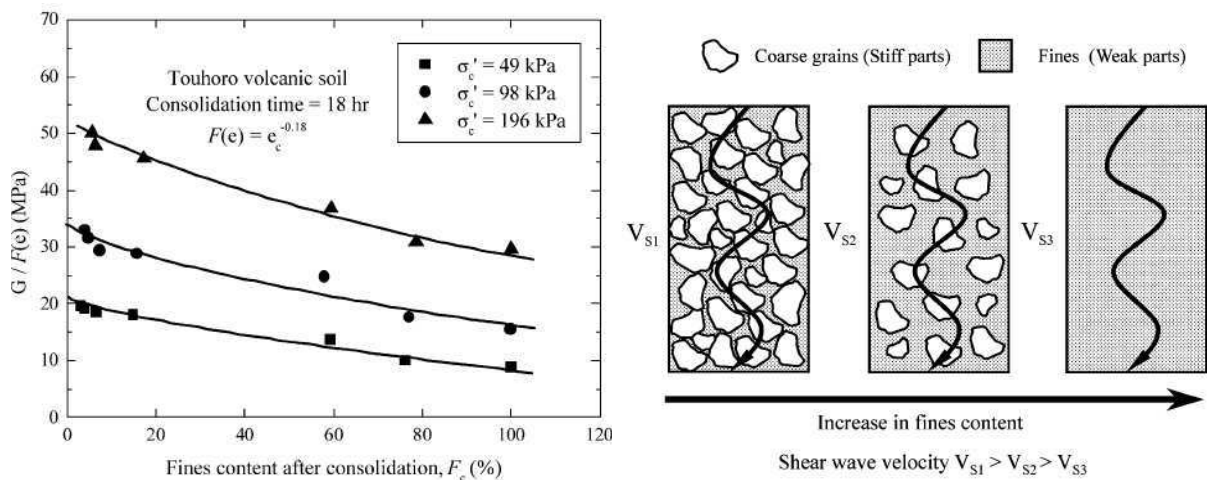


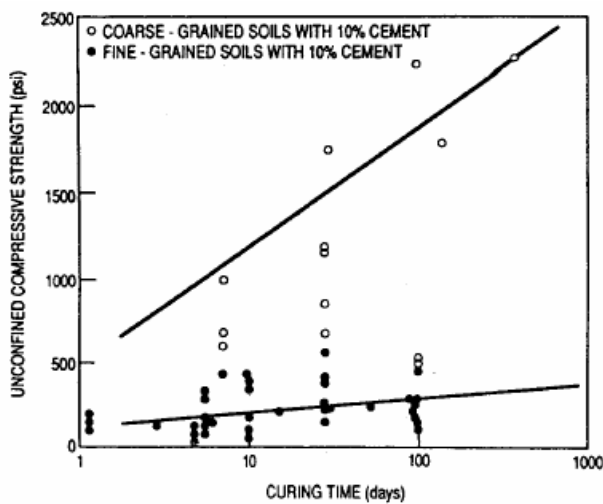
Figure 1-20 Effect of fine content on shear wave velocity (Sahaphol and Miura, 2005)

For treated soils, the effect of grain size/aggregate size may be also fundamental for  $G_{\max}$ . As soil is constituted of grains, its stiffness improvement can be explained by two main mechanisms: 1) a reduction of fines by hydration reactions and 2) an increase of bonding due to the formation of cementitious products coating among grains. Probably, the grain size and aggregate size distributions evolve over time, with firstly coating the particles or aggregates, binding particles or aggregates, and followed by formation of new compounds or cementitious products around these aggregates. This stiffness improvement can be significantly affected by the mixing process.

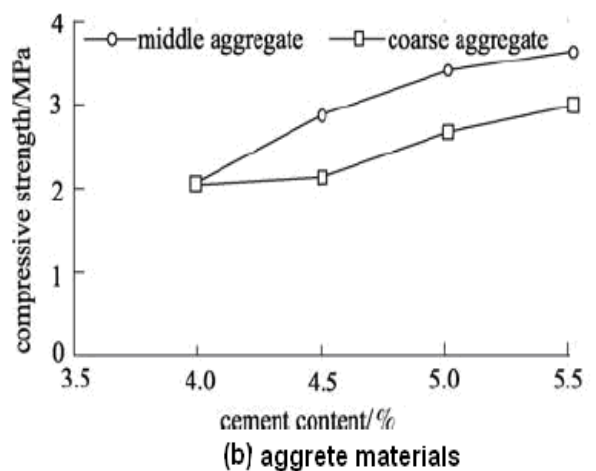
Intuitively, it is logical that the soil treatment mechanism is aggregate-size dependent. However, for lime and/or cement treated fine-grained soils, the grain size effect or aggregates size effect on  $G_{\max}$  is still an open question. In fact, several studies (Mitchell, 1976; Lasisi and Ogunjide, 1984; Anon, 1990; Chiang, 2003; Peng and He, 2009; Tang *et al.*, 2011) involve the grain size effect on the hydro-mechanical behaviour of treated soils, and the results obtained are controversial. Mitchell (1976) reported that cement treated fine-grained

soils present lower UCS than coarse-grained soils after 100-day curing (see Figure 1-21a). Lasisi and Ogunjide (1984) investigated the grain size effect on the strength characteristics of cement-stabilized lateritic soils, and observed that the finer the grains the higher the compressive strength. Later, Anon (1990) reported similar results to that of Mitchell (1976). However, another study on the cement stabilized soils in base pavement structure by Peng and He (2009) provides opposite results: the middle-aggregate soils have higher compressive strength than coarse-aggregate soils (Figure 1-21b).

Recently, as shown in Figure 1-22, this grain size effect was specially studied and evidenced by Tang *et al.* (2011) for the lime-treated Tours clayey silt. The results show that the larger the maximum diameter of aggregate  $D_{max}$  the lower of the  $G_{max}$ . Tang *et al.* (2011) explained this phenomenon by the difference in total surface of grains. The grain size effect may be the motivation for the development of deep mixing techniques (Lorenzo and Bergado, 2006; Shen *et al.*, 2008).



(a) Coarse/fine-grained soil (Modified by Sariosseiri, 2008 from Mitchell 1976)



(b) Middle and coarse aggregate (Peng and He, 2009)

**Figure 1-21 Controversial size effect on the strength of cement-treated aggregate soil**

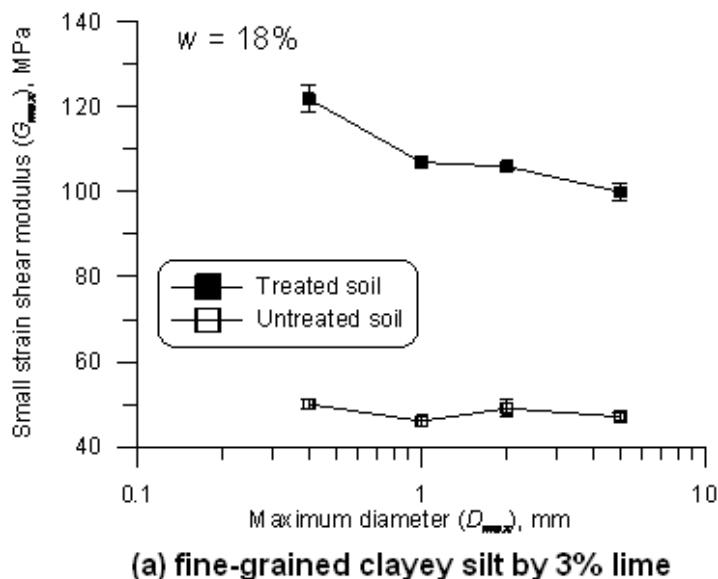


Figure 1-22 Effect of aggregate size for a lime treated clayey silt (Tang *et al.*, 2011)

#### 1.4.2.2. Density

Like other parameters (ex. grain size distribution and particle shape), the soil initial dry density is also a crucial parameter governing the soil's stiffness. The higher the dry density the higher the modulus, as evidenced by Elhakim and Mayne (2003) on a saturated clay. Some stiffness measurements were made using stiffness gauges, allowing establishment of the relationship between dry density and stiffness. However, this kind of relationships is often quite sensitive to changes in water content for fine-grained soils. Sun *et al.* (2007) elaborated a density-dependent elastoplastic hydro-mechanical model for unsaturated compacted soils, allowing consideration of both density and water content effects. It is important to note that two soil samples can have the same dry density but different structures and hence different soil moduli (Briaud, 2001). Indeed, Pokhrel (2009) reported that the soil stiffness depends on the structural organization of particles.

#### 1.4.2.3. Hydric state

When the subgrade soil is affected by wetting-drying cycles, its water content will change. This often causes changes in matric suction and other soil parameters. Since the last decade, several studies were concentrated on the relationship between soil strength/stiffness and soil suction (Fredlund *et al.*, 1978; Peterson, 1990; Fredlund *et al.*, 1995; Vanapalli *et al.*, 1996; 1997; Yuan and Nazarian, 2003; Briaud, 2001; Mancuso *et al.*, 2002; Rassam and

cook, 2002). According to Briaud (2001), the stiffness of soils depends strongly on their moisture contents. At low water contents, water binds the particles (especially for fine-grained soils) increasing the effective stress between the particles. As a result, low water contents increase soil moduli. For example, clay shrinks and becomes very stiff when it is dried. But, for coarse-grained soils, at very low water contents, the maximum density is difficult to be obtained by compaction, and the moduli are generally small. In such cases, the modulus increases with the increase of water content because the effect of compaction is improved. However, if the water content rises beyond the optimum one, the modulus starts to decrease (Briaud, 2001). Similar results are also obtained by Mancuso *et al.* (2002) - see the relationship between matric suction and shear stiffness in Figure 1-23.

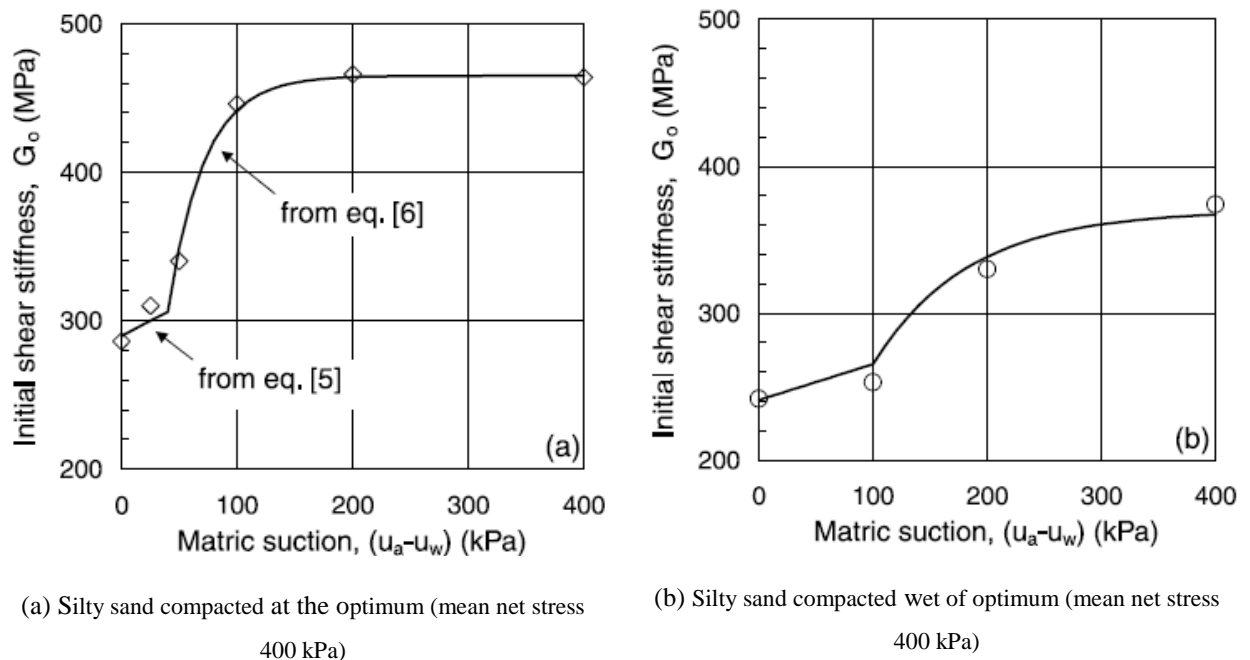


**Figure 1-23 Influence of suction on the shear stiffness (Mancuso *et al.*, 2002)**

Naturally, the  $G_{\max}$  may evolve with the moulding water content (dry side, wet side and optimum water content), especially for cementitious treated soils. Figure 1-24 is a general sketch, showing how the shear modulus changes with water content (Schuettpelz *et al.*, 2009). In a limited range of water contents around the optimum state, the shear modulus decreases with water content increase; however, at dry conditions, the effect of water content is positive for the soils cohesion thus the stiffness. Similar results are also found in terms of  $M_R$  by Yuan and Nazarian (2003). In addition, the strain growth will give rise to decrease in the corresponding stiffness at the same water content. The suction or water content effect on

$G_{\max}$  can be explained by the “glue effect” as termed by Santamarina (2003). Certain quantity of water exists at the contacts between particles, gluing the particles together. On dry side, water in untreated fine-grained soils can result in a significant “glue effect” between particles induced by suction. This effect is temporary as an increase in water content will destroy it (e.g. wet side). For cementitious treated fine-grained soils, the glue effect induced by the reactions is permanent, and water may play a role different with untreated soils. It is still unknown whether the Schuettpelz’s model works or not for the cementitious treated soils. The study by Tang *et al.* (2011) on the  $G_{\max}$  of Tour silt treated with 3% lime and compacted at different water contents and same dry density ( $w = 14\%$  and  $18\%$ , both on dry side) shows similar final modulus value, showing no effect of water content.

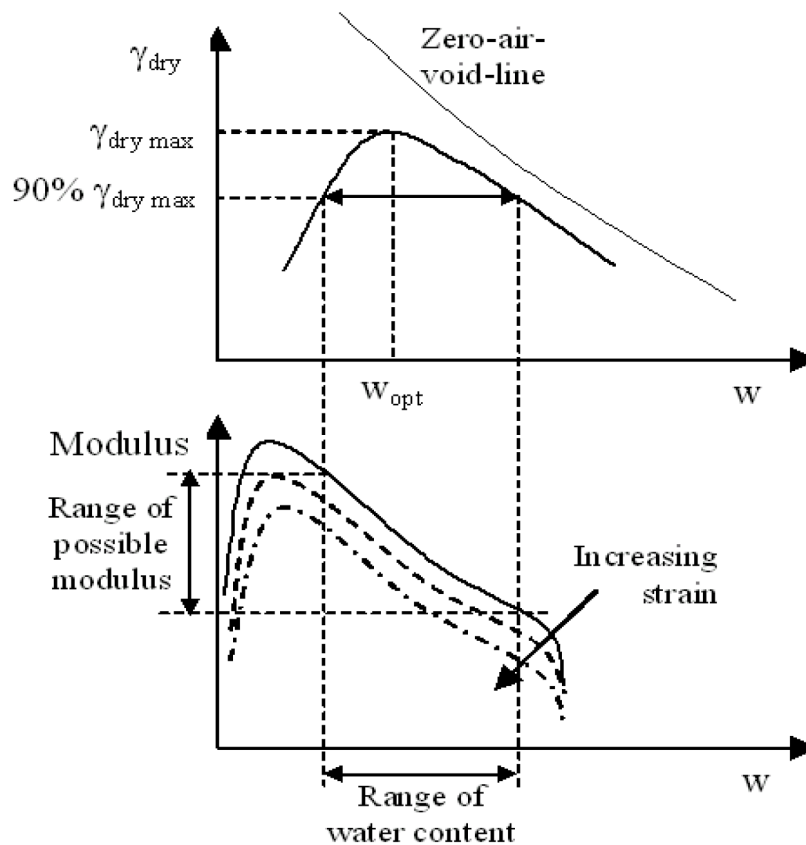


Figure 1-24 Mechanical model of the impact of water content on the soil’s shear modulus, proposed by Schuettpelz *et al.* (2009) (cited by Tascon, 2011)

Water content is a crucial factor affecting the stiffness of both untreated and treated soils (Yuan and Nazarian, 2003; Puppala *et al.*, 2006; Ng *et al.*, 2009; Vaunat *et al.*, 2009; Tang *et al.*, 2011; Stoltz *et al.*, 2012). Normally, in the early stage of curing, the environmental moisture condition has a positive effect for the different reactions, while the

drying-wetting cycles often lead to degradation of soil's stiffness. Yuan and Nazarian (2003) reported that the moisture-modulus relationships are different between drying and wetting process. Ng *et al.* (2009) reported that the measured  $G_{\max}$  increases in a nonlinear fashion with increasing matric suction, and that in a small range of matric suctions, the influence of suction on the stress-induced stiffness anisotropy is not significant. Vaunat *et al.* (2009) investigated the influence of suction and suction history on the  $G_{\max}$  of compacted Boom clay and the results show a significant increase of  $G_{\max}$  when the degree of saturation decreases. In addition,  $G_{\max}$  appears to depend only on the degree of saturation during the drying process. Later, Ng and Xu (2012) studied the effects of suction history/suction magnitude on  $G_{\max}$ . Puppala *et al.* (2006) reported that the enhancement in shear moduli of both cement and lime treated cohesive soils is lower for the specimens continuously soaked in water as compared to those cured in a humidity controlled room. Vanapalli (1999) reported that wetting results in a more significant influence on the matrix suction at the beginning of the wetting, and that when the water content approaches the equilibrium moisture content, this influence becomes less significant. Drying can cause significant changes in soil parameters and give a sudden increase in matric suction. Tang *et al.* (2011) explained that the degradation is caused by the micro-cracks induced by wetting/drying cycles.

#### 1.4.2.4. Curing time

As for the strength gain, curing time is also a very important factor for the stiffness development. If the ageing effect (Delage *et al.*, 2006; Ali *et al.*, 2011) may be responsible for the evolution of the behaviour of untreated soils, the development of cementitious products and cementitious bonds by chemical reactions is responsible for the development of stiffness of cementitious treated soils (Clough *et al.*, 1981; Lade and Overton, 1989; Airey and Fahey, 1991; Reddy and Saxena, 1993; Cuccovillo and Coop, 1998; Bahador and Pak, 2011).

For untreated soils, Ander and Stokoe (1978) reported that the shear modulus is a time-dependent soil property: the increase of the shear modulus is characterized by two phrases: 1) an initial phase induced by the primary consolidation; 2) a second phrase after completion of the primary consolidation, namely the 'long term time effect'. Furthermore, it is emphasized that all soils exhibit a long term time effect, no matter fine-or coarse-grained soil, in both ranges of small strains ( $<10^{-3}$  %) and high shear strains ( $10^{-3}$  to  $10^{-1}$  %). Ali *et al.*

(2011) showed an over 40 years' old embankment soil (Ebina soil in Japan) which is still changing in terms of stiffness as expressed below (see also Figure 1-25).

$$G_{\max}(t) = G_{\max}(t_p) \left[ 1 + \left\{ N_G \log\left(\frac{t}{t_p}\right) \right\} \right] \quad (1-20)$$

where  $G_{\max}(t)$  is the  $G_{\max}$  at time  $t$ ;  $t_p$  is the primary consolidation time;  $G_{\max}(t_p)$  is the  $G_{\max}$  after the primary consolidation;  $N_G$  is the slope of the relationship between the  $G_{\max}$  normalized with respect to  $G_{\max}(t_p)$ , and the logarithm of time.

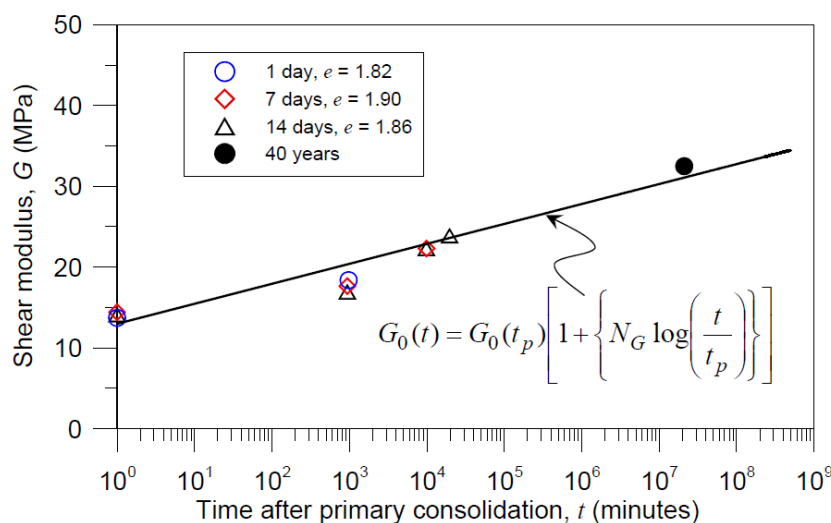


Figure 1-25 Variation of shear modulus over 40 years for an embankment (Ali *et al.*, 2011) (note:  $G_0 = G_{\max}$ )

For cementitious treated fine-grained soils, the stiffness development can last longer, depending on the cementation degree. As the cementitious treatments have similar reaction mechanisms, i.e. short-term hydration/cation exchange and long-term pozzolanic reactions, similar to the strength development, the stiffness evolves with time, also following several phrases and the  $G_{\max}$ -time relationship is usually nonlinear. Santamarina (2003) stated that cementation diagenesis depends on curing time as well as the rate of chemical reactions and diffusion. Holm (1979) reported that the stiffness of lime stabilised clays increases with curing time, by 15 times 3 weeks after the treatment and by 35 times 16 months after the treatment. Puppala *et al.* (2006) measured the  $G_{\max}$  of cement/lime treated sulfate-bearing expansive soils using the bender element, also evidencing the clear curing time effect on the stiffness development.



For the constitutive modelling, several strength-time relationships have been developed based on the hyperbolic equation. Plowman (1956) showed that the plot of compressive and tensile strength of concrete versus the logarithm of time is linear. Based on his work, the first strength development relationship was proposed (Plowman, 1956), as follows:

$$S_T / S_0 = A + B \log(T) \quad (1-21)$$

Where,  $S_T$  is the strength at an age  $T$ ;  $S_0$  is a reference strength (for example, at an age of 28 days as proposed by Flores *et al.*, 2010);  $A$  and  $B$  are constants.

Later, several other models were developed, for example, equation (1-22) of a hyperbolic function, equation (1-23) of a parabolic hyperbolic function and equation (1-24) of an exponential function.

$$S = S_u \frac{k(t-t_0)}{1+k(t-t_0)} \quad (1-22)$$

$$S = S_u \frac{\sqrt{k(t-t_0)}}{\sqrt{1+k(t-t_0)}} \quad (1-23)$$

$$S = S_u \exp\left(\frac{-d}{t-t_0}\right) \quad (1-24)$$

Where,  $S_u$  is asymptotic value of strength;  $k$  is rate constant;  $t_0$  is time at which the strength development is assumed to begin, usually of the order of 0.15 day as proposed by Flores *et al.*, 2010.

The first strength gain relationship for cemented soils was proposed by Mitchell *et al.* (1974):

$$UCS_{T_2} = UCS_{T_1} + K \log(T_2 / T_1) \quad (1-25)$$

Where,  $UCS_{T_2}$  is the UCS at age  $T_2$ ,  $UCS_{T_1}$  is the UCS at age  $T_1$  and  $K$  is a constant.

The hyperbolic equation has been applied in several studies (Nagaraj *et al.*, 1998; Horpibulsuk *et al.*, 2003; Flores *et al.*, 2010). Nagaraj *et al.* (1998) conducted unconfined compressive tests on four clays treated with Portland cement at high water content. Based on the 14-day UCS, they proposed the relationship shown in equation (1-26). Later, Horpibulsuk

*et al.* (2003), based on the work of Nagaraj *et al.* (1998) and a large database, proposed another UCS of 28-day curing (equation 1-27).

$$UCS_T / UCS_{14days} = a + b \ln(T) \quad (1-26)$$

$$UCS_T / UCS_{28days} = a + b \ln(T) \quad (1-27)$$

Where  $UCS_T$  is the UCS at age  $T$ ;  $UCS_{14days}$  is the 14-day UCS;  $UCS_{28days}$  is the 28-day UCS;  $a$  and  $b$  are constants.

In the last two decades, numerous studies were conducted and the results show a reasonably linear correlation between  $G_{max}$  and UCS (Tatsuoka *et al.* 1996; Hird and Chan, 2005; Van Impe *et al.* 2005; Lohani *et al.* 2006; Helinski *et al.* 2007; Flores *et al.*, 2010). However, the relationship for stiffness is rarely reported for treated soils. The only two studies on the  $G_{max}$ -time relationship were conducted by Puppala *et al.* (2006) and Flores *et al.* (2010).

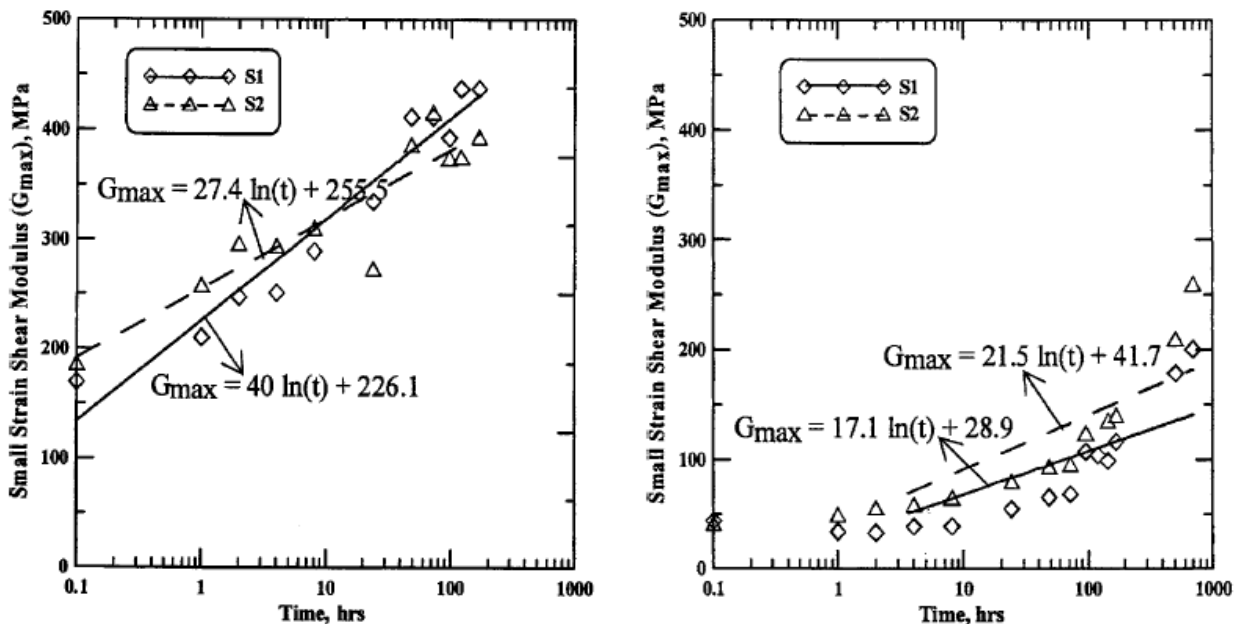
Puppala *et al.* (2006) studied the lime and cement treated expansive soils, and modelled  $G_{max}$  using a linear relationship with the natural logarithm of curing time (equation 1-28). However, it appears that this model cannot well depict the short-term effect (several hours) and long-term effect (over 1000 hours), particularly for the lime treated clays due to the clear nonlinear relationship involved (see Figure 1-26).

$$G_{max} = a \ln(t) + b \quad (1-28)$$

Where  $a$  reflects the ratio of stiffness development with time;  $b$  represents the initial value ( $t = 1$  hour) and  $t$  is the curing time.

Flores *et al.* (2010) investigated both the  $G_{max}$  and UCS development for a cement treated clay. Using an equation similar to that proposed by Horpibulsuk *et al.* (2003), and replacing the UCS by  $G_{max}$  (see Formula 1-29), it was found that the increases of  $G_{max}$  and UCS are closely related. As shown in Figure 1-27, the  $G_{max}$  (normalized  $G_0 = G/G_{max}$ ) of a cement treated clay over logarithm of time shows a two-phase curve.

$$G_{max} / G_{max(28days)} = a + b \ln(T) \quad (1-29)$$



(a)  $G_{max}$  of 10% cement treated clays

(b)  $G_{max}$  of 8% lime treated clays

Figure 1-26 Evolution of  $G_{max}$  over time for the cement /lime treated natural clays (1000 ppm of Sulfates level, compacted at optimum moisture content) (Puppala *et al.*, 2006)

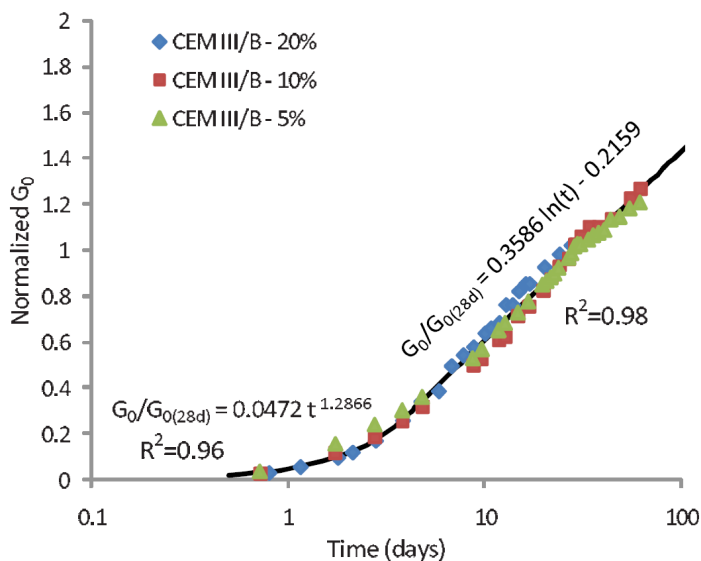


Figure 1-27 Two phrases of  $G_{max}$  development with curing time for a cement treated clay (Flores *et al.*, 2010)

### 1.4.2.5. Cementation

Cementation can significantly influence the stiffness, strength and volume change of soils (Clough *et al.*, 1981; Lade and Overton, 1989; Airey and Fahey, 1991; Reddy and Saxena, 1993; Cuccovillo and Coop, 1998; Bahador and Pak, 2011). For cementitious

treatment soils, the relationship between suction and stiffness may be more complex than for the untreated soils and the water retention properties can be also modified by the treatment (Clare and Cruchley, 1957; Fredlund and Xing, 1997; Stoltz *et al.* 2012). Bahador and Pak (2011) observed that  $G_{\max}$  increases with curing time, water content, confining pressure and cement content. They highlighted that the effect of cement content is the most dominant one, followed by water content, curing time and confining pressure.

According to Santamarina (2003), two regions of cementation can be defined: the low-confinement “cementation controlled” region and the high-confinement “stress-controlled” region. In the cementation-controlled region,  $G_{\max}$ /strength is controlled by cementation: 1) the buckling of chains is hindered at lower initial volume contraction, and 2) the soil tends to brake in blocks immediately after breaking. The inter-block porosity is zero, hence shear tends to cause high dilation, even if the cemented soil within the blocks has high void ratio. Unlike the “glue effect” due to suction effect, the glue effect due to cementation is permanent. The cementation can be due to the deposition of calcium at the particle-to-particle contacts. The cementation degree is normally governed by the reactions between soil and agent, depending on the void/agent ratio, water content, mixing and curing conditions, etc.

Recently, voids/lime ratio and porosity/cement or void/cement parameters have been considered as appropriate parameters to assess both the initial stiffness and unconfined compressive strength (Lorenzo and Bergado, 2004; Consoli *et al.*, 2009; 2011; Consoli *et al.*, 2007; 2010; 2012). Although water-cement ratio is chosen to define the cement dosage for soil-cement stabilization in many studies, this ratio does not appear as effective as voids/cement ratio in assessing the compressive strength (Consoli *et al.*, 2007; 2010; 2012). In contrast, the voids/cement ratio, defined as the ratio between the porosity of the compacted mixture and the volumetric cement content, is revealed to be the most appropriate parameter in assessing the unconfined compression strength. For unsaturated soils, the voids are partially filled by water; therefore, there is not a unique relationship between the voids and the amount of water. The roles played by the porosity and by the water content are different. Consoli *et al.* (2007) stated that the porosity affects the strength through the number of contacts among the soil particles, while the water content affects the strength through the modification of soil structure. Therefore, for the soil cement in the unsaturated state, the use of the relationship between porosity and cement content is more appropriate in the analysis the soil mechanical strength. Indeed, Consoli *et al.* (2010) founded a good relation between the amount of cement, the porosity, the water content and the strength of artificially cemented

soils. A number of unconfined compression tests, triaxial compression tests, and measurements of matric suction were carried out. The results show that the unconfined compression strength increases linearly with the increase of cement content and exponentially with the decrease of porosity. The change in water content has a marked effect as well on the unconfined compression strength. Further, Consoli *et al.* (2012) reported that the porosity/cement ratio is an appropriate parameter in assessing both the initial stiffness and the unconfined compressive strength of the soil–cement mixtures.

### **1.4.3. Climate change effect on the hydro-mechanical behaviour of treated soils**

Numerous studies have been conducted for better understanding the long-term characteristics evolution with respect to the influence of environmental factors, especially the wetting–drying and freezing–thawing cycles. These characteristics include shear strength, volume change and hydraulic behaviour.

#### **1.4.3.1. Wetting/drying cycles**

As soil undergoes drying process, its suction increases, leading to the increase of inter-particle force. An apparent cohesion term is thus created, and consequently, a tensile strength term. There is thus a correlation between suction and tensile strength, which was recognised early in the study in this field. Kim & Hwang (2003) attempted to directly relate tensile strength to the normal inter-particle force that is calculated from micro-scale considerations. Considering the Griffith theory of tensile failure, it is believed that such approaches only give a partial view of the real mechanisms related to macroscopic tensile failure and the way that tensile strength evolves during drying. In fact, Peron *et al.* (2009) stated that the failure mechanisms related to drying–wetting is still not well understood. Charlier *et al.* (2009) stated that any saturation variation induces a variation of suction, internal stress state and strain. Strains are induced by either stress or suction. Some researchers explained the degradation of hydro-mechanical behaviour of soils during wetting–drying cycles by the micro-cracks induced by suction cycles (Pardini *et al.*, 1996; Tang *et al.*, 2011).

Although the cementitious treatment can greatly improve the swelling properties of soils, several studies (Rao *et al.*, 2001; Guney *et al.*, 2007; Khattab *et al.*, 2007; Cuisinier and

Deneele, 2008a; Pedarla, 2009; Kasangaki and Towhata, 2009; Nowamooz and Masrouri, 2010; Stoltz *et al.*, 2010; Akcanca and Aytakin, 2011; Stoltz *et al.*, 2012) investigated the impact of wetting-drying cycles on the swelling properties of lime-stabilized clays, showing the efficiency reduction of the lime treatment under the effect of wetting-drying cycles. Recently, several studies (Zhang and Tao, 2008; Harichane *et al.*, 2010; Tang *et al.*, 2011; Kalkan, 2011; Parsons and Milburn, 2003) showed that for the cementitious treated clayey soils, their mechanical performance is degraded by the effect of wetting-drying cycles. Zhang and Tao (2008) studied the durability of cement stabilized low plastic soils by applying wetting-drying following ASTM559, showing that the soil-cement loss decreases consistently with the increase in cement dosage, but increases with water-cement ratio. This indicates that the water-cement ratio of cement-stabilized soil has a dominant influence on soils durability. Some other studies (Guney *et al.*, 2007; Rao *et al.*, 2001; Yong and Ouhadi, 2007; Cuisinier and Deneele, 2008a; Stoltz *et al.*, 2010; Al-kiki *et al.*, 2011) showed that the swelling pressure and swelling potential increase with wetting-drying cycles for lime treated clayey soils. Many studies consider the wet-dry process by starting with wetting process, while Al-kiki *et al.* (2011) performed their study by performing both wet-dry and dry-wet cycles tests, showing a greater reduction in strength by the wetting-drying cycle than the drying-wetting cycle, and a higher volume change by the drying-wetting cycle. Several studies (Cuisinier and Deneele, 2008a; Lorenzo and Bergado, 2004; Guney *et al.*, 2007; Stoltz *et al.*, 2010; Nowamooz and Masrouri, 2010; Stoltz *et al.*, 2012) investigated the effect of wetting/drying cycles by controlling the suction for the lime treated expansive clays. Lorenzo and Bergado (2004) studied the influence of suction cycles (0~8 MPa) on the mechanical behaviour of a compacted treated bentonite/silt mixture. The results show a swelling accumulation for both lime treated and untreated samples with cycles ongoing. Further, the volumetric strain of treated soils due to changes in suction or stress are different from that of untreated soils in the first few cycles, but the treated soils may finally present the same volumetric strain as the untreated samples after enough cycles applied. Cuisinier and Deneele (2008a) also applied a similar suction amplitude to an *in situ* lime treated clay (A4 according to the French standard): partial cycles of 0~1 MPa and full cycles of 0~8 MPa. They observed that the lime treatment efficiency decreases over time under the effect of drying -wetting cycles: the first wetting leads to an increase of volume and the first cycle leads to an irreversible deformation. This is different from the following cycles. Stoltz *et al.* (2010) reported that the alteration of lime stabilisation effects by wetting/drying cycles depends not only on the amplitude of cycles, but also on the lime content: the lower the lime-

content the higher the alteration of lime stabilisation effects. In addition, Guney *et al.* (2007) reported that the maximum swelling potential reduction is observed at the first cycle, the swelling potential decreasing gradually at the subsequent cycles and reaching equilibrium after 4-6 cycles.

Recent studies have involved the impact of moulding water content (dry, wet side and optimum) on the resistance to the wetting/drying cycles. Tang *et al.* (2011) studied the grain size effect of a lime treated clayey soil compacted dry of optimum at two initial molding water contents of 14 and 18%, respectively. Drying/wetting cycles were applied after the curing time (stability of the  $G_{max}$  after about 200 hours). The results show (Figure 1-28a): 1) a  $G_{max}$  change less sensitive to drying/wetting cycles for treated soil compared to untreated soil; 2) a significant decrease of  $G_{max}$  under first wetting path due to suction change; 3) a slight increase of  $G_{max}$  due to the onset of various physico-chemical reactions within the soil; 4) a notable decrease of  $G_{max}$  due to intensive drying. The results of Al-kiki *et al.* (2011) also show an initial increase in strength during the first few cycles for a lime treated clay soil, under both drying/wetting and wetting/drying cycles (wetting/drying cycling begun after 2-day curing) (Figure 1-28b). It is explained by the continuous reactions and the subsequent strength gain that compensate the deterioration caused by the cycles. However, Harichane *et al.* (2010) reported that the 1<sup>st</sup> wetting path has a quicker degradation rate for a treated soil compacted at optimum, cured for 28 days and then submitted to wetting-drying cycles. Analysis of these confused results shows that the different trends for the first wetting path may be induced by several curing factors: 1) difference in moulding water content (the former compacted at dry side while the latter at optimum); 2) different curing time before wetting/cycles (the former 2 days at 49 °C while the latter 28 days at 20°C); 3) different measurement time after the first wetting (as the ongoing chemical reactions and wetting often cause different trends of stiffness/strength change, the coupled effect of curing and suction change may give different results). On the whole, all these studies indicate that the treatment efficiency decreases with the number of wetting/drying cycles.



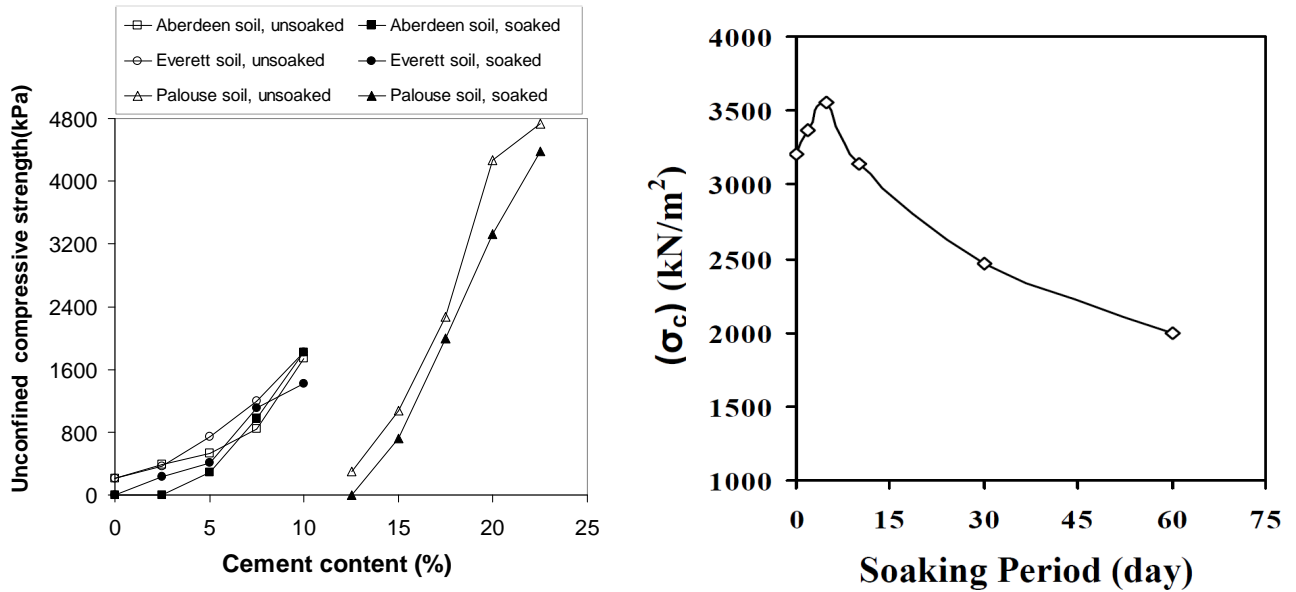


erosion-resistant material may be controlled by weathering rates. Al-kiki *et al.* (2011) also compared the effect of wetting-drying cycles and the effect of F-T on a lime treated clayey soil. The results show that F-T cycles have more detrimental impact on the structure of soils (Figure 1-28b).

#### **1.4.3.3. Long term leaching and soaking effect**

Several studies investigated the physico-chemical effect of cementitious treated fine-grained soils by leaching test (Malhotra and Bashkar, 1983; McCallister, 1990; McCallister and Petry, 1992; Matasović and Jr, 1998; Boardman *et al.*, 2001; Parsons and Milburn, 2003; De Bel *et al.*, 2005, Khattab *et al.*, 2007; Le Runigo, 2008; Le Runigo *et al.*, 2009; Le Runigo *et al.*, 2011; John *et al.*, 2011). Malhotra and Bhasker (1983) and Little *et al.* (1995) showed that leaching has a significant effect on both treated and untreated soils containing soluble salts and minerals. The results of Le Runigo (2008) show that the maintenance of the mechanical performance is highly related to the soil permeability: the higher the permeability, the higher and the faster the loss of the mechanical performances. It appears that the cementitious products can be dissolved in water and gradually lost over circulation time.

The soaking effect on soil strength is different from one study to another, depending probably on the soaking regime and curing conditions before soaking. Over the last 10 years, several studies (Al-kiki *et al.*, 2011; Rogers *et al.*, 2006; Kavak and Akyarh, 2007; Sariosseiri, 2008; Umesha *et al.*, 2009; Burczyk *et al.* 1994; Lee *et al.* 1994; Fahoum *et al.*, 1996; Muhanna *et al.*, 1998; 1999; Puppala *et al.*, 1999; 2003; Qubain *et al.*, 2000; Parsons and Milburn, 2003) involved long-term soaking to investigate the cementitious treatments fine-grained soils resistance to water flooding. Croft (1967) studied the strength of cement treated clay minerals after soaking by considering different curing periods before soaking (1, 4 and 60 weeks), showing that the longer the curing period prior to soaking, the higher the strength obtained after soaking. Sariosseiri (2008) reported that the cement treated soils have higher resistance to water soaking than untreated soils (Figure 1-29a). Al-kiki *et al.* (2011) reported an increase of the strength of lime stabilized soils at early soaking stage, followed by a decrease (Figure 1-29b).



(a) Decrease of UCS by soaking effect for cement treated clays - 2-day soaking (after Sariosseiri, 2008)

(b) Different effect of soaking period on lime treated soils - 2-day curing (Al-kiki *et al.*, 2011)

Figure 1-29 Soaking effect for cement and lime treated soils

#### 1.4.4. Microstructure investigation

Microstructural investigation allows a deep insight into the complex phenomena taking place in the treated soils. Recently, several attempts (MIP, SEM and XRD method) have been made to examine the reaction products formed as well as their distribution.

##### 1.4.4.1. Microstructure change during curing time

The microstructure change during curing time is often examined by the MIP test. The pore size distribution evolution with time can reflect the accumulation of the cementitious products as well as their distribution. Based on the cluster theory (Nagaraj *et al.* 1990; Mitchell JK. 1976, Horpibulsuk *et al.*, 2010), the pores can be classified into two categories: inter-aggregate pores (larger than  $0.1\mu\text{m}$ ) and intra-aggregate pores (smaller than  $0.01\mu\text{m}$ ). Several factors may influence the reaction process and thus control the pore size distribution. In addition to the void ratio, the additive dosage, moulding water content and curing time are also critical factors.

Firstly, the time-dependent microstructure change is strongly related to the initial moulding water content of the sample, especially at the early stage of curing. With the curing times going, the microstructure difference becomes less. As shown in Figure 1-30, Russo *et*

*al.* (2006) studied the variations in porosity induced by lime addition with silt samples in different states (dry, wet and at optimum, curing for 0, 28 days), showing that more effects are detected on optimum and wet samples with an increase of porosity (Figure 1-30a) and less effective changes are observed on samples compacted dry of optimum. The three samples cured for 28 days have very slight difference in porosity (Figure 1-30c), which suggests that the development of pozzolanic reactions and the subsequent cementation of aggregates contribute to the reduction of porosity (Figure 1-30d). In addition, Russo *et al.* (2006) observed that the addition of lime mainly affects the inter-aggregate porosity instead of the intra-aggregate porosity.

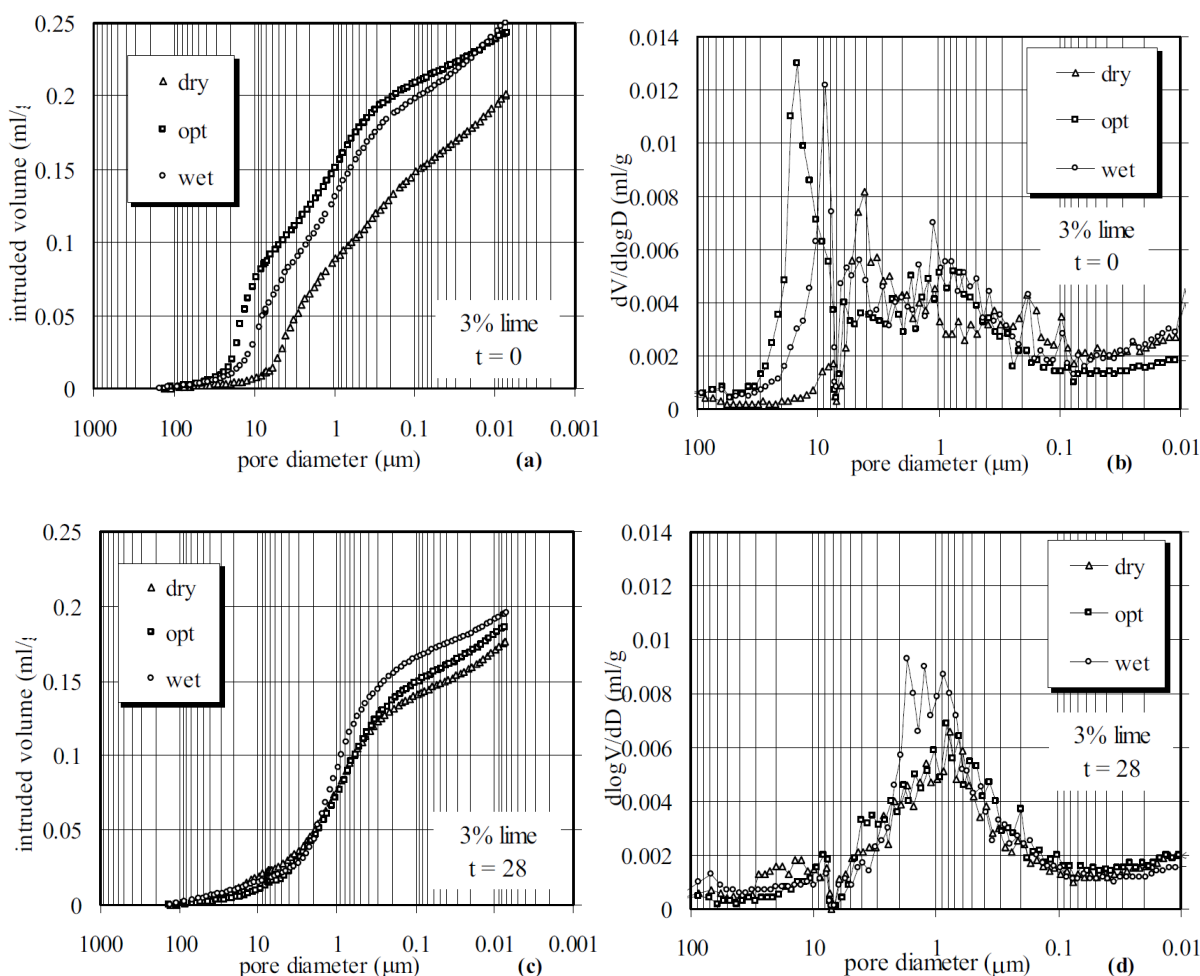


**Figure 1-30** pore size distribution curves of the stabilized soils in different curing time (a, b at  $t = 0$  and c, d at  $t = 28$  days)

Secondly, the treatment dosage and curing time are also factors responsible for the microstructure changes. Figure 1-31 presents the effects of curing time and treatment dosage on the microstructure evolution for lime treated soils (Locat *et al.*, 1996). The large

difference of porous volume is mainly induced by the different void ratio for different lime dosages. It is interesting to note that the highest dosage (10%) does not give a measurable pore entrance radius smaller than  $0.2 \mu\text{m}$ , suggesting that a complete coating of the natural aggregates with cementitious products makes the intra-aggregate pores inaccessible. This case occurs at very high water content (65%), the pozzolanic reactions being fully developed, and the cementitious products induced not only filling the inter-aggregate but also coating the external surface aggregates.

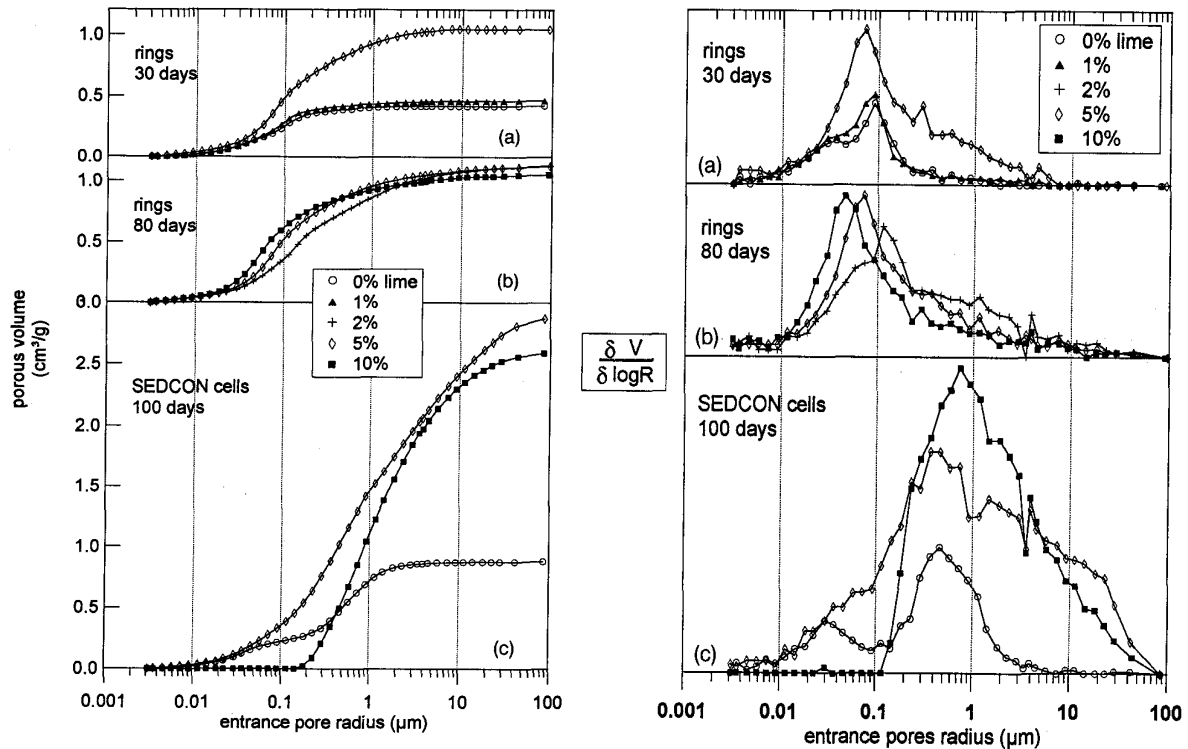
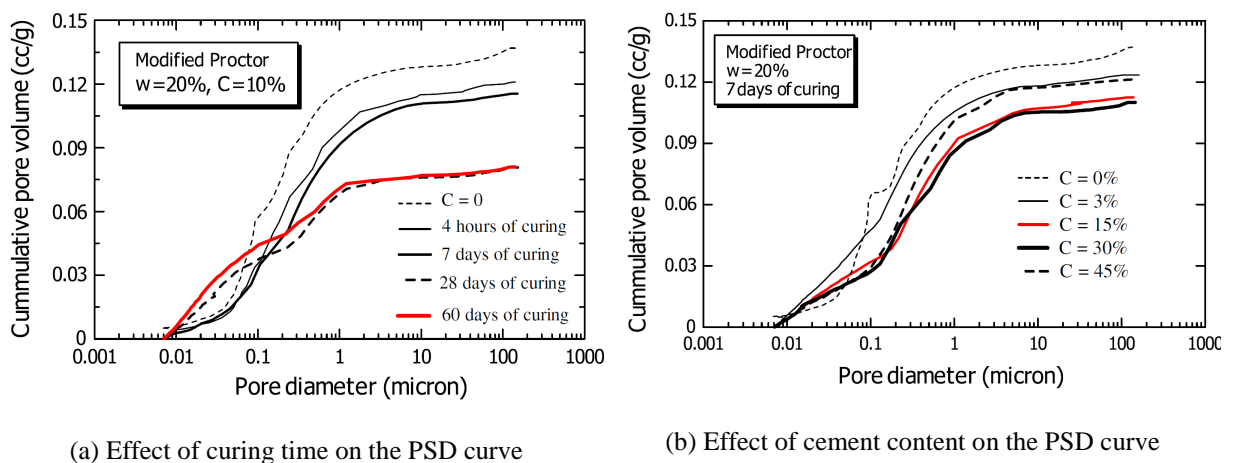


Figure 1-31 Evolution of the microstructure of a lime treated soils (Locat *et al.*, 1996)

Similar to the case of lime treated soils, the formation of clay-cement clusters by the physico-chemical interaction is also responsible for the pore distribution change in the case of cement treated soils. Horpibulsuk *et al.* (2010) reported that, after mixing clay with cement, the volume of small inter-aggregate pore ( $0.01\text{-}0.1 \mu\text{m}$ ) decreases while the volume of the large inter-aggregate pore ( $0.1\text{-}10 \mu\text{m}$ ) slightly increases. Further, because the growth of cementitious products with time, large inter-aggregate pores are filled and thus, the total pore volume decreases. Figure 1-32 presents the microstructure evolution of cement treated silty soils compacted wet of optimum ( $w = 20\%$ , with a modified optimum water content of  $17.2\%$ ). The effect of curing time on the pore size distribution of the cemented samples is illustrated in Figure 1-32a. It is found that, during 7-day curing, the volume of pores smaller

than  $0.1 \mu\text{m}$  significantly decreases while the volume of pores larger than  $0.1 \mu\text{m}$  slightly increases. This result suggests that, during the early stage of curing, the cementitious products fill the pores smaller than  $0.1 \mu\text{m}$  and the coarse particles (unhydrated cement particles) cause large soil-cement clusters and large pores. After 7-day curing, the volume of pores larger than  $0.1 \mu\text{m}$  tends to decrease while the volume of pores smaller than  $0.1 \mu\text{m}$  tends to increase, suggesting that the cementitious products fill the large pores (larger than  $0.1 \mu\text{m}$ ). As a result, the volume of small pores (smaller than  $0.1 \mu\text{m}$ ) increases and the total pore volume decreases. Normally, the higher the dosage of cement is, the more the cementitious products and subsequently the higher the soil strength is. However, this reasoning is based on the condition with sufficient water content for reactions. In the active zone (3% cement in Figure 1-32b), the cementitious products not only enhance the inter-cluster bonding strength but also fill the pore space: the volume of pores smaller than  $0.1 \mu\text{m}$  is significantly reduced with cement, thereby reducing the total pore volume; for the inert zone (15% - 30% cement in Figure 1-32b), the pore size distribution for 15% and 30% cement treated clay is almost the same, indicating similar formation of hydration products and cementitious products; for the deterioration zone (45% cement in Figure 1-32b), compared to the case of 30% cement, both the volume of large pores ( $1.0 - 0.1 \mu\text{m}$  pores) and the total pore tend to increase with cement addition. Horpibulsuk *et al.* (2010) explained that by the significantly reduction of water content with the increase of cement content: the degree of hydration and thus the cementitious products are decreased. This indicates that for a given water content, the addition of cement in excess of the active zone is useless.



**Figure 1-32 Effects of curing time and cement content on the microstructure evolution of cement treated soils (Horpibulsuk *et al.* 2010)**

The curing time strongly influence the soil microstructure (Cai *et al.*, 2006; Russo *et al.*, 2006; Le Runigo *et al.*, 2009; Sakr *et al.*, 2009). Many studies show that the cementitious products can be induced by long-term reactions. However, this process depends on the treatment, soil type, curing time, etc. Table 1-2 and Table 1-3 summarise these cementitious products induced by lime and cement additions, respectively. Note that the cementitious products induced by mix treatments (lime and cement) have been scarcely reported.

**Table 1-2 Summary of cementitious products induced by lime addition**

(Note: d = day; RH = relative humidity; RT= room temperature; Normal Proctor optimum water content (OWC); C = CaO, S = SiO<sub>2</sub>, A = Al<sub>2</sub>O<sub>3</sub> and H = H<sub>2</sub>O, ex.: calcium silicate hydrate = CSH)

Clay	CaO (%)	Curing condition	Water condition	Cementitious products	Reference
5 pure minerals	2 ~ 20	60°C, 3/6/30 d	OWC	CSH	Eades and Grim (1960)
3 pure minerals	29, 80	60/45°C; 55/60 d	57%/91%	CSH, C <sub>3</sub> AH <sub>6</sub> , Ca(OH) <sub>2</sub> / CSH, C <sub>4</sub> AH <sub>13</sub>	Diamond <i>et al.</i> (1964)
Lateric clay	5	RT, 90 d	29%	C <sub>3</sub> AH <sub>11</sub> , CaCO <sub>3</sub> , C <sub>3</sub> AH <sub>6</sub> , CASH, CSH	Rossi <i>et al.</i> (1983)
Buckingham soil	4	23°C; 100% RH; 10/100 d	48%	Larger lumps by flocculation (10 days); CASH and CSH (100 days)	Locat <i>et al.</i> , (1990)
Louisville clay	0~10	80/100 d	122% ~650%	No cementitious products for 2% CaO; CSH for 10% CaO	Locat <i>et al.</i> (1996)
Kaolinite	6	RT; 2~ 140 d	-	C <sub>2</sub> ASH <sub>8</sub> (over 21d)	Wild <i>et al.</i> (1993)
A: Kaolinite; B: Montmorillonite	2, 4, 6, 8, 10	20°C; 365 d	A: 29.5%; B: 20%	A: CSH, C <sub>3</sub> S <sub>2</sub> H <sub>3</sub> , C <sub>4</sub> AH <sub>13</sub> , CAH <sub>10</sub> , C <sub>3</sub> AH <sub>11</sub> ; B: CaCO <sub>3</sub> , CSH and (C <sub>4</sub> AH <sub>13</sub> or C <sub>3</sub> AH <sub>10</sub> )	Bell (1996)
Marine clay	-	RT; 2/7/15/30/45d	-	CSH and CAH	Rajasekaran and Rao (1997)
Ariake clay	5, 10, 20	20°C; RH 90%; 7/28 d	185%	CSH, CAH	Onitsuka <i>et al.</i> (2001)
Clay Foca	10	RH 100%; 7 d	32%	CASH	Khattab (2002)
Jossigny silt	1, 3	20°C; 25 d	21%/23%	CaCO <sub>3</sub> , CSH	Le Runigo (2008)
Lateritic gravels mixtures	0 ~12	RT; 30 d	30%	Ca(OH) <sub>2</sub> , CaCO <sub>3</sub> , CSH (6% CaO)	Millogo <i>et al.</i> (2008)
Kaolinite	60	175°C; 1 d	209%	Ca(OH) <sub>2</sub> , CSH(gel), Tobermorite, hydrogrenat	Rios <i>et al.</i> (2009)
Kaolinite; bentonite	2, 5, 10	20/50°C; 2/510 d	OWC	Kaolinite-lime: C <sub>3</sub> AH <sub>6</sub> , C <sub>4</sub> ACH <sub>11</sub> C <sub>4</sub> AH <sub>13</sub> , C-S-H, CaCO <sub>3</sub>	Maubec (2010)
Manois Argillite	4	20/60°C; 7/90 d	OWC (25%)	CSH, CaCO <sub>3</sub> , Ca(OH) <sub>2</sub>	Deneele <i>et al.</i> (2010)

For lime treated fine-grained soils, as shown in Table 1-2, the main cementitious products are of various forms of  $C_xA_yH_z$ ,  $C_xS_yH_z$ ,  $C_xA_yS_zH_m$ . As stated by Yong and Ouhadi (2007), those cementing agents are CSH  $\{3CaO.2SiO_2.3H_2O\}$  and CAH  $\{3CaO.2Al_2O_3.Ca(OH)_2.12H_2O\}$ . The carbonation product ( $CaCO_3$ ) is not a stable cementitious product as mentioned in several studies (Rossi *et al.*, 1983; Bell, 1996; Le Runigo, 2008; Millogo *et al.*, 2008; Maubec, 2010; Deneele *et al.*, 2010). In addition, Maubec, (2010) identified the product  $C_4ACH_{11}$  in lime treated kaolinite and calcium bentonite. Rogers and Glendinning (2000) detected the presence of aluminium, silicon, and calcium in lime treated clays after 300-day curing using atomic absorption spectroscopy. Cai *et al.* (2006) observed that lime stabilization greatly changes soil microstructure and forms the cementitious gel. Normally, the cementitious products start to be produced after a certain period. Locat *et al.* (1990) reported that for the 4% lime treated Buckingham soil, cementitious products are produced only after 10 days. In addition, the cementitious products occur earlier in case of higher dosages (Locat *et al.*, 1996). This is consistent with the minimum lime content for stabilization as aforementioned in section 1.1.3.2.

These reaction products bind the soil grains together and thereby strengthen the soil (Onitsuka *et al.*, 2001; Nalbantoglu and Gucbilmez, 2001; Mathew and Rao, 1997). Based on the SEM examination, Kavak and Akyarh (2007) reported that the silica and aluminium minerals are dissolved as a result of lime-water reactions. The soil microstructure changes from a particle-based form to a more integrated complex with formation of bonding or chains between grains.

For cement treated fine-grained soils, as shown in Table 1-3, many studies showed that the strength development for lime and cement stabilized clays are mainly through the formation of cementing products (Bergado *et al.*, 1996; Schaefer *et al.*, 1997; Chew *et al.*, 2004; Kawamura and Dimond, 1975; Kamon and Nontananandh, 1991; Rajasekaran *et al.*, 1997; Onitsuka *et al.*, 2001). According to Bergado *et al.* (1996) and Schaefer *et al.* (1997), the primary cementitious materials are formed by hydration reaction and are comprised of hydrated calcium silicates ( $C_2SH_x$ ,  $C_3S_2H_x$ ), calcium aluminates ( $C_3AH_x$ ,  $C_4AH_x$ ) and hydrated lime  $Ca(OH)_2$ . Chew *et al.* (2004) also identified the CSH, CASH compounds in their study. Numerous studies confirmed the formation of these cementing products ( $CaO-SiO_2-H_2O$ ,  $CaO-Al_2O_3-H_2O$ ) through x-ray diffraction and scanning electron microscope (SEM) (Kawamura and Dimond, 1975; Kamon and Nontananandh, 1991; Rajasekaran *et al.*, 1997; Onitsuka *et al.*, 2001).

**Table 1-3 Summary of the cementitious products by hydration pozzolanic reactions for cement-clay mix**

(Note: h = hour; d = day; RH = relative humidity; Normal Proctor optimum water content (OWC); C = CaO, S = SiO<sub>2</sub>, A = Al<sub>2</sub>O<sub>3</sub> and H = H<sub>2</sub>O, ex.: calcium silicate hydrate I = CSHI)

Clay	Cement (%)	Water condition	Curing condition	Products	Reference
7 kinds of clays	1 ~ 20	OWC	50/21°C; various curing period	CSHI and crystallized C <sub>4</sub> AH <sub>13</sub>	Croft (1967)
Ariake and Ashikari clay	10, 20, 30	185%	20°C; 90% RH; 7 d	CSH, CAH	Onitsuka <i>et al.</i> (2001)
Clay	10	90%, 40%	22°C; 7/28 d	CSHs, CSH gel and CaCO <sub>3</sub>	Tremblay <i>et al.</i> (2002)
Singapore Marine clay	10, 30, 50	90%, 120%	32°C; 28 d	CSH, CASH	Chew <i>et al.</i> (2004)
Clayey soil	5, 10, 15 (cement kiln dust)	95%OWC	23±1.7°C 96% RH; 28 d	Net-like crystal formation	Solanki <i>et al.</i> (2007)
Silty clay	3, 7, 10; 15, 20, 25, 30; 35, 40, 45	14%, 17%, 20%, 24%	25±2°C; 4h/7d/28d/60d	CSH, CAH, CASH and ettringite	Horpibulsuk <i>et al.</i> (2010)

As for the lime treated soils, the cementitious products induced by cement addition also bind the soil grains and thereby strengthen the soils. By the MIP test, Horpibulsuk *et al.* (2010) observed that the volume of pores smaller than 0.1µm is significantly reduced with cement addition, thus reducing of total pore volume. This indicates that cementitious products enhance the inter-cluster bonding and fill the pore space. Some other studies show that the strength development is related not only to cementation products but also to the microstructure (Onitsuka *et al.* 2001).

By the SEM test, Locat *et al.* (1996) identified the filling of the inter-cluster and interparticle pores by a highly reticulated cementitious products. Rao and Rajasekaran (1996) and Chew *et al.* (2004) reported that the cementitious products CSH and CASH induced by the dissolution of kaolinite and additives, give rise to cementation of the flocculated clay particles, forming clay-cement clusters. The flocculation causes water to be trapped within these clusters. Then the secondary cementitious products induced by the following pozzolanic reactions are deposited on or near the surfaces of the clay clusters. Shi *et al.* (2007) reported also that the cement or lime particles are often deposited on the surface of aggregates by photography observations. Through EDX analysis of lime treated expansive sample, They



also identified that lime concentrates in pores or on the surface of aggregates, with few effects on the inner of aggregates of dimensions ranging from 5 to 10 mm. In addition, it is observed that the calcite  $\text{Ca}^{2+}$  cannot infiltrate into the centre of aggregates even after a period as long as 8 years in the laboratory, but is concentrated on the surface of aggregates; thereby, it has no influence on the intra-aggregate pores. The SEM analysis of Deneele *et al.* (2010) shows the presence of cementitious products linking the soil particles, covering the soil grains and filling the inter-aggregate pores 90 days after the treatment; these secondary cementitious gel consist of Ca, Si, calcium carbonates ( $\text{CaCO}_3$ ) and portlandite ( $\text{Ca}(\text{OH})_2$ ). Therefore, during the curing time, the proportion of large pores (with a radius more than  $100\ \mu\text{m}$ ) of lime treatment soils decreases, and the cementitious products modify the surface state of aggregates. Figure 1-33a and Figure 1-33b present the SEM observation, where we can observe the coating of cementitious products on the surface of the grains. Figure 1-33c shows the photograph of a lime treated soil after 90-day curing and Figure 1-33d presents the cementitious products and the distributions of silica, calcium and potassium. It can be observed that 1) the cementation coats the grains/aggregates; 2) the treatment is not homogeneous and the centre of the aggregate/grain is not affected.

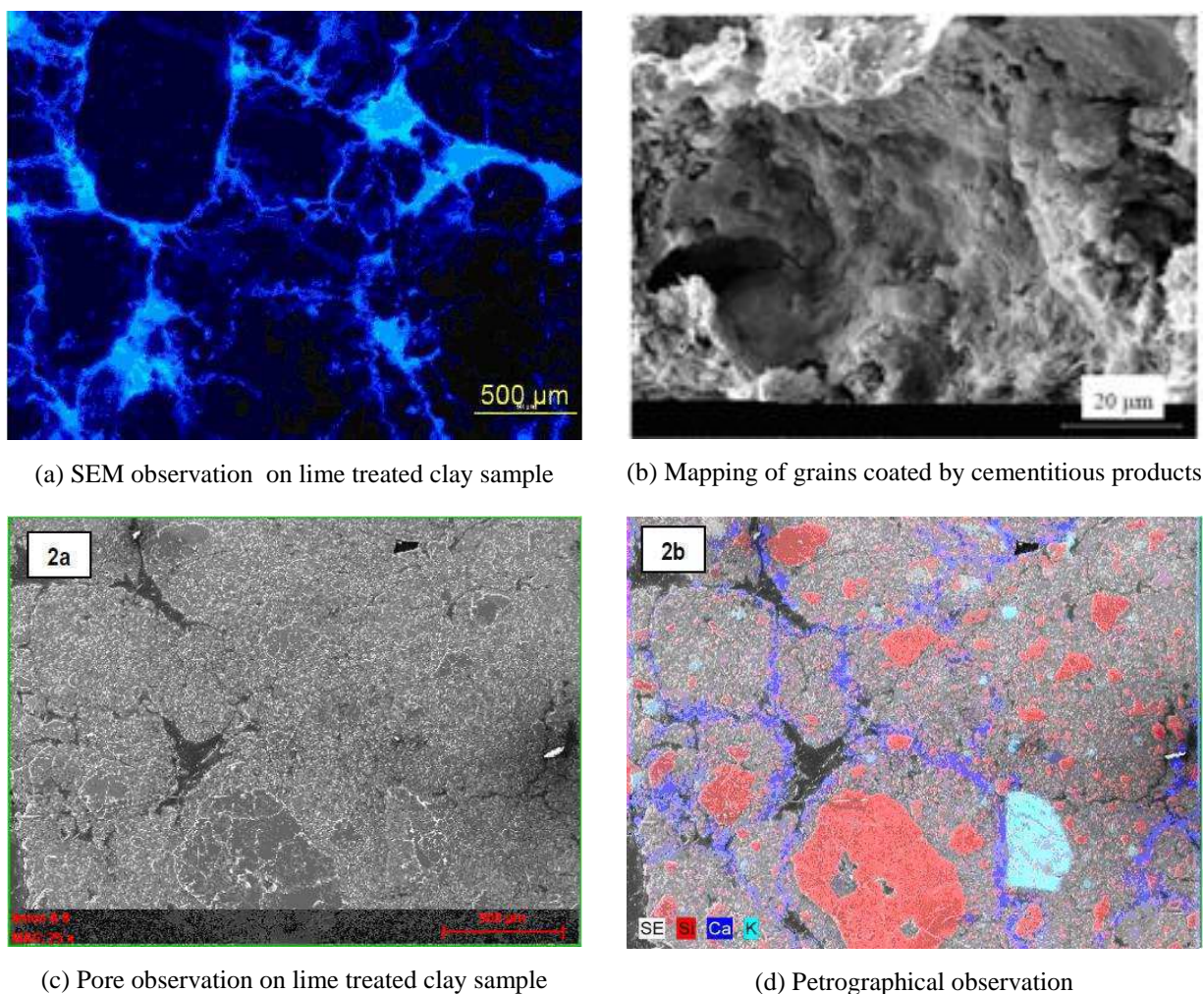


**Figure 1-33** Distribution of cementitious products in lime treated clay (90-day curing) (Deneele *et al.*, 2010)

#### 1.4.4.2. Microstructure analysis by durability tests

Drying-wetting cycles can be destructive for the microstructure of both untreated and treated soils, particularly for the expansive soils. Basma *et al.* (1996) observed the soil particles become almost disoriented after 4-5 cycles for expansive soils and consequently further change in expansibility disappears. Pires *et al.* (2005) evaluated microstructure change of intact samples upon wetting-drying using Gamma ray CT technique, confirming the cyclic wetting/drying effect on both soil porosity and microstructure. Later, Guney *et al.* (2007) observed that the lime stabilized soils are negatively affected by the wetting-drying cycles, suggesting that the lime stabilized expansive clayey soils should not be used in the regions with significant wetting-drying cycles. Figure 1-34 presents the pore distribution curve of a 4% lime treated expansive clay before and after the drying/wetting cycles (Khattab *et al.* 2007), showing a significant increase of pore volume related mainly to the large pores (1-20  $\mu\text{m}$ ). This suggests that the bonding efficacy is reduced by the wetting/drying cycles.

Long-term leaching can modify soil microstructure, leading to loss of the cementitious products (Deneele *et al.*, 2010; Khattab *et al.*, 2007). Figure 1-35 presents the modification of microstructure induced by leaching for 4% lime treated Manois argillite (MA) (Deneele *et al.*, 2010). After 12-month leaching with alkaline fluid circulation, the links between aggregates are visibly destroyed (Figure 1-35a), and the total porosity and porosity of inter-aggregate increases significantly. It is interesting to note that the porosity of intra-aggregate first experiences an increase (6 months, probably due to opening of initial void pores by debonding of aggregates, with no occurrence of cementitious reactions during the previous curing, as shown in Figure 1-7 and Figure 1-34d) followed by a decrease (after 6 months, probably due to the ongoing solidification reactions induced by the saturated  $\text{Ca}(\text{OH})_2$  solution infiltration into the intra-aggregates pores after the breakage of aggregates) (Figure 1-35b). The increase in inter-aggregates porosity indicates the dissolution/loss of cementitious products with leaching.

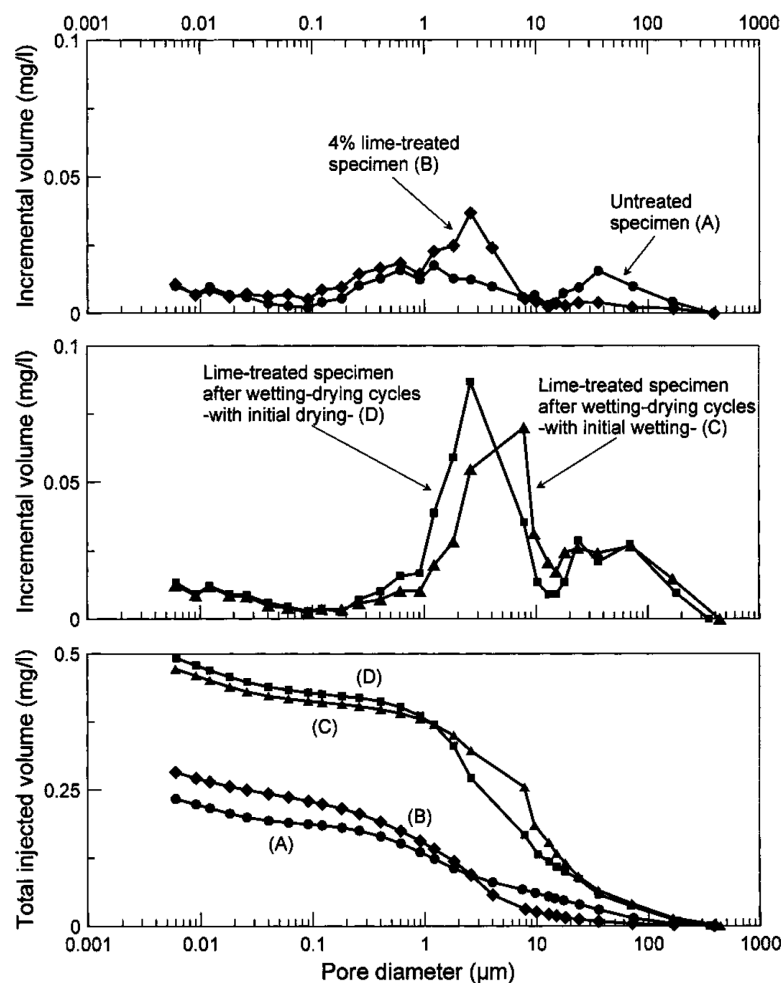
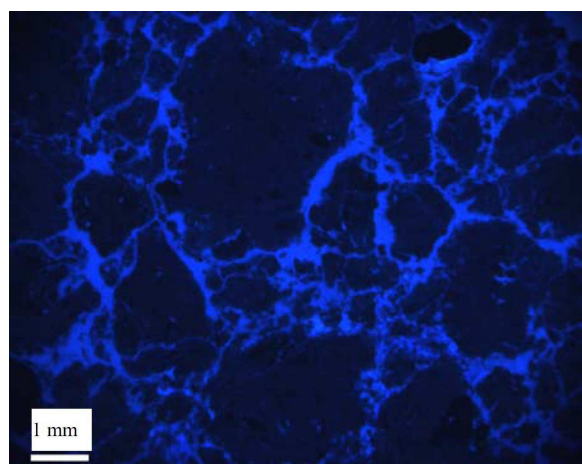
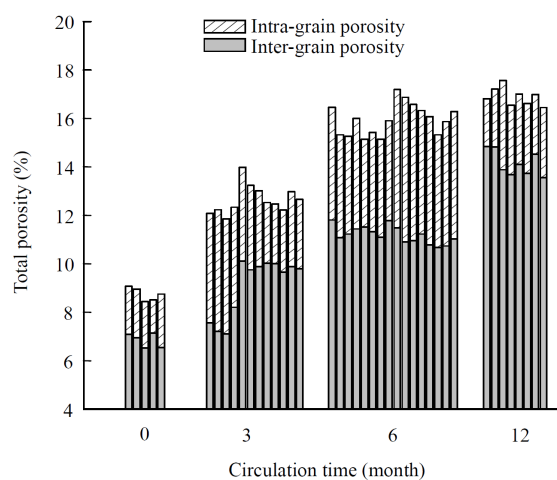


**Figure 1-34 Pore size distribution: A) untreated specimen and B) 4% lime treated specimen (OMC and maximum density); C) 4% lime treated specimen after cyclic wet-dry, starting by wetting; D) 4% lime treated specimen after cyclic wet-dry, starting by drying (Khattab *et al.* 2007)**



(a) Photograph of lime-treated Manois argillite (12-month leaching)



(b) Evolution of the porosity during 12-month leaching

**Figure 1-35 Modification of soil microstructure by leaching (Deneele *et al.*, 2010)**

## 1.5. Correlation between laboratory and field conditions

Several studies (Anderson and Woods, 1975; Arango *et al.*, 1978; Mayne and Rix, 1993; Sully and Campanella, 1995; Viggiani and Atkinson, 1995; Nazarian *et al.*, 1998; Schneider *et al.*, 1999; Szczepanski, 2008) attempted to find out the correlation between the laboratory and field results for untreated soils, and the results are quite promising, albeit the inherent heterogeneity of soils *in-situ* and the sampling perturbation (Table 1-4). Nazarian *et al.* (1998) reported that there is no unique relationship between moduli from laboratory and field tests and that the modulus from laboratory test is normally lower than the *in situ* one. This is in agreement with the observation of Anderson and Woods (1975). Szczepanski (2008) also reported a reasonably good correlation between data from the surface seismic field test and that from the laboratory bender element analysis.

However, for cementitious treated fine-grained soils, even though numerous studies have been performed to analyse the effect of lime and/or cement treatment, almost all works have involved soil specimens prepared in laboratory conditions. Some studies have been performed aiming at correlating the soil strength identified in the laboratory and in field (Bryhn, 1984; Locat *et al.*, 1990; Hopkins, 1996; Puppala *et al.*, 2005; Horpibulsuk *et al.*, 2006; Bozbey and Guler, 2006; Kavak and Akyarh, 2007; Cuisinier and Deneele, 2008a; Snethen *et al.*, 2008).

**Table 1-4 Summary of studies on the correlation between laboratory and field**

Reference	Aim	Method	Material	Observation
Sully and Campanella (1995)	<i>In situ</i> anisotropy	Cross-hole and down-hole	Untreated Clay	The variations of structural anisotropy are the predominant factor controlling the directional shear wave velocities, and almost mask the effect of stress-induced variations.
Nazarian <i>et al.</i> (1998)	Relating laboratory and field moduli	Resilient modulus. Field test by falling weight deflectometer and seismic pavement analyzer tests	Untreated 4 soils: limestone; caliche; iron-ore; sand and gravel etc.	The laboratory moduli are normally lower than the <i>in situ</i> values.
Schneider <i>et al.</i> (1999)	Laboratory/field measurements	$G_{max}$ by resonant column tests in the laboratory; and by seismic piezocones, seismic flat dilatometers, SASW and crosshole tests in field	Untreated residual soils	Good agreement between field and laboratory result
Szczepanski (2008)	Comparisons of $G_{max}$ between <i>in situ</i> and laboratory	Surface waves: SASW, CSWS; Seismic CPT and Seismic DMT; Bender element	Untreated clay, sand (river valley area)	There is a reasonably good correlation between data of the surface seismic field test and laboratory BES analysis.
Puppala <i>et al.</i> (2005)	Effectiveness of deep mixing technology for treated soil columns	Comparisons of $G_{max}$ and strength of soil prepared in laboratory and sampled from field; $G_{max}$ using Bender Elements	Cement and/or lime treated expansive clay	$G_{max, field} / G_{max, lab} = 0.43$ to $0.67$ and $0.56$ to $0.65$ (2 sites); strength ratio ( $q_{ucs, field} / q_{ucs, lab}$ ) = $0.67$ to $0.70$ and $0.83$ to $0.86$ .
Horpibulsuk <i>et al.</i> (2006)	Comparisons of strength UCS of laboratory and field	A phenomenological model to assess the laboratory data and compared to field data.	Cement treated low plasticity and coarse-grained soils	Strength in field is 0.5-1.0 times the value from laboratory test.
Bozbey and Guler (2006)	Feasibility of using a silty soil as landfill liner material	Hydraulic conductivity experiment at both laboratory and <i>in situ</i> scale. Field tests by sealed double ring infiltrometers (SDRI)	Lime-treated silty soil and pure silty silt	Hydraulic conductivity of specimens prepared in the laboratory is one order of magnitude lower than that of undisturbed samples taken from the field
Kavak and Akyarh (2007)	Analysis of the impacts of lime stabilization on road construction	CBR tests for both laboratory and field cured samples (28-day)	Lime treated clay soils	In the laboratory: CBR value increases by 16-21 times; in field: it increases only by 2 times.
Cuisinier and Deneele (2008a)	Comparisons of curing in laboratory and field	Suction-controlled oedometer tests for both <i>in situ</i> and laboratory prepared soils	3-year cured lime treated cores from a n embankment and same soils/treatment in laboratory	Swelling potential (in field) > Swelling potential (in the laboratory); but swelling potential (treated soils in field) > swelling potential (untreated soils).
Snethen <i>et al.</i> (2008)	Rate and magnitude of strength development	Laboratory measuring UCS and $M_R$ for both laboratory mixed and field mixed treated soils and untreated soils.	Several cementitious additives treated subgrade soils	UCS (in field)/UCS (in the laboratory) = 50%; $M_R$ (in field) / $M_R$ (in the laboratory) = 90%; increase rate: field < laboratory.

Quality assessments showed that the treatment in field, due to large area of treatment, often tends to give lower performance when compared with the laboratory condition. Locat *et al.* (1990) stated that the use of laboratory results for selecting field design parameters is quite irrelevant. A few data are available about the field strength values of stabilized clays. Bryhn *et al.* (1984) have found that, over a period of about 30 days, only half of the laboratory strength is obtained in the field for treated clays. Puppala *et al.* (2005) determined the  $G_{\max}$  of lime-cement treated expansive clays in the laboratory, and they compared the results obtained with that obtained in field. They observed that the ratio  $G_{\max, \text{field}}/G_{\max, \text{lab}}$  for two tested sites varies from 0.43 to 0.67 and 0.56 to 0.65, respectively. Further, the strength ratio ( $q_{\text{ucs, field}}/q_{\text{ucs, lab}}$ ) for these two sites varies from 0.67 to 0.70 and 0.83 to 0.86, respectively. This indicates that the stiffness is 40% lower and the strength is 20% to 30% lower for the field treatment. As a result of these variations, reduced strength and stiffness are recommended in the numerical analyses. Horpibulsuk *et al.* (2006) also reported that the field strength is lower than the laboratory one due to the heterogeneity of the soil-cement mixture, and the difference in compaction method and curing condition. Thereby, the field roller-compacted strength is 0.5-1.0 times the laboratory strength for the same cement content, water content and dry unit weight. Bozbey & Guler (2006) investigated the feasibility of using a lime-treated silty soil as landfill liner material by conducting tests at both laboratory and field scales. They found that the hydraulic conductivity measured on the specimens prepared in the laboratory is one order of magnitude lower than that of undisturbed samples taken from the field. Kavak and Akyarh (2007) investigated the improvement of road by lime treatment based on both the laboratory and field CBR tests. They found that the soaked CBR values obtained in the laboratory increase significantly (by 16-21 times) 28 days after the treatment, while that obtained from the field CBR tests increases slightly (by 2 times). Snethen *et al.* (2008) performed both UCS and  $M_R$  tests in both laboratory and field on mixed samples, and the results show that the UCS and  $M_R$  values for field mixed samples are 50% to 90% of the laboratory mixed samples. Generally, the higher the PI of the soils the greater the difference between field and laboratory conditions. No matter laboratory parameters measured by UCS and  $M_R$  or field parameters such as DCI (Dynamic Cone Penetrometer) and PTR (PANDA Penetrometer), typically 70% or more of the strength and structural improvement occurs in 7 days. Field measured parameters exhibit lower rates of improvement as compared to laboratory values. Further, Cuisinier and Deneele (2008a) performed suction-controlled oedometer tests on soil samples taken from an embankment 3 years after the construction. They also performed the same tests on untreated soil and treated

specimens prepared in the laboratory. The results show that the swelling potential of the lime-treated samples taken from the field is significantly larger than that prepared in the laboratory but still remains lower than that of the untreated samples. They attributed this loss of stabilization efficiency in field condition to the effects of drying-wetting cycles related to climatic changes. Many studies aforementioned show that the climatic changes can greatly alter the hydromechanical behaviour of treated soils; and finally the treated soils may behaves as the untreated soils (Lorenzo and Bergado, 2004).

As a conclusion, although considerable studies claim that the laboratory results usually show better soil properties, the correlation between laboratory and field cannot be made easily. The quite large difference in aggregate size between laboratory and field conditions might be the main factor causing this difficulty. Based on this idea, Tang *et al.* (2011) studied the aggregate size effect on the stiffness of lime treated Tour silt in the laboratory. The results show clearly that due to the aggregate size effect the laboratory results cannot be used to design and guide the field operation.

## 1.6. Conclusions

This chapter introduces the cementitious treatment techniques used in the earthwork engineering for improving the soils' strength, stiffness, stability and durability, including the treatment methods, the compaction methods in the laboratory and in field. The fundamental mechanisms of cementitious treatment are also introduced, including the physical/chemical reactions and classic physical microstructure changes. The chemical reaction products and the distribution of these cementitious products in the lime/cement treated soils are depicted, together with different factors involved in these mechanisms. The experimental techniques or tests are presented, permitting to evaluate the strength/stiffness, stability, durability behaviour of cementitious treated soils. The hydro-mechanical behaviour of the treated soils is presented at both macro- and micro- scales. Finally, different studies aiming at correlating the laboratory result to the field one are summarised.

One of the main reasons responsible for the difference between the laboratory and field could be the difference in aggregates size. Indeed, prior to compaction in the laboratory, the soil is usually sieved at a few millimetres and then mixed with additives. On the contrary, in the field, the dimension of clay clods may reach several centimetres before the treatment. From the microstructure analysis of cementitious treated fine-grain soils, we know that the

cementitious products are just on the surface of soil grains. These products bond the grains together, thus increasing hydro-mechanical behaviour of soils. According to the durability tests such as the wetting-drying tests, long-term leaching and soaking tests, the treated soils will lose gradually their cementitious products (by leaching for example) and the efficacy of these cementitious products is decreasing (destruction of bonds by wetting-drying cycles and breakage of soil grains by freezing/thawing effect for example). Thus, over time, the treated soils present more and more properties of natural soils and finally it is probable that the treated soils behave as the untreated soils.



## Chapter 2. Materials and methods

### 2.1. Materials

#### 2.1.1. Soils

Two soils have been studied, one silt and one clay; both were used for the construction of the experimental embankment at Héricourt (70), France, within the TerDOUEST Project.

Table 2-1 shows the main geotechnical properties of the two soils, including the grain size (NF P 94-056 and NF P 94-057), the specific gravity (NF P 94-054), the VBS value (NF P 94-068), the CaCO<sub>3</sub> content (ASTM D4373-02:2007), the Atterberg limits (NF P 94-051), the compaction characteristics (NF P 94-093), etc. The silt studied has a clay fraction (< 2 μm) around 27%, a liquid limit of 40% and a plasticity index of 18.3%. The clay has a clay fraction (< 2 μm) more than 75% and a plasticity index as high as 45%, indicating a very plastic nature and a high sensitivity to moisture changes. According to the French/European standard NF EN P 11-300, these soils are classified into A2 and A4, respectively.

**Table 2-1 Geotechnical properties of the soils studied**

<b>Property</b>	<b>Silt</b>	<b>Clay</b>
Specific gravity, $G_s$	2.70	2.74
Liquid limit, $w_L$ (%)	40	79
Plastic limit, $w_p$ (%)	22	34
Plasticity Index, $I_p$ (%)	18	45
VBS (g/100g)	2.19	5.20
CaCO <sub>3</sub> content (%)	1.4	1.9
Optimum moisture content	17.9	26.4
Maximum dry unit mass	1.76	1.50
Sand (0.06 ~ 2 mm) (%)	38	10
Gravel (2 ~ 5mm) (%)	5	-
Silt/clay ( $\leq$ 0.01 mm) (%)	57	90
Clay (< 2 μm) (%)	27	76

### 2.1.2. Lime for treatment

The lime used in this study was supplied by the Lhoist Company. The main characteristics of this lime are presented in Table 2-2. Its chemical composition indicates a high purity with a content of CaO as high as 97.3%, and a very small quantity lost when burnt (2.4%). Note that the sieves for aggregate size analysis were chosen following the standards EN 459-2 and EN 14227-11: 2006.

**Table 2-2 Characteristics of the quicklime (www.lhoist.com)**

<b>Chemical analysis</b>	
CaO (%)	97.30
CaO + MgO (%)	98.26
MgO (%)	0.96
CO <sub>2</sub> (%)	0.25
Loss of mass when burnt (%)	2.4
Infected maximum temperature (°C)	76.7
Reactivity ratio, t <sub>60</sub> (minute)	4.5
SO <sub>3</sub> (%)	0.06
Free CaO (%)	97.1
<b>Aggregate size analysis</b>	
Passing through 80 µm (%)	82.7
Passing through 200 µm (%)	95.2
Passing through 2 mm (%)	100.0

### 2.1.3. Cement

The cement used in this study is CEMII 42.5, provided by the Cimbeton Company. It is the same cement which was used in the experimental embankment of TerDouest.

According to the European and French standards (NF EN 197-1/A1, CE/CE+ü, NF P15-318, CE+NF, this cement is classified into CEM II / A- LL 42.5 N CE CP2 NF). Table

2-3 presents its main technical characteristics provided by Altkirch Holcim France. We observe that this cement mainly contains alite  $C_3S$  (63.5%), but it is also strongly aluminous with significant quantities of  $C_3A$  (8.2%) and  $C_4AF$  (11%).

Table 2-3 Main characteristics of cement-CEM II

<b>Nominal composition (%)</b>			
<b><u>Composition</u></b>		<b><u>Setting regulator</u></b>	
Clinker (K).....	83	Gypsum (CaSO <sub>4</sub> ).....	3.7
Limestone (L or LL).....	14	Other calcium sulfate.....	2.0
Secondary constituents.....	3	<b><u>Addition</u></b>	
		Sulfate ferrous.....	0.50
		Grinding agent (CXN <sub>2</sub> ).....	0.03
<b>Compressive strength (MPa)</b>			
1 day.....	<b>16</b>	2 days.....	<b>31</b>
		7 days.....	<b>46</b>
		28 days.....	<b>55</b>
<b>Physical characterisation</b>			
<b><u>Powder</u></b>		<b><u>Pure paste</u></b>	
Bulk density (Mg/m <sup>3</sup> ).....	3.07	Water requirement (%).....	27
Surface mass density (m <sup>2</sup> /g).....	0.4450	Stability (mm).....	0.2
Clearness index.....	65	Initial setting (min).....	190
<b>Chemical characterisation (%)</b>			
<b><u>Composition</u></b>			
Calcium oxide (CaO).....	61.5	Silicon dioxide (SiO <sub>2</sub> ).....	18.5
PAF.....	6.2	Aluminum oxide (Al <sub>2</sub> O <sub>3</sub> ).....	4.6
Ferric oxide (Fe <sub>2</sub> O <sub>3</sub> ).....	3.1	Sulfate trioxide (SO <sub>3</sub> ).....	3.2
CO <sub>2</sub> .....	5.2	Magnesium oxide (MgO).....	1.4
INS.....	1.3	Potassium oxide (K <sub>2</sub> O).....	0.91
Na <sub>2</sub> O.....	0.6	Free lime (CaO <sub>free</sub> ).....	0.5
Sodium oxide (Na <sub>2</sub> O).....	0.12	Cl-.....	0.04
<b><u>Potential composition of clinker</u></b>			
C <sub>3</sub> A.....	8.2	C <sub>3</sub> S.....	63.5
		C <sub>4</sub> AF.....	11

## 2.2. Sample preparation in the laboratory

### 2.2.1. Soils preparation

The silty soil was first air-dried and ground. Two sieving methods were then applied.

- **Method 1:** The total quantity of soil was first ground, passed through 5.0 mm sieve. The soil was then well mixed and successively passed through the target sieve sizes 2.0 mm, 1.0 mm and 0.4 mm.

- **Method 2:** The air-dried soil was first ground and passed through one of the four target sieve sizes ( $D_{\max} = 0.4, 1.0, 2.0$  and  $5.0$  mm). The soil aggregates which did not pass through the sieve were ground again. The procedure was repeated until all soil aggregates passed through the sieve except some large stones. Note that this method was also applied by Tang *et al.*, (2011).

After sieving, each sub-series of soil was well mixed and the aggregate size distribution determined by dry sieving. Figure 2-1 shows the grading curves of the soil sub-series, obtained with the two preparation methods. The figure also shows the curve obtained by the wet sieving method (NF P 94-056) and the hydrometer method (NF P 94-057). Note that the hydrometer method is suitable for the portion of soil passing through  $80 \mu\text{m}$  sieve, while the wetting sieving (NF P 94-056) is applicable for particles larger than  $80 \mu\text{m}$ .

Comparison of the curves obtained with the dry sieving method (aggregate size distribution) and wet sieving method (grain size distribution obtained following the standards) shows that the wet sieving method preserves the portion of soil grains larger than 5 mm, while dry sieving preparation crushed all this portion.

Several other points can be observed: 1) the sub-series obtained by the two methods share the same maximum aggregate sizes; 2)  $D_{\max} = 0.4$  powders show similar aggregate size distribution curve with the two methods; 3) the other sub-series ( $D_{\max} = 1.0, 2.0$  and  $5.0$  mm) obtained by method 2 have more fine aggregates ( $<80 \mu\text{m}$ ) than those by method 1; 4) method 1 results in a relatively uniform aggregates size while method 2 gives a well graded aggregates size.

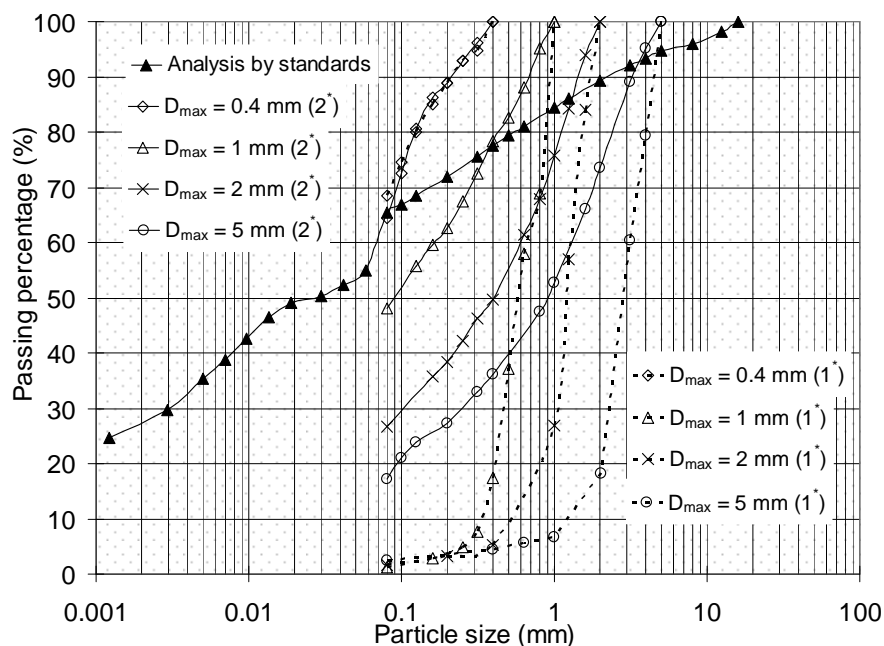


Figure 2-1 Grain and aggregate size distribution of silt powders prepared by the two methods (Note: 1\*, 2\* mean method 1 and 2, respectively)

From the mineral composition point of view, the procedure of method 2 allows preparing the soils with the same mineral composition, whereas method 1 may slightly change the mineral composition of each sub-series. Indeed, in method 1 the clay fraction in coarse sub-series is relatively smaller, leading to a lower content of clay minerals. Table 2-4 presents the fines (<63  $\mu\text{m}$ ), sand (0.063 ~ 2 mm) and gravel size (> 2 mm) fractions of the representative sub-series samples obtained by wet sieving method (XP CEN ISO/TS 17892-4: 2005). These compositions may give an estimation of change in mineral composition induced by method 1. It shows that the sub-series of ' $D_{\text{max}} = 1 / 2 / 5 \text{ mm}$ ' prepared by method 1 have indeed a lower fine fractions, thus slightly coarser than those by method 2, while ' $D_{\text{max}} = 0.4 \text{ mm}$ ' is finer with method 1.

Table 2-4 Comparison of the fines, sand, and gravel contents between method 1 and method 2 by wet sieving method

$D_{\text{max}}$ (mm)	Fines (%) (<0.063 mm)		Sand (%) (0.063 ~ 2 mm)		Gravel (%) (> 2 mm)	
	Method 1	Method 2	Method 1	Method 2	Method 1	Method 2
5	61.7	68.1	21.5	25.5	16.8	6.4
2	65.8	71.9	34.2	28.1	0.0	0.0
1	66.7	73.8	33.3	26.2	0.0	0.0
0.4	79.7	74.9	20.3	25.1	0.0	0.0

Figure 2-2 allows a visual observation of the difference between the two preparation methods: method 1 produces a uniform grain distribution, while method 2 produces a relatively well graded soil.



(a) Silt,  $D_{\max} = 5$  mm by method 1

(b) Silt,  $D_{\max} = 5$  mm by method 2

**Figure 2-2  $D_{\max} = 5$  mm silt powders prepared by method 1 and 2**

In order to avoid any effects related to the mineralogy changes, the clay was prepared using method 2 only. As for the silt, each group of the clay was also well mixed after sieving, and then the representative sample was taken for determining the aggregate size distribution by the dry sieving method. Figure 2-3 presents the grading curves of the four soil sub-series by different maximum soil aggregate diameters, together with the curve determined by the wet sieving method according to the standards NF P 94-056 and NF P 94-057.

Several points can be drawn from the comparison between the curves obtained by the dry sieving and wet sieving methods: 1) the maximum grain size by wet sieving is around 1 mm; 2) the dry sieving permits to preserve a portion of soil aggregate larger than 1 mm. 3) the portion of aggregate size larger than 0.4 mm is entirely crushed during the preparation for sub-series ' $D_{\max} = 0.4$  mm'.

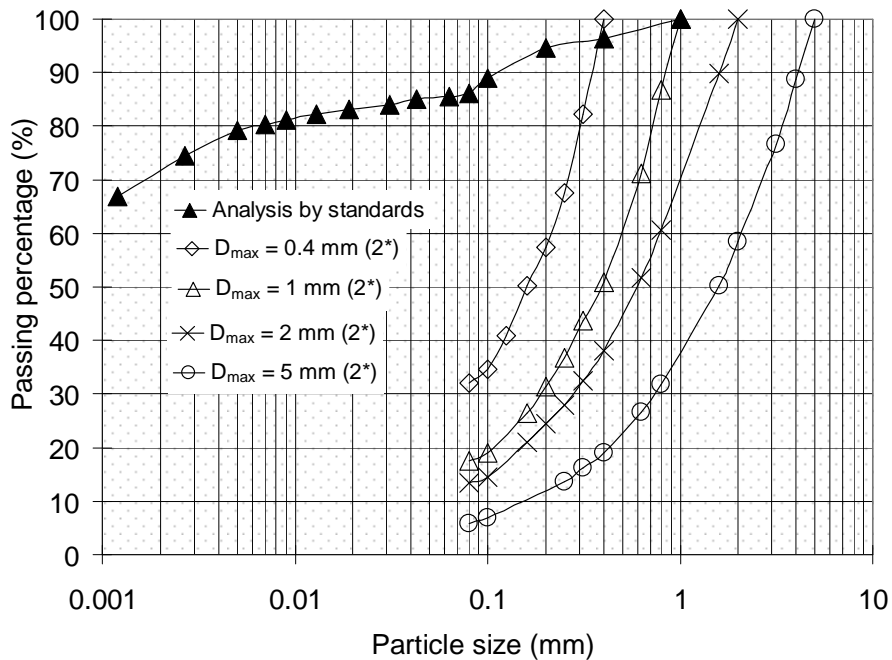
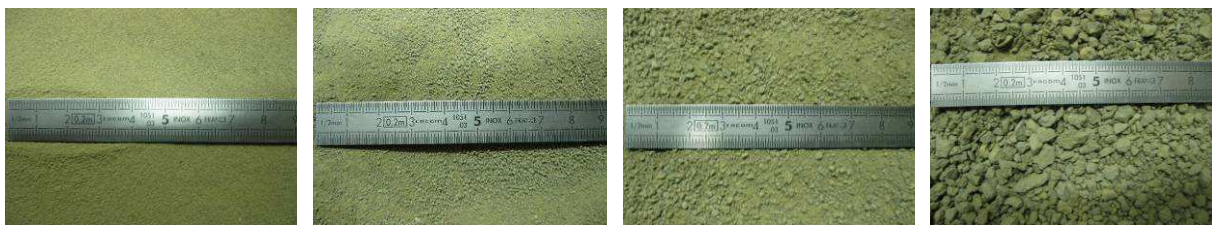


**Figure 2-3 Particle and aggregates size distributions of the clay powders prepared by method 2**

The sub-series of soil powders after grinding and sieving are depicted in Figure 2-4, where the aggregate size difference between the four sub-series of clay can be clearly appreciated.



(a)  $D_{max} = 0.4$  mm      (b)  $D_{max} = 1$  mm      (c)  $D_{max} = 2$  mm      (d)  $D_{max} = 5$  mm

**Figure 2-4 Description of the four sub-series of clay powders prepared by method 2**

When the powders were prepared, the soil was humidified by spraying distilled water, in order to reach the target moisture content  $w_i$ . Then, it was sealed in plastic boxes for water content homogenization (during 48 hours for silt and one week for clay).

In order to obtain a homogeneous soil, the humidification was conducted as follows:  
 1) the required quantity of water is calculated; 2) the soil and the corresponding amount of water are divided into several parts, each part being for a layer; 3) the wet soil is hand-mixed;

4) the quantity of wet soil is re-measured, and the water loss by evaporation during the mixing is compensated; 5) the wet soil is well sealed in a plastic box for 48 hours for the silt and one week for the clay.

### 2.2.2. Compaction of specimens

Prior to the preparation of specimens, we need to determine the ‘water content – density’ relationship for the treated soils by performing Normal Standard Proctor tests. Based on the proctor curves obtained, the states of specimens can be defined.

The compaction tests were carried out following the French standard NF P 94-093. First, as indicated in the soil classification NF P 11-300, the test requires soils with grains smaller than 20 mm. Note that in this study, the soils naturally meet this condition (see curves shown in Figure 2-1 and Figure 2-3). Then, the optimum water content ( $w_{OPN}$ ) of each soil was estimated and five soils at water contents around  $w_{OPN}$  were prepared (at least 3 points and at most 4 points between  $0.8 w_{OPN}$  and  $1.2 w_{OPN}$ ). A homogenisation of the wet soil was conducted by sealing it in a box under room temperature ( $20 \pm 1^\circ\text{C}$ ) for 48 hours.

For untreated soils, the compaction by 3 layers was proceeded directly in a normal Proctor mould (25 blows per layer); for treated soils, according to NF EN 14227-10 (for cement), NF EN 14227-11 (for lime), a hand-mixing with additive and 1 hour mellowing were required before compaction, After compaction, the water content  $w_f$  was determined by taking the mean value of three measurements in different positions of the specimen. Figure 2-5 and Figure 2-6 present the Normal Proctor test results for the silt and clay soils, respectively (data provided by LRPC in Rouen for the silt and by LRPC at Autun for the clay).

The treated soil specimens were prepared on both dry side and wet side of optimum, under the same dry density (Table 2-5). The corresponding untreated soils were also prepared at the same dry density and water content ( $w_f$ ). As the  $w_f$  measurement following standard NF 94-093 destroys the soil specimen, to consider the water loss during specimen preparation, we need to estimate the amount of water loss or to determine  $w_i$  before the specimen compaction. The water loss tests will be presented later.



Table 2-5 Specimens of silt and clay for different treatments

Treatment	Silt		Clay	
Property	2% lime	3% cement	4% lime	2% lime + 3% cement
Height (mm)	50	50	50	50
Diameter (mm)	50	50	50	50
Dry density (g/cm <sup>3</sup> )	1.65	1.70	1.35	1.35
Water content, $w_f$ (%)	17 / 21.8	14 / 21	25 / 35	25 / 35
Maximum grain size (mm)	0.4; 1.0; 2.0; 5.0	0.4; 1.0; 2.0; 5.0	0.4; 1.0; 2.0; 5.0	0.4; 1.0; 2.0; 5.0

Figure 2-5 presents the Normal Proctor curves of natural silt, silt treated by 3% cement and silt treated by 2% lime. By comparing the curves of both untreated silt ( $w_{OPN} = 17.9\%$ ,  $\rho_{dOPN} = 1.76 \text{ Mg/m}^3$ ) and 2% lime or 3% cement treated silts, we can observe that the 3% cement treatment does not change the curve significantly ( $w_{OPN} = 17.7\%$ ,  $\rho_{dOPN} = 1.76 \text{ Mg/m}^3$ ). On the contrary, under the treatment of 2% lime, the optimum moisture content of soil increases ( $w_{OPN} = 17.9\%$  to  $20.3\%$ ) and the maximum dry density decreases significantly ( $\rho_{dOPN} = 1.76 \text{ Mg/m}^3$  to  $1.68 \text{ Mg/m}^3$ ).

As shown in Figure 2-5, in order to prepare the 2% lime treated silt, for each sub-series of soil produced by method 1 and method 2 ( $D_{max} = 0.4, 1.0, 2.0$  and  $5.0 \text{ mm}$ ), the soil was humidified to reach the target water contents  $w_i$ , then mixed (with a mellowing period of 1 hour) with 2% lime powder (calculated by dry soil) prior to static compaction at a dry density of  $1.65 \text{ Mg/m}^3$ , and  $w_f = 17\%$  on dry side and  $w_f = 21.8\%$  on the wet side of optimum ( $w_{OPN} = 20.3\%$ ). Then, the untreated specimens were also compacted, at the same water content and dry density, following the same procedure as for 2% lime treated silt.

Figure 2-5 also shows the  $w_f$  and dry density of the cement treatment of specimens (0% and 3% cement): the nominal dry density of  $1.70 \text{ Mg/m}^3$  for both the dry side ( $w_f = 14\%$ ) and wet side ( $w_f = 21\%$ ) of optimum.

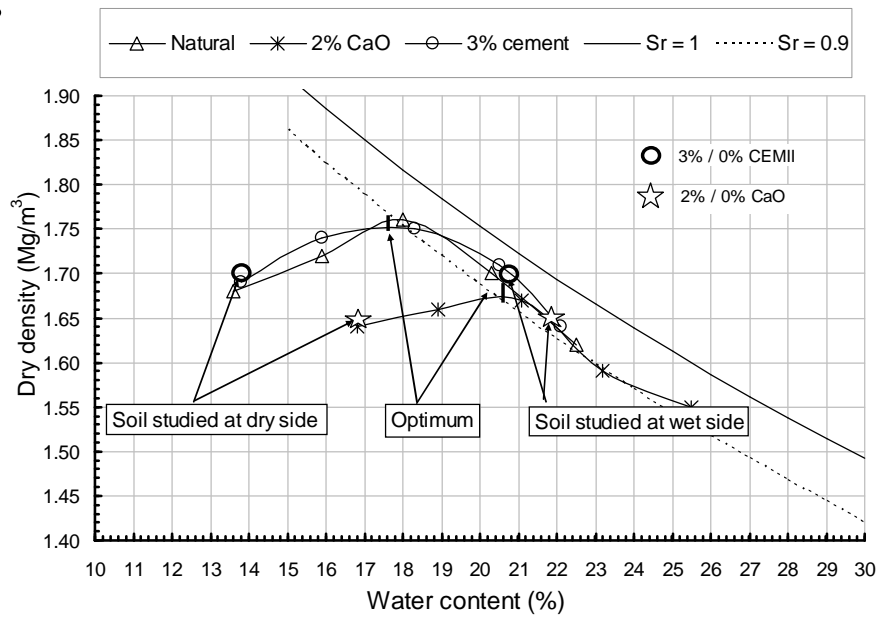


**Figure 2-5 Normal proctor curves of natural silt, silt treated by 2% lime and treated by 3% cement**

Figure 2-6 presents the Normal Proctor curves of natural clay, 2% lime + 3% cement treated clay and 4% lime treated clay. For this plastic clay, it is difficult to determine the optimum water content and the corresponding dry density, as the proctor curves obtained are irregular. By comparing the curves of untreated ( $w_{OPN} = 26.4\%$ ,  $\rho_{dOPN} = 1.50 \text{ Mg/m}^3$ ) with those of treated clays, we can observe that the treatments significantly increase the optimum moisture content ( $w_{OPN} = 32\%$  and  $32.5\%$  for 4% lime and mix treatment, respectively) and reduces the maximum dry density ( $\rho_{dOPN} = 1.30$  and  $1.34 \text{ Mg/m}^3$  for 4% lime and mix treated clay, respectively).

As for the silt specimen preparation, both 4% lime treated and mix 2% lime + 3% cement treated clay specimens were prepared on both dry side and wet side of optimum, at the same dry density (Figure 2-6). The corresponding untreated soils were also prepared, at the same dry density and water content. However, due to the irregular Proctor curves of the clay soils and the small difference of dry density between the two treatments, for both dry side and wet side, it was decided to use, for all the treatments, a unique value of  $w_f$  for each side (dry side  $w_f = 25\%$ ; wet side  $w_f = 35\%$ ) and dry density ( $\rho_d = 1.35 \text{ Mg/m}^3$ ) after treatment.

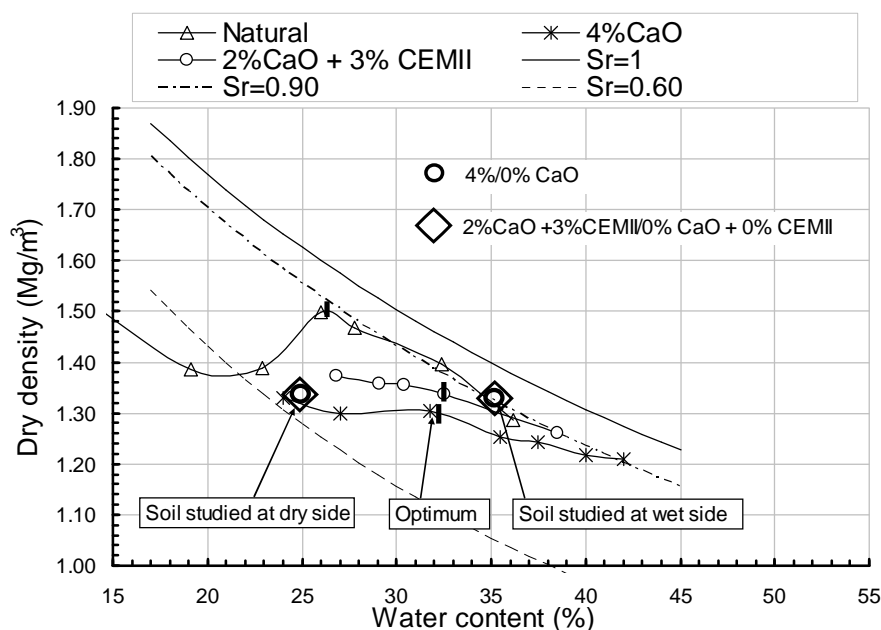


**Figure 2-6 Normal proctor curves of natural clay, clay treated by 4% lime, and treated by 2% lime + 3% cement**

Prior to the compaction of soil specimen, the wet soil at given water content  $w_i$  was mixed with additive for treatment. The quantity of additive was calculated according to the weight of the dry soil (equation 1-2 in chapter 1).

For each specimen, the given quantity of wet soil is equally divided to 6 parts for 6 different layers and put successively in the box, with a given quantity of additive poured uniformly on each layer. Afterwards, two different mixing methods were applied: 1) Method A - mixing with a metal stick; 2) Method B - a simple mixing method consisting in shaking the sealed box containing the soil-additive mix. For method A, the duration is controlled for each sub-series: 20 / 15 / 10 / 7 min of mixing for  $D_{max} = 0.4 / 1 / 2 / 5$  mm respectively, aiming at controlling the aggregate size. For method B, the samples are shaken for 20 minutes for all sub-series.

For the silt, only method B was applied. The aggregates obtained with method 1 after mixing are presented in Figure 2-7 ~ Figure 2-10, involving both dry and wet sides for 2% lime treatment and 3% cement treatment. As the features of soil-additives mixture obtained with method 2 are similar to method 1, the results corresponding to method 2 are not presented.

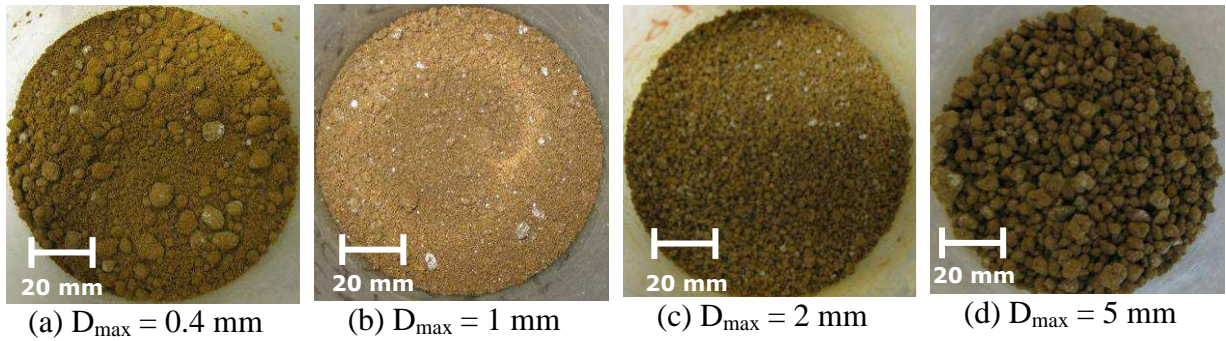


Figure 2-7 Héricourt silt,  $w_f$  of 17%, treated by 2% lime, by mixing method B

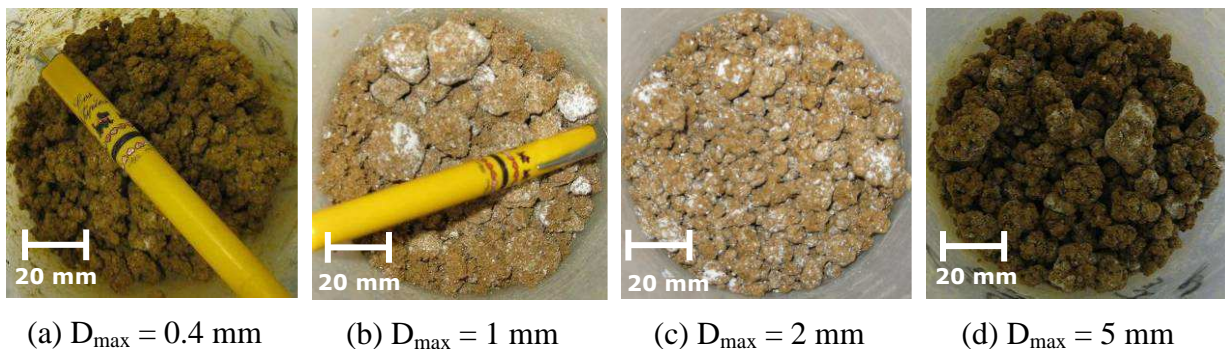


Figure 2-8 Héricourt silt,  $w_f$  of 21%, treated by 2% lime, by mixing method B

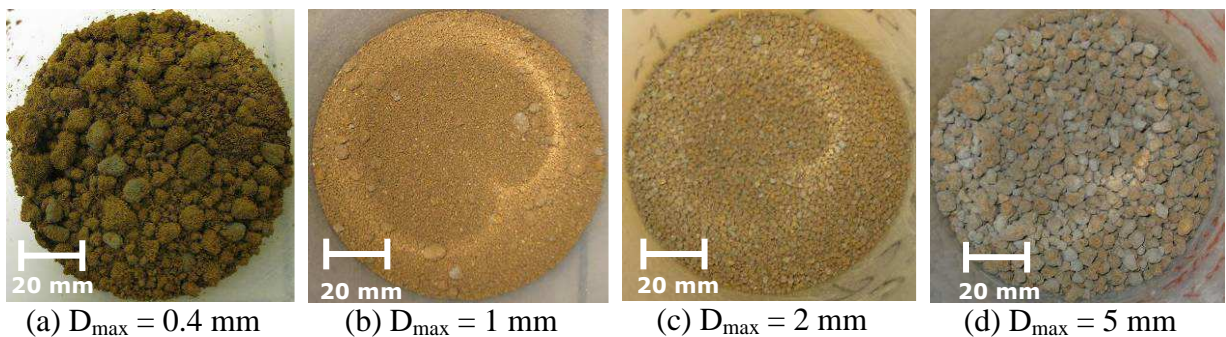


Figure 2-9 Héricourt silt,  $w_f$  of 14%, treated by 3% cement, by mixing method B

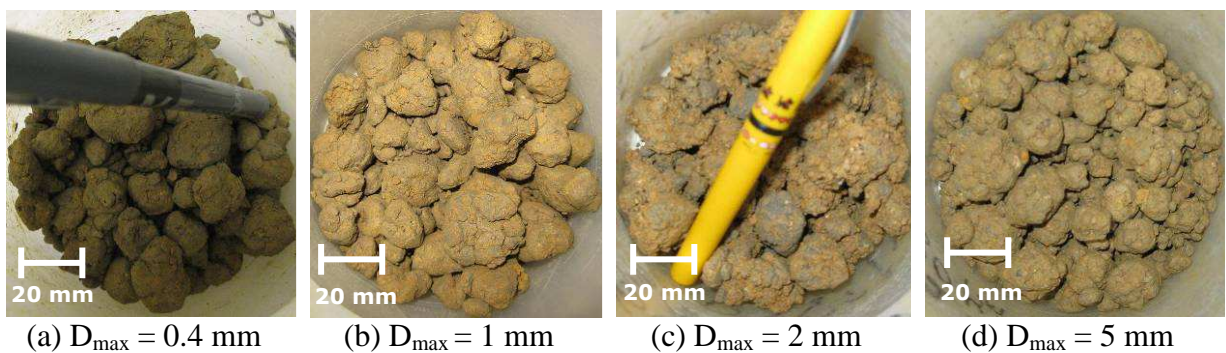


Figure 2-10 Héricourt silt,  $w_f$  of 21%, treated by 3% cement, by mixing method B

For the clay, both mixing method A and B were applied. Figure 2-11 ~ Figure 2-14 present the aggregates by method A and method B. As there is no significant difference between 4% lime and 2% lime + 3% cement treatments, we only show here the case of 4% lime treatment mix.

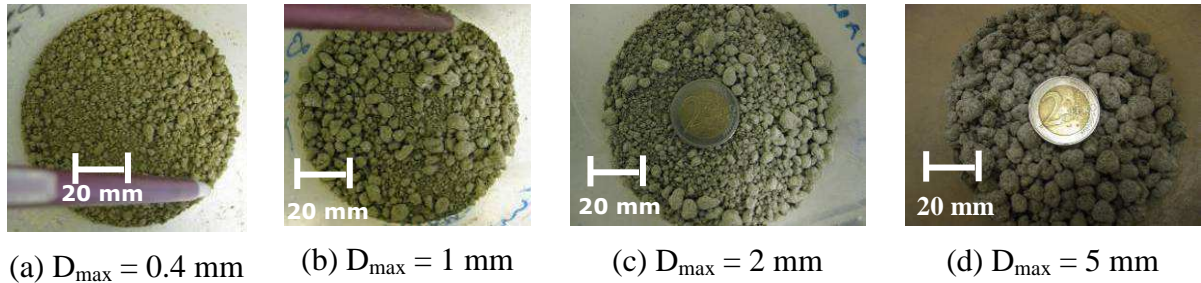


Figure 2-11 Héricourt clay,  $w_f$  of 25% treated by 4% lime, by mixing method A

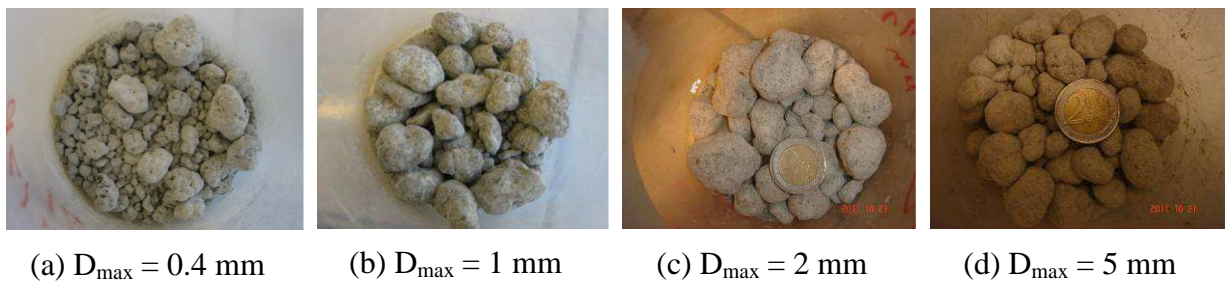


Figure 2-12 Héricourt clay,  $w_f$  of 25% treated by 4% lime, by mixing method B

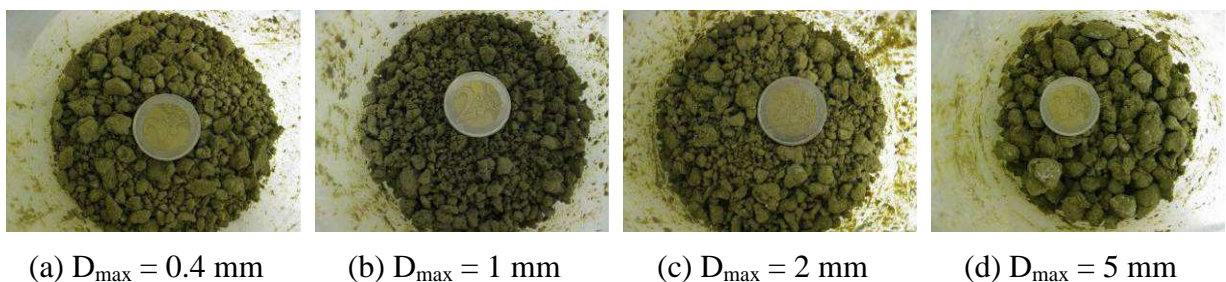


Figure 2-13 Héricourt clay,  $w_f$  of 35%, treated by 4% lime, by mixing method A

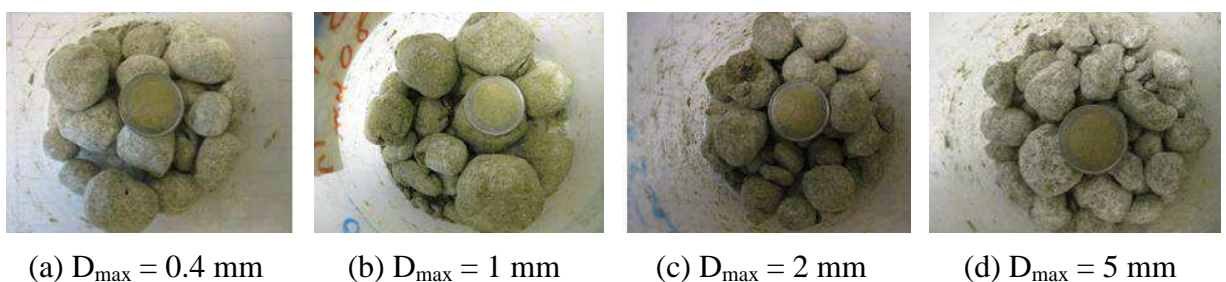
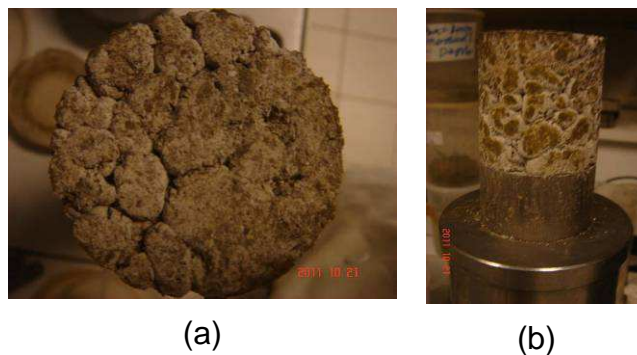


Figure 2-14 Héricourt clay,  $w_f$  of 35%, treated by 4% lime, by mixing method B

Compared to mixing method B (Figure 2-12 and Figure 2-14), mixing method A permits to obtain a relatively more homogenous distribution of additives, for both dry and wet sides (see in Figure 2-11 and Figure 2-13 ). Moreover, the initial aggregates may be totally or partially destroyed. As mentioned before, the main objective of this study is to investigate the effect of aggregate size. It is thereby necessary to have different aggregate sizes after mixing. Note that it is for this purpose that the duration of the mixing operation was specified for each sub-series. It can be seen that the evolution of aggregate size is still clear on the dry side mixed after mixing with method A (see Figure 2-11). On the contrary, the difference in aggregate size is no longer clear on the wet side with the same method because of the effect of water content (see Figure 2-13).

With mixing method B, thanks to the absence of breakage by stick, the initial aggregates are better preserved than with mixing method A, though larger soil blocks are formed. Figure 2-15 presents a dry clay specimen prepared by mixing method B, where newly formed large aggregates can be identified even for the dry side. Note that, using this mixing method, the dry specimens are often broken after compaction. This is probably due to the weakness of the chains formed between the large aggregates with non-hydrated lime as shown in this figure.



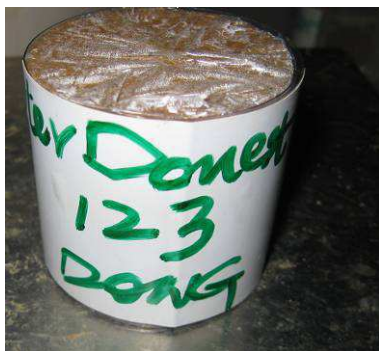
**Figure 2-15 Héricourt clay, initial water content of 25% treated by 4% lime, by mixing method B,  $D_{\max} = 2$  mm, after compaction: (a) face of the specimen; (b) side of the specimen.**

After 1-hour mellowing of the soil-additive mix, the compaction of the specimens began. A ‘Tritest 50 compaction’ machine was used in this test, together with a force transducer (Range 0 ~ 50 KN). This compaction system allows the compaction rate control (0.0001 ~ 5.0 mm/min) and the compaction force/stress control. In order to obtain a homogeneous soil specimen, the compaction was conducted in three layers. The procedure is as follows: 1) grease the mould; 2) pour the given quantity of soil mix for one layer into the

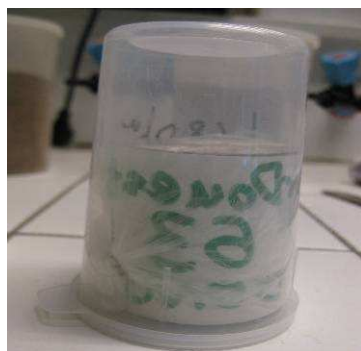
mould; 3) mix the soil-additive aggregates with a metal stick; 4) compact this layer to reach a defined height (marked by a line on the mould); 5) reverse the mould; scarify the surface of this layer and push the soil to leave a space to add another layer of soil mix; 6) repeat the operations above for other layers. Note that the compaction rate adopted was 0.3 mm/min and the final force of each compacted layer was recorded.

After compaction, the soil specimens (with a nominal size: diameter \* height = 50 mm \* 50 mm) were de-moulded and weighed. Immediately, the size of the specimen was measured using a calliper.

Then, the soil specimens were enveloped in a membrane, well wrapped in a plastic film and then put into a plastic bag, in order to prevent any moisture exchange with the atmosphere. Note that the water content was monitored by measuring the soil specimen's weight, omitting the water loss due to chemical reactions in the curing period. During curing, as shown in Figure 2-16, the specimens were confined in hermetic boxes and kept in a chamber at a relative humidity of 100% and a temperature of  $20 \pm 2$  °C.



(a) Enveloped by membrane and wrapped in a film



(b) Sealed in plastic bag and in box



(c) Curing in the chamber with controlled temperature/humidity

**Figure 2-16 Protocol adopted to prevent moisture exchange between soil and atmosphere**

As mentioned before, the specimen preparation is expected to be on the Proctor curves that are different for different treatments, therefore the water content loss test was performed for each treatment to determine  $w_{lost}$ , hence the target  $w_i$ . Furthermore, the water loss induced by hydration reactions, evaporation during mixing and compaction, needs to be determined by tests. In addition, when the saturation exceeds 80%, the loss of water due to spilling over the mould often occurred. The water loss can also be induced during the one-hour mellowing time ( $w_m$ ). The total loss of water content can be determined by measuring

the water content of wet soil before mixing ( $w_i$ ), after mixing and mellowing ( $w_{mix}$ ), and just after compaction ( $w_f$ ).

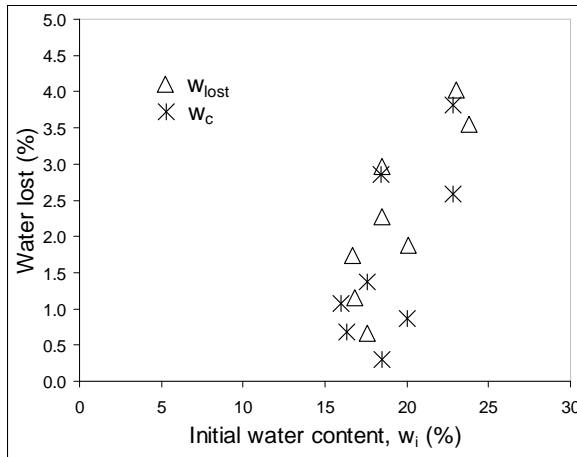
Figure 2-17 shows some specimens after water loss tests. We can see that: 1) for the silt specimens on the dry side, the aggregates size is well defined, while for the wet side the aggregates are merged together; 2) for the clay specimens, both dry and wet sides show large aggregates. Note that only mixing method B was used during the water loss tests for both the silt and clay.



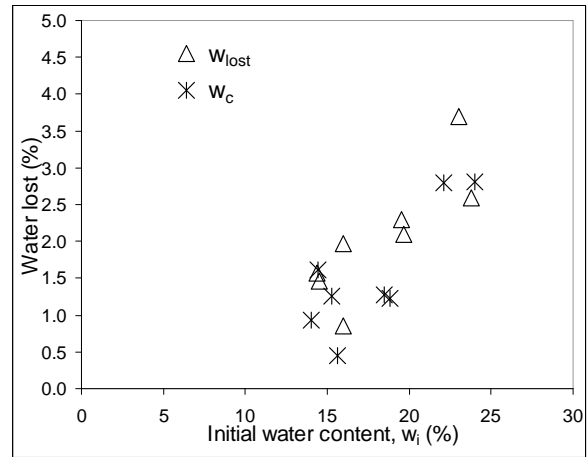
Figure 2-17 Some specimens after water content measurement, during water loss test

The test of water loss was performed in the same fashion as compacting the specimens: 1) different  $w_i$  was firstly estimated (higher than  $w_f$ ) and the quantity of water needed was added to each sub-series powder; 2) then the given quantity of soil was mixed with a additive for each treatment; 3) the water content of the mixture ( $w_{mix}$ ) was measured after one-hour mellowing; 4) the specimen was compacted. After compaction, the water content of the specimen ( $w_f$ ) was measured by oven-drying (105°C) (XP CEN ISO/TS 17892-1). Thereby, the total loss of water ( $w_{lost}$ ) was determined by  $w_{lost} = w_i - w_f$ . The water loss during compaction ( $w_c$ , after mellowing) was determined by  $w_c = w_{mix} - w_f$ , and in turn the part of water loss induced during mellowing ( $w_m$ ) can also be determined by  $w_m = w_i - w_{mix}$ . Figure 2-18 presents the water loss ( $w_{lost}$  and  $w_c$ ) due to the different treatments as a function of the initial water contents ( $w_i$ ). We observe that the loss of water increases almost linearly with the rise of initial water content for all the treatments of both the clay and silt.

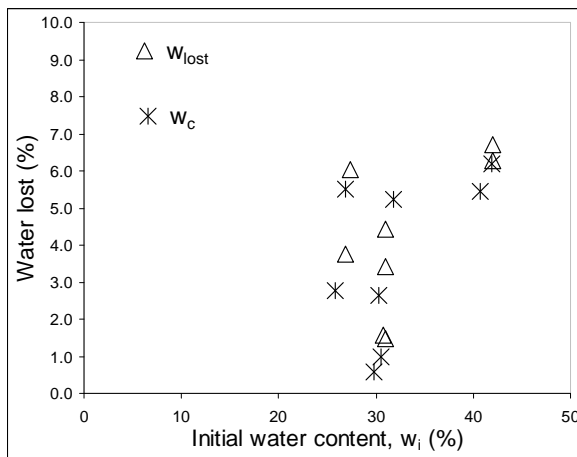




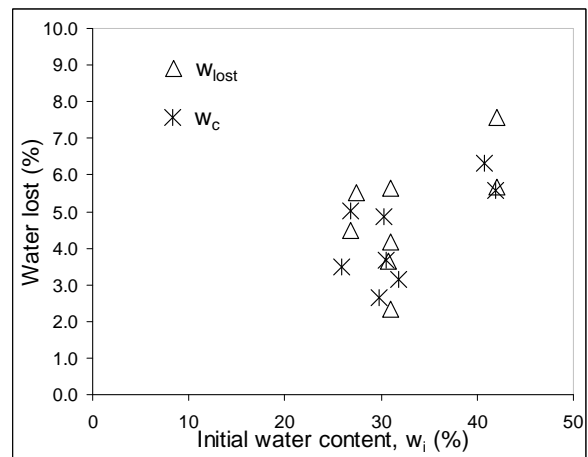
(a) 2% lime treated silt by method 1



(b) 3% cement treated silt by method 1



(c) 4% lime treated clay by method 2



(d) 2% lime + 3% cement treated clay by method 2

**Figure 2-18 Water loss due to different treatments, in function of different initial water contents ( $w_i$ )**

Using a linear relationship between  $w_{lost}$  and  $w_i$ , we can estimate the  $w_{lost}$  for all the treatments of both the silt and clay (see Table 2-6). Mathematically, the  $w_i$  can be back-calculated by the sum of  $w_{lost}$  and  $w_f$  ( $w_i = w_{lost} + w_f$ ): 1) for the 2% lime treated silt, the initial water content ( $w_i$ ) is 19.2% for the dry side and 25.8% for the wet side; 2) for the 3% cement treated, the  $w_i$  is 15.6% for the dry side and 23.6% for the wet side; 3) for the 4% lime treated clay, the  $w_i$  is 28.5% for the dry side and 40.4% for the wet side; 4) for the mix 2% lime plus 3% cement treated clay, the  $w_i$  is 29.3% for the dry side and 41.2% for the wet side.

**Table 2-6 The mean values of  $w_{lost}$  during specimens' preparation using mixing method B**

Position on the Proctor curve	Water loss (%)			
	Silt		Clay	
	2% lime	3% cement	4% lime	2% lime + 3% cement
Dry side	2.2	1.6	3.5	4.3
Wet side	4.0	2.6	5.4	6.2

Figure 2-18 shows clearly that large variation of water loss can be induced with the experimental protocol adopted. Considering this variation, we adopted the following water contents: 1) for the 2% lime treated silt, the  $w_i$  is 19% for the dry side and 25% for the wet side; 2) for the 3% cement treated, the  $w_i$  is 16% for the dry side and 23% for the wet side; 3) for both the 4% lime and 2% lime + 3% cement treated clay, the  $w_i$  is 29% for the dry side and 41% for the wet side.

### 2.2.3. Test program

Table 2-7 shows the tests program with all the specimens prepared (25 cases in total). For each test, three identical specimens are investigated for replicate. This program implies that each maximum soil aggregate size involves two different soils (silt and clay), four treatments, six water contents (on the dry/wet side of optimum), three dry density levels (same density at different sides), two sieving methods (1 and 2) and two mixing methods (A and B). Case 1 ~ case 4 show the 2 % lime treated and untreated silty specimens by sieving method 1 and mixing method B, being compacted on both dry side ( $w = 17\%$ ,  $\rho_d = 1.65 \text{ Mg/m}^3$ ) and wet side ( $w = 22\%$ ,  $\rho_d = 1.65 \text{ Mg/m}^3$ ) of optimum. Case 5 ~ case 8 present the soil specimens by sieving method 2. Case 9 ~ case 16 correspond to the 3% cement treated and untreated silt specimens by both method 1 and method 2. Case 17 ~ case 25 illustrate clay specimens by 4% lime, 2% lime + 3% cement treatments (in Figure 2-6), respectively.

After compaction, several measurements were performed on these specimens in different periods, including: 1) the small strain shear modulus ( $G_{max}$ ) measurement during curing ( $G_{max}$ -time test); 2) the  $G_{max}$  changes induced by wetting/drying cycles (W-D cycles); 3) matrix suction measurement for all the specimens at different states, during the period

when the soil specimen reaches its stability of  $G_{max}$ , and during a drying/wetting cycle (ex. the 3<sup>rd</sup> drying and 4<sup>th</sup> wetting cycles for the clay). As shown in Table 2-7,  $G_{max}$ - time test and matrix suction measurement were performed on all the specimens (case 1 ~ case 25). However, no W-D cycles test was carried out on the silt specimens prepared by method 2 (case 5 ~ case 8 and case 13 ~ case 16).

**Table 2-7 Test program of this study**  
(Note: ✓ tests performed; ✗ tests non-performed)

Soils specimens							Test performed		
No.	Soil	Treatment	w <sub>f</sub> (%)	$\rho_d$ (Mg/m <sup>3</sup> )	Sieving	Mixing	$G_{max}$ -time	W-D cycles	Suction
Case 1	Silt	2% lime	17	1.65	1	B	✓	✓	✓
Case 2	Silt	Untreated	17	1.65	1	B	✓	✓	✓
Case 3	Silt	2% lime	22	1.65	1	B	✓	✓	✓
Case 4	Silt	Untreated	22	1.65	1	B	✓	✓	✓
Case 5	Silt	2% lime	17	1.65	2	B	✓	✗	✓
Case 6	Silt	Untreated	17	1.65	2	B	✓	✗	✓
Case 7	Silt	2% lime	22	1.65	2	B	✓	✗	✓
Case 8	Silt	Untreated	22	1.65	2	B	✓	✗	✓
Case 9	Silt	3% cement	14	1.70	1	B	✓	✓	✓
Case 10	Silt	Untreated	14	1.70	1	B	✓	✓	✓
Case 11	Silt	3% cement	21	1.70	1	B	✓	✓	✓
Case 12	Silt	Untreated	21	1.70	1	B	✓	✓	✓
Case 13	Silt	3% cement	14	1.70	2	B	✓	✗	✓
Case 14	Silt	Untreated	14	1.70	2	B	✓	✗	✓
Case 15	Silt	3% cement	21	1.70	2	B	✓	✗	✓
Case 16	Silt	Untreated	21	1.70	2	B	✓	✗	✓
Case 17	Clay	4% lime	25	1.35	2	B	✓	✓	✓
Case 18	Clay	4% lime	25	1.35	2	A	✓	✓	✓
Case 19	Clay	Untreated	25	1.35	2	B	✓	✓	✓
Case 20	Clay	4% lime	35	1.35	2	B	✓	✓	✓
Case 21	Clay	4% lime	35	1.35	2	A	✓	✓	✓
Case 22	Clay	Untreated	35	1.35	2	B	✓	✓	✓
Case 23	Clay	2% lime + 3% cement	25	1.35	2	A	✓	✓	✓
Case 24	Clay	2% lime + 3% cement	35	1.35	2	A	✓	✓	✓
Case 25	Clay	2% lime + 3% cement	35	1.35	2	B	✓	✓	✓

$G_{\max}$  (cf. 1.3.2 in chapter one) was determined by the bender elements technique which will be presented later.

Matrix suction was measured with the filter paper method following a procedure similar to that specified in ASTM D5298 -03: 1) the specimen was firstly wrapped by three layers of filter paper; 2) It was then sealed with one membrane, scotch and paraffin; 3) the intermediate filter paper was used to determine the water content after a 10 day period for equilibrium. Note that drying filter paper (Whatman 42) was used.

## **2.3. Preparation of samples taken from the experimental embankment**

### **2.3.1. Experimental embankment at Héricourt**

The experimental embankment was constructed at Héricourt. The seasonal environment variability in this zone constitutes the good conditions to investigate the durability of treated soils in long term under the effect of climate changes.

The embankment was constructed between March 15<sup>th</sup> and April 2<sup>nd</sup> 2010 (Figure 2-19). It is 107 m long, 5 m high and 5 m large (21 m at bottom, with a ½ slope). One side is made of silt and the other side is made of clay that is of green color.

Figure 2-20 presents the details of the experimental embankment. From the sub-embankment layer to the upper layers, there are five parts: sub-embankment (1 layer, 0.40 m), embankment (11 layers, 3.30 m), top of earthwork (3 layers, 0.90 m), sub-grade (1 layer, 0.30 m) and base (1 layer, 0.25 m). The silt side received several treatments (17 layers in total: 16 compaction layers + 1 sub-embankment of silt treated by 2% lime). For the 5 surface layers, the silt received 1% lime plus 5% cement, 3% lime, and 3% cement treatments; for the following 11 layers, they are either untreated or treated by 2% lime and 3% cement. The clay side also received different treatments (also 17 layers in total: 16 compaction layers + the same sub-embankment as the silt side). For the five surface layers, the clay side contains a layer of silt treated with 1% lime plus 5% cement, followed by 4 layers of clay with 2% lime plus 3% cement and 5% lime; for the deeper 11 layers, the clay received 2% lime, 4% lime, and 2% lime plus 3% cement treatments.



(a) Silt side in construction

(b) Clay side in construction



(c) Experimental embankment after construction

**Figure 2-19 Silt and clay sides of the experimental embankment**

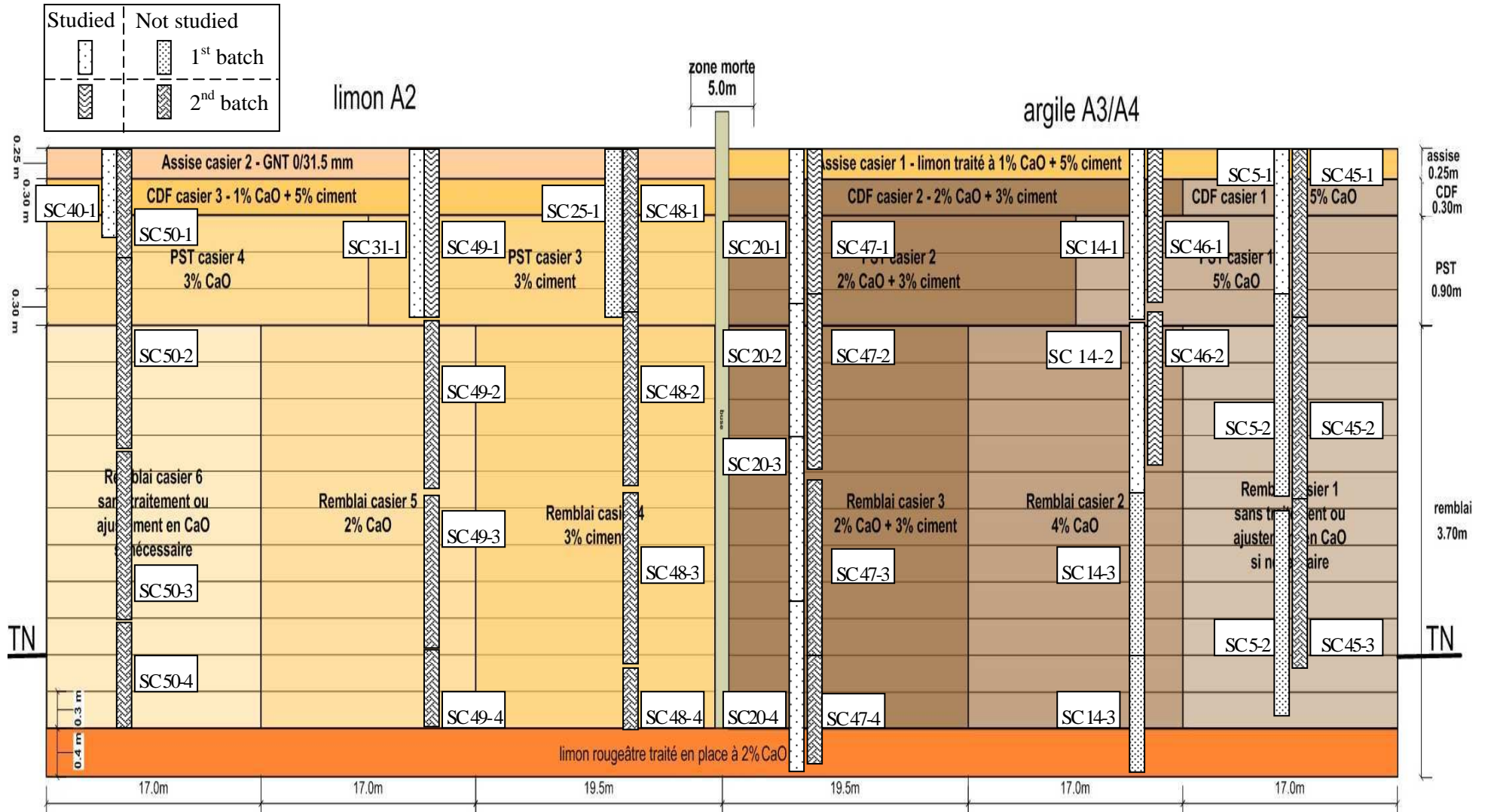


Figure 2-20 Distribution of the core samples in the experimental embankment

### 2.3.2. Cores taken from the embankment

As shown in Figure 2-20, 14 core samples were studied and they were taken from both the silt side and clay side successively from two batches. For example, core sample “SC 40-1” denotes the first sample of core 40. As shown in Table 2-8, on the silt side, core sample SC 31-1 and SC 40-1 were bored in May 2010 (first batch) and core SC 49 was sampled in March 2012 (second batch). On the clay side, the first batch cores (SC 20, SC 14 and SC 5) were sampled at the end of April 2010 while the second batch cores (SC 47 and SC 46) were bored in December 2011.

**Table 2-8 Sampling dates of the cores studied**

Side	Silt side			Clay side			
Batch	First batch		Second batch	First batch		Second batch	
Core No.	SC40	SC31	SC 49	SC 20, 14	SC 5	SC 47	SC 46
Boring date	15/05/2010	04/05/2010	14/03/2012	28/04/2010	27/04/2010	13/12/2011	14/12/2011

We can note that on the silt side, core samples SC 40-1, SC31-1 and SC 49-1 come from the surface layers- base, subgrade and top of earthwork. Core samples SC31-1 and SC 49-1 are located in a similar position in the centre of the silt side. On the clay side, a total of 11 core samples were extracted from 5 cores. Core SC 20 and core 47 are in a similar position. The first batch core SC 20 contains four samples (SC 20-1, SC 20-2, SC 20-3 and SC 20-4), covering all the depth in this position. The second batch core SC 47 consists of two samples, one in the shallow part (SC 47-1) and the other in the deeper part of embankment (SC 47-2). In the centre part of clay side, the first batch core SC14 and the second batch core SC 46 are also in a similar position and at a similar depth as core SC47. In the right part of clay side, the first batch core sample SC 5-1 is near the slope of the embankment.

Figure 2-21 and Figure 2-22 present the description of a silt core sample SC 31-1 and a clay core sample SC 20-1, respectively, both from the first batch. The descriptions of other 12 core samples are in appendix.

Figure 2-21 shows that core sample SC 31-1 is 1.0 m long, involving 0.22 m of base, 0.21 m of sub-grade and 0.57 m of top of earthworks, with four compacted layers (No. 16 ~ No. 13). From the observation of this core sample, we can see that layer No. 16 is made of gravels and broken stones, followed by layer No. 15 of yellow silt treated by 1% lime plus

5% cement that contains many little stones, then layer No. 14 of pure yellow silt treated by 3% cement that also contains a little stones and presents some fissures at the end and finally layer No. 13 of silt treated by 3% cement that contains many little stones. Note that: 1) the silt between -0.69 m and -0.78 m is found to be very fragile and shows many fissures; 2) the parts -0.22 ~ -0.43 m and -0.78 ~ -1.0 m appears very stiff.

Figure 2-22 describes a clay core sample - SC 20-1: it is 1.44 m long, containing 0.25 m of base, 0.265 m of subgrade and 0.825 m of top of earthworks, and involving 5 compaction layers (No. 16 ~ No. 12). Firstly, we can see that layer No. 16 is yellow silt treated with 1% lime plus 5% cement, and other layers are green-grey based multicoloured clay treated solely by 2% lime plus 3% cement. Secondly, in the base part (No. 16, 0 ~ -0.25 m), the core contains many little stones of white or grey colour, especially on the top of the core (0 ~ 5 cm). For the clay part, it is a mix of light-colour and deep-colour parts. In this test, we observed that the light-colour parts are mainly composed of natural clay, while deep-colour parts are clay with a significant amount of additives. From layer No. 15 to layer No. 13, the clay mostly shows light-colour, especially in the zones near the interface of compaction layers (ex. near 51.5 cm, 77.5 cm, 88 cm ~ 112 cm). Layer No. 12 mainly presents homogeneous and deep-coloured clay, showing concentrated additives and well mixed clay. In addition to the interfaces due to compaction, there are some fissures (ex. 34 cm; 88 cm; 129 cm) and stones occasionally (ex. big stone at 60 cm ~ 70 cm) in the clay.

After visual examination, the core samples were divided into several parts according to the fissures or cracks, and immediately sealed by membrane and scotch in order to prevent from water loss. The divided samples are named “sample”, as shown in Figure 2-21 and Figure 2-22.




Part	Compaction layer	Photo	Description	Sample
Base (0.22m)	0 cm		(0 ~ 22 cm) gravels, grains, asphalt	SC31-1-0 (0.0 m ~ 0.22 m) (layer No.16)
	Limit of layer (22 cm)		(22 ~ 43 cm) limit of layer is frank at 43 cm silt treated by 1% CaO + 5% cement, with many little stones	SC31-1-1 (0.22 m ~ 0.43 m) (layer No.15)
Subgrade (0.21m)	Limit of layer (43 cm)		(43 ~ 78 cm) fissure at 69 ~ 70 cm many fissures between 72 cm ~ 78 cm limit of layer is probably between 78 ~ 80 cm silt treated by 3% cement + with some little stones	SC31-1-2 (0.43 m ~ 0.78 m) (layer No.14)
	Limit of layer (78 cm)		(78 ~100cm) silt treated by 3% cement + many little stones	(0.78 m) SC31-1-3 (w) SC31-1-4 (0.80 m ~ 1.00 m) (layer No.13)
Top of earthworks (0.57m)	Sample end (100 cm)			

Figure 2-21 Description of silt core sample SC 31-1


Part	Compaction layer	Photo	Description	Sample
Base (0.25 m)	0 cm		(0 ~ 25 cm) Silt treated by 1% CaO + 5% cement, little stones 0 - 5 cm, de-aggregate part (two aggregates), strongly foliated traces coated the surface of aggregates	SC20-1-1 (0.0 ~ 0.25 m) (layer No.16)
	Limit of layer (25 cm)		(25 ~ 51.5 cm) Clay multicoloured, treated by 2% CaO + 3% cement, with little stones, a limit at 34 cm, another at 44 cm, and a frank limit at 51.5 cm	SC20-1-2 SC20-1-4 (0.25 ~ 0.51 m) (layer No.15)
Subgrade (0.265 m)	Limit of layer (51.5 cm)		(51.5 ~ 77.5 cm) Clay multicoloured, treated by 2% CaO + 3% cement, little stone presence at 60 ~ 70 cm (big pebble)	SC20-1-5 SC20-1-6 (0.51 ~ 0.65 m) (0.65 ~ 0.78 m) (layer No.14)
	Limit of layer (77.5 cm)		(77.5 ~ 112 cm) Clay multicoloured, treated by 2% CaO + 3% cement	SC20-1-7 (0.78 ~ 1.12 m) (layer No.13)
Top of earthworks (0.925 m)	Fissure (88 cm)		(112 ~ 144 cm) Clay treated by 2% CaO + 3% cement, clay well mixed, little stones	SC20-1-8 (1.12 ~ 1.44 m) (layer No.12)
	Limit of layer (112 cm)		Fissure (129 cm)	
	Sample end (144 cm)			

Figure 2-22 Description of clay core sample SC 20-1

### 2.3.3. Preparation of specimens from core samples

Figure 2-23 and Figure 2-24 show the experimental procedure and measurements adopted, including: 1) opening and describing the core sample, 2) separating it to several parts and preparing soil specimens, 3) for each specimen, measuring its water content, density and shear wave velocity.

Firstly, the state of the core sample was recorded, including soil type, treatments, positions of fissures and potential compaction interfaces, etc. (Ex. Figure 2-21). Secondly, the core samples were separated into different samples as mentioned before. For each sample, the exact position and direction were recorded. Thirdly, all the samples from this core sample were stored in a sealed barrel to prevent from any water loss. Finally, the sample was re-opened and the real preparation of specimens started: the sample was firstly well fixed with plastic films to prevent any disturbance when cutting it manually with a saw (Figure 2-24), then trimmed to obtain a specimen of 100 mm diameter and 70 mm height (Figure 2-23). The specimen was immediately enveloped by membrane and stored. The upper and lower parts of the specimen were trimmed and used to determine the water contents (Figure 2-23). The volume of the specimen was obtained by an immersion method according to XP CEN ISO/TS 17892-2 (the 3<sup>rd</sup> picture in Figure 2-24). With the values of water content and volume, the dry density was calculated. For each specimen, five  $G_{max}$  measurements by bender elements at different points were performed (see Figure 2-23).

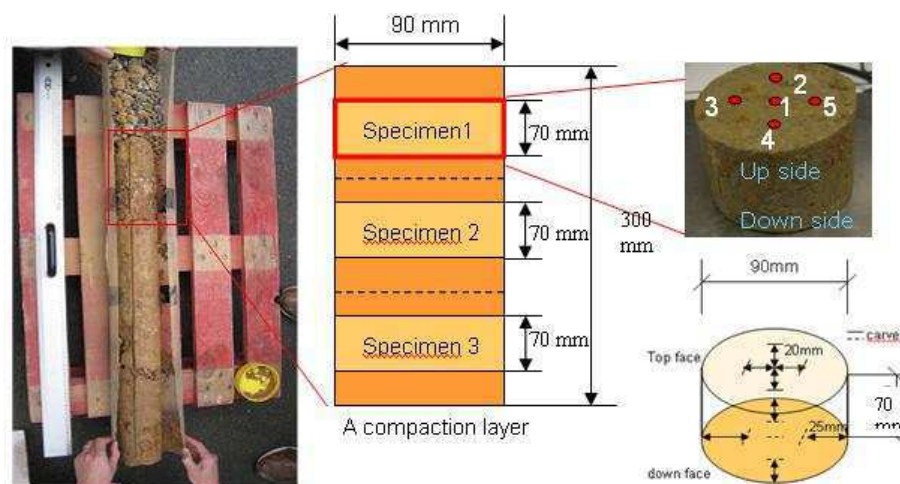


Figure 2-23 Experimental procedure adopted



Figure 2-24 Water content protection and volume measurement

### 2.3.4. Test program

Table 2-9 shows the time table of  $G_{\max}$  measurements for all cores (25 cases in total). As it can be seen, different conditions are involved, allowing the effects of curing, climate and treatment to be investigated by mean of comparing  $G_{\max}$  results of the different cases.



## 2.4. Experimental methods

### 2.4.1. Experimental setup

Figure 2-25 describes the shear wave velocity measurement device - bender element system. It consists of two parts: a pair of benders and the benders box. The benders box contains a function generator, a power amplifier and an oscilloscope. The bender element is made of piezoceramic transducers bonded to a stainless steel plate. When excited by an input voltage, the bender element can change its shape and generate a mechanical excitation, hence acting as a signal transmitter. Moreover, when subjected to a mechanical excitation, the bender element will emit an electrical output, thus acting as a signal receiver. Both the input and output signals are finally transmitted to a computer and stored. The input signal can be triggered by stable single sinusoidal pulses, with a frequency between 0.05 ~ 10 kHz. The size of the benders is 10 mm (width) \* 1.0 mm (thickness) \* 1.25 mm (penetration length).

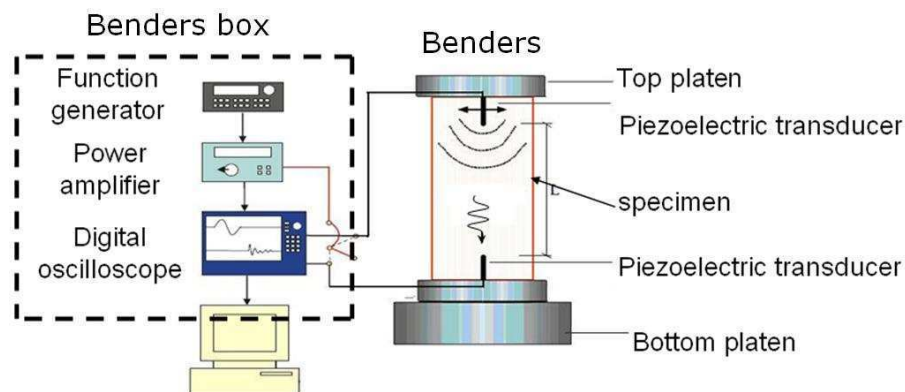


Figure 2-25 Experimental device - Bender elements system

As shown in Figure 2-25, the soil specimens (either with a height of 50 mm for the laboratory specimens or 70 mm for the field samples) were put between the pair of benders. In order to ensure that the contact is well ensured between the benders and the specimen, two bender elements were put into two cavities being prepared previously on the surface of specimen (at the centre with the same orientation). When the function generator gave a shear wave signal (S-wave), the S-wave signal was first amplified by the power amplifier and then transferred to a first bender element. The signal passed through the soil specimen and was transmitted to the other bender element (the receiving one). The received signal was then

amplified and recorded by the oscilloscope. Finally, the travel time of shear wave propagation through the specimen was determined (time difference  $\Delta t$ ).

The travelling distance of s-wave was determined using the current tip-to-tip distance ( $L_{tt}$ ) between the transmitter and receiver bender elements (Dyvik and Madshus, 1985; Viggiani and Atkinson, 1995a, b). In other words,  $L_{tt}$  is equal to the specimen's height, after removing twice of the penetration length (equation 2-4). Then, the shear wave velocity ( $V_s$ ) can be deduced from  $L_{tt}$  and  $\Delta t$  (equation 2-5) and  $G_{\max}$  can be determined using equation 2-6:

$$L_{tt} = L - 0.00025 \quad (2-4)$$

$$V_s = L_{tt} / \Delta t \quad (2-5)$$

$$G_{\max} = \rho V_s^2 \quad (2-6)$$

where  $\rho$  is the soil specimen's unit mass.

The transmitter element was excited using a sinusoidal voltage for S-wave. The accuracy of  $G_{\max}$  depends on the precision of  $\Delta t$  and  $L_{tt}$ . The precision or graduation of  $\Delta t$  is a nominal constant (0.002 ms) which is related to the maximum sampling frequency of the bender element (500 kHz). The stiffer the soil, the shorter the travelling time, and as a result, the lower the accuracy. In other words, for a given length of a specimen, the accuracy of the  $G_{\max}$  measurement depends mainly on the stiffness of the soils. Similarly, as the length of the specimens can also affect the travel time of the shear waves, it can also contribute to the accuracy of  $G_{\max}$  measurement. The longer the sample the higher the accuracy. However, with the increase of the travel path of shear wave, the energy of shear wave signal becomes swiftly weaker. Thus, an increase of the length of specimen is not a good approach to improve the accuracy of  $G_{\max}$  measurement. In fact, two things are important to do for reducing the  $G_{\max}$  error: 1) using a mean value of repeated triggering signals to obtain a credible  $\Delta t$ ; this can also avoid potentially incorrect signals; 2) obtaining the optimum received signals by changing excitation frequencies, by a careful comparison and evaluation of these signals.

### 2.4.2. Travel time identification methods

Figure 2-26 shows a typical S-wave shape of both input and output signals. The output wave starts with a bump-torture at the arrival time that makes difficult the determination of the arrival time using the start-to-start time method. Thereby, the peak-to-peak method, from the first peak of the input wave to the first peak of the output one, is applied to determine the travel time. Note however that the peak-to-peak method should be used with caution as the travelling time may be influenced by the triggering frequencies as mentioned in chapter 1.

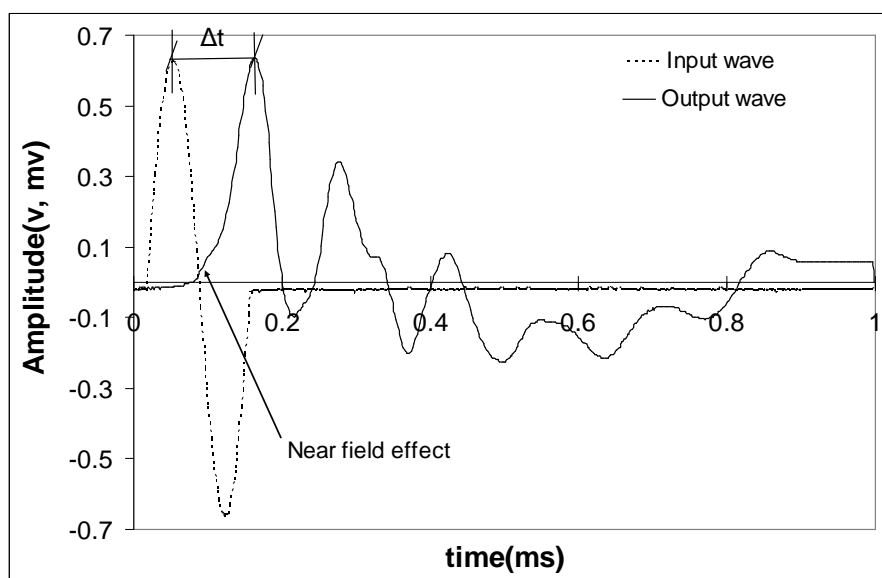


Figure 2-26 Determination of the travel time by the peak to peak method

### 2.4.3. Signals received at various frequencies

Due to the complexity of the bender element and the absence of standards to follow, a large number of Vs measurements have been performed for each test, in order to obtain the optimum excitation frequency and to ensure the reproducibility of measurements. Thanks to the large number of specimens in different states, a large number of S-wave data are available to analyse the frequency effects. These data involve both the silt and clay at different densities and water contents, different treatments – lime and/or cement, different curing conditions – in the laboratory and in field, etc.

As the strongest signal is generated at the resonant frequency of the system, theoretically we can just apply the same frequency as input. However, in practice, as there are noisy waves as sinusoidal S-waves, we must test several input frequencies to determine the

optimum one. Yamashita *et al.* (2005) also reported that, when the peak to peak method is used, it is required to choose the output wave which has the most similar shape as the one of the input wave, i.e. similar period and similar amplitude. In order to examine the response of input frequencies for different soils, a large number of bender element tests were carried out at different input frequencies, and a clearly defined output signals were determined for each specimen. On the whole, we applied: 1) 10, 8.3, 7.1, 6.2, 5.6, 5, 3.8 kHz for high stiffness soils; and 2) 3.8, 3.3, 2.8, 2.5, 2, 1.25 kHz for low stiffness soils. Note that the frequency of 10 kHz is the maximum that can be generated by the apparatus.

Many approaches have been attempted to study the factors which may influence the resonant frequencies of the soil-bender element system. We firstly considered the soil's state (dry samples and wet samples), then the aggregates size ( $D_{\max} = 0.4 / 1 / 2 / 5$  mm), and finally the soil type: silt, clay. Analysis of the results obtained shows clearly that the optimum frequency for a soil is mainly stiffness dependant (see Figure 2-31 and Figure 2-32).

Figure 2-27 ~ Figure 2-30 show some examples of input/output S-wave shapes for different levels of stiffness. In these figures, the excitation frequency was chosen based on the comparison of the wave shapes between the input and output sinusoidal S-waves.

Taking a soft soil with low stiffness as an example, the  $V_s$  of the *in situ* clay specimen ( $S_r = 0.62$ ) is 145.8 m/s at a triggering frequency of 2 kHz. After testing a large range of triggering frequencies (Figure 2-27), it was found that classic S-waves are only located in the range of 1.25 ~ 3.3 kHz. If the triggering frequency is not in this range, the S-wave signals would be masked by noisy waves. In the 1.25 ~ 3.3 kHz range, the evolution of the received S-waves is the clearest. At a 10 kHz triggering frequency, there is no clear output signal. With a triggering frequency decreasing to 5 kHz, the output signal shows a vague peak. At 3.3 kHz, the peak is quite clear, but the wave shape tends to deviate rightward. At 2 kHz, the received S-wave signal seems to have an impartial wave shape and a relatively stronger intensity than that at other input frequencies. At 1.25 kHz, the output shear wave shows a leftward distortion tendency.

Thus, in this example, we choose the 2 kHz triggering frequency to calculate the arrival time, because the corresponding received signal is the most similar to the input one. When the triggering frequency is higher or lower, the received shear waves are twisted or their amplitudes becomes weaker; thus, the arrival time cannot be clearly defined, neither by the first peak-peak method nor by the first start-start method.



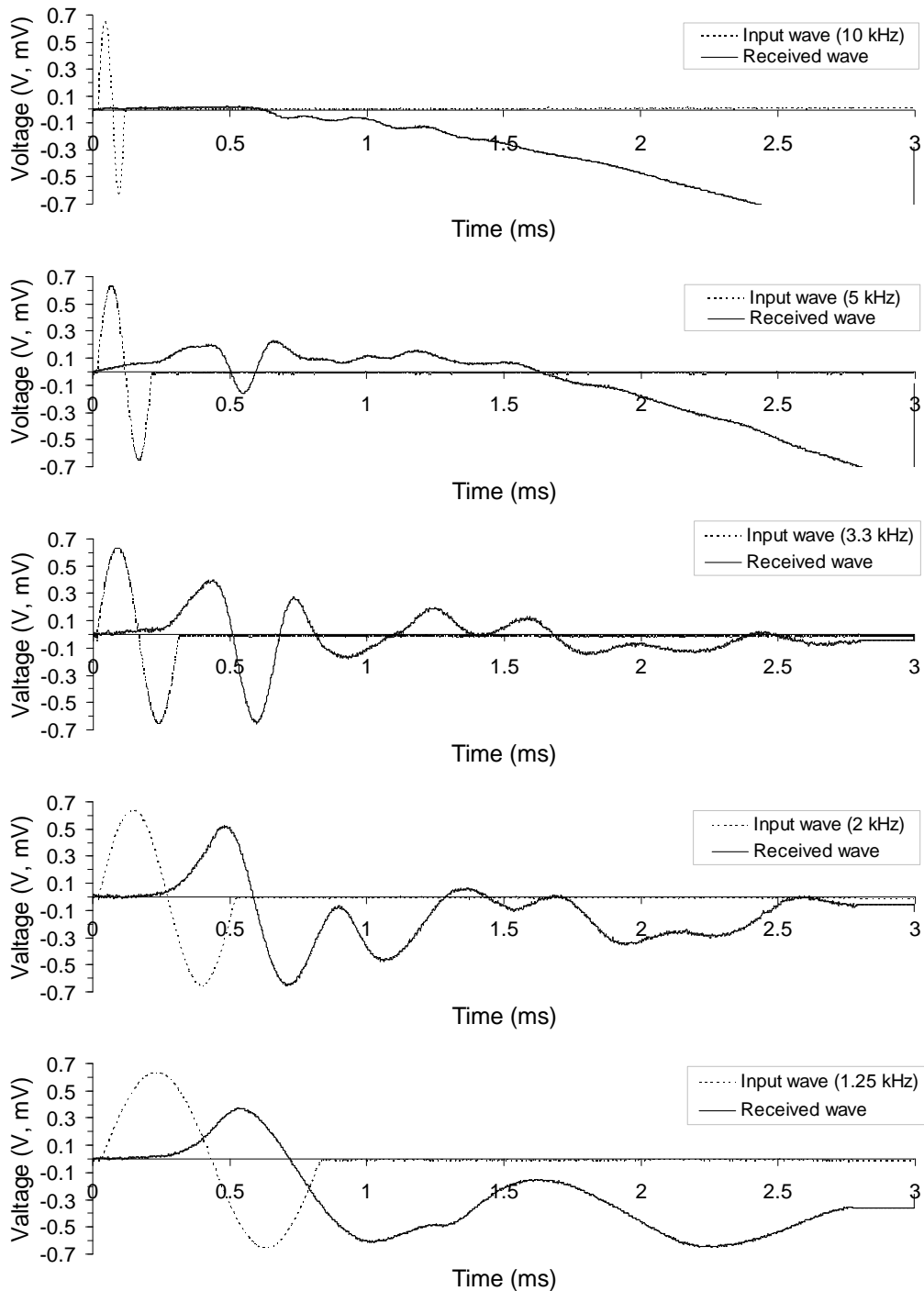


Figure 2-27 Test on low stiffness soils ( $V_s = 146$  m/s at 2 kHz) (*in situ* clay specimen,  $D_{\max} = 31.5$  mm)

The effect of excitation frequency on the stiffness of soils is shown in Figure 2-31 [see *in situ13*, clay, ( $D_{\max} = 31$ mm)]. We can see that the stiffness at the chosen frequency is almost the highest (in terms of shear wave velocity) among the clearly defined received shear waves.

We also tested soil specimens of middle level of stiffness for the same purpose. Figure 2-28 shows a frequency test on a 3% cement treated silt specimen just after its compaction at an initial water content of 14% ( $S_r = 0.61$ ) and a dry density of  $1.72 \text{ Mg/m}^3$ . Similarly, we observe that the clearly defined shear waves are located in the range of  $3.9 \sim 10 \text{ kHz}$ . Visualisation of the wave shapes shows classic sinusoidal signal with a crisp and impartial wave shape at a triggering frequency of  $4.5 \text{ kHz} \sim 5.6 \text{ kHz}$ . Thereby, we can determine that the resonant frequency is around  $4.5 \text{ kHz} \sim 5.6 \text{ kHz}$  and we finally choose a frequency of  $4.5 \text{ kHz}$  with a  $V_s$  of  $325 \text{ m/s}$  ( $\Delta t = 0.15 \text{ ms}$ ). Likewise, if the triggering frequency is not in this range, there is no clearly defined shear wave.

In addition, the effect of excitation frequency on the stiffness of soils can be depicted in Figure 2-31 (see case 9, test 02). We also observed that the stiffness at the chosen frequency is the highest one among the clearly defined received shear waves (at about  $4.5 \text{ kHz}$ ).

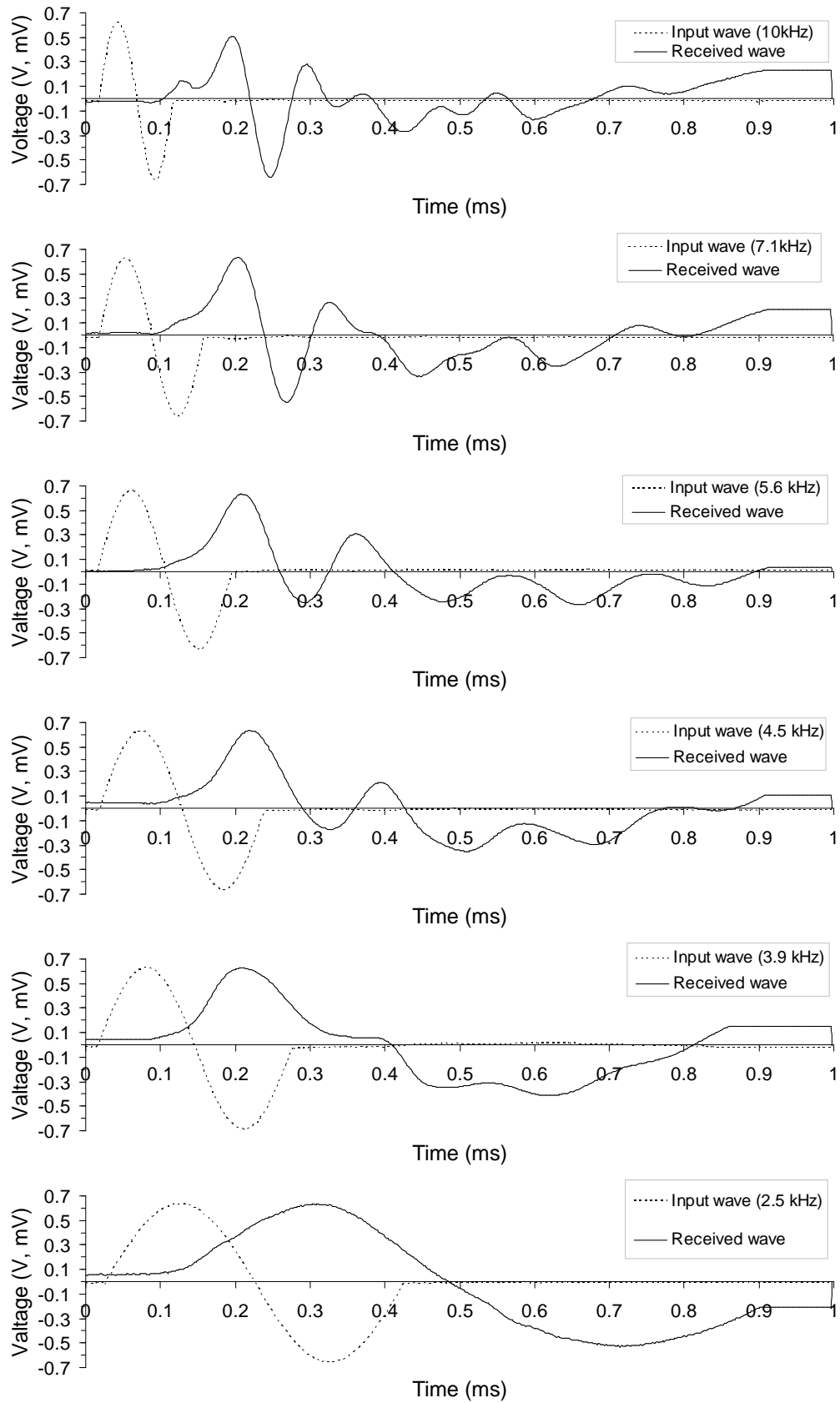
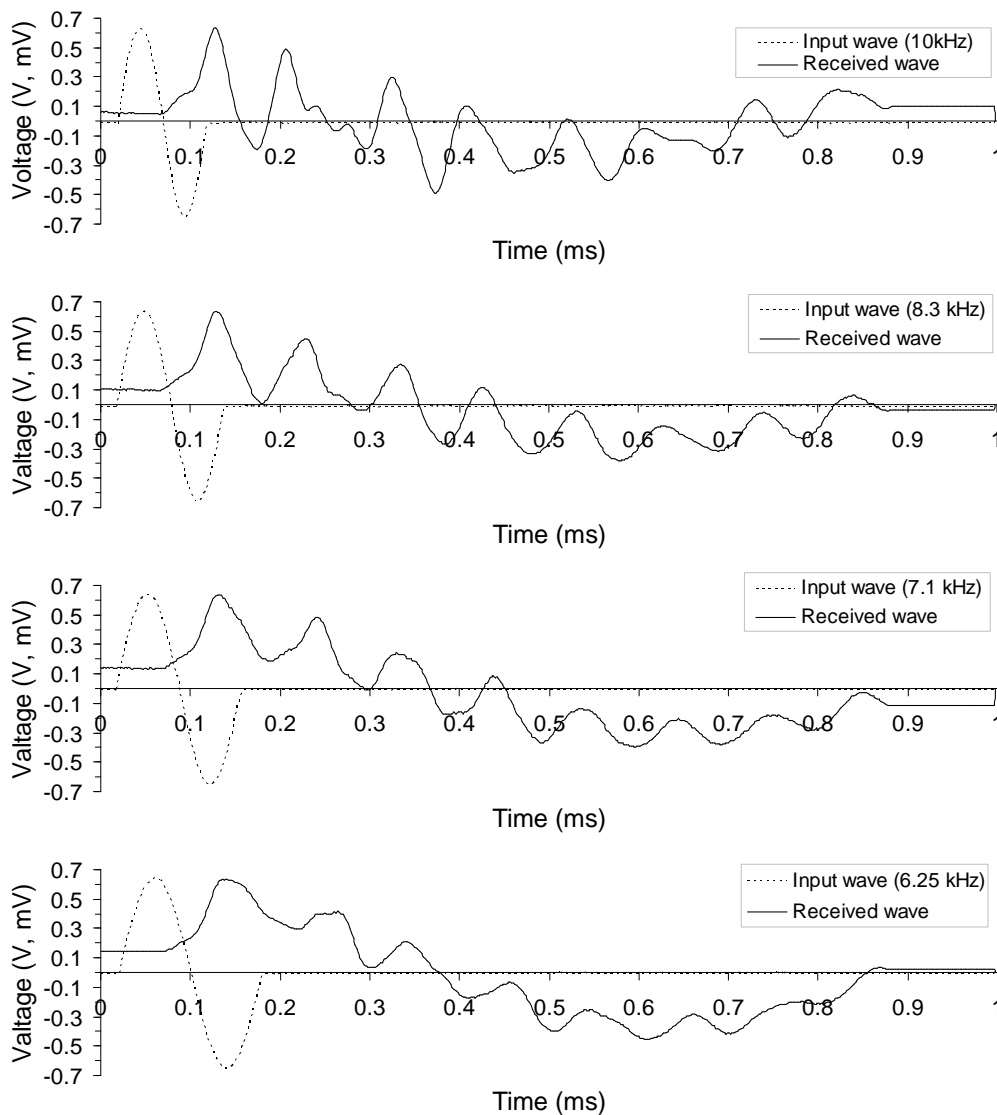


Figure 2-28 Test on soils of middle level of stiffness ( $V_s = 325$  m/s at 4.5 kHz) (case 9, test 02,  $D_{max} = 5$  mm)

For high stiffness soils, this series of clearly defined shear waves still moves to higher triggering frequencies with increasing stiffness: the chosen frequency is 8.3 kHz for  $V_s = 600$  m/s (Figure 2-29) and 10 kHz for  $V_s = 780$  m/s (Figure 2-30). In addition, the excitation frequency range of clear defined S-wave is narrower than that for lower stiffness soils.



**Figure 2-29** Test on soils of high level of stiffness ( $V_s = 600$  m/s at 8.3 kHz) (case 4, test 44, drying state:  $S_r = 0.96 \rightarrow 0.69$ )

Figure 2-29 and Figure 2-30 show the evolution of these S-waves at different triggering frequencies. In Figure 2-29, we can see that there is no large difference in stiffness among 10 kHz, 8.3 kHz and 7.1 kHz. However, when the triggering frequency is lower (6.2 kHz), the stiffness values decrease rapidly. It should be noted that these values are no longer reliable because the distortion of the output shear waves causes fallacious

identification of these output first peaks. Thereby, we should choose the high triggering frequencies in Figure 2-29.

For soils of higher stiffness, as shown in Figure 2-30, the clearly defined S-wave zone becomes still narrower and is limited to a solely imparital one at 10 kHz.

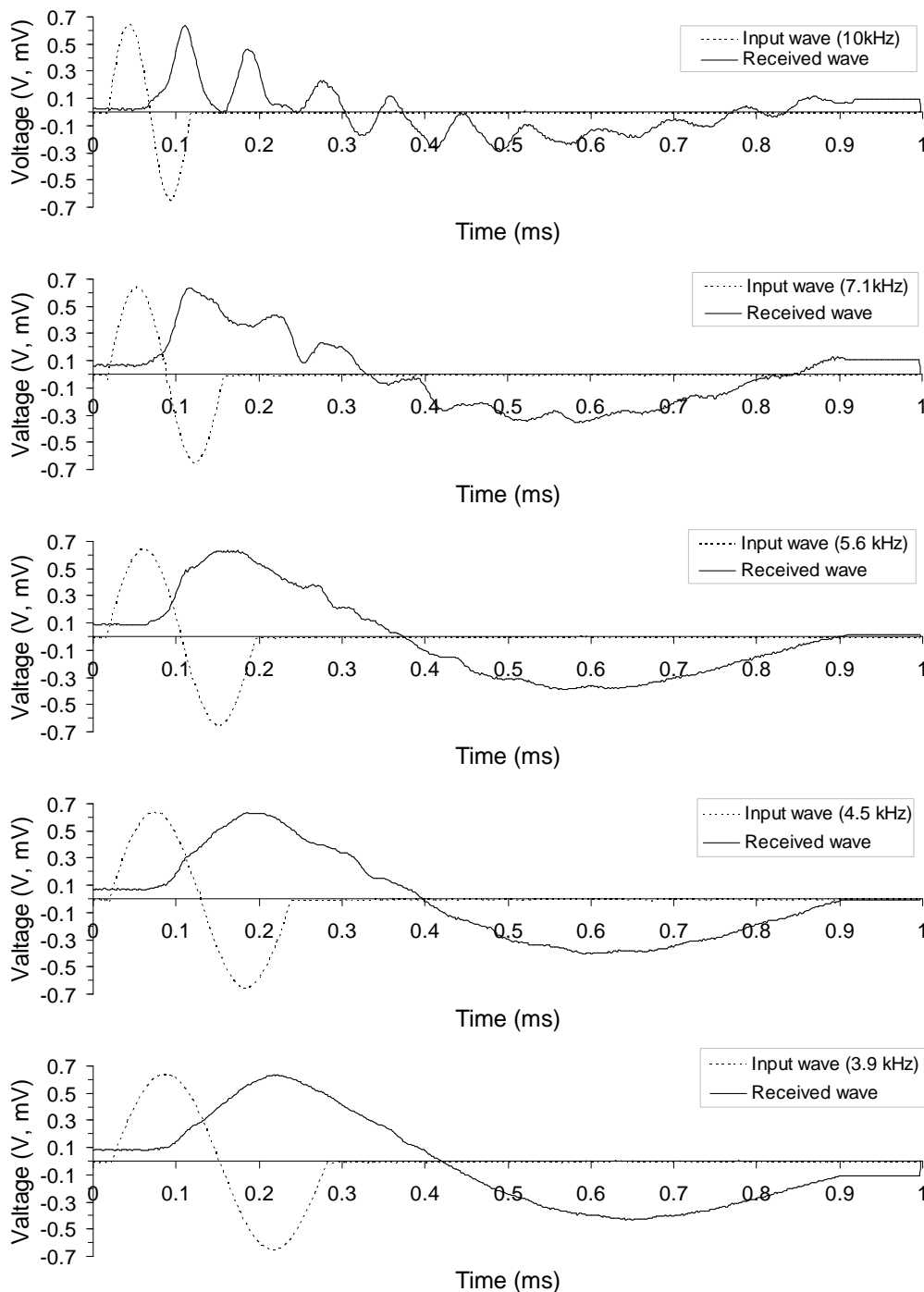


Figure 2-30 Test on soils of high level of stiffness ( $V_s = 780$  m/s at 10 kHz) (case 18,  $D_{max} = 0.4$  mm)

Comparison between Figure 2-27 and Figure 2-30 shows that, 1) a series of clearly defined output S-wave signals are often around the one at the excitation frequency chosen; 2) the chosen frequency increases with the increase of stiffness, together with the frequency zone of the clearly defined S-waves being narrowed; 3) the two sides of the clearly defined waves tend to be an impartial S-wave for low stiffness level; 4) only one side of the clearly defined waves tend to be an impartial one for the high stiffness level (ex. Figure 2-30); 5) the resonant frequency may be higher than the maximum triggering frequency (10 kHz) if the stiffness of soil is still higher. In this case, the maximum frequency is proposed to be chosen.

#### **2.4.4. Effects of frequency on the determination of soil stiffness**

Figure 2-31 shows the  $V_s$  response by various triggering frequencies for each test at its frequency chosen. We observe that the higher the frequency chosen the higher the stiffness of soil. Further, according to the criterion and example introduced previously, the frequency chosen for each level of stiffness corresponds to the highest value among the numerous triggering frequencies. There is a good correlation between the stiffness and frequency.

For stiff soils ( $V_s > 500$  m/s), a high input frequency enables the output S-wave shape to be clearly defined and similar to the input one. As the frequency decreases, the received shear waves become gradually tortured and the corresponding stiffness value decreases sharply. Thus it is better to avoid choosing S-waves in this zone.

For the soils of middle stiffness ( $200$  m/s  $< V_s < 450$  m/s), the peak value of  $V_s$  is moving gradually to a lower frequency when the soil is becoming softer. However, the difference is not as large as for stiff soils.

For low stiffness soils ( $V_s < 200$  m/s), the frequency chosen still moves to a lower value as the soil stiffness decreases. But the stiffness value does not change clearly with the frequency. This indicates that the frequency effect is less significant for soft soil than for stiff one.

In conclusion, due to the large range of triggering frequencies for each specimen, some unfavourable output signals, including not clearly defined shear waves, are mixed with good signals. This can give rise to a significant difference in stiffness estimates for a given specimen. Thereby, in order to choose the optimum frequency by first peak-to-peak method, several measures can be taken: 1) the chosen triggering frequency should be located in a zone that shows a series of clearly defined shear waves, thus minimising the disturbance of

spurious waves; among these frequencies, the corresponding  $V_s$  values are similar to each other, and the frequency chosen is often located at the highest  $V_s$  obtained; 2) the evolution of the received S-waves is rather regular: the upper part of the S-wave is tortured rightward when the frequency is higher than the frequency chosen; on the other hand, it tends to be tortured leftward when the frequency is lower than the chosen one; 3) the frequency chosen often gives a crisp and impartial wave shape; therefore, the identification of the optimum frequency becomes much easier because it can be judged only by the evolution of waveforms, instead of comparing the difference of input/output period for each frequency (Leong et al., 2009).

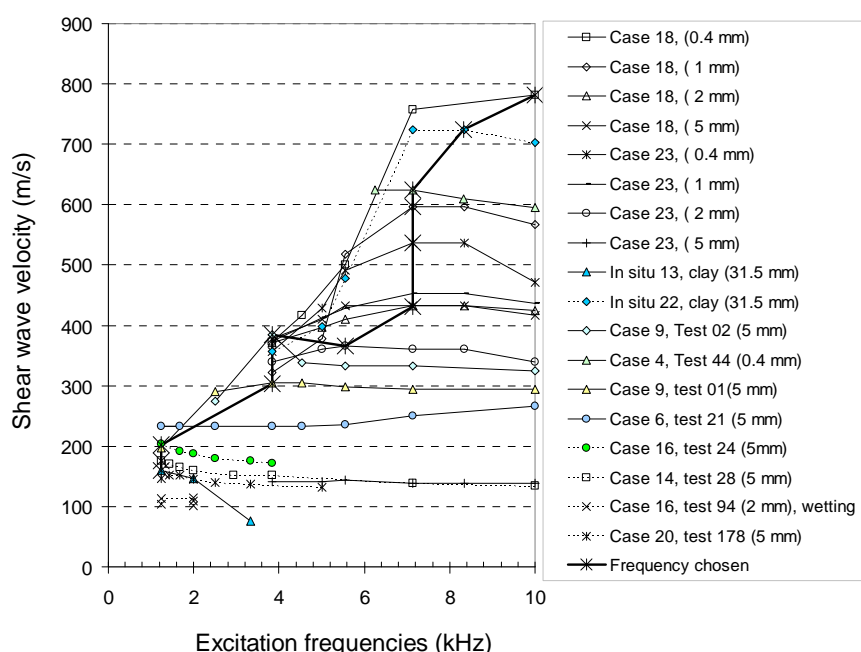


**Figure 2-31 Effect of excitation frequency on the determination of the stiffness of soils in different states**

Figure 2-32 summarises some of the frequencies chosen for the soils of different stiffness levels. At a certain stiffness, we observe a linear relationship between the frequencies chosen and the stiffness: the stiffness increases with the increase of the chosen frequency. As mentioned before, if the soil is still stiffer and the measurement becomes out of the zone represented by the this figure, we propose to change the bender element system with a larger triggering frequency range, or to use the highest triggering frequency (10 kHz) in case of no possibility to replace the device.

Lee and Santamarina (2005) also observed the nearly linear relationship between stiffness and resonant frequency. He also evidenced this relationship at low level of shear

wave velocity of soils ( $<200$  m/s). Comparison between the linear relationship obtained by Lee and Santamarina (2005) and that obtained in the present study shows that, 1) the linearity exists in a similar range of frequency chosen in the case of low stiffness ( $V_s < 100$  m/s); and 2) the difference of frequency chosen is enlarged with increase of stiffness, especially for when  $V_s > 400$  m/s. The differences indicate that the chosen frequency depends not only on the soil's stiffness, but also on the nature of the bender element system. It means that among different bender element systems, the required frequency may be different for a given level of stiffness. This implies the calibration of each bender element system. With this calibration or the relationship between the stiffness and frequency, the shear wave velocity measurement can be conducted without too much difficulty.

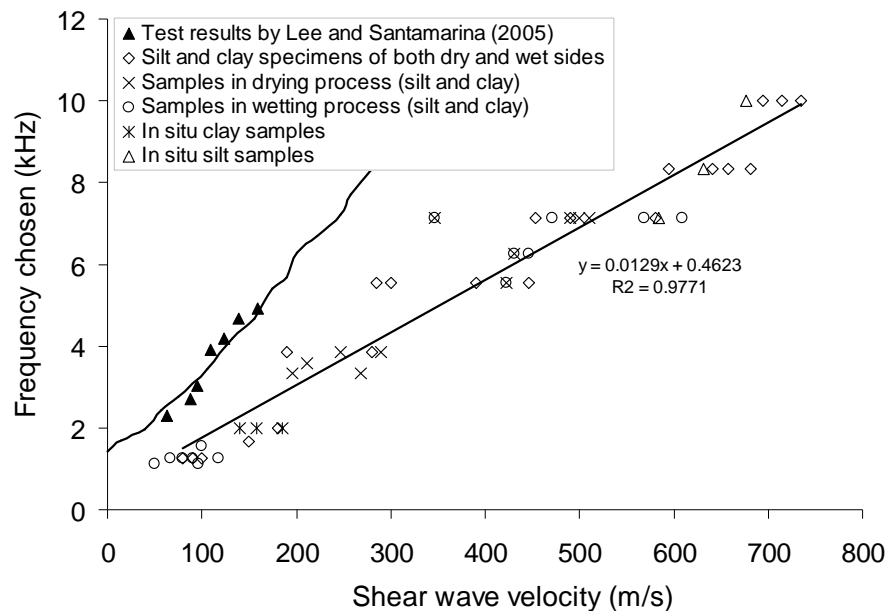


Figure 2-32 Frequency chosen for soils of different stiffness levels

As a conclusion, the shear wave responses to different excitation frequencies are not constant for a given soil, especially for high stiffness soils. The identification of the relationship between the optimum S-wave and  $V_s$  is decisive to solve this problem. The results obtained show that, for a certain stiffness level: (i) when the applied frequency is close to the resonant frequency of the system, the waves are relatively well defined, and the best wave is obtained at the resonant frequency; (ii) the triggering frequency that gives the strongest receiver signal is associated with the resonant frequency of bender element system; (iii) for a given bender element system, the resonant frequency is directly related to the stiffness of a soil. In other words, the triggering optimum frequency is stiffness dependent for



a given bender element system. In addition, it is important to investigate the resonant frequency responses of a given bender element system in order to determine the arrival time with accuracy.

## 2.5. Conclusions

This chapter is devoted to the presentation of the materials studied, the test program and the methods used. Two soils have been studied, one silt and one clay; both were used for the construction of the experimental embankment. The  $G_{\max}$  of the lime and/or cement treatment of soils was measured for soils prepared in the laboratory and taken from the experimental embankment, using bender elements based on the wave propagation technique.

In the laboratory, the soils were firstly air dried and ground into a target maximum soil aggregates size ( $D_{\max}$ ). For each  $D_{\max}$ , the soils were humidified to reach the target water contents  $w_i$ , then mixed with a given quantity of additive powder (calculated by dry soil) prior to the static compaction at a given density and water content ( $w_f$ ) following the normal Proctor curve of each treatment. The water loss during preparation ( $w_{\text{lost}} = w_i - w_f$ ) was determined by tests. The treated soil specimens were compacted at the same dry density on both dry side and wet side of the optimum following the Normal Proctor curve. The corresponding untreated soils were also prepared at same dry density and  $w_f$ . Only mixing method B was used for the silt, whereas two mixing methods (A and B) were applied for the clay. For the silt, two treatments (2% lime, 3% cement), two values of  $w_f$ , and four sub-series of soil powders ( $D_{\max} = 0.4, 1.0, 2.0, 5.0$  mm) prepared by two sieving methods (1 and 2) were considered. For the clay, two treatments (4% lime, 2% lime + 3% cement), two values of  $w_f$  and four sub-series as in the case of silt but prepared only by sieving method 2 were accounted for. After compaction, the soil specimen (50 mm both in diameter and height) was covered by membrane, plastic film to prevent the soil moisture changes. The  $G_{\max}$  was then measured at variable time intervals until the stabilisation. Its matrix suction was measured also at stabilisation. Thereafter, the soil was subjected to wetting/drying cycles, by being fully saturated and then air-dried to its  $w_f$ . The suction measurement was also performed during one wetting/drying cycle where significant  $G_{\max}$  change was observed.

The experimental embankment constructed in the framework of TerDouest project is consisted of both silt and clay treated by lime and /or cement. Compared to the laboratory

condition, the field condition involves larger aggregates size:  $D_{max} = 31.5 \text{ mm}$  for the clay and  $D_{max} = 20 \text{ mm}$  for the silt. As the hydromechanical behaviour of lime and /or cement treated soils changes not only with curing time but also with climate changes, the tests, aiming at investigating the combined effect of curing time and climate, were programmed using the core samples with the same soils/treatments as in the laboratory.

After the construction of the embankment, two batches of core samples were bored after different curing periods. In the laboratory, the cores were cut into small cylindrical specimens of 70 mm high. Five measurements of  $G_{max}$  were performed for each specimen at a given time, allowing any heterogeneity on the cross-section to be identified.

$G_{max}$  was determined by the shear wave velocity ( $V_s$ ) using the bender elements based on the wave propagation technique. As it is normally difficult to identify the arrival time of shear waves using the start to start method because of the near field effect and various wave shapes, the peak to peak method was used in this study. This method should be used with caution as the travelling time may be influenced by the triggering frequency, making the  $V_s$  measurement difficult. In order to solve this problem, we studied the shear wave responses of both the clay and the silt in various states (different densities and water contents, different treatments – lime/cement treated, curing conditions) with respect to the triggering frequency. The optimum frequency is chosen based on the identification of output wave shapes. It is observed that the triggering optimum frequency moves regularly with the stiffness of soils. After determining the relationship between the optimum frequency and soil stiffness, the identification of arrival time can be conducted without difficulty.

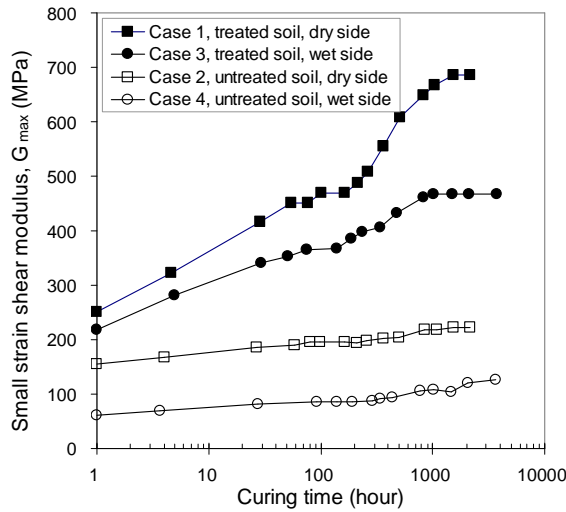
## Chapter 3. Aggregates size effect during curing time

In this chapter, the variations of  $G_{\max}$  with time are first presented. For the silty soil the specimens are prepared by sieving method 1 and 2 and then treated by lime and cement (cf. section 2.2.1). For the clayey soil, the specimens are prepared by sieving method 2 and treated by lime and by lime plus cement. Note that two mixing methods are applied for the clayey soil, namely mixing method A and B (cf. section 2.2.2). The results obtained are finally analysed.

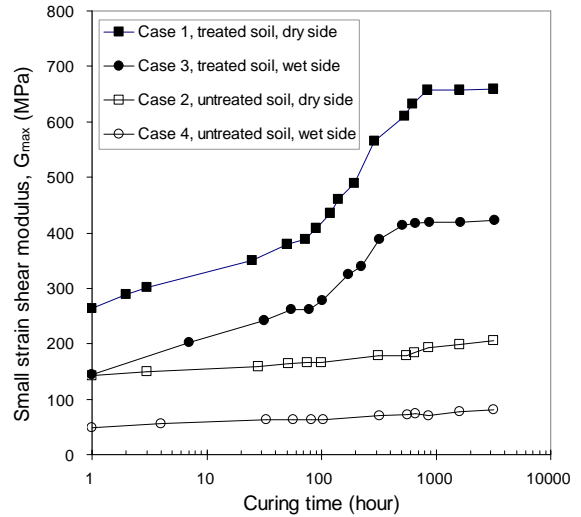
### 3.1. Silty soil treated with lime

#### 3.1.1. Samples obtained by sieving method 1

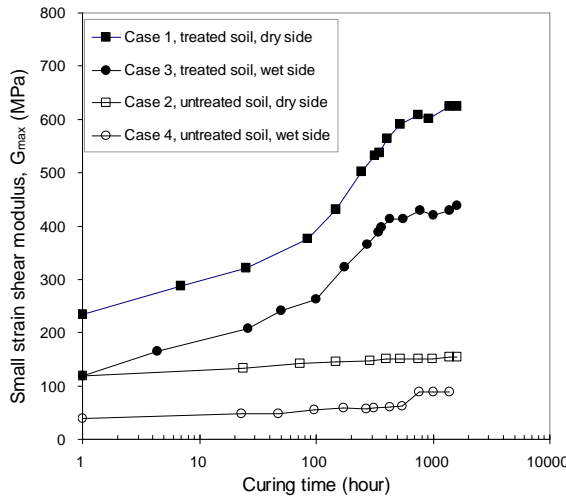
Figure 3-1 depicts the variations of  $G_{\max}$  over time for the silt specimens prepared by sieving method 1 and then treated by 0% and 2% lime. In case of untreated specimens (case 2 and 4) with soil passed through 0.4 mm sieve (Figure 3-1a), the  $G_{\max}$  just after compaction is 155 MPa for the dry side at a water content  $w_f = 17\%$  (case 2), and is 61 MPa for the wet side at a water content  $w_f = 21.8\%$  (case 4). The values increase slightly over time and reach stabilization after 80 hours at 196 MPa and 85 MPa, respectively. Thereafter (at 400 hours), they slightly increase until stabilisation after 2000 hours, at 222 MPa and 121 MPa respectively. In the case of 2% CaO treated specimens (case 1 and 3) with soil passed through 0.4 mm sieve, the  $G_{\max}$  just after compaction is 251 MPa for the dry side at the same water content  $w_f = 17\%$  (case 1), and is 219 MPa for the wet side also at the same water content  $w_f = 21.8\%$  (case 3). Comparison between the values for the untreated and treated specimens shows that the lime treatment has a significant effect on the  $G_{\max}$  just after the compaction. With curing time, the  $G_{\max}$  of treated specimens also increases and achieves a relative stabilization after 80 hours, at 450 MPa for the dry side (case 1) and 368 MPa for the wet side (case 3). Thereafter (about 100 hours), this increasing trend is followed by a much faster evolution, until stabilisation after 1000 hours at 686 MPa and 468 MPa for the dry and wet side, respectively. In other words, there are two phases (phase 1 and phase 2) of development of  $G_{\max}$  on the scale of logarithm of time. The increase is more significant at a lower water content ( $w_f = 17\%$ ). Interestingly, the stabilized  $G_{\max}$  value for the dry side is higher than the one for the wet side, for both the lime-treated and untreated silts.



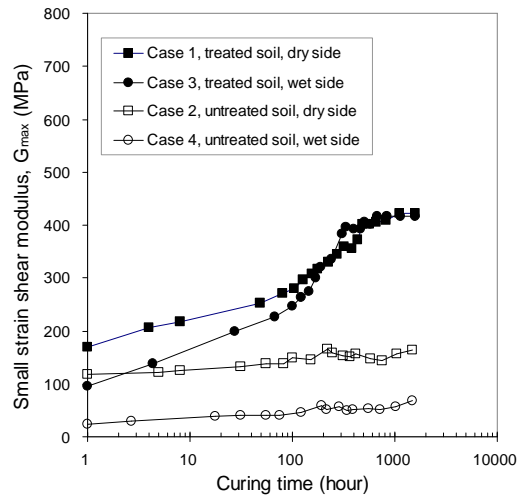
(a)  $D_{max} = 0.4 \text{ mm}$



(b)  $D_{max} = 1 \text{ mm}$



(c)  $D_{max} = 2 \text{ mm}$



(d)  $D_{max} = 5 \text{ mm}$

**Figure 3-1 Small strain shear modulus ( $G_{max}$ ) versus curing time for the silt treated with lime (sieving method 1)**

Similar observations can be made for the results of soil passed through 1.0 mm (Figure 3-1b), 2.0 mm (Figure 3-1c) and 5.0 mm sieves (Figure 3-1d): (i) an immediate effect of lime treatment after compaction, characterised by a significant increase of  $G_{max}$ ; (ii) a slight increase of  $G_{max}$  over time for the untreated specimens; (iii) a higher  $G_{max}$  value for the dry side than that for the wet side, for both the treated and untreated silt (for most cases); (iv) the stabilization of  $G_{max}$  over 1000 hours after the treatment; v) in the logarithmic scale of time, the increase of  $G_{max}$  for the 2% CaO treated specimens clearly shows the two-phase

development, i.e. an increasing nonlinear curve followed by another faster one. This is particularly the case for the dry side.

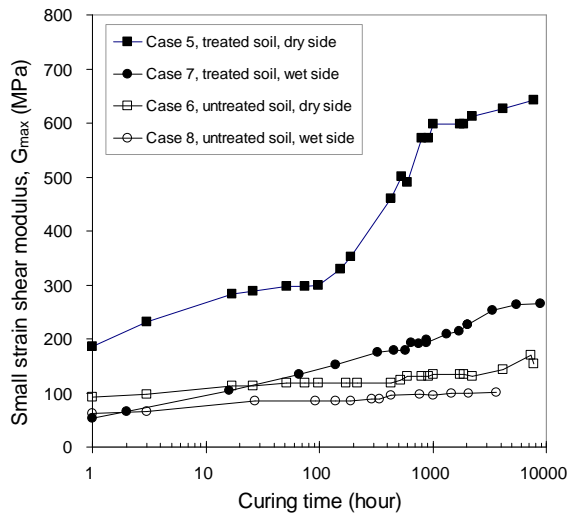
Some slight differences are also observed for the treated ones: 1) for the soil passed through 0.4 mm sieve (Figure 3-1a), we can see a transition period before starting the second  $G_{\max}$ -time phase (ex. 55 ~ 213 hours for the dry side) which is obviously longer than that for other sieves sizes; 2) for the soil passed through 5 mm sieve (Figure 3-1d), the  $G_{\max}$  of wet side reaches the values similar to that of dry side after 200-hour curing.

### 3.1.2. Samples obtained by sieving method 2

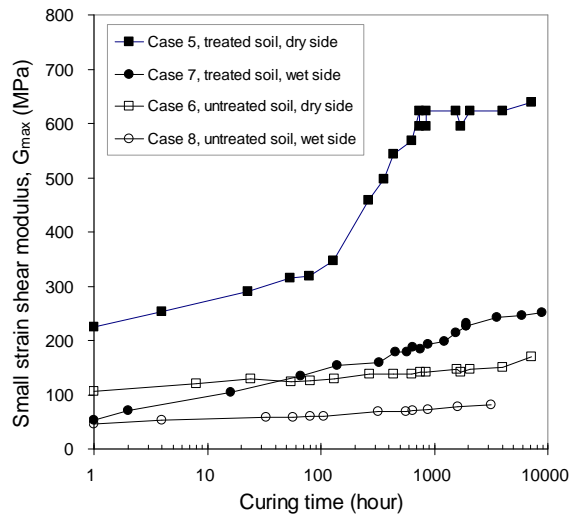
Figure 3-2 depicts  $G_{\max}$  versus time for the silt specimens prepared by sieving method 2 and treated with 0% / 2% lime. We observe globally that the  $G_{\max}$  curves are similar to the corresponding curves with sieving method 1, for both the untreated and treated silt, though the treated wet specimens show significantly lower  $G_{\max}$  values with method 1.

As with method 1, we can observe similar phenomena with method 2: (i) an immediate treatment effect of lime after compaction; (ii) similar  $G_{\max}$  curves over time; and (iii) a significant water content effect (dry and wet side) for both treated and untreated specimens.

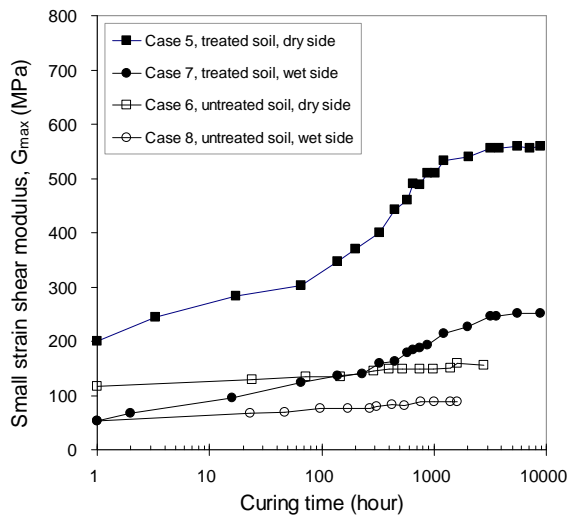
We also observe some differences, especially for the treated specimens: (i) the first relative stabilization of  $G_{\max}$  comes earlier than with method 1 (around 20 hours instead of hundreds of hours); (ii) the initial value and the  $G_{\max}$  over time for the wet side are lower than that with method 1; the transition from phase 1 to phase 2 is less evident than that with method 1; (iii) the gap of  $G_{\max}$  value between the wet and dry sides is larger than with method 1.



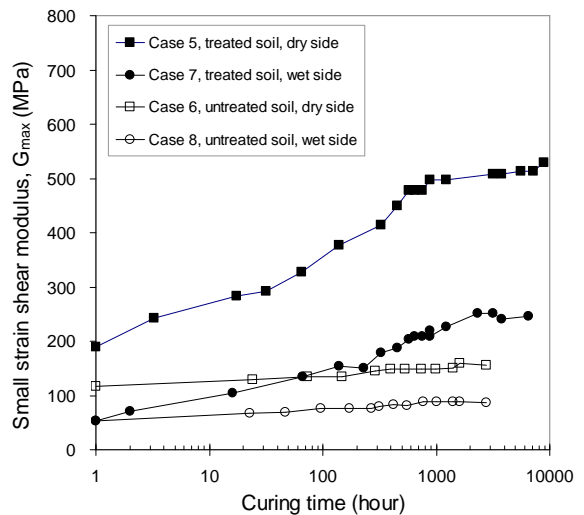
(a)  $D_{max} = 0.4 \text{ mm}$



(b)  $D_{max} = 1 \text{ mm}$



(c)  $D_{max} = 2 \text{ mm}$



(d)  $D_{max} = 5 \text{ mm}$

Figure 3-2 Small strain shear modulus ( $G_{max}$ ) versus curing time for the silt treated with lime (sieving method 2)

## 3.2. Results on silty soil treated with cement

### 3.2.1. Samples obtained by sieving method 1

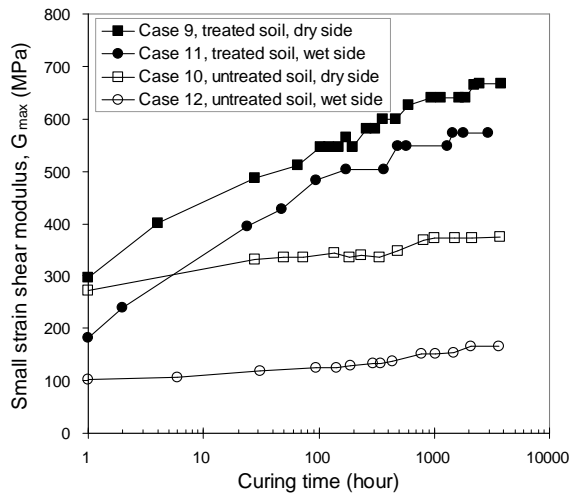
Figure 3-3 shows the  $G_{max}$  development for the silt prepared by sieving method 1 and then treated by 0% / 3% cement. For the sub-series of  $D_{max} = 0.4 \text{ mm}$  (Figure 3-3a), in the case of untreated specimens, just after compaction, the  $G_{max}$  is 272 MPa for the dry side ( $w_f = 14\%$ , case 10), and is 102 MPa for the wet side ( $w_f = 21\%$ , case 12). The values develop

slightly over time and reach their relative stabilization after 80 hours at 335 MPa and 120 MPa, respectively. Then (at around 300 hours), they increase slightly over time, until stabilisation after 1000 hours, at 372 MPa and 152 MPa, respectively. On the other hand, in the case of 3% cement treated specimens (case 9 and 11), after compaction,  $G_{\max}$  is equal to 296 MPa for the dry side ( $w_f = 14\%$ , case 9), and 183 MPa for the wet side ( $w_f = 21\%$ , case 11). Similar to the lime treatment, the cement treatment also has a significant immediate effect on  $G_{\max}$  just after the compaction, especially for the wet side. Over time  $G_{\max}$  also increases and reaches a first stabilization level after 100 hours, at 547 MPa for the dry side (case 9) and at 490 MPa for the wet side (case 11). Thereafter, the values of  $G_{\max}$  increase continuously until reaching another stabilization level after 2000 hours at 666 MPa and 574 MPa, respectively. As for the lime treatment, the stabilized  $G_{\max}$  value for the dry side is also higher than that for the wet side, for both cement treated and untreated silts. Interestingly, the  $G_{\max}$  curves for the dry side and wet side are almost parallel.

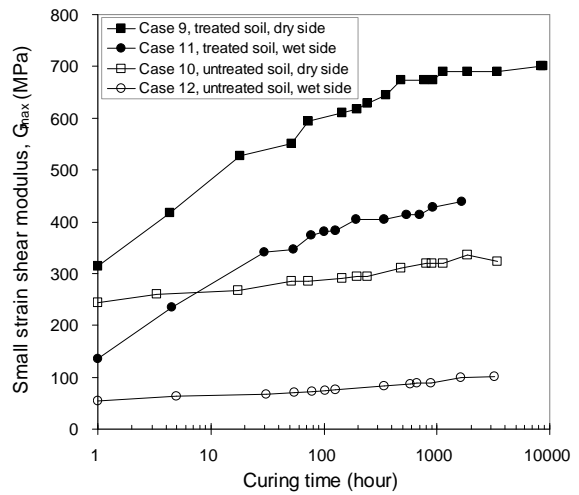
We observe similar phenomena for other sub-series ( $D_{\max} = 1.0 \text{ mm}$  in Figure 3-3b,  $2.0 \text{ mm}$  in Figure 3-3c and  $5.0 \text{ mm}$  in Figure 3-3d): (i) an immediate  $G_{\max}$  gain after compaction due to the cement-treatment effect; (ii) a slight development of  $G_{\max}$  for untreated specimens; (iii) an increase of  $G_{\max}$  with the logarithm of time for the 3% cement treated specimens; (iv) a stabilization of  $G_{\max}$  1000 hours after compaction, with a higher value for the dry side than for the wet side; (v) an almost parallel  $G_{\max}$  curves are obtained for the dry and wet sides.

Comparison of cement treatment and lime treatment shows that: (i) cement treatment gives a more significantly stiffness increase even at the beginning of curing; (ii) the transition between the two  $G_{\max}$  development phases is not as clear as for lime treatment; (iii) the  $G_{\max}$  for the wet side is also increasing significantly; (iv) the curves for the dry and wet sides are almost parallel.

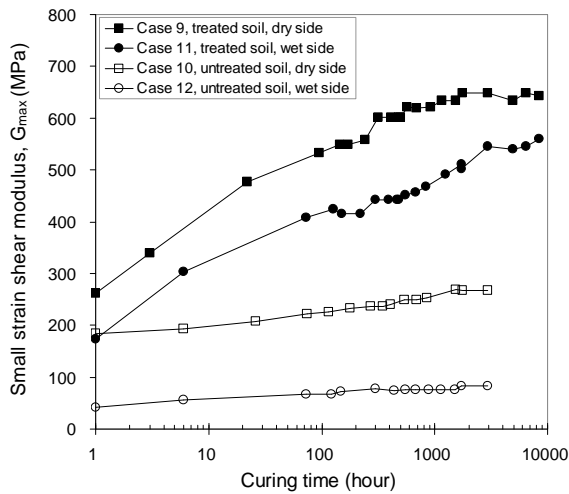
For the cement treatment, the higher  $G_{\max}$  development occurs in the early stage of curing. This is probably due to the immediate reaction of cement with water, forming cementitious compounds that crystallize in this stage. On the contrary, the hydration of lime does not provide cementitious products. The similar  $G_{\max}$  curves between the dry and wet sides for the cement treatment indicate lower water dependency than in the case of lime treatment.



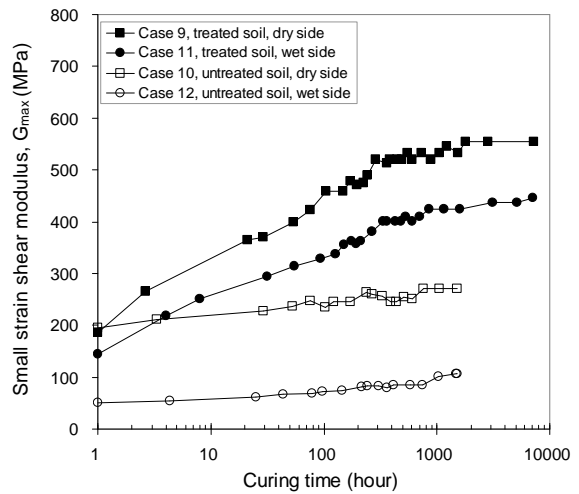
(a)  $D_{max} = 0.4 \text{ mm}$



(b)  $D_{max} = 1 \text{ mm}$



(c)  $D_{max} = 2 \text{ mm}$



(d)  $D_{max} = 5 \text{ mm}$

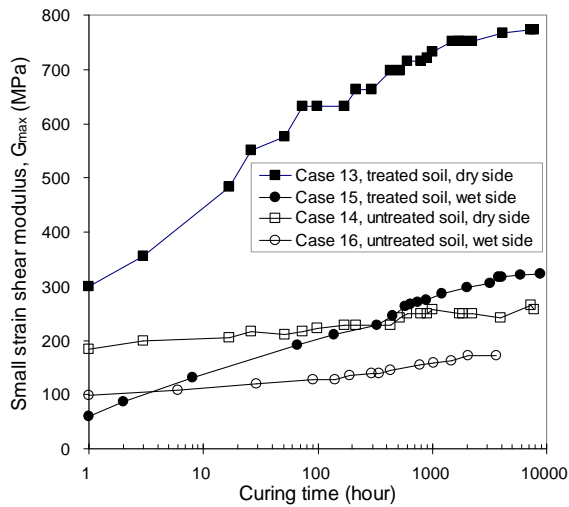
Figure 3-3 Small strain shear modulus ( $G_{max}$ ) versus curing time for the silt treated with cement (sieving method 1)

### 3.2.2. Samples obtained by sieving method 2

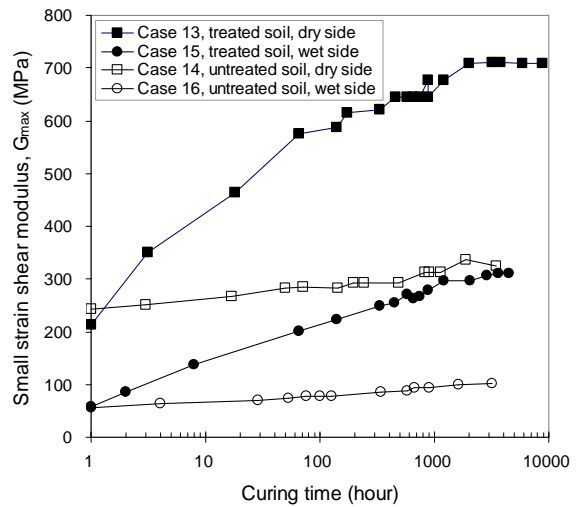
Figure 3-4 presents  $G_{max}$  evolution over time for the silt prepared by sieving method 2 and treated by 0% / 3% cement. Although most observations are similar to that for sieving method 1, some clear differences between treated specimens can be identified (case 13 and 15), especially for the wet side (case 15): (i) both the initial value of  $G_{max}$  and its development for the wet side are largely lower than that obtained with method 1, and even lower than that of the untreated dry specimens in the early stage; (ii) the curves of dry and wet sides are no



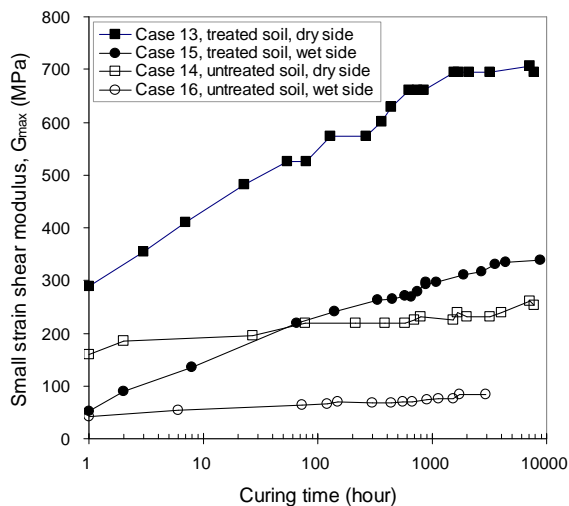
longer parallel; (iii) the difference in  $G_{max}$  value between wet side and dry side seems to be much larger than for method 1.



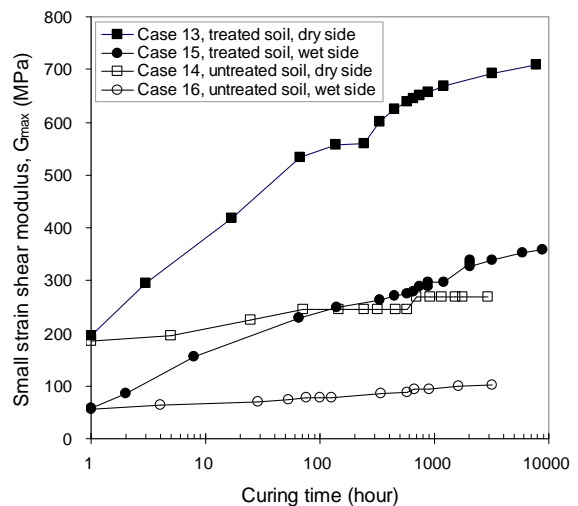
(a)  $D_{max} = 0.4$  mm



(b)  $D_{max} = 1$  mm



(c)  $D_{max} = 2$  mm



(d)  $D_{max} = 5$  mm

Figure 3-4 Small strain shear modulus ( $G_{max}$ ) versus curing time for the silt treated with cement (sieving method 2)

Summarising, the common points and differences between the lime and cement treatments indicate that  $G_{max}$  development is strongly water content and treatment dependent.

1) Water effect: for both treated and untreated silt, the final  $G_{max}$  decreases with water content increase. It is logical because the soil aggregates are stiff when they are at dry state;

by contrast, they are soft at wet state. In other words, the suction may be responsible for the differences;

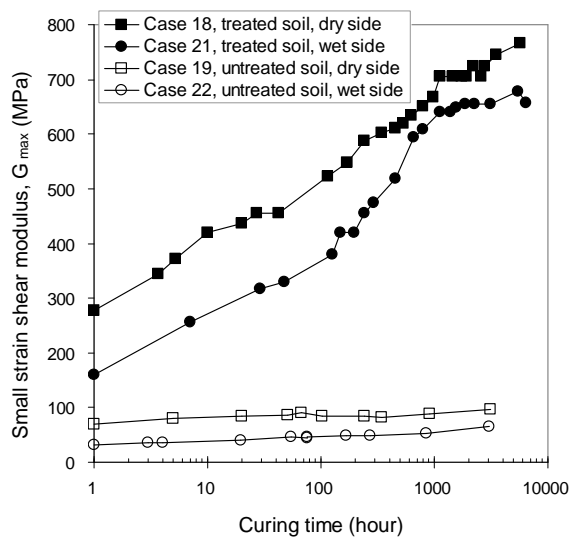
2) Treatment effect: at the same compaction conditions (water content and dry density), the treated silt has a higher  $G_{max}$  value than untreated one. This indicates that the treatment can reinforce the aggregates and strengthen them by bounds of cementitious compounds.

### 3.3. Results for the clay treated with lime

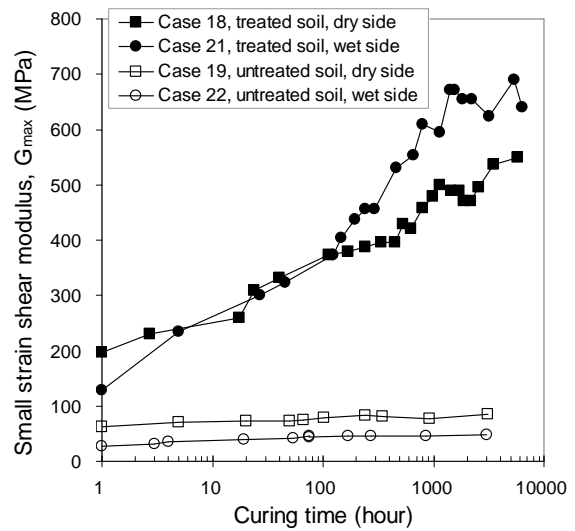
#### 3.3.1. Samples obtained by mixing method A

Figure 3-5 presents the results of  $G_{max}$  change over time for the clay treated by 0% / 4% lime, with mixing method A. For the soil of  $D_{max} = 0.4 \text{ mm}$  (Figure 3-5a), in the case of untreated specimens, just after the compaction,  $G_{max}$  is 68 MPa for the dry side ( $w_f = 25\%$ , case 19), and 31 MPa for the wet side ( $w_f = 35\%$ , case 22). The values increase slightly over time and reach their relative stabilization after 20 hours for the dry side (84 MPa) and 54 hours for the wet side (46 MPa). Then (after about 50 hours), they increase rather slowly and reach the stabilisation after 3000 hours at 97 MPa and 65 MPa for the dry and wet sides, respectively. Note that the second increase for the untreated clay is not as obvious as for the untreated silt. In the case of 4% CaO treated specimens (case 18 and 21), just after compaction,  $G_{max}$  is equal to 277 MPa for the dry side ( $w_f = 25\%$ , case 18), and 160 MPa for the wet side ( $w_f = 35\%$ , case 21). Compared to the untreated specimens, the lime treated ones show an immediate and significant effect of treatment on  $G_{max}$ . Then, the  $G_{max}$  also increases with time and reach a relative stabilization after 28 hours for both the dry side (456 MPa) and wet side (310 MPa). Thereafter (about 100 hours), as for the lime treated silt, the treated clay also shows a first increase phase followed by a second one which is faster until stabilization after 1400 hours (705 MPa and 640 MPa for the dry and the wet sides, respectively). Later, the  $G_{max}$  increases much slower than in the previous periods, especially in the case of high water content ( $w_f = 35\%$ ). Also as for the silt, the stabilized  $G_{max}$  value for lower water content is higher than the one for higher water content, for both the treated and untreated clay. In addition, for the untreated clay, the  $G_{max}$  curves for the dry and wet sides are almost parallel. However, for the 4% lime treated clay, the  $G_{max}$  curve for the dry side seems to be

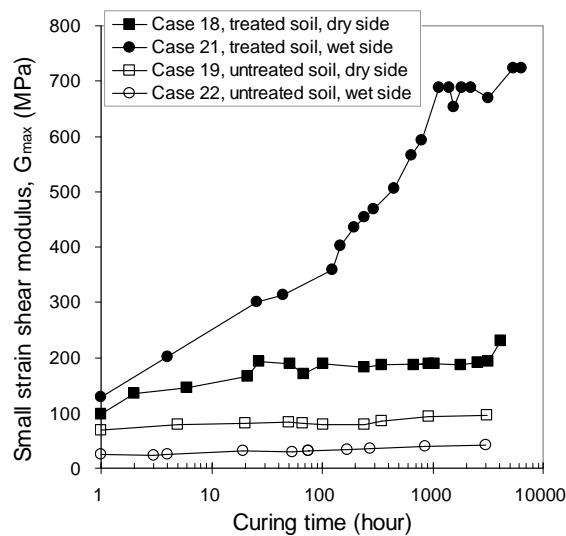
parallel to that for the wet side during the first 200 hours, but approaches the wet side curve afterwards.



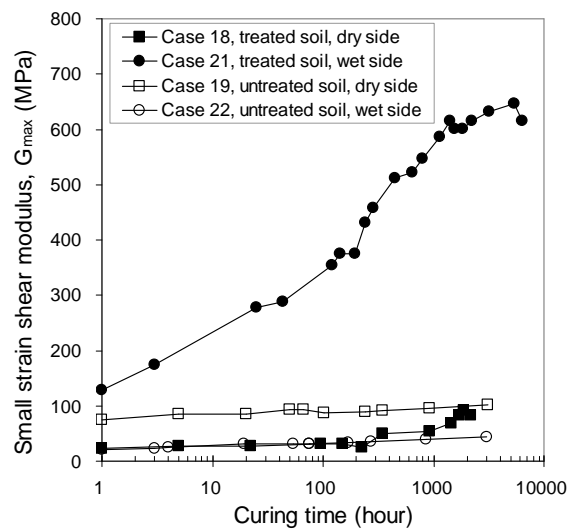
(a)  $D_{max} = 0.4$  mm



(b)  $D_{max} = 1$  mm



(c)  $D_{max} = 2$  mm



(d)  $D_{max} = 5$  mm

**Figure 3-5 Small strain shear modulus ( $G_{max}$ ) versus curing time for the clay treated with 4% lime (mixing method A)**

Examination of the results of soil passed through 0.4 mm sieve (Figure 3-5a), 1.0 mm sieve (Figure 3-5b), 2.0 mm sieve (Figure 3-5c) and 5.0 mm sieve (Figure 3-5d) shows significant difference in  $G_{max}$  curves for treated specimens of dry side (case 18). By contrast, similar curves are obtained for the wet side (case 21). In other words, the initial aggregate

size effect on the specimens of dry side is much more significant than on the specimens of wet side. Thereby, it is worthy to discuss the case of dry side and the case of wet side separately.

For the specimen of wet side (case 21), the  $G_{\max}$  curve seems to be similar to that of lime treated silt (see Figure 3-1 and Figure 3-2): (i) a slight increase of  $G_{\max}$  over time for the untreated specimens; (ii) an immediate treatment effect after compaction; (iii) a two-phase  $G_{\max}$  development for the treated specimens - an increasing nonlinear curve followed by another one much faster (starting at around 100 hours); (iv) a stabilization of  $G_{\max}$  about 1400 hours after the treatment.

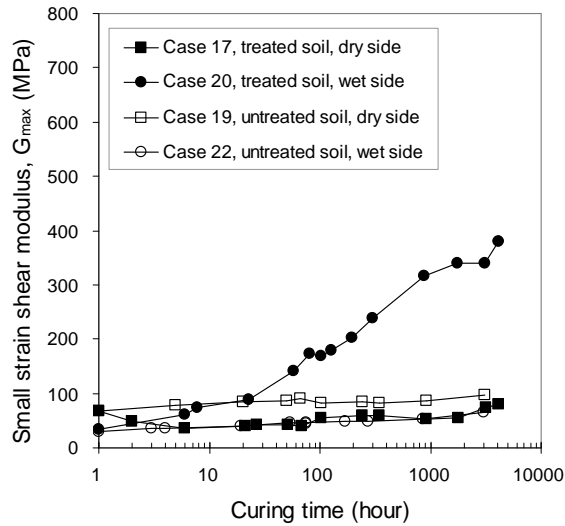
For the 4% lime treated clay on the dry side (case 18), both the initial  $G_{\max}$  value and its development present a significant changes with the increase of soil's  $D_{\max}$ . For the initial value after compaction, it decreases to 198 MPa for  $D_{\max} = 1\text{mm}$ , 96 MPa for  $D_{\max} = 2\text{mm}$  and 23 MPa for  $D_{\max} = 5\text{mm}$ . Note that for  $D_{\max} = 5\text{mm}$ , the treated clay even has a lower initial  $G_{\max}$  than untreated one. During curing time, the  $G_{\max}$  development shows a decreasing effect of lime treatment with increase of  $D_{\max}$ : a significant increase over time for  $D_{\max} = 0.4\text{mm}$  followed in a decreasing order by  $D_{\max} = 1\text{mm}$ ,  $D_{\max} = 2\text{mm}$  and  $D_{\max} = 5\text{mm}$ .

By comparing the  $G_{\max}$  development of the specimens of these sub-series prepared on dry and wet sides, we observe that: 1) for  $D_{\max} = 0.4\text{mm}$ , the  $G_{\max}$  for the dry side is higher than that for wet side; 2) for  $D_{\max} = 1\text{mm}$ , the  $G_{\max}$  for the wet side exceeds that for the dry side after around 100-hour curing; 3) for larger aggregate sizes ( $D_{\max} = 2\text{mm}$  and  $5\text{mm}$ ), the  $G_{\max}$  for the dry side is always lower than for the wet side after compaction.

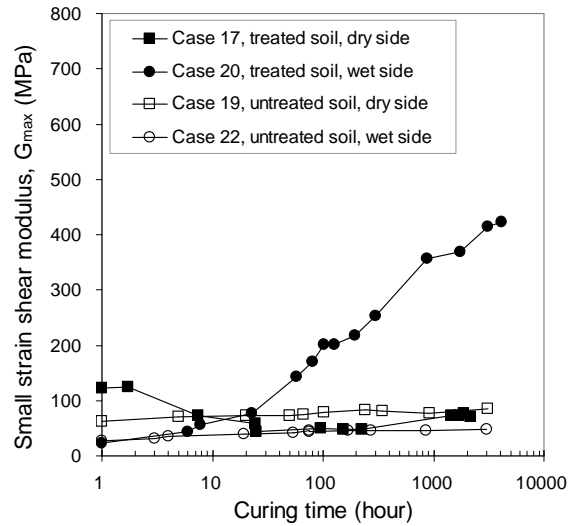
Summarising, for the untreated clay, the wet side corresponds to higher water contents and thereby a lower  $G_{\max}$ . For the 4% lime treated one, the high water content on the wet side allows a fully development of  $G_{\max}$ . Moreover, this development is similar for all values of  $D_{\max}$  considered. On the contrary, the low water content on the dry side enables a limited development of  $G_{\max}$ , but with a clearer effect of  $D_{\max}$ : the larger the aggregate size, the slower the  $G_{\max}$  development.

### 3.3.2. Samples obtained by mixing method B

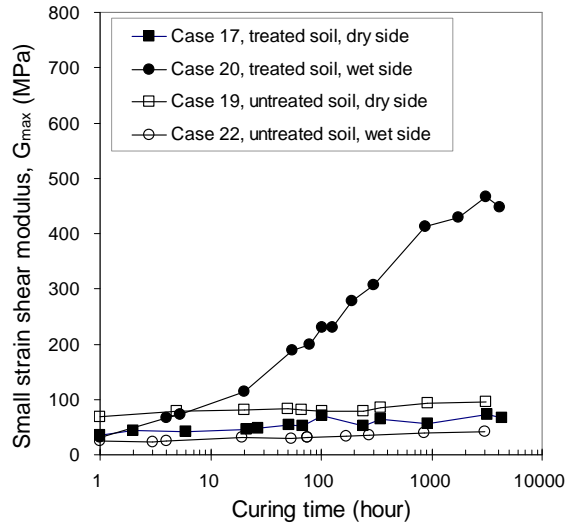
Figure 3-6 describes the  $G_{\max}$  versus time for the untreated and 4% lime treated clay with mixing method B, both compacted on dry side ( $w_f = 25\%$ ) and wet side ( $w_f = 35\%$ ).



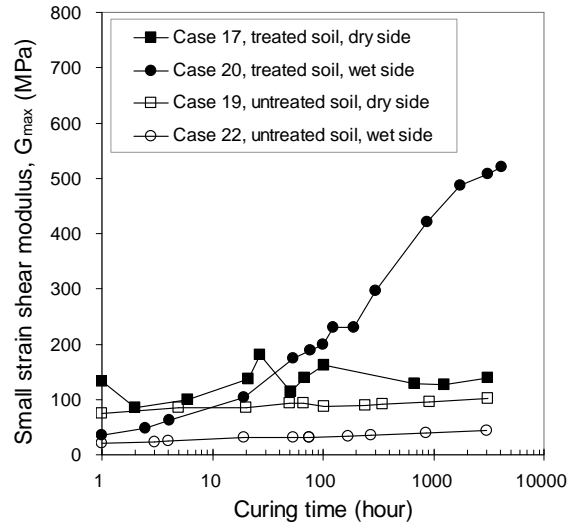
(a)  $D_{max} = 0.4$  mm



(b)  $D_{max} = 1$  mm



(c)  $D_{max} = 2$  mm



(d)  $D_{max} = 5$  mm

Figure 3-6 Small strain shear modulus ( $G_{max}$ ) versus curing time for the clayey soil treated with 4% lime (mixing method B)

In the case of untreated specimens of different sub-series ( $D_{max} = 0.4 / 1 / 2 / 5$  mm), the  $G_{max}$  of dry specimens just after compaction (case 19) ranges from 63 to 75 MPa. These values increase slightly and reached their stabilisation after 1000 hours at 80 ~ 90 MPa. The  $G_{max}$  of wet specimens (case 22) shows nearly parallel evolution to that of dry specimens, though with lower values.

In the case of 4% lime treated specimens, for the dry side (case 17), they show comparable values of  $G_{\max}$  with untreated ones, although their variations are much larger. The  $G_{\max}$  does not well develop over time (ex.  $D_{\max} = 2 \text{ mm}$ ). By contrast, it often decreases during several hours after compaction (ex.  $D_{\max} = 0.4 \text{ mm}, 1 \text{ mm and } 5 \text{ mm}$ ). On the other hand, for the wet side (case 20), similar curves are obtained for the specimens at different initial  $D_{\max}$ . They all start with a low  $G_{\max}$  value just after compaction, as for the untreated soils, then increase slowly. Thereafter, they increase much faster after about 20 hours, and finally show another slower increase after 1000 hours.

Under the same soil state (water content and density) and treatment as for mixing method A, the wet treated specimens also have a two-phase  $G_{\max}$  development curve (phase 2 begins at about 20 hours). However, different mixing methods give different results: on dry side, instead of having a significant effect of initial  $D_{\max}$  on  $G_{\max}$  for method A, method B results in equivalent values to that of untreated specimens. On wet side, method B shows lower initial values and slower development of  $G_{\max}$  than method A.

### **3.4. Results on the clay treated with mixture**

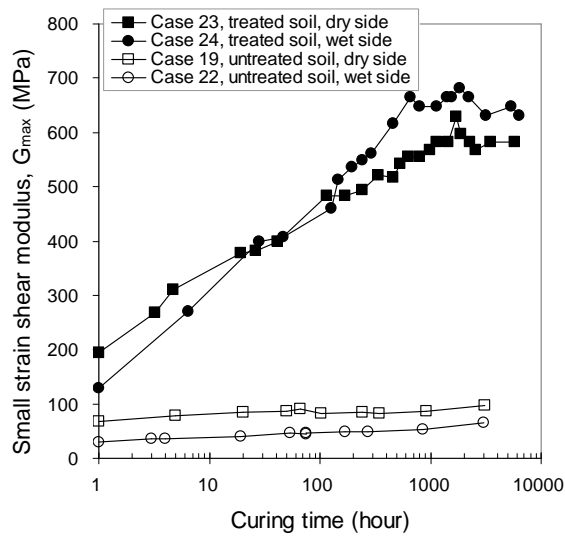
#### **3.4.1. Samples obtained by mixing method A**

Figure 3-7 depicts the  $G_{\max}$  changes over time for the untreated and mixture (2% lime + 3% cement) treated clay with mixing method A, for both the dry side ( $w_f = 25\%$ ) and the wet side ( $w_f = 35\%$ ). For the mixture treated specimens, we observe: 1) an immediate gain of  $G_{\max}$  just after compaction for both the dry and wet sides, apart from the soils on dry side with  $D_{\max} = 5 \text{ mm}$  (case 23, Figure 3-7d); 2) a nearly linear relationship between  $G_{\max}$  and the logarithm of time; and 3) a relative stabilisation starting after around 1000 hours.

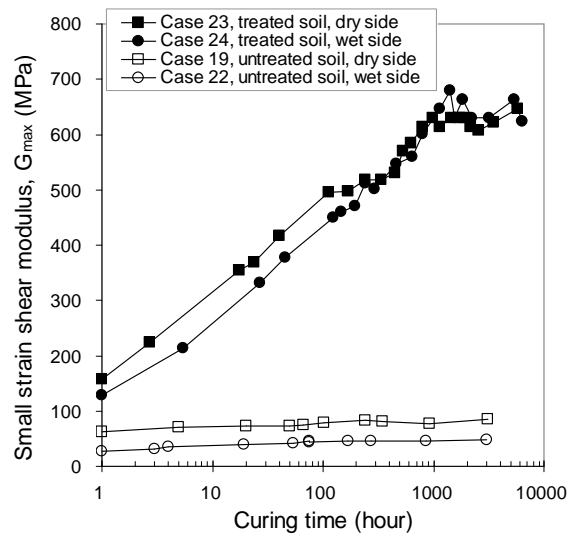
For the treated specimens compacted on the wet side (case 24), the  $G_{\max}$  curves seem to be similar for different  $D_{\max}$ : (i) similar  $G_{\max}$  values after compaction (128 ~ 139 MPa); (iii) similar development - a linear relationship between  $G_{\max}$  and the logarithm of time, unlike the two-phase development in the case of lime treatment; (iv) similar values at stabilization, after around 1000 hours (648 ~ 707 MPa).

For the treated specimens compacted on the dry side (case 23), both the initial value of  $G_{\max}$  and its development present significant effects of  $D_{\max}$ . For the initial value, it

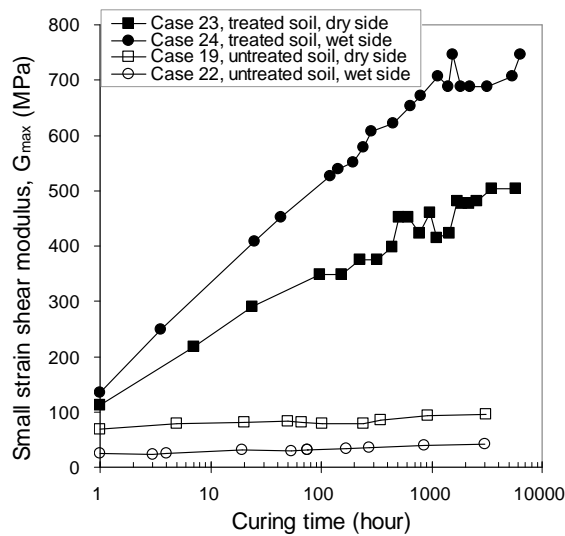
decreases with rise of  $D_{max}$  (195, 157, 113 and 45 MPa for  $D_{max} = 0.4$  mm, 1 mm, 2 mm and 5 mm, respectively). Note the limited development of  $G_{max}$  for  $D_{max} = 5$  mm.



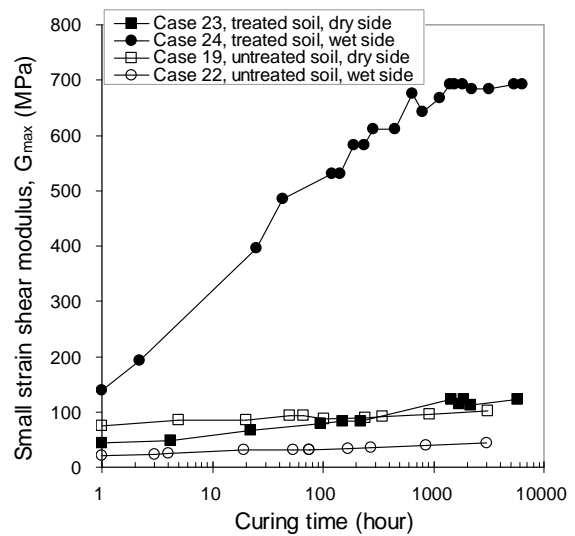
(a)  $D_{max} = 0.4$  mm



(b)  $D_{max} = 1$  mm



(c)  $D_{max} = 2$  mm



(d)  $D_{max} = 5$  mm

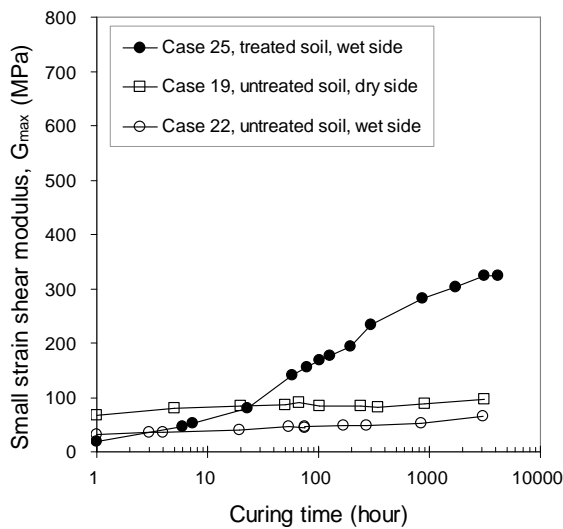
Figure 3-7 Small strain shear modulus ( $G_{max}$ ) versus curing time for the clayey soil treated with 2% CaO + 3% cement (mixing method A)

As for the lime treated soils with mixing method A, the results of mixture treated clays show: 1) an evolution of  $G_{max}$  curve with  $D_{max}$  for the dry side (less significant than for lime treatment); 2) similar phenomena for different  $D_{max}$  values for the wet side. In other words, the effect of  $D_{max}$  on  $G_{max}$  is much more significant for dry side than for wet side.

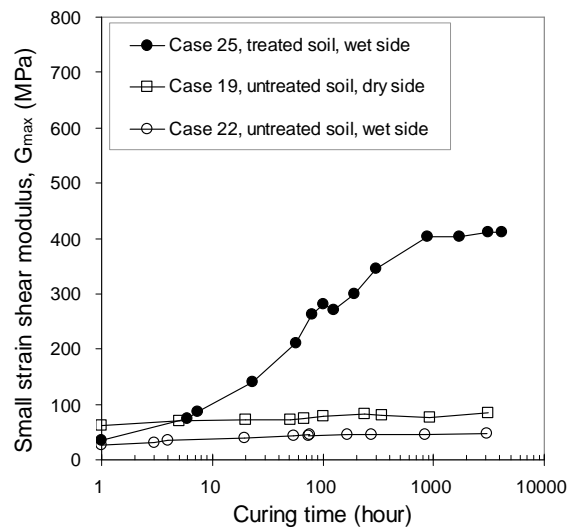
Compared to the lime treated clay, the mixture treated one show: 1) a one-phase curve instead of two-phase one; 2) a less significant reduction of  $G_{max}$  with the rise of  $D_{max}$  for the dry side.

### 3.4.2. Samples obtained by mixing method B

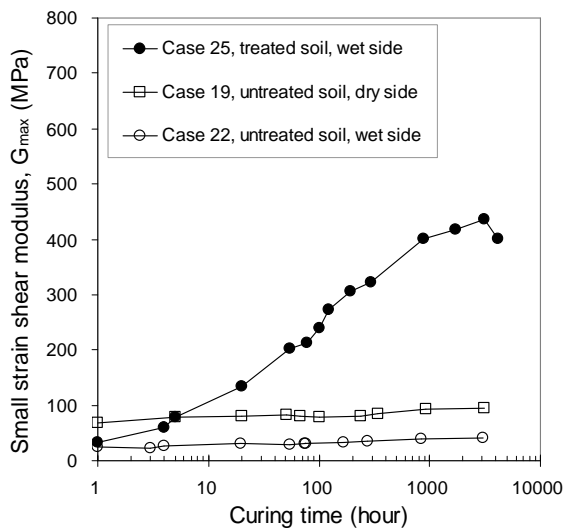
Figure 3-8 depicts the  $G_{max}$  variations over time for the mixture treated (2% lime + 3% cement) clay with mixing method B.



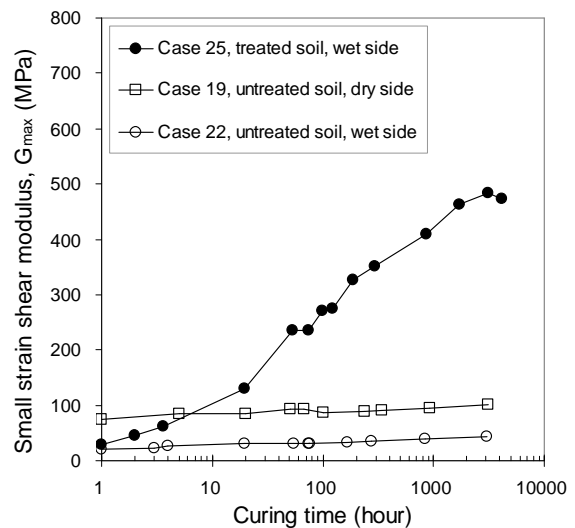
(a)  $D_{max} = 0.4$  mm



(b)  $D_{max} = 1$  mm



(c)  $D_{max} = 2$  mm



(d)  $D_{max} = 5$  mm

Figure 3-8 Small strain shear modulus ( $G_{max}$ ) versus curing time for the clayey soil treated with 2% CaO + 3% cement (mixing method B)



For the dry side ( $w_f = 25\%$ ), the test was not performed as the dry specimens cannot be well prepared at a preparation water content as low as  $w_i = 29\%$  because of the marked concentration of non-hydrated additives within the visible inter-aggregates pores. This concentration leads to weakening of the contacts between aggregates. Thereby, even a feeble disturbance produced by the measurements may result in visible fissures on the specimens. Note that the fissures may also be responsible for the large variations of  $G_{\max}$  in case of 4% lime treated clay mixed with the same method B and compacted at the same water content (see Figure 3-6). In fact, the water loss test (cf. Chapter 2) also shows a higher  $w_{\text{lost}}$  for the mixture treated clay than for the 4% lime treated clay, indicating the shortage of available water for different reactions.

The treated specimens compacted on wet side (case 25,  $w_f = 35\%$ ) share similar initial values of  $G_{\max}$  as untreated ones (case 22). Moreover, they also have similar  $G_{\max}$  curves during curing. Surprisingly, this two-phase curve of  $G_{\max}$  development is similar to that with lime treatment, also with mixing method B. Comparison of the linear curve obtained with mixing method A indicates that the  $G_{\max}$  development is strongly influenced by the mixing methods.

### 3.5. Aggregate size effect on shear modulus

As mentioned in chapter 1, chemical reactions occur immediately after adding lime and/or cement to a wet soil. These reactions may result in short-term modification of soil by hydration (ex. cation exchange, flocculation/agglomeration, etc.) or long term solidification (ex. hydration in case of cement treatment and/or pozzolanic reaction in case of lime treatment, etc.). Both the modification and the solidification processes change the  $G_{\max}$  value of soils. In the literature, the microstructure analysis of treated soil also indicates that these two processes may also be affected by the aggregate size.

#### 3.5.1. For the silty soil

We investigate the initial small strain shear modulus value ( $G_0$ ) for short term modification analysis.  $G_0$  is defined as the immediate  $G_{\max}$  just after compaction - after one hour mellowing or treatment (omitting the compaction period in the moulding state). Physically,  $G_0$  mainly reflects the effect of modification induced by the initial hydration process. Figure 3-9 and Figure 3-10 depict  $G_0$  versus  $D_{\max}$  for the 2% lime treated (Figure

3-9) and 3% cement treated (Figure 3-10) silt, compacted on dry and wet sides, respectively. Note that two preparation methods (method 1 and method 2) of soil powders are involved for each treatment.

For the 2% lime treated silt, in the case of sieving method 1 (Figure 3-9a), the  $G_0$  of treated specimens (case 1 and 3) decreases with the rise of  $D_{max}$ , for both dry and wet sides. For the corresponding untreated specimens (case 2 and 4), the  $G_0$  is lower than that of treated ones; it also decreases with the rise of  $D_{max}$ . In the case of method 2 (Figure 3-9b), however, on dry side, the trend for the treated specimens (case 5) is not clear, as it first rises and then decreases unlike the untreated ones that show slight increases (case 6). On the wet side, it is constant for both treated (case 7) and untreated (case 8) specimens. Note that the wet specimens have similar  $G_0$  values for both treated and untreated cases (case 6 and 8). In addition, for the two preparation methods, the  $G_0$  of dry specimens is obviously decreasing with the rise of  $D_{max}$ , except  $D_{max} = 0.4 \text{ mm}$ . The exception is probably related to the difficulty of mixing soils as fine as  $D_{max} = 0.4 \text{ mm}$  (see the mixing effect in Figure 2-7 and Figure 2-9).

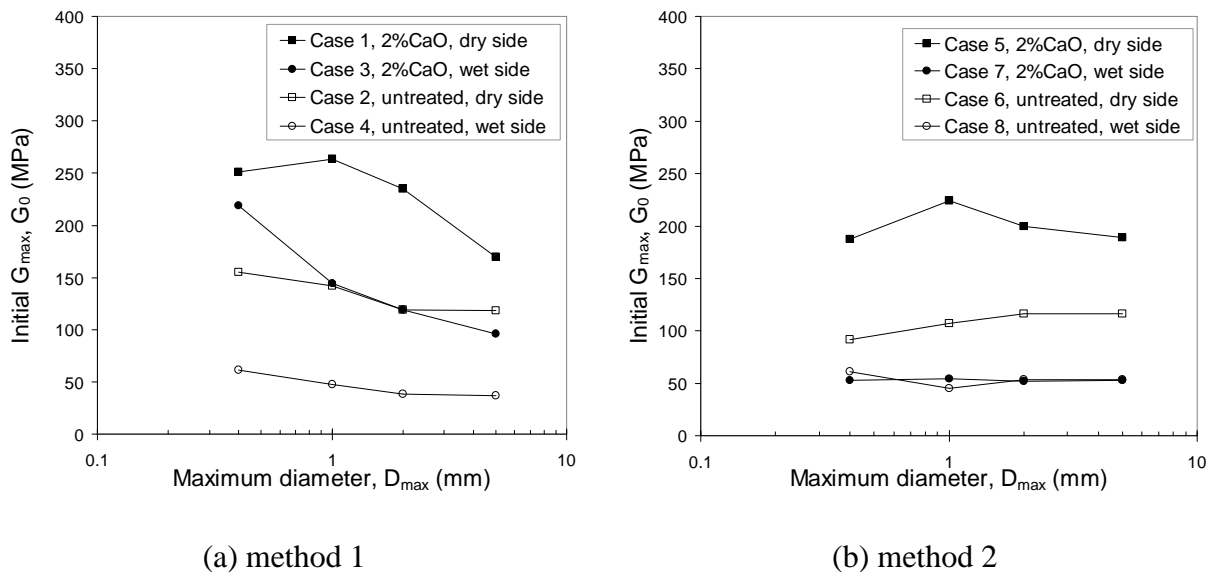


Figure 3-9 Aggregates size effects on  $G_0$  for the 2% CaO treated silt with mixing method B

For the 3% cement treated silt (Figure 3-10), despite a large variation of  $G_0$  with  $D_{max}$ , similar observations can be made as in the case of lime treatment: 1) for the treated and untreated soils with method 1 (Figure 3-10a),  $G_0$  is globally decreasing with the rise of  $D_{max}$ ;

2) for the soils with method 2 (Figure 3-10b),  $G_0$  is also decreasing for the dry side but it seems to be constant for the wet side.

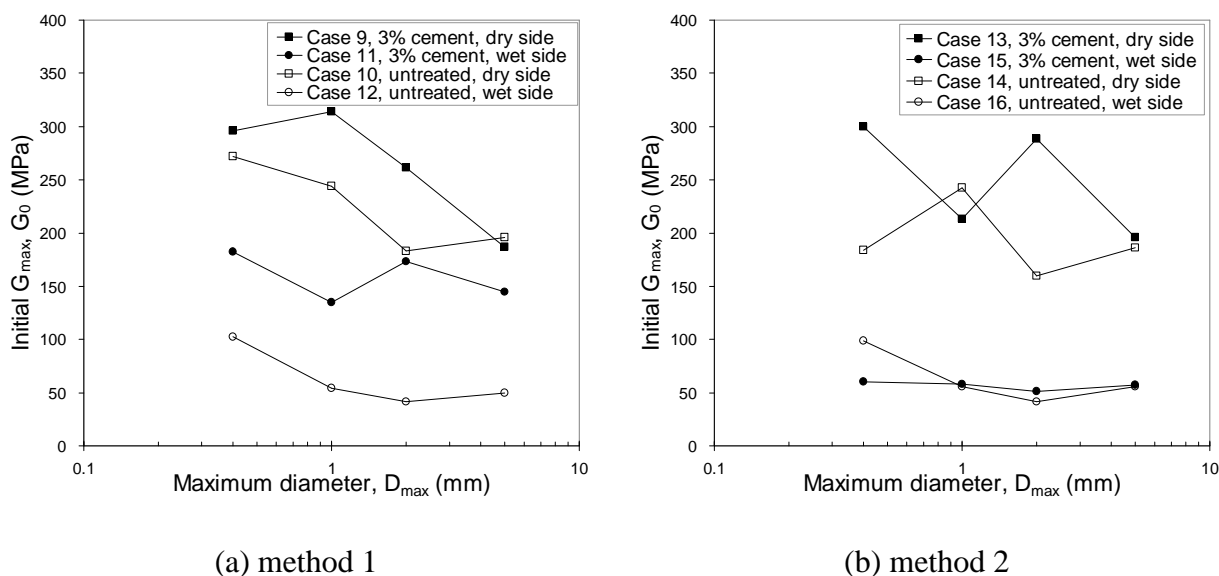
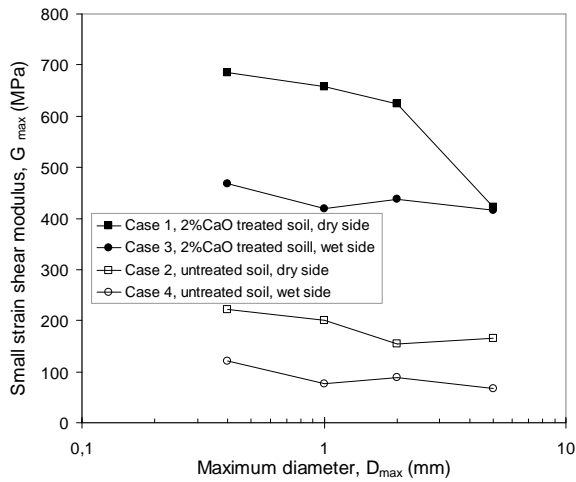


Figure 3-10 Initial stiffness value  $G_0$  for the 3% cement treated silt with mixing method B

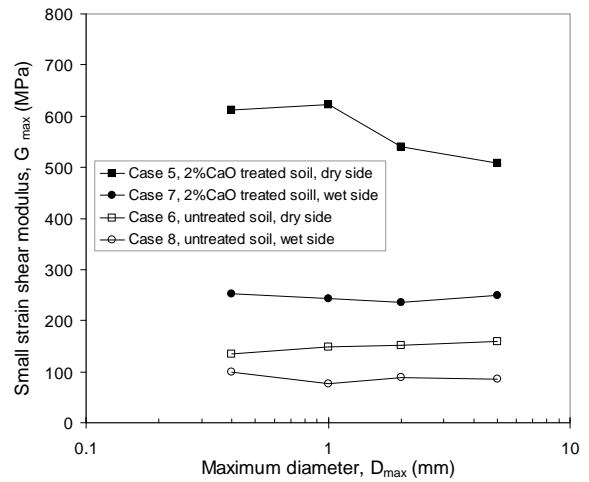
In other words,  $G_0$  globally decreases with the rise of  $D_{max}$  for both lime and cement treated silt; the decreasing rate is higher for the dry side than for the wet side; the decreasing rate is more notable for soils prepared by method 1 than by method 2.

In order to analyse the long term effect, in the following, the final  $G_{max}$  values are compared as a function of  $D_{max}$ .

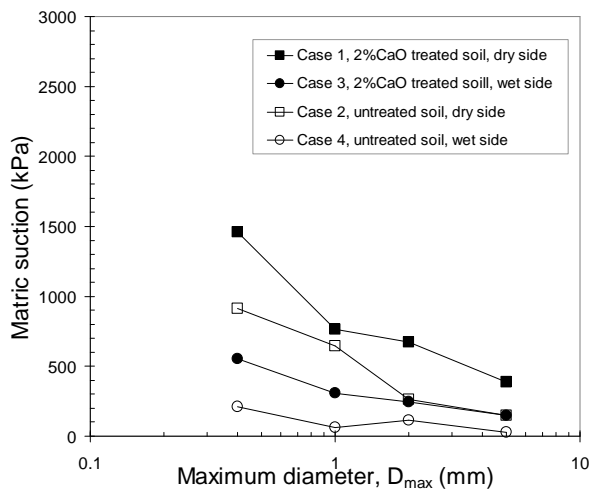
Figure 3-11 presents the final values of  $G_{max}$  (at around 2000 hours) versus  $D_{max}$  for the 2% treated silt by sieving method 1 and 2. Considering the close relationship between the shear modulus and suction (c.f. chapter 1), the corresponding matrix suction -  $D_{max}$  relationship is also given.



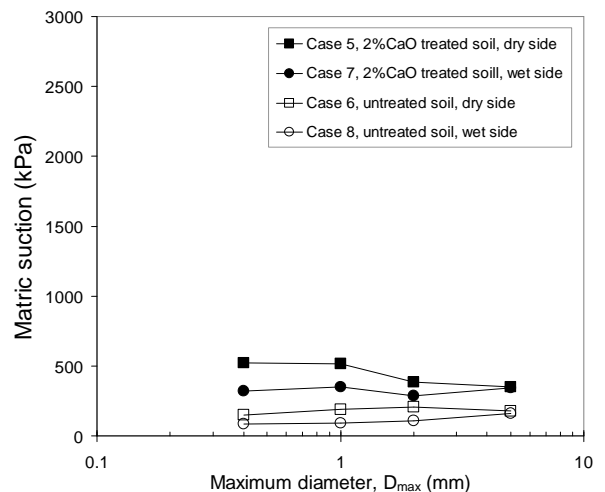
(a)  $G_{max}$  versus  $D_{max}$  (method 1)



(b)  $G_{max}$  versus  $D_{max}$  (method 2)



(c) Matrix suction versus  $D_{max}$  (method 1)



(d) Matrix suction versus  $D_{max}$  (method 2)

**Figure 3-11** Relative stabilization  $G_{max}$  (about 2000 hours) versus  $D_{max}$  for the lime treated silt prepared by sieving method 1 and 2, mixing method B

For sieving method 1, the  $G_{max}$ - $D_{max}$  curve shows that (Figure 3-11a): (i) on the dry side (case 1),  $G_{max}$  decreases with the rise of  $D_{max}$  for treated silt, with the highest value of 685 MPa for  $D_{max} = 0.4 \text{ mm}$  and the lowest value of 422 MPa for  $D_{max} = 5.0 \text{ mm}$ ; (ii) on the wet side (case 3), the decrease trend for  $G_{max}$  is not as clear as in the case of dry side, with the highest value of 468 MPa for  $D_{max} = 0.4 \text{ mm}$  and the lowest value of 416 MPa for  $D_{max} = 5 \text{ mm}$ ; (iii) for the untreated silts (case 2 and 4), the final  $G_{max}$  also shows a slightly decreasing trend with the rise of  $D_{max}$ , for both the dry and wet sides, within a range of 222 ~ 154 MPa for the dry side and a range of 121 ~ 68 MPa for the wet side. Apparently, this aggregate size effect on  $G_{max}$  is less obvious for the wet side than for the dry side. On the

other hand, the corresponding matrix suction- $D_{max}$  curve (Figure 3-11c) also shows that the matrix suction globally decreases with the increase of  $D_{max}$ , for both treated and untreated silts. It is particularly the case for the dry side with a trend similar to that of  $G_{max}$ - $D_{max}$  curves. Furthermore, the matrix suction of treated specimens is often higher than that of the corresponding untreated ones.

For sieving method 2 (Figure 3-11b and Figure 3-11d), similar observations can be made for the dry side (case 5): the higher the  $D_{max}$ , the lower the  $G_{max}$  and matrix suction values. However, for both the untreated and 2% lime treated specimens compacted on wet side, the effect of  $D_{max}$  on  $G_{max}$  is no longer appreciable, with negligible difference of  $G_{max}$  at various  $D_{max}$ .

Comparison between sieving method 1 and method 2 shows that the decreasing trend is globally more notable for method 1 than for method 2.

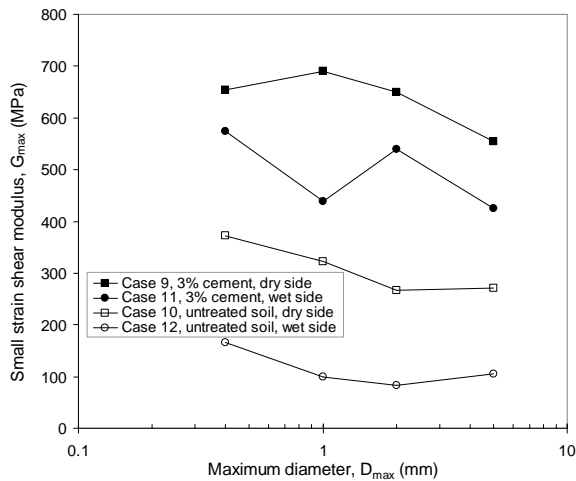
Figure 3-12 presents the stabilised values of  $G_{max}$  and the corresponding values of matrix suction versus  $D_{max}$  in the case of cement treated silt.

For the silt prepared by sieving method 1 (Figure 3-12a) and method 2 (Figure 3-12b), although some variations of  $G_{max}$  exist,  $G_{max}$  is also found to be decreasing with the rise of  $D_{max}$ , particularly for the dry side.

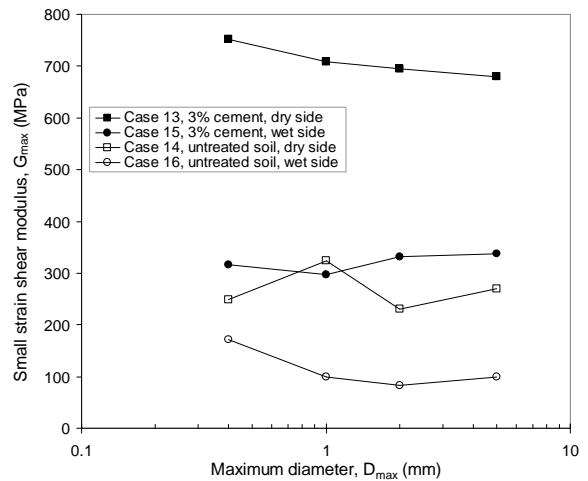
For sieving method 1, the treated silt compacted on dry side (case 9) shows the highest value of 690 MPa for  $D_{max} = 1 \text{ mm}$  and the lowest value of 555 MPa for  $D_{max} = 5.0 \text{ mm}$ ; However, the treated silt compacted on wet side (case 11) shows the highest value of 574 MPa for  $D_{max} = 0.4 \text{ mm}$  and the lowest value of 425 MPa for  $D_{max} = 5.0 \text{ mm}$ . In the case of untreated silt, both compaction sides show a slight decreasing trend, with the highest value of 372 MPa for  $D_{max} = 0.4 \text{ mm}$  and the lowest value of 271 MPa for  $D_{max} = 5.0 \text{ mm}$  for the dry side (case 10), and with the highest value of 165 MPa for  $D_{max} = 0.4 \text{ mm}$  and the lowest value of 83 MPa for  $D_{max} = 2.0 \text{ mm}$  (case 12).

For sieving method 2, similarly, the treated silt compacted on dry side (case 13) also shows a decreasing trend, the highest value being 752 MPa for  $D_{max} = 0.4 \text{ mm}$  and the lowest value being 680 MPa for  $D_{max} = 5.0 \text{ mm}$ . However, for the treated silt compacted on wet side (case 15) as well as the untreated silt (case 14 and 16), the decreasing trend is no longer clear.

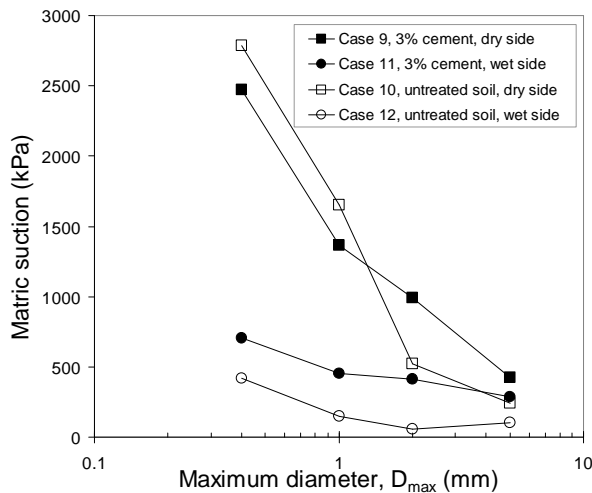
The corresponding suction changes with  $D_{max}$  show that the larger the  $D_{max}$ , the lower the suction, especially for method 1 (Figure 3-12c).



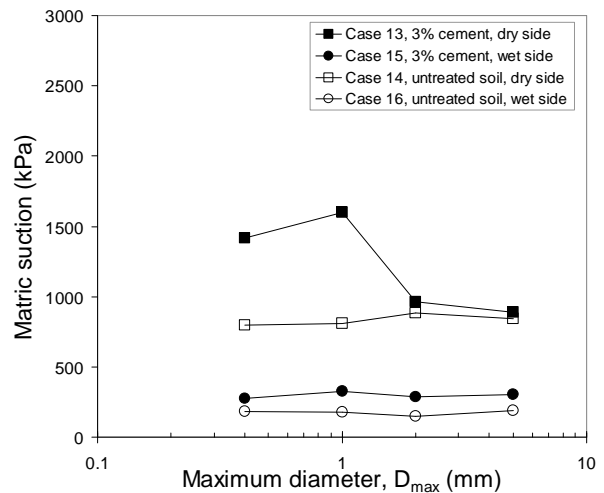
(a)  $G_{max}$  versus  $D_{max}$  (method 1)



(b)  $G_{max}$  versus  $D_{max}$  (method 2)



(c) Matrix suction versus  $D_{max}$  (method 1)



(d) Matrix suction versus  $D_{max}$  (method 2)

**Figure 3-12 Stabilised values of  $G_{max}$  (about 2000 hours) versus  $D_{max}$  for the cement treated silt by method 1 and method 2**

By comparing the 2% lime treated silt with the 3% cement treated one prepared by the two sieving methods, the following conclusions can be drawn: (i) both  $G_{max}$  and matrix suction are strongly influenced by the aggregate size as well as its distribution; (ii) a similar trend of  $G_{max}$  and the corresponding matrix suction versus  $D_{max}$  exists; (iii) the aggregate size effect (effect of  $D_{max}$  on  $G_{max}$ ) for the soil prepared by method 1 is more notable than that by method 2; (iv) the aggregate size effect is more significant for the dry specimens than for the wet specimens; (v) at the same  $D_{max}$ , sieving method 2 allows a lower suction value than method 1, especially for  $D_{max} = 0.4$  mm; (vi) at the same  $D_{max}$ , the dry side always results in a higher matrix suction than the wet side.

### 3.5.2. For the clayey soil

Figure 3-13 and Figure 3-14 depict the  $G_0$  variations with  $D_{max}$  for the 4% lime and 2% lime+3% cement treatments of clay specimens prepared by mixing method A (Figure 3-13) and method B (Figure 3-14), respectively.

For mixing method A, the  $G_0$  of 4% lime treated clay compacted on dry side (Figure 3-13a) is decreasing swiftly with the rise of  $D_{max}$  (case 18): from 277 MPa for  $D_{max} = 0.4 \text{ mm}$  to 23 MPa for  $D_{max} = 5 \text{ mm}$ ; it is also decreasing but less obviously in the case of wet side (case 21). For the untreated specimens,  $G_0$  changes with  $D_{max}$  are observed neither on dry side nor on wet side. Similar observations can be made for the mixture treatment (Figure 3-13b), but with a less sharply decreasing trend than for the lime treatment and compaction on dry side (case 23), and an almost constant trend for the wet side (case 24). In addition, for both treatments, we observe that: 1) the  $G_0$  of treated soils is often higher than that of untreated ones (an exception for  $D_{max} = 5 \text{ mm}$ ); 2) the  $G_0$  of the dry treated specimens is often higher than that of wet specimens for  $D_{max} \leq 1 \text{ mm}$ , except for  $D_{max} \geq 2 \text{ mm}$ .

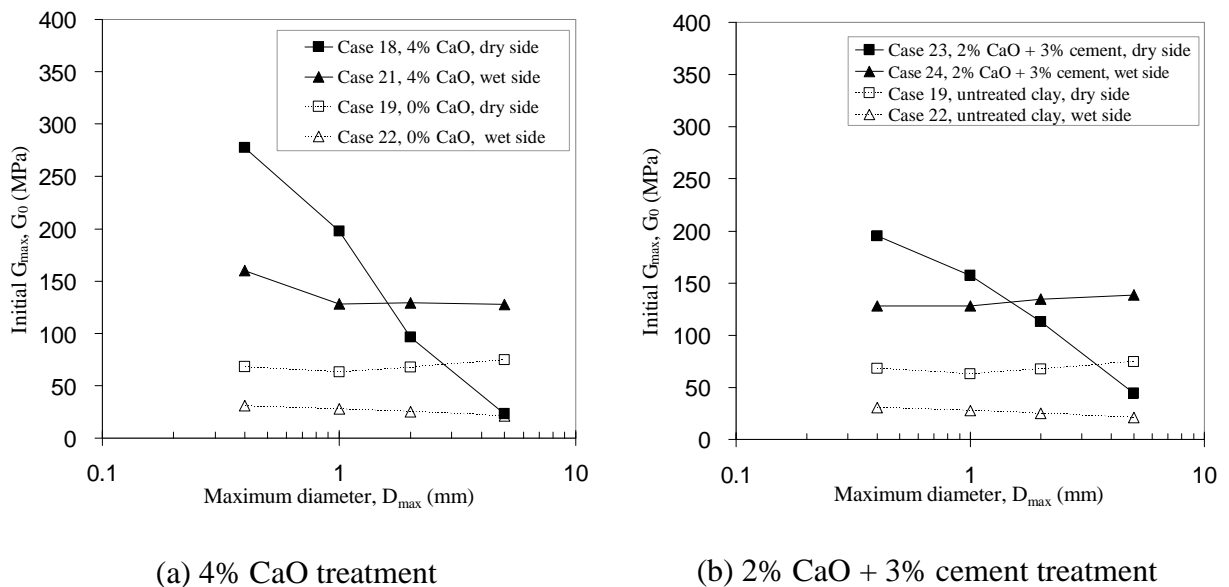


**Figure 3-13 Initial stiffness value  $G_0$  for the 4% lime treated and mixture (2% lime + 3% cement) treated clay involving mixing method A and soil powder preparation method 2**

For mixing method B (Figure 3-14), we observe that  $G_0$  does not change significantly with  $D_{max}$  for both lime (Figure 3-14a) and mixture treatments (Figure 3-14b). On the other hand, comparable values of  $G_0$  are obtained for treated and untreated specimens, despite the higher variation of data for the dry side (case 17 in Figure 3-14a). The absence of obvious

effect of  $D_{max}$  on  $G_{max}$  indicates a similar aggregate size distribution after compaction. Indeed, on both dry and wet sides, the hydration of lime results in a similar distribution of large aggregate size (Figure 2-12 and Figure 2-14), hence in a similar  $G_0$  for various  $D_{max}$ . The comparable  $G_0$  for the treated and untreated clay evidences the effect of the formed large aggregates, reducing different reactions. The large variation in the case of dry side indicates that it is more difficult to obtain a homogeneous treatment than in the case of wet side. Note that the dry specimens are not studied for the mixture treatment because of the high heterogeneity caused by this treatment.

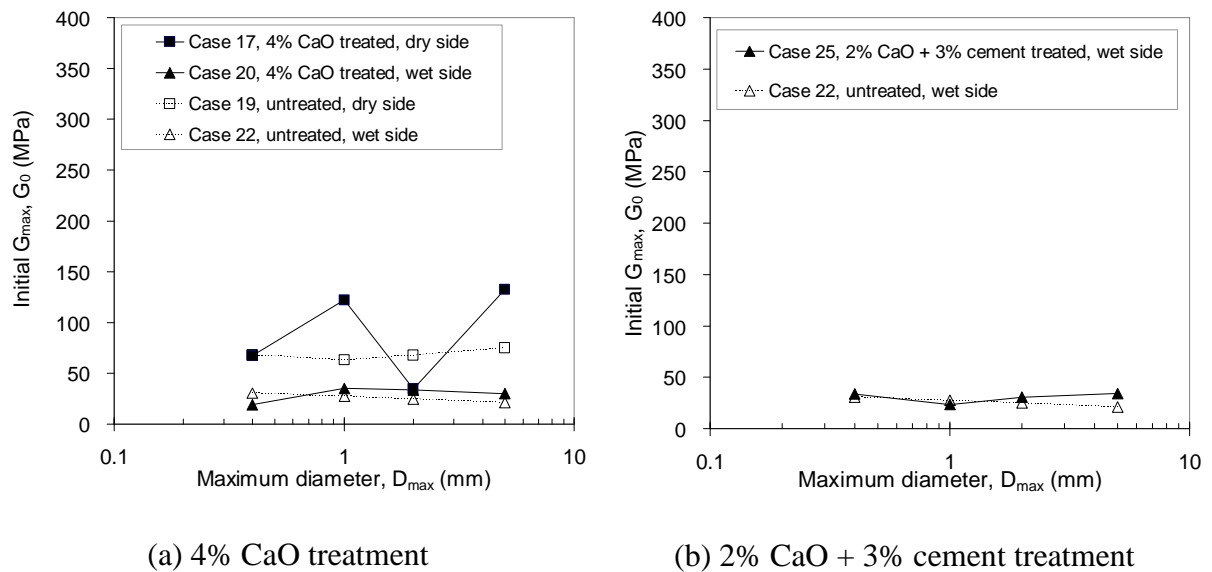


**Figure 3-14 Initial stiffness value  $G_0$  for the 4% lime treated and mixture (2% lime + 3% cement) treated clay involving mixing method B and soil powder preparation method 2**

As a conclusion, the  $G_0$  of both treatments is decreasing with the rise of  $D_{max}$  for mixing method A, particularly for the dry side, while there is no clear aggregate size effect for mixing method B. In addition, mixing method A results in a higher  $G_0$  for the treated specimens than for the untreated ones, whereas mixing method B gives rise to similar  $G_0$  values for the treated and untreated specimens. This indicates that the effect of  $D_{max}$  on  $G_0$  is strongly influenced by the mixing method and water content. It is logical because: 1) mixing method B often results in larger aggregates than mixing method A, giving rise to smaller contact surface between soil and additive, and thus enabling less hydration reactions in the first hours (almost no treatment effect on  $G_0$  for mixing method B); 2) water content can also significantly influence the  $G_0$  value but this influence is mainly through the aggregates



formation that is water content dependent. Thereby,  $G_0$  is mainly governed by the aggregate size after treatment.

As for the silt, the effect of  $D_{max}$  on  $G_{max}$  during long term curing (at around 3000 hours) for clay specimens is also studied with both lime and mixture treatments, in the case of mixing method A (Figure 3-15) and mixing method B (Figure 3-16). Changes of the corresponding suction with  $D_{max}$  are also presented.

For mixing method A, Figure 3-15 shows the stabilised  $G_{max}$  and the corresponding matrix suction versus  $D_{max}$  in the case of 4% lime treated clay (Figure 3-15a and c) and mixture treated clay (Figure 3-15b and d).

Figure 3-15a presents the relationship between  $G_{max}$  and  $D_{max}$  in the case of 4% lime treatment. It can be observed that: 1) the  $G_{max}$  of treated specimens compacted on dry side is decreasing sharply with the rise of  $D_{max}$ ; 2) for the wet side, the  $G_{max}$  seems to be constant; 3) there is no clear effect of  $D_{max}$  on  $G_{max}$  for untreated specimens, for both the dry and wet sides (case 19 and 22). For the dry side (case 18), the highest value is 735 MPa for  $D_{max} = 0.4 \text{ mm}$  and the lowest value is 89 MPa for  $D_{max} = 5.0 \text{ mm}$ . For the wet side (case 21), the highest value is 688 MPa for  $D_{max} = 2 \text{ mm}$  and the lowest value is 631 MPa for  $D_{max} = 5.0 \text{ mm}$ . For the untreated specimens, they show quite small variations of  $G_{max}$  with  $D_{max}$  change: 85 ~ 101 MPa for the dry side and 44 ~ 65 MPa for the wet side. On the other hand, as shown in Figure 3-15c, the corresponding suction- $D_{max}$  relationship shows: 1) a sharp decrease of suction with the rise of  $D_{max}$  for the dry side (case 18); 2) a smaller variation of suction for the wet side (case 21, ranging from 1500 to 3000 kPa); 3) an almost unchanged value of  $G_{max}$  with increasing  $D_{max}$  for untreated specimens (674 ~ 966 kPa for case 19 and 320 ~ 530 kPa for case 22). In addition, the suction of treated specimens is often higher than that of untreated specimens, apart from the case of larger aggregates for the dry side ( $D_{max} = 2 \text{ and } 5 \text{ mm}$  of case 18). In other words, a suction- $D_{max}$  trend similar to the  $G_{max}$ - $D_{max}$  one is identified.

Figure 3-15b shows the results of clay compacted at the same water content and dry density in the case of mixture treatment. It can be observed that: 1) for the dry side (case 23),  $G_{max}$  seems first to stay unchanged at high values (576 ~ 614 MPa) when  $D_{max} < 2 \text{ mm}$ , and then it decreases sharply when  $D_{max} > 2 \text{ mm}$  - a drop of  $G_{max} = 120 \text{ MPa}$  at  $D_{max} = 5 \text{ mm}$  is identified; 2) for the wet side (case 24),  $G_{max}$  seems to be constant or slightly increasing with rise of  $D_{max}$ . Correspondingly, Figure 3-15d shows a suction- $D_{max}$  trend similar to that of

$G_{max}$ - $D_{max}$  in Figure 3-15b, except for the dry side (case 23) where a steady decrease is observed for suction.

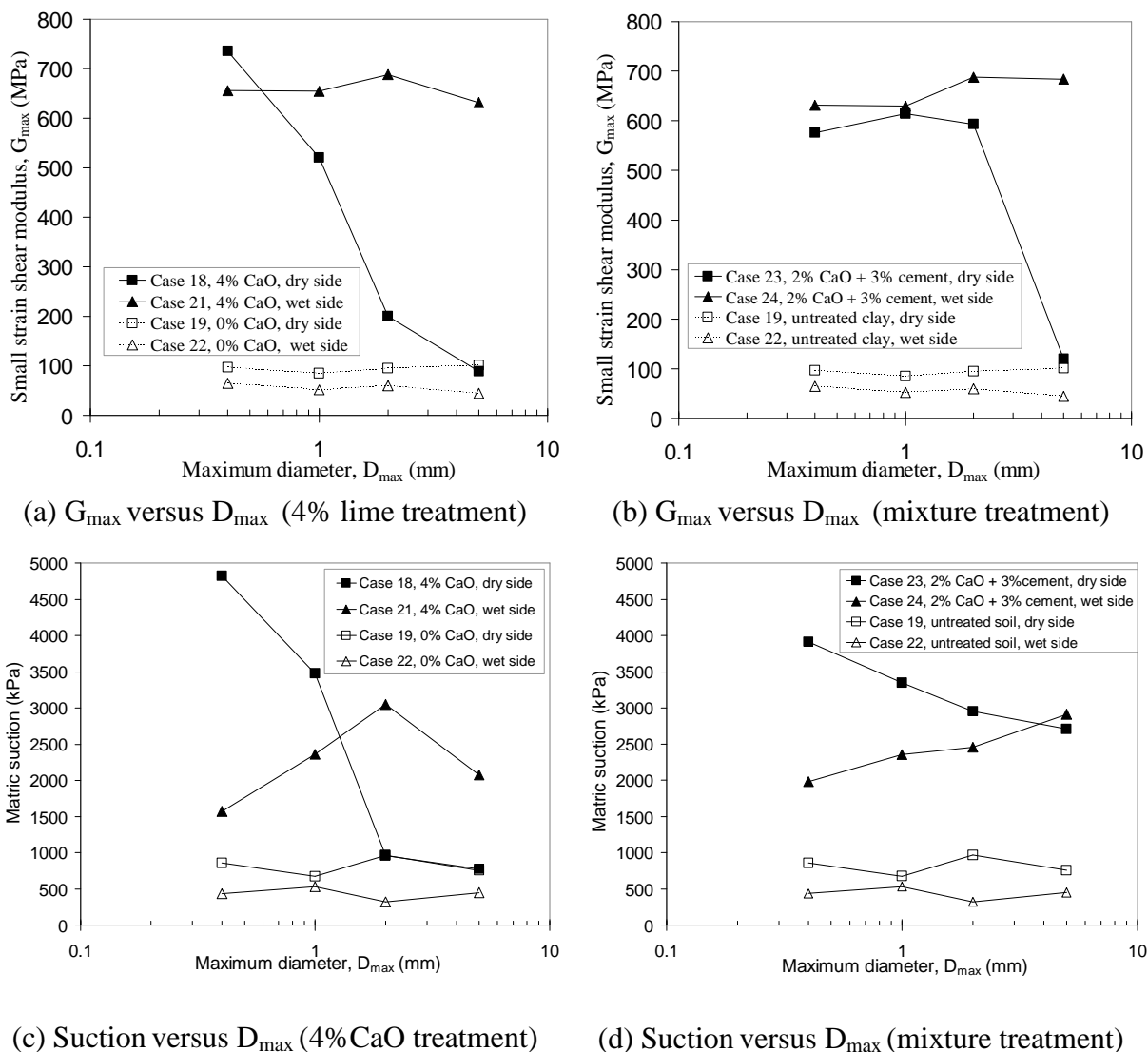
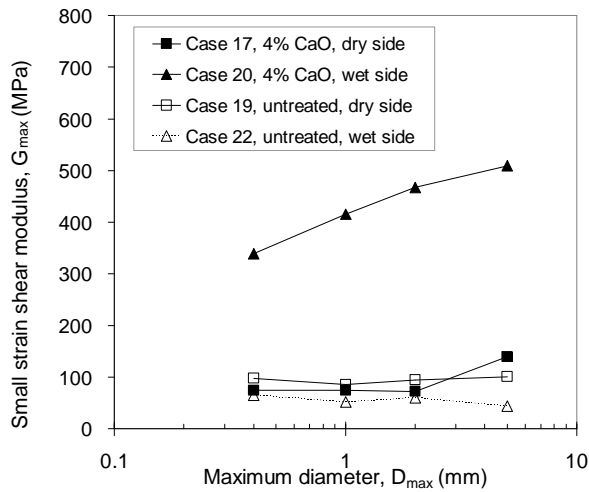


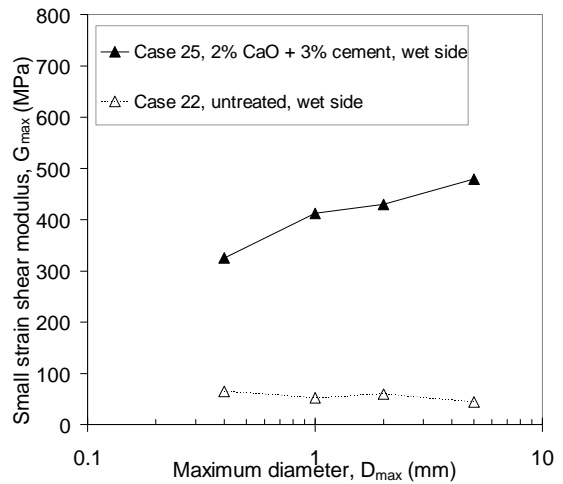
Figure 3-15 Aggregate size effects for the treated clay with mixing method A

For mixing method B, the aggregate size effect is shown in Figure 3-16 through the variation of final  $G_{max}$  and suction with  $D_{max}$  for the clay treated by 4% lime and 2% lime + 3% cement and at the same moulding water content and dry density as that shown in Figure 3-15. We observe rather different results compared to mixing method A. In the case of lime treatment (Figure 3-16a), we observe: 1) an increase of stabilised  $G_{max}$  with the rise of  $D_{max}$  for the wet side (*case 20*); 2) a rather small variation of stabilised  $G_{max}$  for the dry side (*case 17*), the values of stabilised  $G_{max}$  being close to or even lower than those for the untreated specimens. In the case of mixture treatment (Figure 3-16b), the stabilised  $G_{max}$  of wet

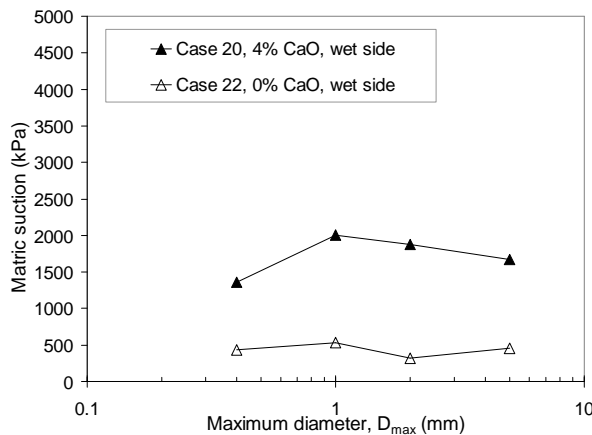
specimens has a similar increasing trend as that of wet lime treated ones. On the other hand, the corresponding suction globally increases with the rise of  $D_{max}$  for both lime treated (case 20 in Figure 3-16c) and mixture treated clays (case 25 in Figure 3-16d), compacted on wet side.



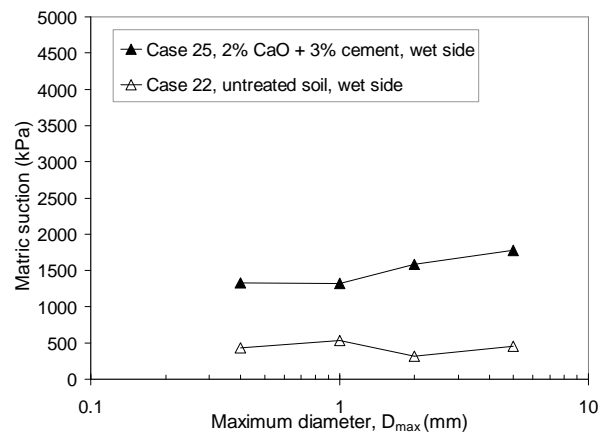
(a)  $G_{max}$  versus  $D_{max}$  (4% lime treatment)



(b)  $G_{max}$  versus  $D_{max}$  (mixture treatment)



(c) Suction versus  $D_{max}$  (4% CaO treatment)



(d) Suction versus  $D_{max}$  (mixture treatment)

**Figure 3-16 Aggregate size effects for the treated clay with mixing method B**

We observe a trend of suction changes with  $D_{max}$  similar to that of  $G_{max}$  changes with  $D_{max}$  for both treatments with mixing method A and B.

## 3.6. Discussion

### 3.6.1. For the silt

#### 3.6.1.1. Treatment mechanisms for $G_{\max}$ -time curves

For the untreated silt, the  $G_{\max}$  gain over time shows also a two-phase development as for the lime treated one. In fact, Anderson and Stokoe (1978) also reported two phases for the shear modulus evolution over time, explaining that the first phase is related to the primary consolidation and the second phase is related to the “long term time effect”. Following Delage *et al.* (2006), the  $G_{\max}$  gain over time for untreated soils can be attributed to aging effects: the microstructure changes in long term due to exchange of water between the inter-aggregate and intra-aggregate pores. Tang *et al.* (2008) observed a slight increase of soil suction after compaction. In recent years, several studies showed that the  $G_{\max}$  gain of untreated soils is induced by suction changes (Mancuso *et al.*, 2002; Sawangsuriya *et al.*, 2008; Ng *et al.*, 2009; Tang *et al.*, 2011).

The treatment effect is responsible for both the immediate  $G_{\max}$  increase after compaction:  $G_0$  (treated) >  $G_0$  (untreated) and the increase of  $G_{\max}$  during curing (Figure 3-1 ~ Figure 3-4).

Firstly, lime treatment results in immediate soil drying due to lime hydration, followed by a rapid decrease of clay content due to cation exchange and pozzolanic reactions. This increases the soil stiffness (Sahaphol and Miura, 2005). For the cement treatment, although the modification of aggregate size distribution is not clear, except for the little contribution of the lime contained in the cement product (Osula, 1996), the hydration of cement in wet soils immediately produces cementitious formations of CSH or CASH, giving rise to an immediate increase of stiffness.

Secondly, over time, lime and cement treatments give different  $G_{\max}$  developments (Figure 3-1 ~ Figure 3-4): two-phase development for the lime treated silt and a single phase for the cement treated one. Note that the shape of  $G_{\max}$  curves reflects the complex chemical reactions that take place at different times. For the 2% lime treated silt, the  $G_{\max}$  is in general increasing over time in two phases (sieving method 1 in Figure 3-1 and method 2 in Figure 3-2). The nonlinear development of  $G_{\max}$  of lime treated clayey soil was also reported by Tang *et al.* (2011). In phase 1, the lime hydration only results in a quite limited increase of

soil stiffness ( $G_0$  increase during the mellowing period). Because the hydration of lime does not provide cementitious products (phase 1), the main solidification comes from the subsequent pozzolanic reactions over long term (phase 2). The cementitious products induced by pozzolanic reactions can bond the aggregates or aggregates and thus increase the soil stiffness. For the 3% cement treated silt, the two-phase  $G_{\max}$ -time curve does not exist any more: the transition stage does not appear, instead, the increase of  $G_{\max}$  maintains a high ratio over long term (sieving method 1 in Figure 3-3 and method 2 in Figure 3-4). Compared to the lime treated silts, the cement treated one shows higher shear modulus at the early stage of curing, which is probably due to the fact that cement reacts immediately with water to form cementitious compounds that crystallize at the early stage of curing.

Thirdly, lime and cement treatments result in different  $G_{\max}$ -time curves for the dry and wet sides: 1) for the cement treatment, the  $G_{\max}$  curves are almost parallel for the dry and wet sides; 2) for the lime treatment, the solidification phase (phase 2) presents a quite different ratio between dry and wet sides. This suggests a different water effect on the solidification process involving the hydration of cement or pozzolanic reactions of lime/soil. The solidification induced by lime treatment is found to be more water-dependent than by cement treatment. This solidification process also results in suction change, hence affects the  $G_{\max}$ . The suction effect on  $G_{\max}$  is also evidenced in the present study. Indeed, the treated specimens compacted on dry side (lower water content and higher suction) often have a higher  $G_{\max}$  value than those compacted on wet side (Figure 3-1 ~ Figure 3-4). It is logical because, normally, soil aggregates are more resistant at dry state than at wet state due to the difference in suction and aggregation force. As reported in the literature, the cementitious products induced by treatment are located on the surface of aggregates. Thereby, the water content may still play a role in the aggregation force and suction changes after the treatment, hence in changes of  $G_{\max}$ . It was evidenced in the present study that the higher the water content, the lower the suction; it is particularly the case for the lime treated silt (Figure 3-11 and Figure 3-12). This water effect also depends on the coating or solidification process of aggregates. The water content can also impact the starting time of the solidification. The curve of phase 2 in the case of lime treatment seems to appear earlier for the dry side than for the wet side, especially for the specimens obtained by method 2 (Figure 3-2). This is in accordance with the study reported by Locat *et al.* (1990), where the shear strength-curing time curve is also governed by the moulding water content. This is probably because higher

water contents often result in lower concentrations of ions in the pore-water environment, thus initiates slower pozzolanic reactions.

### 3.6.1.2. Aggregate size effect

The aggregate size effect is evidenced not only on the value of  $G_0$  (Figure 3-9 and Figure 3-10), but also on the final value of  $G_{max}$  (Figure 3-11 and Figure 3-12).

Firstly, the  $G_0$  and  $G_{max}$  decrease globally with the rise of  $D_{max}$ . This is related to the decrease of total contact surface between soil and additives with increasing  $D_{max}$  (Tang *et al.*, 2011). This aggregate size effect is more marked with method 1 (uniform soil powder) as compared to method 2 (graded soil powders), probably because of the effect of aggregate size distribution. With different distribution of aggregate size, the total contact surface of soil-additive is different. The aggregate size effect gives rise to different reaction process: the finer the soil, the more the reactions and the more the number of bonding created. Furthermore, the same trend for the  $G_{max}$ - $D_{max}$  and suction- $D_{max}$  curves also confirms that the suction generated depends strongly on the aggregates size and their distribution. This proves that the solidification process by coating and bonding of aggregates or aggregates is aggregate size dependent. The cementitious products induced by the chemical reactions form bonding chains between the aggregates. The larger the aggregate after treatment, the smaller the additive/soil contact surface. This also leads to a lower number of bonding chains a lower suction. The solidification/cementation process results in an increase of suction, which is clearly evidenced in the present study (Figure 3-11 and Figure 3-12).

Secondly, the moulding water content can also influence the formation of aggregates after mixing, thus controlling the  $G_{max}$  by aggregate size effect. It is observed that the aggregate effect for the dry side is often more significant than for the wet side. This is mainly because of the difference in the preparation of soil specimens. For the dry side, the initial aggregates are clearly defined, while for the wet side, mixing method B leads to formation of larger soil blocks/aggregates. Thereby, the total soil/additives contact surface is much smaller than that for the dry side, and is similar to each other (Figure 3-17). This observation also suggests that the moulding water content affects the additive distribution and hence the soil treatment.



(a) Dry side (case 1) (b) Dry side (case 9) (c) Wet side (case 3) (d) Wet side (case 11)

**Figure 3-17 Description of  $D_{max}$  of 5 mm silt after mixing at water contents corresponding to dry and wet sides**

Thirdly, the mixing method also affects the  $G_{max}$  measurement, especially for the dry side. This is because the finer the soil is, the more difficult it is to mix the soils to obtain a homogeneous additive distribution. The difficulty of mixing also makes the aggregate size effect more significant in case of mixing method 1 (uniform soils, easy to mix) than in case of mixing method 2 (well graded soils, difficult to mix). For some dry treated specimens, we observe that the aggregate size effect does not follow a general and logic rule ( $G_{max}$  of  $D_{max} = 0.4 \text{ mm} < G_{max}$  of  $D_{max} = 1 \text{ mm}$ , see in Figure 3-10a, Figure 3-11b and Figure 3-12a, b). This is to be explained by the difficulty of mixing fine-aggregated soil with additives using mixing method B (cf. in section 2.2.2).

Fourthly, the aggregate size effect is sometimes influenced by water availability, especially for soils with large aggregate size and at dry conditions. In Figure 3-1d, a similar final value of  $G_{max}$  for the 2% lime treated silt prepared by method 1 ( $D_{max} = 5 \text{ mm}$ ) was reached for both the dry and wet sides. This is probably related to the competition between water availability and aggregate size effect. In fact, in case of large aggregate sizes, although the dry specimens has a more homogeneous distribution of lime and thus has a larger total contact surface than the wet side, most water is located inside the aggregates, leaving a certain quantity of additives non hydrated. In other words, the lower quantity of available water for the dry side leads to a limited lime hydration and pozzolanic reactions. On the contrary, on the wet side, there is sufficient water ensuring full development of reactions. On the other hand, the high water content also results in larger aggregate size and thus a smaller total contact surface. However, on the dry side, the limited development of stiffness for large aggregate size is scarcely observed in this study, probably because the proctor curve is relatively narrow for the treated silt, and the reaction induced by silt/lime or silt/cement is relatively slow as compared to the treated clay. In the field condition, the aggregates being

larger, the water availability would be a decisive factor for the various reactions, especially for the clay.

In addition, although the aggregate size is a decisive factor for the  $G_{\max}$  development, the mineral composition of soil particles may also play an important role on the  $G_{\max}$  of silt with different treatments. As shown in chapter 2, for the two sieving methods (1 and 2), the aggregate size distributions for sub-series  $D_{\max} = 0.4 \text{ mm}$  are almost the same. However, method 1 results in higher fines percentage than method 2 (a difference of about 5%). After compaction, for the lime treated silt of this sub-series, both the  $G_0$  (Figure 3-9a) and final  $G_{\max}$  (Figure 3-11a) obtained with method 1 are higher than with method 2 (Figure 3-9b and Figure 3-11b). When the silt is treated by 3% cement, a similar  $G_0$  value is obtained (Figure 3-10), whereas the final  $G_{\max}$  by method 1 (Figure 3-12a) is lower than by method 2 (Figure 3-12b). This comparison between method 1 and method 2 confirms that lime treatment is particularly efficient for clayey soils (Little *et al.*, 1995b; Thagesen, 1996; Muhunthan and sariosseiri, 2008), whereas cement treatment is more suitable for granular soils (Currin *et al.*, 1976; Thagesen, 1996).

### 3.6.2. For the clay

#### 3.6.2.1. Treatment mechanisms for $G_{\max}$ -time curves

As for the treated silt, the untreated clay also shows a slight increase of  $G_{\max}$  over time, which can be explained by the aging effect (Delage *et al.*, 2006) or the suction change after compaction (Tang *et al.*, 2008). The higher  $G_{\max}$  for the dry side is probably due to the suction effect (Figure 3.15 and Figure 3.16).

For the treated clay, we also observe the effect of additive type on the  $G_{\max}$  development: 1) two typical phases for the 4% lime treated clay with both mixing method A (Figure 3-5) and method B (Figure 3-6), especially for the wet side - an increasing nonlinear curve followed by another faster one; 2) a single phase development for the mixture treatment by method A (Figure 3-7). This can be explained by the two reaction mechanisms mentioned before: the short term modification due to hydration and long term pozzolanic reactions. The mixing method as well as water content can also influence the solidification process. For the mixture treatment (2% lime + 3% cement), for the wet side, the two-phase  $G_{\max}$ -curve is also obtained for method B (Figure 3-8), whereas it is not obvious for method A. On the dry side,



the  $G_{max}$  does not increase significantly over time for both treatments with mixing method B, whereas for mixing method A, the  $G_{max}$  is strongly influenced by the aggregate size effect: the larger the aggregate, the less significant the development, particularly for the 4% lime treated clay.

The  $G_{max}$  development is strongly moulding water content dependent. The  $D_{max}$  evolution indicates that the water availability can also be a decisive factor, especially for large aggregate on the dry side. Indeed, we have a significant evolution of  $G_{max}$  development due to mixing method A but a less significant development of  $G_{max}$  by mixing method B. In case of large aggregate size, either hydration or subsequent pozzolanic reactions cannot be fully developed due to the limited available water. Thereby, the choice of mixing method affects the aggregate size, hence governs the  $G_{max}$  value. For the treated clay with mixing method B, the values of  $G_0$ ,  $G_{max}$  and suction are much lower than those with mixing method A. In addition, similar  $G_{max}$  development over time for method B was obtained with different values of  $D_{max}$ . In other words, the total contact surface of wet soil-additive is essential for the  $G_{max}$  development of treated soils.

As in the case of silt, the treatment effect is also responsible for the immediate  $G_{max}$  increase ( $G_{0treated} > G_{0untreated}$ ) for clay due to the modification effect. Although hydration of lime does not produce cementitious products, it can significantly reduce the fine aggregates percentage by flocculation/agglomeration (Osua, 1996). The reduction of fines percentage enables the increase of stiffness of soil, as reported by Sahaphol and Miura (2005).

For the lime treated clays prepared by mixing method B and compacted on dry side, we surprisingly observe that the  $G_{max}$  decreases with time in a few hours after compaction (ex.  $D_{max} = 0.4 / 1 / 5 \text{ mm}$  in Figure 3-6 ). In fact, this can be explained by the water availability as mentioned before. Compared to the silt, the clay by mixing method B has much larger aggregates (see Figure 2-12 and Figure 2-14). Thereby, the hydration of lime can not develop well, leading to aggregates coated by non-hydrated lime. Within a few hours, solidification by pozzolanic reactions may not occur, instead, the ongoing hydration of lime consumes a certain quantity of water existing between aggregates/aggregates. Water can play a “glue effect” (Santamarina, 2003) on the extreme dry side where the  $G_{max}$  increases with the rise of water content as proposed by Schuettpelz *et al.* (2009). Therefore, the decrease of water by lime addition leads to a decrease of this glue effect and thus makes the  $G_{max}$  diminish. The slight increase of  $G_{max}$  in long term may be induced by the subsequent pozzolanic reactions.

In addition, we observed larger variation of  $G_{\max}$  for treated clay than for untreated clay. This is probably due to the higher heterogeneity of the treated clay due to the treatment.

### 3.6.2.2. Aggregate size effect

Concerning  $G_0$  ( $G_{\max}$  after one-hour curing), the aggregate size effect is revealed for the treated clay by mixing method A, especially for the dry side (Figure 3-15). For mixing method B, this aggregate size effect is no longer obvious because of the similar and larger aggregate size obtained after mixing. This suggests that  $G_0$  is mainly governed by the aggregate size after treatment. The larger the aggregate size, the lower the  $G_0$ . This can also be explained by the difference in the total contact surface between soil aggregates and additives (Tang *et al.*, 2011).

For the final value of  $G_{\max}$ , as shown in Figure 3-15 and Figure 3-16, when  $D_{\max}$  increases, no clear aggregate size effect on  $G_{\max}$  and on suction can be observed for untreated clay. However, for the treated clay, several observations can be made: (i) for mixing method A, the final suction and  $G_{\max}$  show obvious decreasing trends for the dry side and slight increasing trends for the wet side. This indicates that the aggregate size effect due to coating and bonding after compaction is strongly influenced by the moulding water content or suction. (ii) the  $G_{\max}$  obtained with mixing method A is much higher than with mixing method B at the same  $D_{\max}$ , suggesting that the aggregate size effect is correlated with the total contact surface that is related to the aggregate size after mixing; (iii) for the wet specimens with both mixing method A and method B, the final  $G_{\max}$  values are similar for different values of  $D_{\max}$ . This is probably due to a similar aggregate distribution after mixing (Figure 2-13); (iv) for the wet specimens with mixing method B, the slight increasing trend also reflects the difference in coating for different values of  $D_{\max}$ . This is probably induced by a good preservation of the initial aggregates with mixing method B; (v) for the dry specimens with method A, a sharp decreasing trend is observed for the 4% lime treated clay, whereas for the mixture treatment, the  $G_{\max}$  firstly stays at relatively similar level for  $D_{\max} = 0.4 \text{ mm}$ ,  $1 \text{ mm}$  and  $2 \text{ mm}$ , and then presents a drop value at  $D_{\max} = 5 \text{ mm}$  to reach a value similar to that of untreated clay and lime treated clay in this aggregates size level. This phenomenon indicates that the 4% lime treated clay requires more water for different reactions than the mixture treated one (2% lime + 3% cement). This aggregate size effect can also be explained by the difference in water availability for different  $D_{\max}$ . The finer the soil after mixing, the more the wet soil/additives contact surface and thus the more the available water for the

chemical reactions, especially for the dry side. If water is sufficient and the total surface of aggregate is large enough, the  $G_{\max}$  development can last over 5000 hours or longer (ex. case 18,  $D_{\max} = 0.4\text{mm}$  in Figure 3-5).

Summarising, the aggregate size has significant effect on the soil stiffness: the larger the aggregates, the lower the  $G_{\max}$ . However, cautions need to be taken when it comes to the wet side because the aggregate size may be changed by different mixing methods. In addition, the coated aggregate size depends also on the soil type and mixing condition: we observe a slight decreasing or constant trend for the treated silt compacted on wet side but a slight increasing trend for the treated clay.

### 3.7. Conclusions

$G_{\max}$  evolution during curing is studied on the silt and clay of different sub-series prepared by sieving method 1 and 2, treated by lime and/or cement, mixed with method A and method B, and compacted at various moulding water contents corresponding to dry and wet sides, respectively. After compaction, an increase of  $G_{\max}$  over time is observed for both the untreated and treated soils. The aging effect (Rammah *et al.*, 2004; Delage *et al.* 1996) or suction effect (Tang *et al.*, 2008) can explain the increase for untreated soils, whereas hydration and/or pozzolanic reactions can explain the increase for treated soils.

Several effects are identified, as follows:

**1) Water effect and suction effect:** the stiffness of soil on dry side is normally higher than that of soil on wet side under the same conditions of compaction and treatment, because soil aggregates are softer at higher water content. For both treated and untreated soils of different sub-series, the suction shows an evolution trend similar to that of  $G_{\max}$ . Thereby, the  $G_{\max}$  of both untreated and treated soils is probably controlled by suction.

**2) Treatment effect:** The treated soils show higher stiffness than the untreated ones for the immediate value after compaction ( $G_0$ ) and the final value after thousands of hours of curing. Moreover, a two-phase  $G_{\max}$  development with corresponds to two phases: phase I related to additive hydration; phase II related to pozzolanic reactions.

**3) Aggregate size effect:** for the same soil with same treatment and then compacted at identical moulding water content, the  $G_{\max}$  development is often different for the soils prepared from different sub-series. The larger the aggregate size, the lower the stiffness after

treatment. This is due to the different contact surface between soil and additives: the larger the aggregates, the less the contact surface, thus the lower the soil stiffness. This aggregate size effect exists in both short (just after compaction, 1 hour of treatment) and long terms (several thousands of hours). Note that it is the size of aggregates after treatment that affects the soil stiffness. Thereby, the mixing method is crucial because it governs the aggregate size distribution after treatment, hence influencing the soil stiffness, especially for clayey soils.

4) **Water availability:** water availability is also a key factor for the stiffness development, especially in dry conditions. As this factor is aggregate size dependent, the mixing method can also play a decisive role in soil stiffness development. In this study, we observe that mixing method A changes the distribution of aggregates, thereby controlling the water availability for different reactions.

5) **Mineral composition of soil:** For the same aggregates size distribution (sub-series  $D_{max} = 0.4 \text{ mm}$ ), method 1 provides higher fines percentage of silt (about 5% higher) than method 2, and therefore a higher final  $G_{max}$  value for the lime treatment. But a lower  $G_{max}$  value was identified in the case of cement treatment with method 1. This confirms that lime treatment is particularly efficient for clayey soils (Little *et al.*, 1995b; Thagesen, 1996; Muhunthan and sariosseiri, 2008), whereas cement treatment is more suitable for granular soils (Currin *et al.*, 1976; Thagesen, 1996). This also indicates that the mineral composition of soils is important in the stiffness development.

## Chapter 4. Aggregates size effect during drying/wetting cycles

After reaching stability in terms of  $G_{\max}$  evolution, the specimens presented in chapter 3 underwent cyclic wetting/drying tests, aiming at investigating the aggregates size effect during wetting/drying cycles. The  $G_{\max}$  values of the specimens during application of the cycles were recorded. The matric suction during drying or wetting was also punctually measured.

### 4.1. Wetting/drying process

Once the stabilization of  $G_{\max}$  was reached, the specimens were first wetted and then dried to complete the first wetting/drying cycle. Figure 4-1 shows the wetting/drying methods applied to both silt and clay specimens. For wetting, the immersion in water during 24 hours was applied for the silt; the immersion in a saturated sand bath for 5 days was performed for the clay. For drying, the soil specimens were air-dried until they reached their initial water content  $w_f$ ; the required air-dry period ranged from 1 to 10 days according to the initial water content  $w_f$  and the treatment. After wetting or drying to the target water content value, the soil specimens were wrapped in plastic film for 3 days for moisture homogenisation and then  $G_{\max}$  measurements were performed.



(a) Silt wetting by immersion in water



(b) Silt drying in air



(c) Clay wetting in a saturated sand bath



(d) Clay drying in air

**Figure 4-1 Wetting/drying cycles application for both silt and clay soils**

In fact, the duration of immersion regime was determined according to the immersion test. It corresponds to the time for water content to be stabilized (two mass differences  $\leq 0.1g$ ). The duration of drying was specified at a temperature of  $20 \pm 2$  ( $^{\circ}C$ ) and an average humidity of 33%. Figure 4-2 shows the water content/saturation degree change during a wetting and a drying of a mixture-treated clay specimen compacted on the dry side (case 23). For wetting, the water content increases drastically during the first day (1440 min), then it grows gradually and then levels off (Figure 4-2a). For drying to  $w_f$ , the water content decreases almost linearly (Figure 4-2b). Note that the drying time is calculated without considering the period when the soil specimen was conserved in sealed box (ex. maintaining 1 hour in box after three-hour drying). This can avoid any cracks on the soil surface induced

by intensive drying. Thereby, it requires a period of about 4 days to complete the 1-day drying (see Figure 4-2b). Note that it was difficult to wet the treated soils to saturated state (Figure 4-2a). This may be due to coating effect induced by curing - the cementitious products on the surface of aggregates prevent water infiltration. In order to investigate the aggregates size effect on the drying rate, the time needed for drying was also recorded for each treatment of different sub-series.

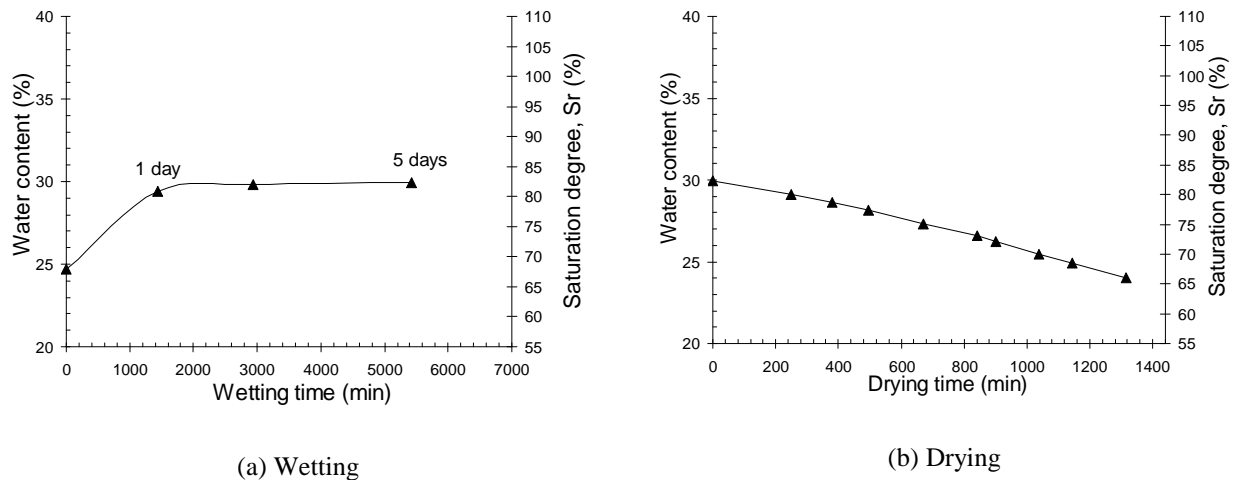


**Figure 4-2 Water change during a wetting and a drying for a mixture (2% lime + 3% cement) treated clay specimen (test 151, dry side, case 23)**

During wetting or drying, the water content of the specimen was controlled by monitoring the changes of its mass as reported by Tang *et al.* (2011). This wetting/drying procedure was repeated until the soil had a significant degradation of  $G_{max}$  - water content can no longer be controlled by measuring weight due to falling off of soil particles. At least five wetting-drying cycles were applied for each treated silt specimen. For the untreated specimens, the number of cycles varied depending on their degradation conditions.

In addition, the changes in dimensions of the specimens were measured by a calliper, aiming to monitor the volume change caused by wetting/drying cycle. Note that this volume change was also considered in calculating both shear wave velocity and soil density for  $G_{max}$  measurement.

## 4.2. Results of silt treated with lime

As indicated in chapter 3, the aggregates size effect on  $G_{\max}$  for the treated silt prepared by sieving method 1 is more significant than by sieving method 2. Thereby, to study this aggregates size effect on the  $G_{\max}$  development of treated silt during wetting/drying cycles, sieving method 1 was adopted.

### 4.2.1. Results for dry side

Cyclic wetting/drying was carried out by controlling the water content of soil specimen. Figure 4-3 shows the  $G_{\max}$  changes with wetting-drying cycles for the untreated silt specimens of different sub-series (initial  $D_{\max}$ ) prepared by sieving method 1 and compacted on dry side of optimum (case 2,  $w_f = 17\%$ ). In this figure, the corresponding water content and saturation degree are also indicated for each wetting/drying path.

The starting points (No.0) correspond to the stabilised  $G_{\max}$  (chapter 3). As shown in Figure 4-3, with the initial water content  $w_f = 17\%$  (corresponding to a value of  $S_r$  about 73.8%) at No.0, the specimens show different  $G_{\max}$  values for different  $D_{\max}$  (156 ~ 216 MPa). Wetting to a common water content of 22% (corresponding to a value of  $S_r$  about 90.7%) at No.1 decreases  $G_{\max}$  to similar values (24 ~ 39 MPa). The subsequent drying to the same initial water content of 17% increases  $G_{\max}$ , but to the values lower than the initial ones (106 ~ 178 MPa). Further wetting/drying cycles result in similar  $G_{\max}$  change to that during the first cycle, indicating a high sensibility of  $G_{\max}$  to water content changes. A degradation of  $G_{\max}$  in both wetting and drying paths is observed for each soil. In addition, the wetting No. 3 decreases the  $G_{\max}$  of soils to a few MPa. Interestingly, for the wetting paths, the cycles gradually increase the degree of saturation of soils, especially for the finer aggregates soils (ex.  $D_{\max} = 0.4 \text{ mm}$ ). Moreover, the cycles also slightly decrease the  $G_{\max}$  of soils.

The  $G_{\max}$  variation range is significantly different for drying paths and wetting paths of, whatever the sub-series soil is - with much larger variation in drying paths.

Summarising, wetting/drying cycles cause cyclic change of  $G_{\max}$ , evidencing the sensibility to the moisture change /suction change.



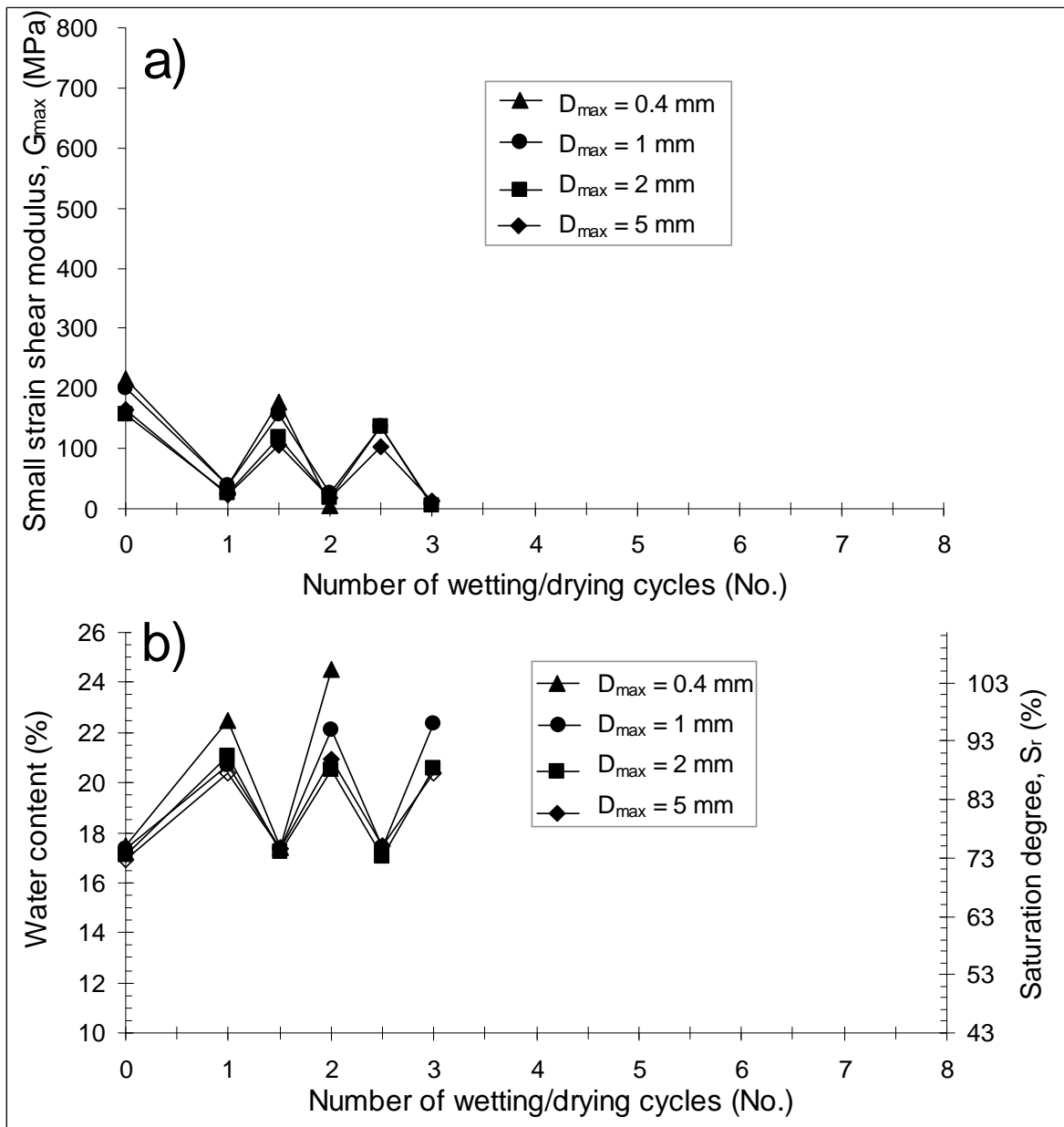


**Figure 4-3 a) Changes in  $G_{max}$  upon wetting/drying cycles for untreated silt of different sub-series prepared by method 1, on dry side; b) the corresponding water content and saturation degree change with cyclic wetting/drying (case 2)**

Figure 4-4 shows the  $G_{max}$  changes with wetting-drying cycles for the 2% lime treated silt, compacted at the same water content (case 1,  $w_f = 17\%$ ). As for untreated silt, the corresponding water content/saturation degree values are also shown in this figure. On the whole, the effect of  $D_{max}$  on the  $G_{max}$  evolution with cycles is quite clear. In the light of this evolution with  $D_{max}$ , it is worthy describing the results for each aggregates size separately.

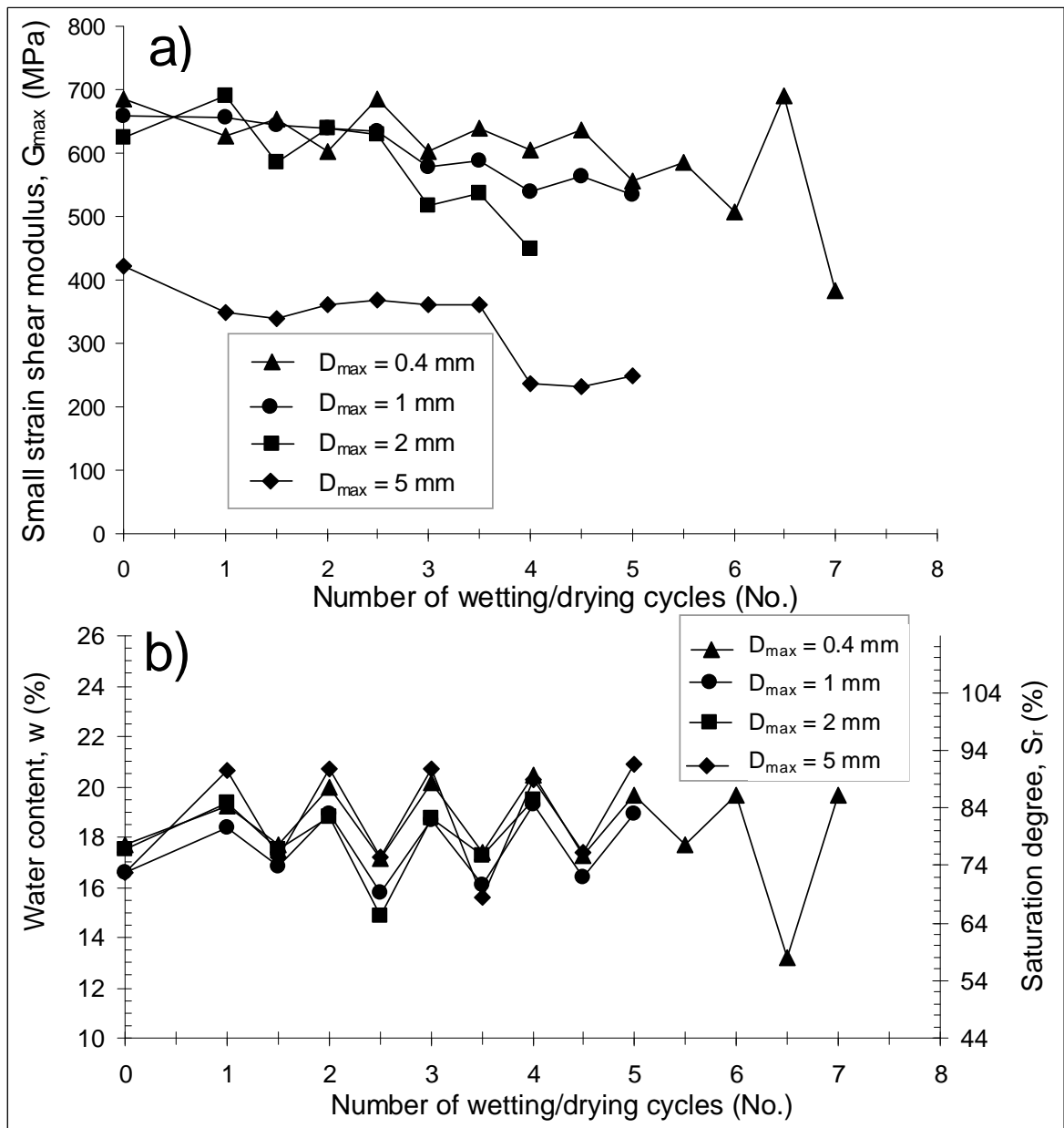


Figure 4-4 a) Changes in  $G_{max}$  upon cyclic wetting/drying for 2% lime treated silt of different sub-series prepared by method 1, with mixing method B, and then compacted on dry side; b) water content and saturation degree change with cyclic wetting/drying (case 1)

For the soil specimens of sub-series  $D_{max} = 5$  mm at water content  $w_f = 17\%$  (corresponding to a saturation degree  $S_r = 70\%$ ),  $G_{max}$  is equal to 422 MPa for 2% lime treated specimen. Wetting to a water content of 20.64% ( $S_r = 86\%$ ) decreases the  $G_{max}$  to 348 MPa (No.1). The subsequent wetting/drying cycles only changes the  $G_{max}$  slightly until No.3.5 (stage I). Then, it decreases sharply when re-wetting at No.4 - a drop of  $G_{max}$  value (236 MPa) is identified (stage II). This suggests the breakage or damage of aggregates by debonding. Then the  $G_{max}$  changes slightly again with the subsequent cycles, at a low stiffness

level. This suggests that the breakage of aggregates is progressed in steps, and it is believed that further cycles may give rise to other decrease of  $G_{\max}$ .

For the soils of other sub-series ( $D_{\max} = 0.4/ 1/ 2$  mm), they begin with a similar initial  $G_{\max}$  value (685 ~ 624 MPa). Before No.2.5 they show a slight variation of  $G_{\max}$  with cycles (stage I). After No.2.5 (stage II), the  $G_{\max}$  changes show an increasing effect of cycles with increase of  $D_{\max}$ : a slight degradation of  $G_{\max}$  with cycles for  $D_{\max} = 0.4$  mm followed in an increasing order of degradation by  $D_{\max} = 1$  mm and 2 mm. This suggests the different breakage degrees of aggregates for different sub-series.

For the wetting paths, the saturation degree seems to be almost at stable values, though a quite slight change of  $G_{\max}$  at stage I and another steadily decreasing of  $G_{\max}$  at stage II. In other words, the first few cycles only results in a limited change of  $G_{\max}$ ; no clear degradation effect is observed. Moreover, intensive drying followed by wetting accelerates the breakage or de-bonding of aggregates. Taking the cycle No.7 of the soil  $D_{\max} = 0.4$  mm for example, an intensive drying ( $w = 13.2\% < 17\%$ ) results in a significant increase of  $G_{\max}$  and the subsequent wetting gives rise to a drop of  $G_{\max}$  value ( $G_{\max} = 382$  MPa at No.7 against  $G_{\max} = 507$  MPa at No.6). This indicates that the effect of cycles can give rise to a breakage of aggregates and a certain limit suction change induced by intensive drying can accelerate the breakage of the aggregates.

Comparison of the results between the treated and untreated silts shows that: 1)  $G_{\max}$  of untreated soils is very sensible to water content change, whereas it is less sensible for treated specimens; 2) unlike untreated soils, the  $G_{\max}$  change of treated specimens is strongly influenced by soil aggregates size  $D_{\max}$  during wetting/drying cycles; 3) the saturation of wetting paths for untreated silt is 4% higher than for treated silt.

#### **4.2.2. Results for wet side**

For the silt compacted on the wet side,  $G_{\max}$  changes with wetting-drying cycles are shown in Figure 4-5 for untreated silt, and in Figure 4-6 for 2% lime treated one.

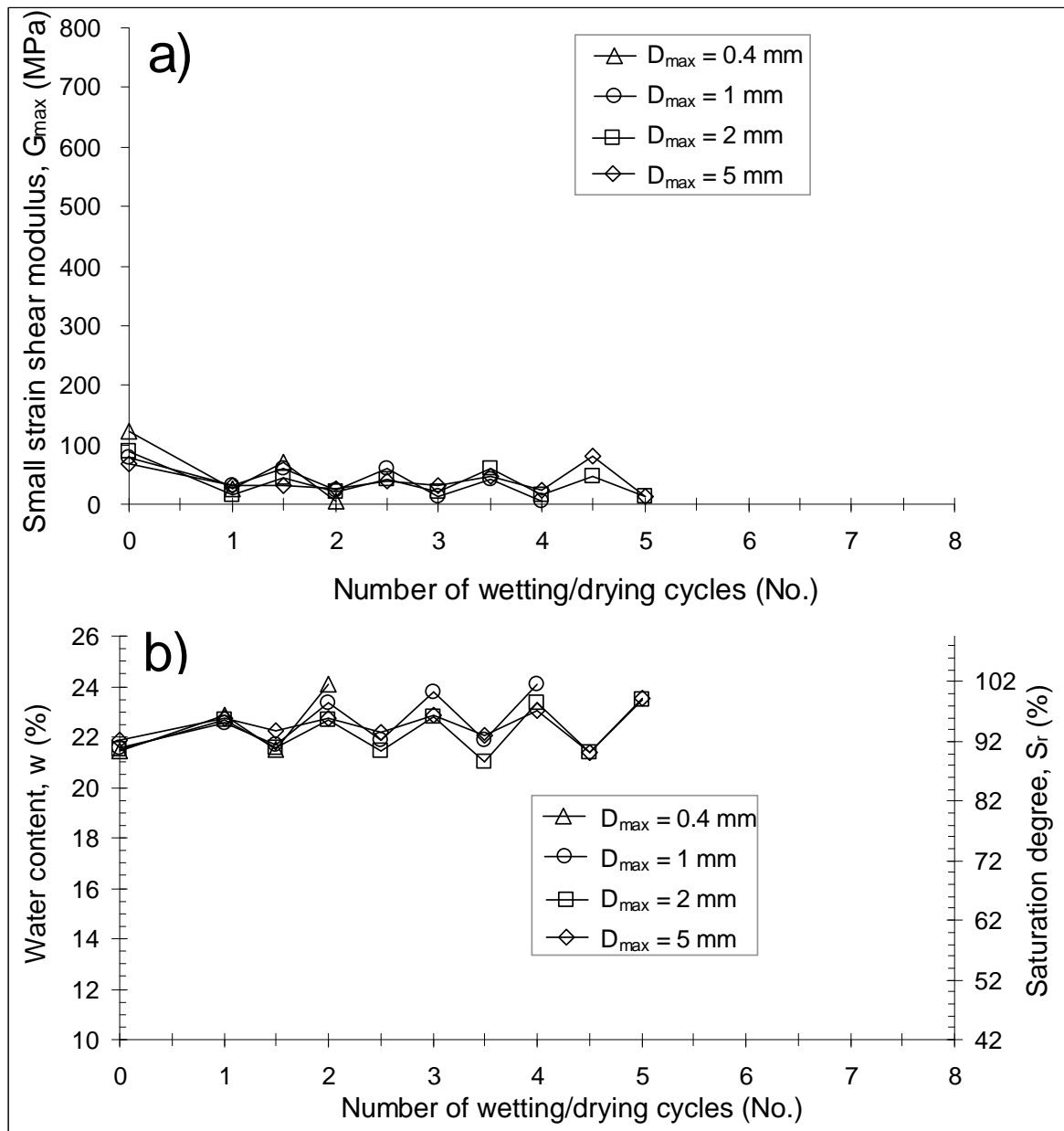


**Figure 4-5 a) Changes in  $G_{max}$  upon cyclic wetting/drying of untreated silt in different sub-series prepared by method 1, on wet side; b) corresponding water content and saturation degree changes with wetting/drying cycles (case 4)**

As for the dry side, the wet untreated soils ( $D_{max} = 0.4$  mm, 1 mm, 2 mm and 5 mm) are also sensible to the water content change during cycles (Figure 4-5): the  $G_{max}$  values follow the wetting/drying cycles. As for the dry side, the cycles also slightly decrease the  $G_{max}$  of soils. At No.4 (Figure 4-5a), wetting decreases the  $G_{max}$  of soils to only tens of MPa. We also observe that the water content or saturation degree for the wetting paths increases slightly with the cycles (ex.  $S_r$  from 97% at No.1.0 to 100% at No. 5.0 for  $D_{max} = 2$  mm) (Figure 4-5b).

Unlike the dry side treated silt, the wet side treated four sub-series ( $D_{max} = 0.4$  mm, 1 mm, 2 mm and 5 mm) present similar  $G_{max}$  development with wetting/drying cycles (Figure 4-6a). They have a similar initial  $G_{max}$  value of (420 - 474 MPa), and this value decreases slightly during the first wetting (410.6 MPa ~ 433 MPa). On the whole, the samples show a visible and very slight change of  $G_{max}$  until cycle No.6 (stage I). The low variation range of  $G_{max}$  is probably due to the fact that the range of water content/saturation change ( $\Delta w = 0.79\%$ ,  $\Delta Sr = 3.64\%$ ) is much lower than for the dry side ( $\Delta w = 2.60\%$ ,  $\Delta Sr = 10.06\%$ ). At No.6.5, the finer soils ( $D_{max} = 0.4$  mm and 1 mm) have a significant increase of  $G_{max}$  to reach a value similar to that of dry side at No.5.5. This is due to an intensive drying that decreases the water content to a value of 17%, similar to the initial water content of dry side ( $w = 16.7\%$  and 17.9% respectively, Figure 4-6b). Re-wetting at No.7 significantly decreases the  $G_{max}$ : a drop of  $G_{max}$  value is identified (from 551, 475 MPa to 248, 339 MPa for sub-series  $D_{max} = 0.4, 1$  mm respectively). This evidences that intensive drying followed by re-wetting can heavily change the microstructure of soil or de-bond the chains between aggregates, thereby decreasing the value of  $G_{max}$ .

Comparison between the results of dry side and wet side shows that: 1)  $G_{max}$  of untreated soils is very sensible to water content changes; it is not sensible for treated specimens; 2) unlike untreated soils that have similar  $G_{max}$ -cycles curves for different values of  $D_{max}$ , the dry side treated specimens have the  $G_{max}$ -cycles curves strongly dependent on the values of  $D_{max}$ ; 3) by contrast, the wet treated specimens show no clear effect of  $D_{max}$  on  $G_{max}$  development - similar  $G_{max}$  variation with cycles are identified; 4) in general, dry side treated specimens show typical two-stage degradation curves, whereas wet side treated specimens show one-stage development; 6) an intensive drying followed by rewetting can significantly decrease the  $G_{max}$  of the treated silt of both the dry and wet sides.

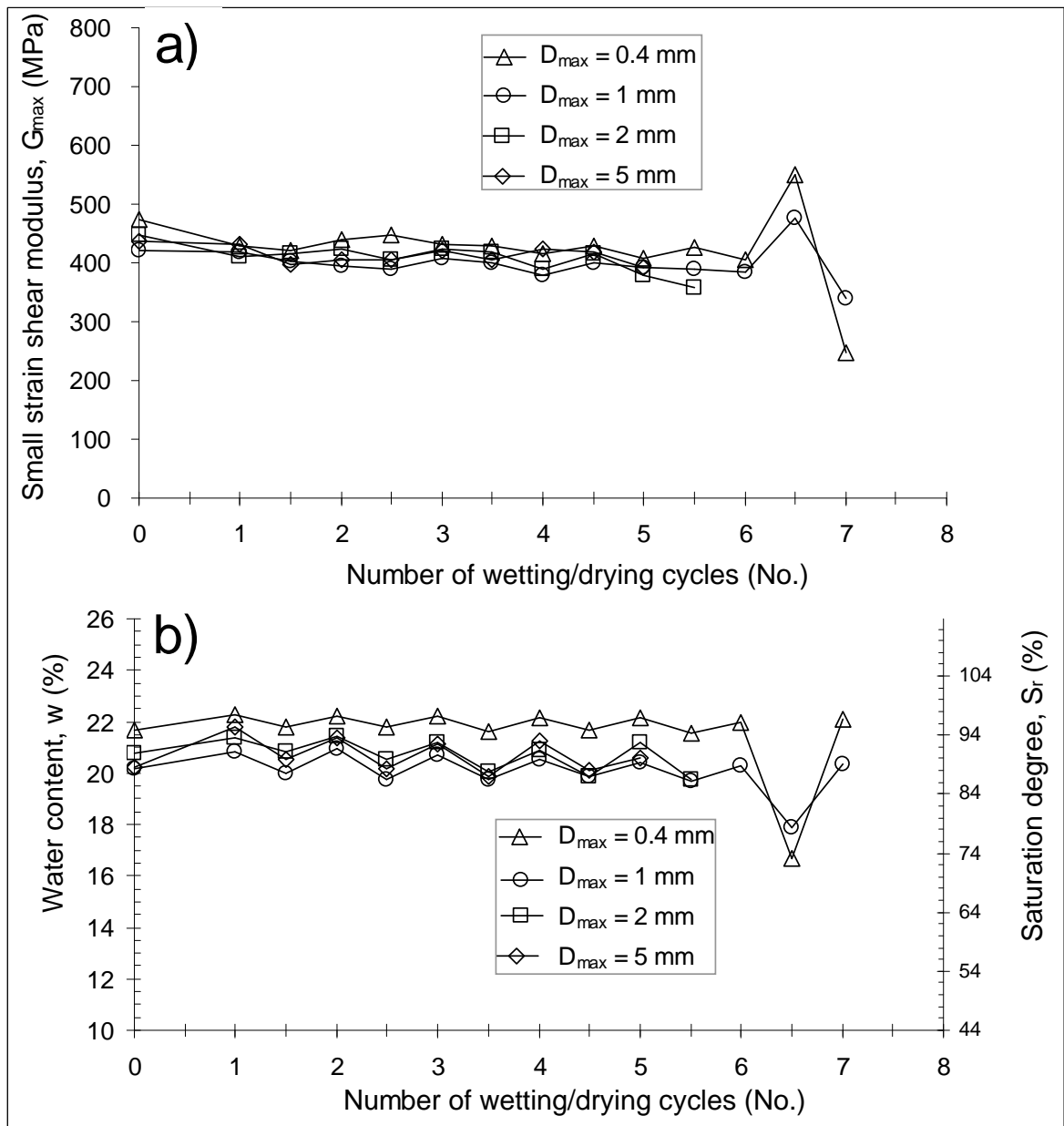


Figure 4-6 a) Changes in  $G_{max}$  upon cyclic wetting/drying for 2% lime treated silt of different sub-series prepared by method 1, with mixing method B, and then compacted on the wet side; b) corresponding water content and saturation degree changes with wetting/drying cycles (case 3)

### 4.2.3. Matric suction change

Figure 4-7 presents the suction change during one wetting/drying cycle for the lime treated silt.

On the whole, for the drying path, we observe a clear aggregates size effect - the larger the aggregates size, the lower the suction. By contrast, for wetting path, the aggregates size effect is not as noticeable as for the drying paths. Comparison of suction between drying

and wetting paths shows a large variation of suction values during drying paths and a relatively small variation of suction values during wetting paths.

For the untreated silt (case 2, 4) of the drying paths, as for the  $G_{\max}$ , we observe that the larger the  $D_{\max}$  the lower the suction (ex. No. 2.5,  $s = 877 \sim 140$  kPa). For the wetting paths, the suction variation for the four sub-series is negligible (ex. No. 3,  $s = 24 \sim 14.5$  kPa). Similar to the significant difference of  $G_{\max}$  variation range between drying and wetting in Figure 4-3a and Figure 4-5a, a much lower variation of suction in wetting paths is observed, whatever the sub-series is. Thereby, changes of  $G_{\max}$  of untreated silt during wetting or drying are mainly controlled by the suction change, as reported by Mancuso *et al.* (2002). The slight decrease of  $G_{\max}$  in the wetting paths or drying paths indicates the effects of the cyclic suction (wetting/drying).

For the treated silt (case 1, 3), the trends of suction with increase of  $D_{\max}$  are found to be similar to that for untreated silt. Moreover, comparison of the suction between the treated silt and the untreated one shows that the treated silt presents larger range of suction change during wetting/drying. This is probably induced by the coating effect due to cementation, as much higher  $G_{\max}$  for treated silt is also identified (Figure 4-3a ~ Figure 4-6a). However, the treated silt is much less sensible to suction changes, as less pronounced  $G_{\max}$  change is identified for the treated silt during wetting/drying (Figure 4-4a and Figure 4-6a). In addition, for the treated silt, the dry side specimens present higher variation of  $G_{\max}$  than the wet side ones. This suggests that  $G_{\max}$  change for treated silt also depends on the range of suction change.

Summarizing, for the untreated silt, the  $G_{\max}$  is mainly suction change dependent; for the treated silt, the  $G_{\max}$  is influenced by the combined effects of suction and cementation degree of the silt.

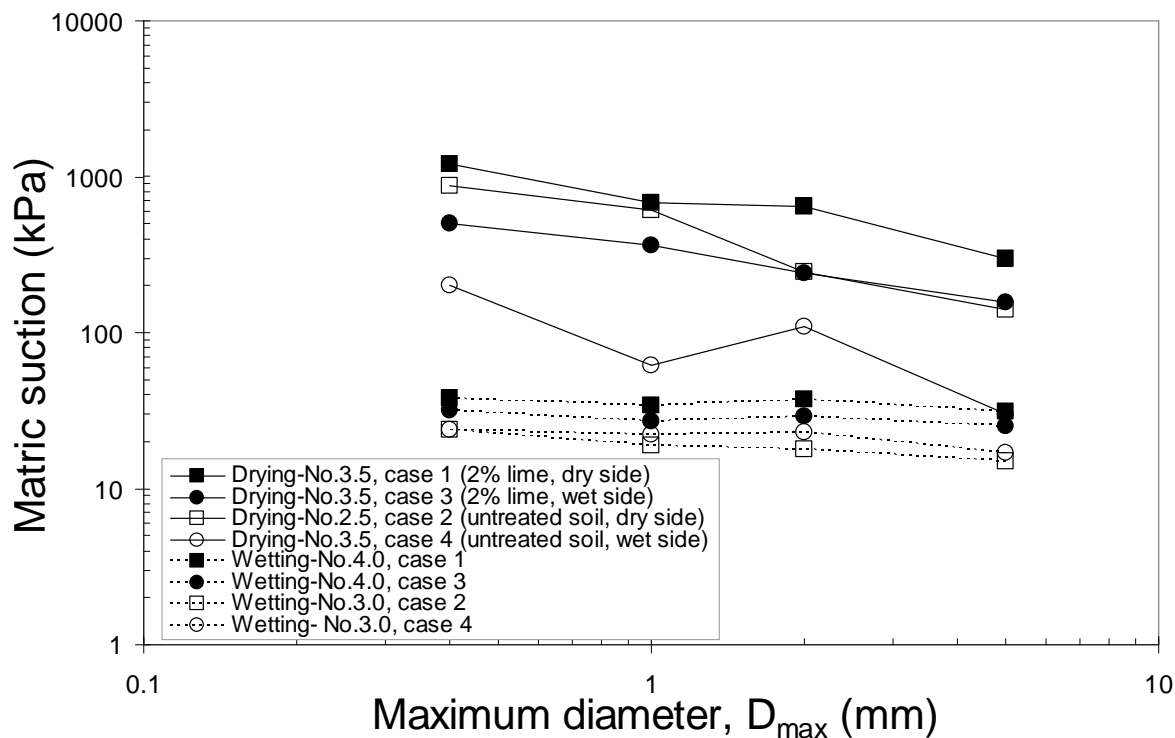


Figure 4-7 Matric suction change during drying and wetting for the lime treated silt

#### 4.2.4. Results with intensive drying

As mentioned in section 4.2.1 and 4.2.2, intensive drying to a water content lower than the initial value  $w_f$  increases the  $G_{max}$  and the subsequent rewetting (from No.6 to No.6.5) significantly decreases the  $G_{max}$ . In order to investigate the  $G_{max}$  evolution during this intensive drying, several measurements were performed on a same specimen at different water contents. Figure 4-8a presents the results of the specimen compacted on the dry side and Figure 4-8b shows the results for the wet side.

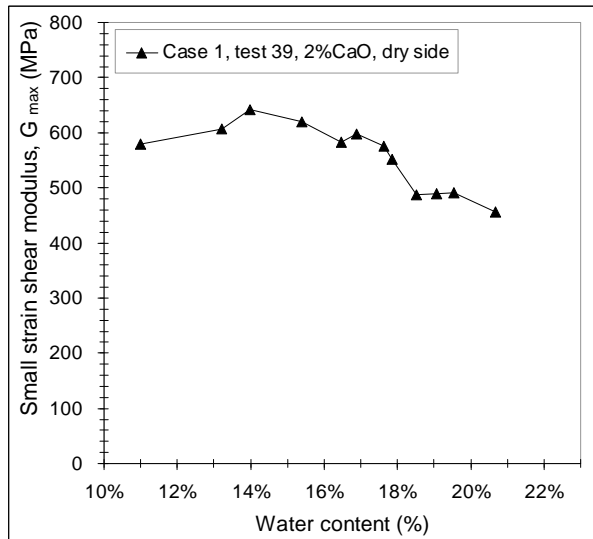
For the dry side specimen (case 1),  $G_{max}$  is 457 MPa at wetting state. Drying gradually increases the  $G_{max}$  value until reaching the peak value of 642 MPa at  $w = 14\%$ . Thereafter, further drying surprisingly decreases the  $G_{max}$  value.

For the wet side (case 3), the  $G_{max}$  at wetting state is about 406 MPa (ex. 388 MPa and 424 MPa for test 43 and test 44, respectively). Similarly, continuous drying also increases their  $G_{max}$  until a water content of about 18%. The subsequent intensive drying does not increase the  $G_{max}$ .

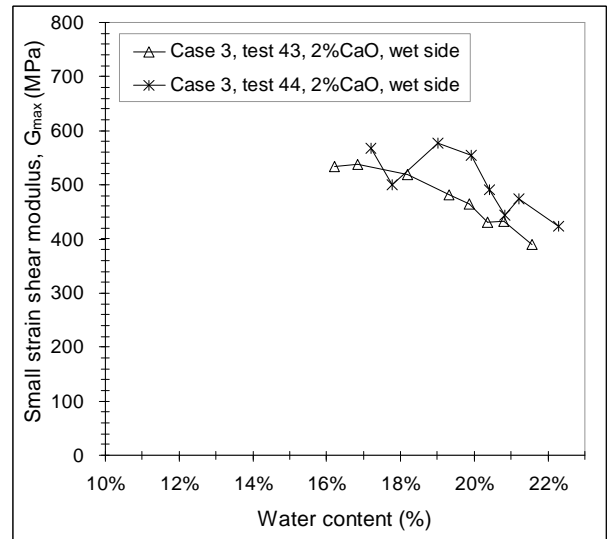
This suggests a notable change in microstructure or organization of soil grains. The intensive drying followed by wetting causes a negative effect on the soil microstructure.



Normally, as evidenced on the soils of  $D_{max} = 5$  mm compacted on the dry side (Figure 4-4a), after the negative effect at No.4, the  $G_{max}$  cannot return to the previous levels with the subsequently cycles. Thereby, the intensive drying probably results in a significant suction change which causes significant breakage of the aggregates (suction limit). For the 2% lime treated silt, the limit suction probably occurs at water content 14% and 18% for the dry side and the wet side, respectively.



(a) Case 1, dry side, 2% lime,  $D_{max} = 0.4$  mm



(b) Case 3, wet side, 2% lime,  $D_{max} = 0.4$  mm

Figure 4-8  $G_{max}$  evolution with intensive drying from saturated condition to very dry states for the 2% lime treated silt, prepared by method 1 (case 1 and case 3)

### 4.3. Results on cement treated silt

As for the silt treated with lime, only the silt prepared by sieving method 1 and then treated with cement was tested.

#### 4.3.1. Results for dry side

For the soils compacted on dry side, the results for untreated silts (case 10) are shown in Figure 4-9. The corresponding 3% cement treated silts (case 9) are shown in Figure 4-10. Their variations of water content/saturation degree during cyclic wetting-drying are also presented.

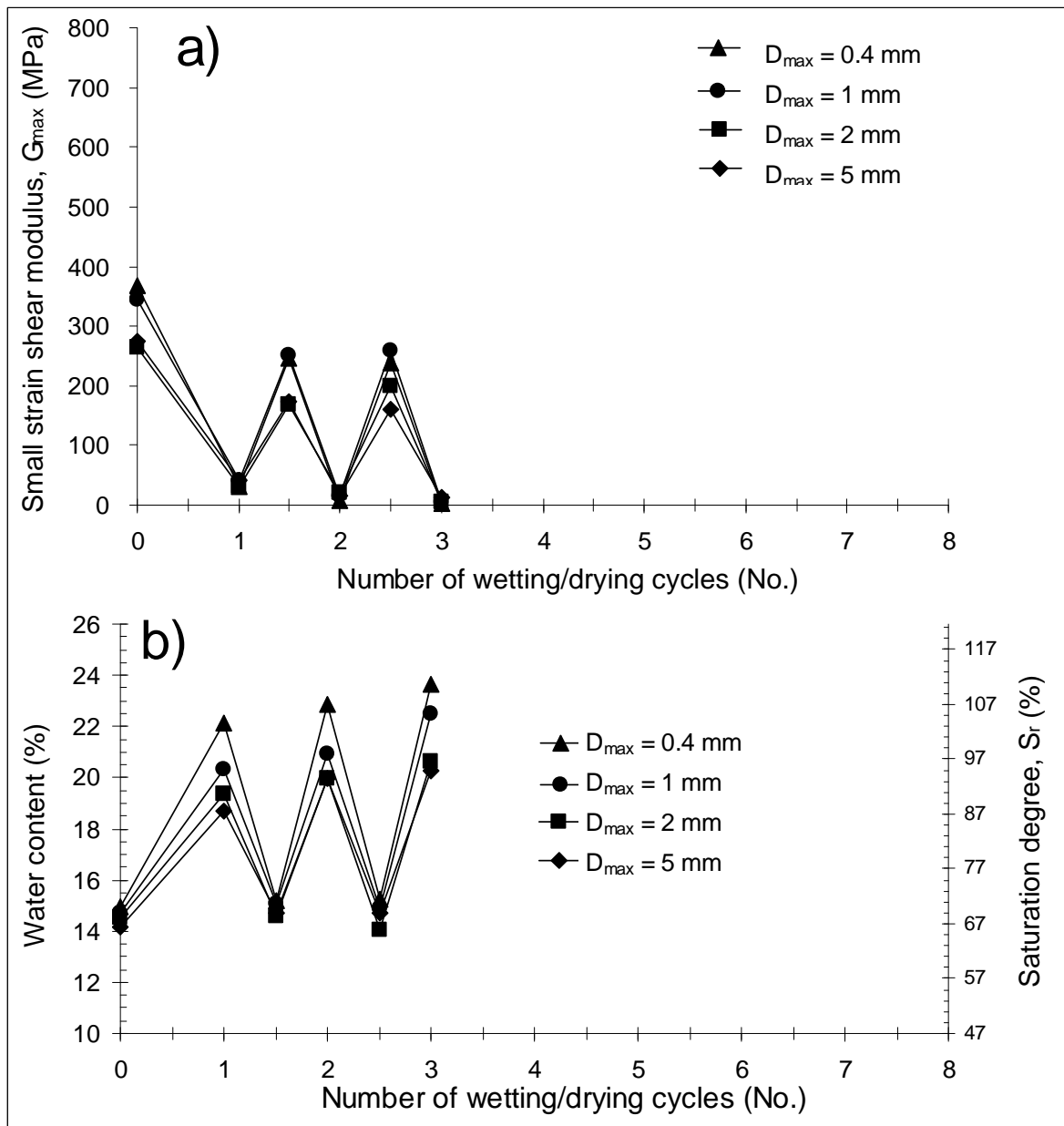


**Figure 4-9 a) Changes in  $G_{max}$  upon cyclic wetting/drying for untreated silt of different sub-series prepared by method 1, compacted on the dry side; b) water content and saturation degree change with cyclic wetting/drying (case 10)**

For the untreated silts (case 10), as it can be seen in Figure 4-9, similar observations can be made as for the untreated silts on dry side: 1) the soils are very sensible to the water content changes; 2) in the wetting paths, the water content increases with the cycles, especially for the finer aggregates soils (ex.  $D_{max} = 0.4$  mm); 3) no clear aggregate size effect on  $G_{max}$  in wetting paths is observed as opposed to the case in drying paths.

Similar to the untreated silt, on the whole, the cement treated soil (Figure 4-10) shows typical cyclic variations of  $G_{max}$  with wetting/drying cycles before a serious degradation

finally occurs. This is very different from lime treated one. It suggests that the water content effect is no longer negligible for the cement treated silt.

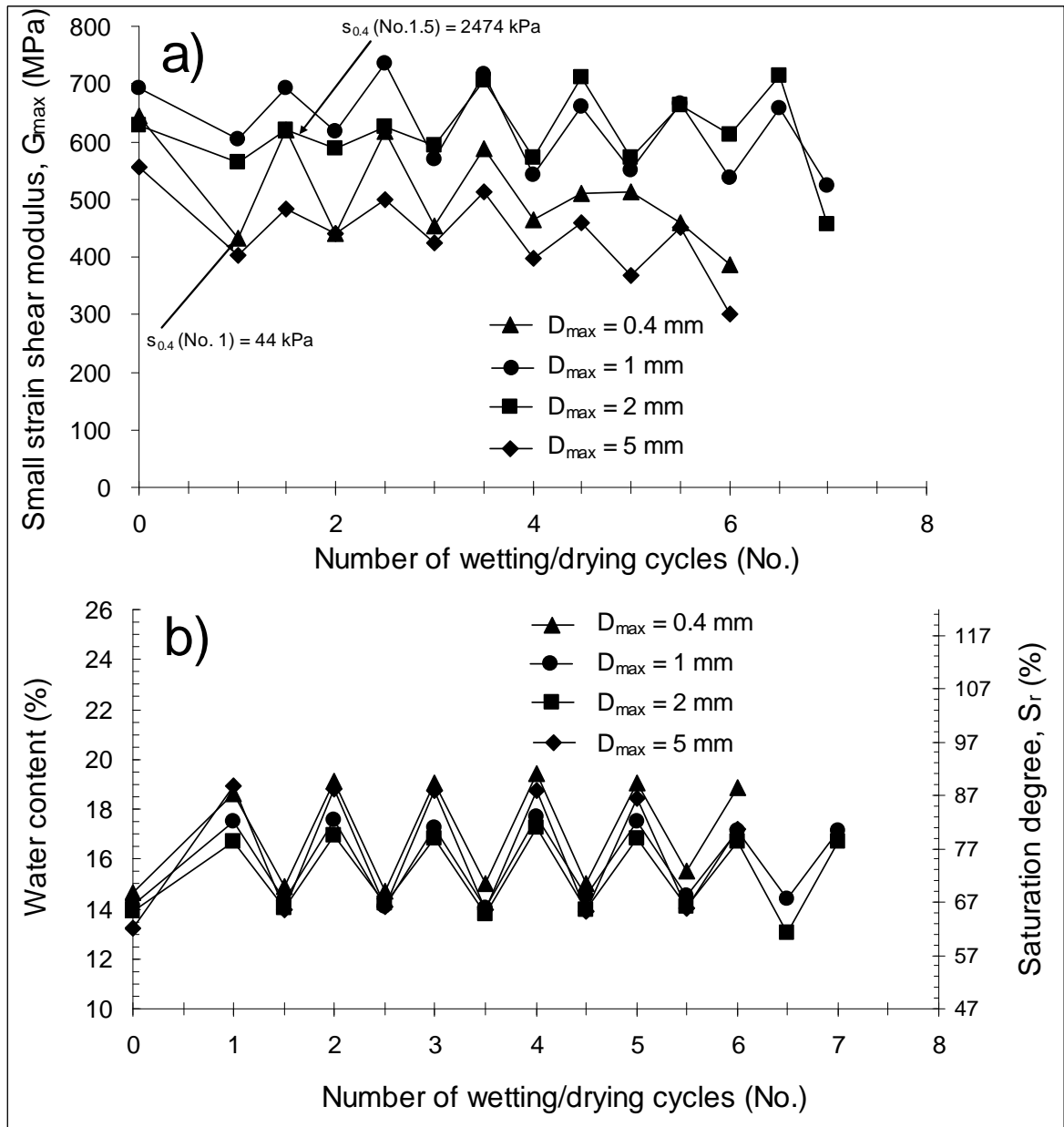


**Figure 4-10 a) Changes of  $G_{max}$  upon cyclic wetting/drying for 3% cement treated silt of different sub-series prepared by method 1, with mixing method B, then compacted on the dry side; b) corresponding water content and saturation degree changes with wetting/drying cycles (case 9)**

For the treated specimens of sub-series  $D_{max} = 0.4$  mm, the first wetting (No.1) decreases the  $G_{max}$  value from 644 MPa to 431 MPa. Then, the subsequent wetting/drying cycles No.1 ~ No.3 results in cyclic variations of  $G_{max}$  within an almost constant range. Thereafter, the range of cyclic  $G_{max}$  values decreases rapidly until No.5, suggesting a lower sensibility of  $G_{max}$  to water content changes. Finally, the wetting/drying cycles No.5~ No.6

steadily decreases the  $G_{max}$ , showing a serious degradation of soil sample. It is worth noting that the  $G_{max}$  in wetting paths changes very slightly during the first 3 cycles, and it increases then slightly until No.5. If the first five cycles are induced by the coating effect related to the chemical reactions (stage I), the subsequent degradation is probably due to the de-bonding effect related to the steadily breakage of aggregates (stage II). Tang *et al.* (2011) also observed an increase of  $G_{max}$  after a few wetting/drying cycles for a lime treated silt compacted on the dry side.

For the treated soils from other sub-series (case 9), similarly, the first wetting also decreases their  $G_{max}$  values. Then, the subsequent wetting/drying cycles cause an increasing range of cyclic  $G_{max}$  followed by a constant range of cyclic  $G_{max}$ , and finally a serious decrease of  $G_{max}$ . Note that, for  $D_{max} = 2 \text{ mm}$ , the  $G_{max}$  at No.6.5 slightly higher than in the previous drying paths is probably due to the lower water content.

Under similar wetting/drying conditions, the different  $G_{max}$  evolutions for the soils from different sub-series suggest that the  $G_{max}$  value depends not only on the effect of water content/suction, but also on the effect of aggregates size. The aggregates size effect is related to the ongoing chemical reactions within the silt during these cycles, building chains by cementation or de-bonding them. Comparison between the curves of lime treated and cement treated silt shows that the cement treated silt is more sensible to water content changes. This indicates that the lime treatment may result in more cementitious chains than the cement treatment.

### 4.3.2. Results for wet side

In the case of the wet side, Figure 4-11 shows the  $G_{max}$  changes with cyclic wetting-drying for the untreated silt (case 12). Similarly, Figure 4-12 presents the results for the 3% cement treated silt (case 11). Their water content /saturation degree variations during cyclic wetting-drying are given.

For the untreated silt, as shown in Figure 4-11, some similar observations can be made. The  $G_{max}$  value is strongly influenced by the soil water content changes.

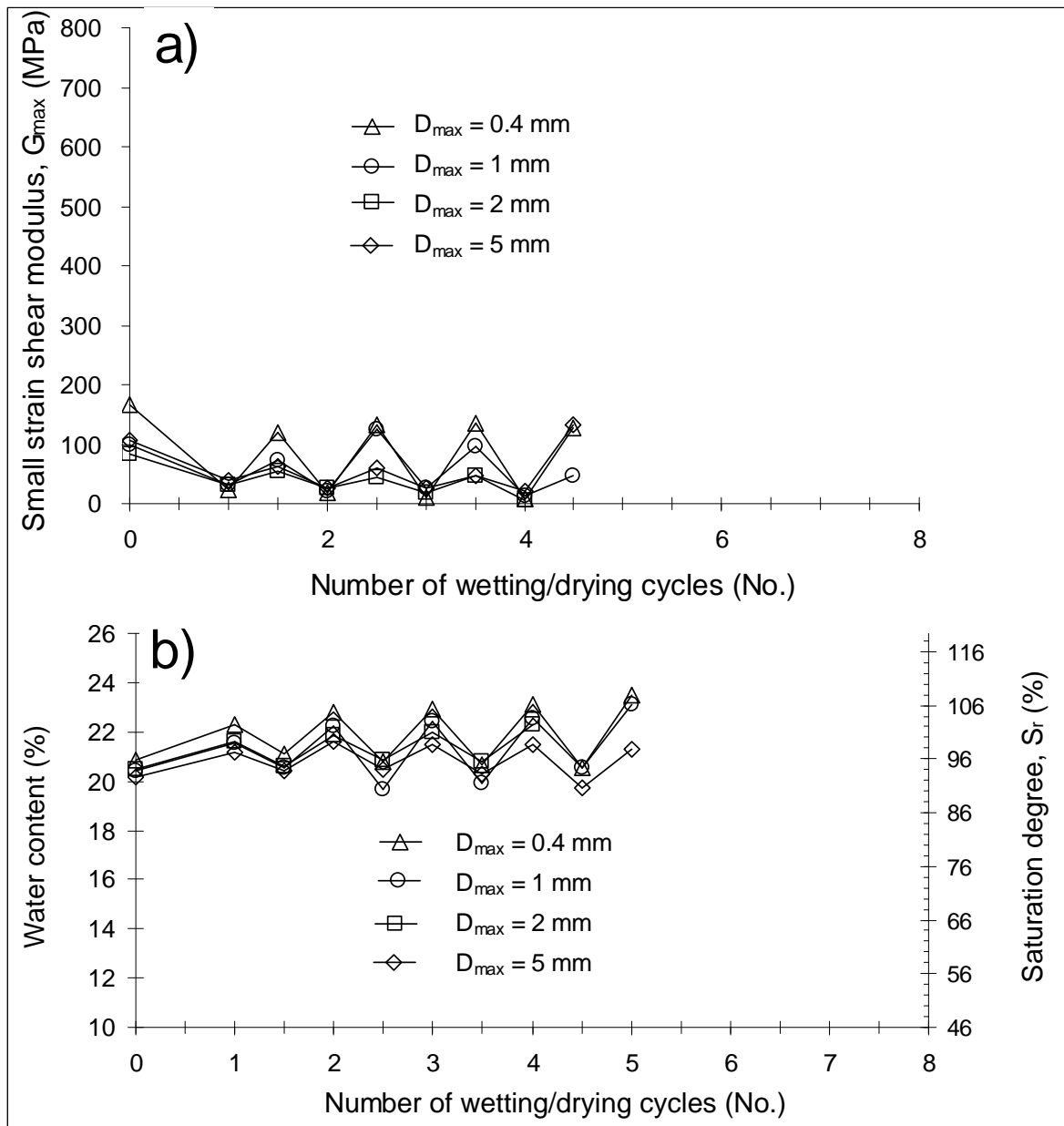


**Figure 4-11 a) Changes of  $G_{max}$  upon cyclic wetting/drying for the silt of different sub-series prepared by method 1, then treated by 0% cement and compacted on the wet side of optimum; b) corresponding water content and saturation degree change with wetting/drying cycles (case 12)**

For the 3% cement treated silt, as shown in Figure 4-12a, all the samples show a decreasing  $G_{max}$  after the first wetting path. Then, the subsequent wetting/drying cycles No.1 ~ No.5 result in a limited variation of  $G_{max}$ , probably due to a lower range of water content changes than for the dry side. Thereafter, the following wetting/drying cycles No.5 ~ No.6 present a slightly enlarged variation range of  $G_{max}$ , indicating a higher water content sensibility than that in the previous cycles. Finally, the enlarged variation range of  $G_{max}$  changes in No.6.5 ~ No.7 is due to the intensive drying followed by wetting (Figure 4-12b).

The normal (non intensive) wetting/drying cycles only lead to a very slight degradation of  $G_{max}$  (stage I), whereas the intensive drying (No.6.5) and wetting (No.7) can result in a noticeable degradation of  $G_{max}$  value. This phenomenon is also identified for the lime treated silt. This indicates that breakage of aggregates occurs due to the de-bonding effect. The de-bonding of aggregates may be the result of the previous cycles and the present intensive drying. Obviously, the intensive drying accelerates the de-bonding process.

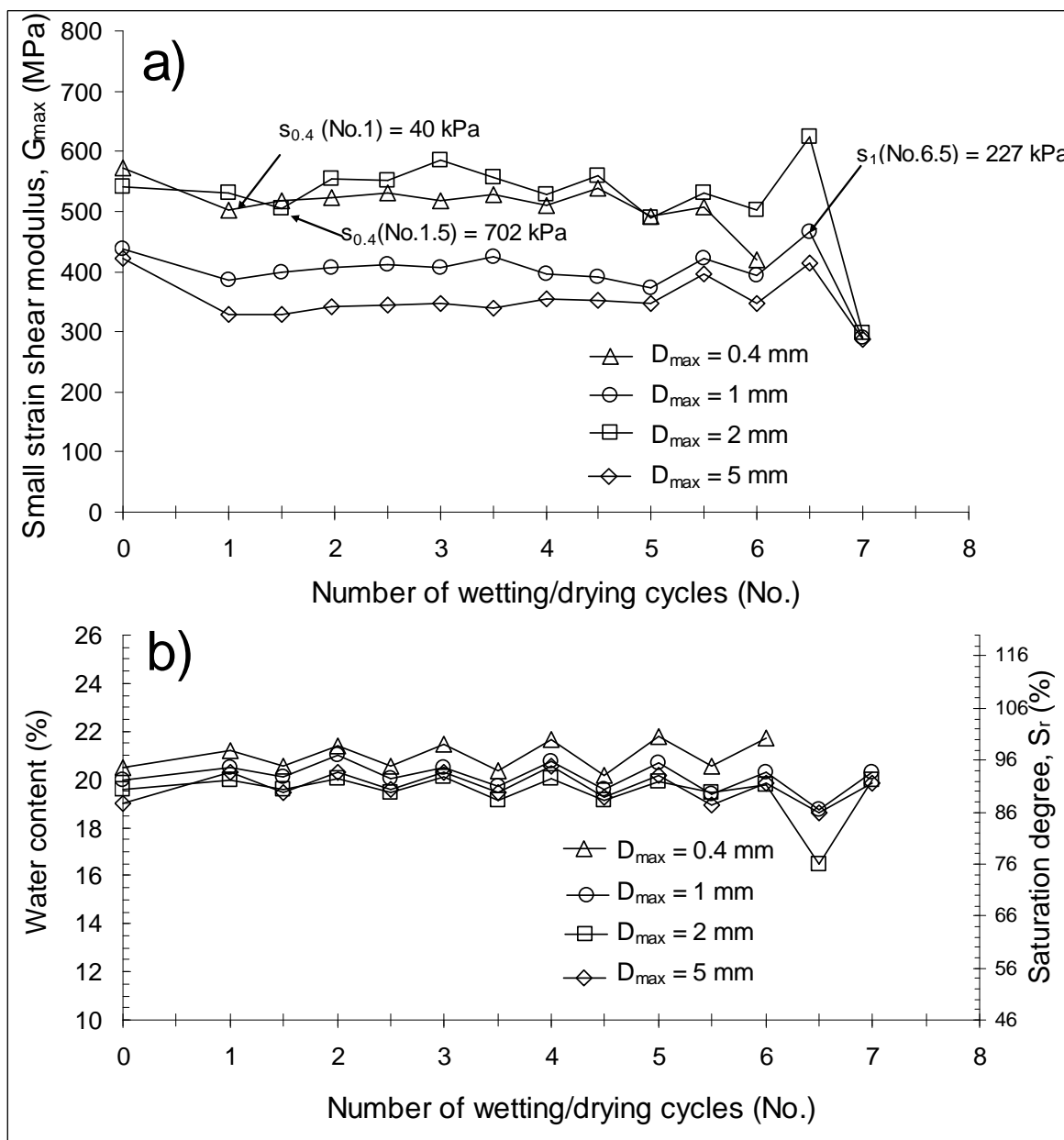


Figure 4-12 a) Changes of  $G_{max}$  upon cyclic wetting/drying for 3% cement treated silt of different sub-series prepared by method 1, with mixing method B, and then compacted on the wet side; b) corresponding water content and saturation degree changes with wetting/drying cycles (case 11)

On the whole, for the treated specimens compacted on wet side, the  $G_{\max}$  is no longer sensible to water content changes, whereas the  $G_{\max}$  of untreated ones is still very sensible to water content change but less noticeable than that of dry side. This difference is probably due to the range of suction change, as the wet side specimens have much higher saturation degrees than the dry side specimens.

### 4.3.3. Matric suction change

Figure 4-13 presents the suction change with  $D_{\max}$  during a cycle of wetting/drying for the cement treated silt. Similar to the lime treated silt, in the drying path, a clear aggregates size effect is noticeable - the larger the aggregates size, the lower the suction. For the wetting path, this aggregates size effect is not noticeable. Compared to the lime treated silt, the suction of wetting state is obviously much higher for both dry side and wet side. This is probably due to the different conditions of compaction and cementation (treatments).

Similar to the untreated silt (case 2, 4), the cement treated one (case 10, 12) also shows high sensibility of  $G_{\max}$  (Figure 4-9a, Figure 4-11a) to suction changes (Figure 4-13). The more pronounced cyclic changes of  $G_{\max}$  in case 10 (dry side) as compared to case 2 are also to be related to the larger range of suction changes.

For the 3% cement treated silt compacted on dry side (case 9), as shown in Figure 4-10, the cyclic  $G_{\max}$  changes with wetting/drying cycles are also due to the significant suction changes between drying (ex. mean value 1253 kPa at No.3.5) and wetting (ex. mean value 39 kPa at No.4). The range of suction changes is almost doubled to that for the 2% lime treated silt (35 ~ 700 kPa). This is confirmed by the 3% cement treated specimens compacted on wet side (case 11) – with lower variations of  $G_{\max}$  and lower range of suction changes (42 ~ 448 kPa). Thereby, the range of suction changes affects the stiffness of treated soils.

It is worth noting that the suction of treated soils can be influenced by the effect of wetting/drying cycles, especially for the drying state. In fact, the normal wetting/drying cycles changes its suction very slightly (ex. case 9 for sub-series  $D_{\max} = 0.4 \text{ mm}$ : 2474 kPa at No.1.5 in Figure 4-10a and 2282 kPa at No.3.5 in Figure 4-13; case 11: 702 kPa of No.1.5 to 689 kPa at No.4.5), whereas intensive drying can significantly decrease the suction of treated soils - as intensive drying surprisingly decreases the soil suction to 227 kPa at No.6.5 from 452 kPa at No.4.5 in Figure 4-12(a) (ex. case 11,  $D_{\max} = 1.0 \text{ mm}$ ). This indicates that breakage of aggregates occurs due to the large range of suction changes or intensive drying.

This phenomenon is confirmed by the significantly decrease of  $G_{\max}$  due to the subsequent wetting.

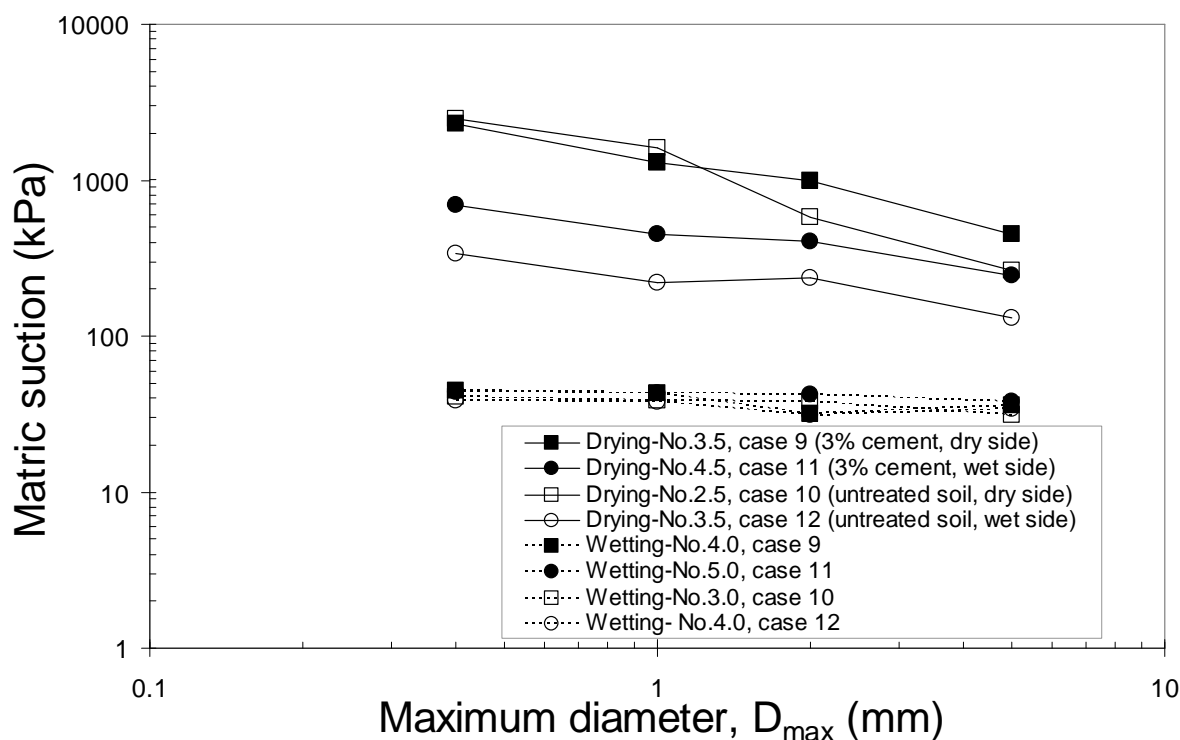


Figure 4-13 Matric suction changes during drying and wetting for the cement treated silt

#### 4.3.4. Results with intensive drying

As for the results of intensive drying of the lime treated silt, Figure 4-14 presents the  $G_{\max}$  changes with different water contents when drying the 3% cement treated silt. Both dry side ( $w_f = 14\%$ , case 9) and wet side ( $w_f = 21\%$ , case 11) are presented.

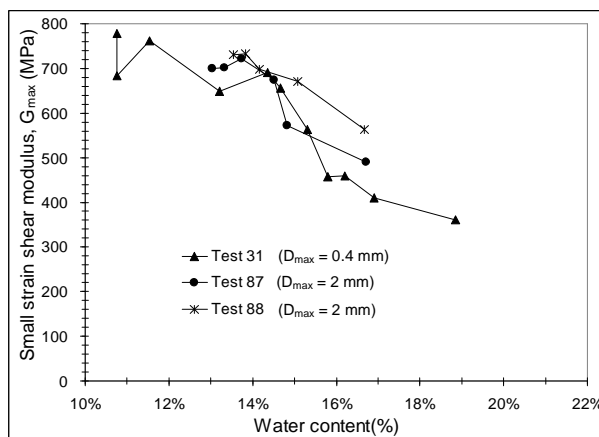
For the dry side (case 9), although a large variation of  $G_{\max}$  is obtained at very dry state, drying steadily increases the  $G_{\max}$  until its value at the initial water content  $w_f$ , and then the  $G_{\max}$  seems to level off upon further intensive drying.

For the wet side (case 11), drying from the near saturation state firstly increases  $G_{\max}$  until a peak value at about  $w = 17.5\%$ , then further drying surprisingly decreases the  $G_{\max}$  of soils of different sub-series. The high variation of  $G_{\max}$  indicates the heterogeneity of the treatment.

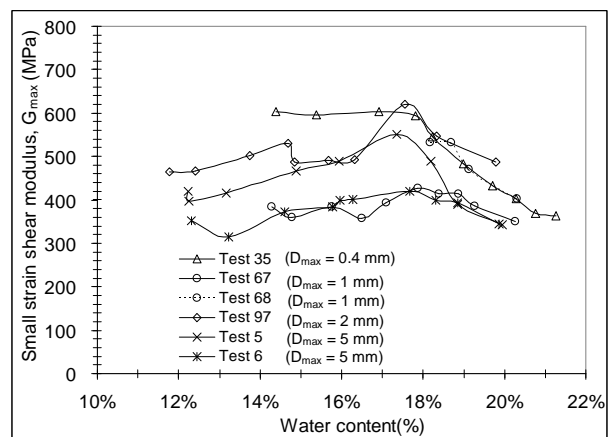
A drop of  $G_{\max}$  is often identified in case of intensive drying followed by wetting (ex. 623 MPa at No.6.5 to 298 MPa at No.7.0 of case 11  $D_{\max} = 2 \text{ mm}$  in Figure 4-12). This indicates that intensive drying (lower than the  $w_f$ ) can cause significant microstructure change



for treated soils or induce de-bonding of the aggregates. As mentioned before, in some extreme cases, the intensive drying even decreases the suction of treated soils (ex. case 11,  $D_{max} = 1.0$  mm, the suction at normal cycle at No.4.5 is significantly higher than at the intensive drying at No.6.5). Comparison of the results between the dry side and wet side indicates that this modification of microstructure depends strongly on its moulding water content. As in the case of lime treatment, the limit of water content to enable breakage of aggregates may be defined by the peak values of  $G_{max}$ , i.e. about 13% and 17.5% for the dry side and wet side treated specimens, respectively.



(a) Case 9, dry side, 3% cement,



(b) Case 11, wet side, 3% cement

Figure 4-14  $G_{max}$  evolutions with intensive drying from saturated condition to very dry states for 3% cement treated silt of different sub-series prepared by method 1(case 9 and case 11)

Comparison of the results of intensive drying followed by wetting between lime treatment and cement treatment shows a common point - accelerated soil degradation. As the cyclic suction change can de-bond the cementitious chains of aggregates during normal wetting/drying cycles, the acceleration of the degradation induced by intensive drying followed by wetting indicates that the degradation is strongly suction range dependent.

#### 4.4. Results on the lime treated clay

For the clay, we will firstly present the results with mixing method A and then with mixing method B.

### 4.4.1. Mixing method A

#### 4.4.1.1. Results for dry side

Figure 4-15a depicts the variations of  $G_{max}$  with wetting/drying cycles for the untreated clay specimens prepared from soil powders of different sub-series ( $D_{max} = 0.4\text{ mm}$ ,  $1\text{ mm}$ ,  $2\text{ mm}$ ,  $5\text{ mm}$ ) by method 2, compacted dry of optimum ( $w_f = 25\%$ ,  $S_r = 67.6\%$ ) (case 19). Figure 4-15b gives the corresponding water content/saturation changes during these wetting/drying cycles.

In Figure 4-15a, similar  $G_{max}$  evolutions with wetting/drying cycles are observed for different sub-series. The starting points of  $G_{max}$  (No.0) are similar, ranging from 85 MPa to 101 MPa. The first wetting (No.1) to a mean water content of 34.6% ( $S_r = 92\%$ ) decreases the  $G_{max}$  value to only several MPa (9 MPa - 12 MPa). Then, drying to  $w_f$  increases their  $G_{max}$  (70 MPa ~ 112 MPa). Thereafter, the rewetting (No.2) decreases these values to several MPa again. As for the silt, the untreated clay is also very sensible to water content changes from the beginning of the application of cycles. For the wetting paths, the similar  $G_{max}$  values for different sub-series suggest the absence of aggregates size effect on  $G_{max}$ . As for the silt, we also observe that the  $G_{max}$  variation range is larger for the drying paths than for the wetting paths.

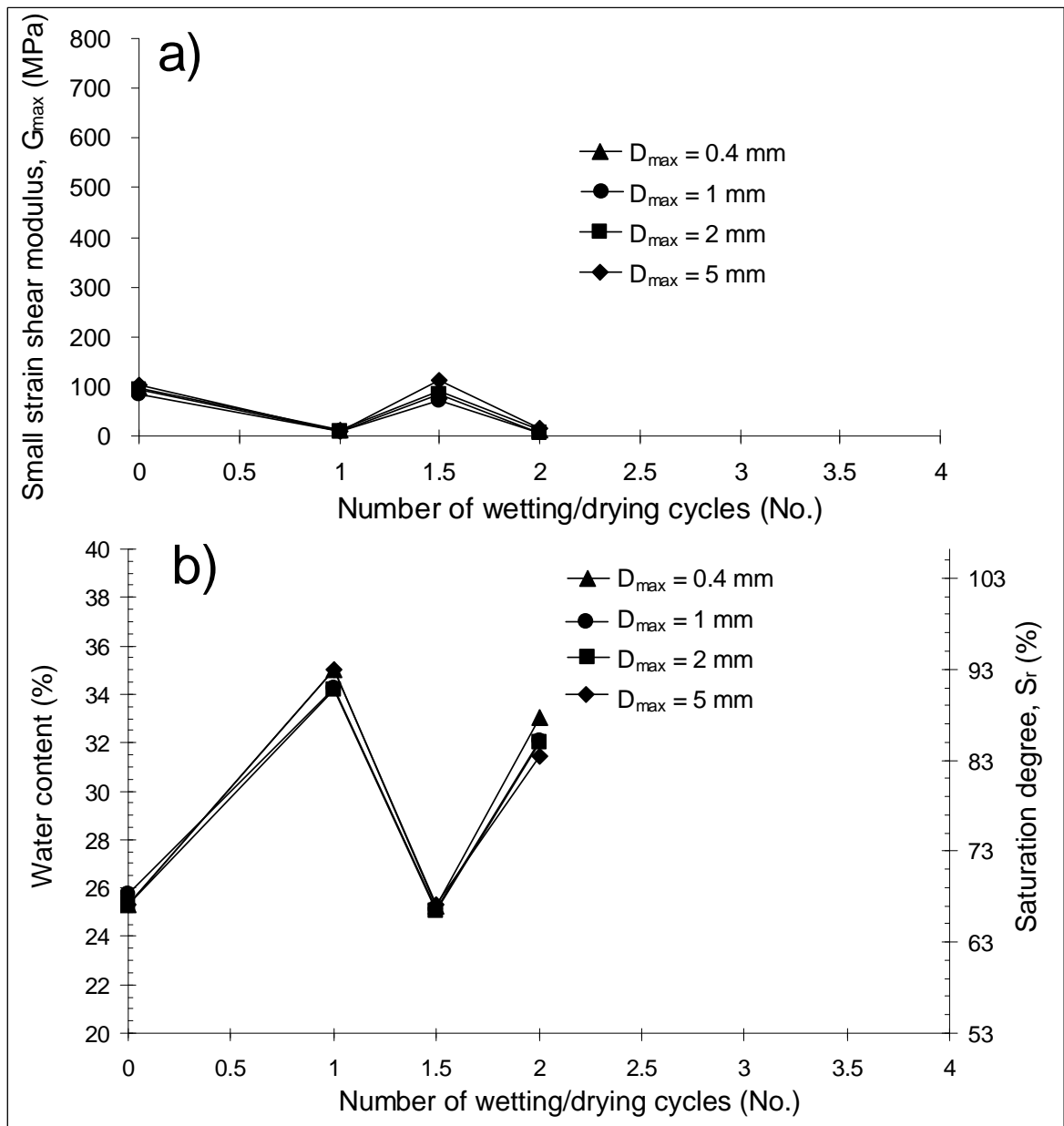


**Figure 4-15 a) Changes of  $G_{max}$  upon cyclic wetting/drying for the untreated clay of different sub-series prepared by method 2, compacted on the dry side; b) corresponding water content and saturation degree changes with wetting/drying cycles (case 19)**

Figure 4-16a depicts the  $G_{max}$  variations with wetting/drying cycles for the 4% lime treated clay, also compacted on the dry side ( $w_f = 25\%$ ,  $S_r = 67.6\%$ ) (case 18). Figure 4-16b presents the water content/saturation changes during these wetting/drying cycles. On the whole, the  $G_{max}$  varies in different levels for different sub-series, depending on their suction and aggregates size effects (see chapter 3).

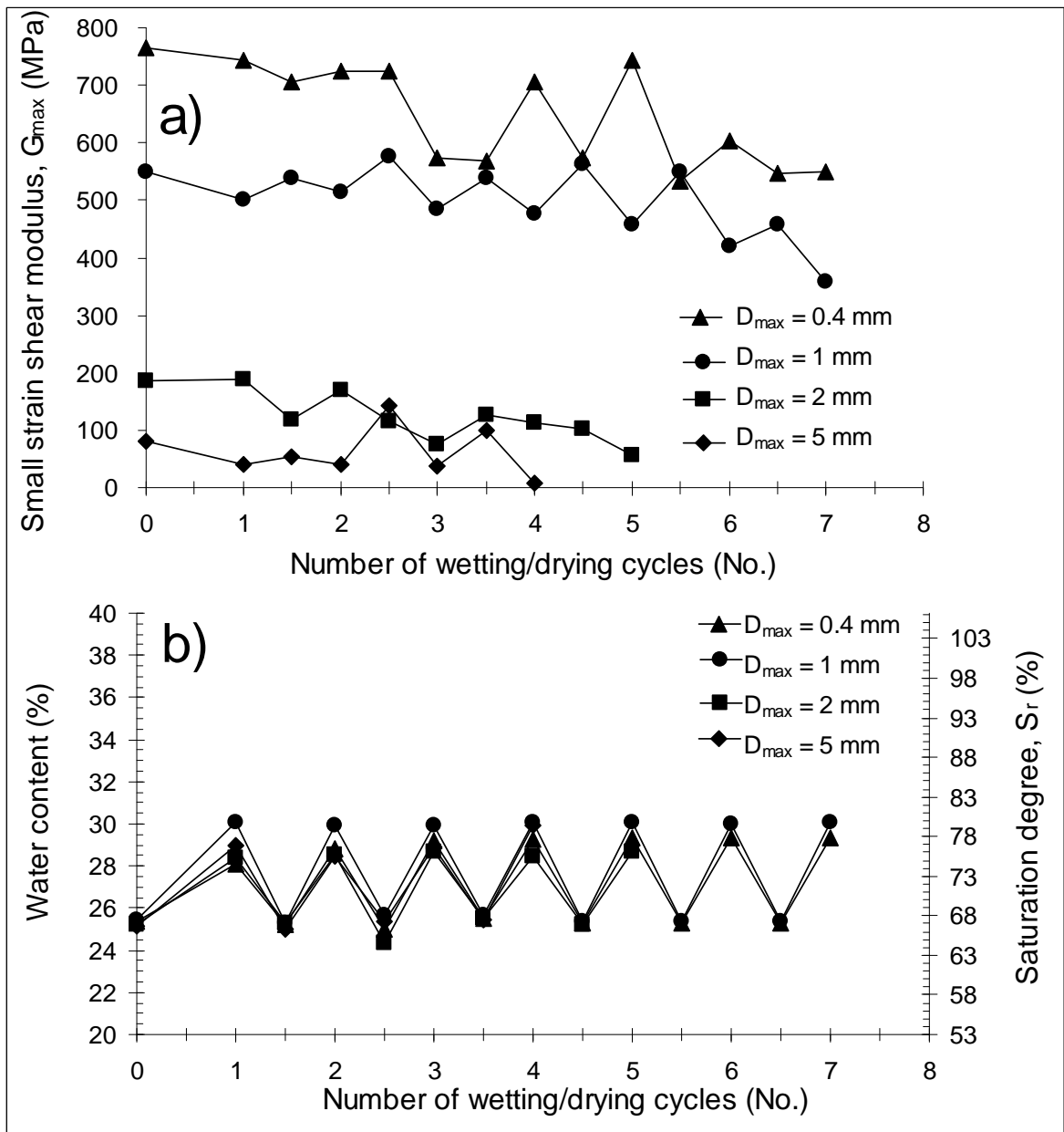


Figure 4-16 a) Changes of  $G_{max}$  upon cyclic wetting/drying for the clay of different sub-series prepared by method 2, then treated by 4% lime with mixing method A, compacted on dry side; b) corresponding water content and saturation degree changes with wetting/drying cycles (case 18)

For the 4% lime treated soil specimens with  $D_{max} = 0.4$  mm, at the initial water content  $w_f = 25.4\%$  ( $S_r = 67.6\%$ ),  $G_{max}$  is 745 MPa. Wetting to a water content of 28.1% ( $S_r = 74.7\%$ ) only slightly decreases its  $G_{max}$  to 348 MPa (No.1). The subsequent wetting/drying cycles do not visibly change the  $G_{max}$  until No.2.5 (stage I). Then, the third wetting (No.3) decreases the  $G_{max}$  value sharply- a drop of  $G_{max}$  value (567 MPa) is identified. This indicates the breakage of aggregates. Thereafter, the  $G_{max}$  variation range increases with the cycles

No.3 to No.5.5. In these cycles, the  $G_{\max}$  shows similar values in drying paths, whereas it increases sharply in wetting paths. Finally, the  $G_{\max}$  changes slightly again with values similar to that in the previous drying paths. A slight degradation from No.6 to No.7 is also observed. In addition, the water content increases gradually in the wetting paths to 29.4% ( $S_r = 78.1\%$ ) at No.7.

For the other sub-series, under the similar wetting/drying cycles, they also firstly experience a negligible variation of  $G_{\max}$  during several cycles (stage I), then a cyclic variation of  $G_{\max}$  (stage II), finally a negligible variation again with a steady degradation. It seems that stage II occurs earlier for the coarser aggregates soils (ex. No.1 and No.2 for  $D_{\max} = 2 \text{ mm}$  and  $5 \text{ mm}$ , respectively) than for the finer one  $D_{\max} = 1 \text{ mm}$  (No.4). Note that the sub-series  $D_{\max} = 5 \text{ mm}$  resists only to four cycles. After the fourth wetting, the soil often presents obvious horizontal fissures and is thus damaged. In addition, as for  $D_{\max} = 0.4 \text{ mm}$ , the water content also increases slightly during the wetting paths.

Comparison between the results of the four sub-series shows that the  $G_{\max}$  change with wetting/drying cycles is strongly aggregates size dependent. The larger the aggregates, the lower the  $G_{\max}$  value and the lower the resistance to wetting/drying cycles.

#### 4.4.1.2. Results for wet side

Figure 4-17 shows the  $G_{\max}$  change with wetting-drying cycles for the untreated clay specimens of the same sub-series as in Figure 4-15 ( $D_{\max} = 0.4 \text{ mm}, 1 \text{ mm}, 2 \text{ mm}, 5 \text{ mm}$ ), but compacted on the wet side ( $w_f = 35\%$ , case 22). The corresponding water content/saturation changes are also presented.

As for the dry side specimens, the wet side specimens of the four sub-series present similar  $G_{\max}$  evolutions with wetting-drying cycles, but a lower variation level of  $G_{\max}$  between the drying and wetting paths. In Figure 4-17, the specimens start with similar  $G_{\max}$  values (65 ~ 44 MPa) at No.0 ( $S_r = 92.6\%$ ). The first wetting No.1 ( $S_r = 100.1\%$ ) decreases the values to only 13 ~ 15 MPa. The second drying No.1.5 to their initial water contents  $w_f$  increases their  $G_{\max}$  to almost the same values as the initial ones. The final rewetting No.2 decreases the values to several MPa. Similar to the dry side specimens, the wet side clay specimens are also very sensible to water content changes.

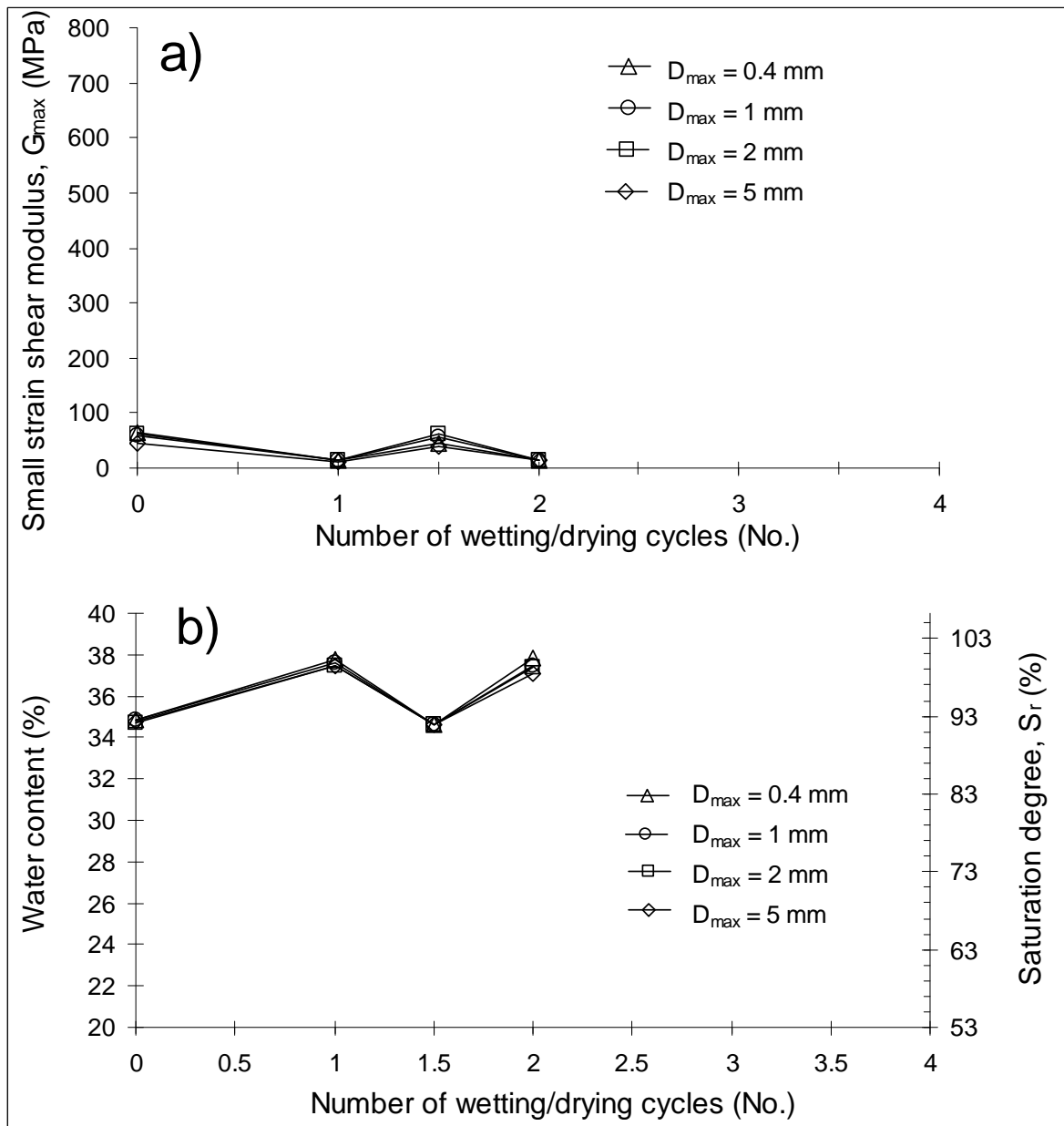


**Figure 4-17 a) Changes of  $G_{max}$  upon cyclic wetting/drying of the untreated clay of different sub-series prepared by method 2, then compacted on the wet side; b) corresponding water content and saturation degree change with wetting/drying cycles (case 22)**

Figure 4-18 presents the results of 4% lime treated clay, also from the same four sub-series being mixed with method A and then compacted wet of optimum ( $w_f = 35.29\%$ ,  $S_r = 93.9\%$ ) (case 21). The water content/saturation degree of wetting paths almost remains constant with wetting/drying cycles. The water content increases to a mean value of 35.53% ( $S_r = 94.54\%$ ) at the first wetting No.1 and at the last wetting to 35.6% ( $S_r = 94.72\%$ ).

Considering the slight water content variation between wetting and drying, the  $G_{max}$  change can be regarded as significant.

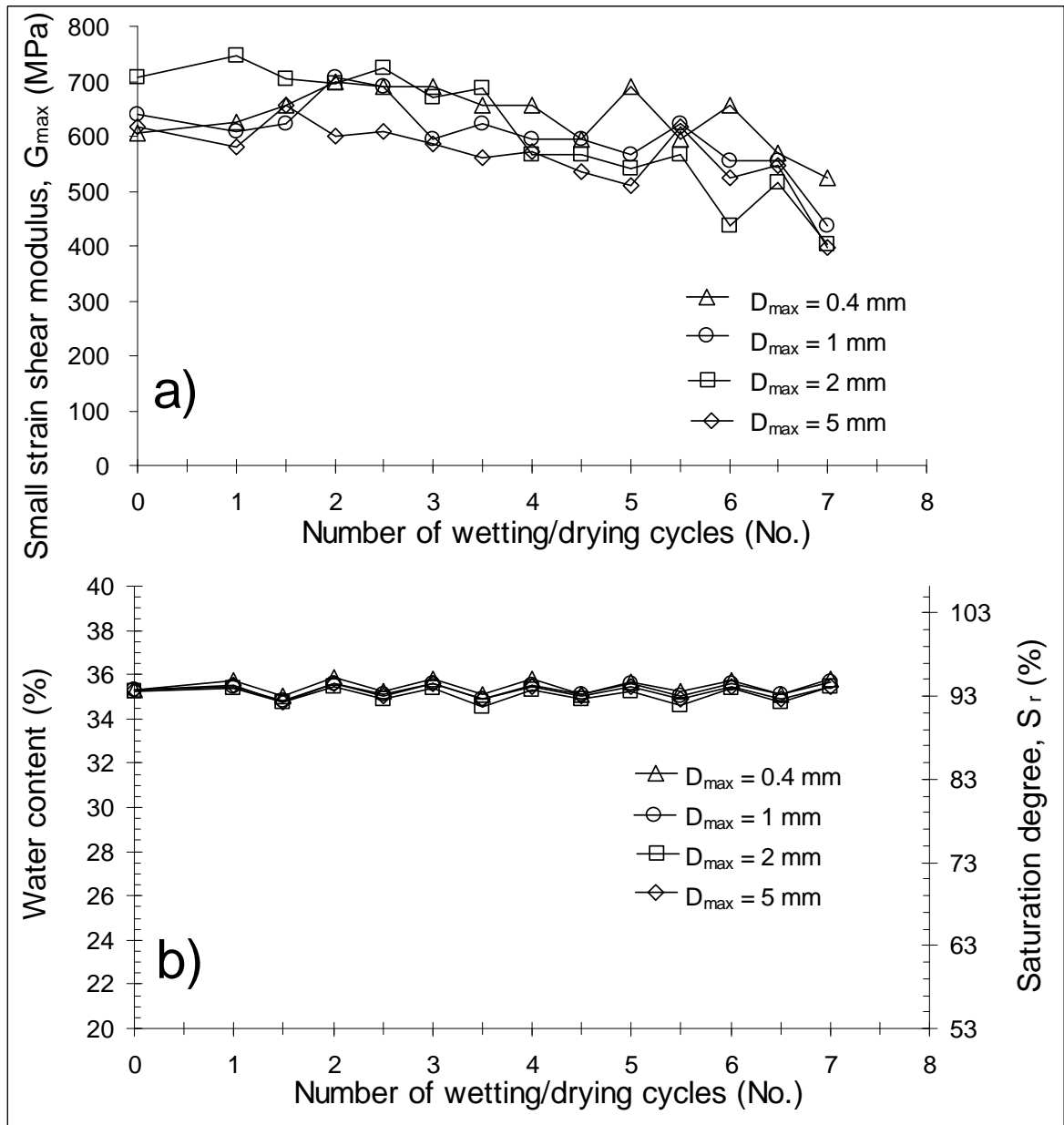


Figure 4-18 a) Changes of  $G_{max}$  upon cyclic wetting/drying for the 4% lime treated clay of different sub-series prepared by method 2, with mixing method A, and then compacted on the wet side; b) corresponding water content and saturation degree change with wetting/drying cycles (case 21)

Similar to the dry side specimens, the wet side specimens for the four sub-series also present the  $G_{max}$  variations starting with relative stable values in the first several cycles (stage I, about 4 cycles, No. 1.5 ~ 4), then cyclic variations (stage II, about 2 cycles, No. 4 ~ 6), and finally a steady degradation (stage III, one cycle No. 6 ~ 7). Unlike in the case of dry side, stage II for the finer aggregates soil ( $D_{max} = 0.4$  mm) appears slightly earlier than the other

sub-series. Moreover, the variation of  $G_{\max}$  during the first two cycles is mainly due to the combined effects of suction change and coating related to chemical reactions. The cyclic  $G_{\max}$  (stage II) is probably mainly influenced by the significant different suction between drying and wetting paths. The accelerated decrease of  $G_{\max}$  (stage III) indicates the breakage of aggregates or de-bonding of chains. On the whole, a series of similar  $G_{\max}$ -cycle curves are observed for the four sub-series. Thereby, the effect of aggregates size on  $G_{\max}$  is not as noticeable as for the dry side. In addition, the increase of  $G_{\max}$  in early cycles is probably induced by the ongoing chemical reactions. This phenomenon was also identified by Tang et al. (2011) for the lime treated Tours silt compacted on dry side.

## 4.4.2. Mixing method B

### 4.4.2.1. Results for dry side

For the lime treated clay compacted on dry side, the specimens prepared by both mixing method A and mixing method B underwent cyclic wetting/drying. However, only the results of the wet specimens with method B are analysed in the following section, because, as mentioned before, the  $G_{\max}$  values of dry specimens with mixing method B are during curing as low as that of untreated clay. In fact, large aggregates were formed even compacted on the dry side, leading very weak chains formed between them. During wetting/drying cycles, these chains between aggregates do not develop as expected, in stead, they are easily destroyed. Thereby a very scattered  $G_{\max}$  data are obtained.

### 4.4.2.2. Results for wet side

Similar to mixing method A, Figure 4-19 presents the  $G_{\max}$  change against wetting-drying cycles for the 4% lime treated clay specimens of the same sub-series as in Figure 4-18 ( $D_{\max} = 0.4 \text{ mm}, 1 \text{ mm}, 2 \text{ mm}, 5 \text{ mm}$ ), mixed with method B and compacted on the wet side at the same dry density (mean  $w_f = 35.14\%$ , case 20). Its corresponding water content/saturation changes during these cycles are also given. As for mixing method A, mixing method B also results in a slight water content/saturation changes ( $\Delta w = 0.23\% \sim 0.70\%$ ,  $\Delta S_r = 0.61\% \sim 1.87\%$ ) and significant changes of  $G_{\max}$  during wetting/drying cycles.



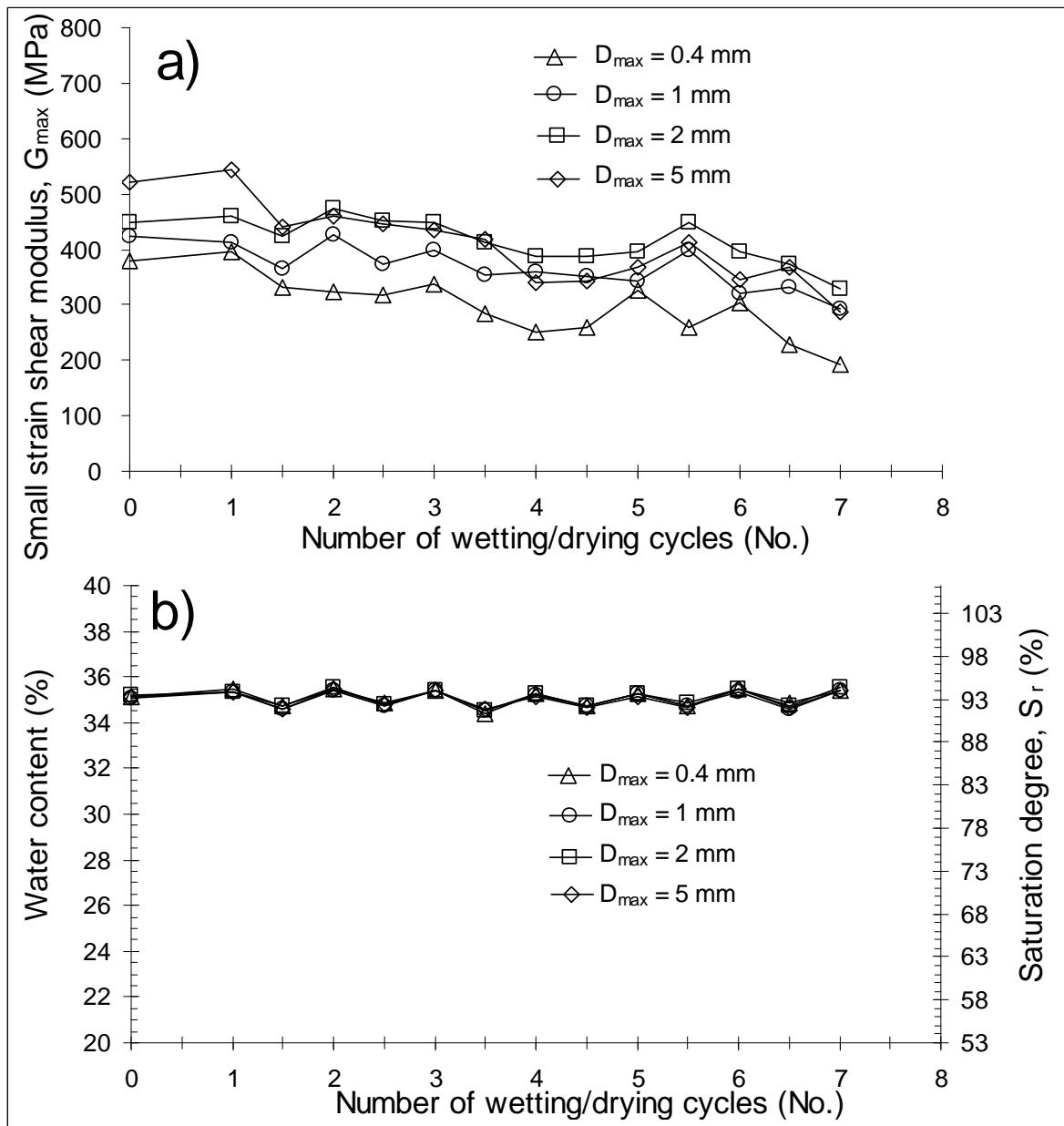


**Figure 4-19 a) Changes of  $G_{max}$  upon cyclic wetting/drying for the 4% lime treated clay in different sub-series prepared by method 2, with mixing method B, then compacted on wet side; b) corresponding water content and saturation degree changes with wetting/drying cycles (case 20)**

As with mixing method A, as shown in Figure 4-19, the  $G_{max}$  of different sub-series have different initial values (379 ~ 520 MPa) due to the effect of aggregates size as discussed in chapter 3: the finer the aggregates, the higher the  $G_{max}$ . Then the values slightly increase with the first wetting No.1 (394 ~ 544 MPa) and decrease with the first drying No.1.5, showing a high sensibility to water content changes. After a stabilized values at a lower stiffness level during No.1.5 ~ No.3, they begin to decrease steadily until No.4. Thereafter, they show large variations again in response to water content changes during No.4 ~ No.5.5.

Finally, they steadily decrease during No.5.5 ~ No.7. On the whole, they all show similar decreasing trends with cycles, with more obviously variation at the beginning and at No. 4.5. The development of  $G_{max}$  with cycles can also be classified into three stages: stage I (No.1 ~ No.4.5) due to effects of coating and suction, stage II (No.5 ~ No.6) due to breakage of aggregates and stage III (No.6 ~ No.7) related to the accelerated breakage of aggregates by de-bonding effect.

Compared to mixing method A, some differences can be observed for mixing method B: 1) the first wetting slightly increases the  $G_{max}$ , indicating that more significant chemical reactions occurred; 2) lower  $G_{max}$  values are obtained because less cementation is expected for larger aggregates by mixing method B; 3) a decreasing order of  $G_{max}$  level is obtained with the decrease of  $D_{max}$ .

### 4.4.3. Matric suction change

Figure 4-20 presents the suction change with  $D_{max}$  during a cycle of wetting and drying for the lime treated clay. Similar to the treated silt, the treated clay also presents higher suction than untreated one, especially noticeable for the drying paths. Unlike the treated silt, the treated clay shows negligible aggregates size effect on suction values.

For the untreated clay (case 19, 22), as shown in Figure 4-20, significant difference between the suction values upon wetting and drying is identified (No.1.5 and No.2). Unlike the untreated silt, the untreated clay shows no clear aggregate size effect on suction as similar suction values are identified between different sub-series. As for the untreated silt, the  $G_{max}$  value for the clay is also controlled by suction. We also observe that the higher the variation range of  $G_{max}$ , the higher the variation range of suction (the dry side and wet side specimens, case 19 versus case 22).

For the treated clay, the  $G_{max}$  change during wetting/drying cycles is also influenced by the significant suction changes (ex. case 18 of different aggregates size soils, drying path No.3.5: 725 ~ 3423 kPa; wetting path No.4: 17 ~ 22 kPa).

In the case of dry side specimens (mixing method A, case 18), a clear aggregates size effect upon drying (No.3.5) is observed, with higher suction for the smaller aggregates size soil (ex. 3423 kPa for  $D_{max} = 0.4 \text{ mm}$ ). Correspondingly, we also observe the different variation levels of  $G_{max}$  during wetting/drying cycles, with a decreasing order of the stiffness level with increase of the aggregates size (case 18 in Figure 4-16).

In the case of wet side specimens, with both mixing method A (case 21) and mixing method B (case 20), upon drying (No.3.5), different sub-series present similar suction values, showing no noticeable aggregates size effect on suction. Correspondingly, similar  $G_{max}$  variations with cycles are identified for different sub-series in Figure 4-18 and Figure 4-19. Moreover, compared to mixing method A, mixing method B results in lower  $G_{max}$  values and suction values (ex. No.3.5, 1333 kPa ~ 1778 kPa for method A; 1572 ~ 3045 kPa for method B). This is probably due to the different cementation with different aggregates sizes, considering that the aggregates mixed by method A are normally much smaller than by method B.

Summarising, the correlation between suction and stiffness of the clay is observed during wetting/drying cycles. The effect of aggregates size on suction or stiffness is highly mixing method dependent. This size effect reflects the different degree of cementation.

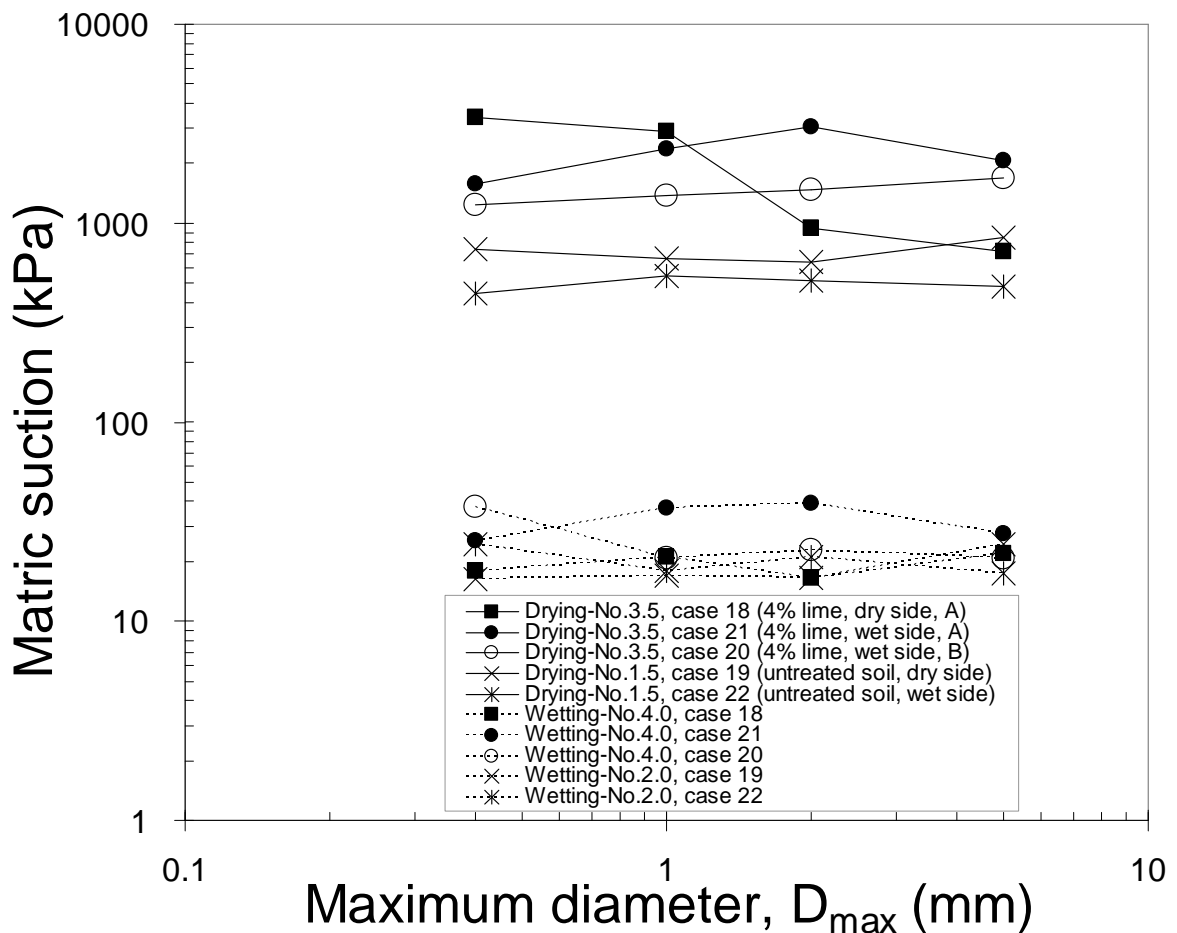


Figure 4-20 Matric suction changes during drying and wetting for the lime treated clay

## 4.5. Results of the mixture treated clay

As for the results of the clay treated by 4% lime using both mixing method A and B, in the following, we will present the results of clay with mixture treatment (2% lime + 3% cement) by these two mixing methods, A and B.

### 4.5.1. Mixing method A

In the case of mixing method A, following the same order as previously, the results for the clay compacted on the dry side and then on the wet side are analysed.

#### 4.5.1.1. Results for dry side

Figure 4-21 depicts the  $G_{max}$  evolutions with cyclic wetting-drying for the 2% lime + 3% cement treated clay, compacted dry of optimum ( $w_f = 25\%$ ,  $S_r = 65.79\%$ , case 23). The corresponding water content/saturation degree variations during the cyclic wetting-drying are also shown.

For soil specimens of sub-series  $D_{max} = 0.4 \text{ mm}$  (Figure 4-21), at the initial water content  $w_f = 24.70\%$  ( $S_r = 65.74\%$ ), the  $G_{max}$  is 583 MPa. Wetting to a water content of 29.95% ( $S_r = 79.69\%$ ) decreases the  $G_{max}$  to 555 MPa (No.1). The subsequent drying (No.1.5) and wetting (No.2) both increase the  $G_{max}$  significantly to 613 MPa and 717 MPa, respectively. Then the following wetting/drying cycles result in relatively stabilised values or slightly decreasing values until No.3.5. From cycle No.4, a clear decreasing trend is observed, with cyclic variations of  $G_{max}$  (higher values in wetting paths) during cycles No.4 ~ No.6 and with steady decreasing  $G_{max}$  from No.6. In addition, the increase of  $G_{max}$  during the first few cycles No.0 ~ No.4 is probably due to the coating of the soil aggregates (stage I), thereby the following cycles No.4 ~ No.6 correspond to the breakage of aggregates (stage II), and the final cycles accelerate this breakage phenomenon (stage III). Note that the increase of  $G_{max}$  was also identified for the 3% lime treated Tours silt with wetting/drying cycles in the study of Tang et al. (2011). This indicates that chemical reactions occur during the application of cycles because sufficient water is available during wetting.

For other sub-series, first, they present different initial  $G_{max}$  values, the higher ones being for the finer aggregates ( $D_{max} = 1 \text{ mm}$  and  $0.4 \text{ mm}$ ) due to the aggregates size effect (see chapter 3). Then, they present different trends of  $G_{max}$  development. For sub-series  $D_{max}$

$= 1 \text{ mm}$ ,  $G_{\max}$  first increases slightly at No.0 ~ No.1.5 (stage I), then varies at No.1.5 ~ No.3 (stage II) and finally decreases steadily from No.3 (stage III). For the sub-series  $D_{\max} = 2 \text{ mm}$ , it begins with a lower value than for the finer aggregates mentioned previously. After an increase of  $G_{\max}$  induced by the first wetting No.1 (stage I), a significant decrease is observed until No.3 (stage II). Thereafter,  $G_{\max}$  remains at a very low level, with first an increase then a cyclic variation in the end. For the sub-series  $D_{\max} = 2 \text{ mm}$ ,  $G_{\max}$  begins with a value as low as 113 MPa and decreases during the first wetting No.1. Then, it presents a slight increase from No.1.5 to No.2.5 (stage I) and a decrease at No.3 (stage II and III). Finally, it remains at a level as low as that for the untreated clay under the effect of wetting/drying cycles, indicating significant breakage of aggregates.

Comparison between the four sub-series shows that the  $G_{\max}$  evolutions with cyclic wetting-drying depend strongly on the effect of aggregates size. As for the results during curing, the finer the aggregates size, the higher the resistance to wetting/drying cycles. Due to the difference in available water during curing and cycles, the cycles result in more significant size effect. It appears that the  $G_{\max}$  value is governed by the combined effects of suction and treatment.

It is worth noting that  $G_{\max}$  does not show a well defined increase or decrease during the first wetting. This suggests that the  $G_{\max}$  changes depend not only on the suction but also the ongoing chemical reactions. The chemical reactions also depend on the hydrate state of the microstructure environment in soils and on the current states of additives. The ongoing reactions after wetting can significantly increase  $G_{\max}$  as it was identified on the subseries  $D_{\max} = 0.4 \text{ mm}$ . However, the ongoing chemical reactions may not significantly increase the  $G_{\max}$  if the non-hydrated additives between the aggregates are negligible in quantity (see for example  $D_{\max} = 1 \text{ mm}$ ).

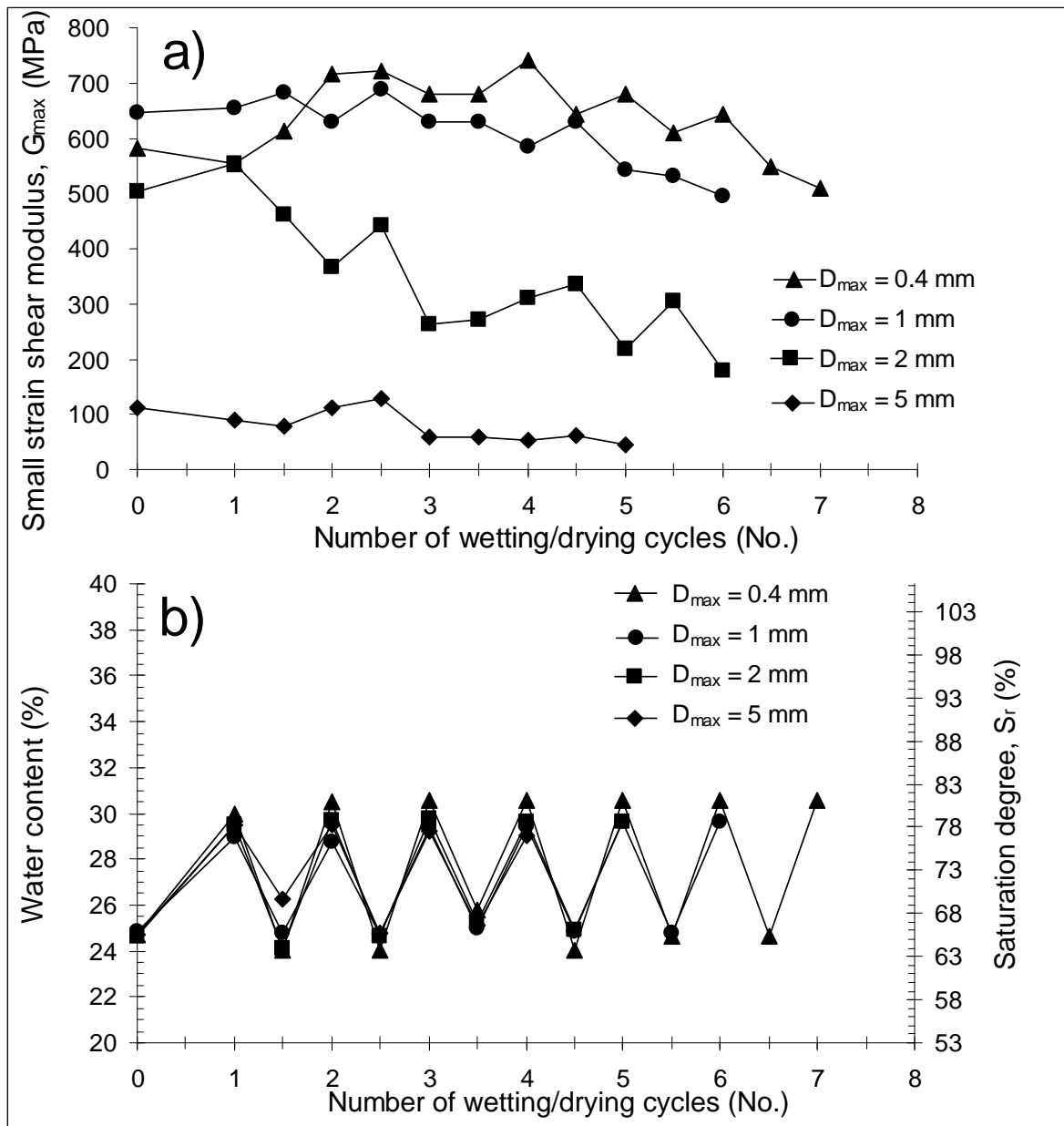


Figure 4-21 a) Changes of  $G_{max}$  upon cyclic wetting-drying for the 2% lime + 3% cement treated clay of different sub-series prepared by method 2, with mixing method A, and then compacted on the dry side; b) corresponding water content and saturation degree changes with wetting/drying cycles (case 23)

#### 4.5.1.2. Results for wet side

Figure 4-22 presents the variation of  $G_{max}$  with cyclic wetting-drying also for the 2% lime + 3% cement treated clay, but compacted on the wet side of optimum ( $w_f = 35\%$ ,  $S_r = 92\%$ , case 24). On the whole, similar to lime treated clay, the water content/saturation degree during the wetting paths increases slightly with cycles. The  $G_{max}$  changes are rather significant, especially for the first few cycles and in the end. Moreover, similar  $G_{max}$  – cycles

curves are obtained for the four sub-series, suggesting a negligible aggregates size effect. This is quite different from the results of the specimens compacted on dry side.

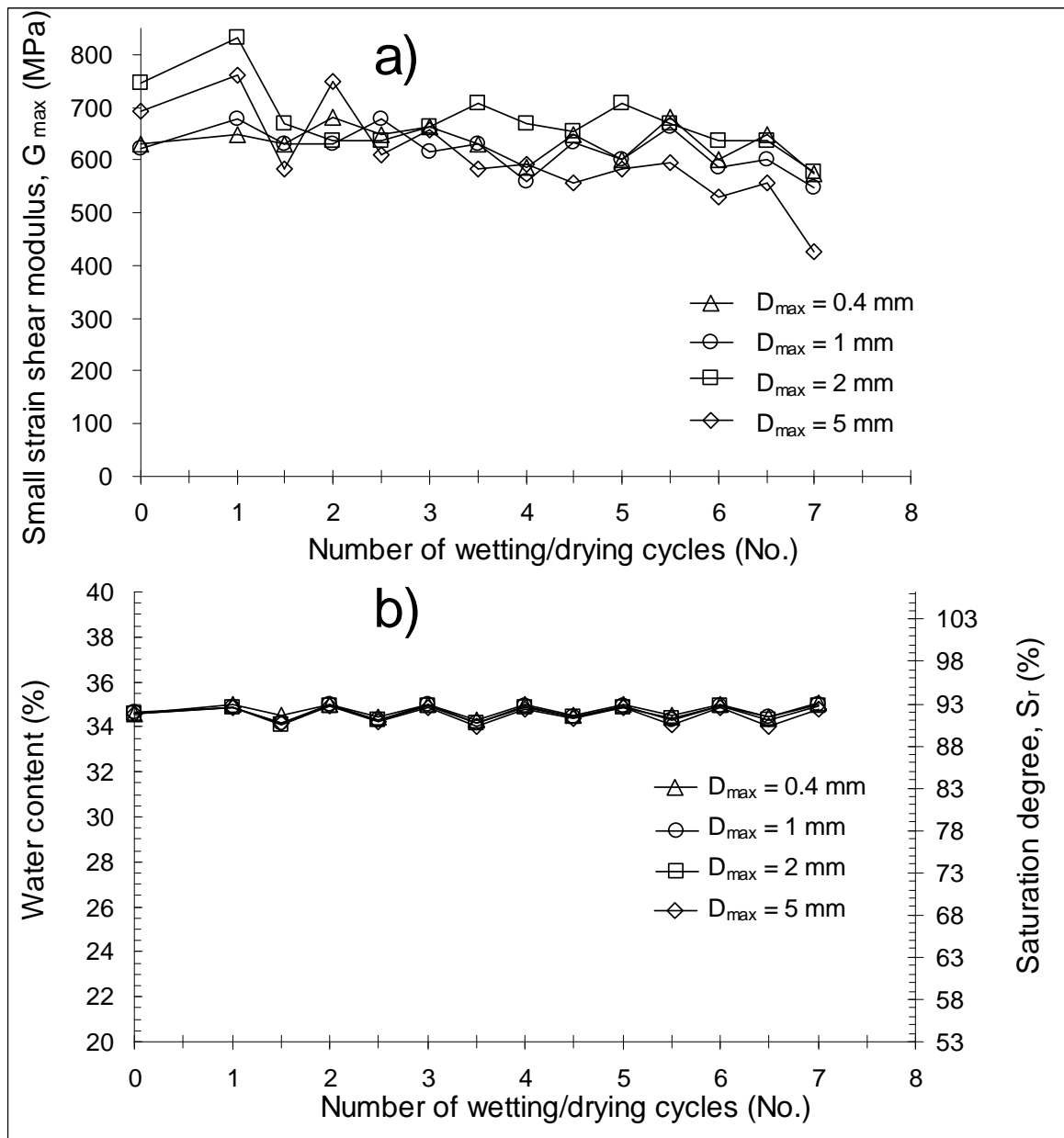


Figure 4-22 a) Changes of  $G_{max}$  upon cyclic wetting-drying for the 2% lime + 3% cement treated clay of different sub-series prepared by method 2, on wet side; b) corresponding water content and saturation degree changes with wetting/drying cycles (case 24)

In Figure 4-22, different from the dry side specimens, the wet side specimens of the four sub-series show similar  $G_{max}$  values (623 ~ 745 MPa) at No.0 and an increase of  $G_{max}$  during the first wetting at No.1 (648 ~ 833 MPa). Then the  $G_{max}$  values stabilise at a lower variation range until cycle No.3 (stage I). Thereafter, the  $G_{max}$  values decrease slightly with a

higher sensibility to water content changes during No.3 ~ No.6 (stage II) and finally decrease steadily during No.5 ~ No.7 (stage III).

Firstly at stage I, compared to the lime treatment, the mixture treatment shows more chemical reactions during the first wetting. The decreasing variation range of  $G_{max}$  during wetting/drying cycles suggests the coating effect. Then at stage II, the slight decreasing trend of  $G_{max}$  is probably due to the significant cyclic suction changes during drying and wetting. This suction effect can de-bond the chains between aggregates. Finally, the wetting/drying cycles at stage III accelerate this de-bonding effect.

The absence of aggregates size effect suggests that the aggregates sizes are similar between these sub-series after compaction, with mixing method A.

### 4.5.2. Mixing method B

The tests on specimens compacted on dry side were not performed and only the results for wet side are presented in this section.

#### 4.5.2.1. Results for wet side

Figure 4-23 depicts the  $G_{max}$  variations with wetting/drying cycles for the clay of different sub-series treated by 2% lime + 3% cement and compacted on the wet side ( $w_f = 35\%$ ,  $S_r = 92\%$ ), with mixing method B (case 25). The water content/saturation changes during these cycles are also presented. On the whole, compared to the results with mixing method A, the results with mixing method B also show a slight water content/saturation changes ( $w = 34.1\% \sim 34.7\%$ ,  $S_r = 90.7\% \sim 92.4\%$ ) but a more significant change of  $G_{max}$  during wetting/drying cycles, especially during the first few cycles.

For the soil specimens of sub-series  $D_{max} = 0.4 \text{ mm}$ , before wetting with a water content of 34.44% ( $S_r = 91.65\%$ ),  $G_{max}$  is equal to 325 MPa that is much lower than that with mixing method A (632 MPa). Wetting to a water content of 34.76% ( $S_r = 92.49\%$ ) slightly decreases  $G_{max}$  to 301 MPa (No.1). The following drying surprisingly and significantly decreases  $G_{max}$  to 204 MPa. The subsequent wetting/drying cycles result in a cyclic  $G_{max}$  change with higher values in wetting paths, until cycle No.3.5 (stage I). During cycle No.3.5 ~ No.6 (stage II), slight variations of  $G_{max}$  are observed and similar  $G_{max}$  values are identified (158 MPa ~ 182 MPa). Finally, from No.6, the  $G_{max}$  value steadily decreases with cycles



(stage III). For stage I, 1)  $G_{max}$  also shows decreasing trends either during drying paths or during wetting paths; 2) drying causes the decrease of  $G_{max}$ .

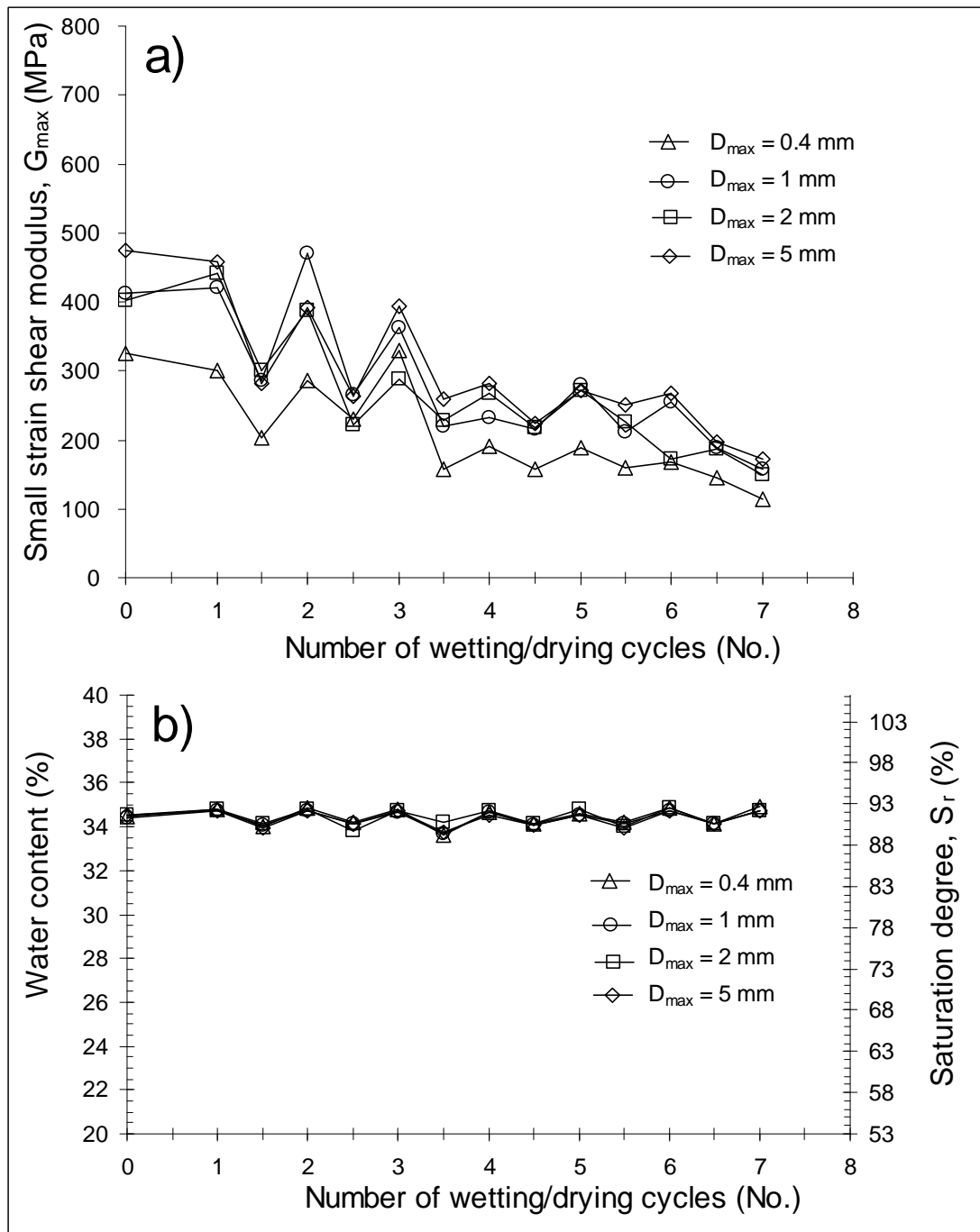


Figure 4-23 a) Changes of  $G_{max}$  upon cyclic wetting/drying for the 2% lime + 3% cement treated clay of different sub-series prepared by method 2, with mixing method B, and then compacted on wet side; b) corresponding water content and saturation degree changes with wetting/drying cycles (case 25)

For the specimens of other sub-series ( $D_{max} = 1/2/5\text{ mm}$ ), although higher stiffness levels are identified, some similar observations can be made: 1) a similar 3-stage

development with cycles; 2) a similar variation range; 3) a similar  $G_{\max}$  change due to drying or wetting after the first cycle. In other words, different trends of  $G_{\max}$  change due to the first wetting are identified for these sub-series. This is probably related to the combined effects of coating and suction.

Comparison between the results of the four sub-series shows that specimens of coarser aggregates present higher resistance to wetting/drying cycles.

As similar  $G_{\max}$ -cycles curves are observed for both mixing method A and mixing method B, in order to investigate the mixing effect, we analyse here the mean  $G_{\max}$  value of the four sub-series. Compared to the results with mixing method A, the results with mixing method B show, 1) a much lower initial  $G_{\max}$  value at No.0,  $G_{\max}(B) = 403 \text{ MPa} < G_{\max}(A) = 673 \text{ MPa}$ ; 2) a less noticeable ongoing cementation after the first wetting No.1.0 - the  $G_{\max}$  value remains almost unchanged for method B (405 MPa), whereas it increases significantly to 730 MPa for method A; 3) a sharper decreasing slope; 4) a much lower final value after cycle No.7 ( $G_{\max}(B) = 148 \text{ MPa} < G_{\max}(A) = 532 \text{ MPa}$ ). The difference indicates that the soil specimens with mixing method A have a higher resistance to the wetting/drying cycles as compared to mixing method B. As mixing method A results in smaller aggregates, a higher homogeneity of treatment can be expected. This shows that the higher the aggregates size after mixing, the lower the resistance to wetting/drying cycles.

### 4.5.3. Matric suction change

Figure 4-24 presents the suction change with  $D_{\max}$  during a cycle of wetting and drying for the 2% lime plus 3% cement treated clay. As in the case of lime treated clay, the aggregates size effect in drying paths is not noticeable as opposed to the case of the dry side clay with mixing method A (case 23).

In the case of the dry side clay with mixing method A (case 23), upon drying path (ex. No.3.5), the suction is observed to be decreasing with increase of  $D_{\max}$ , with a suction 4213 kPa for sub-series  $D_{\max} = 0.4 \text{ mm}$  and 2708 kPa for  $D_{\max} = 5 \text{ mm}$ . Upon wetting (No.4.0), the suction shows similar low values (21 ~ 38 kPa). As for the lime treated clay, the corresponding  $G_{\max}$  variation with cycles is in different levels: a higher level for small aggregates sizes. This evidences the aggregates size effect on suction or stiffness during wetting/drying cycles. If the significant increase of  $G_{\max}$  at beginning for sub-series  $D_{\max} =$

0.4 mm is due to the ongoing chemical reactions, the decreasing  $G_{max}$  during the subsequent cycles is probably due to the de-bonding effect by cyclic suction changes.

In the case of the wet side specimens with both mixing method A (case 24) and mixing method B (case 25), the variation range of  $G_{max}$  is related to suction changes as similar suction values are identified between these sub-series (ex. drying at No.3.5 and wetting at No.4 in Figure 4-24). As for the lime treated clay, mixing method B results in a lower suction than mixing method A, upon both drying path (ex. No.3.5, mean suction  $s(B) = 1728 \text{ kPa} < s(A) = 2424 \text{ kPa}$ ) and wetting path (ex. No.4, mean suction  $s(B) = 19 \text{ kPa} < s(A) = 34 \text{ kPa}$ , Figure 4-24). Correspondingly, mixing method B also leads to a lower  $G_{max}$  variation and a more pronounced degradation of  $G_{max}$  with wetting/drying cycles as compared to mixing method A. The cyclic suction changes are also responsible for the degradation of  $G_{max}$ .

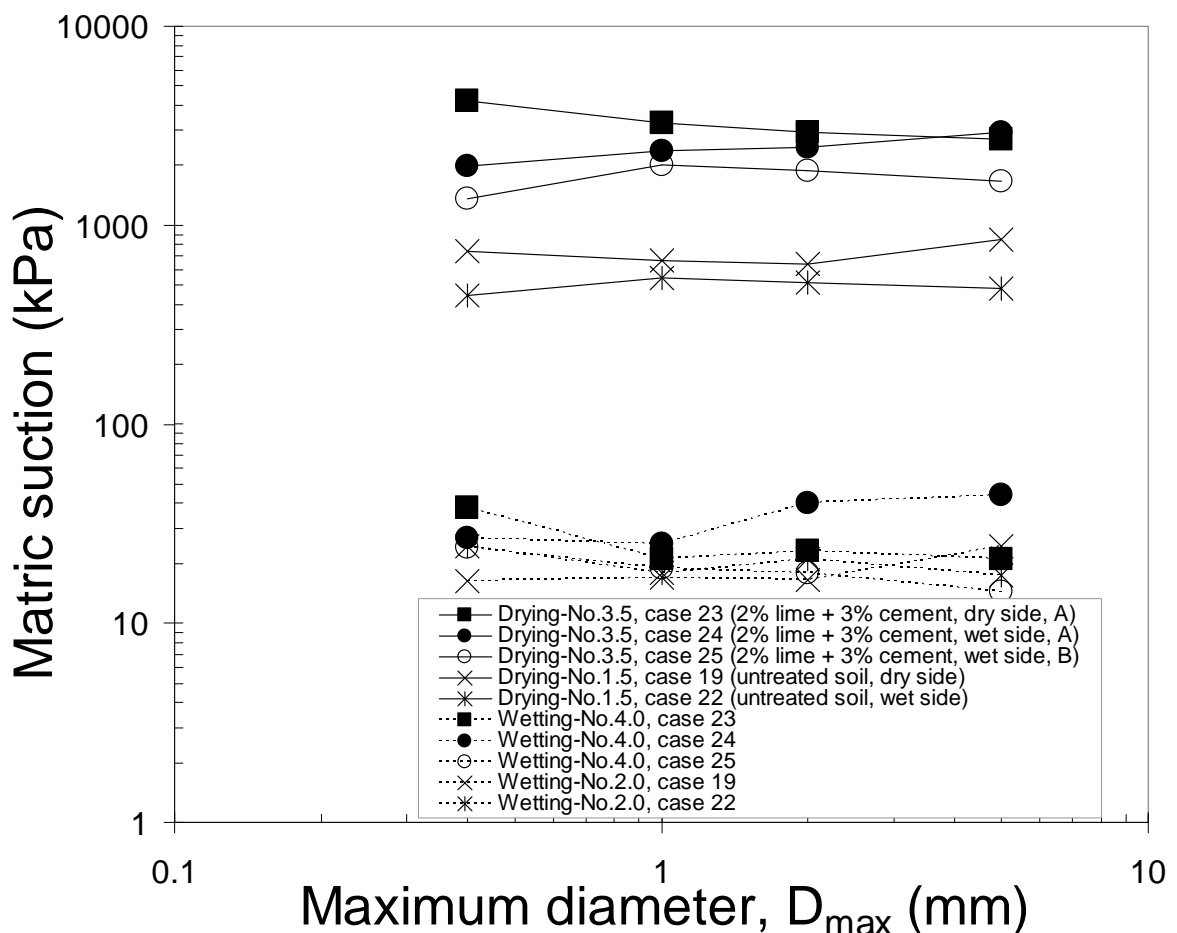


Figure 4-24 Matric suction change during drying and wetting for the mixture (2% lime + 3% cement) treated clay

Summarising, similar to lime treated clay, the mixture treated clay also shows that the effect of aggregates size on suction or stiffness is highly mixing method dependent. It is deduced that the aggregates size effect is mainly due to the ongoing chemical reactions (coating) and the de-bonding by cyclic suction changes.

#### **4.6. Aggregates size effect through the failure number of cycles**

As aforementioned, though the experimental phenomena are various for the different treatments of silt or clay during the application of wetting/drying cycles, they can be characterized by two physical stages: 1) stage I with coating aggregates, characterized by a very slight change and no clear degradation trend of  $G_{\max}$ ; 2) stage II with breakage of aggregates (failure), characterized by a decrease of  $G_{\max}$  and/or by a high sensibility to water content/suction changes. It is worth noting that the specimens often present an accelerated breakage of aggregates (stage III) at the end of the application of cycles, characterized by an accelerated decrease of  $G_{\max}$ . To simplify the analysis, stage III is combined with stage II in this study.

The classification of the two stages for the silt and the clay of the four sub-series can be appreciated in Table 4-1.

For the untreated silt compacted on both dry (case 2, case 10) and wet sides (case 4, case 12), the specimens of four sub-series all show high sensibility to water content/ suction changes from the beginning of wetting/drying cycles, characterized by cyclic  $G_{\max}$  changes (stage II). On the whole, the untreated clay (case 19, 22) show the same stage patterns as untreated silt - stage II begins immediately after the first wetting.

For the 2% lime treated silt (case 1 and 3), the dry side and wet side specimens show different  $G_{\max}$  development for different sub-series. On the dry side (case 1), it mainly shows a two-stage development: with slight  $G_{\max}$  change at stage I and a higher variation and degradation at stage II. For the wet side (case 3), except in case of intensive drying followed by wetting (No.6 ~ No.7), all the sub-series only show stage I, suggesting negligible degradation.

For the 3% cement treated silt, as for the lime treated one, the experimental data for the dry side specimens can also be classified into stage I and stage II (case 9). On the wet side (case 11), except the points corresponding to intensive drying followed by wetting (No.6 ~ No.7), nearly all the data stay at stage I, also suggesting negligible degradation.

**Table 4-1 Classification of the physical stages for the silt and the clay**

Case No.	Soil	Method	w <sub>f</sub> (%)	D <sub>max</sub> (mm)	Stage I (No.)	Stage II (No.)
2 / 4	Untreated silt	1	17 / 21.8	0.4 ~ 5	-	0-
10 / 12	Untreated silt	1	14 / 21	0.4 ~ 5	-	0-
19 / 22	Untreated clay	2	25 / 35	0.4 ~ 5	-	0-
1	2% lime treated silt	1	17	0.4	0 ~ 4.5	4.5 ~ 6.0
				1	0 ~ 2.5	2.5 ~ 5.0
				2	0 ~ 2.5	2.5 ~ 4.0
				5	1 ~ 3.5	3.5 ~ 5.0
3	2% lime treated silt	1	21.8	0.4	0~ 6.0	> 6.0
				1	0~ 6.0	> 6.0
				2	0~ 4.5	4.5 ~ 5.5
				5	0~ 6.0	> 6.0
9	3% cement treated silt	1	14	0.4	0 ~ 4.0	4.0 ~ 6.0
				1	0 ~ 3.5	3.5 ~ 6.0
				2	0 ~ 3.0	3.0 ~ 7.0
				5	0 ~ 3.0	3.0 ~ 6.0
11	3% cement treated silt	1	21	0.4	0 ~ 5.5	5.5 ~ 6.0
				1	0 ~ 6.0	6.0 ~ 7.0
				2	0 ~ 6.0	> 6.0
				5	0 ~ 5	5.5 ~ 7.0
18	4% lime treated clay	A	25	0.4	0 ~ 2.5	2.5 ~ 7.0
				1	0 ~ 2.0	2.0 ~ 7.0
				2	0 ~ 1.0	1.0 ~ 5.0
				5	0 ~ 2.0	2.0 ~ 4.0
21	4% lime treated clay	A	35	0.4	0 ~ 4.0	4.0 ~ 7.0
				1	0 ~ 4.5	4.5 ~ 7.0
				2	0 ~ 3.5	3.5 ~ 7.0
				5	0 ~ 4.0	4.0~ 7.0
20	4% lime treated clay	B	35	0.4	0 ~ 1.0	1.0 ~ 7.0
				1	0 ~ 1.0	1.0 ~ 7.0
				2	0 ~ 1.0	1.5 ~ 7.0
				5	0 ~ 1.0	1.0 ~ 7.0
23	2% lime + 3% cement treated clay	A	25	0.4	0 ~ 3.5	3.5 ~ 7.0
				1	0 ~ 2.0	2.0 ~ 6.0
				2	0 ~ 1.0	1.0 ~ 6.0
				5	0~ 1.5	1.5 ~ 5.0
24	2% lime+3% cement treated clay	A	35	0.4	0 ~ 7.0	>7.0
				1	0 ~ 6.0	6.0 ~ 7.0
				2	0 ~ 5.5	5.5 ~ 7.0
				5	0 ~ 5.5	5.5 ~ 7.0
25	2% lime+3% cement treated clay	B	35	0.4	0 ~ 1.0	1.0 ~ 7.0
				1	0 ~ 1.0	1.0 ~ 7.0
				2	0 ~ 1.0	1.0 ~ 7.0
				5	0 ~ 1.0	1.0 ~ 7.0

For the 4% lime treated clay with mixing method A (case 18 and case 21), stage II begins at about No. 2.0 and No.4.0 for the dry and wet sides, respectively. For the same soil with mixing method B (case 20), stage II comes much earlier, at about No.1.0 for the wet side.

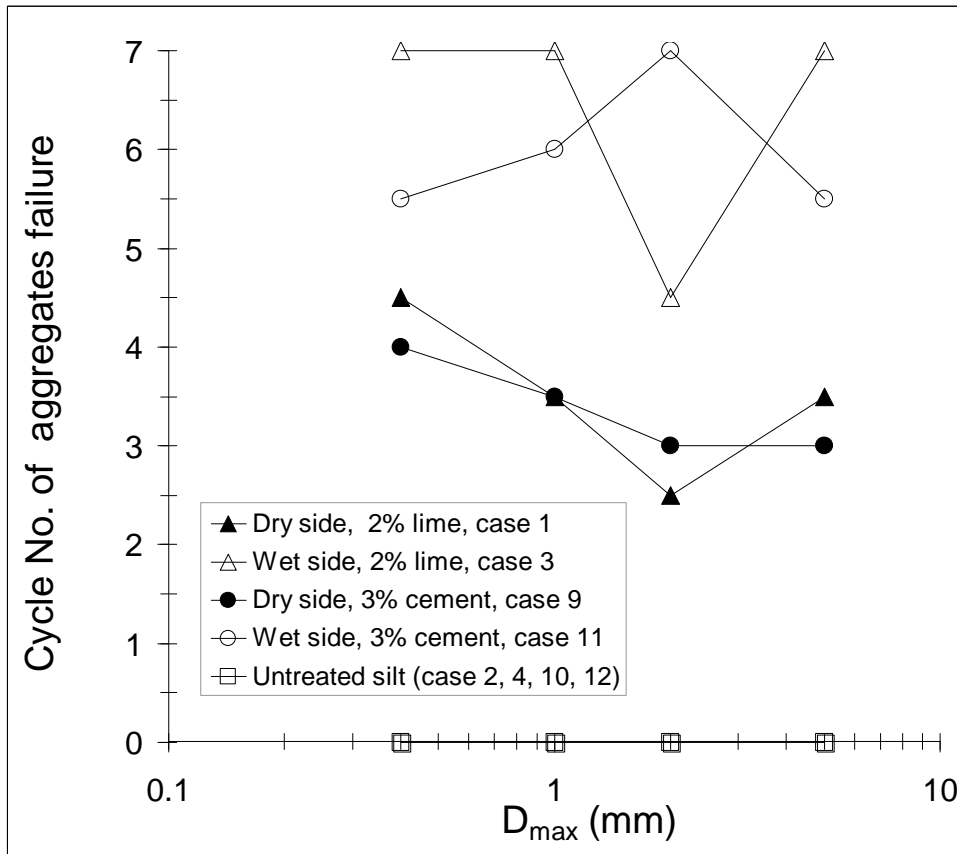
For the 2% lime plus 3% cement treated clay, with mixing method A (case 23, 24), stage II for the dry side specimens also begins at about No. 2.0, as in the case of lime treatment. For the wet side specimens, stage II begins a little later, at about No.6.0. With mixing method B (case 25), the wet side specimens also begins stage II after No.1.0, as in the case of lime treatment.

Figure 4-25 presents the number of cycles ( $N_f$ ) corresponding to the beginning of aggregates failure (stage II) as a function of the maximum aggregates diameter ( $D_{max}$ ) for both the silt and the clay.

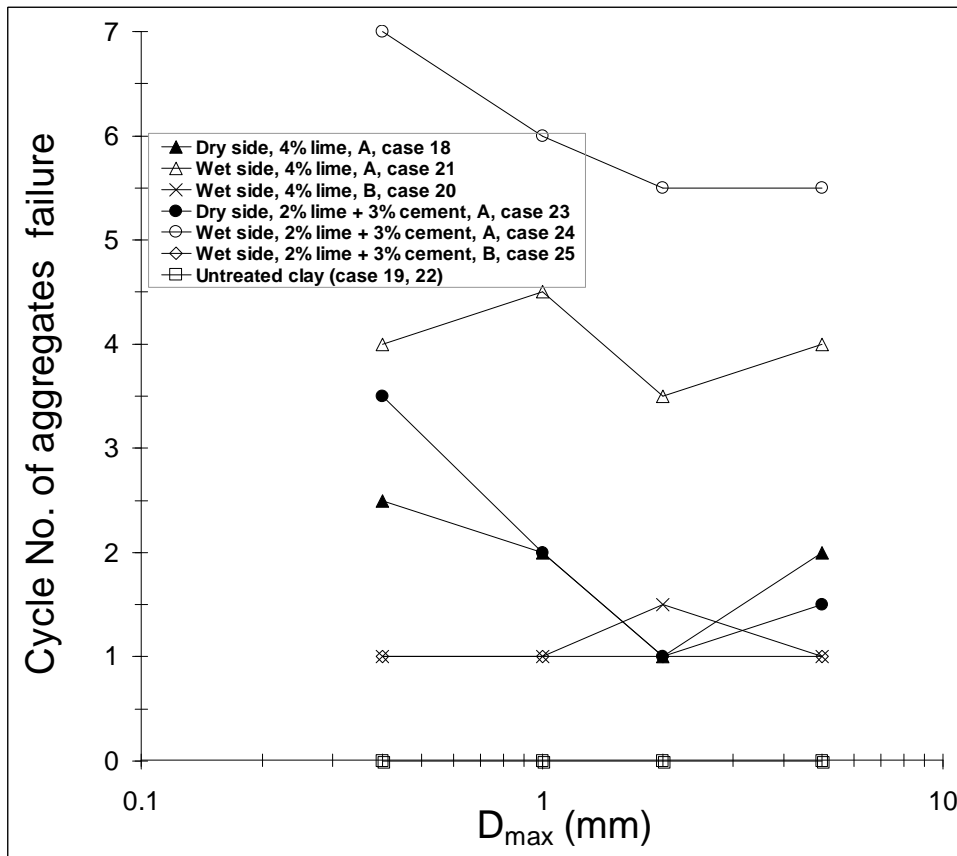
For the silt, as shown in Figure 4-25a, we observe that the dry side treated specimens (case 1, 9) show smaller  $N_f$  than the wet side treated ones (case 3, 11), the untreated specimens having  $N_f$  equal to zero (case 2, 4, 10 12). This indicates a decreasing order of resistance to wetting/drying cycles: wet side treated specimens, dry side treated specimens and untreated specimens.

For the clay, as shown in Figure 4-25b, with mixing method A, the wet side treated specimens (case 21 and case 24) show larger values of  $N_f$  than the dry side treated ones (case 18 and case 23). The untreated clay also has stage II initiated at the beginning of cycles. For the wet side specimens, mixing method A results in much larger value of  $N_f$  than mixing method B for both 4% lime treated clay (case 21 versus case 20) and mixture treated clay (case 24 versus case 25).

Comparison between the results of treated and untreated soils show that the treatment highly increases the  $N_f$  value. This indicates that the treatment can significant improve the performance of soils in terms of resistance to wetting/drying cycles.



(a) Lime / cement treated silt by method 1, method B



(b) Lime / mixture treatment of clay by method 2, with mixing method A and B

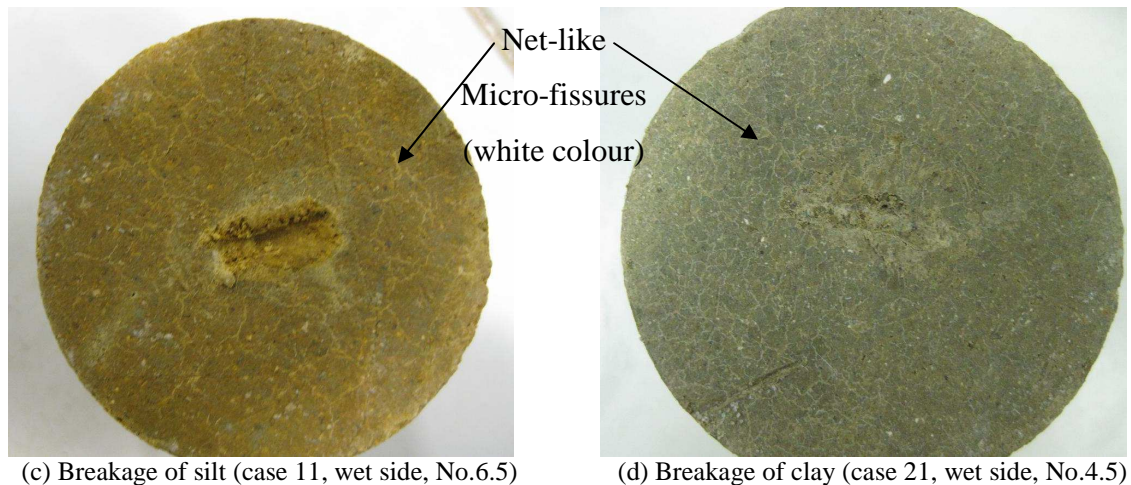


**Figure 4-25 Cycle No. of aggregates failure for the silt and the clay with different treatments**

It is worth noting that the  $N_f$  value of treated soils is strongly influenced by the aggregates size effect, especially for the dry side. For the silt,  $N_f$  is decreasing with increase of  $D_{max}$  for the dry side (case 1 and case 9), but this trend is not observed for the wet side. For the clay of different treatments with mixing method A (case 18, case 23 and case 24),  $N_f$  is also influenced by this aggregates size effect - the larger the  $D_{max}$ , the lower the  $N_f$ . For the same clay with mixing method B (case 20 and case 25), this aggregates size effect is no longer noticeable. This indicates that the larger the aggregates, the easier or earlier the breakage of aggregates by wetting/drying cycles.

Moreover, the breakage of aggregates (stage II) often occurs at the drying state for treated soils whereas it often occurs at the wetting state for untreated ones. Figure 4-25c, d clearly presents the breakage of aggregates after drying for the wet side treated soils. For these wet side treated specimens, the net-like surface suggests the de-bonding effect by these micro-fissures.

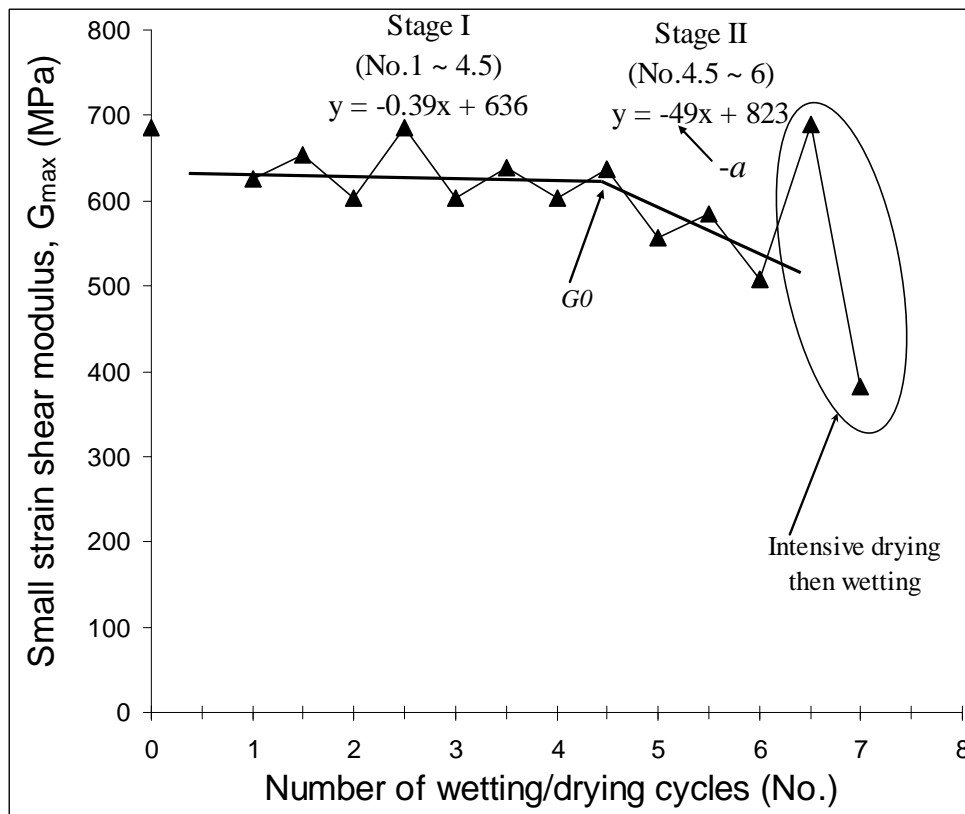
## 4.7. Aggregates size effect on shear modulus

### 4.7.1. Results for silt treated with lime

As mentioned before, the  $G_{max}$  sensibility to wetting/drying cycles is different during different stages. Thereby, it is necessary to investigate the aggregates size effect for each stage. For this purpose, the relationship between the  $G_{max}$  and wetting/drying cycles is fitted for each stage.



Figure 4-26 shows the two degradation slopes with cycles ( $\Delta G_{\max}/\Delta \text{cycle}$ ) for the 2% lime treated silt of sub-series  $D_{\max} = 0.4\text{mm}$  (case 1, dry side). In order to compare the effects of cycles for the different sub-series, only the normal cycles are analyzed, without the intensive drying points. Stage I presents a linear relationship that is nearly parallel to x-axis, showing no clear degradation with cycles. Stage II also presents a linear relationship with much higher slope value. The slope value ( $a = \Delta G_{\max}/\Delta \text{cycle}$ ) reflects the degradation because it shows the reduction of  $G_{\max}$  value due to each cycle. Another parameter, namely degradation ratio ( $R = a/G_0$ ), represents the reduction ratio. The data in both drying and wetting paths are used to show a general degradation, i.e. without taking into account the very slight difference by the wetting paths and by the drying path (Yuan and Nazarian, 2003).



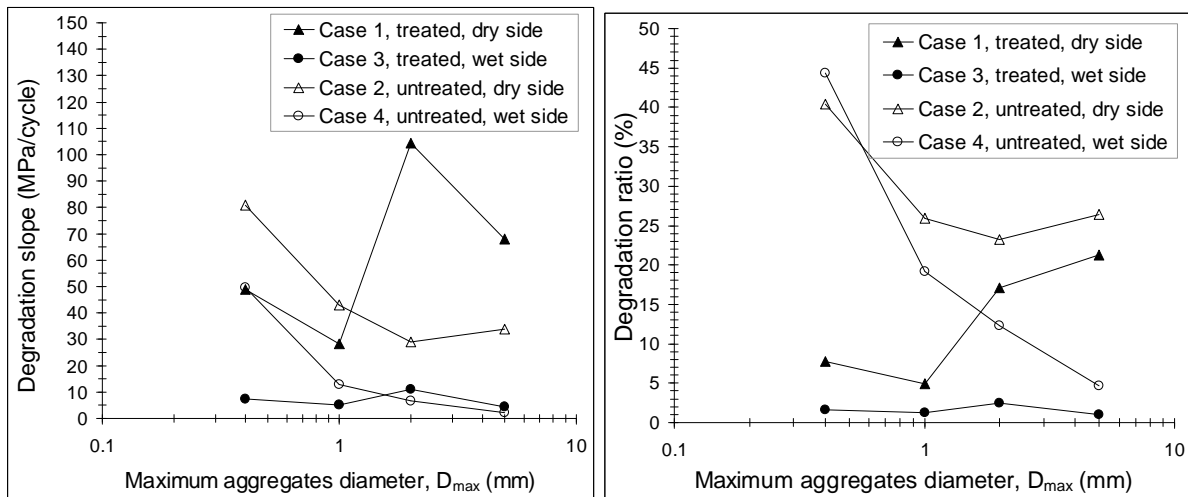
**Figure 4-26** Degradation slope of  $G_{\max}$  with cycles for the 2% lime treated silt, on the dry side of optimum ( $D_{\max} = 0.4$  mm of case 1)

Figure 4-27 presents the degradation slope/degradation ratio versus  $D_{\max}$  in the case of both untreated and 2% lime treated silt, compacted on both dry (data from stage II) and wet sides (data from stage I).

For the untreated silt compacted on both dry and wet sides (case 2 and case 4), as shown in Figure 4-27a, the degradation slope decreases with increase of  $D_{\max}$ . This is

probably due to the range of suction changes: the finer the aggregates the larger the range of suction changes, as identified before.

The 2% lime treated silt shows different trends of slopes with  $D_{max}$ . For the dry side, we observe that the larger the  $D_{max}$  the larger the degradation slope. This evidences that the coarser soils have a lower resistance to wetting-drying cycles. This can be explained by the total contact surface of aggregates: the larger the soil aggregates, the less the cementation after treatment, thereby the easier the de-bonding of aggregates. For the wet side, the degradation slope is as low as several MPa per cycle. Moreover, the trend is no longer increasing with  $D_{max}$ , showing no clear aggregates size effect. This is explained by the soil preparation as mentioned in chapter 3 - with mixing method B, the soil aggregates after mixing are similar. In addition, the low degradation slope is due to the much lower suction range as compared to the case of dry side.



(a) Degradation slope versus  $D_{max}$  (b) Degradation ratio versus  $D_{max}$   
 Note: the slope  $a = \Delta G_{max} / \Delta cycle$ ; the degradation ratio,  $R = a / G_0$ .

**Figure 4-27 Aggregates size effect for 2% lime treated silt by method 1**

The parameter degradation ratio in Figure 4-27b shows similar trends for both the untreated and the 2% lime treated silt. However, the untreated silt shows higher degradation ratio than the treated silt. This difference is to be related to the very different  $G_{max}$  values between treated silt and untreated silt.

### 4.7.2. Results for silt treated with cement

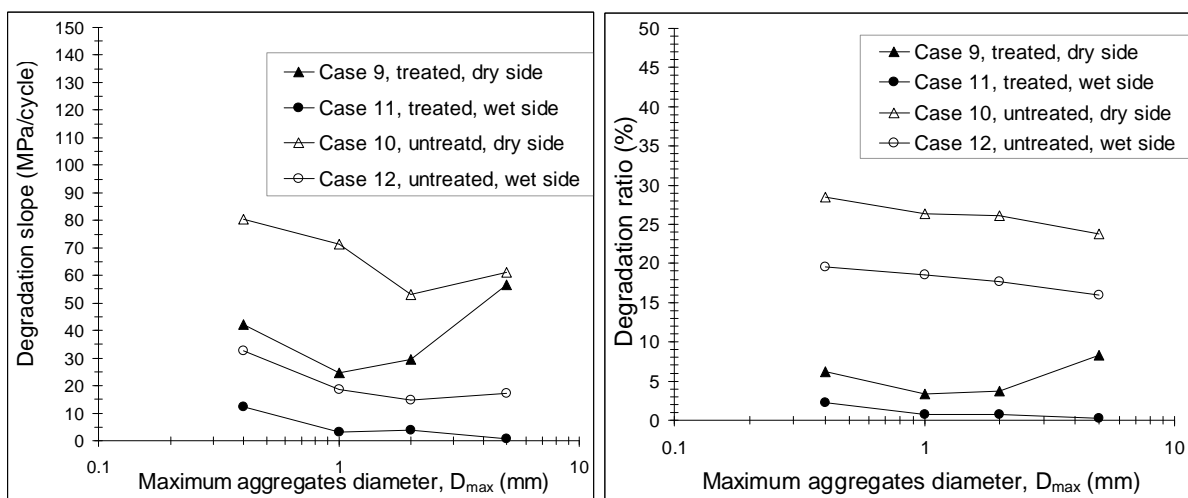
Figure 4-28 presents the degradation slopes/ratio versus  $D_{max}$  for the untreated and 3% cement treated silt, also compacted on both dry side (data from stage II) and wet side (data from stage I). In order to better analyze the aggregates size effect, both the degradation slope and ratio are compared between different sub-series.

For the untreated soil, the degradation slope is decreasing with  $D_{max}$ , especially for the dry side. This can also be explained by the suction effect between different sub-series. The finer the aggregates size, the higher the suction change during wetting/drying cycles, thus the higher the degradation.

Similar to the 2% lime treated silt, the 3% cement treated silt also shows different trends between dry and wet sides. This is significantly different from the untreated silt.

For the treated silt compacted on the dry side (case 9), the trend is not clear, as it first decreases and then increases with  $D_{max}$ . The first decrease is related to the difficulty of mixing a soil as fine as  $D_{max} = 0.4$  mm. Except for the sub-series  $D_{max} = 0.4$  mm, the increasing trend of the degradation slope with  $D_{max}$  also evidences that the larger the aggregates size after treatment the lower the resistance to wetting-drying cycles.

For the treated silt compacted on the wet side (case 11), it shows a slight decreasing trend. This is different with the lime treated silt as mentioned before. Nevertheless, these changes are so slight that we can consider the aggregates size effect negligible.



(a) Degradation slope versus  $D_{max}$  (b) Degradation ratio versus  $D_{max}$   
 Note: the slope  $a = \Delta G_{max} / \Delta cycle$ ; the degradation ratio,  $R = a / G_0$ .

**Figure 4-28 Aggregates size effect for cement treated silt by method 1**

Comparison the degradation slope between the wet side and dry side shows that the wet side specimens show much lower values. This can be explained by the lower suction range during wetting/drying cycles.

For the degradation ratio (Figure 4-28b), similar trends can be observed: it decreases with increase of  $D_{max}$  for the untreated silt, and increases with increase of  $D_{max}$  for the 3% cement treated silt on the dry side. The untreated silt shows higher degradation ratio than the treated silt. This evidences that the cement treatment can significantly improve the resistance to wetting/drying cycles. The higher degradation ratio for the dry side is to be attributed to the much higher suction change range.

### 4.7.3. Results for the lime treated clay

Figure 4-29 presents the degradation slopes/ratio versus the  $D_{max}$  for the untreated and 4% lime treated clay, compacted on both dry and wet sides (data from stage II).

On the whole, we observe significant difference between the variations of the two parameters with  $D_{max}$ . For the degradation slope ( $a = \Delta G_{max}/\Delta cycle$ ), the trends are not clear (Figure 4-29a), making the analysis difficult. On the contrary, for the degradation ratio ( $R = a/G_0$ ), the trends are clearly observed (Figure 4-29b). Moreover, the trends of degradation ratio with  $D_{max}$  are similar to that for the silt.

As shown in Figure 4-29b, the degradation ratio of untreated clay (case 19 and case 22) is decreasing with the increase of  $D_{max}$ . This is due to the suction change during wetting/drying cycles: the larger the aggregates size, the lower the suction during drying and wetting; thus the smaller the degradation ratio.

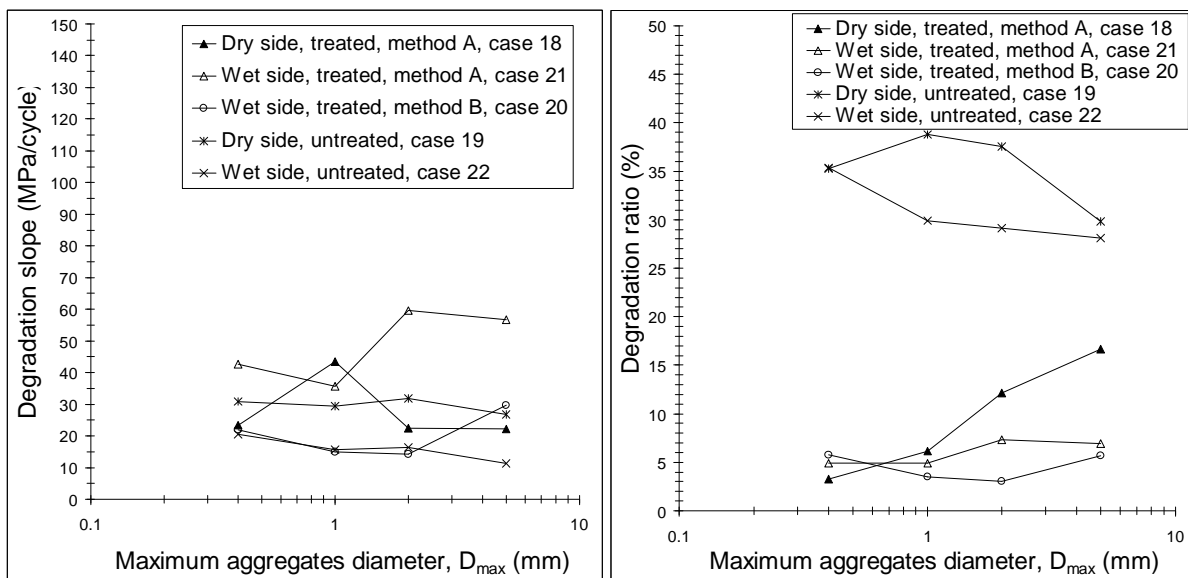
The 4% lime treated clay shows different trends for the dry side (case 18) and the wet side (case 20, 21).

For the clay compacted on the dry side with mixing method A (case 18), the trend is clear: the larger the  $D_{max}$  the higher the degradation ratio. The lowest degradation ratio is 3.11% for sub-series  $D_{max} = 0.4$  mm and the highest one is 18.09% for  $D_{max} = 5$  mm. This proves that the coarser the soils, the lower the resistance to wetting-drying cycles.

For the clay compacted on the wet side with mixing method A (case 21), the increasing trend with  $D_{max}$  is no longer obvious: 4.93% for  $D_{max} = 0.4$  mm and 6.93% for  $D_{max} = 5$  mm. With mixing method B (case 20), similar low degradation ratios are obtained

with unclear trend. This indicates that the aggregates size effect is not clear for the wet side. The low value is to be attributed to the narrow range of suction changes during wetting/drying cycles.

Comparison between the results of dry side and wet side shows that the dry side specimens are much more influenced by the aggregates size effect.



(a) Degradation slope versus  $D_{max}$  (b) Degradation ratio versus  $D_{max}$

Note: the slope  $a = \Delta G_{max} / \Delta cycle$ ; the degradation ratio,  $R = a / G_0$ .

**Figure 4-29 Aggregates size effect for the 4% lime treated clay, with both mixing method A and B**

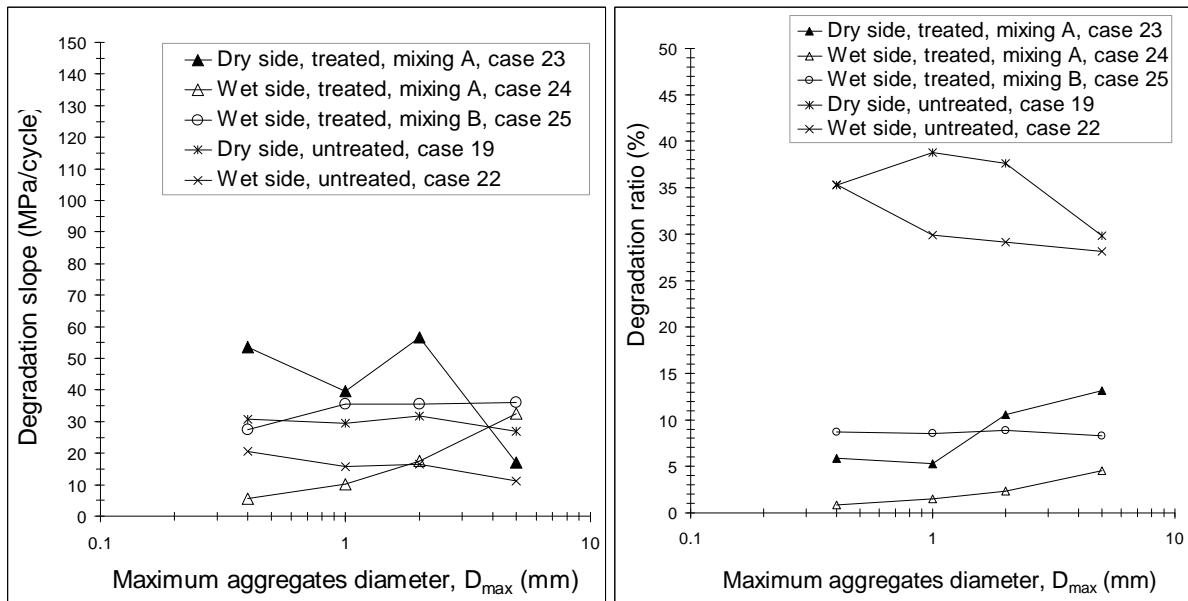
As opposed to the case of silt, the variation of the degradation slope with  $D_{max}$  is no longer in accordance with that of degradation ratio. Because the slope ( $a = \Delta G_{max} / \Delta cycle$ ) reflects the degradation of  $G_{max}$  with cycles, it cannot express the ratio of stiffness change in different levels. By contrast, the degradation ratio ( $R = a / G_0$ ) can show the degradation percentage with respect to the initial value. As the 4% lime treated clay shows quite different stiffness between different sub-series, it is difficult to use the degradation slope for a comparison, and it is better to use the degradation ratio for this purpose.

#### 4.7.4. Results for the mixture treated clay

In order to compare the degradation slope with the degradation ratio, the two parameters are used to investigate the aggregates size effect for the mixture treated clay.

Figure 4-30 presents the degradation slopes/ratio versus  $D_{max}$  for the 2% lime + 3% cement treated clay, compacted on both dry (data from stage II) and wet sides (data from both stage I and stage II).

As for the 4% lime treated clay, the degradation slope presents unclear trends for both the treated and untreated clay (Figure 4-30a). By contrast, the degradation ratio can well separate these different treatments (Figure 4-30b).



(a) Degradation slope versus  $D_{max}$  (b) Degradation ratio versus  $D_{max}$   
 Note: the slope  $a = \Delta G_{max}/\Delta cycle$ ; the degradation ratio,  $R = a/G_0$ .

**Figure 4-30 Aggregates size effect for the 2% lime + 3% cement treated clay, with both mixing method A and B**

As shown in Figure 4-30b, the dry side treated specimens with mixing method A (case 23) show clear aggregates size effect — the higher the  $D_{max}$  the higher the degradation ratio. In other words, the coarser the soils, the lower the resistance to wetting-drying cycles. Moreover, the wet side treated specimens by mixing A (case 24) present less significant aggregates size effect. For the wet side specimens by mixing method B (case 25), the degradation ratio changes slightly with increase of  $D_{max}$ , showing no aggregates size effect. In addition, the values for mixing method B are higher than for mixing method A. This proves that the aggregates size effect is also influenced by the mixing method. This indicates that the aggregates size effect mainly depends on the cementation degree (ex. aggregates size effect for the dry side treated specimens). Comparison of the values between the dry side and wet side shows that the degradation ratio depends strongly on the range of suction changes, as

higher values are obtained for both untreated clay and treated clay. The degradation ratio for the treated clay is less dependent on the cyclic water content /suction changes as compared to the untreated one. Unlike the treated clay, untreated clay shows a trend of degradation ratio- $D_{max}$  similar to that of suction- $D_{max}$ : a decreasing trend with increase of  $D_{max}$  is identified.

Comparison between the results of treated and untreated specimens shows that, 1) the treatment significantly reduces the degradation ratio; 2) the aggregates size effect is related to suction effect for the untreated clay; 3) the aggregates size effect depends on the cementation degree, ongoing chemical reactions, etc.

Comparison of the degradation ratio results between the 4% lime and 2% lime + 3% cement treatments of clay shows that the aggregates size effect is evidenced for mixing method A, but not noticeable for mixing method B. This indicates that the aggregates size effect refers to the soil aggregates size after treatment and mixing. Note that this is also proved by the results of curing in chapter 3.

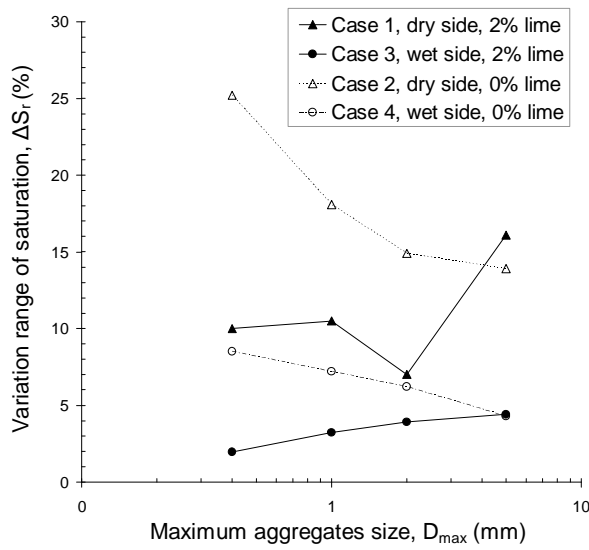
#### **4.8. Aggregates size effect on the saturation degree change**

As a close relationship between suction and  $G_{max}$  is identified, the variation range of saturation degree between wetting and drying may also change with maximum aggregates sizes ( $D_{max}$ ). Figure 4-31 presents the variation range of saturation degree (mean value of these cycles) versus  $D_{max}$  for the silt and the clay with different treatments.

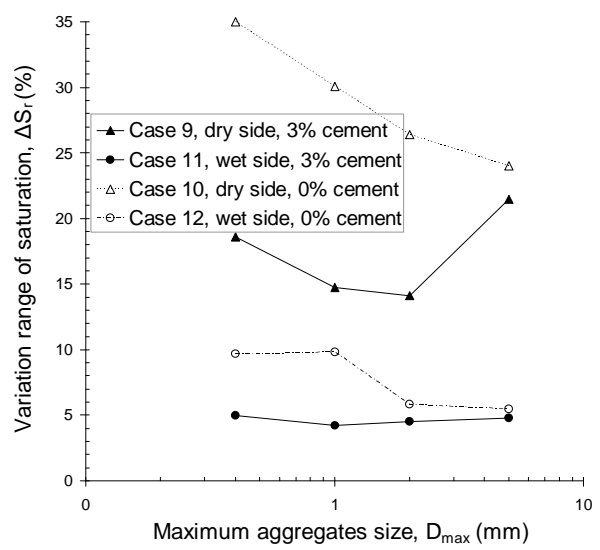
For the treated silt, the variation range of saturation degree is increasing with the increase of  $D_{max}$ , whereas it is decreasing for the untreated soils. This is in accordance with the trends of the degradation ratio with  $D_{max}$  (Figure 4-27 and Figure 4-28). For the untreated silt, this phenomenon can be explained by the suction effect. For the treated silt, it can be explained by the different cementation degrees for the different aggregates sizes. During curing, the coarser the soils, the smaller the total surface of aggregates, thus the fewer the cementitious bonds or chains. Thereby, during the wetting/drying cycles, these low cementitious bonds let water infiltrate more easily to the soils than for the finer soils. This is also evidenced by the comparison between untreated and treated soils.

On the whole, for the silt (Figure 4-31a, b), we observe the trends similar to those of degradation ratio -  $D_{max}$  curves. For the clay (Figure 4-31c, d), the trends are not noticeable. This indicates that the saturation degree change is not as clear as the  $G_{max}$  change, especially

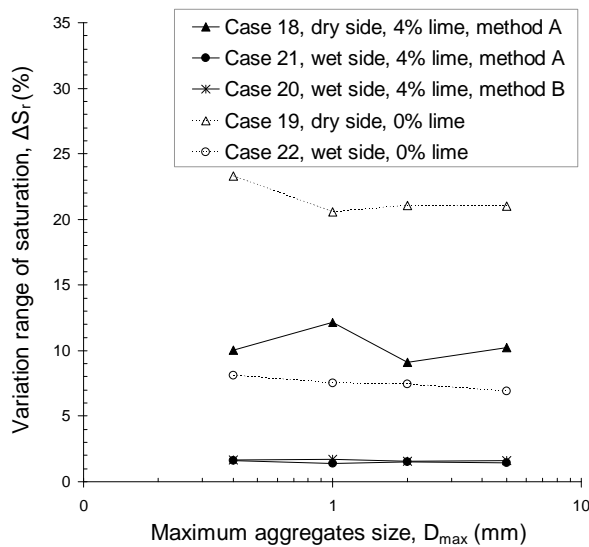
for the clay. For both the silt and clay, sub-series  $D_{max} = 0.4$  mm often shows a slightly higher value.



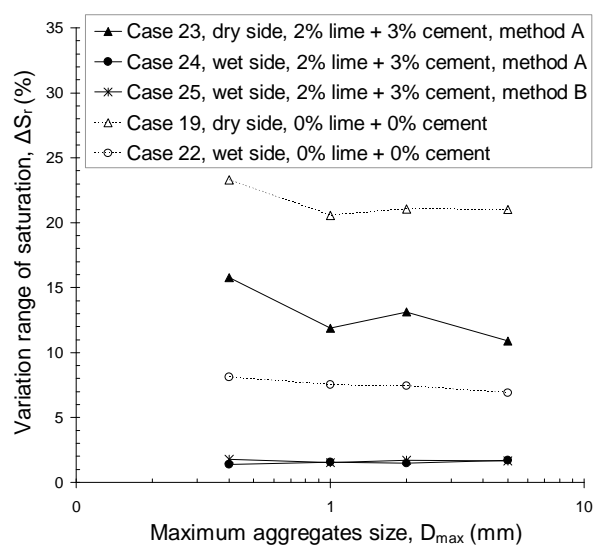
(a) Lime treated silt



(b) Cement treated silt



(c) Lime treated clay



(d) Mixture treated clay

Figure 4-31 Variations of saturation degree with aggregates size during wetting and drying for the silt and the clay

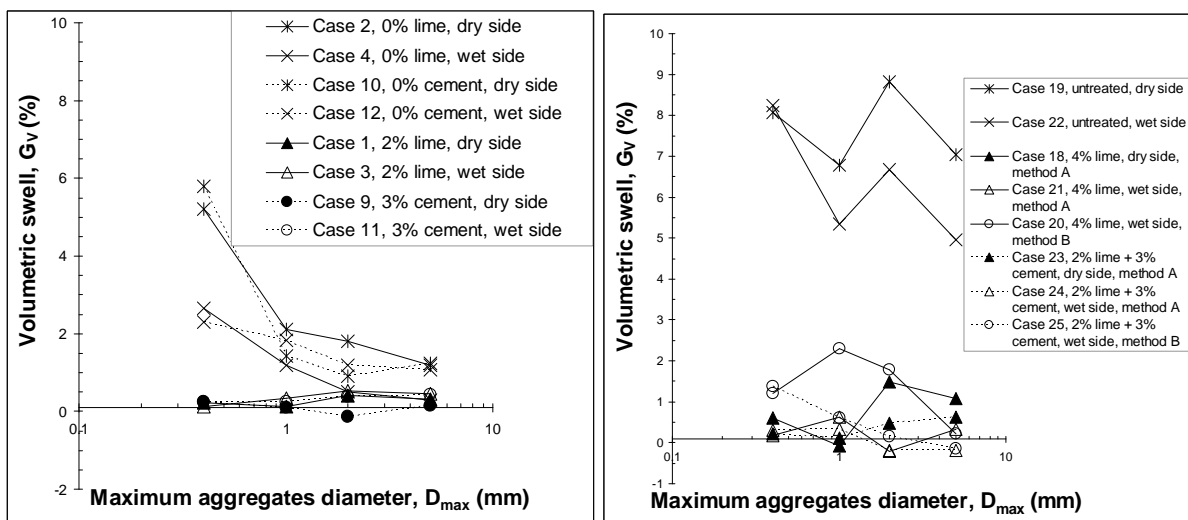
## 4.9. Aggregates size effect on volume change

Figure 4-32 presents the volumetric swell versus the maximum aggregates size for the silt and the clay with different treatments on a wetting path (ex. cycle No.3.0 for the silt and No.4.0 for the clay).



For the untreated soils, firstly they show much larger volumetric swell than the treated ones. Then, they decrease with the increase of aggregates size, especially for the silt. Moreover, they show higher values for the dry side than for the wet side. This is related to the difference in suction range during wetting/drying cycles.

For the treated soils, the trends are not as clear as untreated soils. For the silt, a slight increasing trend is observed in most cases except case 9, with small range of variations. For the clay, it seems to increase for the dry side with mixing method A, whereas it shows globally decreasing trends for the wet side, with higher values for mixing method B. These different trends indicate the aggregates size effect induced by different coating states for the soils with different mixing methods.



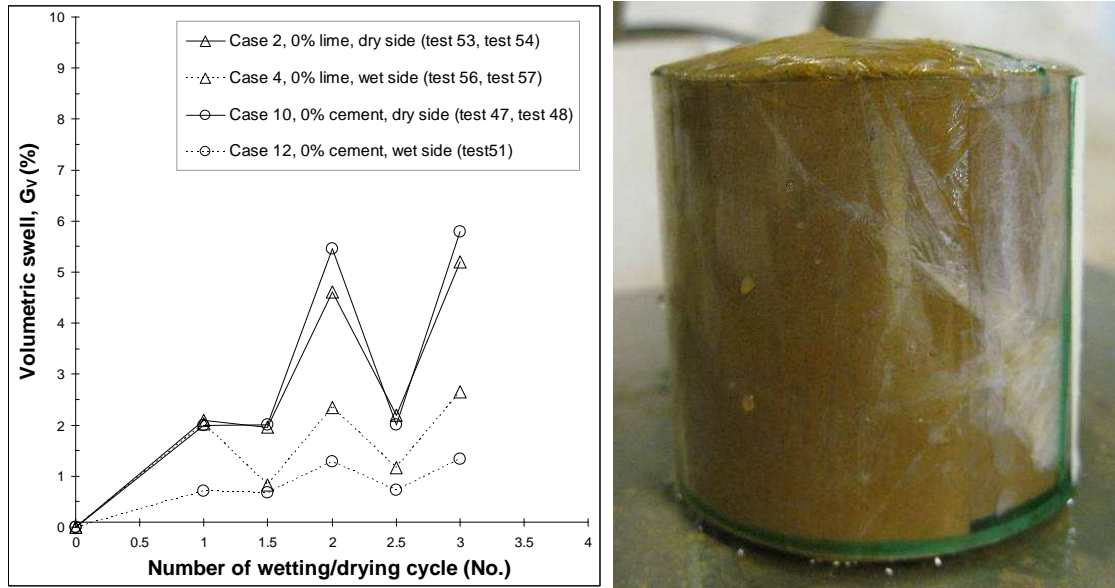
(a) Silt with different treatments (No.3.0) (b) clay with different treatments (No.4.0)

Figure 4-32 Aggregates size effect on the volumetric swell of the silt and the clay

In general, the volumetric swell is slight for the treated clay specimens (<5%). The untreated clay presenting larger swell (about 7%) is normal due to its high plasticity index. The silt show a large value for sub-series  $D_{max} = 0.4$  mm (about 2.5%, 5.5% for the wet side and dry side, respectively). This is to be attributed to its different microstructure with normally less macro-pores.

It is worth noting that during the swelling of the sub-series  $D_{max} = 0.4$  mm, a visible dimension change was observed (Figure 4-33b). Figure 4-33a presents the volumetric swell versus number of cycles for the untreated silt at different densities and moulding water

contents (case 2, 4, 10, 12). For the different cases of silt, the first wetting increases its volume. The subsequent drying cannot bring back to its initial volume. Similar observation was reported by Cuisinier and Deneele (2008) for a clayey soil.



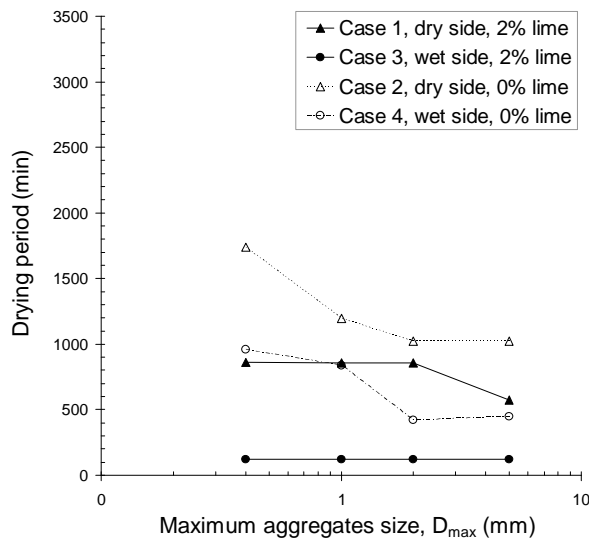
(a) Volumetric swell versus cycles (b) Visible swell (case 10 at No.2, T47)

Figure 4-33 Volumetric swell versus wetting drying cycles for the untreated silt of sub-series  $D_{max} = 0.4 \text{ mm}$

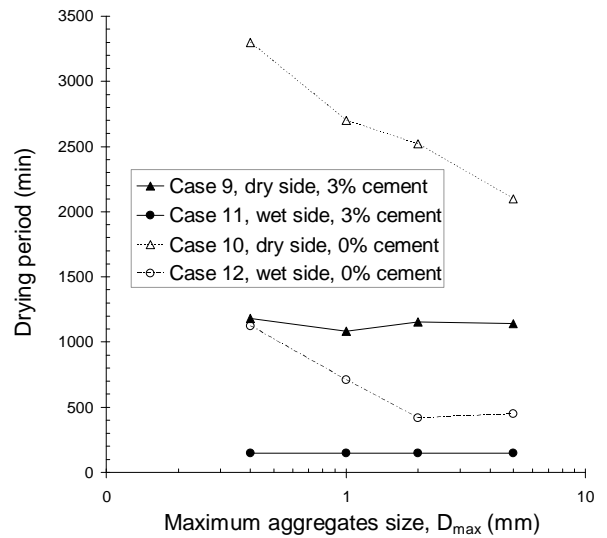
#### 4.10. Aggregates size effect on the drying period

As shown before in Figure 4-2b, a linear relationship exists between water content change and drying time, and the time of drying required to bring back to the initial water content is different for different sub-series. Following the same drying time calculating method, Figure 4-34 presents the drying time required to bring back to the initial water content for the different sub-series of silt and clay. It can be observed that the drying period is longer for the untreated soils than for the treated ones. It is longer for the dry side than for the wet side. For the untreated soils, the drying period shows clear aggregates size effect - the larger the  $D_{max}$ , the shorter the drying period required, especially for the dry side. This is in accordance with the aggregates size effect on suction changes as mentioned before. This indicates that the evaporation rate is correlated to the suction gradient between the soils and the environment. However, for the treated soils, this aggregates size effect is no longer noticeable under similar effect of suction gradients/suction changes. This suggests that some

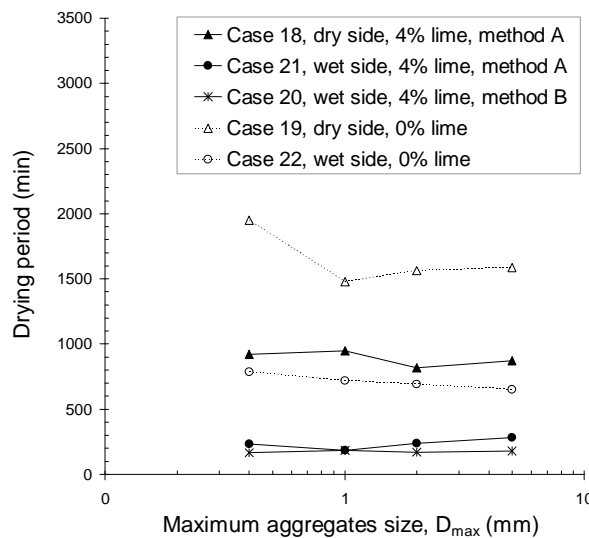
other phenomena occur (chemical reactions for example) in addition to the evaporation mechanism in the treated soils.



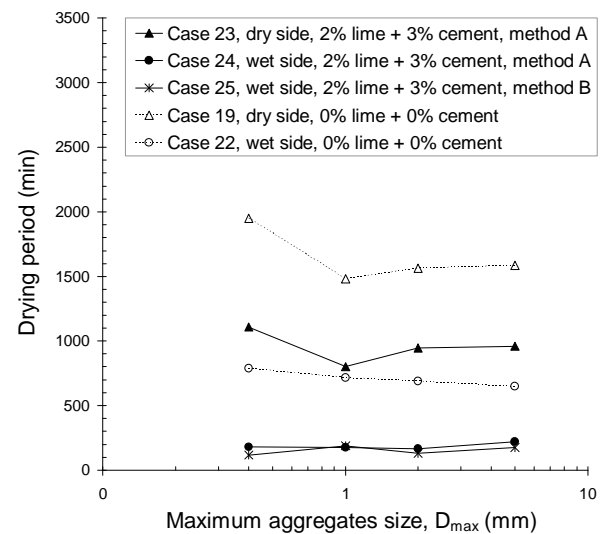
(a) 2% lime treated silt



(b) 3% cement treated silt



(c) 4% lime treated clay



(d) 2% lime plus 3% cement treated clay

Note: drying condition: average temperature  $20 \pm 2$  °C and average humidity 33%

Figure 4-34 Aggregates size effect on the drying time required to bring back to the initial water content for the lime treated, cement treated or mixture treated silt or clay

## 4.11. Discussion

For the untreated silt / clay compacted on both dry and wet sides, the  $G_{max}$  and water content vary in a cyclic fashion with wetting/drying cycles, with higher values in drying

paths. The higher the change in water content/saturation degree, the larger the range of  $G_{max}$  changes. As discussed in chapter 3, the stiffness of treated soils is suction dependent. This cyclic  $G_{max}$  change is also found to be related to the soil suction change. However, the degradation and failure mechanism related to drying-wetting is still an open question (Peron *et al.*, 2009). Recently, several researchers (Pardini *et al.*, 1996; Tang *et al.*, 2011) explained the degradation of hydro-mechanical behaviour of soils during wetting-drying cycles by the micro-cracks induced by suction cycles.

For the treated silt /clay, the  $G_{max}$  change with wetting/drying cycles is often classified into several stages in the present study (ex. 1 ~ 3 three stages). This indicates that the alteration of stabilization effect by wetting/drying cycles is much more complicated than for the untreated soils. In fact, apart from the higher range of suction changes during wetting/drying cycles, the complicated chemical reactions also play an important role for the  $G_{max}$  changes.

Firstly, the first wetting often decreases the  $G_{max}$  value, especially for the silt. This decrease is due to the significant decrease of suction. On the other hand, the first wetting can also increase the  $G_{max}$  value and sometimes the increase is for the first few cycles, especially for the dry side (ex.  $D_{max} = 0.4 \text{ mm}$  in Figure 4-21a). This can be explained by the ongoing pozzolanic reaction during the wetting process. This increase trend is also identified in Tang *et al.* (2011) and Al-kiki *et al.* (2011). The first wetting often induces a  $G_{max}$  change that is different from that in the following cycles. Cuisinier and Deneele (2008) also reported that the first wetting leads to an increase of volume and the first cycle leads to an irreversible volume change (Figure 4-33). This irreversibility is due to the combined effects of suction changes and pozzolanic reactions.

After the first cycle, a two-stage development of  $G_{max}$  is often observed, with more significant degradation in stage II (failure stage) than in stage I (coating stage). This is particularly noticeable for the dry side. This suggests that the soils compacted on the wet side are more durable than on dry side. Several studies (Seed and Chan 1960; Lambe and Whitman 1969; Barden and Fice, 1974; Holtz and Kovacs, 1981; Daniel and Benson, 1990; Daita *et al.*, 2005; Russo *et al.*, 2006) also reported the good engineering properties of soil-additive mixture compacted at or near the optimum. This is probably related to the much less suction change range during wetting/drying cycles as compared to that on dry side. In addition, the higher cementation before wetting/drying by coating thanks to the presence of more cementitious products is also beneficial to the durability of soils.

Most importantly, both the initiation cycle number for stage II (Figure 4-25) and the degradation ratio of stage II (Figure 4-26 ~ Figure 4-30) are strongly influenced by the aggregates size effect, especially for the dry side. The higher the aggregates size, the earlier the stage II (breakage or failure of aggregates) and the higher the degradation ratio. For the silt, this aggregates size effect is obvious for the dry side, but not noticeable for the wet side. This is explained by a good preservation of aggregates on the dry side but destruction of initial aggregates on the wet side. As mentioned in chapter 3, this size effect depends strongly on the mixing method, especially for the clay: a clear aggregates size effect is identified with mixing method A but not with mixing method B. As the larger the aggregates size, the lower the cementation obtained (see chapter 3), the soil with larger aggregates size has lower resistance to wetting/drying cycles.

Finally, although the aggregates size effect on saturation degree and volume changes is less pronounced than on the change of  $G_{\max}$ , the general trends identified are in agreement with the variations of degradation ratio with  $D_{\max}$ . This also evidences the aggregates size effect during application of wetting/drying cycles.

### 4.12. Conclusions

$G_{\max}$  changes during wetting/drying cycles are studied on the silt and clay of different sub-series by sieving method 1 (for the silt) and method 2 (for the clay), treated by lime and/or cement, mixed with mixing method A and method B, and compacted at both dry and wet sides. The corresponding water content/suction changes are also investigated. Several conclusions can be drawn from the results obtained:

1. Untreated soils are quite sensitive to water content/saturation degree/suction changes, and this sensitivity is significantly reduced for treated soils. The treated soils often experiences coating (stage I) and/or breakage of aggregates (stage II). At stage I, the treated soils present low sensitivity to water content changes and no noticeable degradation of  $G_{\max}$ . At stage II, higher sensitivity to water content appears together with noticeable degradation sign. In this study with application of 7 wetting/drying cycles, the dry side specimens often show typical two-stage behaviour (stage I and II), whereas the wet side specimens often present one stage only (stage I). The treated soils show larger failure initiation number of cycles and lower degradation ratio than untreated soils, evidencing much higher resistance to wetting/drying cycles. The degradation is related to the cyclic suction changes. Intensive

drying followed by re-wetting is greatly harmful to the stiffness of soils, with an accelerated breakage of aggregates.

2. Both the failure initiation number of cycles  $N_f$  (beginning of stage II) and the degradation ratio at stage II are strongly influenced by the aggregates size effect, especially for the dry side. The higher the aggregates size, the smaller the  $N_f$  and the higher the degradation ratio. This aggregates size effect depends strongly on the mixing method and molding water content, especially for the clay.

3. The sensitivity to water content changes is related to the suction of soil, the cementation degree and the range of suction change during wetting/drying cycles. The breakage of aggregates can lead to a decrease of soil suction and thus an increase of the sensibility to water content changes. Thereby, this sensitivity is treatment dependent. Cement treated silt is more sensitive than lime treated one. Mixture (2% lime + 3% cement) treated clay is more sensitive than solely lime treated one, especially in case of large aggregates size (ex. mixing method B, case 25 versus case 17).

4. The water content after each wetting changes with wetting/drying cycles. For untreated soils, the water content/saturation degree increases with cycles, whereas for treated soils, no noticeable changes take place. Further examination shows that the water content/saturation degree often decreases during the coating phase (stage I) and then slightly increases during the degradation phase (stage II). This phenomenon is found to be aggregates size dependent. For untreated soils, the larger the aggregates, the lower the increase of saturation degree. For treated soils at stage II, the larger the aggregates, the higher the increase of the saturation degree. This indicates that the saturation degree (suction) changes are closely correlated to the breakage process of the aggregates.

## Chapter 5. *In-situ* specimens from the experimental embankment in Héricourt

In this chapter, the profiles of  $G_{\max}$ , dry density and water content will be first depicted for the two batches of cores. For each treatment on the silt and clay, the effects of heterogeneity, curing time and climate are analyzed.

### 5.1. Results of silt side

For the silt side of the embankment, because of lack of core samples of silt treated by 2% lime, only SC40-1 with the silt treated by 3% lime was tested.

SC40-1 is a core sample of the first batch. It consists of silt treated by 1% lime plus 5% cement (*in-situ* 5, 0 m ~ 0.54 m, see chapter 2 for the *in-situ* numbers) and by 3% lime (*in-situ* 4, at 0.57 m). It is situated at sub-grade and on the top of the earthwork part of this embankment.

Figure 5-1 presents changes of  $G_{\max}$ ,  $\rho_d$  and  $w$  over depth for core sample SC40-1. The corresponding designed values of  $w$  and  $\rho_d$  are also shown in this figure. Figure 5-2 shows the section observation of these specimens. We observe that: 1) the  $G_{\max}$  data is very scattered between the five measurements on each specimen; 2) the dry density and water content vary with depths, indicating the high heterogeneity of *in-situ* soil. Figure 5-2 presents the heterogeneity due to the presence of stones and the non homogeneous additive distribution. Based on the photos of these core specimens, we observe that more stones/additives exist in the specimens of *in-situ* 5 than in the specimen of the *in-situ* 4. This heterogeneity is typical for the *in-situ* soil that is compacted at a large aggregates size scale.

Apart from the heterogeneity of the *in-situ* soil, comparison of the  $G_{\max}$  values between *in-situ* 5 and *in-situ* 4 shows that the treatment with 1% lime plus 5% cement is much more efficient than with 3% lime treatment, considering their similar values of water content and dry density.

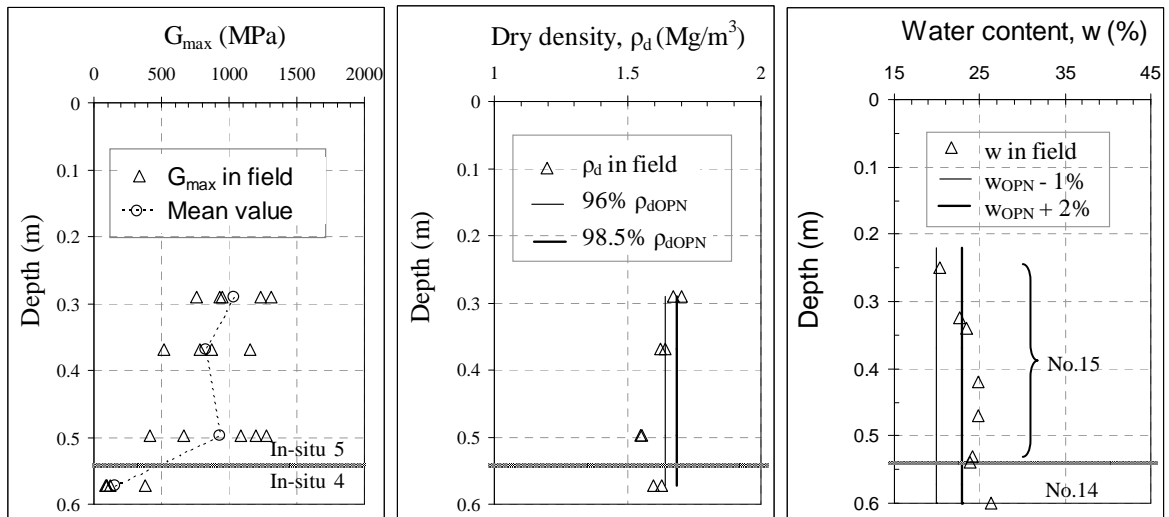


Figure 5-1 Stiffness, density and water content versus depths for SC40-1 (*In-situ* 5 and *In-situ* 4)

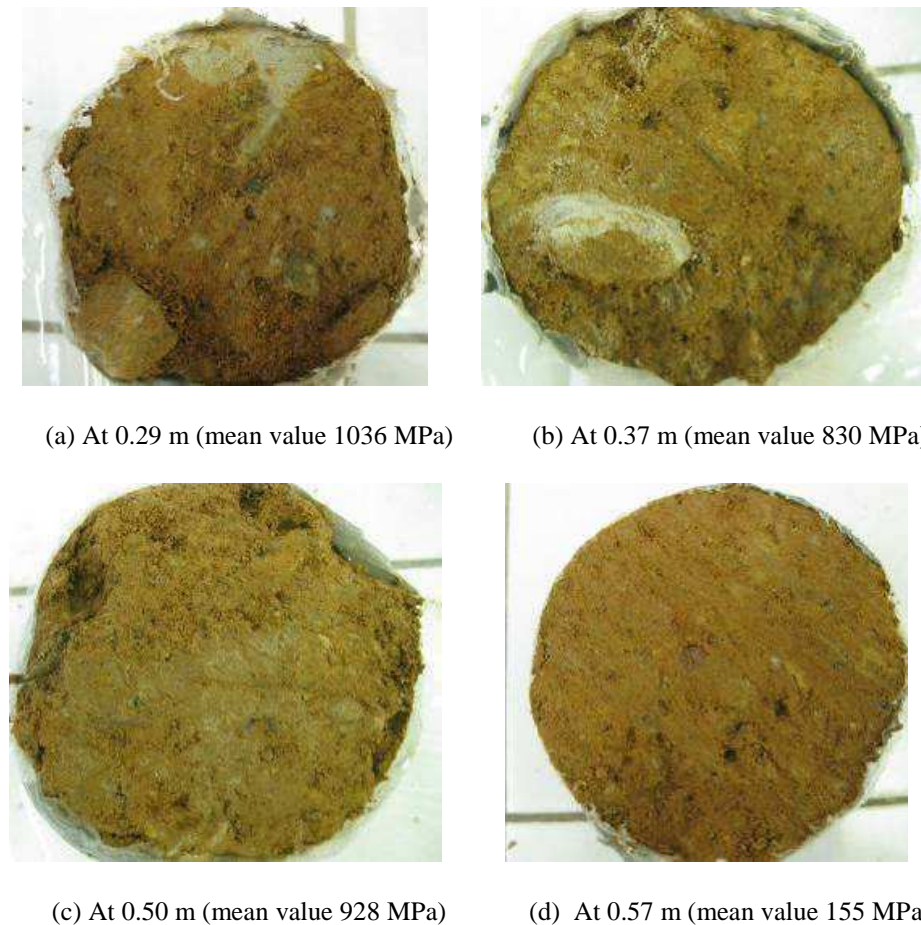


Figure 5-2 Photos of the core specimens of SC40-1



## 5.2. Results on the silt treated with cement

### 5.2.1. First batch of core sample SC31-1

SC31-1 is a silt core sample constituted of stones at base (No.16: 0 ~ 0.22 m), of sub-grade silt treated by 1% lime plus 5% cement (*in-situ* 6, No.15: 0.22 ~ 0.43 m) and of earthwork silt treated by 3% cement at top (*in-situ* 1, No.14: 0.43 ~ 0.78 m; No.13: 0.78 ~ 1.00 m). Globally, this core sample is quite stony. Moreover, Layer No.15 and No.13 show relative higher content of stones and higher concentration of additives than layer No.14.

Figure 5-3 shows changes of  $G_{\max}$ ,  $\rho_d$  and  $w$  over depth for a core sample-SC31-1 also of the first batch. The corresponding values of  $w$  and  $\rho_d$  designed according to the GTR (1992, 2000) are also shown in this figure. On the whole, we observe the large variation of  $G_{\max}$  and a certain variation of  $\rho_d$  and  $w$  with depth, indicating the high heterogeneity of the *in-situ* silt.

Firstly, for the  $G_{\max}$  (Figure 5-3a), the variation range is huge even for the same nominal treatment (ex. *in-situ* 1, from the mean value of about 60 MPa at 0.55 m / 0.65 m to over 1000 MPa in layer No.13). Further examination shows that the high stiffness values (0.22 m ~ 0.43 m; 0.78 m ~ 1.00 m) are induced by the high concentration of additives and stones (ex. at 0.81m, in Figure 5-4f); the lower  $G_{\max}$  values of layer No.14 (0.43 m ~ 0.78 m) are related to the lower contents of stones and cement than in other layers (ex. at 0.45 m, 0.55 m and 0.65 m in Figure 5-4a, b, c). Note that no tests were performed on the soil between 0.70 m and 0.78 m because of the fragility of the silt with low concentration of additives. For the same reason, a low stiffness value of specimen at 0.96 m is identified although it is very stony (Figure 5-4e).

Then, the dry density presents relatively lower variation in layer No.15 and No.14 than in layer No.13, almost all with slightly higher values than the designed ones (Figure 5-3b). At 0.96 m of layer No.13, the dry density values ranges from 1.47 to 1.57 Mg/m<sup>3</sup>. This high variation is due to the scattered water content data induced by the presence of stones.

Finally, for the water content (Figure 5-3c), it does not change noticeably over depth in layer No.15 and No.14 ( $w = 19.5\% \sim 22.37\%$ ). All values are greater than the designed ones, with an exception at 0.96 m of layer No.13. This is probably due to the

difficulty of sampling as this layer contains many stones as mentioned before (Figure 5-4d, e). The *in-situ* water content is found close to the water content of the specimens compacted in the laboratory on the wet side of optimum.

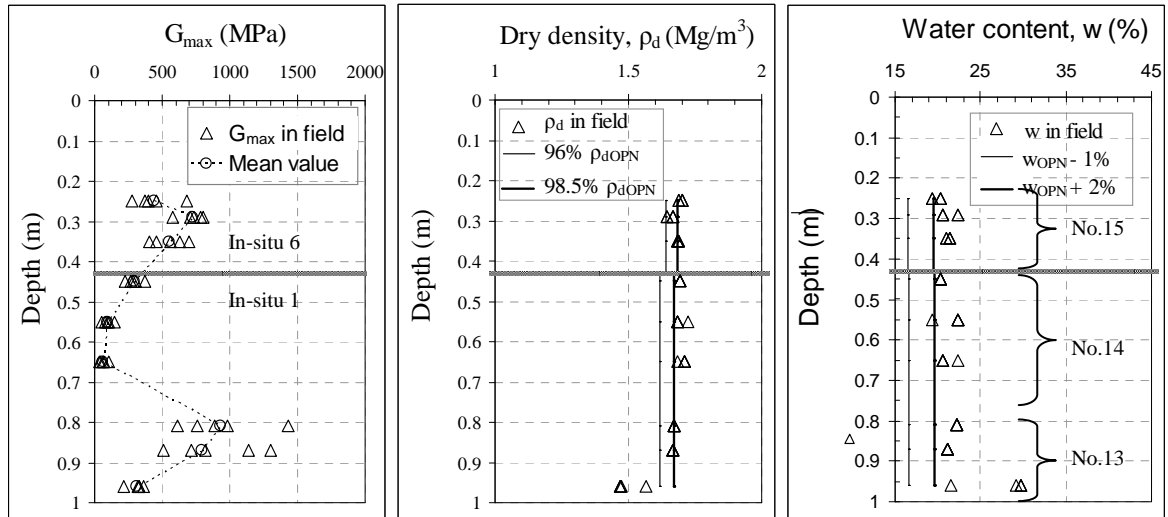


Figure 5-3 Stiffness, density and water content versus depths for SC31-1 (*In-situ* 6 and *In-situ* 1)



(a) 219 MPa at 0.45m



(b) 61 MPa at 0.65m



(c) 95 MPa at 0.55m



(d) Stony but low concentration of cement (0.90 ~ 1.00 m)



(e) 300 MPa at 0.96 m, very stony and high w



(f) 935 MPa at 0.81 m, stony and concentrated of cement

Figure 5-4 Some specimens of SC31-1 with their mean stiffness values

As a conclusion, we observe that: 1) the heterogeneity of the additives distribution is responsible for the variations of stiffness. This can be explained by the aggregates size

of the *in-situ* soil: the larger the aggregates, the lower the concentration of additives, hence the lower the stiffness (ex. layer No.14); 2) the heterogeneity in terms of stone presence comes to strengthen this aggregates effect: the less the stones presence, the narrower the variation range and the lower the  $G_{max}$  value (ex. less stones presence in layer No.14 than in layer 13 for the specimens at 0.96 m, with similar additive distribution). The high stone presence and concentration of additives significantly increase the soil stiffness (ex. at 0.81 m,  $G_{max}$  range: 613 ~ 1433 MPa).

### 5.2.2. Core SC49-1 of the second batch

Core SC49-1 is similar to core SC31-1, with 1% lime plus 5% cement treated silt (*in-situ* 12, No.15: 0.25 ~ 0.46 m) and 3% cement treated silt (*in-situ* 2, No.14: 0.48 ~ 0.80 m; No.13: 0.80 ~ 1.00 m). For each compaction layer, a slightly greater depth of the limit is observed than in the case of SC31-1. This is related to the long term volume change behavior under *in-situ* conditions.

Figure 5-5 presents changes of  $G_{max}$ ,  $\rho_d$  and  $w$  over depth also for core SC49-1. Globally, we also observe the large variation of  $G_{max}$ ,  $\rho_d$  and  $w$  over depth. The high heterogeneity of the *in-situ* silt can also be explained by the heterogeneity of additive distribution and of stones presence (Figure 5-6). The stone presence/high concentration of additive results in both large variation range of stiffness and high stiffness level in terms of mean values.

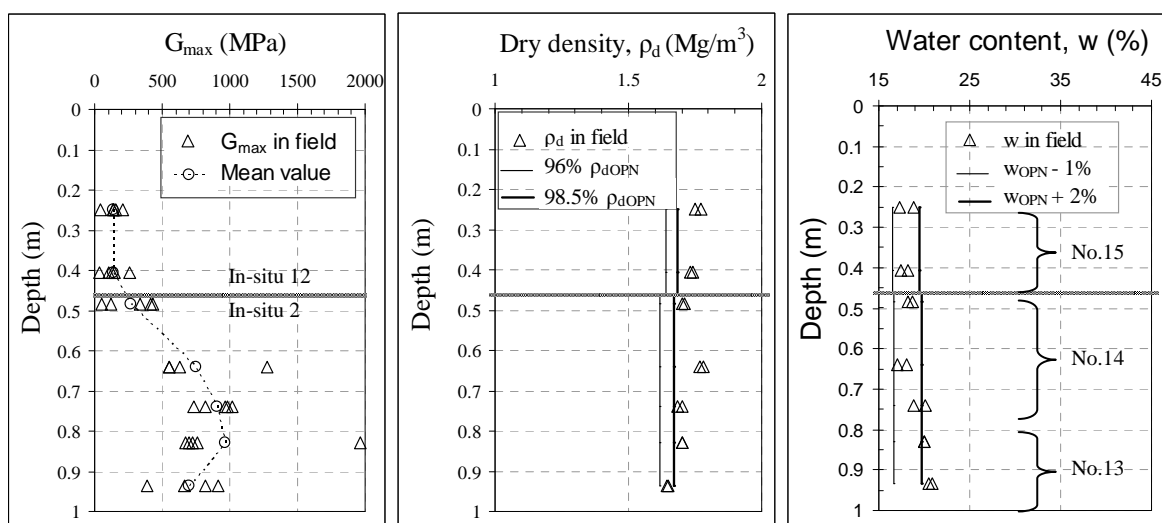


Figure 5-5 Stiffness, density and water content versus depth for SC49-1 (*In-situ* 12 and 2)

It is worth noting that the significant difference of stiffness level (mean value) between *in-situ* 12 (No.15) and *in-situ* 2 (No.14, 13) reflects the different climate effects.



(a) 36 ~ 255 MPa at 0.405 m



(b) Mean value 135 MPa also at 0.405 m



(c) 47 ~ 219 MPa at 0.25 m



(d) 554 ~ 1271 MPa at 0.64 m very stony



(e) 554 ~ 1271 MPa at 0.83 m, stony and high concentration of cement



(f) Very stony in layer No.13 (near 0.83 m)

**Figure 5-6 Some specimens of SC49-1 with their different stiffness values**

### 5.2.3. Time effect

As for the laboratory compacted specimens, we have observed that the behaviour of lime/cement treated soils changes with curing time. The pozzolanic reactions can last several months, even longer. For the *in-situ* core sample, due to the presence of large aggregates, the effect of curing time can be more pronounced. This effect was investigated by performing five  $G_{\max}$  measurements at different curing periods.

Figure 5-7 presents the  $G_{\max}$  of the silt specimens of SC31-1 (3% cement and 1% lime plus 5% cement treatments) with the curing periods of 7 months, 11 months and 29 months. These tests involve five measurements of each specimen presented in Figure 5-7a and the time effect by considering the mean value of these measurements in Figure 5-7b. The near surface layer (layer No.15, *in-situ* 6) consists of 1% lime plus 5% treated silt, followed by two layers of 3% cement treated silt (*in-situ* 1).

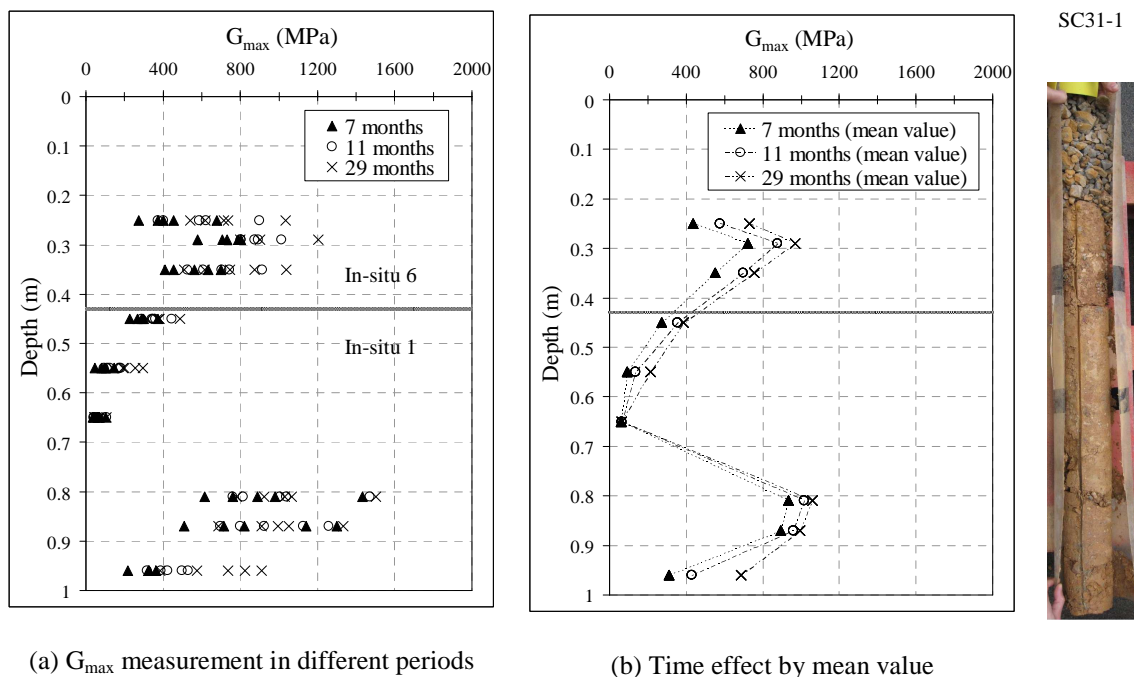


**Figure 5-7** Curing time effect for the 3% cement treated silt (*in-situ* 1) and 1% lime plus 5% cement treated silt (*in-situ* 6) of SC31-1

As shown in Figure 5-7a, the values of the five measurements during these curing periods are not well ordered due to the high heterogeneity of soils, and the time effect is not clear. However, their mean values (Figure 5-7b) show that the evolution of  $G_{\max}$  changes with time can be identified. In Figure 5-7b, we observe that the stiffness gain due to the curing

effect is different for different soils. For the 3% cement treated silt, the  $G_{\max}$  values of the specimen at 0.65 m remain almost unchanged, whereas the values of the specimens at other depths increase significantly, especially for the specimen at 0.96 m. This indicates that the curing effect is strongly dependent on the heterogeneity of soils, especially in terms of additive distribution and stone presence. The more the additives and stones are, the higher the curing effects is. This is logical because with higher dosage of additives, a higher solidification degree by pozzolanic reactions is expected.

#### 5.2.4. Climate effect

The effect of climate on the stiffness of the core samples is mainly through the effect of water content change and the effect of wetting/drying cycles. Of course, as the heterogeneity of the soils plays a very important role to the stiffness of soils, we need also pay attention to it when analysing the data. Note that the stiffness measurements were performed at similar periods between the two batches of cores.

Figure 5-8 presents the 23-month climate effect on the stiffness, dry density and water content by the comparison of the results between the two batches of core sample SC31-1 and SC49-1. These two cores are situated in the near surface part of the silt side, containing 1% lime plus 5% cement treated silt (*in-situ* 1 and *in-situ* 2) and 3% cement treated silt (*in-situ* 6 and *in-situ* 12), respectively.

In Figure 5-8a, although a large variation of  $G_{\max}$  values for the two batches specimens is identified due to their high heterogeneity, we observe that the mean value of the first batch soils show much higher values than the second batch soils in the near surface layer No.15 (0.25 ~ 0.43 m). Then the gap decreases until 0.50 m depth. For the deeper levels (0.50 ~ 1.00 m), the mean values are close, showing the negligible effect of climate on  $G_{\max}$ . This indicates that the climate effect plays a significant role within a depth of 0.50 m for the silt core sample SC49-1. Note that we also observe many fissures and cracks in the near surface layers. This can also explain the decrease of  $G_{\max}$  due to the climate effect.

In Figure 5-8b, we observe similar values of dry density over depth for SC31-1 and SC49-1, with a slightly higher mean value for SC49-1. This is to be attributed to the slight volume change of SC49-1.

In Figure 5-8c, we observe slightly higher water content values for SC31-1 as compared to SC49-1. This can be explained by the drying effect due to the climate changes.

However, the drying of SC49-1 does not increase its  $G_{max}$  at 0.25 ~ 0.43 m, suggesting the significant effects of the climate by wetting/drying cycles.

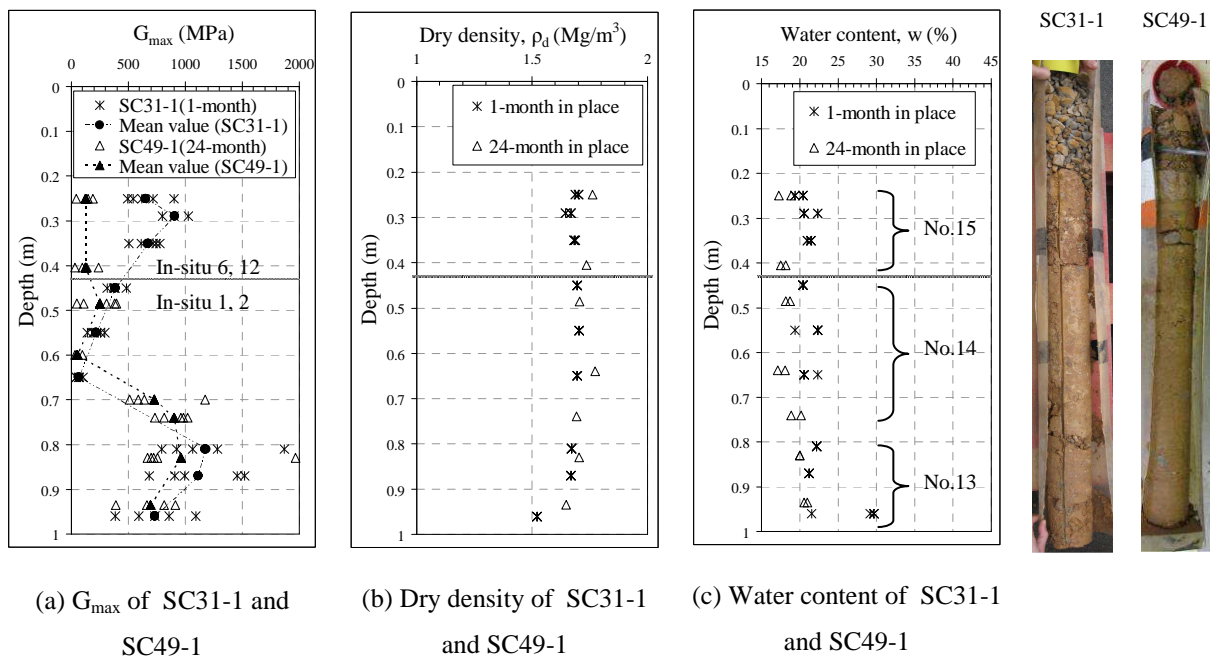


Figure 5-8 Climate effect (23 months) on the 3% cement treated silt (*in-situ* 1 and *in-situ* 2) and 1% lime plus 5% cement treated silt (*in-situ* 6 and *in-situ* 12) of SC31-1 and SC49-1, respectively

### 5.3. Results of clay side

#### 5.3.1. Cores dominantly treated by lime

##### 5.3.1.1. SC5-1

The first batch core sample SC5-1 is situated in the near surface part of the sub-grade, involving the base, sub-grade and top of earthwork. The base is made of the silt treated by 1% lime plus 5% cement (0 ~ 0.22 m, layer No.16, *in-situ* 9). The sub-grade contains one layer of the clay treated by 5% lime (0.22 ~ 0.5 m, layer No.15, *in-situ* 25). The top of earthwork is constituted of 3 layers of clay also treated by 5% lime (0.50 ~ 1.30 m, layer No.12, No.13 and No.14, *in-situ* 25). Visually, we observe that the clayey soils contain less stones than the silty soils.

Figure 5-9 presents changes of stiffness, density and water content over depth for the clay sample SC5-1. On the whole, similar to the silt cores mentioned before, the clay core

still shows a large variation of  $G_{max}$  over depth, even at a scale of a single specimen (Figure 5-9a). The water and density also vary significantly with depths (Figure 5-9 b and c).

Firstly, for each compaction layer, though there is also a large variation of  $G_{max}$ , globally, we observe a common relationship between the average stiffness and water content for each specimen of this core:

- 1) For layer No.16, from 0 to 0.22 m, with the increase of water content and slight decrease of dry density, logically, the mean value of  $G_{max}$  decreases. Thereby, the high stiffness level of this silt layer is due to its treatment effect with high additive dosage (1% lime plus 5% cement), stony presence, high dry density and low water content.
- 2) For layer No.15 (0.22 ~ 0.5 m), with relative stable values of dry density and water content, a significant increase of mean  $G_{max}$  value with depth is observed, from 246 MPa at 0.25 m to 708 MPa at 0.41 m.
- 3) For the following layers, No.14 ~ No.12 (0.50 ~ 1.30), similarly, the mean  $G_{max}$  value of each specimen also increase significantly with steady decrease of water content.

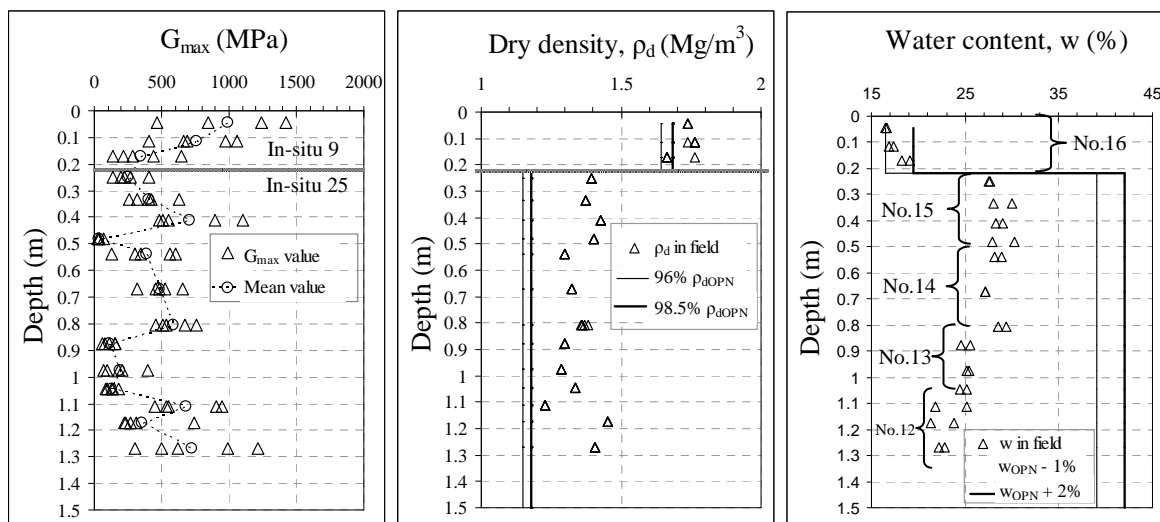


Figure 5-9 Variations of stiffness, density and water content over depths for SC5-1 (*In-situ* 9, 25)

Normally such a slight change of dry density/water content cannot result in such a large range of  $G_{max}$  variation (from several MPa to several hundreds of MPa). As we scarcely observe the stones presence in the *in-situ* clay, the heterogeneity of the additive distribution/aggregates size may be the main reason for this result.



Indeed, from observation of the specimens we can see how the heterogeneity of aggregates size/additives distribution affects the stiffness of the *in-situ* clay. The extreme case of low stiffness level (mean value) at 0.48 m and 0.876 m corresponds to the large size of untreated aggregates (see Figure 5-10). As the large aggregates size means low concentration of additives, the  $G_{\max}$  value is lower.

It is worth noting that high  $G_{\max}$  is often observed at the bottom of each compaction layer. This phenomenon occurs particularly in the case of high dosage of lime (5% lime), and this may not be just a coincidence. It is probably related to the effect of mixing method applied in field conditions.



(a) 37 MPa at 0.48 m in face



(b) 37 MPa at 0.48 m in face



(c) 37 MPa at 0.48 m profile



(d) 113 MPa at 0.876 m (in face)



(e) 113 MPa at 0.876 m (in face)



(f) 113 MPa at 0.876 m (in profile)

**Figure 5-10 Photos of some specimens of SC5-1 with low stiffness level (mean value) and large aggregates size**

### 5.3.1.2. SC14-1

Similar to SC5-1, SC14-1 is also a first batch core sample from the near surface part. It also contains 5 compaction layers: layer No.16 made up of silt treated by 1% lime plus 5% cement (0 ~ 0.22 m, *in-situ* 8); layer No.15 constituted of clay treated 2% lime plus 3%

cement (0.22 ~ 0.5 m, *in-situ* 20); the following 3 layers constituted of clay treated by 2% lime plus 3% cement (No.14: 0.50 ~ 0.80 m; No.13: 0.80 ~ 1.14 m; No.12: 1.14 ~ 1.50 m).

Figure 5-11 presents changes of  $G_{max}$ , density and water content over depth for SC14-1. For layer No.16, the  $G_{max}$  values are scattered probably due to the stones presence as shown in Figure 5-12b and c. Only one specimen was tested due to a big stone in the upper part (Figure 5-12a). For the following layers, with similar density and water content values, the mean  $G_{max}$  values first decrease with depth from 763 MPa for layer No.15 to 324 MPa for layer No.13, and then increase a little to 526 MPa for layer No.12. The difference is particularly noticeable between layer No.15 and the layers below. This is probably due to the effect of treatment: higher values for the mixture treatment (2% lime plus 3% cement) than for the 5% lime treatment. We can also observe the difference in solidification from their profile (Figure 5-12d, e, f). In addition, as for core sample SC5-1, the *in-situ* clay also shows much higher dry density and lower water content than the designed values.

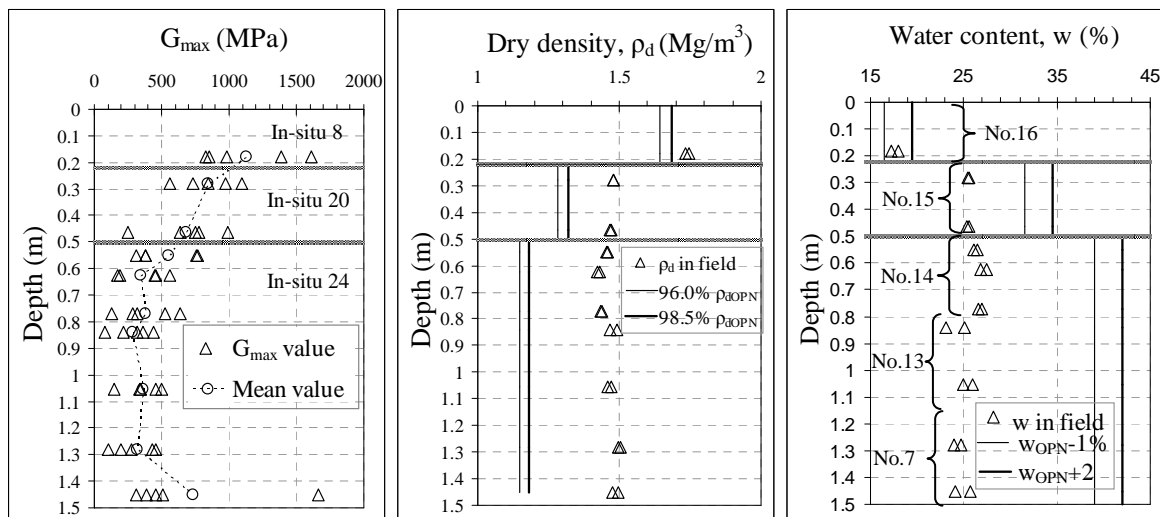
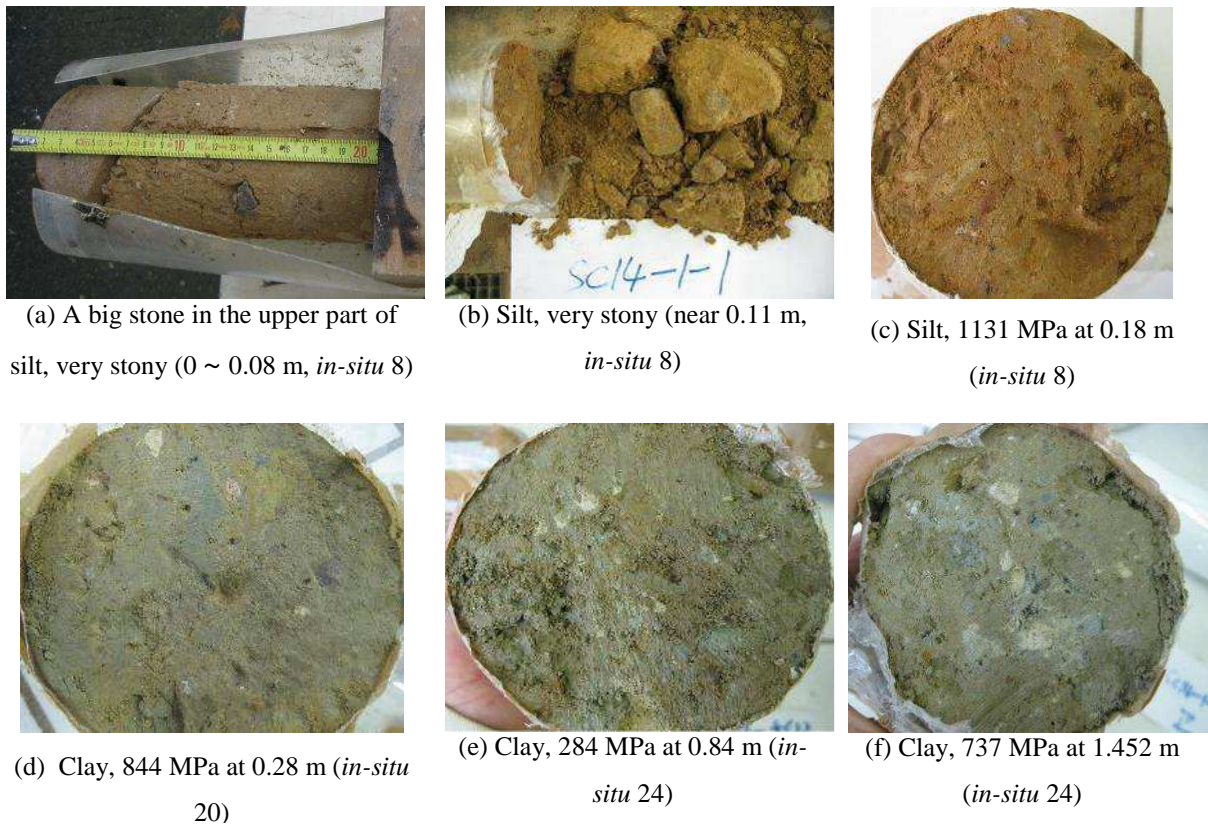


Figure 5-11 The variation of stiffness, density and water content over depth for the silt treated by 1% lime plus 5% cement (*in-situ* 8), the clay treated by 2% lime plus 3% cement (*in-situ* 20) and by 5% lime (*in-situ* 24) from SC14-1



**Figure 5-12** Photos of some specimens and their stiffness levels (mean value) for SC14-1

### 5.3.1.3. SC14-2

The core sample SC14-2 is the second sample of core SC14 (1.5 m ~ 3.0 m). It involves six compaction layers (No.11~ No.6), solely treated by 4% lime. In case of 4% lime treated clay, the stiffness is still strongly affected by the heterogeneity of soils. This heterogeneity can be related to the additive distribution/aggregates size, the stone presence as well as the moisture change.

Figure 5-13 presents changes of stiffness, density and water content over depths for SC14-2. On the whole, the  $G_{max}$  increases with depth at a large scale from 1.50 to 3.0 m (Figure 5-13), although the variation range is large. This variation is probably due to the different concentration of additives (aggregates size effect in Figure 5-14 and Figure 5-15) and the combined effects of aggregates size and stone presence at 2.056 m and 2.424 m (Figure 5-15). The dry density remains at a relative constant level except two points at 2.056 m and 2.424 m (Figure 5-13b). The significant dry density of the two specimens is probably induced by the presence of big stones. The water content decreases slightly with depths (Figure 5-13c).

Firstly, significant difference in heterogeneity is identified in terms of additive concentration/aggregates size. Figure 5-14 and Figure 5-15 clearly show the additive presence in several specimens. As for SC5-1, we also observe that the  $G_{max}$  depends mainly on the additives distribution/aggregates size. The soils with low stiffness clearly show pure clay (in green, yellow or brown) and large aggregates. As the stiffness increases, the spots of cementitious products are gradually visible (1.73 m ~ 1.902 m). Thereafter, with the cementitious spots accumulated, the natural large aggregate blocks are separated into small aggregates (ex. at 2.056 m, 2.424 m). In addition, the high stiffness level (about 600 MPa) at 2.6 ~ 3.0 m also presents small aggregates size similar to that at 2.424 m.

Then, apart from some exceptional points due to the heterogeneity factors (aggregates size), as for SC5-1, the classic relationship between  $G_{max}$ , dry density and water content can be observed - the higher the water content and / or the lower the dry density the lower the stiffness (ex. water content effect at 1.5 ~ 2.1 m; combined effect of density and water content at 2.2 ~ 2.4m and 2.4 ~ 2.6 m). Moreover, the water content effect on the stiffness of soils at a large scale (1.5 ~ 3.0 m) also justifies this classic relationship.

Nevertheless, the effects of water content or dry density are often masked by the heterogeneity of the additive distribution for the clay. As the stone presence can significantly increase  $G_{max}$  value, it can be assimilated to the effect of very high concentration of additives/ small aggregates size.

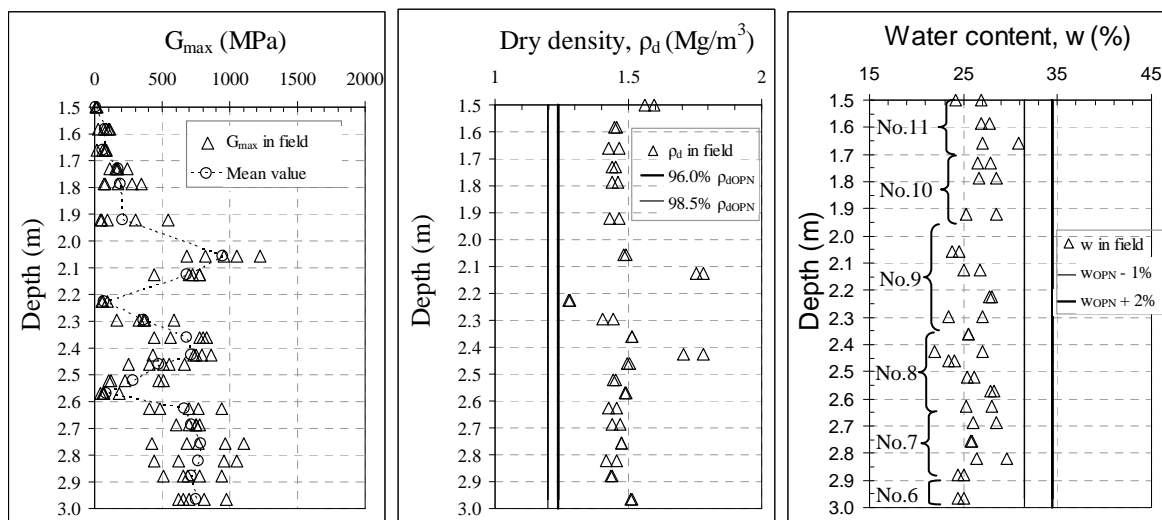


Figure 5-13 Variation of stiffness, density and water content over depth for the 4% lime treated clay (*In-situ* 21) (SC14-2)



(a) 7 MPa at 1.50 m



(b) 79 MPa at 1.584 m



(c) 62 MPa at 1.66 m



(d) 168 MPa at 1.73 m



(e) 191 MPa at 1.789 m



(f) 209 MPa at 1.902 m

**Figure 5-14 Photos of specimens with low  $G_{max}$  values and large aggregates**



1025 MPa at 2.056 m

750 MPa at 2.424 m

**Figure 5-15 Photos of specimens with high  $G_{max}$  values and small aggregates**

The second batch core samples SC46-1 and SC46-2 close to SC14 were bored in December of 2011, 20 months after their compaction in field. The first measurements of the specimens from them were performed in April of 2012. These results are presented in this section.

## 5.3.1.4. SC46-1

SC46-1 contains 5 compaction layers, one layer of base No.16 ( 0.000 m ~ 0.250 m, 1% lime plus 5% cement treated silt), one layer of sub-grade No.15 (0.270 m ~ 0.515 m, 2% lime plus 3% cement treated clay) and three layers of the top of earthwork ( 0.515 m ~ 1.300 m, 5% lime treated clay).

Figure 5-16 presents changes of  $G_{max}$ , density and water content over depth for SC46-1. On the whole, as all the results mentioned before, scattered values over depth are observed because of the heterogeneity of soils. It is worth noting that the effect of climate can also play a role in the change of stiffness, because a foliated structure caused by climate effect is observed for both clay (Figure 5-17c) and silt (Figure 5-17a, b) (SC46-1 in appendix). A report of TerDOUEST project (Muzahim Al-Mukhtar, 2007) also identified a leafage degradation of lime treated clayey soil (A3/A4 according to NF EN P 11-300) in near surface layers of an embankment only 3 years after its construction. In addition, the  $G_{max}$  sensibility to the change of water content is often observed in this core sample.

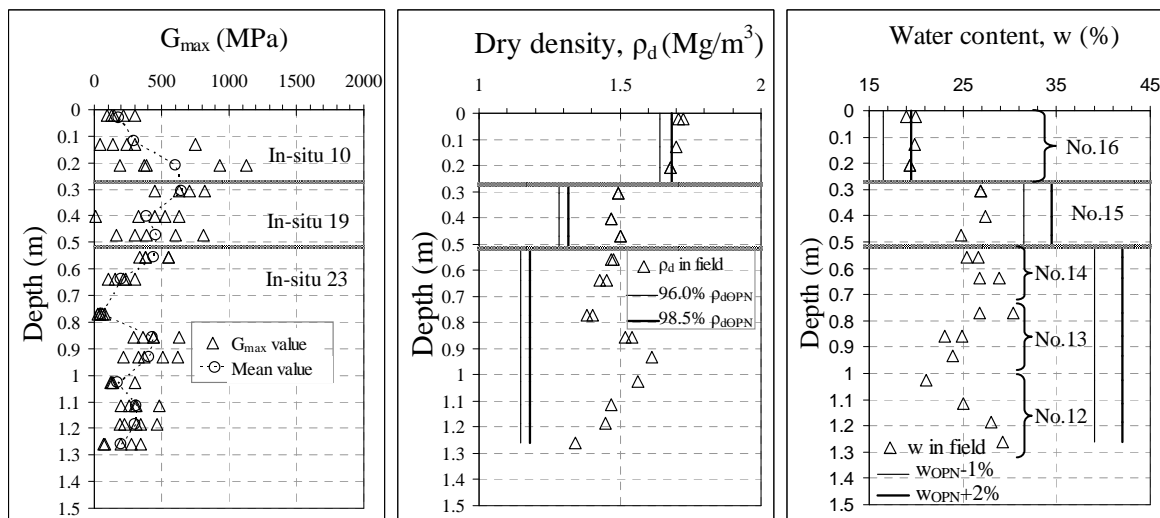


Figure 5-16 Stiffness, density and water content versus depth (SC46-1) (*In-situ* 10, 19 and 23)

For layer No.16 (0.000 m ~ 0.250 m), the mean value of  $G_{max}$  increases significantly with depth; the water content remains almost constant and the dry density decreases slightly. The  $G_{max}$  variation for each specimen is mainly governed by the heterogeneity of the soils. The effect of degradation may be induced by the climate effect (SC46-1 in Appendix). For layer No.15 (0.270 ~ 0.515 m), the mean  $G_{max}$  is higher than that for the following layers. This is due to the treatment effect as mentioned before. For the following layers, NO.14

(0.515 ~ 0.720 m), No.13 (0.735 ~ 0.970 m) and No.12 (1.060 ~ 1.300 m), the classic  $G_{max}$ -density/water content relationship can be observed. This is very different from SC14-1, suggesting that the  $G_{max}$  for SC46-1 is more sensible to water content changes as compared to SC14-1.



(a) Low stiffness values of the silt at 0.02 m (the foliated trace structure )



(b) Low stiffness values of the silt at 0.130 m (the foliated trace structure)



(c) Large aggregates size for low stiffness values of the clay at 0.77 m (the foliated trace structure)



(d) Small aggregates size for high stiffness values of the clay at 0.86 m

**Figure 5-17** Photos of specimens from for SC46-1 with low and high values of stiffness and aggregates size

### 5.3.1.5. SC46-2

SC46-2 is situated at the deeper position in core SC46. It contains four compaction layers (No.11 ~ No.8, 1.30 ~ 2.60 m, 2% lime plus 3% cement treated clay).

Figure 5-18 presents the scattered  $G_{max}$  values, the limited change of water content and dry density for SC46-2. The increasing trend of  $G_{max}$  with depth is noticeable. This is obviously due to the heterogeneity of additive distribution/ aggregates size (Figure 5-19).

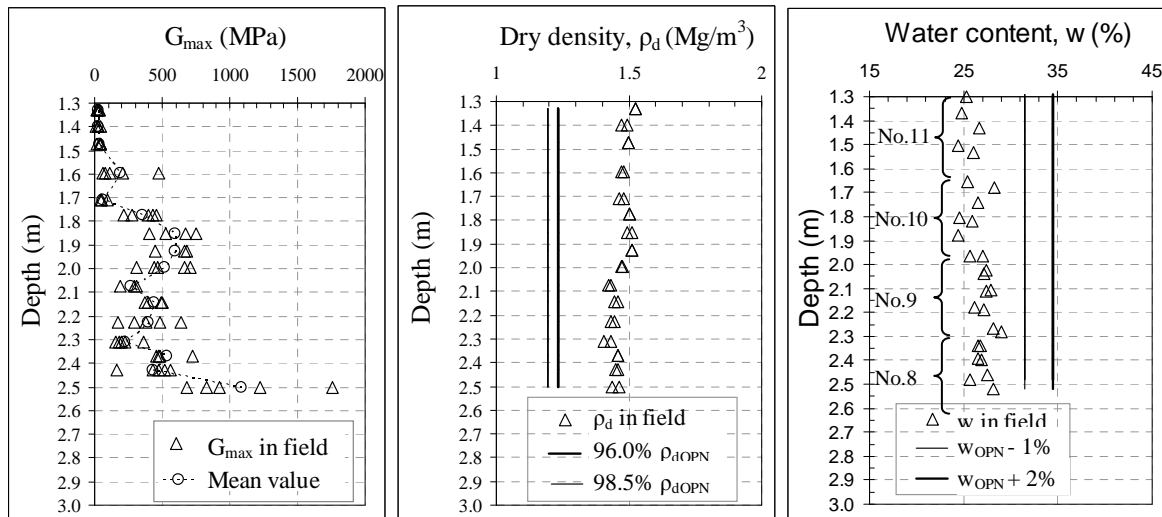


Figure 5-18 Stiffness, density and water content versus depth (SC46-2) (*in-situ* 22)



(a) Large aggregates size for low stiffness level  
(mean value 25 MPa) at 1.33 m



(b) Small aggregates size for high stiffness level (mean value 1082 MPa) at 2.50 m

Figure 5-19 Photos of specimens from SC46-2 with low and high values of stiffness (mean value) and aggregates size

### 5.3.2. Time effect

Figure 5-20 presents the  $G_{max}$  measurements of the same clay specimens (4% lime treated clay) after the curing period of 7 months, 16 months and 30 months for SC14-2 (*in-situ* 21).

As for the silt, the values of the three measurements in Figure 5-20a present high heterogeneity. On the other hand, using the mean value for each measurement can minimize the effect of heterogeneity. Figure 5-20b shows the slight increase of  $G_{max}$  due to the curing



time effect. Two points are observed after in-depth examination: 1) the stiffness gain due to curing is related to the stiffness level of soils: the higher the stiffness, the larger the stiffness gain; 2) for the high stiffness levels (ex. at 2.056 m), the values between the second and third measurements are very close, indicating different increase rates with curing time - the stiffness increases significantly during the first 7 months, whereas it remains almost constant after 12-month curing.

This different effect of curing time can be explained by the different heterogeneity levels of the clay specimens. As stones are less present in the clay than in the silt, the time effect may be mainly related to the additive distribution effect/ aggregate size effect in the case of clay. This also suggests that the stiffness gain is due to the pozzolanic reactions. Indeed, the larger the aggregates, the less the pozzolanic reactions. The different increase rates suggest diminishing reactions with curing.

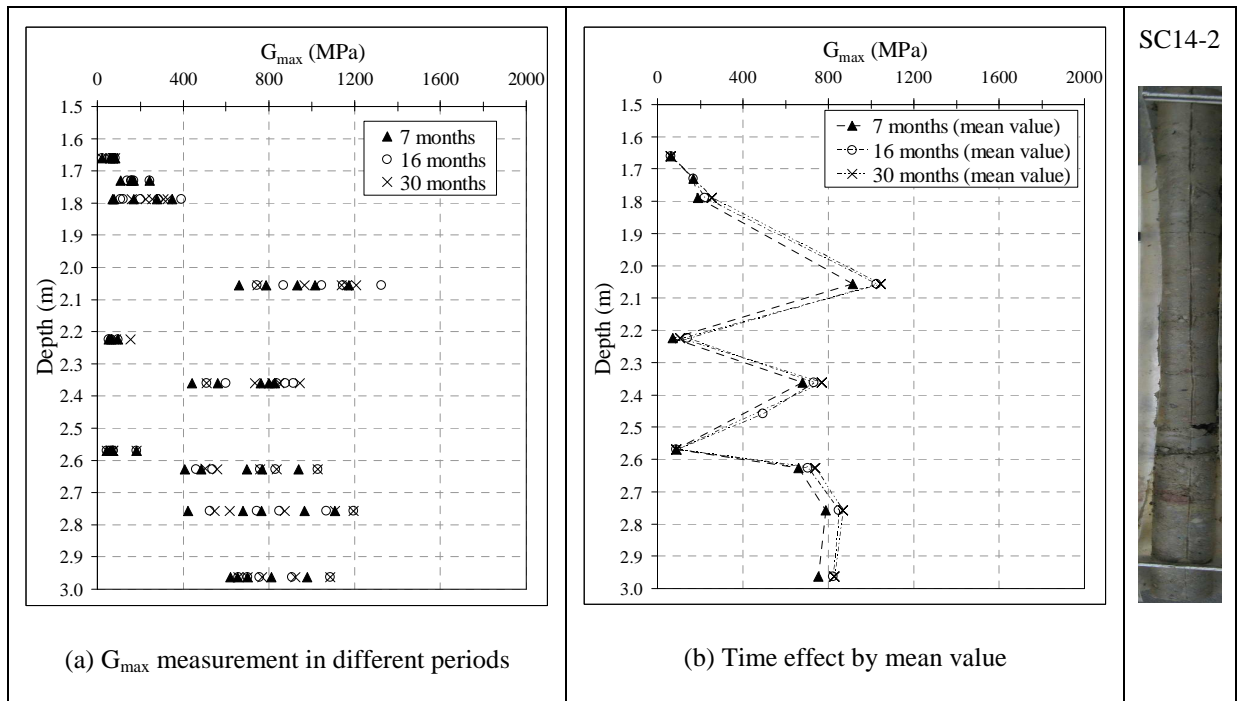


Figure 5-20 Curing time effect on the 4% lime treated clay of SC14-2 (*in-situ* 21)

### 5.3.3. Climate effect

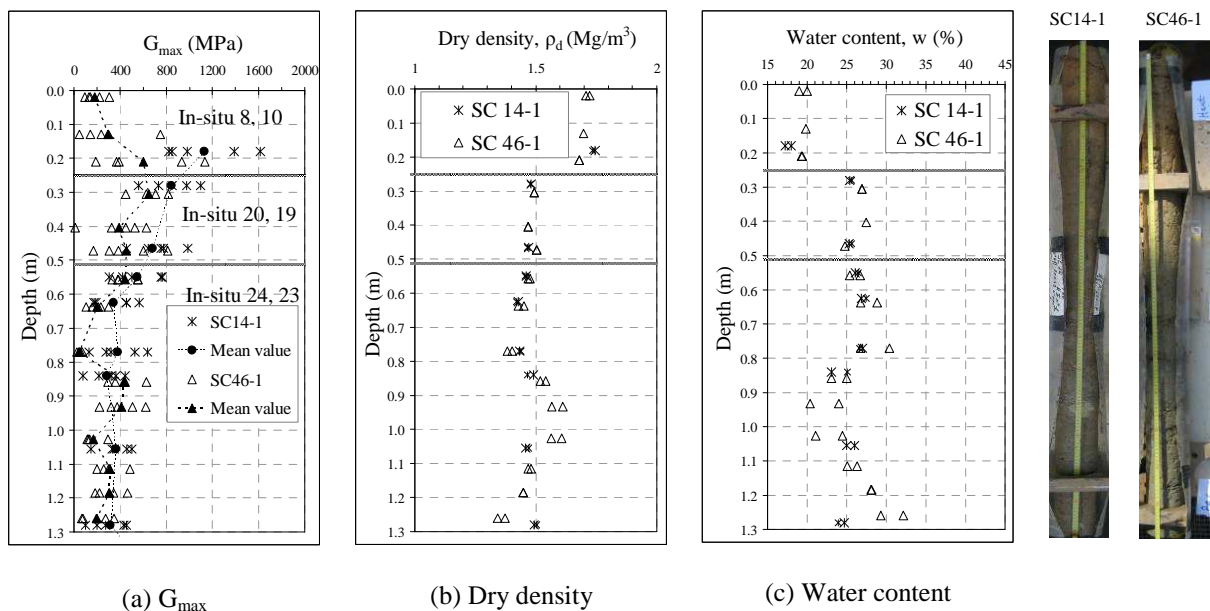
#### 5.3.3.1. The near surface layers of clay side (SC14-1, SC46-1)

Figure 5-21 presents the stiffness, dry density and water content of the two batches of core samples SC14-1 and SC46-1. The observations of the two samples are also given beside. To minimize the effects of curing, all tests were performed in October of 2012. Thereby, the

two batches of cores count 19-month difference of curing in place. The comparison of the results enables the 19-month effect of climate to be investigated.

For the  $G_{max}$ -depth curve (Figure 5-21a), firstly, the  $G_{max}$  values of each specimen are scattered in a large variation range due to the high heterogeneity. As mentioned before, we can use the mean values to minimize the effect of heterogeneity. For the specimens at 0 ~ 0.840 m, we observe that the mean values of the first batch specimen are greater than those of the second batch; the difference decreases with depth. For the specimens deeper than 0.840 m, the two batches share similar values.

For the dry density-depth curve (Figure 5-21b), similar values are observed for the specimens of the two batches. This indicates that the effect of climate does not result in noticeable volume change for the treated soils.



**Figure 5-21 Climate effect (19 months) on the 1% lime plus 5% cement treated silt (*in-situ* 8 and *in-situ* 10), 2% lime plus 3% cement treated clay (*in-situ* 20 and *in-situ* 19) and 5% lime treated clay (SC14-1 and SC46-1)**

For the water content-depth curves (Figure 5-21c), the water content of second batch soil (SC46-1) is in general higher than that of the first batch (SC14-1), especially for the near surface layers at 0 ~ 0.80 m. Then, at 0.80 ~ 1.10 m, the values of the two batches are very close. Thereafter, at 1.10 ~ 1.30 m, the water content of the second batch is higher again than that of the first batch; it increases significantly with depth. If the first wetting at 0 ~ 0.80 m is due to rainfalls before boring (SC46-1), another wetting at 1.10 ~ 1.30 m is probably induced

by the long term re-humidification between the compaction layers. This long term re-humidification may be induced by the different suctions between the layers.

The observation shows that the second batch soils present more fissures and foliated traces than the first batch soils, evidencing also the climate effect.

Comparison of the results between SC14-1 and SC46-1 shows that the climate effect changes not only the stiffness but also the water content of the clay. The effect plays a significant role within a depth of 0.80 m for the treated clay. This is deeper than for the cement treated silt as mentioned before (about 0.5 m).

### 5.3.3.2. Central layers of the embankment (SC14-2 and SC46-2)

Figure 5-22 shows the comparison of the stiffness, dry density and water content between the two batches of core samples SC14-2 and SC46-2. Similar values over depth are observed. This suggests that the climate effect plays a negligible role in the centre of embankment. This evidences again that the effect of climate on the treated clay is limited to the near surface layers (0.80 m depth).

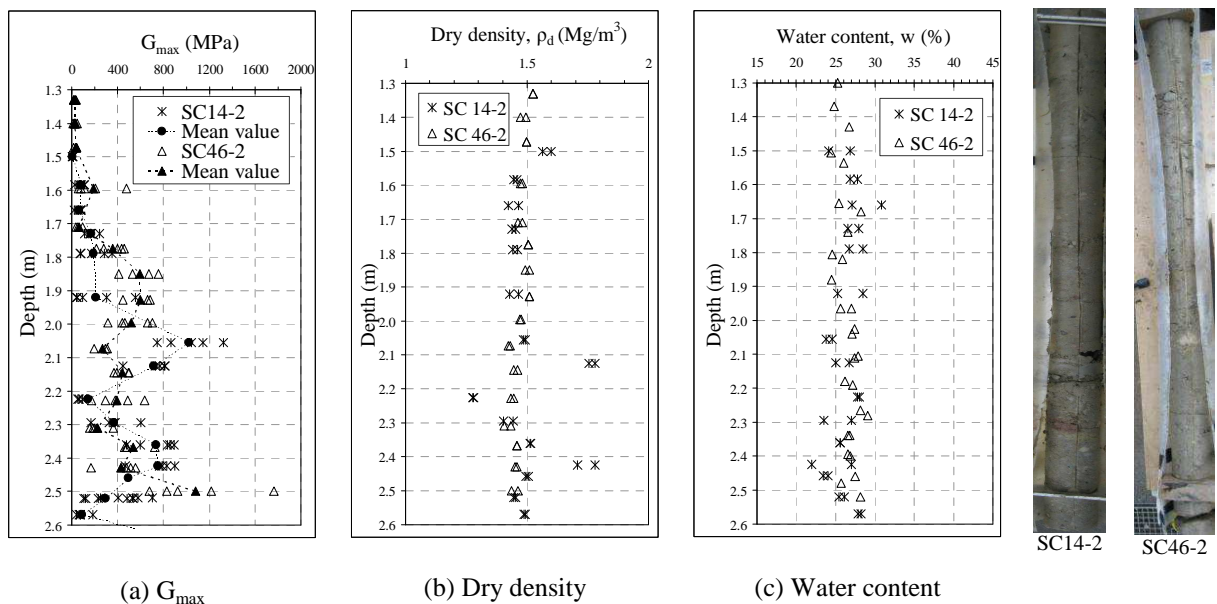


Figure 5-22 Climate effect (19 months) on the 4% lime treated clay (*in-situ* 21/SC14-2, *in-situ* 22/SC46-2)

## 5.4. Cores dominantly treated by mixture

### 5.4.1.1. SC20-1

The first batch core sample SC20-1 involves the base (0 m ~ 0.25 m, layer No.16), the sub-grade (0.25 m ~ 0.515 m, layer No.15) and the top of earthworks (0.515 m ~ 1.44 m, layer No.14, No.13, No.12) on the clay side. The base is made of silt treated by 1% lime plus 5% cement; both the sub-grade and the top of earthworks are constituted of clay treated by 2% lime plus 3% cement.

Figure 5-23 shows the  $G_{\max}$ , dry density and water content evolution over depth for SC20-1. The designed values of water content/dry density are also shown.

A large variation range of  $G_{\max}$  is identified between different compaction layers, event between the specimens from a same compaction layer or between the five measurements on a same specimen. Moreover, the variations of density and water content over depth are also identified. All these data present a high heterogeneity. For layer No.16 (0 m ~ 0.25 m) and layer No.12 (1.120 ~ 1.440 m), most of  $G_{\max}$  measurements range from 400 MPa to 1200 MPa, with a mean value of 781 MPa and 645 MPa, respectively. For layers No.15, 14 and 13 (0.250 m ~ 1.12 m), most values are lower than 400 MPa, with the mean values as low as 127 MPa, 178 MPa and 157 MPa, respectively.

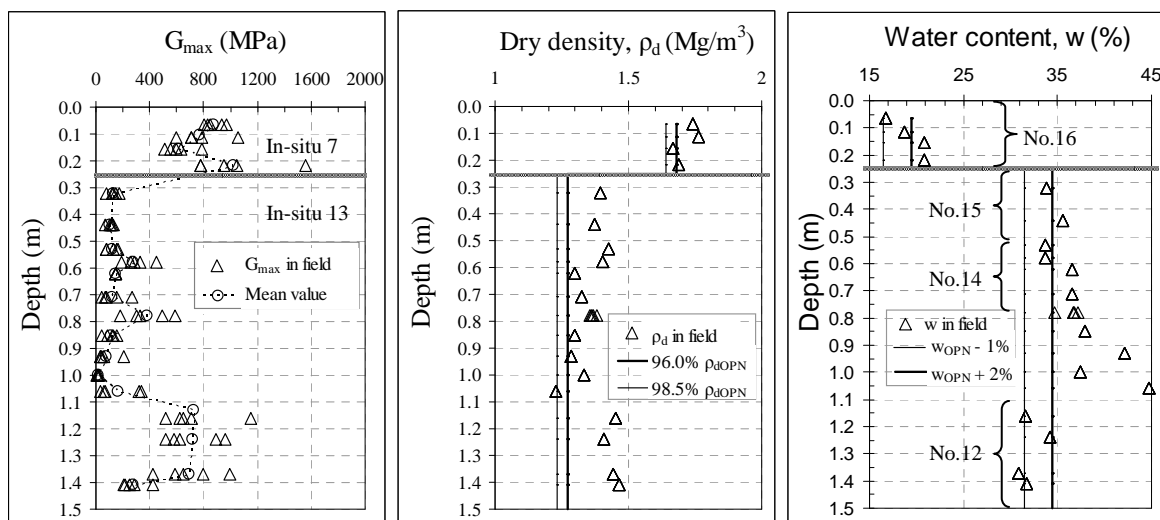
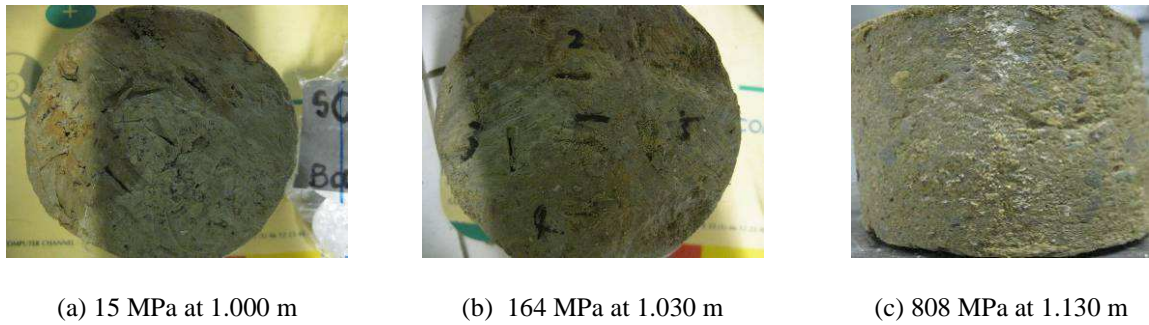


Figure 5-23 Variation of  $G_{\max}$ , dry density and water content over depth for SC20-1 (*In-situ* 7 and *in-situ* 13)

Both the water content and dry density are scattered over depth. For the near surface layers (No.16 ~ No.13), on the whole, the dry density decreases with depth for both the treated silt (0 m ~ 0.25 m, No.16) and treated clay (0.25 ~ 1.12 m, No.15 ~ No.13), whereas the water content increases with depth, especially for layer No.13 (0.780 ~ 1.120 m,  $\Delta w = 14.4\%$ ,  $\Delta \rho_d = 0.13 \text{ Mg/m}^3$ ). For layer No.12, the dry density is about  $1.45 \text{ Mg/m}^3$ ; the water content decreases to 31.5%, much lower than for No.13. The different trends of water content change between No.12 and other layers suggest that the soil may be affected by the climate effect (drying by evaporation or wetting by rainfalls etc.), as for a near surface core sample with a curing period of 1 month in place.

Thereby, the change of  $G_{\max}$  cannot be correlated to the changes of water content/ dry density. The large variation range is probably induced by the effect of heterogeneity of the *in-situ* soils. The aggregates size effect, stones presence and additive distribution may be the main factors for this heterogeneity.

Firstly, the aggregates size can significant affect the stiffness of the *in-situ* soils. Under the field compaction conditions, the percentage of additives is nominal because of the difficulty related to mixing, especially for clayey soils. In this experimental embankment, the maximum initial aggregates size was controlled at 31.5 mm before compaction for the clay, while it was only 5 mm in laboratory. This leads to the higher heterogeneity of additive distribution than in laboratory conditions. Figure 5-24 presents the different aggregates sizes and their corresponding stiffness for the clay specimens. For the large aggregates size soils, as shown in Figure 5-24a and Figure 5-24b for layer No.13, they show a quite low  $G_{\max}$  – 15 MPa and 164 MPa (mean value), respectively. As for the laboratory results, the initial aggregates are observed to be formed together when compacted wet of optimum. It is identified that the aggregates size can reach the same diameter as the core (90 mm). For the small aggregate size soils, as shown in Figure 5-24c for layer No.12, a high stiffness level is obtained (mean value 808 MPa). Thereby, this aggregates size effect is evidenced: the larger the aggregates size, the lower the  $G_{\max}$  value. Moreover, the large aggregates size soils often show high sensibility to moisture change (ex. layer No.13).



**Figure 5-24** Photos of SC20-1 with its aggregates size and different stiffness levels (mean values)

Secondly, the difference in stone presence also plays a decisive role for the variation range of  $G_{max}$ . With the presence of stones, the variation range is enlarged. Layers No.13, No.14 and No.15 have low stiffness levels (mean values) with similar additive distribution, but the variation range of  $G_{max}$  is enlarged when the specimen contains stones (Figure 5-25).

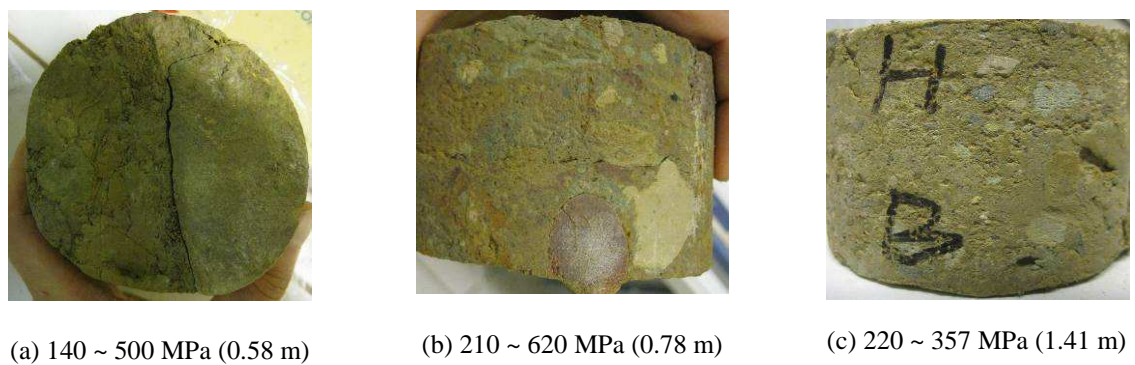


**Figure 5-25** Specimens with similar additive distribution at 0.3 ~ 1.1 m but enlarged variation range of  $G_{max}$  values due to stones presence

Thirdly, the additive distribution can be also an important factor for the variation range of  $G_{max}$ . Large difference of aggregate size gives rise to different additive distribution between layer No.12 and other layers (No.13, 14, 15), therefore to different stiffness values. The former shows high concentration of additives, hence a higher stiffness level. By contrast, the latter shows large aggregates sizes corresponding to a low concentration of additives, hence a low stiffness level. Even in a same layer, the distribution of additive can be quite different (Figure 5-24c and Figure 5-25c of layer No.12). The deep-colour at 1.130 m indicates a higher concentration of additives and a higher  $G_{max}$  level (808 MPa) than the light-colored zone at 1.410 m (265 MPa). The variation range depends also on its additive

distribution. Thereby, the additive distribution effect is in accordance with the aggregates size effect.

Summarizing, the  $G_{\max}$  of the treated *in-situ* soils depends significantly on their heterogeneity levels. The heterogeneity is induced by the effect of aggregates size, additive distribution, stone presence and water content, etc.

Moreover, these factors are also suitable for explaining the large variation of  $G_{\max}$  for the silt. The high stiffness level is induced by high concentrated lime/cement mix. The variation range depends strongly on the stone presence (Figure 5-26).



**Figure 5-26 High concentration of additives and stones for the 1% lime plus 5% cement treated silt (at about 0.220 m)**

#### **5.4.1.2. SC20-2**

The first batch core sample SC20-2 contains five layers, involving the clay treated by 2% lime plus 3% cement. As for SC20-1, SC20-2 also presents large variations of  $G_{\max}$  over depth, and limited variations of dry density and water content, showing a high heterogeneity in terms of  $G_{\max}$  (Figure 5-27). Globally, the water content of this core sample is much lower than the first sample of this core (about 25% for SC20-1).

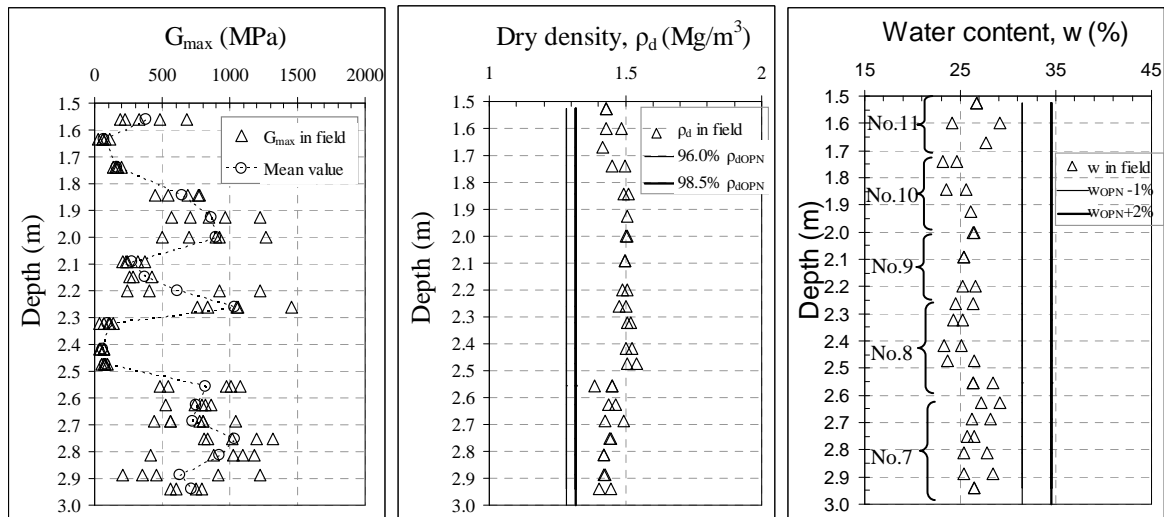


Figure 5-27 Variations of  $G_{max}$ , dry density and water content over depth for SC20-2 (*In-situ* 15)

The effect of aggregates size/additives distribution is still responsible for the variation of  $G_{max}$  (Figure 5-28). Large aggregates are identified for the low stiffness level at 1.60 ~ 1.80 m (ex. at 1.67 m in Figure 5-28a) and at 2.30 ~ 2.50 m (ex. at 2.473 m in Figure 5-28b). Small aggregates are identified for the high level of stiffness, with well clear cementitious products around the aggregates (ex. at 2.00 m in Figure 5-28c). Thereby, the aggregates size effect is confirmed for SC20-2.



(a) Low stiffness at 1.67m (b) Low stiffness at 2.473m (c) High stiffness at 2.000 m

Figure 5-28 Specimens from SC20-2 with different stiffness values and different aggregates sizes

### 5.4.1.3. SC20-3

The core sample SC20-3 is the third sample of the first batch core SC20 (3.000 ~ 4.000 m). As for SC20-2, SC20-3 is also constituted of the clay treated by 2% lime plus 3% cement, involving four compaction layers (No.6~ No.3).



Figure 5-29 presents changes of  $G_{max}$ , density and water content over depth for SC20-3. On the whole, the increase of dry density and decrease of water content with depth correspond to two significantly different stiffness levels. In layer No.6 (3.0 m ~ 3.25 m), the  $G_{max}$  starts from a very low level due to the presence of large aggregates (Figure 5-30a, b); High  $G_{max}$  values are then observed with similar water content at 3.20 m. Thereafter, the  $G_{max}$  remains at the high level albeit the changes of dry density and water content (ex. 1132 MPa at 3.8 m in Figure 5-30c). This difference suggests the aggregates size effect on the heterogeneity of soils.

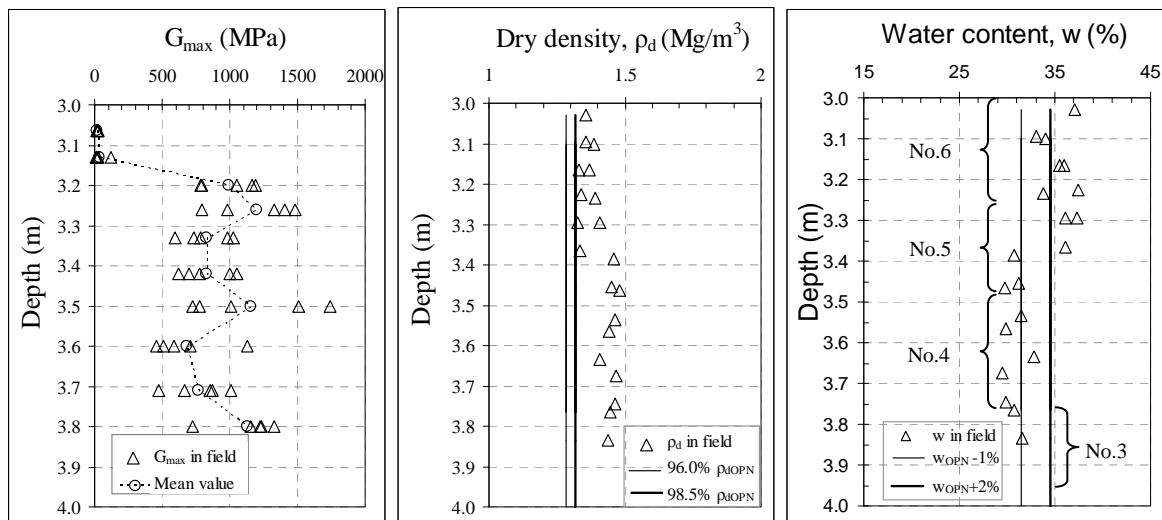


Figure 5-29 Variations of  $G_{max}$ , dry density and water content over depth for SC20-3 (*in-situ* 16)



(a) Low stiffness at 3.065 m (21 MPa)



(b) Low stiffness at 3.13 m (37 MPa)



(c) High stiffness at 3.8 m (1132 MPa)

Figure 5-30 Different stiffness levels (mean values) and the presence of large aggregates size for SC20-3

#### 5.4.1.4. SC20-4

SC20-4 is the fourth sample of core SC20. It is situated at the bottom of the embankment, involving three layers of clay (No.3 ~ No.1) and two layers of silt (No.0 ~ No.-

1). As for SC20-3, the clay is treated by 2% lime plus 3% cement. For the silt, one layer is treated by 2% lime (No.0, 4.80 m ~ 5.17 m) and the other is natural without treatment (No.-1, 5.17 m ~ 5.46 m).

Figure 5-31 presents changes of  $G_{max}$ , density and water content over depth for this sample.

For the clay, the  $G_{max}$  also begins with low stiffness level (mean value 242 MPa) due to its large aggregates size at 4.035 m (ex. Figure 5-32a) and high water content ( $w = 37\%$  in Figure 5-31c) and low dry density ( $1.36 \text{ Mg/m}^3$ ). Then (at 4.1 ~ 4.8 m) it varies at a high stiffness level around 1300 MPa, with a slightly decreasing trend with depth. But the trend cannot be correlated to changes of dry density and water content. The high variation of  $G_{max}$  (800 MPa ~ 2000 MPa) is probably due to the high concentration of additives, small aggregates size and stone presence (ex. Figure 5-32b, c).

For the silt, in layer No.0, the decrease of dry density and the increase of water content surprisingly correspond to an increase of  $G_{max}$ . This is also due to the heterogeneity of the lime distribution. In layer No.-1, for the untreated silt, it is in good accordance with the classic relationship- an increase of water content results in a decrease of  $G_{max}$ .

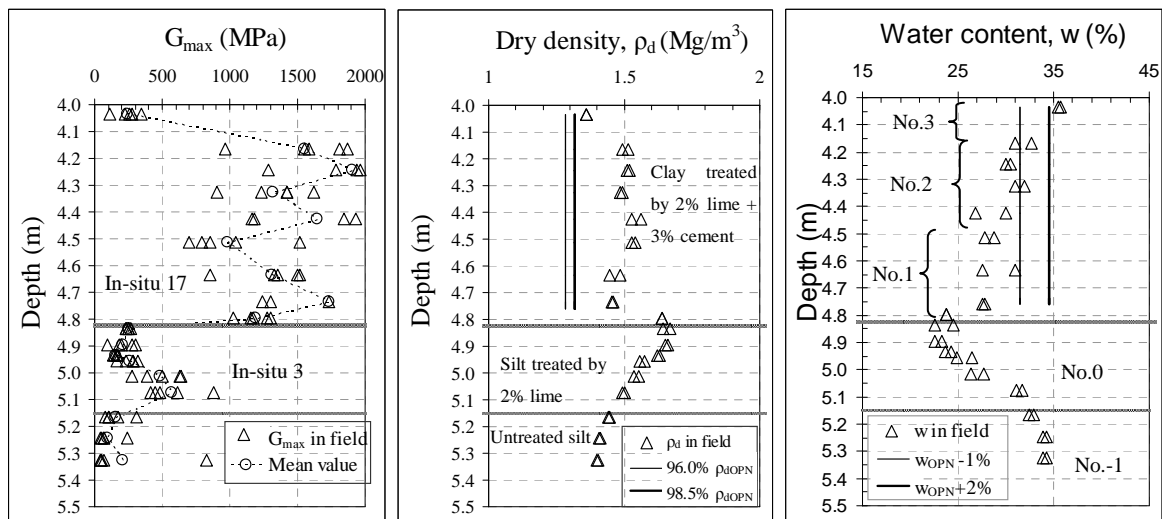
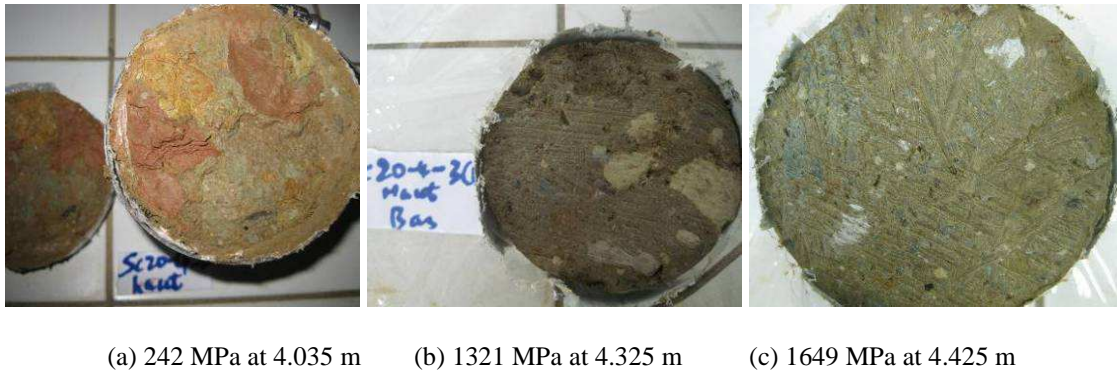


Figure 5-31 Changes of  $G_{max}$ , dry density and water content over depth for SC20-4 (*in-situ* 17 and *in-situ* 3)



**Figure 5-32 Different stiffness levels (mean values) due to difference in aggregates size, stone presence and concentration of additives for SC20-4**

It is worth noting that opposite trends of water content change are identified between the silt and the clay. This is attributed to the combined effects of chemical reactions and water re-distribution due to matric suction effect.

The second batch core samples SC47-1 and SC47-2 are located near SC20. They were both bored in December of 2011, 20 months after the compaction in field. The first measurements on the specimens were performed in September and April of 2012. These results are presented in this section.

#### 5.4.1.5. SC47-1

As for SC20-1, SC47-1 also contains six compaction layers (No.16 ~ No.12, 0 m ~ 1.30 m, 2% lime plus 3% cement treated clay). Figure 5-33 presents the  $G_{\max}$ , density and water content versus depth for SC47-1. Similar to the first batch of clay cores, this sample has the  $G_{\max}$  also depending significantly on its heterogeneity. This heterogeneity is mainly induced by the additive distribution, aggregates size, stone presence, micro-fissures, etc. Further examination of the stiffness levels (Figure 5-34b, c, d) shows that the  $G_{\max}$  depends mainly on the aggregates size - the larger the aggregates, the lower the stiffness. The fissures induced by the climate effect may be also an important factor for the degradation of the near surface layer No.16 in terms of stiffness (Figure 5-34a).

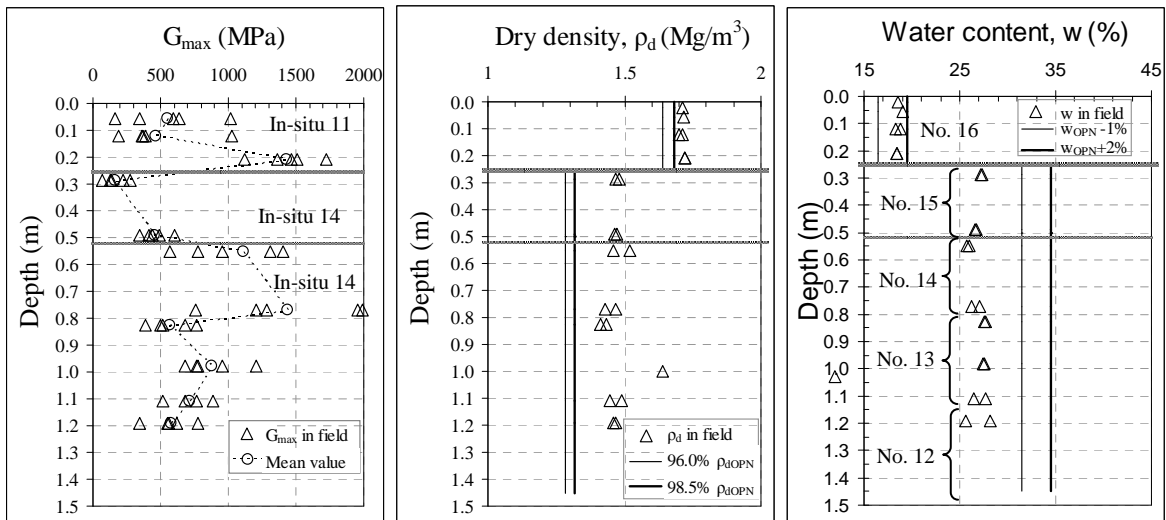


Figure 5-33 Stiffness, density and water content versus depth (SC47-1) (*In-situ* 11 and 14)



(a) Fissures for low stiffness levels due to climate effect (silt)



(b) Small aggregates size for high stiffness level at 0.210 m (silt)



(c) Large aggregates size for low stiffness level at 0.285 m (clay)



(d) Small aggregates size for high stiffness level at 0.550 m (clay)

Figure 5-34 Low and high stiffness levels of the specimens and in the corresponding aggregates sizes for SC47-1

5.4.1.6. SC47-2

SC47-2 is the second sample of core SC47. Figure 5-35 presents the large variation of  $G_{max}$  values over depth and a relatively stable dry density and a low variation of water content (Figure 5-35). Using the mean values of  $G_{max}$  (Figure 5-35a), it is observed that a very low level exists at 1.70 m ~ 2.00 m (57 MPa), a increasing level at 2.00 m ~ 2.20 m (440 MPa) and a high level in other parts (825 MPa). The high heterogeneity observed is mainly due to the aggregates size effect - the larger the aggregates, the lower the stiffness (Figure 5-36).

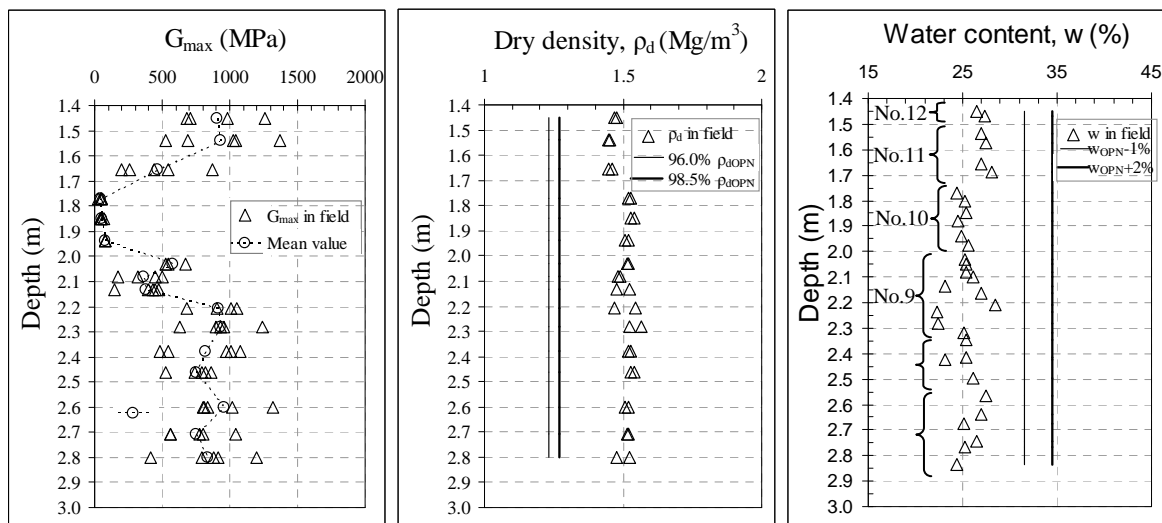


Figure 5-35 Stiffness, density and water content versus depth (SC47-2)



(a) Large aggregates size for low stiffness level at 1.85 m



(b) Small aggregates size for high stiffness level at 2.82 m

Figure 5-36 Low and high stiffness levels and the corresponding aggregates sizes for SC47-2

### 5.4.2. Time effect

Figure 5-37 presents changes of  $G_{\max}$  over depth by the three measurements on core sample SC20-1 during the periods of 7-month, 12.5-month and 30-month curing. As mentioned before, the large variations observed are related to the high heterogeneity of soils. As shown in Figure 5-37a, for the five measurements on each specimen, the  $G_{\max}$  values for the three curing periods are not well ordered showing a large variation range due to the high heterogeneity of soil. Following the same analysis method used before based on the mean values (Figure 5-37b), the evolution of  $G_{\max}$  with curing time for the mixture treated silt (layer No.16, by 1% lime plus 5% cement, *in-situ* 7) and clay (layers No. 15 ~ 12, by 2% lime plus 3% cement, *in-situ* 13) can be evidenced. In fact, as identified before for other treatments, the time effect is strongly influenced by the heterogeneity of soils, especially in terms of additive distribution/aggregates size. The observation of SC20-1 shows that the stiffness gain in case of high additive concentration as in layer No.12 (deep-colour) is much higher than that with low additive concentration as in layers No. 15 ~ 13 (light-colour). In addition, the stiffness gain after the second measurement (12.5 ~ 30 months) is lower than after the first one (7 ~ 12.5 months), especially for the layers with high concentrations of additives (ex. layer No.12). This suggests that the curing effect due to pozzolanic reactions is diminishing after 12.5-month curing.

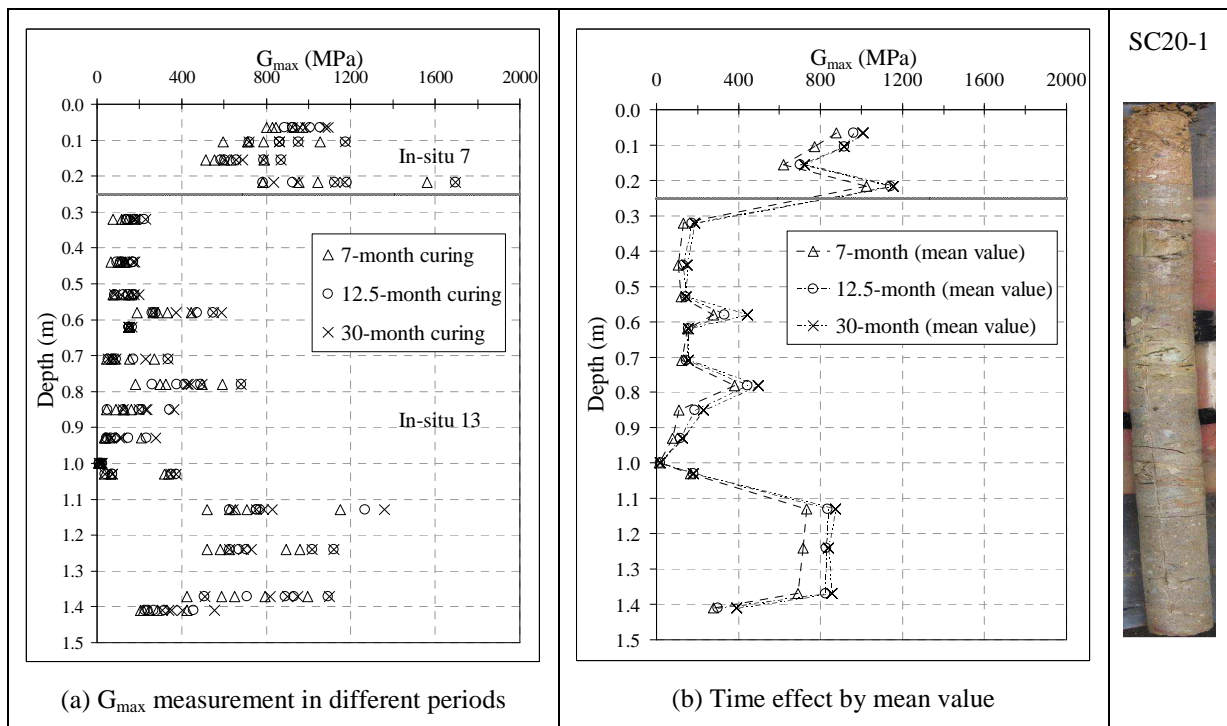


Figure 5-37 Curing time effect on the 1% lime plus 5% cement silt (*in-situ* 7) and 2% lime plus 3% cement treated clay (*in-situ* 13) (SC20-1)

For the clay treated by 2% lime plus 3% cement of core sample SC20-2 (*in-situ* 15), this time effect is also identified (Figure 5-38). In case of lime treated silt (*in-situ* 3), as shown in Figure 5-39, similar observations can be made in terms of time effect.

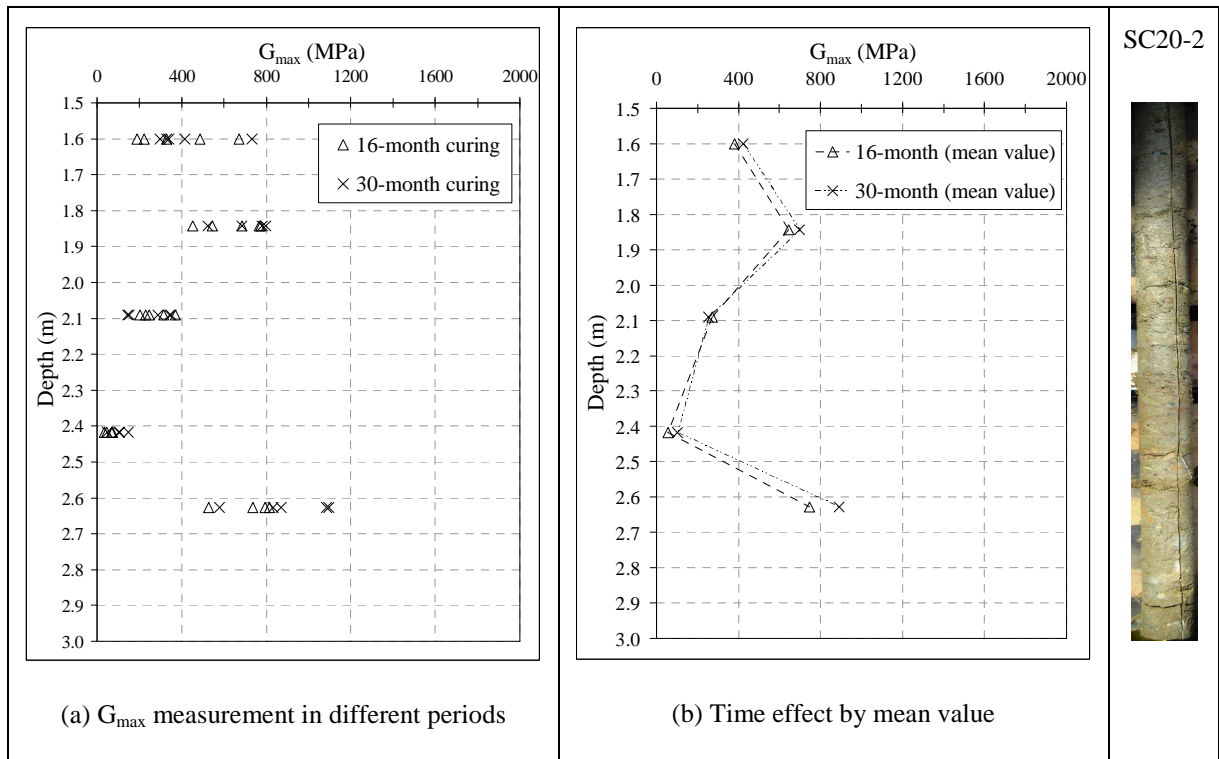


Figure 5-38 Curing time effect on the 2% lime plus 3% cement treated clay of SC20-2 (*in-situ* 15)

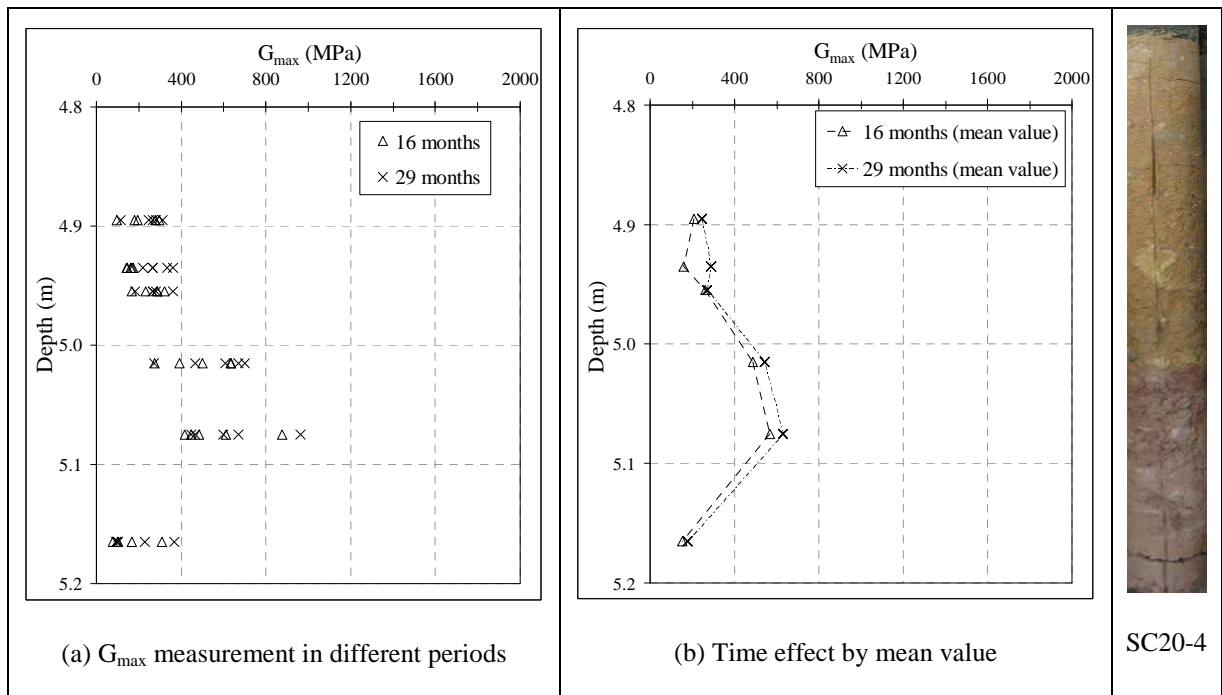


Figure 5-39 Curing time effect on the 2% lime treated silt of SC20-4 (*in-situ* 3)

### 5.4.3. Climate effect

In order to analyze the climate effect, we compare the  $G_{\max}$ , dry density and water content of the specimens from the cores of two batches during the same curing period (the  $G_{\max}$  measurements conducted in September 2012 on SC20 and SC47).

#### 5.4.3.1. Comparison between SC20–1 and SC47–1

Figure 5-40 presents changes of  $G_{\max}$ , dry density and water content over depth for the 1% lime plus 5% cement treated silt (*in-situ* 7 for SC20-1 and *in-situ* 11 for SC47-1) and 2% lime plus 3% cement treated clay (*in-situ* 13 for SC20-1 and *in-situ* 14 for SC47-1), respectively. The different period of curing time in place is 19 months between the two batches, i.e. a period of 19 months under the climate effect.

On the whole, for the near surface layers, as shown in Figure 5-40, despite the large variations of  $G_{\max}$  values, the comparison of the results of the second batch with those of the first batch show: 1) a significant decrease of  $G_{\max}$  under similar density and water content for the silt; 2) a great rise of mean values of  $G_{\max}$  with decrease of water content for the clay; 3) similar  $G_{\max}$ , dry density and water content values at 1.1 m to 1.3 m; and 4) a quite limited water content variation. These differences can be attributed to the effect of climate.

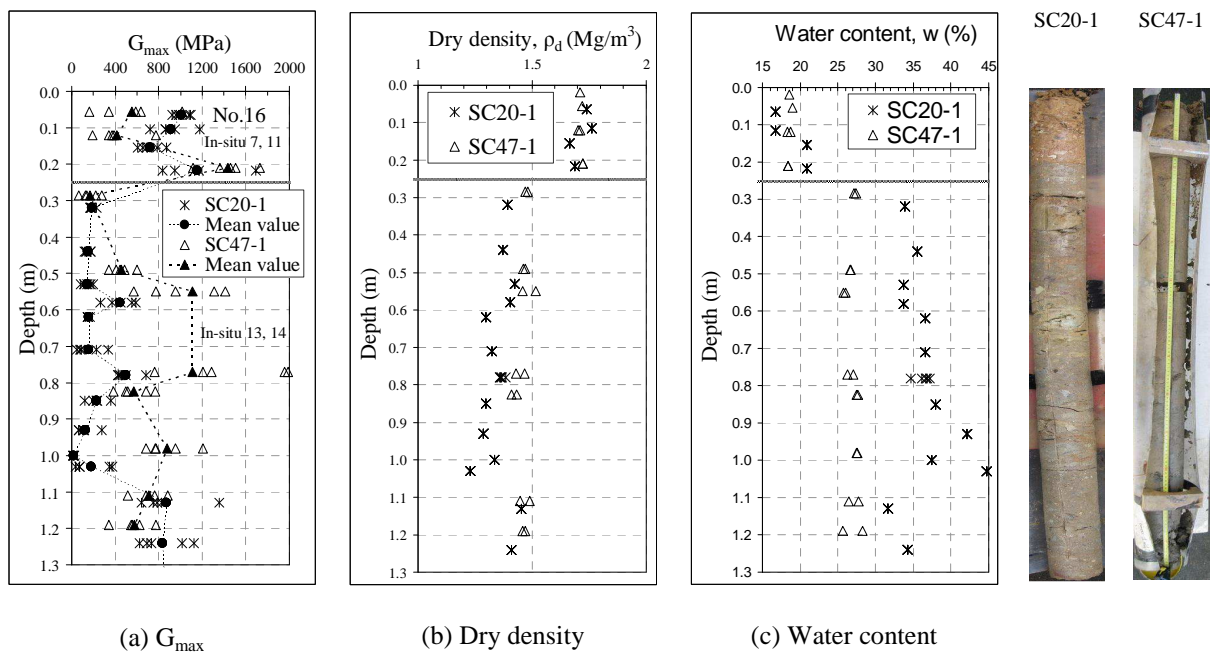


**Figure 5-40 Climate effect (19 months) on the 1% lime plus 5% cement treated silt (*in-situ* 7 and *in-situ* 11) and 2% lime plus 3% cement treated clay (*in-situ* 13 and *in-situ* 14) (SC20-1 and SC47-1)**



Firstly, for the silt, the two batches have similar dry density and water content values over depth, whereas the stiffness of the first batch shows much higher mean value ( $G_{\max} = 961$  MPa against 481 MPa) at 0 ~ 0.200 m. The values become close to each other at 0.220 m. The degradation of stiffness could be induced by the climatic wetting/drying cycles, as mentioned in chapter 2. Moreover, many fissures are observed on the near surface layer soils, justifying the climate effect.

Secondly, for the clay, the first batch soil (SC20-1) mostly presents higher  $G_{\max}$  than the second one at 0.25 ~ 1.100 m (an exception at 0.30 m). Similar mean values are observed at 1.100 ~ 1.300 m. This can be explained by the higher dry density and lower water content of SC47-1 as compared to SC20-1. The increase of dry density is related to the volume change of soil, whereas the water content change may be due to the drying of SC47-1 or wetting of SC20-1. It is worth noting that both the values of dry density and water content get closer between the two batches at 1.100 ~ 1.300 m, indicating the diminishing climate effect.

Thirdly, the significant difference of water content between the two batches (36% against 27%) suggests that the effect of climate is strongly influenced by the aggregates size effect - the larger the aggregates (low  $G_{\max}$ ), the larger the water content change (ex. near 1.00 m). In fact, it is also evidenced by the laboratory results that wetting untreated soils is easier than wetting treated soils. For SC20-1, the  $G_{\max}$  values of several specimens are close to those of the untreated clay compacted in laboratory conditions (<100 MPa); their large aggregates sizes can explain this phenomenon.

#### **5.4.3.2. Comparison between SC20–2 and SC47– 2**

For the central part of the embankment (deeper layers), as shown in Figure 5-41, the stiffness as well as their dry density and water content are comparable for the two batches, indicating that the climate effect did not affect this level.

Comparison between the near surface layers and the deeper layers shows that the climate effect plays a significant role for the near surface zone with a depth until 1.1 m. The effect of climate by cyclic wetting/drying can significantly decrease the  $G_{\max}$  for layer No.16 (silt). It can also dry the soil and increase its sensibility to moisture changes for the following layers. Below 1.1 m, the climate effect is no longer noticeable.

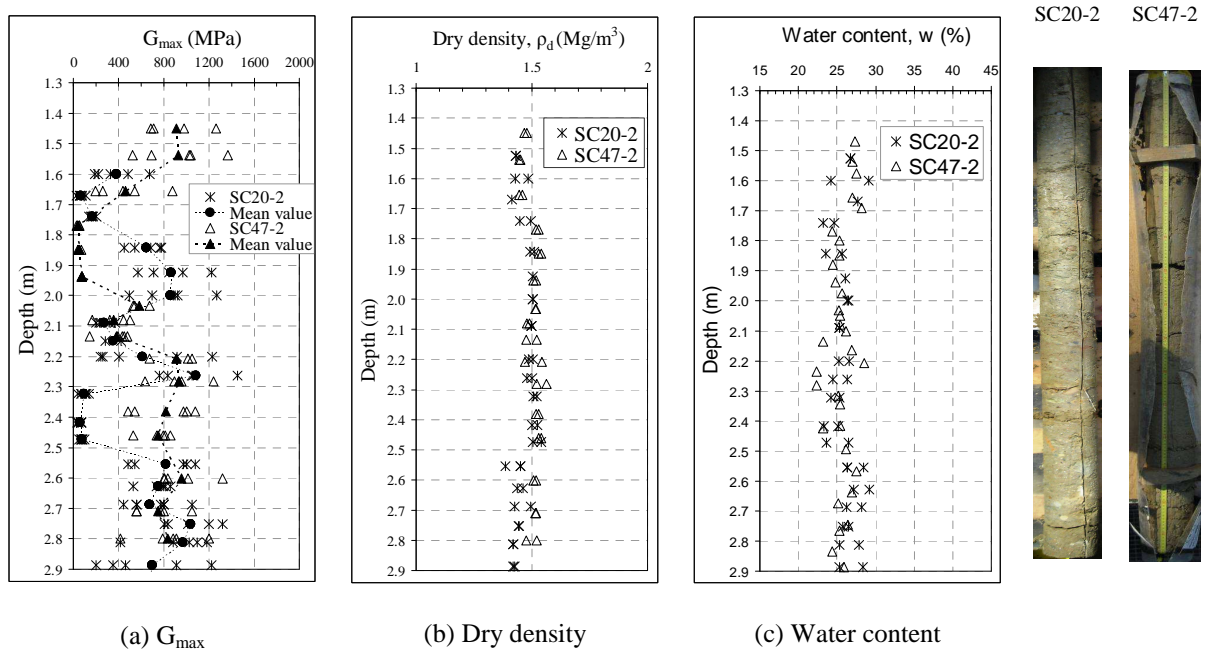


Figure 5-41 Climate effect on the 2% lime plus 3% cement treated clay (*in-situ* 13 and *in-situ* 14) (SC20-2 and SC47-2)

## 5.5. Discussion

### 5.5.1. Heterogeneity of *in-situ* soils

The large variation of  $G_{max}$ ,  $\rho_d$ , and  $w$  over depth are observed for these core samples. Thanks to five measurements on each specimen, the high heterogeneity of *in-situ* soils is identified. According to the analysis of the results, several factors can influence the stiffness of *in-situ* soils, such as the additive distribution/aggregates size, the stones presence, the formation of fissures, etc.

#### 5.5.1.1. Additive distribution effect

Figure 5-42 explains how the additive distribution affects the stiffness of soils. The higher the concentration of additives the higher the stiffness. By contrast, the lower the concentration of additives, the larger the aggregates and the higher the sensibility to water content changes. Figure 5-42c depicts the cementitious distribution, justifying this additive/aggregates size effect (Deneele et al. 2010) - the cementitious products are located just on the surface of the aggregates.

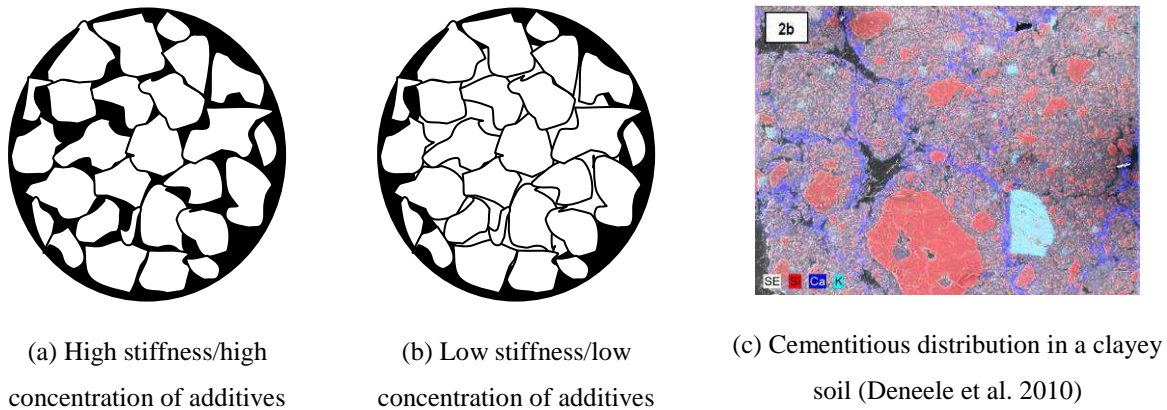


**Figure 5-42 Different configurations with different distributions of additives**

As mentioned before, the distribution of additives can be very different, and some specimens show almost similar  $G_{max}$  values to the untreated ones (layer No.14 of SC31-1; layer No.16, No.15, No.14 of SC20-1; layer No.11 of SC14-2, etc.). Visual observation confirms that these specimens are poorly treated - almost no cementitious products are identified. Other specimens show high values of stiffness (layer No.13 of SC31-1, layer No.12 of SC20-1, layer No.7 of SC20-2 and layer No.2 and No.3 of SC20-4, etc), evidencing a good treatment. This is also easily confirmed by the visual observation - concentrated cementitious products are observed in these specimens.

### 5.5.1.2. Aggregates size effect

Figure 5-43 depicts how the aggregates size impacts on the stiffness of the *in-situ* soils. As shown in Figure 5-43a, in extreme conditions, an *in-situ* core specimen may have an aggregate size as large as the core diameter ( $\Phi = 90$  mm or 100 mm). The  $G_{max}$  is found to be the same as that of untreated specimen in this case. On the other hand, when the distribution of additives is relatively homogeneous, as shown in Figure 5-43b, the stiffness of a specimen depends mainly on the number of large aggregates. The more the large aggregates, the lower the stiffness.

Number of studies indicates that the additives are located on the surface of aggregates (Locat et al, 1990; Ingles and Metcalf, 1973; Choquette, 1988; Le Runigo, 2008). Different aggregates sizes in a soil lead to inhomogeneous treatment. At given nominal dosage, a large aggregates size soil has relatively less cementitious products and chains. By contrast, a smaller aggregates size soil contains more chains or cementitious products, hence a higher

$G_{max}$ . The aggregates size effect is similar to the effect of additive distribution on the stiffness. This is consistent with the aggregates size effect identified in the laboratory conditions (see chapter 3).

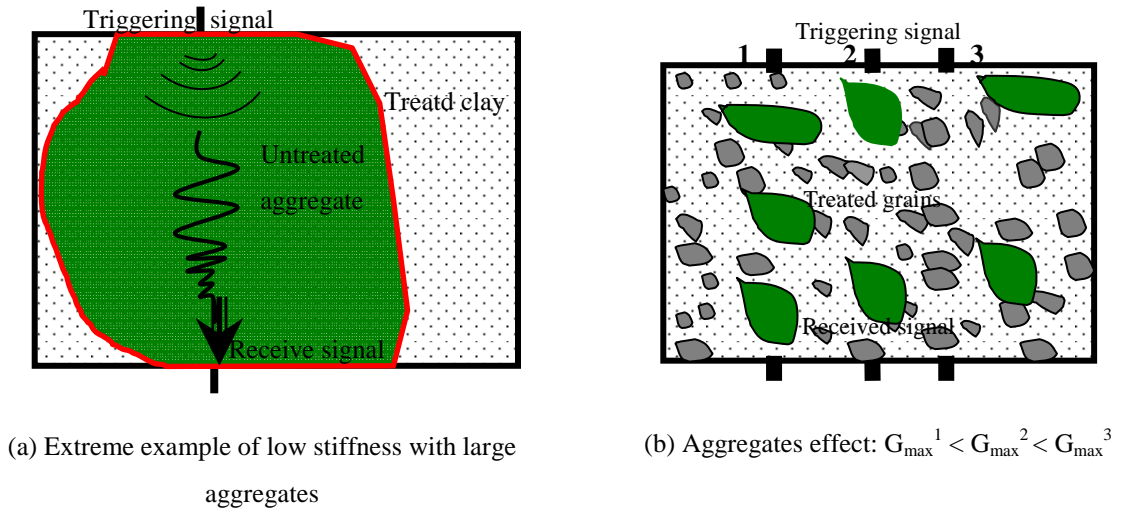


Figure 5-43 Aggregates size effect on the soil stiffness

### 5.5.1.3. Effect of stone presence

Figure 5-44 shows the effect of stone presence on the stiffness of soils. Obviously, a single stone stiffness is much higher than that of soil. At the same additive distribution, the more the stones the higher the  $G_{max}$  and the larger the range of  $G_{max}$ . Some specimens present large variation of  $G_{max}$  over depth just because of the presence of stones. In the present study, stones are observed more frequently in the silt than in the clay.

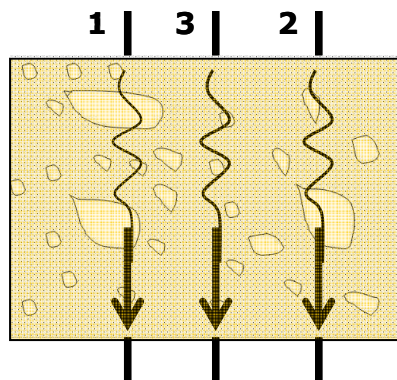


Figure 5-44 Impact of the presence of stones on the soil stiffness:  $G_{max}^1 > G_{max}^2 > G_{max}^3$

Sahaphol and Miura (2005) reported that in laboratory conditions the fines correspond to the soft part and the coarse grains correspond to the stiff part for the contribution to  $G_{max}$ .

Likewise, in field conditions, stones can be the stiff part as compared to the untreated or treated soil aggregates. With similar distribution of additives, the  $G_{\max}$  value depends mainly on the presence of stones. In fact, the increase of soil aggregates stiffness due to treatment also plays a similar role as the effect of stone presence.

#### 5.5.1.4. Water content effect

After compaction, water content changes over depth mainly because of: 1) the heterogeneity of treatment as the complex reactions consume water; 2) the exposure to the exterior conditions, such as rainfalls, evaporation, etc; 3) the water transfer due to suction difference; 4) the heterogeneity factors such as aggregates size, additive distribution, stone presence, etc.

Firstly, the water content with depth depends strongly on the initial molding water content. Taking the first batch soil SC20-1 for example, the initial water content is about 35%, close to that of the wet side specimens in the laboratory. This water content is much higher than those of other clay core samples (SC46, SC14, SC47, SC20-2, SC20-3, SC20-4, SC5-1) and can lead to different suctions between them. Wetting due to rainfalls before boring is also possible if weather permits. If wetting is responsible for the lower stiffness level of layers No. 15 ~ No.13, it is however difficult to explain the slight change of water content in layer No.12 and No.16. Moreover, the large difference of  $G_{\max}$  can be only induced by the heterogeneity of soils, as the laboratory results show a quite limited change of both  $G_{\max}$  and water content during wetting/drying cycles. Finally, the specimens with high water content (SC20-3 at 3.0 ~ 3.4 m; SC20-1 at 0.25 ~ 1.10 m; SC20-4 at 4.0 m) are found to have very low stiffness and large aggregates size. As the decrease of water content due to chemical reactions is very limited for large aggregates size soil, it can be concluded that the high water content of SC20-1 is mainly related to its high initial water content.

Secondly, water content change also depends significantly on the complex reactions, especially for the central part of the embankment where the climate effect is evidenced to be negligible. In the central part, two batches show the similar water content / $G_{\max}$  over depth, suggesting that the several-month curing between the measurements of two batches of cores does not results in significant water content change. This indicates that the majority of additives involved in reactions have been consumed after the first measurement of first core, indicating the diminishing effect of treatment after 7 ~16 month curing.

Thirdly, the water content of soils is affected by the weather conditions before boring, especially for the near surface layers with large aggregates (ex. layer No. 15 ~ No.13 of SC20-1). The two batches taken indicate that they underwent climate effect. Note that for the first batch, the clay cores SC20 and SC14 were bored on 28<sup>th</sup> April 2010, one month after the embankment construction; the silt cores SC31 and SC40 were taken on 4<sup>th</sup> May 2010, one week after the clay cores. For the second batch of cores, the clay cores of SC47 and SC46 were bored on 13<sup>th</sup> and 14<sup>th</sup> December of 2011, respectively.

Fourthly, for the first batch core sample, only one month curing in place may be not enough for the water content homogenization, considering the large aggregates size in field conditions. The larger variation of water content for SC20-1 compared to SC47-1 also indicates this point. After the long term moisture redistribution, the large aggregates size soils often show noticeable nature of untreated soils: high capacity to absorb water and high sensitivity to water content change (ex. layer No.15 ~ No.13 of SC20-1). As mentioned before, the water content redistribution is related to the different suction between large aggregates soils and small aggregates soils.

Finally, the water content is influenced by the heterogeneity of soils. Firstly, the water content can be scattered due to stones presence - the more the stones are, the higher the water content data is scattered (ex. the low water content at 0.96 m for SC31-1). Then, for the large aggregates size soils, high water contents and low stiffness are identified for many layers (layer No.15 ~ No.13 of SC20-1, No.16 of SC20-2, No.3 of SC14-2, No.7 of SC14-2, No.15 ~ No.12 of SC5-1, No.13 of SC31-1, No.15 ~ No.12 of SC46-1, etc.). The large aggregates size soils also show higher sensibility of  $G_{max}$  to water content change as compared to the smaller aggregates size soils. Wetting significantly decreases the stiffness in case of large aggregates size soils (ex. layer No.13 of core SC20-1, layer No.12 and layer No.13 of SC5-1, etc); by contrast, for the small aggregates size soils, this water content effect is no longer noticeable. This is in accordance with the laboratory results (chapter 4).

#### **5.5.1.5. Dry density effect**

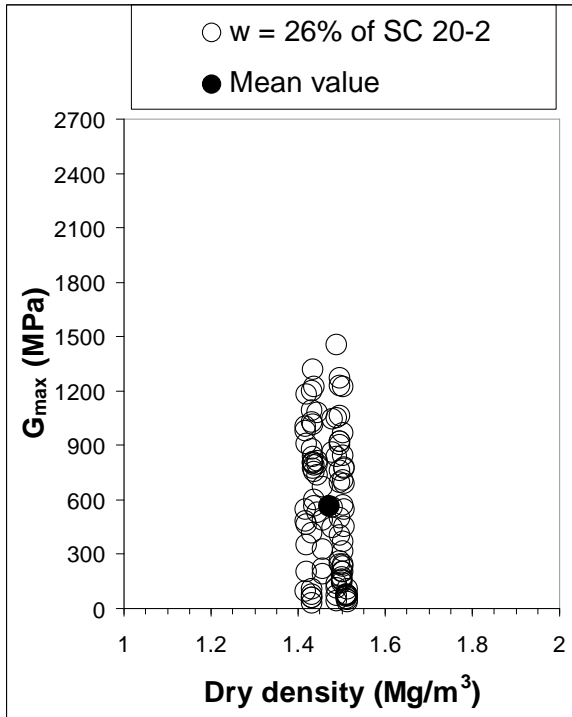
It is well known that the dry density and water content are important factors for the stiffness of soils. Very often, the results present the combined effect of water content and dry density (ex. 1.9 ~ 2.1 m, 2.2 ~ 2.4 m and 2.4 ~ 2.6 m for SC14-2; 0.5 ~ 0.86 m and 0.90 ~ 1.3 m of SC46-1). Moreover, the density effect and the water effect are often masked by the heterogeneity of additive distribution. However, by analysing a large quantity of data, it can

be expected that the main trends of dry density effect and water content effect can be evidenced.

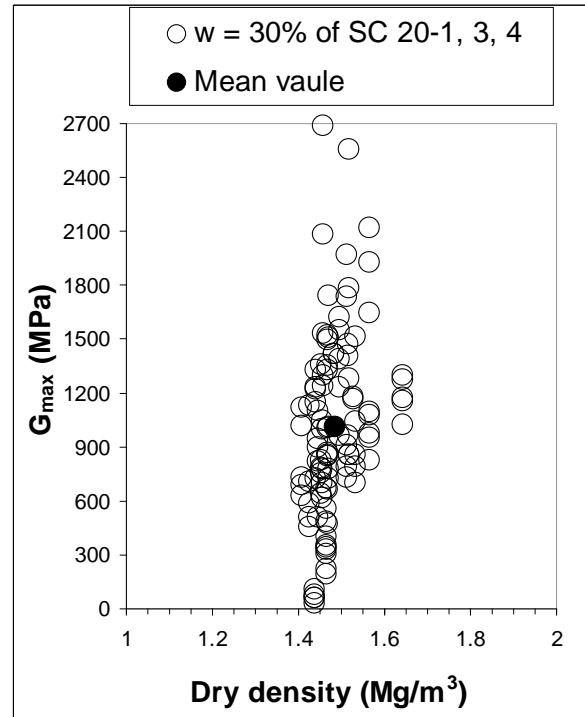
Figure 5-45 presents the  $G_{\max}$  data for the 2% lime plus 3% cement treated clay versus dry density for each water content ( $w = 26\%$ ,  $30\%$  and  $35\%$  in Figure 5-45a, b, c, data from core SC20-1, SC20-2, SC20-3 and SC20-4). In all cases, large variations of  $G_{\max}$  with limited changes of dry density are observed, showing no noticeable dry density effect.

From the mean values in Figure 5-45d, we observe that, 1) the combined effect of dry density and water content is noticeable, as high water content and low density result in low stiffness ( $w = 35\%$ ); 2) for similar higher dry densities, the specimens at the near optimum water content  $w = 30\%$  present higher stiffness than the specimens on either dry side or wet side. The good engineering properties at optimum are also reported by many researchers (Seed and Chan 1960; Lambe and Whitman 1969; Barden and Fice, 1974; Holtz and Kovacs, 1981; Daniel and Benson, 1990; Daita *et al.*, 2005; Russo *et al.*, 2006; Schuettpelz *et al.*, 2009).

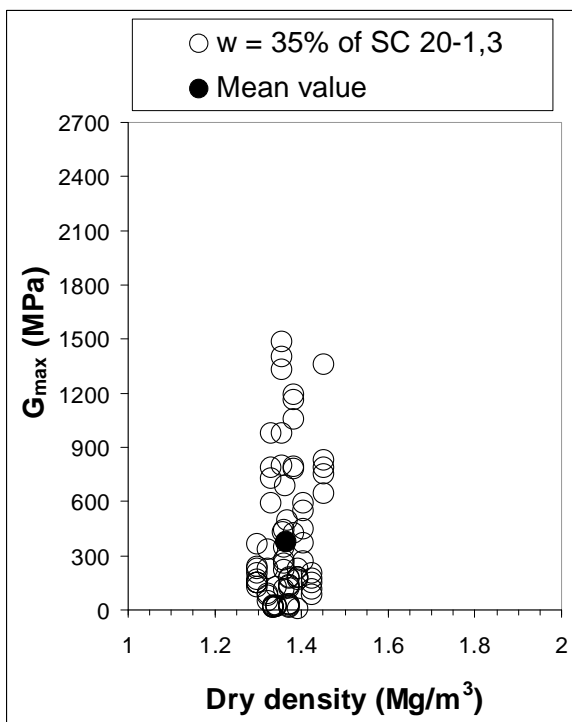
Nevertheless, as mentioned before, due to the high heterogeneity of the *in-situ* soils, the effect of dry density is often masked.



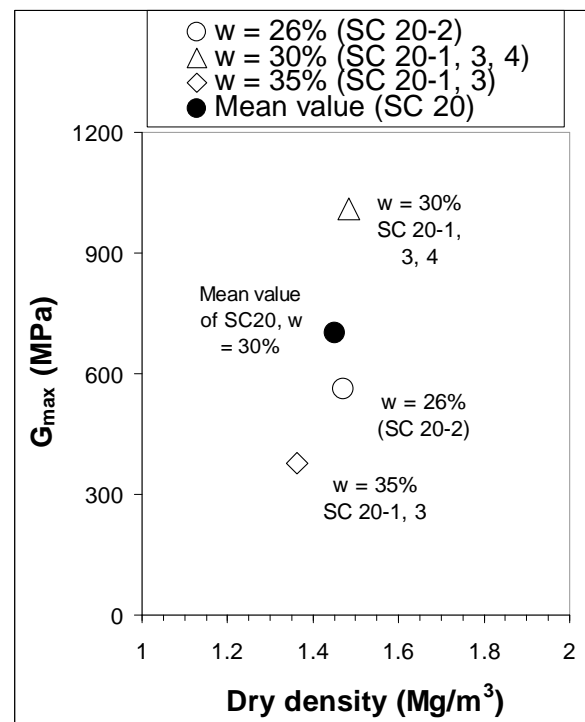
(a) Near  $w = 26\%$  (data from SC20-2)



(b) Near  $w = 30\%$  (data from SC20-1,3, 4)



(c) Near  $w = 35\%$  (data from SC20-1,3)



(d) Mean value (data from SC20)

**Figure 5-45 No clear density/water content effect on the 2% lime plus 3% cement treated clay due to the heterogeneity of soils**



### 5.5.1.6. Compaction process effect

As the soils are constituted of aggregates, their stiffness depends mainly on the stiffness of aggregates and their connection chains. Based on the previous analysis on the heterogeneity of the *in-situ* soils, the aggregates size distribution seems to be fundamental for the definition of heterogeneity. Besides, the heterogeneity level of soils also depends on other factors such as soil type, mixing method, compaction water content, stones presence, etc.

In field conditions, the aggregates size level is designed at  $D_{\max} = 31.5$  mm and 20 mm for the clay and the silt, respectively (Hung, 2010; Froumentin, 2012). The soils were prepared by the following process. They were firstly dried near the embankment site, then pulverized and mixed with the additives, thereafter transported to the experimental embankment site (Figure 5-46 a, b, c). A representative quantity of soils was then tested to meet the designed values (ex. the clay in Figure 5-46c). In Figure 5-46c, we observe that these soil aggregates are coated by additives.



(a) Pulverization process for preparation of clay

(b) Large clay aggregates before mixing

(c) Additives on the surface of aggregates after mixing

**Figure 5-46 Field preparation and storage at a site near the experimental embankment**

Prior to compaction, the pulverization process was proceeded again and water was added to reach the designed water content ( $w = w_{\text{optn}}-1 \sim w_{\text{optn}}+2$  in most cases) (Hung, 2010). This pulverization process may change the size of aggregates, as the soil was compacted at high water content (wet of optimum). Some large soil blocks or new aggregates can be formed after compaction, as identified before. This phenomenon is also confirmed by the laboratory tests, especially for the clay. On the other hand, adding water may result in diffusion of additives into water and then sedimentation at the low side of a compaction layer, leading to a higher concentration of additives at the bottom of each compaction layer, thus a

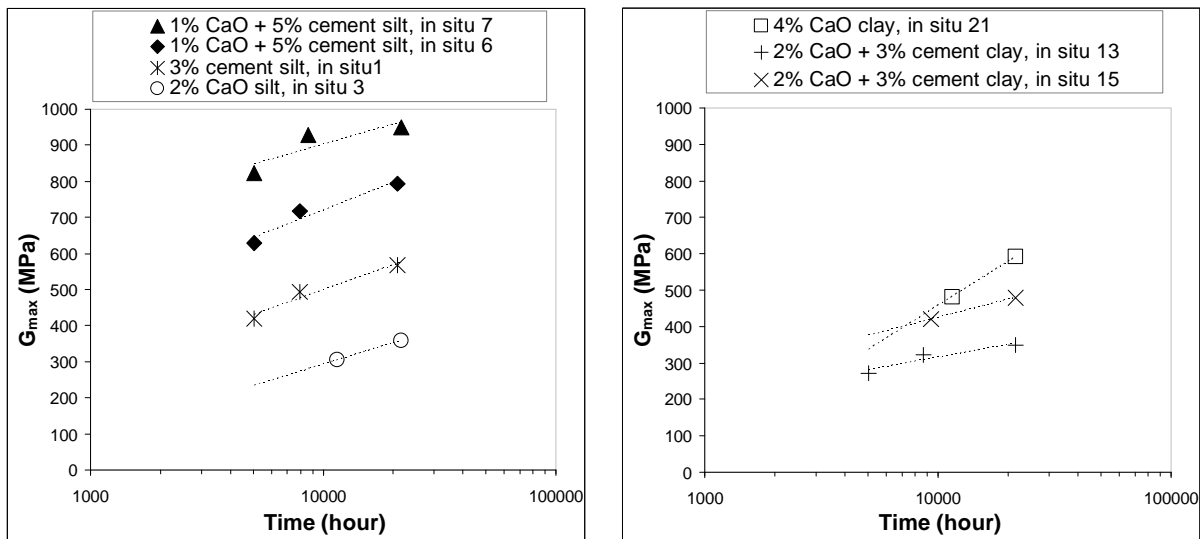
higher  $G_{\max}$ , especially for the clay treated by high dosages of lime (ex. the 5% lime treated clay for SC5-1).

In addition, the dry density of the *in-situ* soil is found to be much higher than the designed value. This is because of the different compaction mode applied in field (vibratory roller compaction) than in the laboratory (normal Proctor test).

### 5.5.2. Time effect

Due to the high heterogeneity of *in-situ* soils, the curing time effect is investigated using the mean value of each measurement for a given curing period.

Figure 5-47 presents the time effect for various treatments of silt and clay. For all treatments, the stiffness increases with curing time, showing clearly the time effect. As discussed before, the ratio of stiffness gain often decreases at the second measurements (11 ~ 16 months), indicating the diminishing effect of chemical reactions. In order to better analyse the stiffness gain ratio for different soils, the function  $G_{\max} = a \ln(t) + b$  is used to fit the  $G_{\max}$ -time curves.



(a) Time effect for treated silts

(b) Time effect for treated clays

**Figure 5-47 Curing time effects of both silts and clays**

The stiffness gain ratio  $a$  is shown in Table 5-1. For the silt, the dominantly cement treated silt (3% cement, 1% lime plus 5% cement) presents slightly higher ratio than the lime treated silt (2% lime). The stiffness level presents a decreasing order with the decrease of

dosage of additives. For the clay, the ratio of 4% lime treatment is higher than that of 2% lime plus 3% cement treatment at the second measurements, indicating the typical long term effect of pozzolanic reactions.

**Table 5-1 Stiffness gain ratio for different treatments and soils (all by mean values)**

Soil type	Silt			Clay	
Treatment	1% lime plus 5% cement	3% cement	2% lime	4% lime	2% lime plus 3% cement
Ratio <i>a</i>	96	100	86	175	61

Nevertheless, the present study evidences that the curing time effect on the treated silt and the treated clay can last as long as 30 months, although it is more obvious in the first 11 ~ 16 months (the second measurement). The pozzolanic reactions contribute to this time effect. As mentioned in chapter 1, the time effect induced by pozzolanic reactions (phase II) is still an open question, especially for the start and the duration of phase II. We also observe that the pozzolanic reactions can last as long as several years in the soil prepared *in-situ* (Little, 1999).

### 5.5.3. Climate effect

Climate change can modify the stiffness, water contents, dry densities of soils. It can also cause soil fissures.

#### 5.5.3.1. Water content-stiffness change

For the near surface layers, climate effect can significantly decrease their  $G_{max}$ , mainly by wetting/drying cycles (Figure 5-8a, Figure 5-21a and Figure 5-40a). This degradation of treated soils caused by cyclic wetting/drying were also identified in several laboratory studies (Rao *et al.*, 2001; Guney *et al.*, 2007; Khattab *et al.*, 2007; Cuisinier and Deneele, 2008a; Pedarla, 2009; Kasangaki and Towhata, 2009; Nowamooz and Masrouri, 2010; Stoltz *et al.*, 2010; Akcanca and Aytakin, 2011; Stoltz *et al.*, 2012). The climate effect also plays a significant role in changes of water content in the near surface layers. For a similar clay treated by 3% lime in the near surface layers of a subgrade, Cuisinier and Deneele (2008b) also reported its high sensitivity to water content changes 3 years after the compaction.

For the first batch of cores, water content has a larger variation over depth when soils contain larger aggregates as mentioned before (SC20-3 at 3.0 ~ 3.4 m; SC20-1 at 0.25 ~ 1.10 m; SC20-4 at 4.0 m), showing a high heterogeneity of treatment or additive distribution. For the second batch of cores, the water content change in the near surface layers may be mainly induced by evaporation or precipitation (Figure 5-8c and Figure 5-40c), whereas for the deep layers (Figure 5-22c and Figure 5-41c) where climate changes are limited, the water content reduction is mainly due to the chemical reactions. Comparison between the two batches shows that the second batch has quite limited water content variations (Figure 5-8c, Figure 5-21c, Figure 5-22c, Figure 5-40c and Figure 5-41c). This shows that the chemical reactions lead to limited water content changes.

Figure 5-48, Figure 5-49 and Figure 5-50 present the mean values of the three water content measurements ( $w$ ) versus compaction layer (No.) for the predominantly 2% lime plus 3% cement treated clay, 4% lime treated clay, 5% lime treated clay:  $w_0$ , measurement in place after compaction,  $w_1$ , first measurement on the first batch (7 ~ 16 months) and  $w_2$ , measurement on the second batch (about two-year curing in place). Both the curves of water content change versus No. ( $\Delta w_1 = w_1 - w_0$ ;  $\Delta w_2 = w_2 - w_0$ ) and the corresponding curves of  $G_{\max}$  versus No. are shown to depict the correlations between them. Note that the data  $w_0$  are taken from a report of TERDOUEST project (Froumentin, 2012).

For the predominantly 2% lime plus 3% cement treated clay (Figure 5-48), firstly we observe that the water content  $w_0$ ,  $w_1$  and  $w_2$  with depth can be globally divided into three zones. Zone I (No.16 ~No.11) shows significant difference between  $w_0$ ,  $w_1$  and  $w_2$ ; it is related to the combined effects of time and climate. Zone II (No.11 ~No.7) presents similar  $w_1$  and  $w_2$ , much lower than  $w_0$ , indicating the pure time effect. Zone III (No.6 ~No.-1) presents similar  $w_1$  and  $w_0$  (in this part, the test of  $w_2$  was not performed). Zone III is influenced by the combined effects of curing and underground water table. In other words, Zone I is a active zone for the climate effect, involving the near surface layers; Zone II is a untouched zone by the climate effect, involving the centre of embankment; zone III is a active zone for the effect of water table.

For  $\Delta w_1$  and  $G_{\max}$ , a good relationship can be observed. In zone I (No.16 ~No.11 in Figure 5-48b), most points of  $\Delta w_1$  are positive; this suggests the wetting behaviour of SC20-1. The  $\Delta w_1$  first increases and then decreases from No.16 to No.12. Surprisingly, the corresponding  $G_{\max}$  (Figure 5-48c) shows opposite trends with  $\Delta w_1$ . Then for both zone II and zone III, the same correlation between  $G_{\max}$  and  $\Delta w_1$  can be observed. For  $\Delta w_2$  and  $G_{\max}$ ,

as for  $G_{max}$  and  $\Delta w_1$ , similar correlation is also obtained. This indicates that the process of wetting or drying governs the changes of soil  $G_{max}$ .

In the same fashion, three zones can be defined for SC14 and SC46 (Figure 5-49). The definition of the three zones is summarised in Table 5-2. This allows the pure treatment effect to be separated from the climate effect.

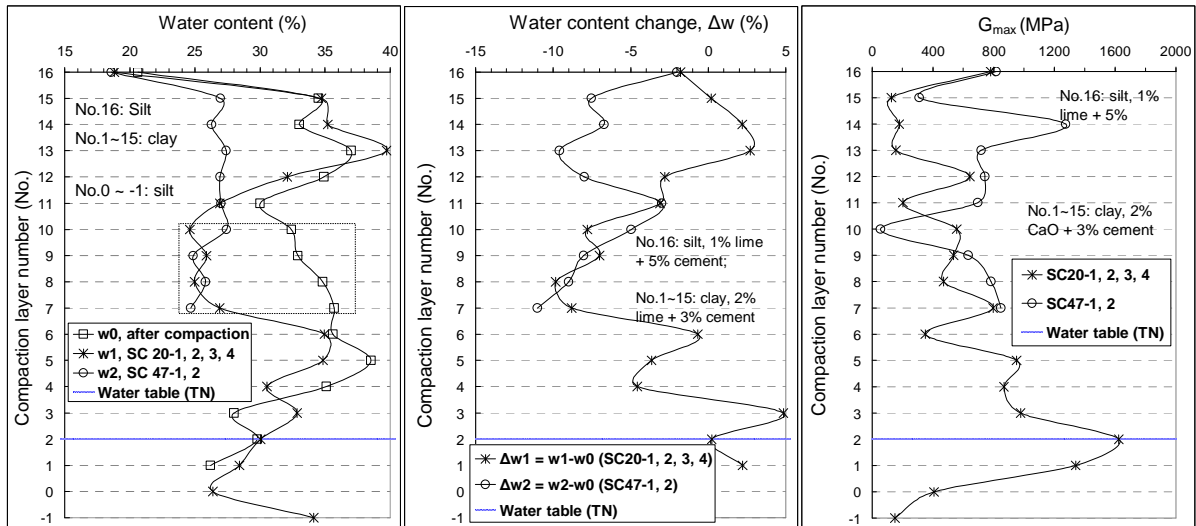


Figure 5-48 Water contents of the treated clay in different periods: measurement just after compaction, measurement on the first batch (SC20) and measurement on the second batch (SC47)

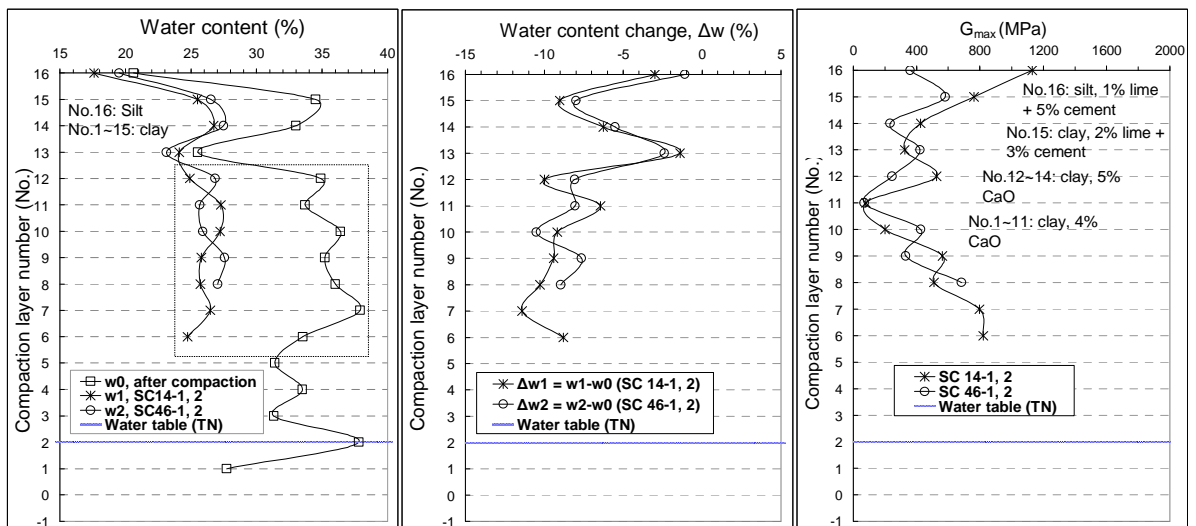


Figure 5-49 Water contents of treated clay in different periods: just after compaction, on the first batch (SC14) and on the second batch (SC46)

Note that for SC5-1 (5% lime treated clay in Figure 5-50), the zones cannot be defined due to the limited data. However, it can be observed that the water content change

( $\Delta w_1$ ) in No. 15 is higher than those in other layers No. 14 ~ 12, indicating a higher drying effect in the near surface layers.

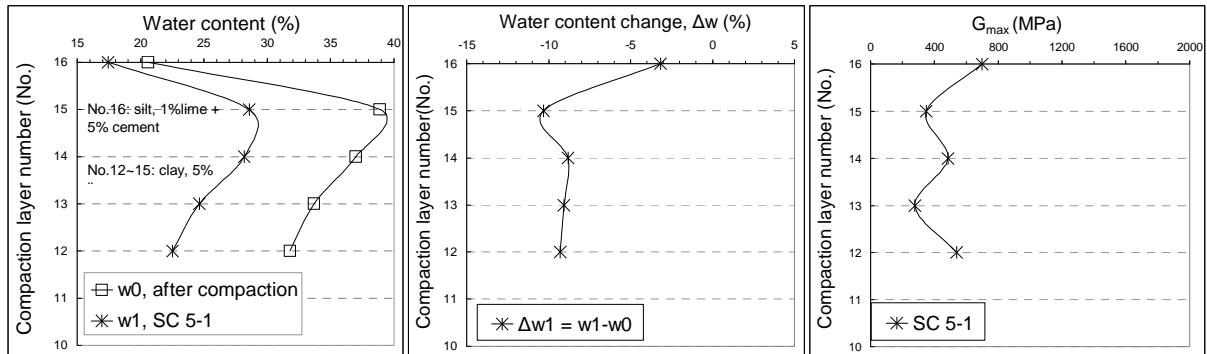


Figure 5-50 Water contents of the treated silt and clay in different periods: just after compaction and on the first batch of core SC5-1

Table 5-2 Active zone for climate effect (Zone I), untouched zone by the climate effect (Zone II) and active zone for the water table change (Zone III) in the clay side of the embankment

Core	Treatment (near surface layers)	Zone I	Zone II	Zone III
SC20	2% lime plus 3% cement	1.45 m (No.16 ~ No.12)	1.50 m (No.11 ~ No.7)	1.20 m (clay, No.6 ~ No.2)/1.0 m (silt, No.2 ~ No.-1)
SC47	2% lime plus 3% cement	2.05 m (No.16 ~ No.10)	1.50 m (No.9 ~ No.7)	- (short of data)
SC14/46	5% lime	0.85 m (No.16 ~ No.14)	1.50 m (No.13 ~ No.7)	- (short of data)

From Table 5-2, we observe that, 1) the impact depths by the climate effect range from 0.85 m to 2.05 m for the two batches; 2) the depth increases with curing time as the a higher depth is observed for the second batch core SC47 (2.05m) than for the first batch core SC20 (1.45 m); 3) the 2% lime plus 3% cement treated clay cores (SC20/47) show higher depth than the 4% lime treated clay cores (SC14/46). This indicates that the mix treated clay (2% lime plus 3% cement) is more sensible to water content changes than lime treated one, in agreement with the laboratory results presented in chapter 4.

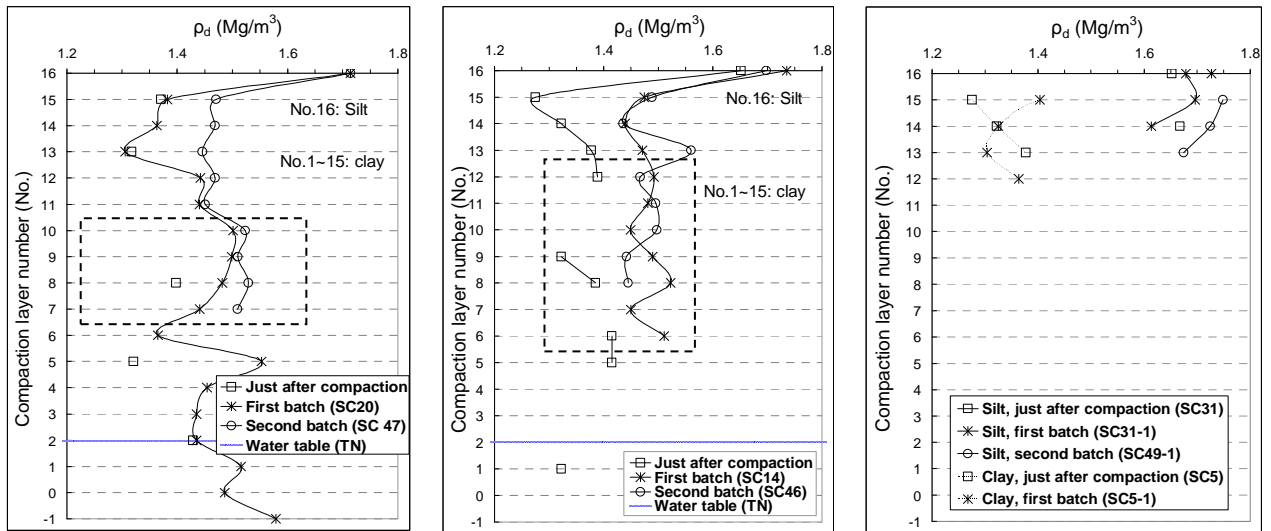
The drying induced by evaporation influences the *in-situ* soils as deep as 0.85 ~ 2.05 m (Table 5-2). However, Ta (2010) indicates that the thickness of water exchange by evaporation for a similar untreated clay (A4) is only about 30 cm in his environmental chamber under laboratory conditions. In addition to the treatment effect, the different homogeneity levels between the laboratory and field conditions can also play an important role. In the work of Ta (2010), the largest soil aggregates size is 2 mm whereas it is 20 mm for the silt and 31.5 mm for the clay in the embankment. Sometimes, even larger aggregates are identified. Normally, the breakage of large aggregates is easier as compared to small aggregates under similar loading. The drying/wetting cycles applied in the laboratory also engender breakage or fissures of soil specimens, especially for the large aggregates size soils (chapter 4). Thereby, in field conditions, the water exchange thickness is larger because of the larger aggregates size.

### 5.5.3.2. Dry density change

Normally, both the chemical reactions due to treatment and the volume change due to climate effect can change the dry density of the *in-situ* soils. Firstly, the dry density increases as water content decreases with curing time due to chemical reactions. Then, the volume change induced by climate effect depends on the soil behaviour upon wetting or drying, particularly for the untreated clay or the treated clay with large aggregates (chapter 4).

Figure 5-51 presents the mean value of the three dry density measurements ( $\rho_d$ ) versus compaction layer (No.) for the 2% lime plus 3% cement treated clay, 4% lime treated clay, 5% lime treated clay, 1% lime plus 5% cement treated silt and 3% cement treated silt:  $\rho_{d0}$ , measurement in place just after compaction (Gamma-dosimeter method, data from Froumentin, 2012 in TerDOUEST project);  $\rho_{d1}$ , measurement on the first batch (7 ~ 16 months); and  $\rho_{d2}$ , measurement on the second batch (about two-year). On the whole,  $\rho_{d1}$  and  $\rho_{d2}$  are much higher than  $\rho_{d0}$ .

In zone II, for mixture treated clay, we observe that the dry density presents an increasing order following  $\rho_{d0}$ ,  $\rho_{d1}$  and  $\rho_{d2}$  in Figure 5-51a (about No.11 ~ 7). For the lime treated clay, we also observe an increasing trend from  $\rho_{d0}$  to  $\rho_{d1}$  and  $\rho_{d2}$  in Figure 5-51b (about No.13 ~ 7). This shows obvious treatment effect. Moreover, the similar values for  $\rho_{d1}$  and  $\rho_{d2}$  also suggest the diminishing effect of treatment.



(a)  $\rho_{d0}$  (in place),  $\rho_{d1}$ ,  $\rho_{d2}$  for SC20 and SC47      (b)  $\rho_{d0}$  (in place),  $\rho_{d1}$ ,  $\rho_{d2}$  for SC14 and SC46      (c)  $\rho_{d0}$  (in place),  $\rho_{d1}$ ,  $\rho_{d2}$  for SC31 and SC49;  $\rho_{d0}$ ,  $\rho_{d1}$  for SC5-1

**Figure 5-51 Dry density changes after compaction (SC20/47, SC14/46, SC31/49, SC5)**

Figure 5-51a shows that in zone I (No.16 ~ No.12) the dry density of the second batch soil SC47-1( $\rho_{d2}$ ) is significantly higher than  $\rho_{d0}$  and  $\rho_{d1}$ , evidencing the treatment effect. In layer No.15~ No.13, the similar values for  $\rho_{d1}$  and  $\rho_{d0}$  suggest the negligible combined effects of treatment and wetting-induced swelling. Comparison of  $\rho_{d1}$  between No.12 and No.15~ No.13 evidences the significant difference in treatment effect. This difference is attributed to the effect of large aggregates sizes in No.15 ~ No.13. In Figure 5-51b, also for the clay in zone I (No.15 ~ No.14), similar result to that of zone II can be observed. Comparison of  $\rho_{d1}$  between the first batch soils SC20-1 and SC14-1 also shows that the small aggregates size soils (SC14-1) is less sensitive to climate changes. In Figure 5-51c, comparable dry densities of  $\rho_{d0}$  and  $\rho_{d1}$  are obtained for the clay. This can be explained by the high heterogeneity of the *in-situ* soil and the climate effect. Obviously, the clay on slope receives more climate effect than other part due to the more contacts with exterior environment. For the silt, the dry density also increases with curing in a global way albeit a large variation of data. For the slope part, the different results between the silt and clay indicate that the volumetric swell of the clay due to the effect of climate is compensated by the volume decrease due to the treatment.



### 5.5.3.3. Fissures development

Many fissures were observed on the *in-situ* cores, especially for the second batch of cores, indicating the strong effect of climate changes. For example, for the core specimen at 0.285 m of SC47-1, the stiffness decreases from 500 ~ 550 MPa to 66 ~ 276 MPa because of a horizontal fissure in the middle of this specimen. Axtell et al. (2008) also indicates that the fissures in core specimens can significantly decrease their stiffness.

Moreover, as mentioned before in the description of core samples in chapter 2, we observe that the mixture treated clay shows more frequent fissures than the 4% lime or 5% cement treated clay. This is probably due to the high sensitivity of  $G_{max}$  to water content change due to the cement addition, especially for the large aggregates size soils, as shown by the laboratory results (ex. case 25, method B for mixture treated clay; case 9 for cement treated silt in chapter 4).

Thus, apart from the heterogeneity factor, the different treatments also play a role on the fissures development. This can impact the depth of the climate effect. As mentioned before, the depth of climate effect (Zone I) for the predominantly mixture treated clay (SC20/SC47) is greater than that for the predominantly lime treated clay (SC14/SC46).

### 5.5.4. Treatment effect

#### 5.5.4.1. Water content change

Water loss reflects the treatment effect as pozzolanic reactions consume water (ex. Chew *et al.*, 2004). In order to minimize the climate effect, the water loss in Zone II is analysed for both the first batch and the second batch (Table 5-3).

**Table 5-3 Water change induced by treatment effect (zone II)**

Core	Treatment	Layer No.	Period (months)	$\Delta w_1$ (w1-w0)	$\Delta w_2$ (w2-w0)	$\Delta w_2 - \Delta w_1$ (w2-w1)
SC20-2 (w1) / SC47-2 (w2)	2% lime plus 3% cement	11 ~ 7 / 9 ~ 7	13 / 25	-7.31%	-8.11%	-0.81%
SC14-2 (w1)/ SC46-2 (w2)	4% lime	11 ~ 7 / 11 ~ 8	16 / 25	-9.35%	-9.32%	+0.03%

For the 2% lime plus 3% cement treated clay, the water loss is 7.31% after 13-month curing (ex. SC20-2), whereas it is 8.11% after 25-month curing. The difference of 0.81% can be considered as the water loss by pozzolanic reactions. In other words, the stiffness gain observed before is attributed to pozzolanic reactions.

For the 4% lime treated clay, similar observations can be made. Note that the small value of 0.03% indicates a slight change after 16-month curing. The large water loss  $\Delta w_1$  (close to 10%) for both treatments suggests the significant treatment effects in the early term after the construction of the embankment.

#### 5.5.4.2. Stiffness change

Considering the complicated effects of time, climate and heterogeneity for the *in-situ* soils, it appears necessary to investigate the treatment effect using the specimens with similar curing time and depth. Mean values are also used to minimize the heterogeneity effect for both the treated silt (Table 5-4) and treated clay (Table 5-5).

**Table 5-4 Treatment effect for the silt**

Treatment	Sample	Curing period	$\rho_d$ (Mg/m <sup>3</sup> )	w (%)	$G_{max}$ (MPa)
0% lime	SC20-4	29 months	1.40	34.3	150
2% lime	SC20-4	29 months	1.58	26.4	297
3% lime	SC40-1	30 months	1.60	25.1	376
3% cement	SC31-1	29 months	1.66	21.3	518
1% lime plus 5% cement	SC31-1, SC40-1, SC20-1, SC14-1, SC5-1	29.5 months	1.69	20.4	833

For the silt, as shown in Table 5-4, all the first batch cores are used. On the whole, the results show that the predominantly cement treated silt (1% lime + 5% cement, 3% cement)

presents higher stiffness than other treatments after about 29-month curing. This is in accordance with the conclusion that cement treatment is especially suitable for soils of low plasticity (Currin *et al.*, 1976; Engineering manual 1110-3-137, 1984; Little *et al.*, 1995c; Prusinski and Bhattacharja, 1999; Texas Department of Transportation, 2005).

For the clay, as shown in Table 5-5, three treatments are evaluated. Firstly, for the 2% lime plus 3% cement treated clay and the 4% lime treated clay, the soil specimens from Zone II are used to minimize the effect of climate. For the 5% lime treated clay, the data of first batch SC5-1 in Zone I is used because no core in Zone II is studied. Under similar compaction conditions ( $w$ ,  $\rho_d$ ) and after a similar curing period (29 ~ 30 months), a decreasing order of stiffness is observed for the 2% lime plus 3% cement treatment (581 MPa), the 5% lime treatment (420 MPa) and the 4% lime treatment (403 MPa). This indicates that the mixture treated clay has more cementitious products than the lime treated one. For expansive soils under same dosage of treatments, Puppala *et al.* (2005) also reported the larger  $G_{max}$  for the predominantly cement treated soil as compared to the predominant lime treated one. For estuarine silt, Jauberthie *et al.* (2010) also reported a higher UCS with mix treatment (cement plus lime) as compared to lime or cement treatment.

Summarising, reasonable results have been obtained by using the mean values that allow the effect of heterogeneity to be minimized and by considering the specimens far from the embankment surface.

Table 5-5 Treatment effect for the treated clay

Treatment	Sample 1	Sample 2	Curing period	$\rho_d$ (Mg/m <sup>3</sup> )	w (%)	$G_{max}$ (MPa)	Mean $G_{max}$ (MPa)
2% lime plus 3% cement	SC20-2 (layer No.7~11)	SC47-2 (layer No.7~11)	29 months	1.473 / 1.50	25.9 / 25.7	513/603	581
4% lime	SC14-2 (layer No.7~11)	SC46-2 (layer No.7~11)	29 months	1.479 / 1.469	26.49 / 26.53	429/377	403
5% lime	SC5-1	SC14-1	30 months	1.467 / 1.36	25.25 / 25.98	425/414	420

## 5.6. Conclusions

In field conditions, the stiffness of cementitious treated soils changes not only with curing but also with climate. In this chapter, the combined effects of curing and climate were investigated on two batches of cores taken from the experimental embankment in Héricourt through the measurements of  $G_{\max}$  using the technique of bender elements. Five measurements were performed for each specimen at a given time, allowing any heterogeneity in the plane of cross-section to be identified. Several observations can be made:

A large variation of  $G_{\max}$  values over depth is identified, showing high heterogeneity of the *in-situ* soil. In field conditions, the water content and dry density are not the main factors governing the stiffness. The heterogeneity due to the presence of stones and additive distribution is decisive for the  $G_{\max}$  value as well as its development.

Owing to these heterogeneity factors, the effects of dry density, water content, curing time, treatment method and dosage, climate effect are often masked. The use of mean values allowed the heterogeneity to be minimized, and thus the time effect, climate effect and treatment effect to be reasonably analyzed.

The climate effect was revealed to be a negative factor, particularly for the near surface layers. The climate effect can be divided into three zones according to the water content changes of the core specimens. Zone I is the active zone for the climate effect; Zone II is the zone untouched by the climate effect; zone III is the active zone for the water table change. The climate change can influence the *in-situ* soils as deep as 0.85 ~ 2.05 m (zone I) in the case of the embankment of Héricourt. This is related to the effect of wetting/drying cycles applied by the climate and to the large aggregates size.

The effect of curing was evidenced to be a positive factor for the stiffness. This curing effect is diminishing after 7 ~ 16 months for different treatments. This effect is strongly influenced by the heterogeneity soils (ex. aggregates size). The  $G_{\max}$  gain due to curing is also strongly stiffness level dependent, with significant increase for soils with high stiffness. The water loss induced by time effect (pozzolanic reactions) was identified in Zone II.

The effect of treatment shows that the predominantly cement treatment has higher stiffness than the lime treatment for both the silt (1% lime + 5% cement > 3% cement > 3% lime > 2% lime) and clay (2% lime + 3% cement > 5% lime > 4% lime).

## Chapter 6. Modelling of curing behaviour in both laboratory and field conditions

In chapter 3, the aggregates size effects on the stiffness development during curing time were investigated in the laboratory for both the silt and clay at an aggregates size scale from 0.4 to 5 mm. A clear nonlinear  $G_{\max} - \log(t)$  relationship was identified, especially for the lime treated soils. In chapter 5, the aggregates size effect was also identified on the *in-situ* core specimens with similar treatments but compacted at a larger aggregates size scale:  $D_{\max} = 20 \text{ mm}$  for the silt and  $D_{\max} = 31.5 \text{ mm}$  for the clay.

In this chapter, this nonlinear relationship for stiffness development is firstly simulated using a hyperbolic model, aiming at better analysing the aggregates size effect on the laboratory scale. This model is then extended to the *in-situ* aggregates size scale.

### 6.1. Model proposed

The increase of strength/stiffness over time for the cementitious treated soils was investigated for several decades. For cement treated soils, several authors (Neville, 1995; Carino and Lew, 2001; Horpibulsuk *et al.*, 2006; Flores *et al.*, 2010) analysed the compressive or tensile strength after curing under isothermal and constant moisture conditions, and obtained linear relationships between the strength and the logarithm of time. But very often, these empirical curves can only fit the test points at the beginning (ex. for several days) and at the end of the strength development (Porbaha *et al.*, 2000; Liu *et al.*, 2008; Horpibulsuk *et al.*, 2008). This is due to the nonlinear nature of the curves. This is particularly the case for lime treated soils (see Tang *et al.*, 2011). Stocker (1974) (cited by Prusinski and Bhattacharja, 1999) reported nonlinear calcium production as a function of the logarithm of time for a clay after addition of cement and lime, evidencing that the stiffness/strength evolution is directly related to the production of cementitious compounds by pozzolanic reactions.

Several models exist allowing the nonlinear behaviour to be described with number of parameters (McNeal, 1970; Curiel Yuste *et al.*, 2007; Estop-Aragonés and Blodau, 2012; Rajeev *et al.*, 2012; Gao *et al.*, 2013). The hyperbolic model (Komine and Ogata, 1997; Al-

Shayea *et al.*, 2003; Muntohar, 2003; Al-Mhaidib, 2008) is one of the simplest models that can satisfactorily describe the nonlinear  $G_{\max}$  development for lime and/or cement treated soils. This model is adopted in this study.

Figure 6-1 shows a typical  $G_{\max}$  development curve for the lime treated silt (ex. case 1,  $D_{\max} = 1 \text{ mm}$ , dry side, 2% lime). In the first two-day curing, the  $G_{\max}$  development is nonlinear; a much faster second nonlinear part follows the first part; finally stabilization is reached after more than 1000 h. This relationship may correspond to the well known mechanisms for cementitious treated soils. The first mechanism is the cation exchange due to hydration of additives, and the second one is related to the pozzolanic reactions. Basically, the cation exchange occurs much earlier than the pozzolanic reactions. We can intend to assimilate the first stage of the  $G_{\max}$  development curve to the cation exchange and the second stage to the pozzolanic reactions.

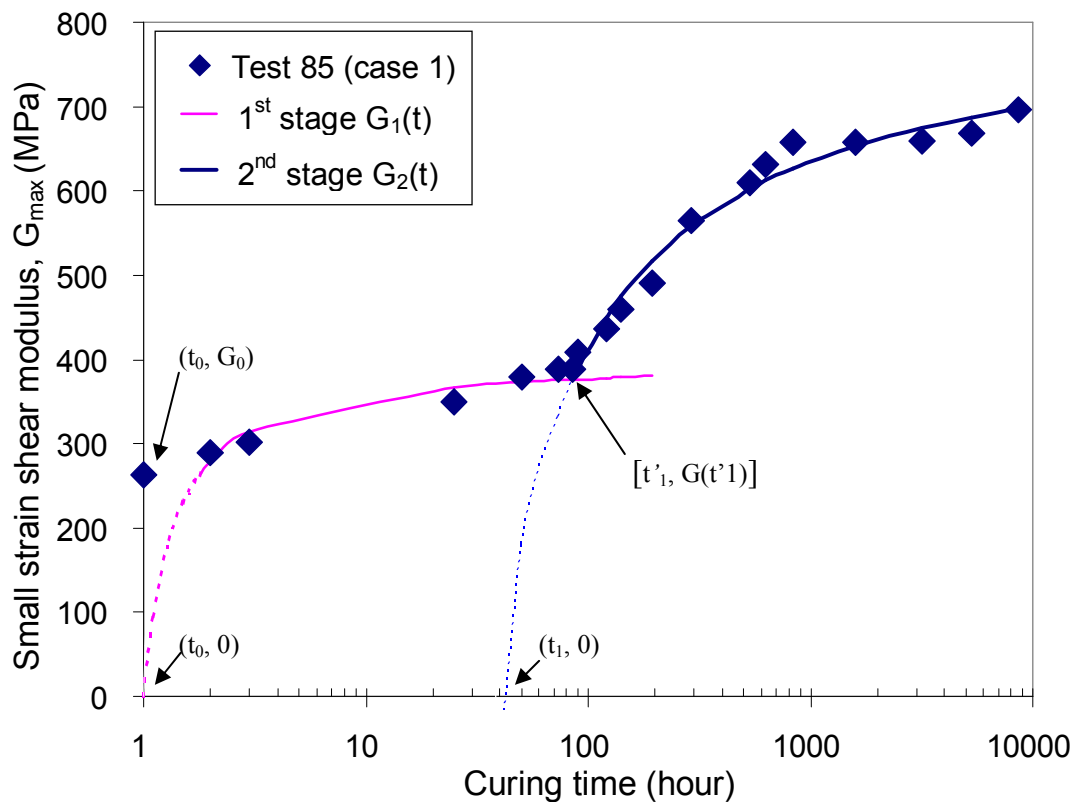


Figure 6-1 Description of  $G_{\max}$  development by a hyperbolic model

In Figure 6-1,  $G_1(t)$  and  $G_2(t)$  express the two stages of  $G_{\max}$  development versus the logarithm of time, and both are of hyperbolic functions as follows:

$$\text{First stage } (t_0 < t < t'_1): G_{\max} = G_1(t) = \frac{\log\left(\frac{t}{t_0}\right)}{\frac{1}{V_1} + \frac{1}{G_{f1}} \cdot \log\left(\frac{t}{t_0}\right)} \quad (6-1)$$

$$\text{Second stage } (t > t'_1): G_{\max} = G_2(t) = \frac{\log\left(\frac{t}{t_1}\right)}{\frac{1}{V_2} + \frac{1}{G_{f2}} \cdot \log\left(\frac{t}{t_1}\right)} \quad (6-2)$$

$$\text{At } t = t'_1: G_{\max} = G_1(t'_1) = G_2(t'_1) \quad (6-3)$$

where,

- $V_1$  is the initial maximum slope (curvature) for the first stage;
- $G_{f1}$  is the asymptote of the first stage;
- $t_0$  is a reference time for the first stage ( $t_0 = 1$  h);
- $t_1$  is a reference time for the second stage;
- $t'_1$  is the starting time of the second stage;
- $V_2$  is the maximum slope for the second stage;
- $G_{f2}$  is the asymptote of the second stage.

The parameters of model can be determined as follows:

1) We firstly present the experimental data in the plane  $[1/G_{\max}, 1/\log(t/t_0)]$  (see Figure 6-2). This enables parameters  $V_1$  and  $G_{f1}$  to be determined because  $1/V_1$  is the slope and  $1/G_{f1}$  is the intersection of the straight line obtained.

2) The obtained parameters  $V_1, G_{f1}$  are substituted into Eq. (6-1), and  $G_1(t)$  can be obtained (see Figure 6-1).

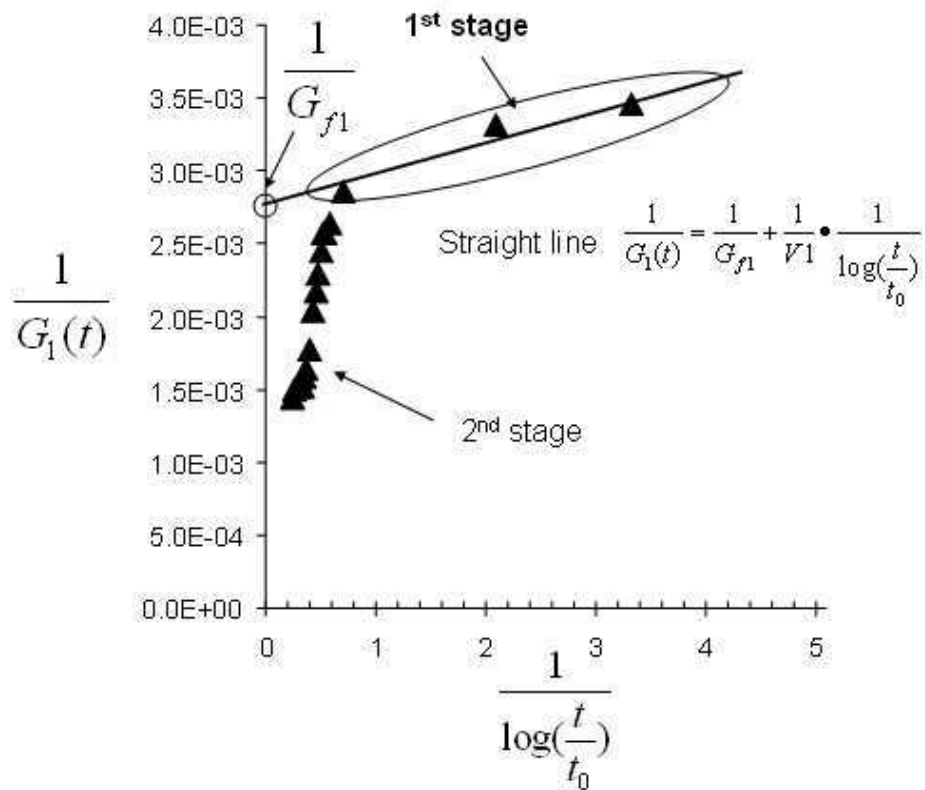


Figure 6-2 Determination of  $1/V_1$ ,  $1/G_{f1}$  for the first stage

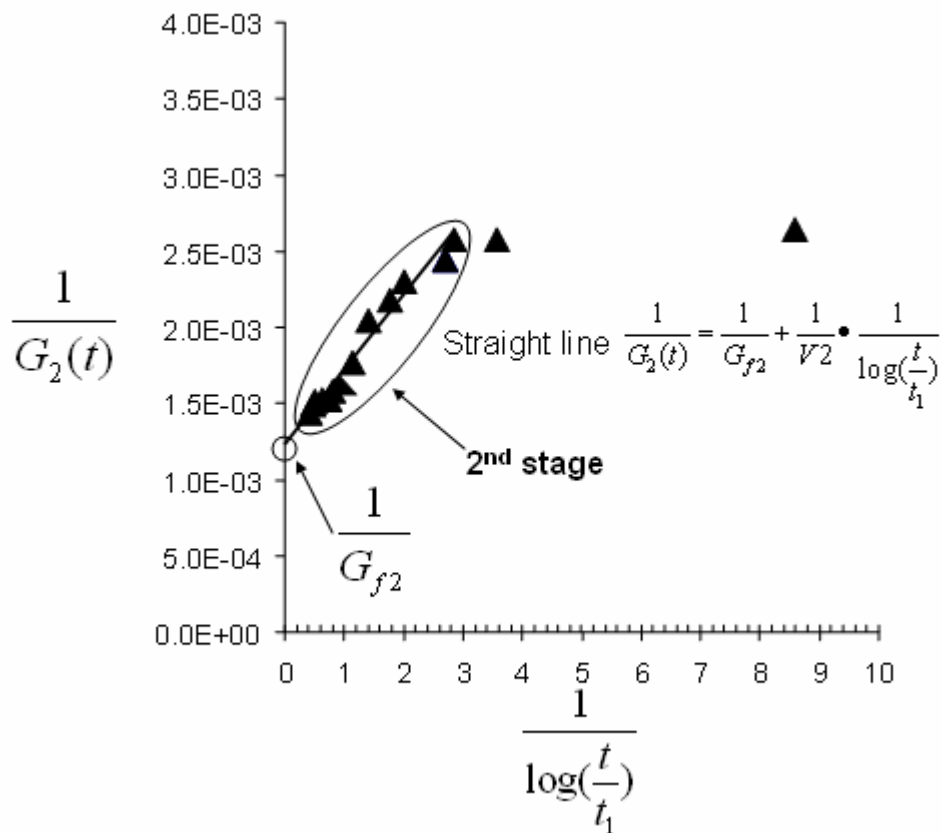


Figure 6-3 Determination of parameters  $V_2$  and  $G_2$  for the second stage



3) For the second stage, as shown in Figure 6-1, we need to translate the coordinate system from  $t = t_0$  to  $t = t_1$ . Based on the general trend of results, firstly, we choose a value of  $t_1$  near the starting time of the second stage  $t'_1$  ( $1 < t_1 < t'_1$ ). As for the first stage, the experimental data are presented in the plane  $[1/G_{max}, 1/\log(t/t_1)]$ , and a linear relationship is also obtained. This enables parameters  $V_2$  and  $G_{f2}$  to be determined because  $1/V_2$  is the slope and  $1/G_{f2}$  is the intersection (see Figure 6-3). Then the parameters  $V_2$ ,  $G_{f2}$  and  $t_1$  are optimized finally by least-squares of the difference between the test and the model.

4)  $t'_1$  can be determined using Eq. (6-3):

$$t'_1 = 10^{\frac{\log t_1}{2} \frac{(V_1 - V_2)G_{f1} \cdot G_{f2}}{2V_1 \cdot V_2 (G_{f1} - G_{f2})} + \sqrt{\left[ \frac{\log t_1}{2} \frac{(V_1 - V_2)G_{f1} \cdot G_{f2}}{2V_1 \cdot V_2 (G_{f1} - G_{f2})} \right]^2 - \frac{G_{f1} \cdot G_{f2} \cdot \log t_1}{V_1 \cdot (G_{f1} - G_{f2})}} \frac{G_{f1} \cdot G_{f2} \cdot \log t_1}{V_1 \cdot (G_{f1} - G_{f2})}} \quad (6-4)$$

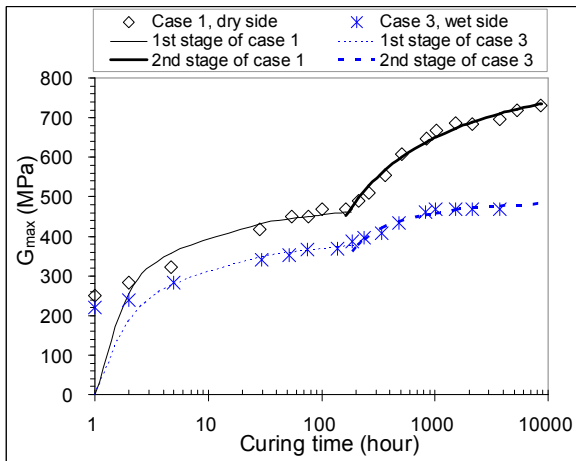
The parameters of this model are determined for all the treated soils presented in chapter 3. The variation of each parameter with  $D_{max}$  (0.4 mm ~ 5 mm) is analysed by the trends.

## 6.2. Modelling of the curing behaviour of lime treated silt

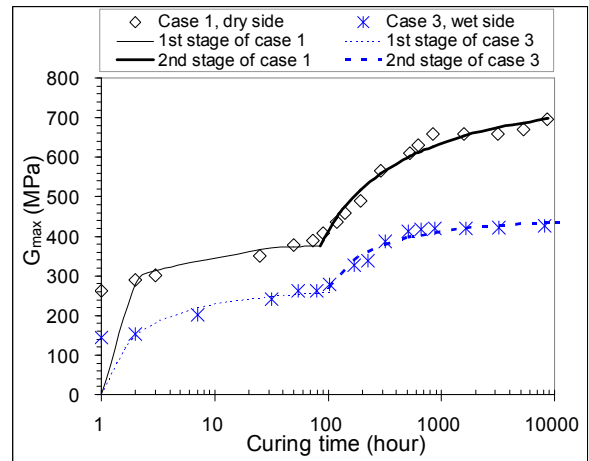
In the laboratory conditions, for the lime treated silt, only the 2% lime treated silt was tested, involving different sub-series prepared by method 1 and method 2 (see chapter 3).

### 6.2.1. Curing behaviour

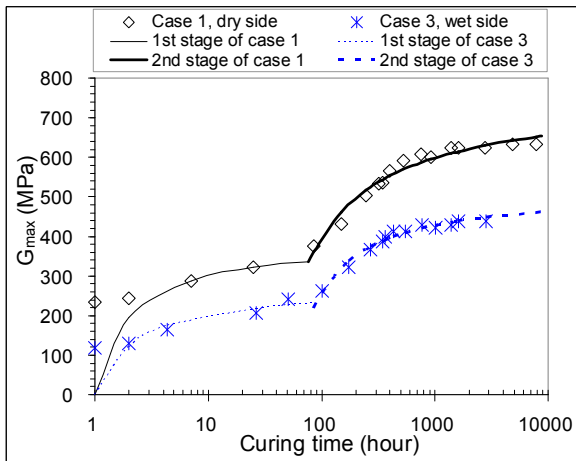
The typical nonlinear two-stage  $G_{max}$  development is modelled for the 2% lime treated silt of different sub-series with method 1 in Figure 6-4 (case 1, 3) and with method 2 in Figure 6-5 (case 5, 7). Apart from the initial value ( $G_{max} = G_0$ , when  $t = 1$  hour), a good agreement is obtained between the measurements and modelling. On the whole, both method 1 and method 2 shows typical two-phase development - phase I is related to the hydration of lime and phase II to the pozzolanic reactions. The significant difference between the two methods is mainly for the wet side specimens: method 2 results in a very limited  $G_{max}$  development as compared to method 1. This leads to a larger difference between the dry and wet sides for method 2, indicating the different cementation for the two methods.



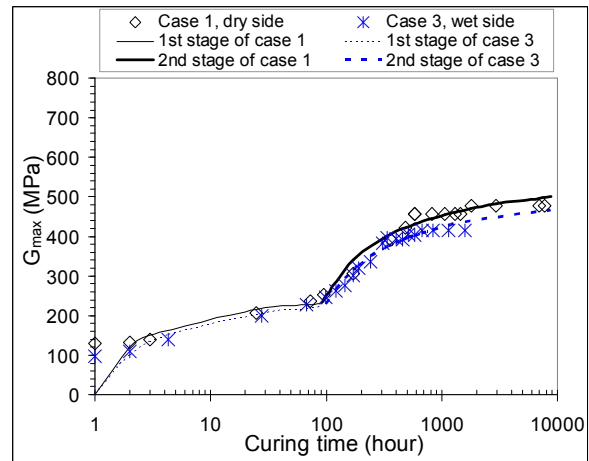
(a)  $D_{max} = 0.4 \text{ mm}$



(b)  $D_{max} = 1 \text{ mm}$



(c)  $D_{max} = 2 \text{ mm}$



(d)  $D_{max} = 5 \text{ mm}$

Figure 6-4 Modelling of the curing behaviour of the 2% lime treated silt by method 1 (case 1, 3)

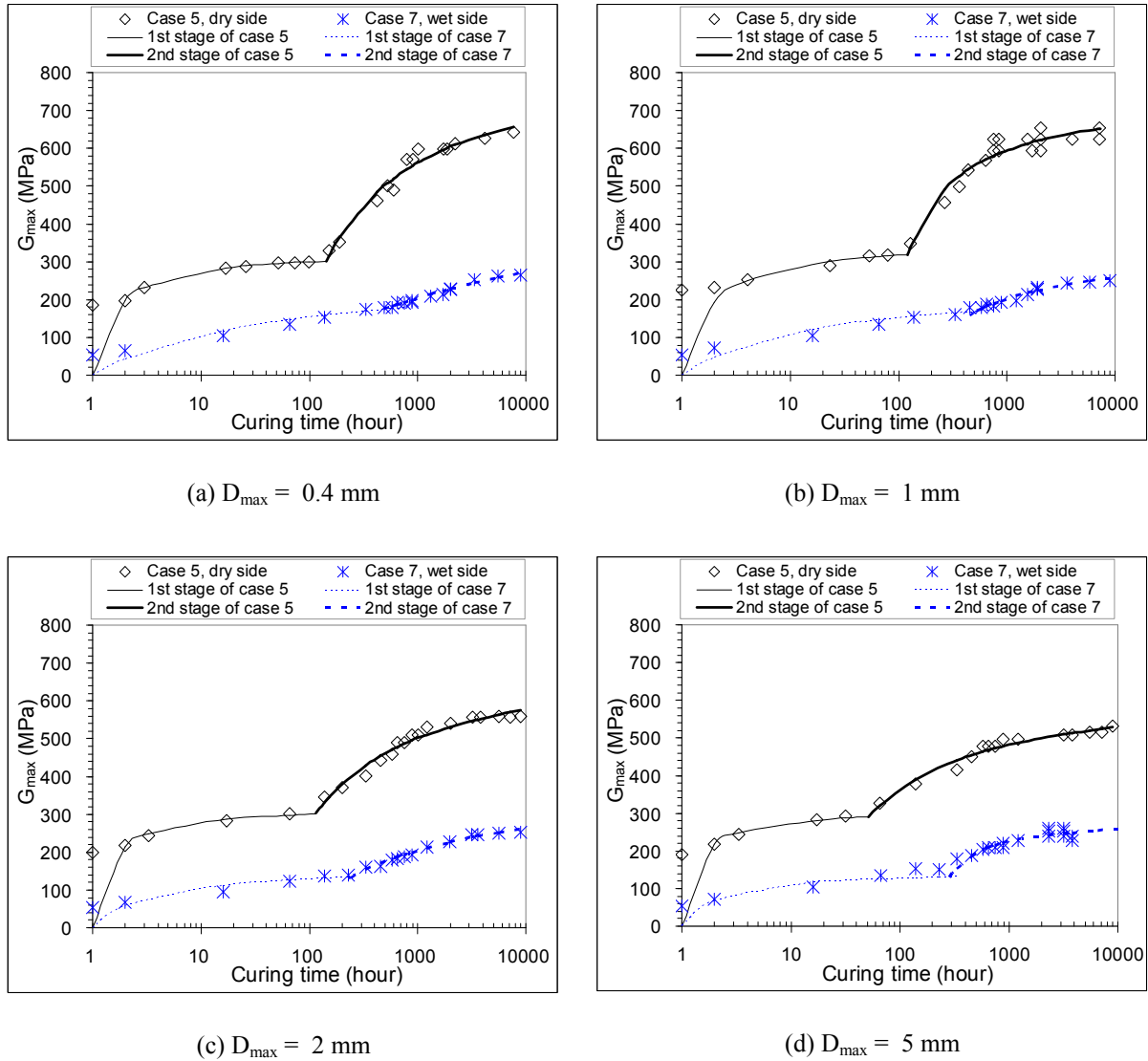


Figure 6-5 Modelling of the curing behaviour of the 2%lime treated silt by method 2 (case 5, 7)

### 6.2.2. Aggregates size effect for the parameters

As mentioned before, parameter  $V_1$  represents the maximum slope of the first stage, related to the hydration of soil/additives and the cation exchange. Figure 6-6 presents  $V_1$  versus  $D_{max}$  for the 2% lime treated silt prepared by two methods. For method 1,  $V_1$  shows a decreasing trend for both the dry and wet sides (case 1, 3), whereas for method 2,  $V_1$  is independent of  $D_{max}$  for the dry side (case 5) but increasing with  $D_{max}$  for the wet side (case 7).

$G_{fl}$  corresponds to the final value of  $G_{max}$  at the first stage, related mainly to the hydration process. For lime treated soils, the hydration process gives rise to a decrease of

water content, a modification of grain size distribution by the flocculation and agglomeration. This process does not contribute significantly to the improvement of soil stiffness.

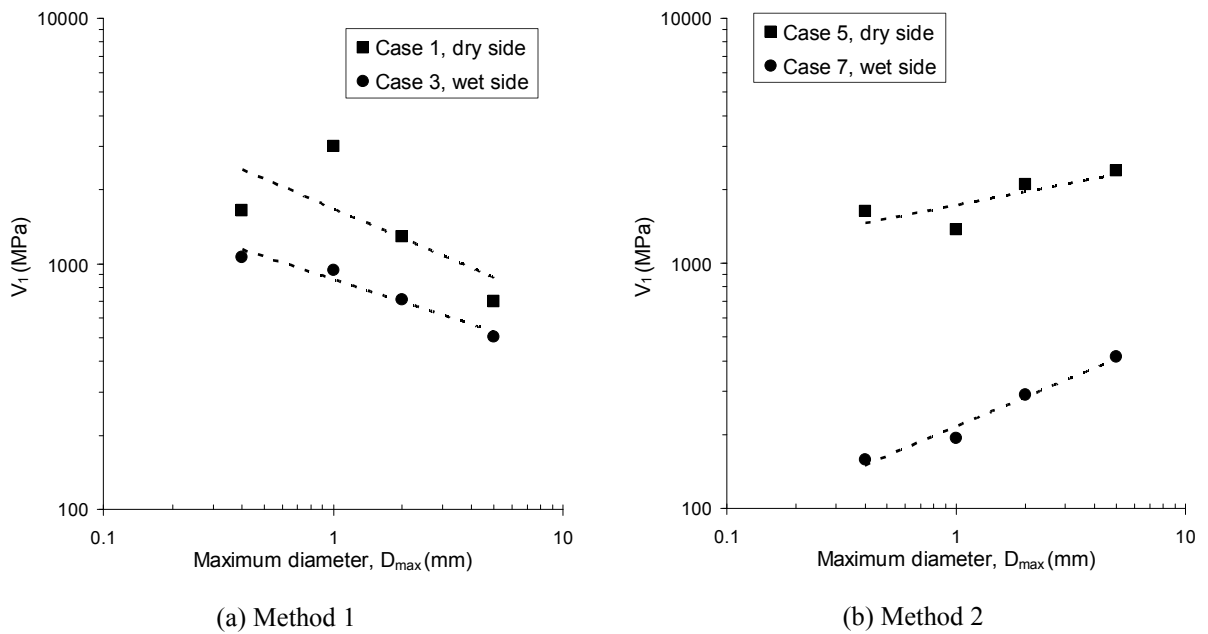


Figure 6-6 Parameter  $V_1$  versus  $D_{max}$  for the 2% lime treated silt

Figure 6-7 presents the  $G_{fl}$  versus  $D_{max}$  for the 2% lime treated silt. We observe that the  $G_{fl}$  is decreasing with increase of  $D_{max}$  for both method 1 (Figure 6-7a) and method 2 (Figure 6-7b).

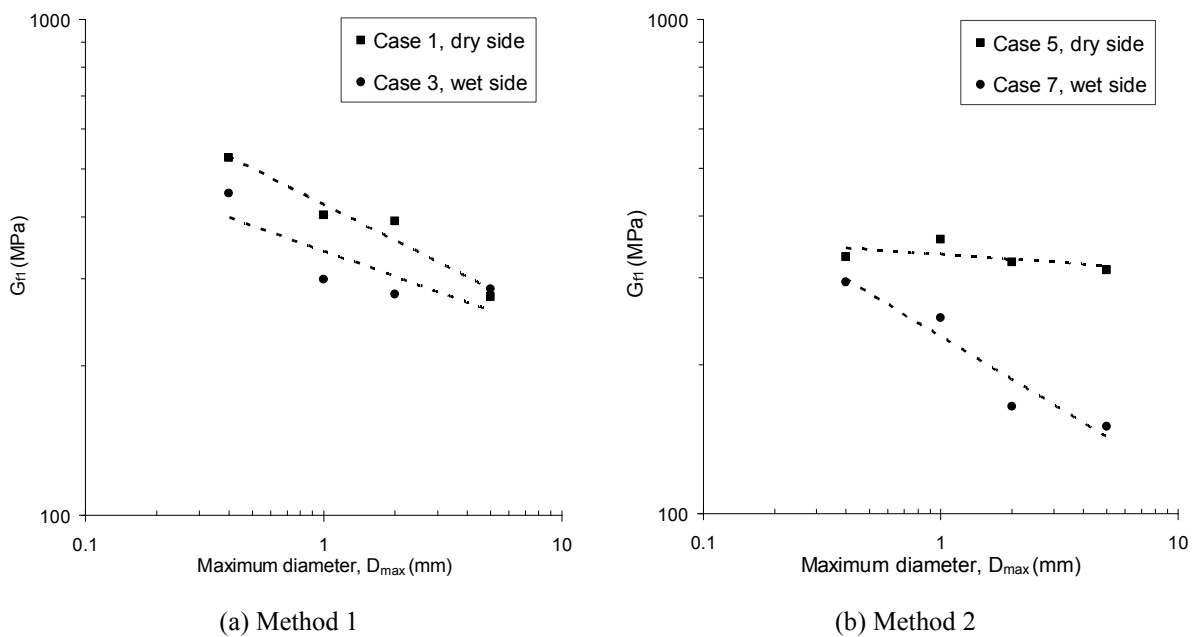
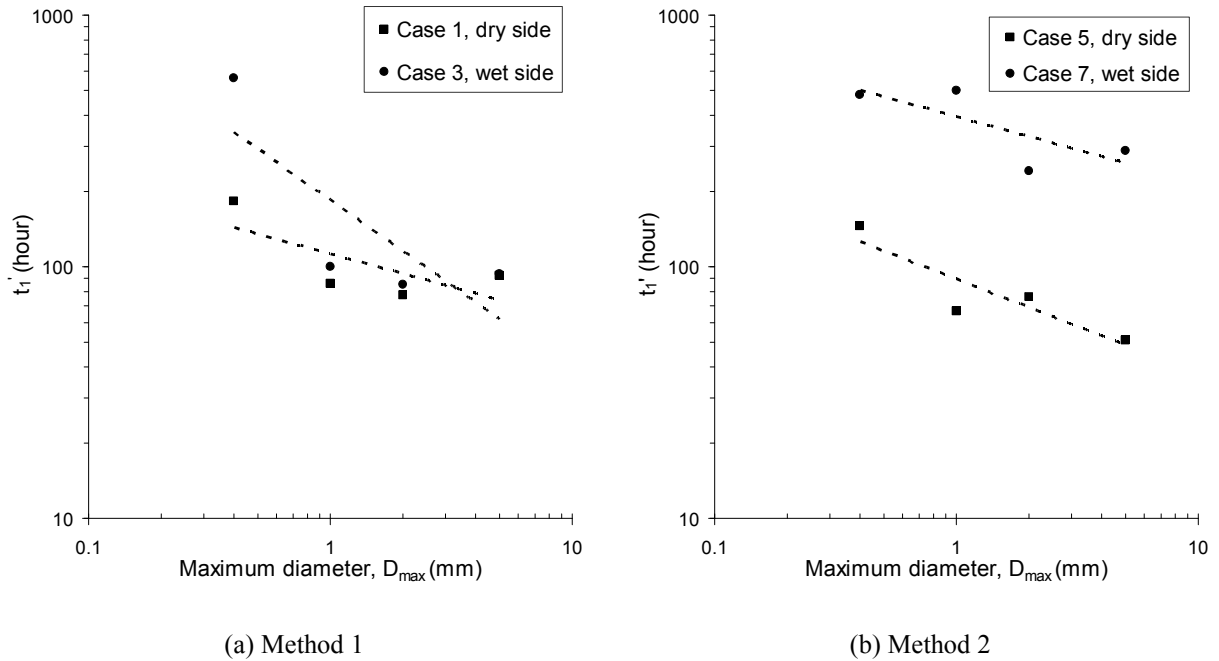


Figure 6-7 Parameter  $G_{fl}$  versus  $D_{max}$  for the 2% lime treated silt

The starting time of the second stage  $t_1'$  is an important parameter in determining the mellow time for lime treated soils. It is the time that separates the modification due to hydration and cation exchange from the stabilization due to pozzolanic reactions. Figure 6-8 presents  $t_1'$  versus  $D_{max}$  for the 2% lime treated silt. We observe obvious decreasing trends with the increase of  $D_{max}$  for both method 1 and method 2.



**Figure 6-8 Starting time of the second stage  $t_1'$  versus  $D_{max}$  for the 2% lime treated silt**

Similar to  $V_1$ ,  $V_2$  is the maximum slope of the second stage and related to the pozzolanic reactions. Figure 6-9 shows  $V_2$  versus  $D_{max}$  for the 2% lime treated silt prepared by both method 1 and method 2. For method 1,  $V_2$  decreases with the increase of  $D_{max}$  for both the dry side (case 1) and wet side (case 3), with more significant decrease for the wet side. For method 2, different trends are observed for the two sides – a noticeable increasing trend for the wet side (case 7) but a decreasing trend for dry side (case 5).

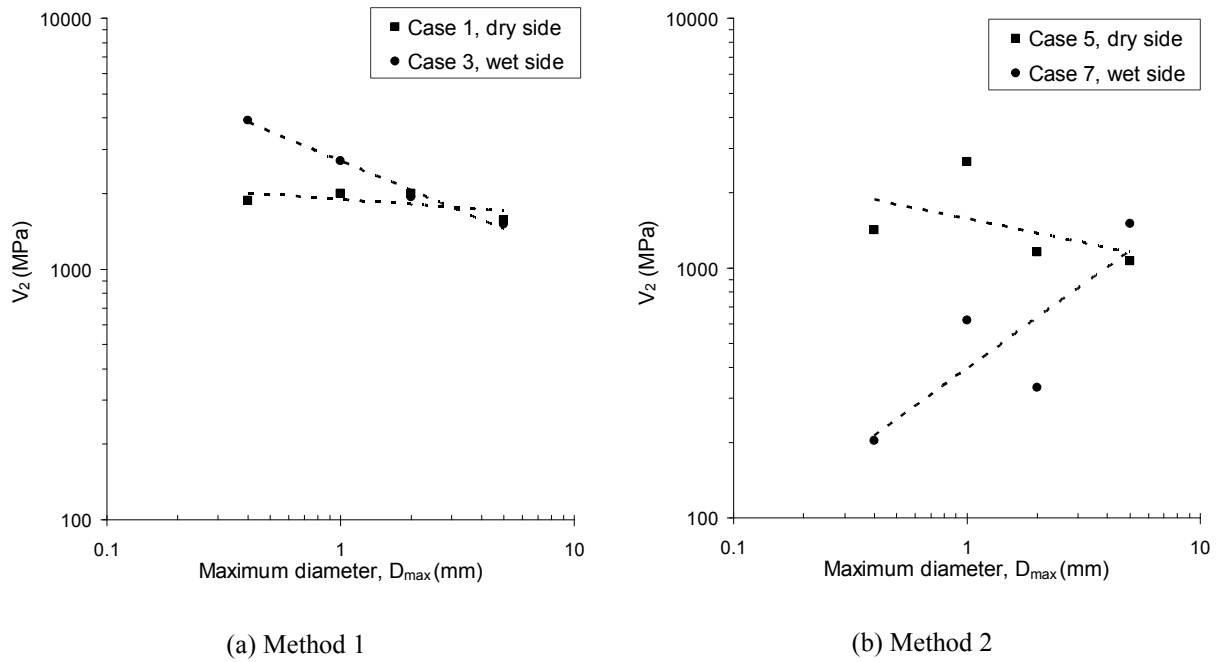


**Figure 6-9 Parameter  $V_2$  versus  $D_{max}$  for the 2% lime treated silt**

Parameter  $G_{f2}$  is the final value of  $G_{max}$  at the second stage, related mainly to the pozzolanic reactions. Figure 6-10 presents the  $G_{f2}$  versus  $D_{max}$  for the 2% lime treated silt prepared by both method 1 and method 2. For method 1,  $G_{f2}$  decreases significantly with the increase of  $D_{max}$  for the dry side (case 1), whereas it increases slightly or remains constant for the wet side (case 3). For method 2,  $G_{f2}$  decreases noticeably with  $D_{max}$  for both dry and wet sides.

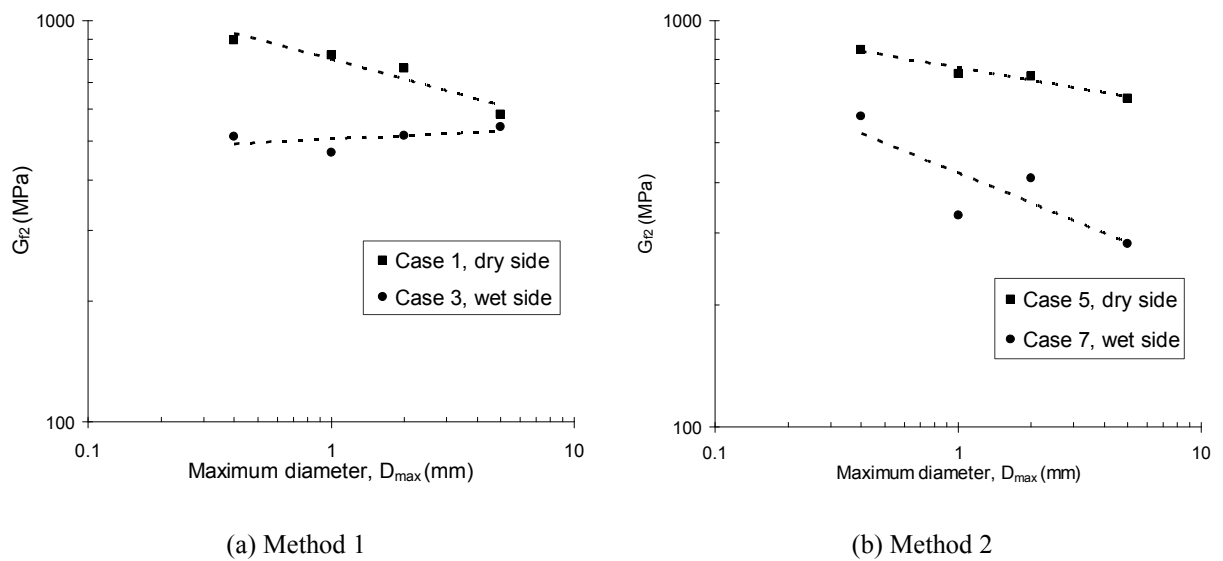


**Figure 6-10 Parameter  $G_{f2}$  versus  $D_{max}$  for the 2% lime treated silt**

### 6.3. Modelling of the curing behaviour of the cement treated silt

In laboratory conditions, for the cement treated silt, only the 3% cement treated specimens were tested, involving different sub-series prepared by method 1 and method 2 (see chapter 3).

#### 6.3.1. Curing behaviour

The modelling results are shown in Figure 6-11 and Figure 6-12 for the 3% cement treated silt of different sub-series with method 1 and method 2, respectively.

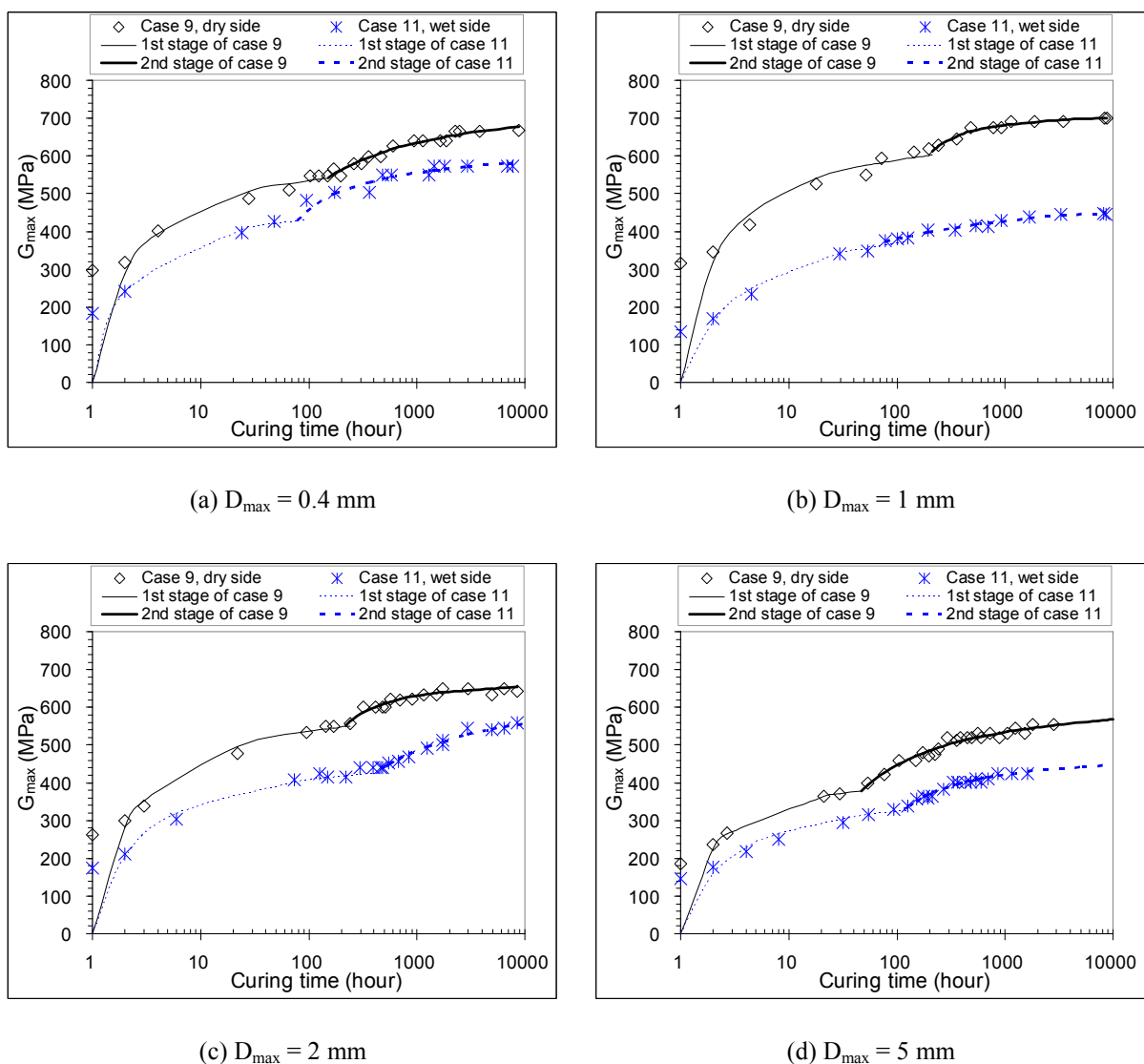


Figure 6-11 Modelling for the 3% cement treated silt of method 1 (case 9, 11)

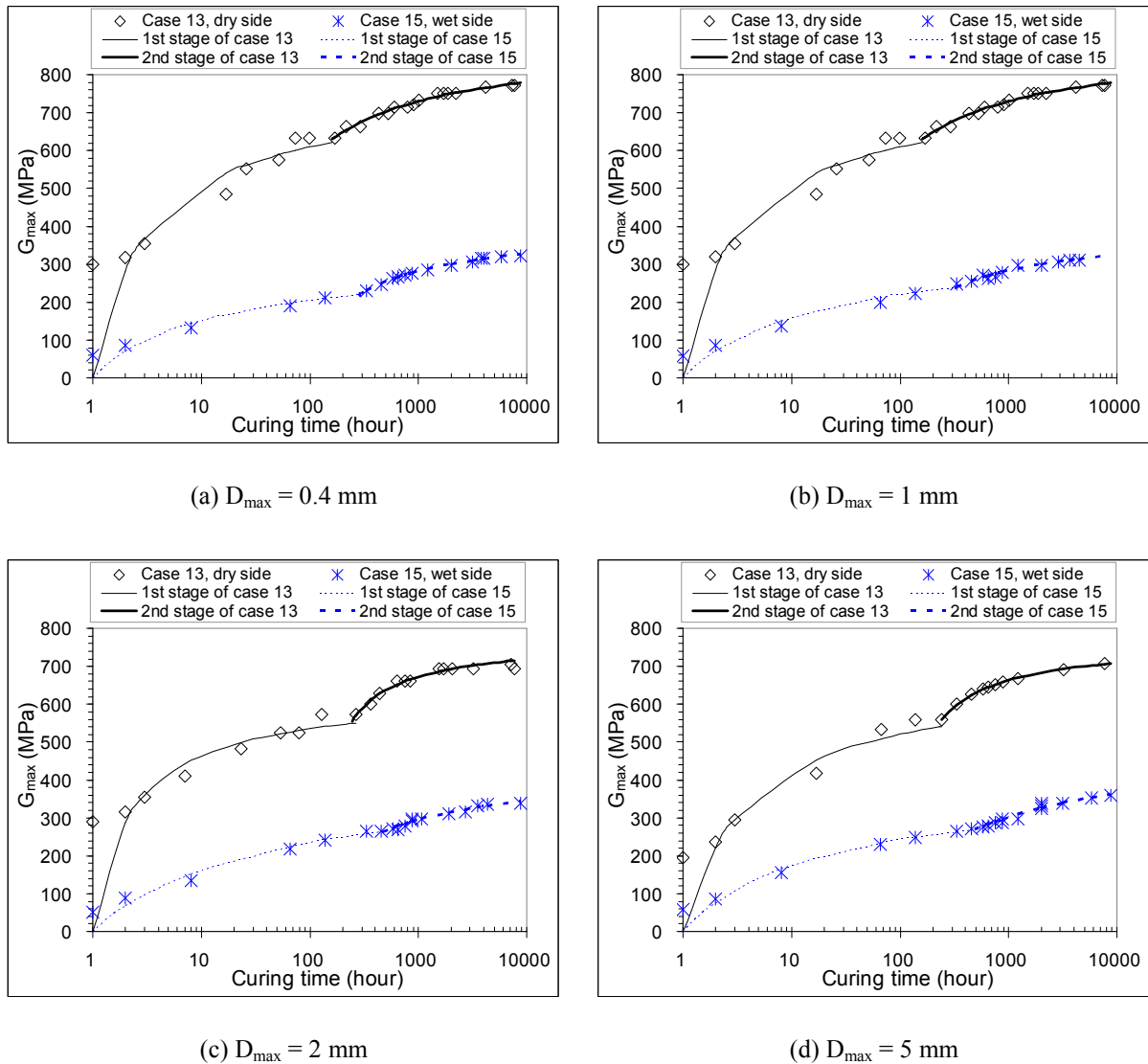


Figure 6-12 Modelling of the curing behaviour of the 3% cement treated silt of method2 (case 13, 15)

On the whole, the two-stage nonlinear  $G_{\max}$  development is not as noticeable as for the lime treated silt. The difference is due to the different effects for the two treatments. For the lime treated silt, the first mechanism of hydration does not produce cementitious compounds. Thus, it is a minor process for the stiffness gain as compared to the pozzolanic reactions. On the contrary, for the cement treated silt, the first mechanism of hydration is the primary process for the stiffness gain as it can produce large quantity of cementitious compounds such as hydrated calcium silicates ( $C_2SH_x$ ,  $C_3S_2H_x$ ) and calcium aluminates ( $C_3AH_x$ ,  $C_4AH_x$ ). The pozzolanic reactions with the silica and alumina from the clay minerals are thereby a secondary process for the cement treated silt.



### 6.3.2. Aggregates size effect

Figure 6-13 presents  $V_1$  versus  $D_{\max}$  for the 3% cement treated silt prepared with both method 1 and method 2.

For method 1,  $V_1$  shows a decreasing trend for both dry and wet sides (case 9, 11), with less noticeable decrease for the dry side. For method 2, it decreases slightly with increase of  $D_{\max}$  for the dry side (case 13) but remains constant for the wet side (case 15).

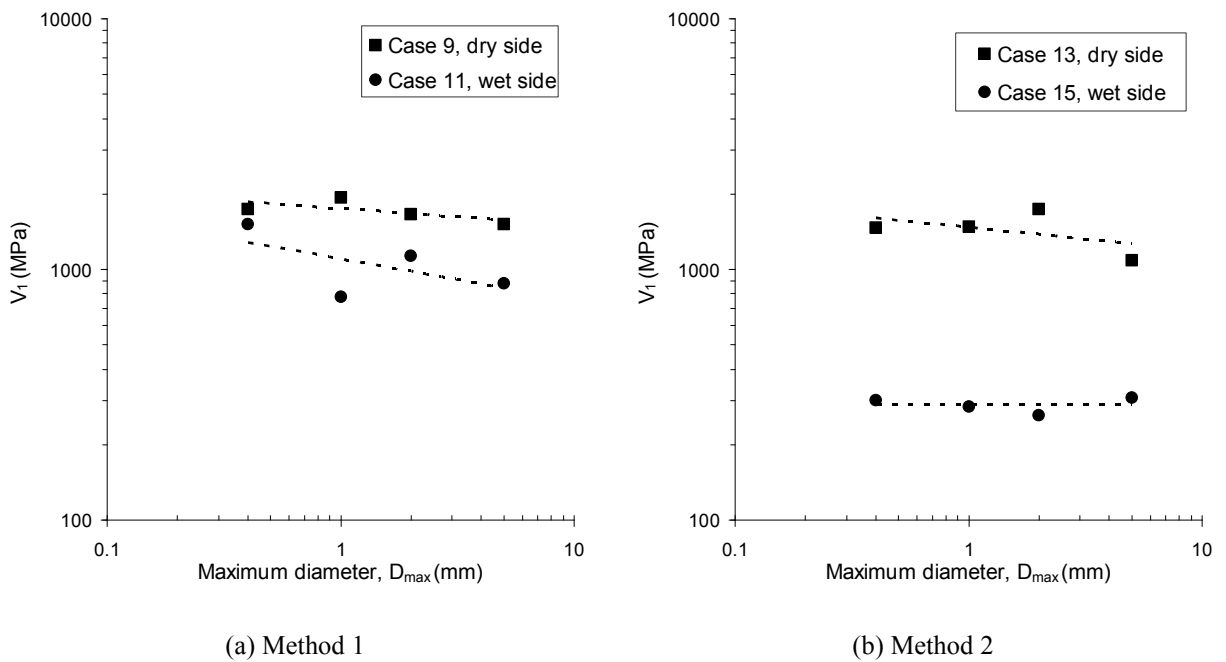
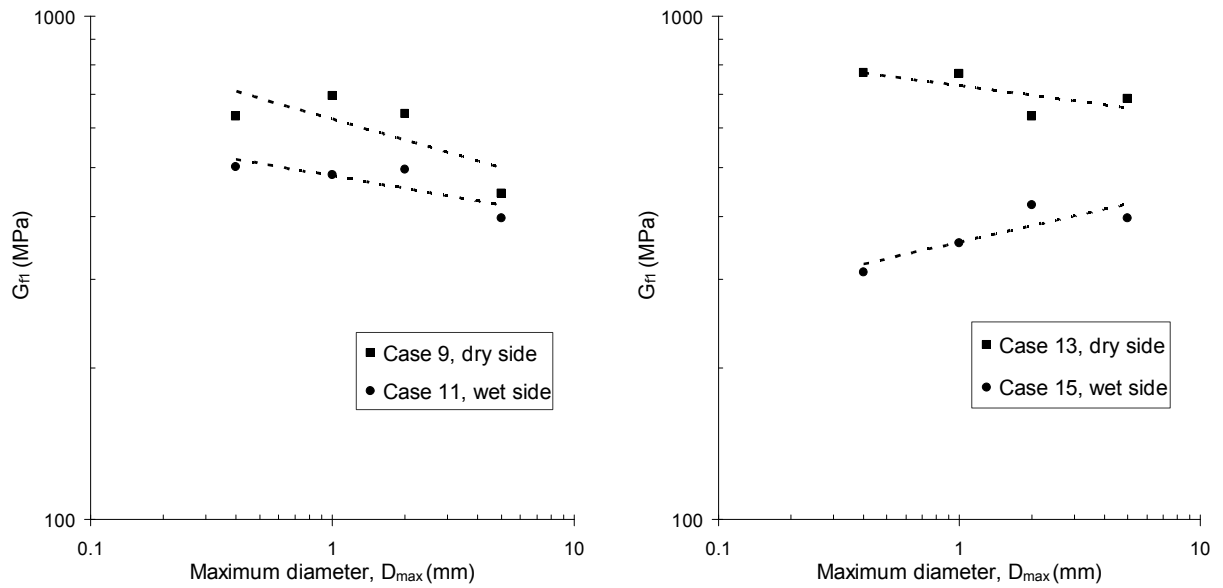


Figure 6-13 Parameter  $V_1$  versus  $D_{\max}$  for the 3% cement treated silt

Figure 6-14 presents  $G_{fl}$  versus  $D_{\max}$  for the 3% cement treated silt prepared by both method 1 and method 2. On the whole, except the wet side of method 2 (case 15),  $G_{fl}$  decreases significantly with increase of  $D_{\max}$ .

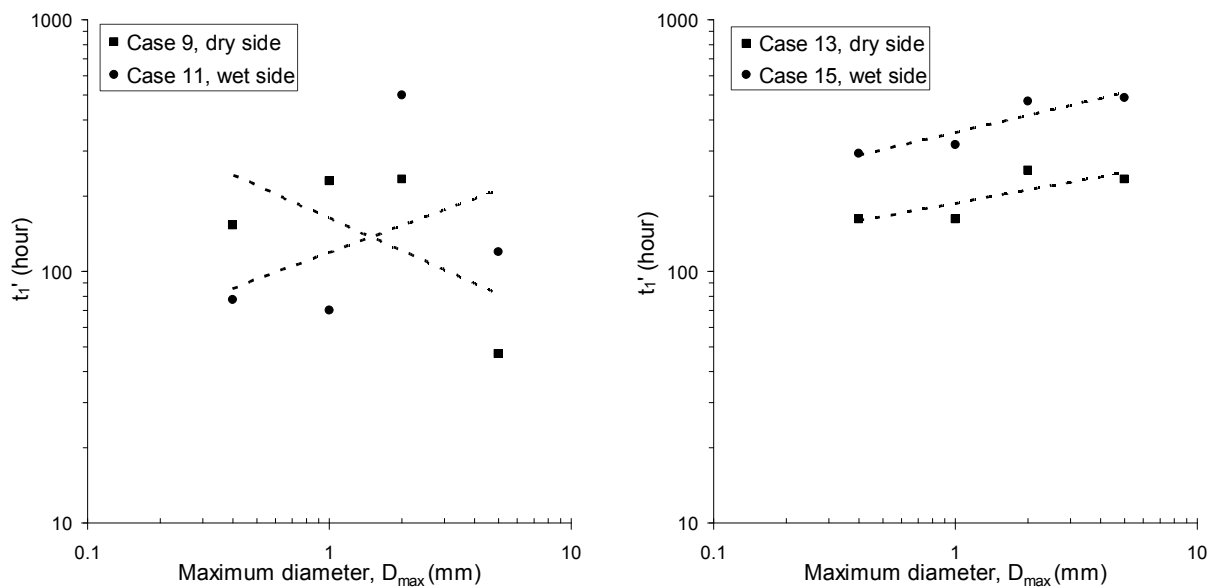


(a) Method 1

(b) Method 2

Figure 6-14 Parameter  $G_{fi}$  versus  $D_{max}$  for the 3% cement treated silt

Figure 6-15 presents  $t_1'$  versus  $D_{max}$  for the 3% cement treated silt. For method 1,  $t_1'$  shows very scattered variations with  $D_{max}$ . A global decreasing trend for the dry side (case 9) and slightly increasing trend for the wet side (case 11) can be identified. For method 2,  $t_1'$  increases slightly with increase of  $D_{max}$  for both the dry side and wet side, with relatively higher values for the wet side.



(a) Method 1

(b) Method 2

Figure 6-15 Starting time of the second stage  $t_1'$  versus  $D_{max}$  for the 3% cement treated silt

Figure 6-16 presents parameter  $V_2$  versus  $D_{max}$  for the 3% cement treated silt. For method 1,  $V_2$  decreases with increase of  $D_{max}$  for both the dry and wet sides, with higher variations for the dry side. For method 2,  $V_2$  decreases with increase of  $D_{max}$  for the wet side, whereas it increases with increase of  $D_{max}$  for the dry side.

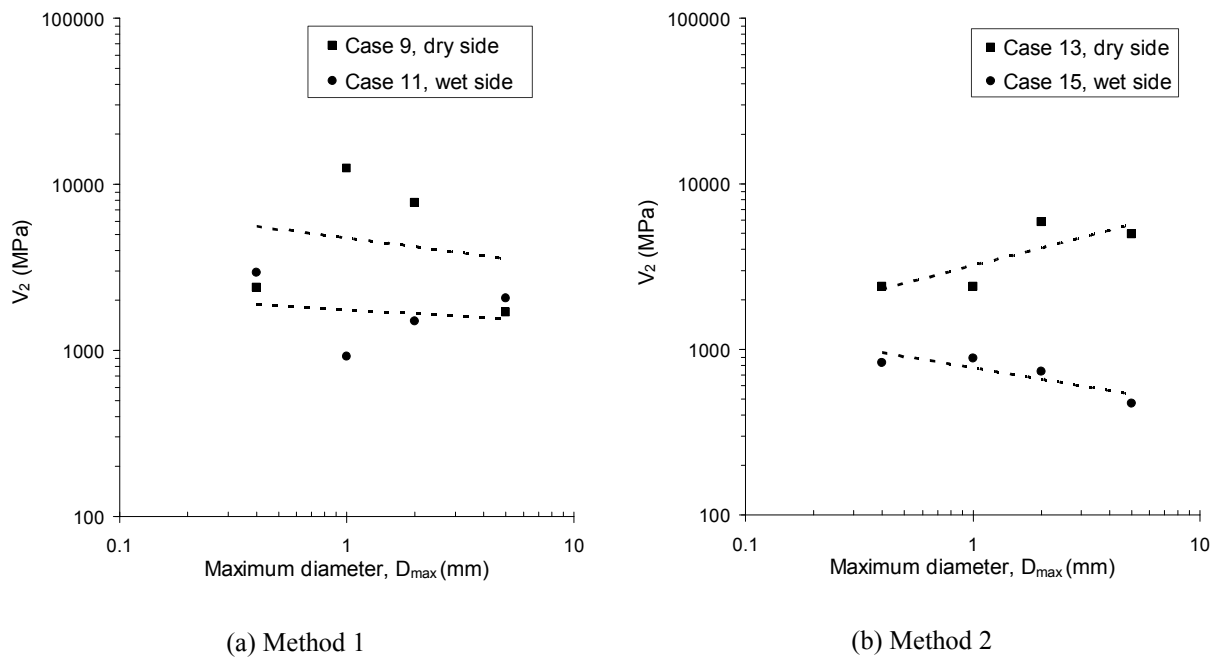


Figure 6-16 Parameter  $V_2$  versus  $D_{max}$  for the 3% cement treated silt

Figure 6-17 presents  $G_{f2}$  versus  $D_{max}$  for the 3% cement treated silt. For method 1,  $G_{f2}$  shows almost parallel decreasing trends with increase of  $D_{max}$  for the dry and wet sides, with higher values for the dry side. For method 2,  $G_{f2}$  also decreases with increase of  $D_{max}$  for the dry side. However, for the wet side, it increases slightly with increase of  $D_{max}$ , with much lower values as compared to those for the dry side.

Summarising, for the silt, comparison of the results between the dry side and wet side shows that method 2 often results in higher difference than for method 1 for all the five parameters. This indicates that method 2 results in larger difference in terms of homogeneity between the wet side and dry side. In other words, the effect of water content changes is more significant for the silt prepared by method 2 than by method 1.

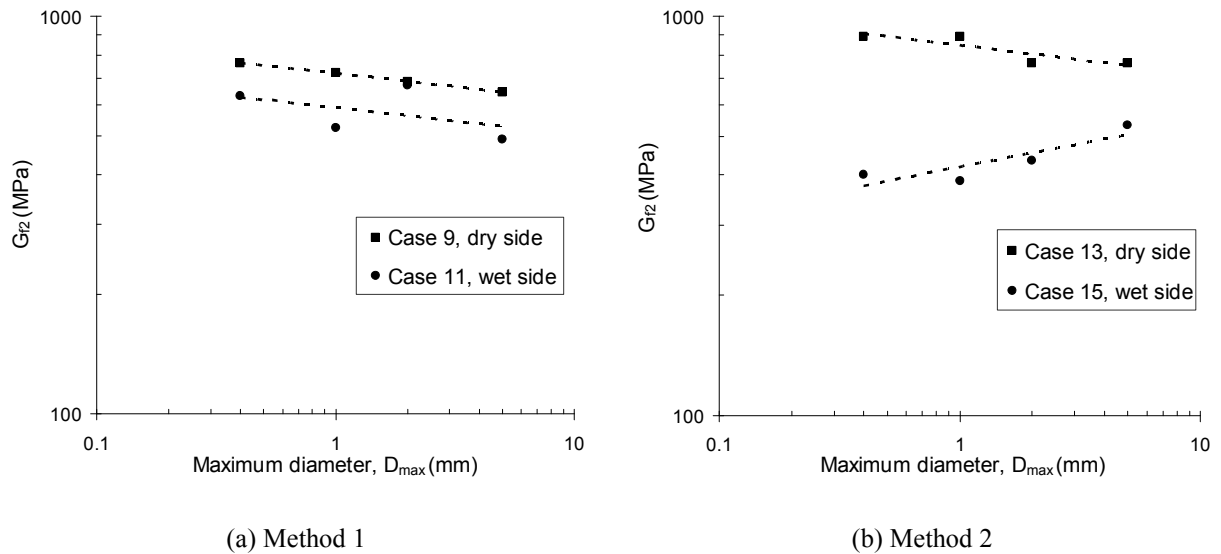


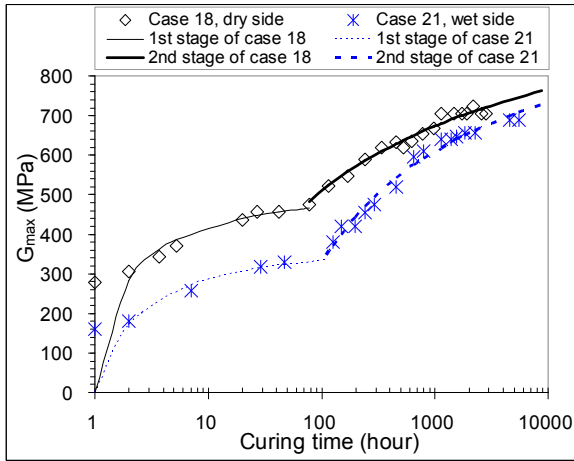
Figure 6-17 Parameter  $G_{12}$  versus  $D_{max}$  for the 3% cement treated silt

## 6.4. Modelling of the curing behaviour of lime treated clay

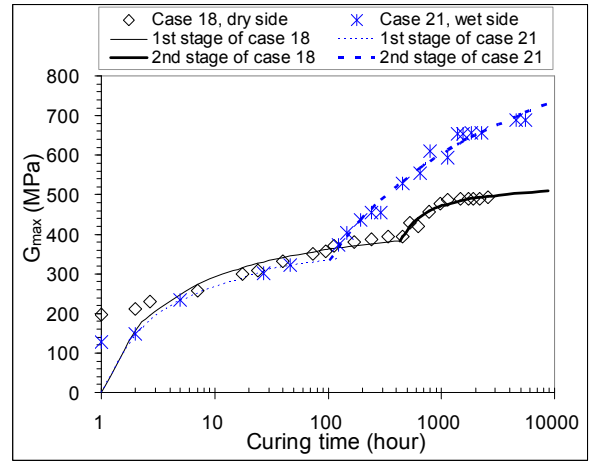
### 6.4.1. Curing behaviour

In the case of lime treated clay, the  $G_{max}$  development curves are significantly different for the soils compacted on the dry side and wet side. Moreover, they are also aggregate size dependent.

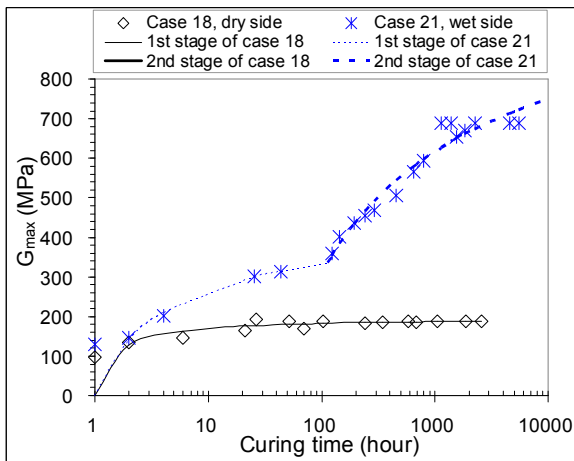
Figure 6-18 presents the modelling results for the 4% lime treated clay of different sub-series prepared with mixing method A. Good agreement is obtained between the measurements and calculations. Comparison between the curves of different subseries shows that for the dry side, the two-stage nonlinear  $G_{max}$  development is decreasing with increase of  $D_{max}$ , whereas for the wet side, a typical two-stage development is identified for all the four aggregate sizes.



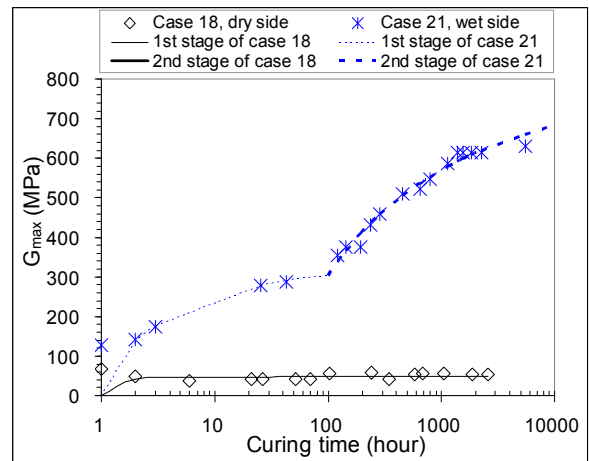
(a)  $D_{\max} = 0.4 \text{ mm}$



(b)  $D_{\max} = 1 \text{ mm}$



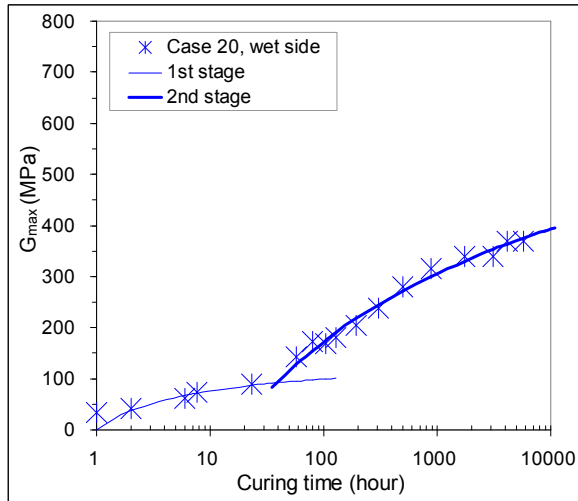
(c)  $D_{\max} = 2 \text{ mm}$



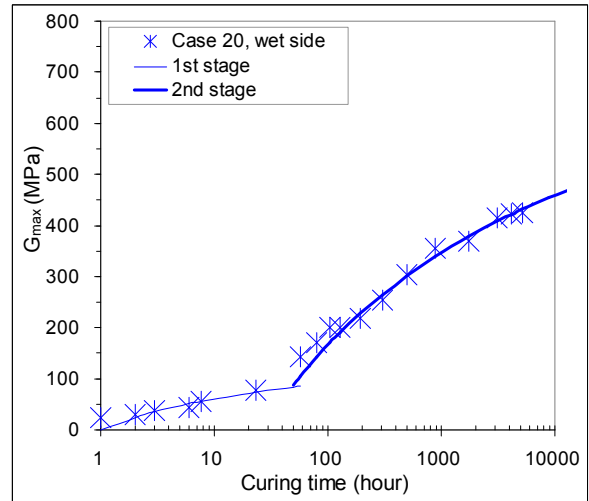
(d)  $D_{\max} = 5 \text{ mm}$

**Figure 6-18 Modelling of the curing behaviour of the 4% lime treated clay by mixing method A (case 18, 21)**

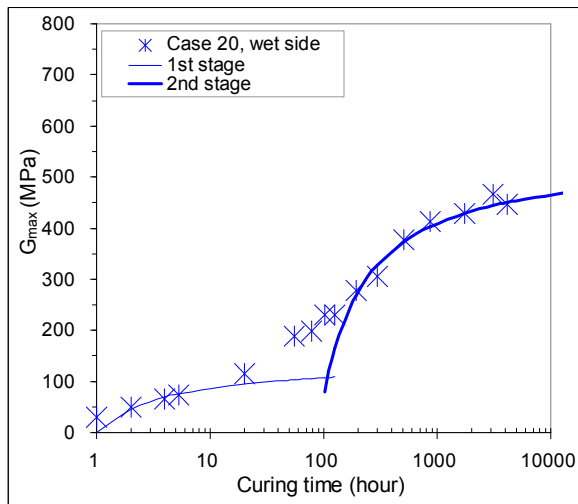
For mixing method B, Figure 6-19 shows the results of specimens with the same treatment but compacted on the wet side. A typical two-stage development is also observed. For the dry side specimens of the large aggregates size sub-series (ex.  $D_{\max} = 2 \text{ mm}$ ,  $5 \text{ mm}$ , case 18), the second stage does not seem to start.



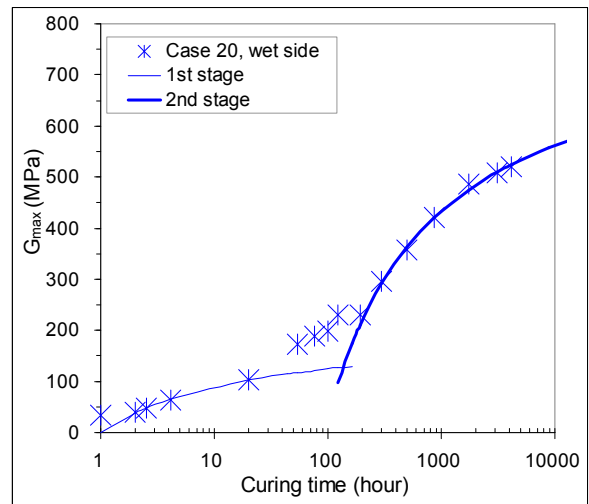
(a)  $D_{\max} = 0.4$  mm, wet side



(b)  $D_{\max} = 1$  mm, wet side



(c)  $D_{\max} = 2$  mm, wet side



(d)  $D_{\max} = 5$  mm, wet side

Figure 6-19 Modelling of the curing behaviour of the 4% lime treated clay by mixing method B (case 20)

### 6.4.2. Model parameters for different aggregates sizes

Figure 6-20 presents parameter  $V_1$  versus  $D_{\max}$  for the 4% lime treated clay. For mixing method A, the decreasing trends for both the dry and wet sides are observed (case 18, 21), with less noticeable decrease for the wet side. For mixing method B,  $V_1$  varies slightly with  $D_{\max}$ , showing no significant aggregates size effect of  $D_{\max}$  (case 20).

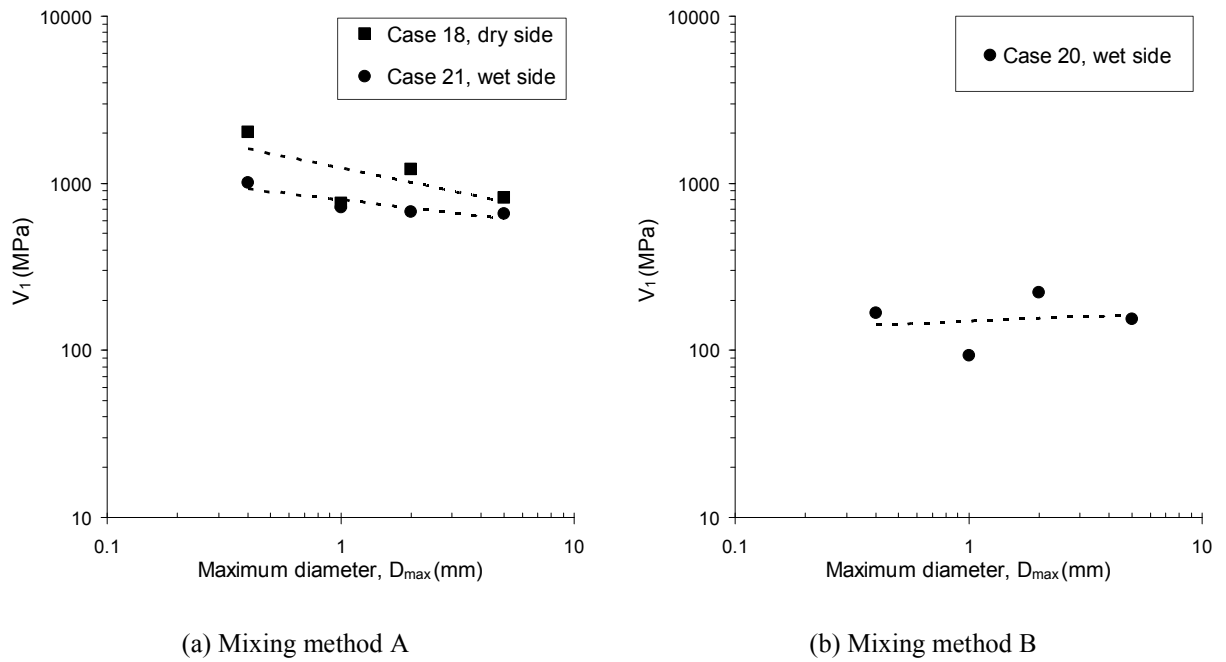


Figure 6-20 Parameter  $V_1$  versus  $D_{max}$  for the 4% lime treated clay (case 18, 21 and 20)

Figure 6-21 presents the final soil stiffness value of the first stage  $G_{f1}$  versus  $D_{max}$  for the 4% lime treated clay. For the dry side,  $G_{f1}$  decreases significantly with increase of  $D_{max}$  for mixing method A. For the wet side, it is almost constant with increase of  $D_{max}$  for both mixing method A and B.

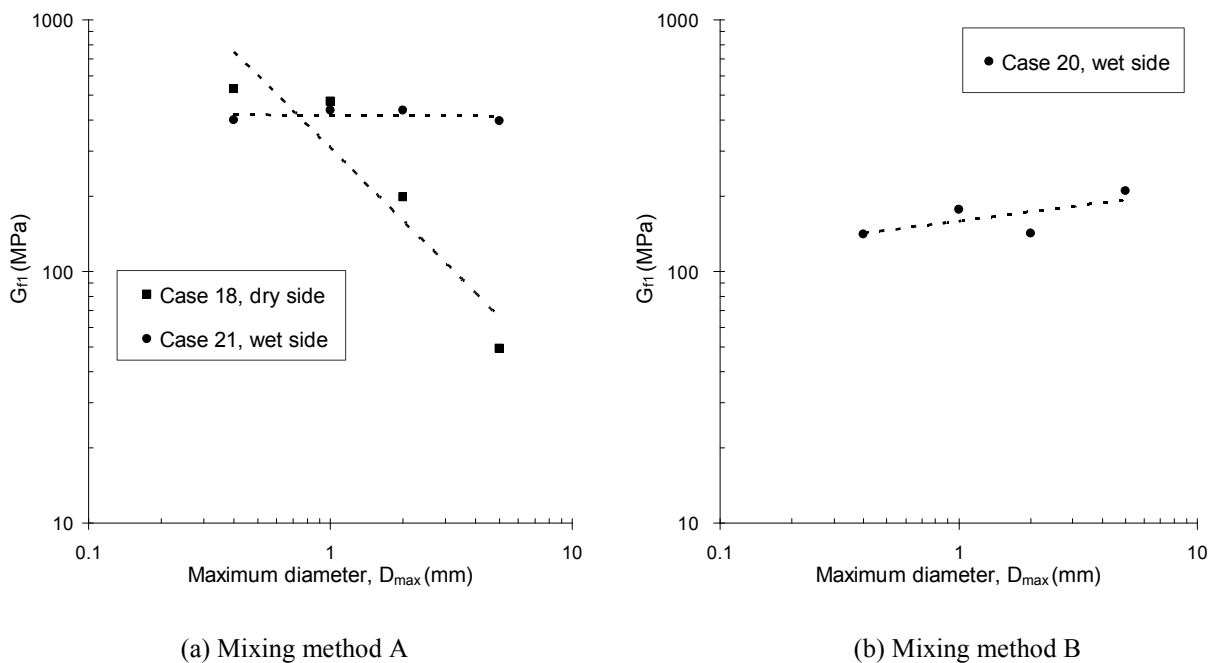


Figure 6-21 Maximum stiffness value of the first stage  $G_{f1}$  versus  $D_{max}$  for the 4% lime treated clay

Figure 6-22 presents the starting time of the second stage  $t'_1$  versus  $D_{max}$  for the 4% lime treated clay. For mixing method A,  $t'_1$  is constant with increase of  $D_{max}$  for the wet side, whereas it is increasing for the dry side (case 18). For mixing method B and compacted on wet side,  $t'_1$  is increasing with increase of  $D_{max}$ .

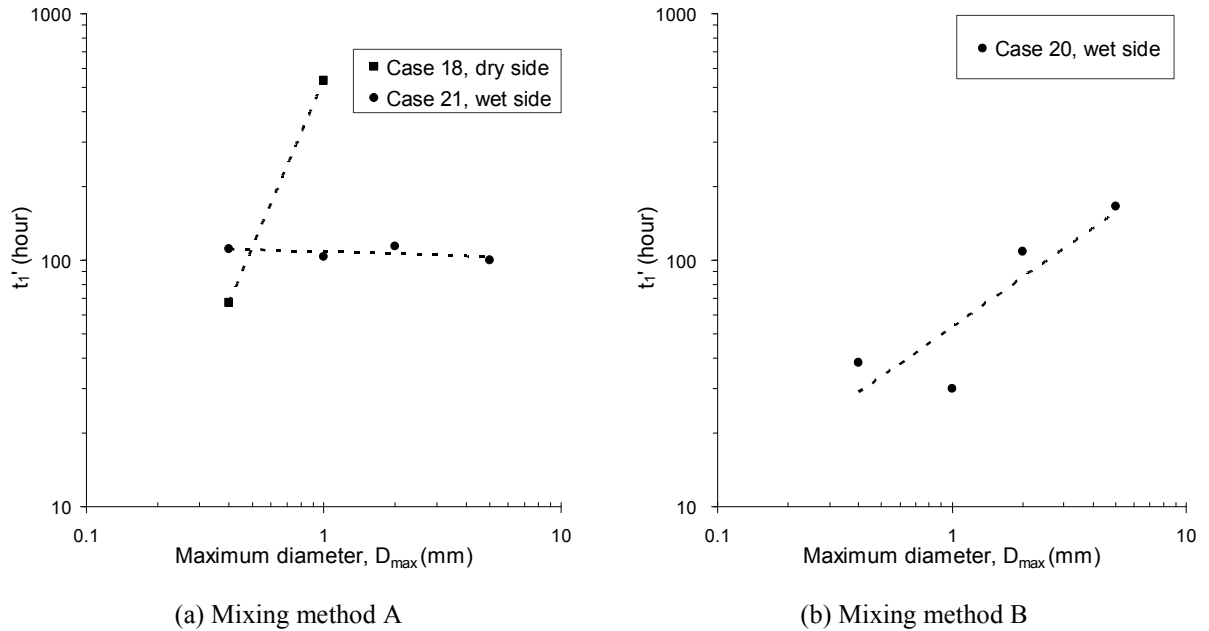


Figure 6-22 Starting time of the second stage  $t'_1$  versus  $D_{max}$  for the 4% lime treated clay

Figure 6-23 shows parameter  $V_2$  versus  $D_{max}$  for the 4% lime treated clay. On the whole, the trends are similar to that for  $t'_1$ .

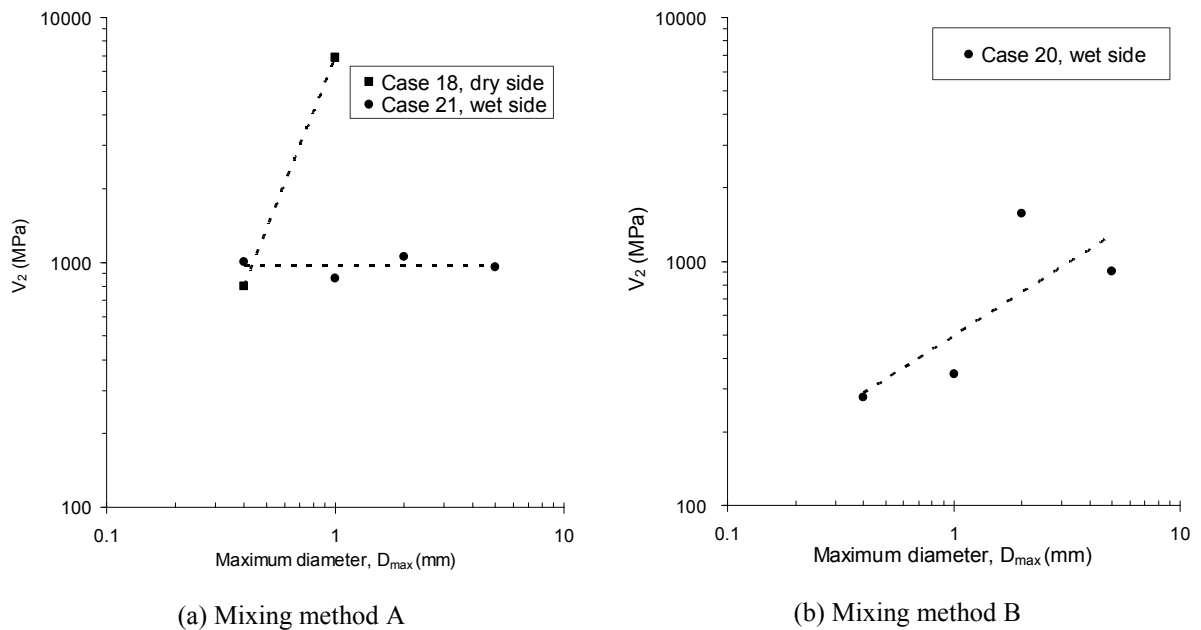


Figure 6-23 Parameter  $V_2$  versus  $D_{max}$  for the 4% lime treated clay



Figure 6-24 presents the maximum value of the second stage  $G_{f2}$  versus  $D_{max}$  for the 4% lime treated clay. On the whole, for mixing method A, decreasing trends with increase of  $D_{max}$  are observed for both the dry and wet sides, particularly for the dry side. For mixing method B, it is also decreasing, with a much greater data scatter.

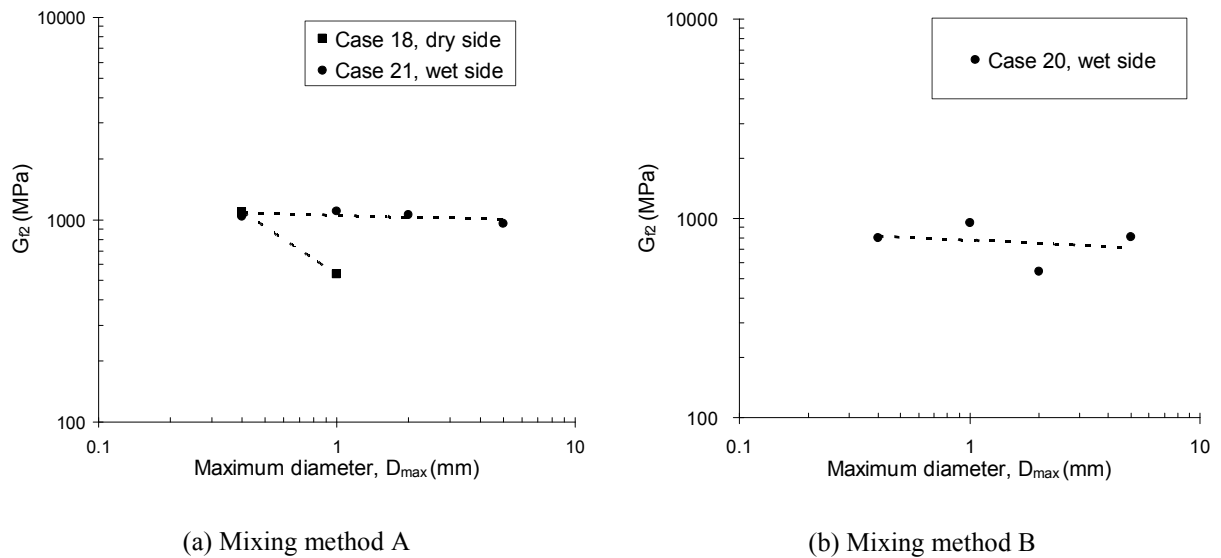


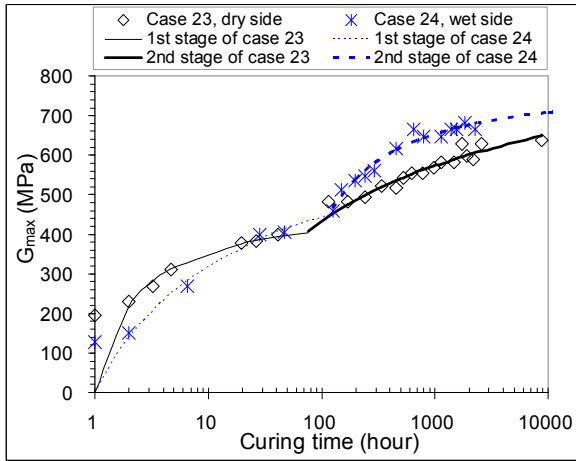
Figure 6-24 Maximum value of the second stage  $G_{f2}$  versus  $D_{max}$  for the 4% lime treated clay (case 18, 21, 20)

## 6.5. Modelling of the curing behaviour of mixture treated clay

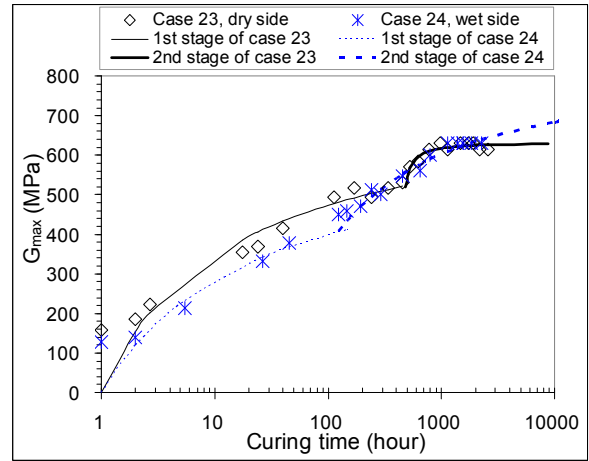
### 6.5.1. Curing behaviour

Figure 6-25 and Figure 6-26 present the modelling of the curing behaviour of the mixture (2% lime plus 3% cement) treated clay prepared by mixing method A and mixing method B, respectively.

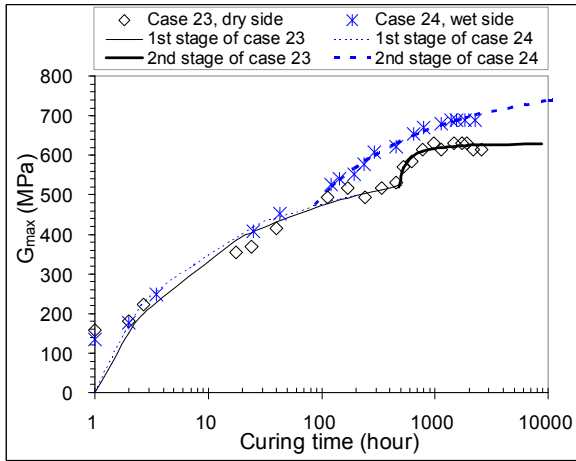
Similar to the lime treated clay, the mixture treated clay also presents significant difference in  $G_{max}$  development between the dry side and the wet side. For mixing method A, one of the main differences is that the mixture treated clay shows less typical two-stage development as compared to the lime treated one. As for the lime treated clay, for the large aggregates size sub-series  $D_{max} = 5$  mm (dry side, case 23), the second stage does not seem to begin.



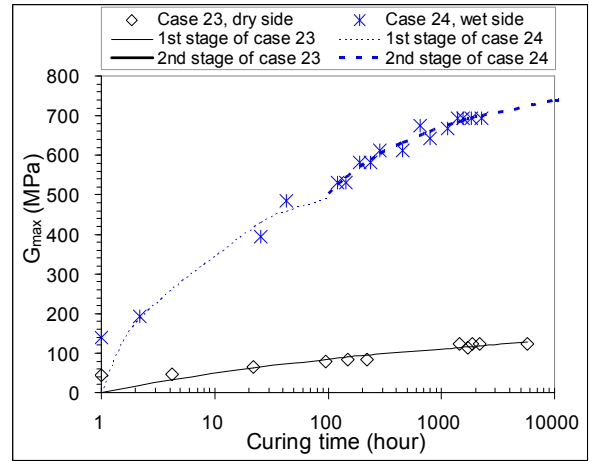
(a)  $D_{max} = 0.4 \text{ mm}$



(b)  $D_{max} = 1 \text{ mm}$

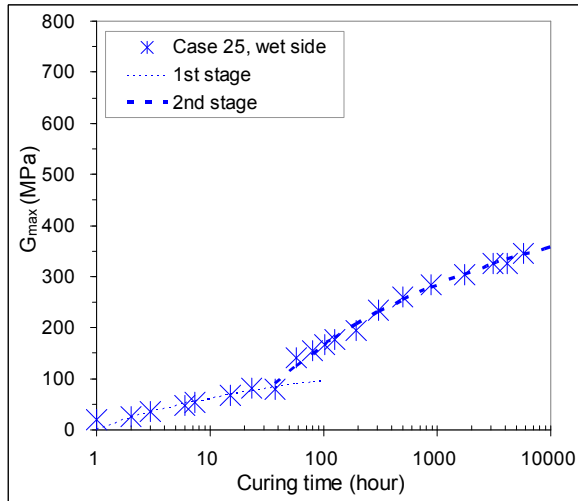


(c)  $D_{max} = 2 \text{ mm}$

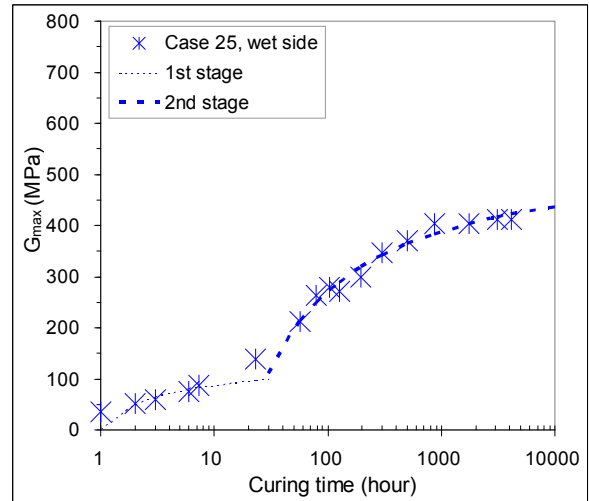


(d)  $D_{max} = 5 \text{ mm}$

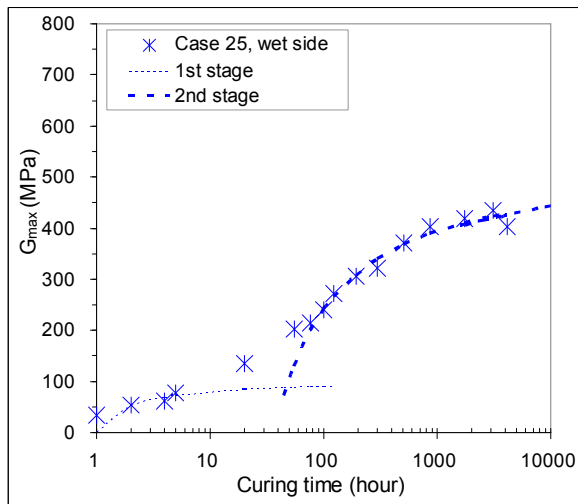
Figure 6-25 Modelling of the curing behaviour of the 2% lime plus 3% cement treated clay by mixing method A (case 23, 24)



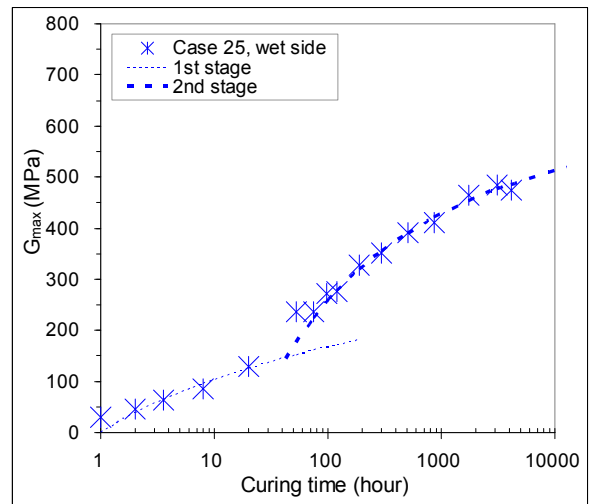
(a)  $D_{max} = 0.4$  mm, wet side



(b)  $D_{max} = 1$  mm, wet side



(c)  $D_{max} = 2$  mm, wet side



(d)  $D_{max} = 5$  mm, wet side

**Figure 6-26 Modelling of the curing behaviour of the 2% lime plus 3% cement treated clay by mixing method B (case 25)**

### 6.5.2. Model parameters for different aggregates sizes

Figure 6-27 presents parameter  $V_1$  versus  $D_{max}$  for the 2% lime plus 3% cement treated clay. For mixing method A,  $V_1$  significantly decreases with increase of  $D_{max}$  for the dry side (case 23). Note that a very low value of 60 MPa is observed for  $D_{max} = 5$  mm, suggesting a negligible  $V_1$  for the large aggregates soils. A slight increase with increase of  $D_{max}$  is identified for the wet side (case 24). For mixing method B,  $V_1$  also slightly increases with  $D_{max}$ , but with larger scatter of data.

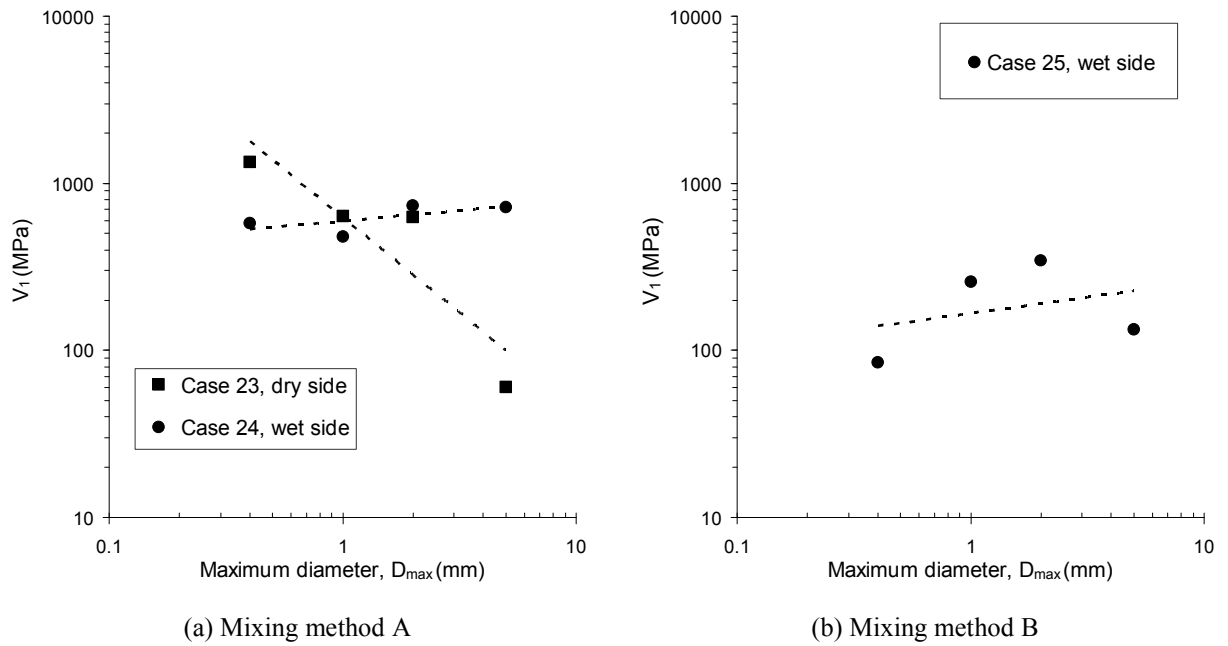


Figure 6-27 Parameter  $V_1$  versus  $D_{max}$  for the 2% lime plus 3% cement treated clay (case 23, 24, 25)

Figure 6-28 shows the maximum value of the first stage  $G_{f1}$  versus  $D_{max}$  for the 2% lime plus 3% cement treated clay. For mixing method A,  $G_{f1}$  is significantly decreasing with  $D_{max}$  with a large data scatter, whereas it is slight increasing with  $D_{max}$  for the wet side. For mixing method B, it is also slightly increasing with  $D_{max}$  for the wet side, but with much data scatter.

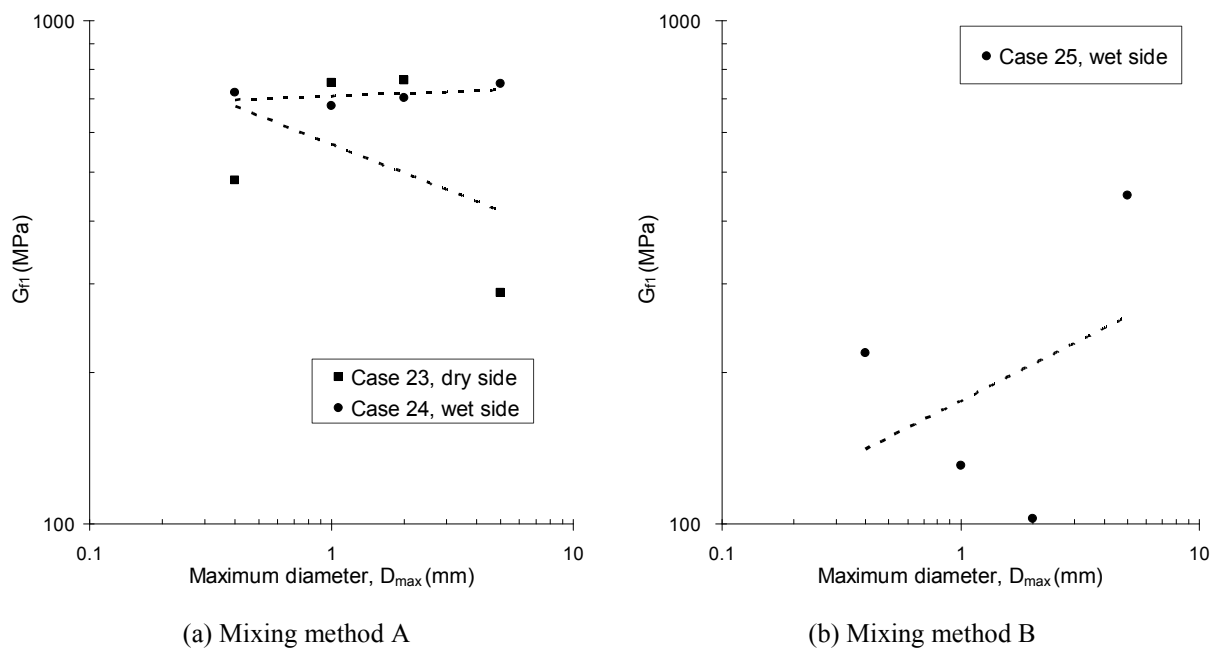


Figure 6-28 Maximum value of the first stage  $G_{f1}$  versus  $D_{max}$  for the 2% lime plus 3% cement treated clay

Figure 6-29 presents the starting time of the second stage  $t'_1$  versus  $D_{max}$  for the 2% lime plus 3% cement treated clay. For mixing method A,  $t'_1$  increases significantly with increase of  $D_{max}$  for the dry side, whereas it decreases slightly with  $D_{max}$  for the wet side. For mixing method B and compacted on the wet side, it is slightly increasing with  $D_{max}$ .

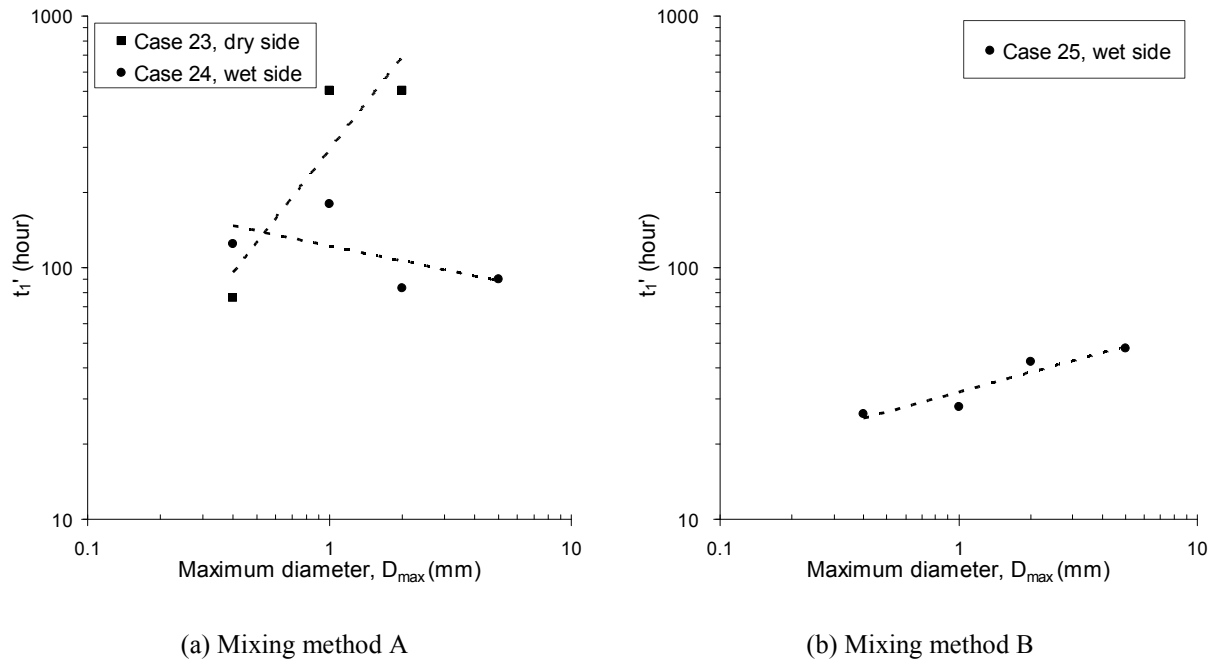
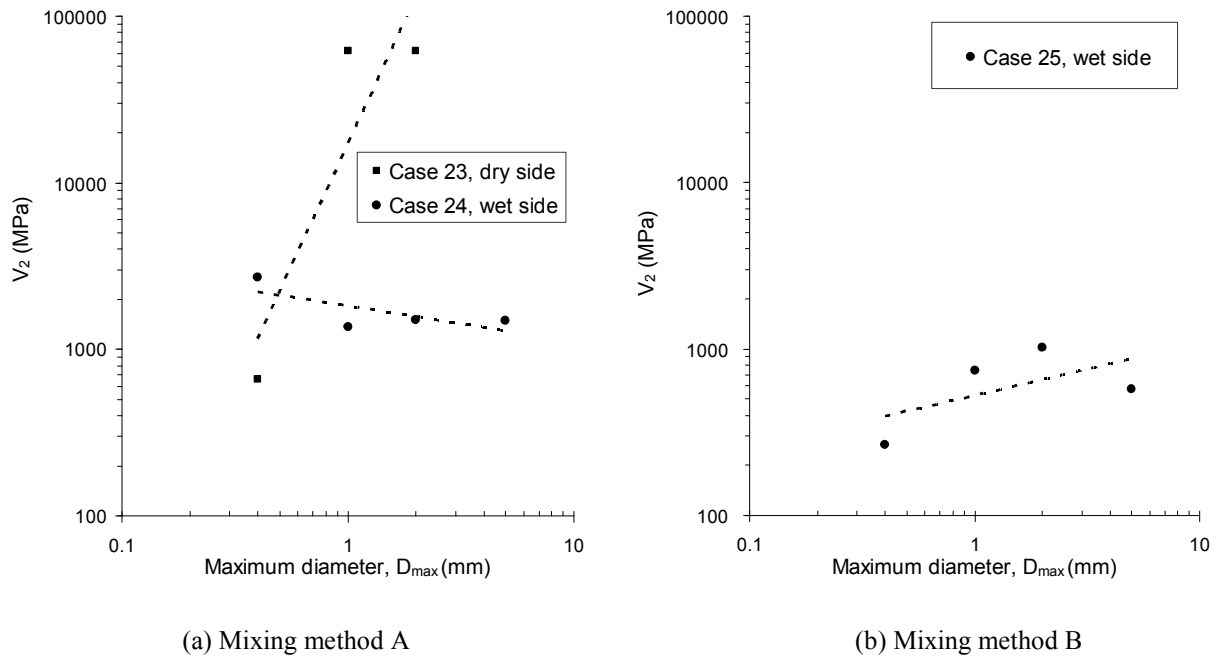


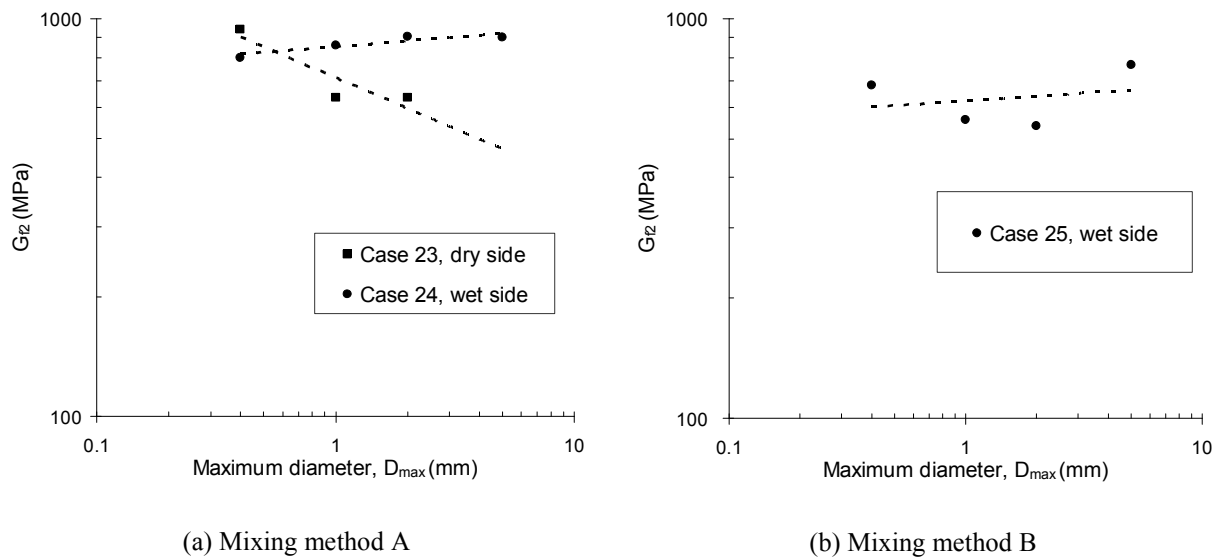
Figure 6-29 Starting time of the second stage  $t'_1$  versus  $D_{max}$  for the 2% lime plus 3% cement treated clay

Figure 6-30 presents parameter  $V_2$  versus  $D_{max}$  for the 2% lime plus 3% cement treated clay. For mixing method A,  $V_2$  is increasing with  $D_{max}$  for the dry side, whereas it is slightly decreasing with  $D_{max}$  for the wet side. For the clay with mixing method B and compacted on the wet side, it showing a slightly increasing trend with  $D_{max}$ .

Figure 6-31 shows the maximum stiffness value of the second stage  $G_{f2}$  versus  $D_{max}$  for the 2% lime plus 3% cement treated clay. For mixing method A,  $G_{f2}$  decreases significantly with increase of  $D_{max}$  for the dry side, whereas it increases slightly with increase of  $D_{max}$  for the wet side. For mixing method B and compacted on wet side, it is also slightly increasing with  $D_{max}$ , but with much higher data scatter.



**Figure 6-30 Parameter  $V_2$  versus  $D_{max}$  for the 2% lime plus 3% cement treated clay**



**Figure 6-31 Maximum stiffness value of the second stage  $G_{12}$  versus  $D_{max}$  for the 2% lime plus 3% cement treated clay (case 23, 24 and 25)**

Summarising, for all the five parameters of the model, comparison between the dry side and wet side for the clay by mixing method A shows that similar values are obtained for the small aggregates size ( $D_{max} = 0.4$  mm). Then, the difference increases with increase of

$D_{\max}$ . For the wet side, mixing method B often results in larger data scatter as compared to mixing method A.

As all results show a linear relationship between each model parameter and  $D_{\max}$  in a logarithmic plane, a power function has been used to describe the relationships identified (Eq. 6-5).

$$y = m * D_{\max}^n \quad (6-5)$$

where,  $m$ ,  $n$  are constants.

## 6.6. Synthesis of the aggregates size effect

Based on the modelling results for the treated soils, the evolutions of the model parameters with increase of  $D_{\max}$  have been determined. The values for all the parameters are available in Table 6-1.

Table 6-2 summarises all the evolution trends of these parameters, involving the silt and clay of different sub-series prepared by sieving method 1 and 2, treated by lime and/or cement, mixed with method A and method B, and compacted at various moulding water contents on dry and wet sides of optimum. We observe that the variation trend of the model parameters with increase of  $D_{\max}$  depends on the soil powder preparation methods, mixing methods, treatments, and water contents. In general, most of these parameters decrease (-) or remain constant (0) with the increase of  $D_{\max}$ , especially for the dry side. Different trends often appear for the wet side, the cement treatment, the clay mixed with additives by mixing method B. It is worth noting that the aggregates size effect is especially noticeable for parameter  $G_{f2}$ , as it is almost decreasing with increase of  $D_{\max}$  in all cases.

These variation trends of parameters suggest that the stiffness of cementitious treated soils depends mainly on three factors: 1) aggregates size and their distribution that define the total contact surfaces and contact chains; 2) water availability (depending on the aggregates size) as well as water content; 3) additive distribution that depends on the aggregates size distribution and the mixing method.

Table 6-1 Values of parameters for all the treated soils in laboratory conditions

Soil type		Héricourt Silt (A2)								Héricourt Clay (A4)					
Treatment		2% lime				3% cement				4% lime			2% lime + 3% cement		
Sieving method		1*	1*	2*	2*	1*	1*	2*	2*	2*	2*	2*	2*	2*	
Mixing method		B	B	B	B	B	B	B	B	A	A	B	A	A	B
Compaction state		dry	wet	dry	wet	dry	wet	dry	wet	dry	wet	wet	dry	wet	wet
Case		1	3	5	7	9	11	13	15	18	21	20	23	24	25
V <sub>1</sub>	D <sub>max</sub> = 0.4 mm	1654	1066	1633	158	1742	1517	1466	301	2021	1005	167	1329	576	85
	D <sub>max</sub> = 1 mm	3003	942	1374	193	1935	778	1479	283	765	713	93	635	478	256
	D <sub>max</sub> = 2 mm	1287	716	2099	291	1656	1127	1741	261	1215	670	221	624	736	343
	D <sub>max</sub> = 5 mm	702	502	2383	416	1519	875	1087	308	817	657	154	60	716	133
G <sub>fl</sub>	D <sub>max</sub> = 0.4 mm	527	446	330	294	631	501	770	310	529	400	141	482	719	219
	D <sub>max</sub> = 1 mm	402	299	358	249	696	483	768	355	474	437	177	754	679	131
	D <sub>max</sub> = 2 mm	392	279	323	164	639	496	632	422	197	437	142	761	702	102
	D <sub>max</sub> = 5 mm	275	285	311	150	445	397	685	398	49	395	209	288	749	450
t <sub>1</sub>	D <sub>max</sub> = 0.4 mm	53	91	68	30	25	27	20	75	6	34	16	6	49	15
	D <sub>max</sub> = 1 mm	38	59	76	147	100	3	20	66	277	29	26	431	33	19
	D <sub>max</sub> = 2 mm	38	54	41	62	94	70	112	60	-	38	89	431	19	37
	D <sub>max</sub> = 5 mm	52	54	16	198	14	38	90	35	-	34	-	-	17	21
t <sub>1</sub> '	D <sub>max</sub> = 0.4 mm	182	564	145	483	152	77	162	294	67	111	38	76	125	26
	D <sub>max</sub> = 1 mm	85	100	66	501	229	70	162	319	534	103	30	506	180	28
	D <sub>max</sub> = 2 mm	77	85	76	241	233	500	251	475	-	113	109	507	83	42
	D <sub>max</sub> = 5 mm	92	94	51	288	47	119	232	489	-	100	165	-	90	48
V <sub>2</sub>	D <sub>max</sub> = 0.4 mm	1869	3925	1423	203	2388	2924	2393	836	800	1008	276	663	2697	266
	D <sub>max</sub> = 1 mm	1993	2688	2671	617	12479	916	2393	883	6891	861	346	61830	1360	741
	D <sub>max</sub> = 2 mm	1998	1928	1157	332	7705	1507	5925	735	-	1050	1570	61830	1498	1018
	D <sub>max</sub> = 5 mm	1566	1499	1064	1508	1694	2072	4938	474	-	955	-	-	1478	577
G <sub>2</sub>	D <sub>max</sub> = 0.4 mm	893	515	848	583	761	631	889	400	1095	1032	802	942	800	683
	D <sub>max</sub> = 1 mm	819	469	742	331	721	524	889	388	537	1101	945	634	858	558
	D <sub>max</sub> = 2 mm	760	516	730	409	684	671	764	436	-	1058	543	634	902	538
	D <sub>max</sub> = 5 mm	584	542	645	283	643	490	761	532	-	959	-	-	899	768



**Table 6-2 Evolution of the model parameters with increase of  $D_{max}$  [(+): increase; (-): decrease; (0): constant]**

Soil type	Héricourt Silt (A2)								Héricourt Clay (A4)					
Treatment	2% lime				3% cement				4% lime			2% lime plus 3% cement		
Sieving method	1*	1*	2*	2*	1*	1*	2*	2*	2*	2*	2*	2*	2*	2*
Mixing method	B	B	B	B	B	B	B	B	A	A	B	A	A	B
Compaction state	dry	wet	dry	wet	dry	wet	dry	wet	dry	wet	wet	dry	wet	wet
Case	1	3	5	7	9	11	13	15	18	21	20	23	24	25
$V_1$	(-)	(-)	(+)	(+)	(-)	(-)	(-)	(-)	(-)	(-)	(+)	(-)	(+)	(+)
$G_{fl}$	(-)	(-)	(-)	(-)	(-)	(-)	(-)	(+)	(-)	(-)	(+)	(-)	(+)	(+)
$t_1$	(-)	(-)	(-)	(+)	(-)	(+)	(+)	(-)	(+)	(+)	(+)	(+)	(-)	(+)
$t_1'$	(-)	(-)	(-)	(-)	(-)	(+)	(+)	(+)	(+)	(-)	(+)	(+)	(-)	(+)
$V_2$	(-)	(-)	(-)	(+)	(-)	(-)	(+)	(-)	(+)	(0)	(+)	(+)	(-)	(+)
$G_p$	(-)	(+0)	(-)	(-)	(-)	(-)	(-)	(+)	(-)	(-)	(-0)	(-)	(+0)	(0/+)

Note: A- mixing method A; B- mixing method B; 1\*- soil powders prepared by method 1; 2\*- soils powders prepared by method 2.

Compacted soils are constituted of aggregates and their stiffness depends on the stiffness of individual aggregates as well as the force/chains between them. Lime and/or cement treatments can significantly increase the stiffness of aggregates and the chains between them thanks to the reactions between soil minerals and additives. Obviously, the aggregates size effect is mainly defined by the total contact surface between soils and additives. This is also evidenced by Tang *et al.* (2011). Normally, Small aggregates correspond to a higher stiffness. This is identified on both the soils treated in laboratory (chapter 3) and *in-situ*.

Water content impacts the stiffness of soils through the suction effect as identified in chapter 3. Moreover, water content can impact the mixing effect as discussed in chapter 2 and chapter 3. On other hand, water availability is essential for the stiffness development because the production of cementitious compounds consumes water. Note that water availability can be different under the same water content, and it depends on the aggregates size distribution and mixing method. A good mixing allows the reactions to be fully developed if sufficient water is available (ex. the finer soils with mixing method A).

Additive distribution also significantly affects the soil stiffness. At the same dosage of additives, a higher stiffness can be expected with homogenous distribution of additives. In the

laboratory conditions, the aggregates size considered is often limited. Thus, the difference in stiffness is not significant. In contrast, in the field conditions, much larger aggregates size is expected and this aggregates size effect can be much pronounced.

## **6.7. Application of the hyperbolic model to the field aggregates size level**

Due to the aggregates size effect mentioned before, it is impossible to directly compare the laboratory results with the field ones. Indeed, in the laboratory, the initial maximum aggregate size is only 0.4 mm to 5 mm, whereas in field, it is up to 31.5 mm for the clay and 20 mm for the silt. Moreover, the measurements time is also different for the laboratory and field specimens: it is 3 ~ 7 months for the measurements on laboratory specimens, and 7 ~ 31 months for the measurements on field specimens.

Based on the hyperbolic model developed using the laboratory results, the field aggregates size scale can be investigated. Firstly, using the tendencies of each parameters obtained in the laboratory (parameter  $y = m \cdot D_{\max}^n$ ), we can obtain the value of each parameter at any corresponding aggregates size. Then, the  $G_{\max}$ -time curve in field aggregate size scale can be established for each case. Figure 6-32 and Figure 6-33 present the extension of  $G_{\max}$  development to the field aggregates size scale for the silt and the clay by different preparation methods for soil powders, different mixing methods, different water contents (dry and wet side) and different treatments. The two-stage development induced by the two reaction mechanisms can be observed clearly. Note that the values of all parameters at *in-situ* aggregates size scale are available in Table 6-3.

**Table 6-3 Model parameters at in-situ aggregates size scale ( $D_{max} = 20$  mm and 31.5 mm for the silt and the clay, respectively)**

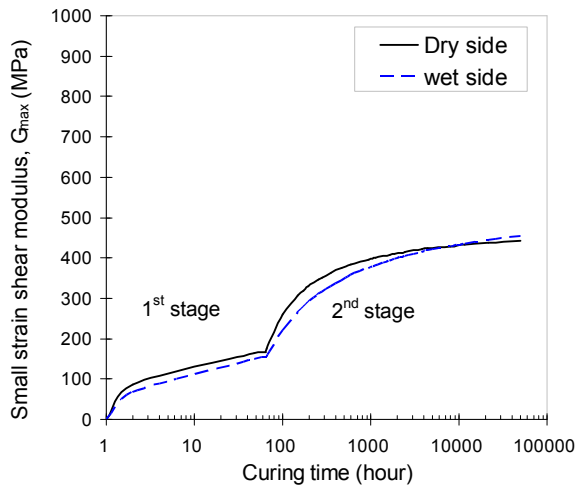
Soil type	Héricourt Silt (A2)								Héricourt Clay (A4)					
	2% lime				3% cement				4% lime			2% lime plus 3% cement		
Treatment	1*		2*		1*		2*		2*		2*		2*	
Sieving method	1*	1*	2*	2*	1*	1*	2*	2*	2*	2*	2*	2*	2*	2*
Mixing method	B	B	B	B	B	B	B	B	A	A	B	A	A	B
Compaction state	dry	wet	dry	wet	dry	wet	dry	wet	dry	wet	wet	dry	wet	wet
$V_1$	503	345	2964	708	1433	670	1110	287	457	453	181	99	906	324
$G_{fl}$	205	204	303	96	413	375	602	492	11	411	242	296	754	403
$t_1$	44	37	9	428	23	71	309	26	1295	38	474	1258	7	40
$V_2$	1556	841	885	2995	2793	1389	9297	390	22888868	967	3811	16960	875	1560
$G_p$	489	550	562	202	586	480	680	594	37	941	644	294	1003	712

Figure 6-32a and b present the  $G_{max}$  development for the 2% lime treated silt at the field aggregate size level ( $D_{max} = 20$  mm) prepared by method 1 and method 2, then compacted on both dry and wet sides. For method 1 (Figure 6-32a),  $G_{max}$  increases with time for the silt compacted on both dry and wet sides, with slightly higher value for the dry side. For method 2 (Figure 6-32b), a much higher  $G_{max}$  value is obtained for the dry side as compared with that for the wet side. Comparison between method 1 and method 2 shows that the  $G_{max}$  values are quite different between the dry and wet sides, suggesting that water effect is much more significant with method 2.

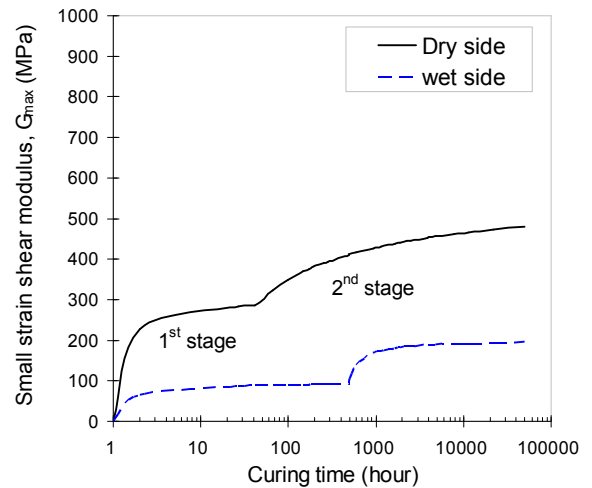
Figure 6-32c and Figure 6-32d present the  $G_{max}$  development at the field aggregate size level ( $D_{max} = 20$  mm) for the 3% cement treated silt prepared by method 1 and method 2 then compacted on both dry and wet sides. On the whole, the  $G_{max}$  of dry side presents much higher values than that of wet side for the both preparation methods, showing a larger stiffness difference between the dry side and wet side in case of method 2. In most cases, the second stage comes later for the wet side as compared to the dry side.

These different  $G_{max}$ -time curves reflect the coupled effects of the total contact surface between soil and additives, the water availability and suction. Firstly, for a given mixing method (method B), mixing on the wet side often leads to larger aggregates or lower suction. This explains why the  $G_{max}$  on dry side is often higher than on wet side. For method 1, the similar development curves for the 2% lime treated silt compacted on dry and wet sides are to be related to the combined effects of aggregate size, water availability and suction. For the

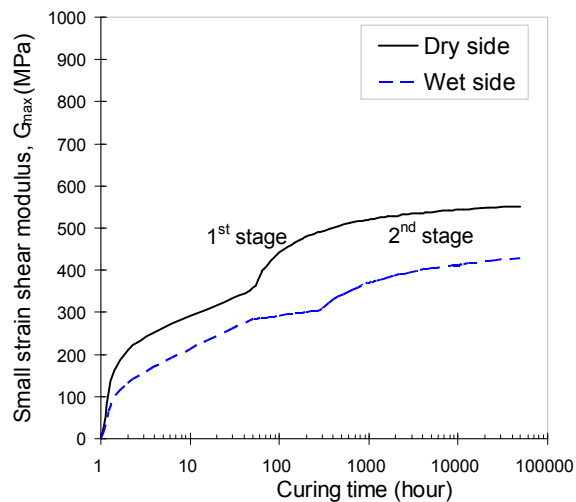
3% cement treatment, the different values of  $G_{max}$  between dry side and wet side suggest less water demand as compared to the 2% lime treatment. Moreover, the significant difference between the dry and wet sides for the two preparation methods (Figure 6-32) indicates the significant difference in aggregates size distribution with mixing method B.



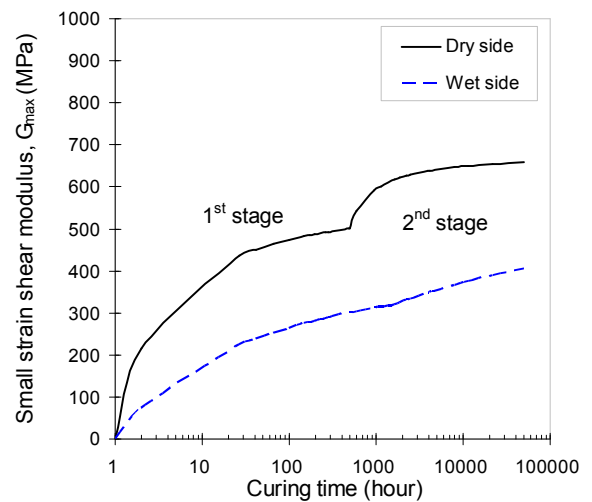
(a) 2% lime treated silt, sieving method No. 1



(b) 2% lime treated silt, sieving method No. 2



(c) 3% cement treated silt, method 1



(d) 3% cement treated silt, method 2

**Figure 6-32 Up-scaled modelling of  $G_{max}$  – time curve for the silt at  $D_{max} = 20$  mm prepared by mixing method B and compacted on both dry and wet sides**

For the clay at the field aggregate size level ( $D_{max} = 31.5$  mm), it is observed that (Figure 6-33): 1) for the wet side,  $G_{max}$  is higher than that for the dry side for both the 4% lime and mix treated clay prepared by method 2 then mixed by both method A and method B; 2) the  $G_{max}$ –time curve corresponding to mixing method A is above that corresponding to

mixing method B for the both treatments; 3) unlike the case of treated silt, the second stage comes earlier for the wet side than for the dry side for the both treatments.

Firstly, the  $G_{max}$  of wet side is higher than that of dry side. This indicates that the effect of water availability prevails on the effect of suction in this large aggregate size level. For the dry state, the water available for the chemical reactions is limited and thus the chemical reactions cannot be fully developed. As a result, the concentrated non-hydrated additives lead to a quite limited contribution to the soil stiffness gain. For the wet state, the difference between method A and method B allows the aggregate size effect to be clearly analysed. The earlier second stage for the wet side indicates the importance of sufficient water to the hydration process and the pozzolanic reactions.

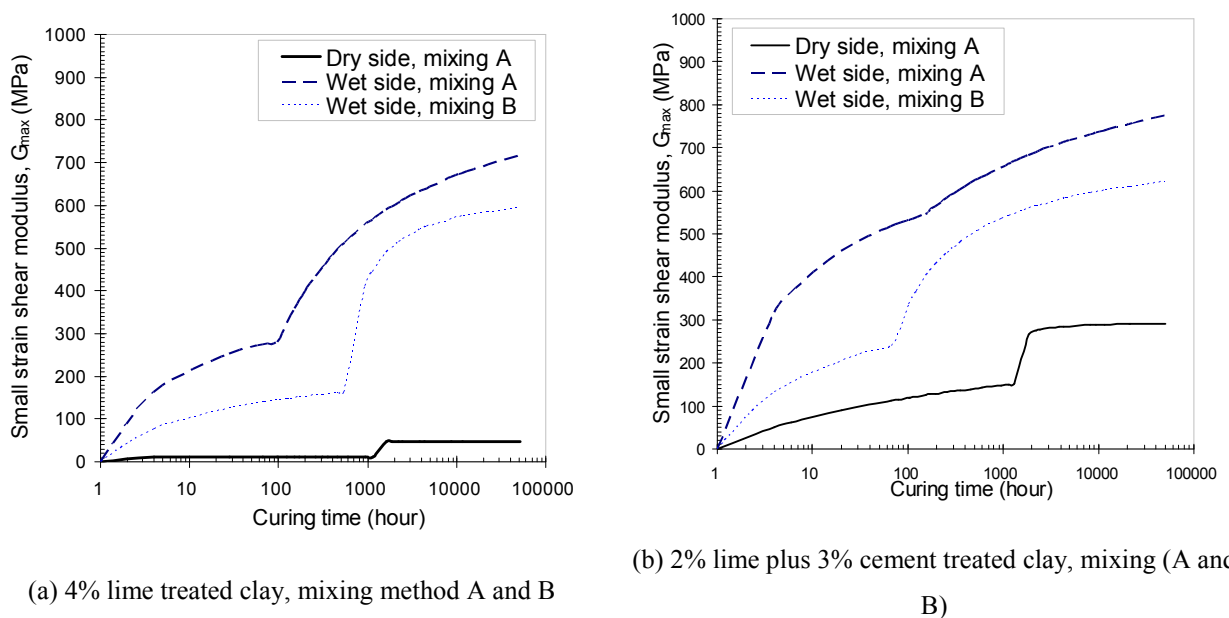


Figure 6-33 Up-scaled modelling of  $G_{max}$  – time curve for the clay at  $D_{max} = 31.5$  mm prepared by both mixing method A and B and compacted on dry and wet sides

## 6.8. Comparisons between laboratory and field conditions

After application of the  $G_{max}$ -time model to the field aggregate size scale, the comparison between laboratory and field can be completed for different curing periods. As observed in chapter 5, the moulding water content of the field compaction is close to that of wet side in the laboratory compaction. Moreover, it is identified that the dry density effect is negligible as compared to the effect of heterogeneity of the *in-situ* soils. Thereby, the comparison is completed only for the compaction of wet side.

Figure 6-34 shows the comparisons of results between field and laboratory for the 2% lime and 3% cement treated silt. Note that both treatments, the first batch core samples - sub-embankment core sample SC20-4 and core sample SC31-1 were used to minimize the effect of climate.

For the 2% lime treated silt (Figure 6-34a), the measurements after 16-month and 30-month curing present a very large data scatter. However, if we consider the mean values, it can be observed that they are close to the predicted ones, between the silt prepared by method 1 and method 2. For the 3% cement treated silt (Figure 6-34b), the three measurements after 7-month, 11-month and 29-month curing also present the very large scatter. The mean values are slightly higher than the predicted ones. This indicates that the mean value of a large number of tests allows the effect of heterogeneity of the *in-situ* soils to be minimized. Moreover, these measurements were identified at the second stage of the stiffness development curves. As mentioned in chapter 5, the increase of  $G_{max}$  by mean value with curing time is attributed to the pozzolanic reactions.

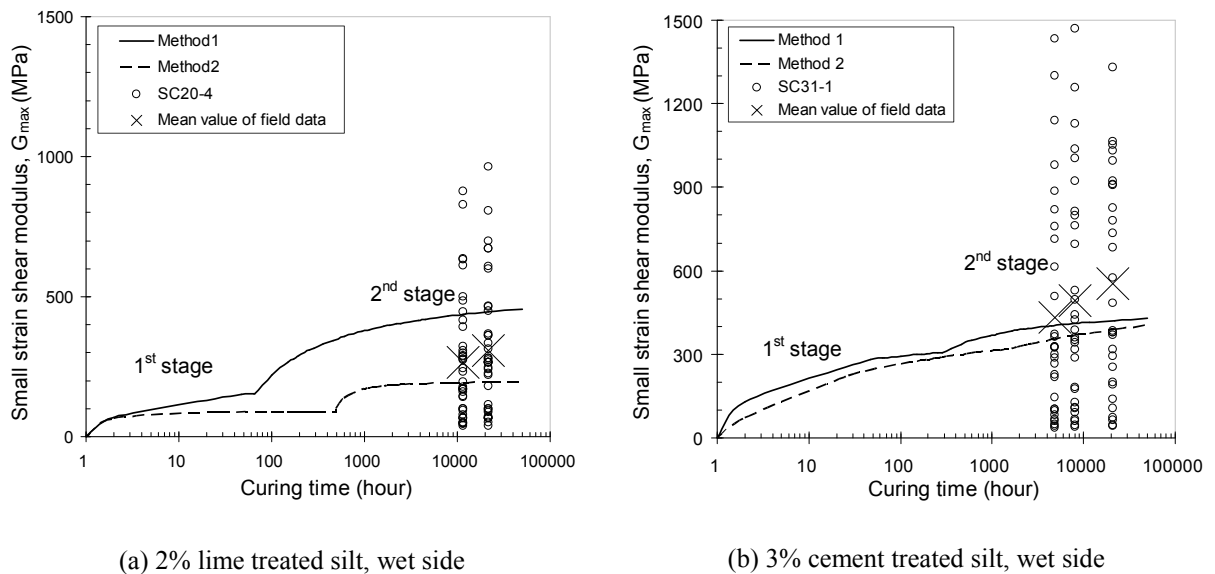
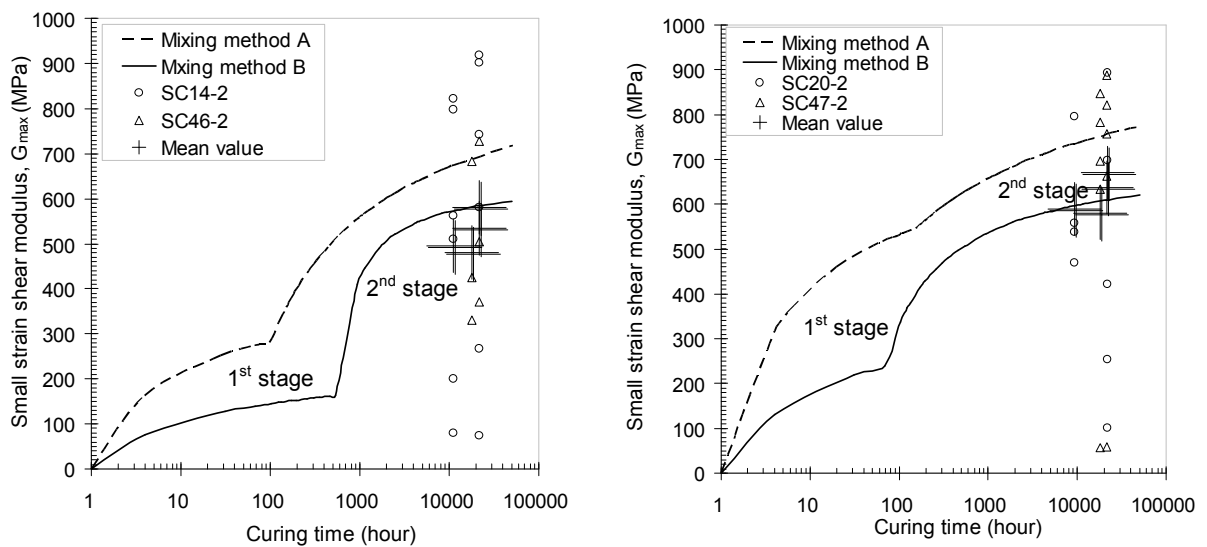


**Figure 6-34 Comparison of the results between the laboratory and field conditions for the silt**

For the clay cores, in order to avoid the effect of climate and underground water, the core samples situated at 1.50 ~ 3.0 m, Zone II (see chapter 5), were considered (SC14-2 / SC46-2 of 4% lime treated clay; SC20-2 / SC47-2 of 2% lime plus 3% cement treated clay). As the mean values of the measurements are proved to be close to the predicted ones for the silt cores, we use the mean value for each compaction layer here. There are about fifteen

measurements for each compaction layer (three specimens per layer and five measurements per specimen).

Figure 6-35 presents the comparisons of the results between the field and laboratory conditions for the 4% lime and 2% lime plus 3% cement treated clay. Though the mean value is used for each compaction layer, large scatter is still observed for both the treatments. The mean values range from less than 100 MPa (similar to that of untreated clay) to more than 900 MPa (due to high concentration of additives). As for the silt, the mean values are also close to predicted ones as (Figure 6-35a and Figure 6-35b), especially in the case of mixing method B. This indicates the difficulty of mixing clay in field conditions.



(a) 4% lime treated clay, wet side

(b) 2% lime plus 3% cement treated clay, wet side

**Figure 6-35 Comparison of the results between the laboratory and field conditions for the clay**

Summarising, the mean values of the *in-situ* results are in agreement with the prediction by the model developed using the parameters identified from the laboratory tests at small aggregate size scale. This shows that it is possible to link the results of laboratory conditions to the results of field conditions based on the consideration of aggregate size effect.

## 6.9. Discussion

### 6.9.1. Modelling and aggregates size effect in laboratory size level

A hyperbolic model is proposed to analyse the  $G_{\max}$ -time development for the soils treated in the laboratory. The non-linger two-stage  $G_{\max}$  development is then characterized using five parameters:  $V_1$ ,  $G_{f1}$ ,  $t_1'$ ,  $V_2$  and  $G_{f2}$ .

All the parameters were globally decreasing with increase of  $D_{\max}$ . It is particularly the case for the final stiffness value  $G_{f2}$  (Table 6-2). This aggregate size effect proves that the effect of soil treatment is controlled by the total contact surface between soil and additives. The larger the aggregate size, the smaller the total contact surface and the less the chemical reactions occurs and thus the lower the soil stiffness gain.

However, sometimes the trends can be different according to the initial aggregates size (Table 6-2), especially for the 3% cement treated silt and the treated clay with mixing method B. This is probably due to the difference in aggregate size distribution before and after mixing. As discussed in chapter 3, the aggregates size is strongly influenced by the moulding water content (ex. dry and wet sides for the silt) and mixing method (ex. for the clay). The changing trends of the five parameters are often different between the wet side and the dry side. This difference is related to the different aggregates contact surface. For the soils compacted on dry side, the aggregates size effect is noticeable as the aggregates are clearly defined, especially in the case of silt. For the wet side, the contact surface between soil and additives becomes smaller when the initial aggregate size is smaller. For example, Figure 6-36 depicts the aggregate size evolution for the soil of sub-series  $D_{\max} = 0.4 \text{ mm}$  and  $5 \text{ mm}$  with mixing method B and compacted on the wet side of optimum. As shown in Figure 6-36(a), for the initially small aggregate size soil (ex.  $D_{\max} = 0.4 \text{ mm}$ ), the hydrated additives mainly locate at the surface of the newly formed larger aggregates and the following pozzolanic reactions occur also only at the surface of the new aggregates (coating stage). Thereby, the real total contact surface between aggregates and additives increases with the increase of  $D_{\max}$  at wet side. Note that the thickness of coating should change with curing time, depending on soil type and moulding water content. As identified by Shi *et al.* (2007), the thickness of coating examined by EDX analysis ranges from 5 to 10  $\mu\text{m}$  for a lime treated expansive soil after 8-year curing.



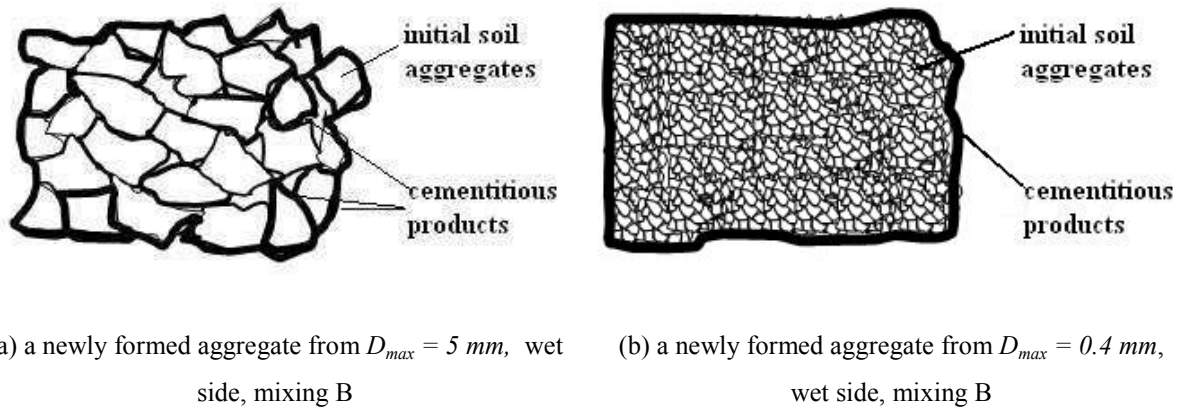


**Figure 6-36 Newly formed aggregates for two different sub-series with mixing method B and compacted on wet side**

For the clay compacted on the wet side, comparison of the parameters between mixing method A and B confirms that the stiffness depends on the total contact surface of the aggregates after mixing. For the 2% lime plus 3% cement treated clay, the larger aggregates induced by method B (case 25) lead to a much larger value of  $V_1$  (Figure 6-27), shorter time for the beginning of the second stage  $t'_1$  (Figure 6-29) and much lower final stiffness value of the first stage  $G_{f1}$  (Figure 6-28) as compared to mixing method A (case 24). Naturally, the finally value  $G_{f2}$  with mixing method B is also lower than that with mixing method A (Figure 6-31). For the 4% lime treated clay, we also observe that most parameters ( $V_1$ ,  $G_{f1}$ ,  $G_{f2}$  in Figure 6-20, Figure 6-21 and Figure 6-24, respectively) obtained is noticeably lower for mixing method B (case 20) as compared to mixing method A (case 21).

For both the 2% lime treated and 3% cement treated silt compacted on the wet side, comparison of the parameters between the sub-series prepared by method 1 and method 2 also indicates that the stiffness depends on the real total contact surface between aggregates after treatment. Note that method 1 results in more uniform aggregates than method 2. Most parameters ( $V_1$ ,  $G_{f1}$ ,  $V_2$ ,  $G_{f2}$ ) for the silt prepared by method 1 are greater than those by method 2, except the starting time for the second stage  $t'_1$ . Comparison of the parameter values between dry and wet side shows that the difference is greater for method 2 than for method 1. As mentioned before, this is mainly induced by the very limited  $G_{max}$  development for the wet side specimens prepared by method 2. This difference suggests that the mixing effect for the sub-series soils prepared by method 1 is better than that by method 2. In other words, it is more difficulty to mix the same sub-series by method 2. The different mixing effects were also observed on the dry side soils (Figure 2-7 in chapter 2): it was more difficult

to mix  $D_{max} = 0.4 \text{ mm}$  than other sub-series. Similarly, as method 2 often results in much higher percentage of finer aggregates ( $< 400 \mu\text{m}$ ) as compared to method 1 (except for  $D_{max} = 0.4 \text{ mm}$ , see Figure 2-1 in chapter 2), it appears logical to have less developed cementation for the wet side specimens by method 2.

Summarising, the changing trends of all parameters confirm that the aggregates size effect is related to the total contact surface between soil and additives. The variations of parameters  $V_2$  and  $t_1'$  with  $D_{max}$  appear in a more complex fashion.

For the 2% lime treated silt compacted on wet side (Figure 6-9), the hydrated lime in the silt prepared by method 1 can enter the inter-aggregate pores easily and participate in the pozzolanic reactions. This is characterised by a higher value of  $V_2$ . In case of well graded silt by method 2, the initial aggregates are still visible within the newly formed larger aggregates especially in the case of large  $D_{max}$  (ex.  $D_{max} = 5 \text{ mm}$  in Figure 6-36). Thereby, the trend opposite to that of method 1 is identified. For the cement treated silts (Figure 6-16), the trends opposite to those for the lime treated silt are due to the different contact surfaces obtained by the different treatments. In fact, in case of lime treated soils, the hydration related mechanism does not result in soil solidification because no cementitious compounds are produced. The hydration products can diffuse freely depending on the water availability. The pozzolanic reactions correspond therefore to the primary process for the stiffness gain. On the contrary, for the cement treatment, the hydration process is the primary reaction due to the large quantity of cementitious compounds produced during this process. In this case, parameter  $V_2$  mainly depends on the mixing conditions. For the dry side, the larger the aggregates size, the easier the soil to be mixed. For the wet side, an opposite mixing effect can be expected. Moreover, the changes in aggregate size depend also on soil type. In the case of clay treated by 4% lime (Figure 6-23) and by mixture (Figure 6-30), a higher sensitivity to water content changes can be expected. The aggregates are prone to form larger aggregates, even for the dry side. Thus, parameter  $V_2$  depends mainly on the mixing effect. For the wet side, the aggregates are more or less similar to each other. Thus, we observe similar value of  $V_2$  in case of mixing method A (Figure 6-23a and Figure 6-30a) but increasing value with increase of initial aggregate size in case of method B (Figure 6-23b, Figure 6-30b) because of the mixing effects as shown in Figure 6-36. Thereby, although  $V_2$  is a complex parameter, it still depends on the real contact surface between the aggregate and additives. The contact surface depends strongly on the treatment method, water content and mixing condition. This is particularly the case for clay.

The time needed for the second stage to start,  $t_1'$ , has been widely discussed for several decades but it remains an open question. For lime treated soils, some authors (Osula 1996; Osinubi *et al.*, 1998) reported  $t_1'$  is equal to several hours but some others indicated that it is about several days to several weeks: 7 days for Bell (1996), Maubec (2010) and Little and Nair (2009), 10 days for Locat *et al.* (1990) and Rao *et al.* (2001), more than 14 days for Rogers *et al.* (2006), 21 days for Wild *et al.* (1993). For cement treated soils, it is also reported that  $t_1'$  is equal to several hours to several days or weeks. Osula (1996) reported that several-hour mellowing time is suitable for the cement treated laterite soils; Chew *et al.* (2004) showed that the water loss by pozzolanic reactions occurs after 7-day curing. The work of Deneele *et al.* (2010) and Froumentin (2012) shows an obvious increase of UCS after 20 day - 30 day curing for the lime and/or cement treated silt and clay of Héricourt, indicating changes on the mechanisms involved. As far as the hydration process is concerned, it lasts often 1 to 72 h for lime treated soils and a few hours for cement treated soils in laboratory conditions, whereas it is can last 1 to 7 days in field conditions (National Lime Association, 2004).

Comparison of the mellowing time between laboratory and field conditions also suggests that the time required for the reaction process change is significant different. This is normal because both hydration and pozzolanic reaction processes depend on the aggregate size after treatment. Firstly, due to the complexity of the chemical reactions in treated soils,  $G_{max}$ -time curves often of typical two-stage nonlinear shape, especially for lime treated soils (treated silt in Figure 6-4 and Figure 6-5; treated clay in Figure 6-18 and Figure 6-19). Normally, the coating process for lime treatment lasts longer period than for cement treatment; this explains the more noticeable aggregates size effect in case lime treatment than in case of cement treatment (see Table 6-2). Comparison of the stiffness development for the 2% lime plus 3% cement treated clay compacted on wet side between method A and B also shows that mixing method B results in typical two-stage development. This also indicates that the chemical process is strongly influenced by the aggregates size after mixing. Because mixing method B often results in larger aggregates than method A, mixing method B leads to very limited  $G_{max}$  development induced by the first phase.

### **6.9.2. Comparison of the results between laboratory and field conditions**

Some studies were performed aiming at correlating the soil strength identified in the laboratory and in field (Bryhn, 1984; Locat *et al.*, 1990; Hopkins, 1996; Puppala *et al.*, 2005;

Horpibulsuk *et al.*, 2006; Bozbey and Guler, 2006; Kavak and Akyarh, 2007; Cuisinier and Deneele, 2008; Snethen *et al.*, 2008). The conclusion is quite divergent. The quite large difference in aggregate size between laboratory and field conditions must be the main factor for this divergence. The comparison between the mean values of the *in-situ* specimens in chapter 5 and the predicted values by the hyperbolic model illustrates well the aggregates size effect and at the same time confirms the performance of the model proposed in up-dating the laboratory conditions to the field ones (Figure 6-34 and Figure 6-35). Besides, the mean values of the field specimens in case of mixing method B (Figure 6-35) are found to be closer to the model results. This also indicates the large aggregates induced by the field compaction conditions (see also chapter 5).

It appears that the use of the mean value of a large quantity field data allows the effect of soil heterogeneity to be masked (Figure 6-34 and Figure 6-35). Thus, it is important to perform large quantity measurements when dealing with soils treated in field conditions.

## 6.10. Conclusions

In this chapter, in order to analyse the aggregates size effects on the stiffness development for treated soils, a simple hyperbolic model is proposed involving five parameters:  $V_1$ ,  $G_{f1}$ ,  $t_1'$ ,  $V_2$  and  $G_{f2}$ . The model predictions are compared with the experimental results, showing good agreement.

The aggregates size effect is analysed through changes of the parameters with  $D_{max}$ . Most parameters are found to decrease with the increase of  $D_{max}$ , demonstrating the aggregates size effect.

The changes of parameters with aggregates size identified using the laboratory results are then extended to the aggregates size in the field conditions. Comparison between the mean values of the *in-situ* results in chapter 5 and the predicted results confirms the aggregates size effect and shows the performance of the model proposed in up-scaling the results in laboratory conditions to the results in field conditions.

## General conclusion

The effect of aggregates size on the stiffness of lime and/or cement treated silt and clay from Héricourt was investigated, by measuring the small strain shear modulus ( $G_{\max}$ ) of soils using the technique of bender element at both laboratory aggregates size scale ( $D_{\max} = 0.4 \sim 5 \text{ mm}$ ) and field aggregates size scale ( $D_{\max} = 20 \text{ and } 31.5 \text{ mm}$  for the silt and the clay, respectively). Note that suction measurements were also performed when reaching the stability of stiffness and during one wetting/drying cycle.

In the laboratory conditions, the tests were performed during curing and during the application of wetting/drying cycles on the specimens prepared at different states: two soils of Héricourt with four aggregates size scales prepared by two sieving methods 1, 2, four treatments, two mixing method A and B, six water contents – on the dry and wet sides of optimum. Two dry density values for the silt ( $1.65, 1.7 \text{ Mg/m}^3$ ) and one for the clay ( $1.35 \text{ Mg/m}^3$ ) are considered. In each case, the same density was kept on the dry and wet sides of optimum.

In the field conditions, the measurements of  $G_{\max}$ , dry density and water content were performed on the silt and clay core specimens from the core samples of two batches. Note that the core samples were taken from the experimental embankment in Héricourt.

### Aggregates size effect during curing

In the laboratory conditions, the  $G_{\max}$  of both the treated and untreated specimens of different sub-series ( $D_{\max} = 0.4 \sim 5 \text{ mm}$ ) increases at constant water content during a curing period of several thousands of hours. The slight  $G_{\max}$  gain for the untreated soils is attributed to the aging effect. A two-phase development is identified for the treated soils, to be related to the hydration and pozzolanic reactions: phase I is related to additive hydration and phase II is related to pozzolanic reactions. In field conditions, the  $G_{\max}$  gain due to treatment is also identified. Furthermore, all results shows that the stiffness development is strongly influenced by the aggregates size, the homogeneity of soils, the type of treatment, the water availability and the soil suction. In other words, the aggregates size effect is a fundamental factor to be accounted for when dealing with the stiffness development of treated soils.

**Aggregate size effect:** for the same soil with the same treatment and compacted at identical moulding water content, the  $G_{\max}$  development is different for different aggregates sizes. The

larger the aggregate size, the lower the stiffness. This aggregate size effect is identified in both laboratory and field conditions. In the laboratory conditions, the aggregates size effect is evidenced by both the immediate value of  $G_{\max}$  after compaction ( $G_0$ , related to phase I) and the final value after thousands of hours of curing (related to phase II). Moreover, for both the lime-treated and cement-treated silt, the aggregates size effect is often more noticeable for the dry side than for the wet side, indicating that aggregates size refers to the one after treatment - the aggregates size often changes after compaction and it is this aggregate size that should be considered when dealing with aggregate size effect. This observation is also made for the treated clay with mixing method A. Indeed, mixing method A often results in higher stiffness than mixing method B, which also evidences the dependence of aggregates size on the mixing method. In the field conditions, this aggregates size effect is also identified on core specimens: the large aggregates size core specimens often show a low stiffness level, whereas the smaller aggregates size core specimens present a higher stiffness level.

**Heterogeneity:** The different aggregates sizes give rise to different heterogeneity of treatment: the larger the aggregates size, the higher the heterogeneity of treatment. This is identified by a relative smaller  $G_{\max}$  variation between the different sub-series ( $D_{\max} = 0.4 \sim 5 \text{ mm}$ ) and a larger variation of  $G_{\max}$  between the *in-situ* specimens ( $D_{\max} = 20 \text{ mm}$  and  $31.5 \text{ mm}$ ). In fact, the effects of water content and dry density are found to be negligible for the stiffness of *in situ* soils, due to their high heterogeneity. This heterogeneity, due to the presence of stones, aggregates size and additive distribution, is decisive for the  $G_{\max}$  value as well as its development.

**Treatment effect:** In the laboratory conditions, the treated soils often show higher stiffness than the untreated ones for both phase I and phase II. In the field conditions, when using the mean value of measurements to minimize the heterogeneity of soils, the treatment effect due to curing is found to be also a positive factor for the stiffness development through the core samples from zone II where the climate effect is absent. This effect can last as long as 30 months and is diminishing after 7 ~ 16 months for different treatments, indicating that the treatment corresponds to phase II in the laboratory conditions. The treatment effect is also identified by the water loss due to pozzolanic reactions (zone II). Moreover, as for the laboratory specimens, the treatment effect is also found to be aggregates size dependent. The  $G_{\max}$  gain is strongly stiffness level dependent: a significant increase is observed with high stiffness level.

The treatment effect on the stiffness development is also closely correlated to the mineral composition of soils. It is found that the lime treatment is particularly efficient for clayey soils, whereas the cement treatment is more suitable for silty soils (ex. the comparison of lime and cement treated silt of sub-series  $D_{max} = 0.4 \text{ mm}$  between methods 1 and 2). This is also the case for the larger aggregates size levels in the field conditions when using the mean values. The predominantly cement treated silt has higher stiffness than the lime treated one (3% cement > 3% lime). The mixture-treated clay is also evidenced to have higher stiffness values than solely lime treated one (2% lime + 3% cement > 5% lime). Finally, a reasonable treatment effect related to the dosage is also evidenced for both the silt (1% lime + 5% cement > 3% cement; 3% lime > 2% lime) and the clay (5% lime > 4% lime).

**Water availability:** In the laboratory conditions, water availability is observed to be aggregate size dependent: the larger the aggregates size, the lower the water availability. Thereby the mixing method plays a decisive role in soil stiffness development, as it is identified that mixing method A modifies the distribution of aggregates and controls the water availability for different reactions. In the field conditions, the low stiffness of the large aggregates size core specimens is probably induced by the limited water availability, especially for the clay.

**Suction/water effect:** In the laboratory conditions, the stiffness of soil compacted on dry side is often higher than that of soil compacted on wet side. Meanwhile, the aggregates size effect on suction is also observed to be similar to that on  $G_{max}$ : the higher the suction, the higher stiffness. Thereby, the aggregates size dependent stiffness is probably controlled by the suction effect. In the field conditions, with larger aggregates sizes, a larger suction range can be expected between the specimens of different aggregates sizes even at similar water contents.

**Modelling of curing behaviour and up-scaling of laboratory conditions to field conditions:** A hyperbolic model is proposed to depict the stiffness development of the treated soils at the laboratory scale, with five parameters:  $V_1$ ,  $G_{f1}$ ,  $t_1'$ ,  $V_2$  and  $G_{f2}$ . On the whole, all the parameters are found to decrease with the rise of maximum aggregate size  $D_{max}$ , confirming the aggregates size effect identified. This model is then used to up-scale the laboratory conditions to the field conditions by the considering the maximum aggregates size for the silt and clay used in the construction of the Héricourt experimental embankment. Comparison between the model predictions and the mean values of experimental data shows

good agreement, confirming the performance of the model developed in describing the aggregate size effect on the curing behaviour of treated soils.

### **Aggregates size effect during wetting/drying cycles**

During wetting/drying cycles or under the climatic effect to a certain extent, the treated soils often experience coating (stage I) and/or breakage of aggregates (stage II). At stage I, the treated soils present low sensitivity to water content changes and insignificant decrease of  $G_{\max}$ . However, at stage II, higher sensitivity to water content changes appears together with noticeable decrease of  $G_{\max}$ . Moreover, the water content and suction also changes with the stiffness development due to the cycles. In the field conditions, although climate changes can modify the stiffness, water contents, dry densities and cause fissures, the  $G_{\max}$  cannot be correlated directly to its water content and dry density due to the high heterogeneity of soils. It is interesting to note that changes of water content and dry density due to the combined effects of treatment and climate are found to be good indicators of stiffness changes. Based on this observation, three zones, I, II and III, are defined according to the influence level of climate. Finally, using the mean values of  $G_{\max}$ , the climate effect can be identified. This effect is revealed to be a negative factor for the stiffness development.

**Aggregates size effect:** In the laboratory conditions, both the number of cycles  $N_f$  for failure initiation (beginning of stage II) and the degradation ratio at stage II are found to be strongly influenced by the aggregates size effect, especially for the dry side treated specimens. The larger the aggregates, the smaller the value of  $N_f$  and the higher the degradation ratio. As mentioned before, this aggregates size effect for the clay is influenced significantly by the mixing method and molding water content, mainly due to the different aggregates sizes obtained after treatment. In the field conditions, using the mean values of measurements, the climate effect is also revealed to be a negative factor, particularly for the surface layers. This climate effect is influenced by the heterogeneity of soils: the larger the aggregates size, the lower the stiffness and the higher the sensitivity to water content change. This is in accordance with the aggregates size effect identified in the laboratory conditions. As for the aggregates size effect during curing, a much larger variation range of  $G_{\max}$  change is obtained for the *in-situ* soils, also evidencing the aggregates size effect. Moreover, the active zone for the climate effect (zone I) can reach as deep as 0.85 ~ 2.05 m in the experimental embankment, much deeper than that identified in laboratory environmental chambers as



reported in the literature. This indicates that the effect of wetting/drying cycles depends on the aggregates size scales: the larger the aggregates, the larger the active zone due to climate effect.

**Treatment effect:** Compared to untreated soils, the treated soils show an improvement in terms of sensitivity to water content changes and resistance to wetting/drying cycles. Firstly, the treated soils show larger  $N_f$  and lower degradation ratio. Secondly, the water content/saturation degree upon wetting paths often increases with cycles for the untreated soils, whereas for the treated soils, no noticeable change takes place. The sensitivity of stiffness to water content variations is also different for different treatments: the cement treated silt is more sensitive than the lime treated one; the mixture treated clay (2% lime + 3% cement) is more sensitive than the solely lime treated one, especially in case of large aggregates size (ex. mixing method B, case 25 versus case 17). In the field conditions, the higher cementation of small aggregates size soils often leads to a lower sensitivity to water content changes than that of large aggregates size soils under the similar climate effect. In addition, as in the laboratory conditions, the mixture-treated clay is also observed to be more sensitive to water content changes than the lime-treated one. This may explain why zone I of the mixture treated clay (SC20/SC47) is deeper than that of the lime treated one (SC14/SC46). Finally, treatments also condition the development of fissures: the development is more frequent for the mixture-treated clay than for the predominantly lime treated one. All these phenomena are in accordance with that observed in the laboratory conditions.

**Water/suction effect:** In the laboratory conditions, the stiffness-change during wetting/drying cycles is found to be suction-change dependent, as the aggregates size effect on suction or  $G_{max}$  during curing. Thereby, the range of cyclic suction change is closely correlated to the process of aggregate breakage. Firstly, the dry side specimens often show typical two-stage behaviour (stage I, II), whereas the wet side specimens often present one stage (stage I) only. This is due to the lower range of suction changes for the wet side specimens. Secondly, intensive drying followed by re-wetting is greatly harmful to the stiffness of soils, with an accelerated breakage of aggregates. This is probably due to the higher variation range of suction changes applied. Third, the change in water content after each humidification is observed to be suction/aggregates size dependent. For untreated soils, the larger the aggregate, the lower the suction change and the lower the increase of saturation degree. For treated soils, the water content/saturation degree often decreases during stage I (suction increase due to coating) and then slightly increases during stage II (suction decrease

due to breakage of aggregates): the larger the aggregates, the higher the increase of the saturation degree. Thereby, all these phenomena are related to suction changes. In other words, the sensitivity of soil stiffness to its water content changes is closely related to the suction, the cementation and the range of suction changes during wetting/drying cycles. The breakage of aggregates due to cyclic suction changes can lead to a decrease of soil suction and an increase of the sensibility to water content changes.

In the field conditions, the aggregates size and treatment effects on the stiffness changes under changes of climate are different for different aggregates sizes. In addition to the heterogeneity of soils, the different ranges of suction changes may explain this phenomenon. The degradation of the *in-situ* soils in terms of  $G_{\max}$  is probably due to the decrease of suction related to the creation of fissures under the climate effect. In other words, the resistance to climate changes is closely related to the cementation degree and the suction that are aggregates size dependent.

### **Perspectives**

In the laboratory conditions, the stiffness change during wetting/drying cycles was analysed on the soils with different aggregates sizes (see chapter 4). On the other hand, we have developed a hyperbolic model allowing the effects of curing time and aggregates size to be accounted for. It would be interesting to extend this model to the effect of wetting/drying cycles.


The  $G_{\max}$  measurements have done on core specimens over two years (see chapter 5). Longer curing time should be considered in order to further verify the effects of curing time and climate changes.

As many transducers are installed in the experimental embankment of Héricourt, rich data are available (see Report of TerDouest project Module C by Boussafir and Froumentin, 2010; Froumentin, 2012). It would be interesting to perform numerical investigations to study the interaction between the embankment and atmosphere.


## Appendix

### 1. Description of the core samples on the silt side of the experimental embankment

#### SC40-1

Part	Compaction layer	Photo	Description	Sample
Base (0.25 m)	0 cm		(0 - 25 cm) Gravels, grains, asphalt	Gravels (0.0 m ~ 0.25 m) (layer No.16)
	Limit of layer (25cm)			
Subgrade (0.29 m)	Inclined fissure (41cm)		Silt treated by 1%CaO + 5% cement, red/orange colour , very stony with gravels, inclined fissures at 35 cm and 40 cm, limit of layer is probably at 54 cm	SC40-1-1 (0.25 m ~ 0.54 m) (layer No.15)
	Inclined fissure (46 cm)			
	Limit of layer (54 cm)			
Top of earthworks (0.06 m)	Cracks since (60 cm)	Silt treated by 3% CaO, red/orange colour, very fragile.	SC40-1-2 (0.54 m ~ 0.60 m) (layer No.14 )	

#### SC31-1

Part	Compaction layer	Photo	Description	Sample	
Base (0.22m)	0 cm		(0 ~ 22 cm) gravels, grains, asphalt	SC31-1-0 (0.0 m ~ 0.22 m) (layer No.16)	
	Limit of layer (22 cm)				
Subgrade (0.21m)			silt treated by 1% CaO + 5% cement, with many little stones	(22 ~ 43 cm) limit of layer is frank at 43 cm	SC31-1-1 (0.22 m ~ 0.43 m) (layer No.15 )
	Limit of layer (43 cm)				
Top of earthworks (0.57m)		silt treated by 3% cement, a few little stones	(43 ~ 78 cm) fissure at 69 ~ 70 cm many fissures between 72 cm ~ 78 cm limit of layer is probably between 78 ~ 80 cm	SC31-1-2 (0.43 m ~ 0.78 m) (layer No.14 )	
	Limit of layer (78 cm)				
			Sample end (100 cm)	(78 ~100cm) silt treated by 3% cement, many little stones	(0.78 m) SC31-1-3 (w) SC31-1-4 (0.80 m ~ 1.00 m) (layer No.13 )

**SC49-1**

Part	Compaction layer	Photo	Description	Sample
Base (0.20 m)	0 cm		(0 ~ 20 cm) Granular material (mixture of gravels, grains, the silt and asphalt)	SC49-1-0 (0.0 ~ 0.20 m) (layer No.16)
	Limit of layer (20 cm)		(20 ~ 46 cm) Big fissure at 30 cm due to stones presence; limit of the compaction layer couche near 46 cm; the silt treated by 1%CaO + 3% cement, little stones.	SC49-1-1 (0.20 ~ 0.46 m) (layer No. 15)
Top of earthworks (0.51 m)	Crack (53 cm)		(46 ~ 80 cm) A crack through the core profile at 53 cm; limit of the compaction layer at about 80 cm; the silt treated by 3% cement, little stones.	SC49-1-2 (0.46 ~ 0.80 m) (layer No.14)
	Limit of layer (80cm)		(80 ~ 97 cm) The silt treated by 3% cement, little stones, core sample ends at 97 cm.	SC49-1-3 (0.80 ~ 0.97 m) (layer No.13 )
	Fissure (89 cm) End at 97cm			

**2. Description of the core samples on the clay side of the experimental embankment**

**1). Cores dominantly treated by lime**

**SC5-1**


Part	Compaction layer	Photo	Description	Echantillon
Base (0 ~ 0.22 m)	0 cm - 4 cm		Disintegrated part, the silt treated by 1% lime + 5% cement	SC5 - 1-0 (w)
	Limit of layer at 22 cm		Silt, red/orange, treated by 1% lime + 5% cement	SC5-1-1(0.04 ~ 0.22 m) (layer No.16)
Subgrade (0.22 ~ 0.5 m)	Fissure at 36 cm		Clay treated by 5% lime, grey, fissures at 36 cm; a disintegrated part from 46 cm to 50 cm.	SC5-1-2 (0.22 ~ 0.36 m)
	Fissure at 46 cm			SC5-1-3 (0.36 ~ 0.46 m)
	End of this layer at 50 cm			SC5-1-4 (0.46 ~ 0.50 m) (layer No. 15 )
Top of earthworks (0.5 ~ 1.3 m)	Fissure at 69 cm		Clay treated by 5% lime, grey, fissures at 69 cm	SC5-1-5 (0.50 ~ 0.84 m) (layer No. 14 )
	Limit of this layer at 84 cm			SC5-1-6 (0.84 ~ 0.95 m)
	Fissure at 95 cm		Clay treated by 5% lime, grey, fissures at 95 cm	SC5-1-7 (0.95 ~ 1.14 m) (layer No. 13 )
	Limit of this layer at 114cm	SC5-1-8 (1.14 ~ 1.30 m) (layer No.12 )		
	End at 130 cm			

Appendix: Description of the core samples of the experimental embankment


<b>SC14-1</b>				
Part	Compaction layer	Photo	Description	Sample
Base (0 ~ 0.21 m)	0 ~ 7 cm Fissure at 5 cm		Silt, red/orange, treated by <b>1% lime + 5% cement</b> . A big sandy stone at 0 cm ~ 7 cm (like a cap at the beginning).	SC14-1-1 (0.07 ~ 0.25 m) (layer No.16)
	Limit of layer at 22 cm Fissure at 24.5 cm			Clay treated by <b>2% lime + 3% cement</b> , grey/green, fissures at 24.5 cm, 30 ~ 32 cm and 40 cm. A limit of layer at 50 cm.
Fissure at 30 ~ 32 cm	Clay treated by <b>5% lime</b> , grey/green, fissures at 67 and 71 cm; a limit of layer at 80 cm.		SC14-1-3 (0.50 ~ 0.65 m) (layer No.14 )	
Fissure at 40cm			SC14-1-4 (0.65 ~ 0.80 m) (layer No.14 )	
Top of earthworks (0.5 ~ 1.5 m)	End of layer at 50 cm		Clay treated by <b>5% lime</b> , grey/green, fissures at 92 cm, 102 cm; a limit of layer at 114 cm	SC14-1-5 (0.80 ~ 1.14 m) (layer No.13 )
	Fissure at 67 cm			Clay treated <b>5% lime</b> , grey/green, fissures at 125cm and 137 cm; end of the core sample at 150 cm.
	Fissure at 71cm		SC14-1-7 (1.25 ~ 1.50 m) (layer No.12 )	
	Limit of layer at 80 cm		End at 150 cm	
	Fissure at 92 cm			
	Fissure at 102 cm			
	limit at 114 cm			
	Fissure at 125 cm			
Fissure at 137 cm				
End at 150 cm				

Appendix: Description of the core samples of the experimental embankment


**SC14-2**

Part	Compaction	Photo	Description	Sample
Embankment 1.5 m (1.5 ~ 3.0 m)	Fissure at 11 cm		Clay treated by 4% lime. Distribution : very wet and almost untreated in the upper part, colour: orange/green; a fissure at 11 cm ; at 20cm, a big fissure, which is a probable limit of the layer	SC14-2-1 (1.5 ~ 1.70 m) (layer No.11)
	Limit of layer at 20 cm			
	Limit of layer at 43cm		Clay treated by 4% CaO. The distribution of water and lime is not homogenous. The upper part is more humid and softer than the lower portion. At 43 cm, there is probably the limit of the compaction layer.	SC14-2-2 (1.70 ~ 1.93 m) (layer No.10 )
	Fissure at 70 cm		Clay treated by 4% lime. The distribution of the water and the lime is not homogeneous. Some fissures at 70 cm abd 83 cm; the probable limit of the layer at 83 cm.	SC14-2-3 (1.93 ~ 2.34cm) (layer No.9 )
	Fissure at 83cm			
	Fissure at 95cm			
	Fissure at 107cm		Clay treated by 4% lime. Some fissures at 95 cm and 107 cm. A cavity and a borken zone at 107 cm. The limit of the layer at 113 cm.	SC14-2-4 (2.34 ~ 2.49 m) SC14-2-5 (2.49 ~ 2.63 m) (layer No.8 )
	Limit of layer at 113cm			
	Fissure at 119-120cm		Clay treated by 4% lime. The distribution of additive and water is not homogeneous. a large crack between 119 and 120 cm (unclear if it is a limit of a layer), another fissure at 139 cm which is probably the limit of the layer	SC14-2-6 (2.63 ~ 2.70 m) SC14-2-7 (2.70 ~ 2.89 m) (layer No.7 )
	Limit of the layer at 139cm			
Core sample ends at 150 cm		Clay treated by 4% lime. The distribution of additive and water is not homogeneous. Upper part is more humid than lower part, the core sample ends at 150 cm.	SC14-2-8 (2.89 ~ 3.00 m) (layer No.6 )	

**SC46-1**


Part	Compaction layer	Photo	Description	Sample
Base (0.27 m)	0 cm		Silt treated by 1% lime + 5% cement, little stones at 0 ~ 5 cm, the strongly foliated trace structure.	SC46-1-1(0 ~ 0.06 m)
	Fissure at 6 cm			SC46-1-2 (0.06 ~ 0.27 m) (layer No.16)
Subgrade (0.245 m)	Limit of layer at 27cm			SC46-1-3 (0.27 ~ 0.375 m)
	Fissure at 31 cm	Clay, multi-coloured, treated by 2% lime + 3% cement, little stones, a fissure at 31 cm and another at 41.5 cm; a limit of the compaction layer at 51.5 cm.	SC46-1-4a (41 ~ 0.515 m) (No.15)	
Top of earthworks (0.815 m)	Fissure at 41.5 cm			SC46-1-4b (0.515 ~ 0.72 m) (No.14)
	Limit of layer at 51.5 cm	Clay, multi-coloured, treated by 5% lime, some little stones presence.		
	Limit of layer at 77.5 cm			SC46-1-5 (0.735 ~ 0.82 m); SC46-1-6 (0.825 ~ 0.97 m) (No.13)
	Fissure at 82 cm	Clay, multi-coloured, treated by 5% lime; little stones.		
of the core sample at 130 cm	Limit of layer at 97 cm			
	Fissure at 129 cm	Clay treated by 5% lime, some fissures concentrated at 97 ~ 106 cm, at 129 cm, little stones.	SC46-1-7 (1.06 ~ 1.30 m) (No.12)	


Appendix: Description of the core samples of the experimental embankment

<b>SC46-2</b>				
Part	Compaction layer	Photo	Description	Sample
<b>Embankment 1.3 m (1.30 ~ 2.60 m)</b>	Fissure at 23.5 cm		Clay treated by 4% lime. Distribution: very humid and almost untreated soil in the upper part; colour: from orange to green; some fissures at 23 ~ 24 cm, which is possible of the limit of a layer.	SC46-2-1 (1.3 ~ 1.54 m) (No.11)
	Limit of layer at 36cm		Clay treated by 4% lime; colour: green/grey. The distribution of lime and water is not homogenous, with little stones at the upper part. The limit of layer is probable at 36 cm.	SC46-2-2 (1.54 ~ 1.66 m) (No.11 )
	Limit of layer at 67cm		Clay treated by 4% lime. The distribution of the additive and water is not homogenous. Colour: green/grey. The limit of the compaction layer is probably at 67 cm.	SC46-2-3 (1.66 ~ 1.965 m) (No.10 )
	Fissure at 76 cm		Clay treated by 4% lime. Colour: grey and a little green. Some fissures at 76 cm and 101 cm through the core profile. The crack at 101 cm is probably the limit of the layer.	SC46-2-4 (1.965 ~ 2.055 m) (No.9)
	Limit of layer at 101cm		Clay treated by 4% lime. Colour: grey and a little green. Some fissures at 76 cm and 101 cm through the core profile. The crack at 101 cm is probably the limit of the layer.	SC14-2-5 (2.077 ~ 2.31 m) (No.9 )
	Fissure at 121 cm Crack at 125cm End at 130 cm		Clay treated by 4% lime. The distribution of the additive and water is not homogenous. A fissure is at 121 cm; a crack is at 125 cm; the core sample ends at 150 cm.	SC46-2-6 (2.31 ~ 2.51 m) (No.8 )
				SC46-2-7 (2.51 ~ 2.60 m) (No.8 )

**2). Cores dominantly treated by mixture**

Appendix: Description of the core samples of the experimental embankment


<b>SC20-1</b>					
Part	Compaction layer	Photo	Description	Sample	
<b>Base (0.25 m)</b>	0 cm		(0 ~ 25 cm) Silt treated by 1% CaO + 5% cement, little stones 0 - 5 cm, de-aggregate part (two aggregates), strongly foliated traces coated the surface of aggregates	SC20-1-1 (0.0 ~ 0.25 m) (layer No.16)	
	Limit of layer (25 cm)		(25 ~ 51.5 cm) Clay multicoloured, treated by 2% CaO + 3% cement, with little stones, a limit at 34 cm, another at 44 cm, and a frank limit at 51.5 cm	SC20-1-2 SC20-1-4 (0.25 ~ 0.51 m) (layer No.15)	
<b>Subgrade (0.265 m)</b>	Limit of layer (51.5 cm)		(51.5 ~ 77.5 cm) Clay multicoloured, treated by 2% CaO + 3% cement, little stone presence at 60 ~ 70 cm (big pebble)	SC20-1-5 (0.51 ~ 0.65 m) SC20-1-6 (0.65 ~ 0.78 m) (layer No.14)	
	Limit of layer (77.5 cm)		(77.5 ~ 112 cm) Clay multicoloured, treated by 2% CaO + 3% cement	SC20-1-7 (0.78 ~ 1.12 m) (layer No.13)	
	Fissure (88 cm)		(112 ~ 144 cm) Clay treated by 2% CaO + 3% cement, clay well mixed, little stones	SC20-1-8 (1.12 ~ 1.44 m) (layer No.12)	
	Limit of layer (112 cm)				
<b>Top of earthworks (0.925 m)</b>	Fissure (129 cm)				
	Sample end (144 cm)				

<b>SC20-2</b>				
Part	Compaction layer	Photo	Description	Sample
<b>Embankment (1.46 m)</b>	0 cm		The clay treated by 2% lime + 3% cement, with grey colour with a little red, an obvious limit of layer at 21 cm	SC20-2-1 (1.5 ~ 1.71 m) (layer No.11)
	Limit or fissure ? (21cm)		The clay treated by 2% lime + 3% cement, mixture colours of grey, red and green, fissure at 38 cm, a limit of layer at 47 cm	SC20-2-2, SC20-2-3 (1.71 ~ 1.97 m) (layer No.10)
	Fissure (38 cm)		The clay treated by 2% lime + 3% cement, colour of grey and a little red, fissures at 57 cm and at 68 cm; a limit of the layer at 73 cm.	SC20-2-4 (1.97 ~ 2.07 m) SC20-2-5 (2.07 ~ 2.23 m) (layer No.9)
	Limit of layer (47cm)		The clay treated by 2% lime + 3% cement, grey/green with a little red, a crack at 101 cm; a limit of layer at 110 cm.	SC20-2-6 (2.23 ~ 2.51 m) SC20-2-7 (2.51 ~ 2.60 m) (layer No.8)
	Fissure (57 cm)		The clay treated by 2% lime + 3% cement, a mixed colour of grey, green and a little red; a crack through the core profile at 141 cm; a limit of the layer at 146 cm.	SC20-2-8 (2.60 ~ 2.91 m) SC20-2-9 (2.91 ~ 2.96 m) (layer No.7)
	Fissure (68 cm)			
	Limit of layer (73 cm)			
	Fissure or limit ? (101 cm)			
	Limit of layer (110 cm)			
	Fissure (141 cm)			
End at 146 cm				






Appendix: Description of the core samples of the experimental embankment


**SC20-3**

Part	Compaction layer	Photo	Description	Sample
Embankment (1.0 m) (3 ~ 4 m)	Crack through (3cm)		Clay treated by 2% lime plus 3% cement, grey colour, with little stones, a crack at 3 cm and many fissures at 17 cm; limit of layer at 25 cm.	SC20-3-1 (3.00 ~ 3.03 m )
	Many fissures (17cm)?			SC20-3-2 (3.03 ~ 3.17 m)
	Limit of layer (25cm)			SC20-3-3 (3.17 ~ 3.25 m) (layer No. 6)
	Crack (38cm)		Clay treated by 2% lime plus 3% cement, dominantly grey/green colour, with a little red colour; a inclined fissure through the core profile at 38 cm	SC20-3-4 (3.25 ~ 3.38 m)
	Limit of layer (47cm)			SC20-3-5 (3.38 ~ 3.47 m) (layer No.5)
	Crack (67cm)		Clay treated by 2% lime plus 3% cement, dominantly grey with a little red/orange; a fissure through the profile at 67 cm; limit of layer at 75 cm.	SC20-3-6 (3.47 ~ 3.67 m)
	Limit of layer (75cm)			SC20-3-7 (3.67 ~ 3.75 m) (layer No.4)
	End at 85cm		Clay treated by 2% lime plus 3% cement, grey/green, with a little white stones; the core sample ends at 85 cm.	SC20-3-8 (3.75 ~ 3.85 m) (layer No.3)


**SC20-4**

Part	Compaction	Photo	Description	Sample
Embankment (0.80 m) 4.0 ~ 4.80 m	Crack at 5cm		Clay treated by 2% lime + 3% cement, grey, a piece of soil.	SC20-4-1 (4.0 ~ 4.05 m); SC20-4-2 (4.05 ~ 4.14 m) (layer No.3)
	Limit of layer at 14cm		Clay treated by 2% lime + 3% cement, grey, with the cementitious products clearly defined.	
	Fissure at 17cm		Clay treated by 2% lime + 3% cement, grey, fissure at 17 cm; a limit of layer at 48 cm.	SC20-4-3 (4.14 ~ 4.48 m) (layer No.2 )
	Limit of layer at 48 cm			SC20-4-5 (4.48 ~ 4.66m) SC20-4-5 (4.66 ~ 4.80m) (layer No.1 )
	Fissure at 66cm			
Limit of layer No.1 End of the embankment at 80 cm	Clay treated by 2% lime + 3% cement, grey and a little red clay, some fissures at 62 cm, a limit of layer / end of the embankment at 80 cm			
Sub-embankment (0.37m)	Fissure at 86 cm		Silt treated by 2% lime, very dry for the silt at connection part with the clay; little fissures at 82 cm and at 97 cm, end of the layer No.0 at 117 cm	SC20-4-6 (SC20-4-6a, b) (4.80 ~ 4.97 m)
	A little fissure at 97 cm			SC20-4-7 (4.97 ~ 5.17 m) (layer No.0)
	End of this layer at 117 cm			
Natural soil (0.29m)	Fissure at 142cm		Natural soil, red, very wet, fissure at 142 cm, end of the core sample at 146 cm	SC20-4-8 (5.17 ~ 5.42 m)
	End at 146 cm			SC20-4-9 (5.42 ~ 5.46 m) (layer No.-1 )

**SC47-1**

Part	Compaction layer	Photo	Description	Sample
Base (0.25m)	Bitumen at 0 ~ 2 cm Fissure at 5 cm		A layer of bitumen 0 ~ 2 cm; then the silt treated by 1% lime + 5% cement, a little stones in the silt; a fissure at 5 cm; and another fissure at 15 cm; a limit of layer at 25 cm.	SC47-1-1 (0 ~ 0.25m); (No.16 )
	Fissure at 15 cm Limit of layer at 25 cm		Clay treated by 2% lime + 3% cement, grey/green and a little orange, fissures at 38cm; a limit of layer at 52 cm.	SC47-1-2 (0.25 ~ 0.52 m) (No.15 )
Limit of layer at 80 cm	Clay treated by 2% lime + 3% cement, grey/green and a little orange; a limit of layer at 80 cm		SC47-1-3 (0.52 ~ 0.80 m) (No.14)	
Fissure at 85 cm Fissure at 95 cm Fissure at 104 cm Limit of layer 114 cm	Clay treated by 2% lime + 3% cement, grey/green and a little red, fissures at 85cm/95cm/104cm; a limit of layer at 114 cm.		SC47-1-4 (0.80 ~ 1.14 m) (No.13)	
Fissure Fissure End at 130 cm	Clay treated by 2% lime + 3% cement, grey/green and a little red, many fissures in this layer (ex. 122 ~ 130 cm); end at 130 cm.		SC47-1-5 (1.14 ~ 1.30 m) (No.12 )	
Subgrade (0.27m)	Fissure at 44 cm Limit of layer 52 cm			
Top of earthworks (0.78m)				

**SC47-2**

Part	Compaction layer	Photo	Description	Sample
Embankment (1.6 m) (1.40 ~ 3.0 m)	0 cm Fissure at 7 cm		Clay treated by 2% lime + 3% cement, a fissure through the core profile at 7 cm which is probable the limit of the layer.	SC47-2-1 (1.4 ~ 1.47 m) (No.12 )
	Fissure at 19 cm		Clay treated by 2% lime + 3% cement, grey and a little red, a fissure at 19 cm and another at 32 cm; the limit of the layer probably at 32 cm.	SC47-2-2 (1.47 ~ 1.59 m) (No.11 )
	Limit of layer at 32 cm		Clay treated by 2% lime + 3% cement, grey/green and a little red, fissures at 44 cm; a limit of layer at 59 cm.	SC47-2-3 (1.59 ~ 1.72 m) (No.11 )
	Fissure at 44 cm Limit of layer at 59 cm		Clay treated by 2% lime + 3% cement, grey/green and a little red, a crack through the profile at 79.5 cm; a limit of layer at 94 cm.	SC47-2-4 (1.72 ~ 1.99 m) (No.10 )
	Crack at 79.5 cm Limit of layer at 94 cm		Clay treated by 2% lime + 3% cement, grey/green and a little red, a limit of layer at 114 cm.	SC47-2-5 (1.99 ~ 2.18 m) SC47-2-6 (2.18 ~ 2.33 m) (No.9)
	Limit of layer at 114 cm		Clay treated by 2% lime + 3% cement, grey/green and a little red, many fissures in this layer (ex. at 127 cm, 131 cm ~ 134 cm), end of the core sample at 146 cm.	SC47-2-7 (2.33 ~ 2.53 m) (No.8)
	Fissure Fissure Fissure End at 146cm		Clay treated by 2% lime + 3% cement, grey/green and a little red, many fissures in this layer (ex. at 127 cm, 131 cm ~ 134 cm), end of the core sample at 146 cm.	SC47-2-8 (2.54 ~ 2.66 m) SC47-2-9 (2.66 ~ 2.86 m) (No.7 )

## Reference

- AASHTO T282 (2000), 'Standard Method of Test for Calibrating a Wheel Force or Torque Transducer Using a Calibration Platform'.
- AASHTO T239: Standard Specification for Moisture Content of Soil and Soil-Aggregate. 1991 (R1996).
- Aderibigbe, D., Akeju, T. & Orangun, C. (1985), 'Optimal water/cement ratios and strength characteristics of some local clay soils stabilized with cement', *Materials and Structures* 18(2), 103–108.
- Airey, D. & Fahey, M. (1991), 'Cyclic response of calcareous soil from the north- west shelf of australia', *Géotechnique* vol. 41, no. 1, pp. 101–121.
- Akbulut, S. & Arsan, S. (2010), 'The variation of cation exchange capacity, pH, and zeta potential in expansive soils treated by additives', Department of Civil Engineering, Engineering Faculty, Ataturk University, Turkey 1, 139–154.
- Akcanca, F. & Aytekin, M. (2011), 'Effect of wetting–drying cycles on swelling behavior of lime stabilized sand–bentonite mixtures', *Environmental Earth Sciences* pp. 1–8.
- Alarcon-Guzman, A., C. J.-L. L. G. & Frost, J. (1989), 'Shear modulus and cyclic undrained behavior of sands', *Soils and Foundations* vol. 29 (4), 105–119.
- Al-Homoud, A., Basma, A., Al Bashabsheh, M. et al. (1995), 'Cyclic swelling behavior of clays', *Journal of geotechnical engineering* 121, 562.
- Alhassan, M. (2008), 'Permeability of lateritic soil treated with lime and rice husk ash', *AU Journal of Technology* 12(2), 115–120.
- Al-Hussaini, M. (1973), 'Influence of relative density on the strength and deformation of sand under plane strain conditions', *Evaluation of Relative Density and Its Role in Geotechnical Projects Involving Cohesionless Soils ASTM STP 523*, 332–347.
- Ali, M., Kuwano, J., Rahman, M. & Tannai, M. (2011), 'Ageing effects on the mechanical properties of forty years old embankment soil', in 'Geo-Frontiers 2011: Advances in Geotechnical Engineering Proceedings of the Geo-Frontiers 2011 Conference', ASCE.

- Al-Kiki, I., Al-Atalla, M. & Al-Zubaydi, A. (2011), 'Long term strength and durability of clayey soil stabilized with lime', *Eng. & Tech. Journal* 29, 725–735.
- Allam, M. & Sridharan, A. (1981), 'Effect of wetting and drying on shear strength', *Journal of the Geotechnical Engineering Division* 107(4), 421–438.
- Al-Mhaidib A. I. (2008), 'Mathematical model to predict swelling of expansive soil', *The 12th International Conference of International Association for Computer Methods and Advances in Geomechanics (IACMAG)* 1-6 October, Goa, India.
- Alonso, E., Romero, E., Hoffmann, C. & Garcia-Escudero, E. (2005), 'Expansive bentonite-sand mixtures in cyclic controlled-suction drying and wetting', *Engineering geology* 81(3), 213–226.
- Alramahi B., Alshibli K., Fratta D., & Trautwein S. (2008), 'A suction-control apparatus for the measurement of p and s-wave velocity in soils', *ASTM geotechnical testing journal* 31(1), 12–23.
- Al-Shayea, N., Abduljauwas, S., Bashir, R., Al-Ghamedy, H., Asi, I. (2003), 'Determination of parameters for a hyperbolic model of soils', *Proceedings of the Institution of Civil engineering – Geotechnical engineering*, Vol. 156, n<sup>o</sup>2, pp. 105-117.
- Altun, S., Sezer, A. & Erol, A. (2009), 'The effects of additives and curing conditions on the mechanical behavior of a silty soil', *Cold Regions Science and Technology* 56(2-3), 135 – 140.
- Amadi, A. (2010), 'Evaluation of changes in index properties of lateritic soil stabilized with fly ash', *Leonardo Electronic Journal of Practices and Technologies* 9(17), 69–78.
- Amr.Farouk.Elhakim (2005), 'Evaluation of shallow foundation displacements using soil small- strain stiffness', PhD thesis, Georgia Institute of Technology.
- Amu, O., Bamisaye, O. & Komolafe, I. (2011), 'The suitability and lime stabilization requirement of some lateritic soil samples as pavemen', *Int. J. Pure Appl. Sci. Technol* 2(1), 29–46.
- Anderson, D. & Stokoe, K. (1978), 'Shear modulus: A time-dependent soil property', *Dynamic Geotechnical Testing*, ASTM STP 654, 66–90.
- Anderson, D. & Woods, R. (1975), Comparison of field and laboratory shear moduli, in '*In Situ Measurement of Soil Properties*', ASCE, pp. 69–92.

- Anon (1990), 'State-of-the-art report on soil-cement', American Concrete Institute Materials Journal 87 (4), 395 – 417.
- Arango, I., Moriwaki, Y. & Brown, F. (1978), *In-situ* and laboratory shear velocity and modulus, in 'From Volume I of Earthquake Engineering and Soil Dynamics– Proceedings of the ASCE Geotechnical Engineering Division Specialty Conference, June 19-21, 1978, Pasadena, California. Sponsored by Geotechnical Engineering Division of ASCE'.
- Asonuma, T., Miura, S., Yagi, K. & Tanaka, H. (2002), 'Dynamic deformation characteristics of volcanic soils and their evaluation methods', in 'Proceedings -Japan Society of Civil Engineers', pp. 161–174.
- ASTM C150 / C 150m - 11 standard specification for portland cement.
- ASTM C593 - 06(2011) standard specification for fly ash and other pozzolans for use with lime for soil stabilization.
- ASTM C977 - 10 standard specification for quicklime and hydrated lime for soil stabilization.
- ASTM C977 - 10 standard specification for quicklime and hydrated lime for soil stabilization.
- ASTM D1556 standard test method for density and unit weight of soil in place by the sand-cone method.
- ASTM D1557 test for laboratory compaction characteristics of soil using modified effort (56,000 ft-lbf/ft<sup>3</sup> (2,700 kn-m/m<sup>3</sup>).
- ASTM D2167 density and unit weight of soil in place by the rubber balloon method.
- ASTM D558 - 04 standard test methods for moisture-density (unit weight) relations of soil-cement mixtures.
- ASTM D560-96 standard test methods for freezing and thawing compacted soil-cement mixtures.
- ASTM D698-07 (2007) test methods for laboratory compaction characteristics of soil using, annual book of ASTM standards, vol. 04.08, ASTM international, west conshohocken, pa.

- ASTM D1633 – 00 (2007) standard test methods for compressive strength of molded soil-cement cylinders.
- ASTM D2901 test method for cement content of freshly-mixed soil-cement.
- ASTM D2922 density of soil and soil aggregate in place by nuclear methods (shallow depth).
- ASTM D3017 test methods for moisture content.
- ASTM D3877 - 08 standard test methods for one-dimensional expansion, shrinkage, and uplift pressure of soil-lime mixtures.
- ASTM D4609 - 08 standard guide for evaluating effectiveness of admixtures for soil stabilization.
- ASTM D5102 - 09 standard test method for unconfined compressive strength of compacted soil-lime mixtures.
- ASTM D559 - 96 standard test methods for wetting and drying compacted soil-cement mixtures.
- ASTM D5982 - 07 standard test method for determining cement content of fresh soil-cement (heat of neutralization method).
- ASTM D806 - 11 standard test method for cement content of hardened soil-cement mixtures.
- Atkinson, J. (2000), 'Non-linear soil stiffness in routine design', *Geotechnique* 50(5), 487–508.
- Atkinson, J. & Sallförs, G. (1991), 'Experimental determination of soil properties', in 'in Proceedings of the 10th European Conference on Soil Mechanics and Foundation Engineering, A.A.Balkema, Rotterdam', Vol. 3, pp. 915–56.
- Attom, M. F. (1997), 'The effect of compactive energy level on some soil properties', *Applied Clay Science* 12(1-2), 61 – 72.
- Axtell, P. & Stark, T. (2008), 'Increase in shear modulus by soil mix and jet grout methods', *DFI Journal* 11, 11 – 21.
- Ayangade, J., Alake, O. & Wahab, A. (2009), 'The effects of different curing methods on the compressive strength of terracrete', *Civil Engineering Dimension* 11(1), pp-41.

- Azadegan, O., Yaghoubi, M. & Pourebrahim, G. (2011), 'Laboratory study on the effects of geogrid layers on mechanical properties of lime/cement treated granular soils', *Electronic Journal of Geotechnical Engineering* 16.
- Baghdadi, Z. (1982), 'Accelerated strength testing of soil-cement.'
- Bagonza, S., Peete, J., Freer-Hewish, R. & Newill, D. (1987), 'Carbonation of stabilised soil-cement and soil-lime mixtures', in 'Proceedings Seminar H. PTRC Transport and Planning Summer Annual Meeting, University of Bath, PTRC Education and Research Services, London'.
- Bahador, M. & Pak, A. (2011), 'Small-strain shear modulus of cement-admixed kaolinite', *Geotechnical and Geological Engineering* pp. 1–9.
- Bandara, N., Rowe, G. M., Sharrock, M. J. & Nickerson, C. R. (2002), 'Seasonal variation of subgrade modulus in different subgrade soils for pavement rehabilitation for non freeze-thaw climates', Vol. 245, *Application of Advanced Technology in Transportation*, ASCE, pp. 473–480. <http://link.aip.org/link/?ASC/245/60/1>
- Barden, L. D. F. (1974), 'Consolidation of clays compacted dry and wet of optimum water content', *Geotechnique* 24(4), 605–625.
- Barstis, W. (2003), 'Long-term effect of lime-fly ash treated soils', Technical report.
- Basha, E., Hashim, R., Mahmud, H. & Muntohar, A. (2005), 'Stabilization of residual soil with rice husk ash and cement', *Construction and Building Materials* 19(6), 448–453.
- Basma, A., Al-Homoud, A., Husein Malkawi, A. & Al-Bashabsheh, M. (1996), 'Swelling-shrinkage behavior of natural expansive clays', *Applied Clay Science* 11(2-4), 211 – 227.
- Beeghly, J. (2003), 'Recent experiences with lime-fly ash stabilization of pavement subgrade soils, base, and recycled asphalt', in 'Proceedings of International Ash Utilization Symposium, 2003, Lexington, KY, 435–452.
- Bell, F. (1989), 'Lime stabilisation of clay soils', *Bulletin of Engineering Geology and the Environment* 39(1), 67–74.
- Bell, F. (1993), 'Engineering treatment of soils', published by E & FN Spon in 1993, Taylor & Francis Group.

- Bell, F. (1996), 'Lime stabilization of clay minerals and soils', *Engineering Geology* 42(1), 223 – 237. <http://dx.doi.org/10.1007/BF02592537>
- Bennert, T., Maher, M., Jafari, F. & Gucunski, N. (2000), 'Use of dredged sediments from newark harbor for geotechnical applications', ASTM Special Technical Publication 1374, 152–164.
- Bergado, D. (1996), 'Soft ground improvement: in lowland and other environments', American Society of Civil Engineers.
- Bin S., Liu Z., Cai Y., Zhang X. (2007), 'Micropore structure of aggregates in treated soils', *Journal of materials in civil engineering* 19, No.1, 99–104.
- Bonal, J., Donohue, S. & McNally, C. (2012), 'Wavelet analysis of bender element signals', *Géotechnique* 62 (3), 243–252.
- Boardman, D., Glendinning, S. & Rogers, C. (2001), 'Development of stabilisation and solidification in lime-clay mixes', *Geotechnique* 51(6), 533–543.
- Borgne, T. L. (2010), 'Caractérisation et quantification des éléments perturbateurs de prise lors du traitement des sols', PhD thèses, école National supérieure de Géologie de Nancy.
- Boussafir, Y., and Froumentin, M., (2010), 'Project TERDOUEST Module C : Ouvrage experimental de référence en sols traités'. Proposition de cahier des charges de réalisation de l'ouvrage expérimental dans le cadre du chantier 'RD438 Héricourt'.
- Bozbey, I. & Garaisayev, S. (2010), 'Effects of soil pulverization quality on lime stabilization of an expansive clay', *Environmental Earth Sciences* 60(6), 1137–1151.
- Bozbey, I. & Guler, E. (2006), 'Laboratory and field testing for utilization of an excavated soil as landfill liner material', *Waste Management* 26(11), 1277 – 1286.
- Brandl, H. (1981), 'Alteration of soil parameters by stabilization with lime', in 'Proceedings of the 10th International Conference on Soil Mechanics and Foundation Engineering, Volume 3, Stockholm.'
- Briaud, J. (2001), 'Introduction to soil moduli', *Geotechnical News*, June 19.02, BiTech Publishers, Richmond, B.C., Canada.



- Brignoli, E., Gotti, M. & Stokoe, K. (1996), 'Measurement of shear waves in laboratory specimens by means of piezoelectric transducers', *ASTM geotechnical testing journal* 19(4), 384–397.
- Bryan, A. (1988), 'Criteria for the suitability of soil for cement stabilization', *Building and Environment* 23(4), 309 – 319.
- Bryhn, O. R., L. T. & Ass, G. (1984), 'Stabilization of sensitive clays with hydroxy-aluminum compared with unslaked lime', Norwegian Geotechnical Institute, Oslo, Publication 151.
- Burczyk, J., Ksaibati, K., Anderson-Sprecher, R. & Farrar, M. (1994), 'Factors influencing determination of a subgrade resilient modulus value', *Transportation Research Record* (1462).
- Cai, Y., Shi, B., Ng, C. W. & sheng Tang, C. (2006), 'Effect of polypropylene fibre and lime admixture on engineering properties of clayey soil', *Engineering Geology* 87(3-4), 230 – 240.
- Carino, N. J., and Lew, H. S. (2001), "The Maturity Method: From Theory to Application," *Proceedings of the 2001 Structures Congress and Exposition, Washington, D.C., National Institute of Standards and Technology, Gaithersburg, MD*, pp. 1–18.
- Chan, C. M., (2006), 'Relationship between shear wave velocity and undrained shear strength of stabilised natural clays', *Proceedings of the 2<sup>nd</sup> International Conference on Problematic Soils, Kuala Lumpur, Malaysia*, 117-124.
- Charlier, R., Dizier, A., Laloui, L. & Collin, F. (2009), 'Multi-physical processes in geomechanics', *European Journal of Environmental and Civil Engineering* 13(7-8), 803–830.
- Charman, J. (1988), *Laterite in road pavements*.
- Chatterji, S. (2001), 'a discussion of the paper: Mercury porosimetry: an inappropriate method for the measurement of pore size distributions in cement-based materials. Author's reply', *Cement and concrete research* 31(11), 1653–1656.
- Chew, S., Kamruzzaman, A. & Lee, F. (2004), 'Physicochemical and engineering behavior of cement treated clays', *Journal of geotechnical and geoenvironmental engineering* 130, 696.

- Chiang, H. (2003), 'Effect of gradation and cement content on the properties of soil-cement mixtures'.
- Chittoori, B. (2008), 'Clay Mineralogy Effects On Long-term Performance Of chemically Treated Expansive Clays', PhD thesis, the Faculty of the Graduate School of The University of Texas at Arlington.
- Choquette, M. (1989), 'La stabilisation à la chaux des sols argileux du Québec'.
- Chou, L. (1987), 'Lime stabilization: Reactions, properties, design, and construction', State of the Art Report 5.
- Christensen, A. (1969), 'Cement modification of clay soils', Portland Cement Assoc R & D Lab Bull .
- Chu, T. & Mou, C. (1973), 'Volume change characteristics of expansive soils determined by controlled suction tests', in 'proc. 3rd int. conf. on expansive soils. Haifa', Vol. 1, pp. 177–185.
- Clayton, C. (2011), 'Stiffness at small strain: research and practice', *Géotechnique* 61(1), 5–37.
- Clough, G., Rad, N., Bachus, R. & Sitar, N. (1981), 'Cemented sands under static loading', *Journal of the Geotechnical Engineering Division* 107(6), 799–817.
- Cokca, E., Erol, O. & Armangil, F. (2004), 'Effects of compaction moisture content on the shear strength of an unsaturated clay', *Geotechnical and Geological Engineering* 22, 285–297.
- Consoli, N. C., Bassani, M. A. A. & Festugato, L. (2010), 'Effect of fiber-reinforcement on the strength of cemented soils', *Geotextiles and Geomembranes* 28(4), 344 – 351.
- Consoli, N., da FONSECA, A., Silva, S., Cruz, R. & Fonini, A. (2012), 'Parameters controlling stiffness and strength of artificially cemented soils', *Géotechnique* 62(2), 177–183.
- Consoli, N., da Silva Lopes Jr, L. & Heineck, K. (2009), 'Key parameters for the strength control of lime stabilized soils', *Journal of Materials in Civil Engineering* 21, 210.
- Consoli, N., da Silva Lopes, L., Prietto, P., Festugato, L. & Cruz, R. (2011), 'Variables controlling stiffness and strength of lime-stabilized soils', *Journal of Geotechnical and Geoenvironmental Engineering* 137, 628.

- Consoli, N., Foppa, D., Festugato, L. & Heineck, K. (2007), 'Key parameters for strength control of artificially cemented soils', *Journal of geotechnical and geoenvironmental engineering* 133, 197.
- Consoli, N., Prietto, P., Carraro, J. & Heineck, K. (2001), 'Behavior of compacted soil-fly ash-carbide lime mixtures', *Journal of Geotechnical and Geoenvironmental Engineering* 127(9), 774–782.
- Consoli, N., Vendruscolo, M. & Prietto, P. (2003), 'Behavior of plate load tests on soil layers improved with cement and fiber', *Journal of geotechnical and geoenvironmental engineering* 129, 96.
- CORREZE, (2009), *Conseil Generale de la CORREZE: Guide Technique pour le remblayage des tranchées et la refection des chaussées sur le domaine public departemental de la CORREZE.*
- Croft, J. (1967), 'The structures of soils stabilized with cementitious agents', *Engineering Geology* 2(2), 63–80.
- Croft, J. (1968), 'The problem in predicting the suitability of soils for cementitious stabilization', *Engineering Geology* 2(6), 397–424.
- Croft, J. B. (1964), 'The processes involved in the lime-stabilization of clay soils'. *Proc. 2<sup>nd</sup> Conf. Aust. Rd Res. Bd. 2: 1169-1203.* (n.d.)
- Cuccovillo, T. & Coop, M. (1998), 'Yielding and pre-failure deformation of structured sands', *Pre-failure deformation behaviour of geomaterials* p. 105.
- Cui, Y.-J., Tang, A.-M., Mantho, A. T. & De Laure, E. (2008), 'Monitoring field soil suction using a miniature tensiometer', *Geotechnical Testing Journal* 31(1), 95 – 100.
- Cuisinier, O., Auriol, J., Le Borgne, T. & Deneele, D. (2011), 'Microstructure and hydraulic conductivity of a compacted lime-treated soil', *Engineering Geology*.
- Cuisinier, O. & Deneele, D. (2008a), 'Long-term behaviour of lime-treated expansive soil submitted to cyclic wetting and drying', in 'Unsaturated soils: advances in geoenvironmental engineering: proceedings of the 1<sup>st</sup> European Conference on Unsaturated Soils, E-UNSAT 2008, Durham, United Kingdom, 2-4 July 2008', Taylor & Francis Group, p. 327.

- Cuisinier O., Deneele D. (2008b), 'Effets de sollicitations hydriques cycliques sur le gonflement d'un sol argileux traité à la chaux', Journées nationales de géotechnique et de géologie de l'ingénieur JNGG'08-Nantes, 18-20 juin 2008, 61-68.
- Cuisinier O., Al-Mukhtar, M., Bouasker M., Buffalo M., Cui Y.-J., Cuinet D., Deneele D., De Windt L., Herrier G., Gaillot A.C., Gandille D., Masrouri F., Mistretta I., Puiatti D., Robinet A., Stoltz G., Tang A.M., (2010) 'Projet ANR TerDOUEST Module B' Report of meeting on 17th December 2009, LCPC Paris.
- Curiel Yuste J., Baldocchi, D.D., Gershenson, A., Goldstein, A., Misson, L., and Wong, S. (2007), 'Microbial soil respiration and its dependency on carbon inputs, soil temperature and moisture', *Global Change Biology*, 13, 1-18.
- Daita, R., Drnevich, V. & Kim, D. (2005), 'Family of compaction curves for chemically modified soils'.
- Daniel, D. & Benson, C. (1990), 'Water content-density criteria for compacted soil liners', *Journal of Geotechnical Engineering* 116(12), 1811–1830.
- Daniels, J., of Transportation. Research, N. C. D., Group, A., of North Carolina at Charlotte. Dept. of Civil, U. & Engineering, E. (2010), 'Subgrade stabilization alternatives to lime and cement', Technical report, North Carolina Dept. of Transportation, Research and Analysis Group.
- Das, B. M. (1990), 'Principle of foundation engineering', PWS-KENT publishing company, Boston.
- Dass, R., Yen, S., Das, B., Puri, V. & Wright, M. (1994), 'Tensile stress-strain characteristics of lightly cemented sand', *Geotechnical Testing Journal* 17(3), 305–315.
- De Bel, R., Bollens, Q., Duvigneaud, P. & Verbrugge, J. (2005), 'Influence of curing time, percolation and temperature on the compressive strength of a loam treated with lime', in 'International symposium TREMTI, paper nC022: 10p'.
- Delage, P., Audiguier, M., Cui, Y. & Howat, M. (1996), 'Microstructure of a compacted silt', *Canadian Geotechnical Journal* 33(1), 150–158.
- Delage, P., Cui, Y., M. A. & Deveughele, M. (2002), 'Water retention properties and microstructure of geomaterials controlled hydration', *Proceedings XI ECSMFE* 3, 43–48.

- Delage, P., Marcial, D., Cui, Y. & Ruiz, X. (2006), 'Ageing effects in a compacted bentonite: a microstructure approach', *Géotechnique* 56(5), 291–304.
- Dempsey, B. (1984), 'Development of a preliminary alternate launch band recovery surface (alrs) stabilized material pavement analysis system (spas)', Technical report, DTIC Document.
- Dempsey, B. & Thompson, M. (1967), 'Durability properties of lime-soil mixtures', Technical report.
- Dempsey, B., Thompson, M., Program, I. C. H. R., of Illinois at Urbana-Champaign. Transportation Research Laboratory, U., of Transportation, I. D. & Administration, U. S. F. H. (1973), 'Effects of Freeze-Thaw Parameters on the Durability of Stabilized Materials', University of Illinois.
- Deneele, D., Cuisinier, O., Hallaire, V. & Masrouri, F. (2010), 'Microstructural evolution and physico-chemical behavior of compacted clayey soil submitted to an alkaline plume', *Journal of Rock Mechanics and Geotechnical Engineering* 2(2), 169–177.
- Deneele D. (resp. module A), Al-Mukhtar, M., Bouasker M., Cui Y-J., Cuisinier O., De Windt L., Herrier G., Gaillot A.C., Guillot X., Lavallee E., Marouri F., Ouvrard G., Paris M., Puiatti D., Robinet A., (2010), 'Processus physico-chimiques et comportement des sols traités', Bilan des actions pour la period Juillet 2008/Juillet 2010 of Module A in TerDOUEST project (Terrassements Durables – Ouvrages En Sols Traités ANR RGCU 2008-2012).
- Diamond, S. (2000), 'Mercury porosimetry: An inappropriate method for the measurement of pore size distributions in cement-based materials', *Cement and Concrete Research* 30(10), 1517–1525.
- Diamond, S. & Kinter, E. (1965), 'Mechanisms of soil-lime stabilization', *Highway Research Record* (92).
- Diamond, S., White, J. & Dolch, W. (1964), Transformation of clay minerals by calcium hydroxide attack, in 'Proc., 12th National Conference of Clays and Clay Minerals', pp. 359–369.
- Dif, A. & Bluemel, W. (1991), 'Expansive soils under cyclic drying and wetting', *Geotechnical Testing Journal* 14(1).

- Dobry, R. & Vucetic, M. (1987) Dynamic properties and response of soft clay deposits. State of the art report. Proc. Int. Symp. Geotech. Eng. Soft Soils, Mexico City 2, 51-87. Eng. Soft Soils, Mexico City 2, 51-87.
- Dyvik R., Madshus C. (1985). Lab measurement of  $G_{max}$  using bender elements. Norwegian Geotechnical Institute, Oslo, Norway. pp. 186-196. Publication No. 161.
- Eades, J. & Grim, R. (1960), 'Reaction of hydrated lime with pure clay minerals in soil stabilization', Highway Research Board Bulletin.
- Eades, J. & Grim, R. (1966), 'A quick test to determine lime requirements for lime stabilization', Highway research record.
- Eades, J. L. (1962), 'Reactions of  $Ca(OH)_2$  with Clay Minerals in Soil Stabilization', PhD thesis, Geology Department, University of Illinois, Urbana.
- Elhakim, A. & Mayne, P. (2003), 'Derived stress-strain-strength of clays from seismic cone tests', Deformation Characteristics of Geomaterials 1, 81-87.
- Engineering manual 1110-3-137. (1984), 'Soil stabilization for pavements mobilization construction', Department of the Army, Corps of engineers office of the chief of engineers.
- EN 13286-40, unbound and hydraulically bound mixtures part 40: Test method for the determination of the direct tensile strength of hydraulically bound mixtures.
- EN 13286-43, unbound and hydraulically bound mixtures part 43: Test method for the determination of the modulus of elasticity of hydraulically bound mixtures.
- EN 13286-47, unbound and hydraulically bound mixtures part 47: Test method for the determination of California bearing ratio, immediate bearing index and linear swelling.
- EN 13286-49, unbound and hydraulically bound mixtures part 49: Accelerated swelling test for soil treated by lime and/or hydraulic binder.
- EN 14227-10, hydraulically bound mixtures - specifications - part 10: Soil treated by cement.2006.
- EN 14227-11, hydraulically bound mixtures - specifications - part 11: Soil treated by lime.2006.
- EN 459-2, Standard for building lime- Part 2: Test methods. 2010

- Esmer, E., Walker, R. & Krebs, R. (1969), 'Freeze-thaw durability of lime-stabilized clay soils', Highway Research Record.
- Estop-Aragonés, C. and Blodau, C. (2012), 'Effects of experimental drying intensity and duration on respiration and methane production recovery in fen peat incubations', *Soil Biology and Biochemistry*, 47(2012), 1-9.
- Eze-Uzomaka, O. & Agbo, D. (2010), 'Suitability of quarry dust as improvement to cement stabilized-laterite for road bases', *Electronic Journal of Geotechnical Engineering* 15, 1053–1066.
- Fahoum, K., Aggour, M. & Amini, F. (1996), 'Dynamic properties of cohesive soils treated with lime', *Journal of Geotechnical Engineering* 122(5), 382–389.
- Fernandez, A. & Santamarina, J. (2001), 'Effect of cementation on the small-strain parameters of sands', *Canadian Geotechnical Journal* 38(1), 191–199.
- Fernando, E., Liu, W., Ryu, D., of Transportation. Research, T. D., Office, T. & Institute, T. T. (2001), 'Development of a Procedure for Temperature Correction of Backcalculated AC Modulus', Texas Transportation Institute, Texas A & M University System.
- Ferber, V. (2005), 'Sensibilité des sols fins compactés à l'humidification apport d'un modèle de microstructure', PhD thesis, L'Ecole Centrale de Nantes et l'Université de Nantes.
- Ferrell, R., Arman, A., Baykal, G. & Louisiana (1988), 'Effects of combined lime and fly ash stabilization on the elastic moduli of montmorillonitic soils', Technical report, Department of Transportation and Development and Louisiana Transportation Research Center.
- Ferreira, C., & da Fonseca, A. V. (2005), 'International parallel tests on bender elements at the university of porto, portugal', Technical report, University of Porto, Portugal.
- Fitzmaurice, R. (1958), 'Manual on stabilised soil construction for housing', United Nations, technical Assistance Programme, New York.
- Fleureau, J. M., Kheirbek-Saoud, S., Soemitro, R., & Taibi, S. (1993), 'Behavior of clayey soils on drying-wetting paths', *Canadian Geotechnical Journal*, 30(2), 287-296.
- Flores, V., Di Emidio, G. & Van Impe, W. (2010), 'Small-strain shear modulus and strength increase of cement-treated clay', *Geotechnical Testing Journal* 33(1), 62.

- Forsssblad, L. (1981), 'Vibratory soil and rock fill compaction', Dynapac Maskin AB, Solna(Sweden).
- Fredlund, D. & Xing, A. (1994), 'Equations for the soil-water characteristic curve', Canadian Geotechnical Journal 31(4), 521–532.
- Fredlund, D., Xing, A., Fredlund, M. & Barbour, S. (1995), 'The relationship of the unsaturated soil shear strength function to the soil-water characteristic curve', Canadian Geotechnical Journal 32, 440–448.
- Fredlund, M., Fredlund, D. & Wilson, G. (1997a), 'Estimation of unsaturated soil properties using a knowledge-based system', in 'Proceedings of the Fourth Congress on Computing in Civil Engineering, ASCE, Philadelphia, PA, June', Citeseer, pp. 16–18.
- Fredlund, M., Fredlund, D. & Wilson, G. (1997b), 'Prediction of the soil-water characteristic curve from grain-size distribution and volume-mass properties', in '3rd Brazilian symposium on unsaturated soils', Rio de Janeiro, Brazil, pp. 22–25.
- Froumentin M. (2012), 'Rapport de construction de l'ouvrage expérimental – RD438 Héricourt (70)', TerDOUEST Projet ANR-07-PCGU-006-10, Rapport de CETE Normandie Centre, DERDI (Département expérimentation, Recherche, Développement et Innovation) et CER (Centre d'Expérimentation et de Recherche), 134 pages.
- Gabriels, P., Snieder, R. & Nolet, G. (1987), '*In situ* measurements of shear-wave velocity in sediments with higher-mode rayleigh waves', Geophysical prospecting 35(2), 187–196.
- Gao, G., Fu, B., Zhan, H., Ma, Y. (2013), 'Contaminant transport in soil with depth-dependent reaction coefficients and time-dependent boundary conditions', Water research 47(2013), 2507-2522.
- Glenn, G. & Handy, R. (1963), 'Lime-clay mineral reaction products', Highway research record .
- Glossop, R. (1968), 'The rise of geotechnology and its influence on engineering practice', Geotechnique 18(2), 107–150.
- Gnanendran, C., Piratheepan, J., Ramanujam, J. & Arulrajah, A. (2011), 'Accelerated laboratory pavement model test on cemented base and clay subgrade', ASTM geotechnical testing journal 34(4), 297–309.



- Goldberg, I. & Kellin, A. (1952), Some effects of treating expansive clays with calcium hydroxide, in 'Symposium on Exchange phenomena In Soils, ASTM special publication', Vol. 141.
- Gourley, C. & Schreiner, H. (1995), 'Field measurement of soil suction', in '1<sup>st</sup> International Conference on Unsaturated Soils', pp. 601–606.
- Graves, R., Eades, J. & Smith, L. (1988), 'Strength developed from carbonate cementation in silica-carbonate base course materials', number 1190.
- Grim, R. (1953), 'Clay mineralogy', *Soil Science* 76(4), 317.
- GTR, (1992), Guide technique « Réalisation des remblais et des couches de forme » LCPC-SETRA (Paris- Bagneux), sept. 1992. pp 204.
- GTR (2000), Guide technique « traitement des sols à la chaux et/ou aux liants hydrauliques. application à la réalisation des remblais et des couches de forme », LCPC-SETRA (paris-bagneux) Jan. 2000. 240p, Technical report.
- Guney, Y., Sari, D., Cetin, M. & Tuncan, M. (2007), 'Impact of cyclic wetting-drying on swelling behavior of lime-stabilized soil', *Building and Environment* 42(2), 681–688.
- Guthrie, W., Roper, M. & Eggett, D. (2008), 'Evaluation of laboratory durability tests for stabilized aggregate base materials', in 'Transportation Research Board 87th Annual Meeting Compendium of Papers'.
- Guthrie, W., Ellis, P. & Scullion, T. (2001), 'Repeatability and reliability of the tube suction test', *Transportation Research Record: Journal of the Transportation Research Board* 1772(-1), 151–157.
- Guthrie, W., Roper, M., Eggett, D. & Board, T. R. (2008), 'Evaluation of laboratory durability tests for stabilized aggregate base materials', in 'Transportation Research Board 87th Annual Meeting Compendium of Papers'.
- Guthrie, W. & Scullion, T. (2003), 'Interlaboratory study of the tube suction test', Report: FHWA/TX-03/0-4114-2.
- Guthrie, W., Sebesta, S., Scullion, T., of Transportation, T. D., Administration, U. S. F. H. & Institute, T. T. (2002), 'Selecting Optimum Cement Contents for Stabilizing Aggregate Base Materials', Texas Transportation Institute, Texas A & M University System.

- Hachum O., Dr. Rafi’M.S., A.-N. H. A. H. (2011), ‘Some engineering characteristics of lime-treated soil of semeel region with emphasis on compaction delay’.
- Hardin, B. (1978), ‘The nature of stress-strain behavior for soils’, in ‘From Volume I of Earthquake Engineering and Soil Dynamics–Proceedings of the ASCE Geotechnical Engineering Division Specialty Conference, June 19-21, 1978, Pasadena, California. Sponsored by Geotechnical Engineering Division of ASCE’.
- Hardin, B. & Drnevich, V. (1972), ‘Shear modulus and damping in soils’, *Journal of the Soil Mechanics and Foundations Division* 98(7), 667–692.
- Harichane, K., Ghrici, M., Khebizi, W. & Missoum, H. (2010), ‘Effect of the combination of lime and natural pozzolana on the durability of clayey soils’, *Electronic Journal of Geotechnical Engineering* 17, 1194–1210.
- Harris, P., von Holdt, J., Sebesta, S. & Scullion, T. (2006), ‘Part 3: Cementitious, chemical, and mechanical stabilization: Recommendations for stabilization of high-sulfate soils in texas’, *Transportation Research Record: Journal of the Transportation Research Board* 1952(-1), 71–79.
- Harty, J. (1971), ‘Factors influencing the lime reactivity of tropically and subtropically weathered soils’, Technical report, DTIC Document.
- Hazaree, C., Wang, K., Ceylan, H. & Gopalakrishnan, K. (2011), ‘Capillary transport in rcc: Water-to-cement ratio, strength, and freeze-thaw resistance’, *Journal of Materials in Civil Engineering* 23, 1181.
- Helinski, M., Fahey, M., and Fourie, A., 2007, “Numerical Modeling of Cemented Mine Backfill Deposition,” *J. Geotech. Geoenviron. Eng.*, Vol. 133, No. 10, pp. 1308–1319.
- Herzog, A. & Mitchell, J. (1963), ‘Reactions accompanying stabilization of clay with cement’, *Highway Research Record*.
- Highways Agency (2000), ‘Treatment of fill and capping materials using either lime or cement or both’, in ‘In Design manual for roads and bridges’, Vol. 4, London: HMSO.
- Hight, D., Bennell, J., Chana, B., Davis, P., Jardine, R. & Porovic, E. (1997), ‘Wave velocity and stiffness measurements of the crag and lower london tertiaries at sizewell’, *Geotechnique* 47(3), 451–474.

- Hilt, G. & Davidson, D. (1960), 'Lime fixation in clayey soils', Highway Research Board Bulletin.
- Hird, C. and Chan, C. M., 2005, 'Correlation of ShearWaveVelocity with Unconfined Compressive Strength of Cement- Stabilized Clay', Proceedings of the International Conference on Deep Mixing Best Practice and Recent Advances, Stockholm, Swedish Geotechnical Institute, Sweden, pp. 79–85.
- Hoar, R. & Stokoe, K. (1978), 'Generation and measurement of shear waves in-situ', Dynamic geotechnical testing, ASTM STP 654, 3–29.
- Holm, G. (1979), 'Lime column stabilization-experiences concerning strength and deformation properties', Vag-Och Vattenbyggaren 25(7/8).
- Holt, C. & Freer-Hewish, R. (1996), Lime treatment of capping layers in accordance with the current specification for highway works, in 'Proceedings, Seminar on Lime Stabilisation', pp. 51–61.
- Holtz, R. & Kovacs, W. (1981), 'An Introduction to Geotechnical Engineering', Prentice Hall.
- Holubec, I. & D'Appolonia, E. (1972), 'Effect of particle shape on the engineering properties of granular soils', ASTM Special Technical Publication (Compendex), 304–318.
- Horpibulsuk, S., Katkan, Sirilerdwattana, W., and Rachan, R. (2006), 'Strength development in cement stabilized low plasticity and coarse grained soils: Laboratory and field study', Soils and foundations 46(3), 351–366.
- Horpibulsuk, S., Miura, N. & Nagaraj, T. (2003), 'Assessment of strength development in cement-admixed high water content clays with abrams' law as a basis', Geotechnique 53(4), 439–444.
- Horpibulsuk S, Kumpala A, Katkan W., (2008), 'A case history on underpinning for a distressed building on hard residual soil underneath non-uniform loose sand', Soils and Found, 48(2), 267–86.
- Horpibulsuk, S., Rachan, R., Chinkulkijniwat, A., Raksachon, Y. & Suddeepong, A. (2010), 'Analysis of strength development in cement-stabilized silty clay from microstructural considerations', Construction and Building Materials 24(10), 2011 – 2021.

- Hossain, K. & Mol, L. (2011), 'Some engineering properties of stabilized clayey soils incorporating natural pozzolans and industrial wastes', *Construction and Building Materials*.
- Hossein Alavi, A., Hossein Gandomi, A., Mollahassani, A., Akbar Heshmati, A. & Rashed, A. (2010), 'Modeling of maximum dry density and optimum moisture content of stabilized soil using artificial neural networks', *Journal of Plant Nutrition and Soil Science* 173(3), 368–379.
- Houlsby, G. & Wroth, C. (1989), 'The influence of soil stiffness and lateral stress on the results of in-situ soil tests', in 'Proceedings of the 12th International Conference on Soil Mechanics and Foundation Engineering, Rio de Janeiro, Brazil', Vol. 1, pp. 227–232.
- Hu, R., Yeung, M., Lee, C. & Wang, S. (2001), 'Mechanical behavior and microstructural variation of loess under dynamic compaction', *Engineering Geology* 59(3-4), 203–217.
- Hung, C. (2010), *Projet de recherche TerDOUEST construction d'un remblai de reference pour tester le reemploi d'argiles très plastiques. Sols et Terrassements. Travaux Revue Technique des Entreprises de Travaux Publics. N°877 Décembre 2010/ Janvier 2011.*
- Hunter, D. (1988), 'Lime induced heave in sulfate-bearing clay soils', *Journal of Geotechnical Engineering, ASCE* 114, No. 2, 150–167.
- Ingles, O. (1987), 'Soil stabilization, Chapter 38, *Ground Engineer's Reference Book*', Butterworths, London, 38/1-38/26.
- Ingles, O. & Metcalf, J. (1973), *Soil stabilization: principles and practice*, Butterworths Sydney.
- Iwasaki, T. & Tatsuoka, F., (1977), 'Effects of grain size and grading on dynamic shear moduli of sands', *Soils Found*, 17, No. 3, 19–35.
- Jauberthie, R., Rendell, F., Rangeard, D. & Molez, L. (2010), 'Stabilisation of estuarine silt with lime and/or cement', *Applied Clay Science*, 50(3), 395 – 400.
- Jesmani, M., Kashani, H. & Kamalzare, M. (2010), 'Effect of plasticity and normal stress on undrained shear modulus of clayey soils', *Acta geotechnica slovenica*,(1) (1), 47–59.
- Joel, M. & Agbede, I. (2010), 'Cement stabilization of igumale shale lime admixture for use as flexible pavement construction material', *Electronic Journal of Geotechnical Engineering* 15, 1661–1673.

- John, U., Jefferson, I., Boardman, D., Ghataora, G. & Hills, C. (2011), 'Leaching evaluation of cement stabilisation/solidification treated kaolin clay', *Engineering Geology*.
- Jovicic, V. & Coop, M. (1997), 'Stiffness of coarse-grained soils at small strains', *Pre-failure deformation behaviour of geomaterials* p. 159.
- Kalkan, E. (2011), 'Impact of wetting-drying cycles on swelling behavior of clayey soils modified by silica fume', *Applied Clay Science*.
- Kamang, E. E. J. (1998), 'Effect of water -cement ratio on the strength properties of stabilized laterite soils', *Nigerian Journal of construction technology and management* 1 No 1, 58–62.
- Kamon, M. & Nontananandh, S. (1991), 'Combining industrial wastes with lime for soil stabilization', *Journal of geotechnical engineering* 117, 1.
- Kang, M., Kim, S., Han, S. & Yoon, M. (2008), 'Comparison and strength characteristics of cements for cement-stabilization for dredged surface soil', in 'ISOPE-2008: Eighteenth(2008) International Offshore and Offshore and Polar Engineering Conference Proceedings', International Society of Offshore and Polar Engineers, P. O. Box 189, Cupertino, CA, 95015-0189, USA,.
- Kasangaki, G. & Towhata, I. (2009), 'Wet compaction and lime stabilization to mitigate volume change potential of swelling clayey soils', *Soils and foundations* 49(5), 813–821.
- Katarzyna.M.L (2008), 'The determination of shear modulus overconsolidated cohesive soils', *Foundations of Civil and Environmental Engineering* pp. 61–71.
- Kavak, A. & Akyarh, A. (2007), 'A field application for lime stabilization', *Environmental Geology* 51(6), 987–997.
- Kawamura, M. & Diamond, S. (1975), 'Stabilization of clay soils against erosion loss: Technical paper'.
- Kawaguchi, T., Mitachi, T., Shibuya, S. (2001), 'Evaluation of shear wave travel time in laboratory bender element test', *Proc. of the 15th International Conference on Soil Mechanics and Geotechnical Engineering*, Vol.1, pp.155-158.
- Kelley, C. (1977), 'A Long Range Durability Study of Lime Stabilized Bases at Military Posts in the Southwest', *National Lime Association*.

- Kennedy, T., Smith, R., Holmgreen Jr, R. & Tahmoressi, M. (1987), 'an evaluation of lime and cement stabilization', number 1119.
- Khattab, A. (2002), 'Comportement mécanique d'une argile gonflante stabilise à la chaux', PhD thesis, Université d'Orléans.
- Khattab, S. A., Al-Mukhtar, M. & Fleureau, J.-M. (2007), 'Long-term stability characteristics of a lime-treated plastic soil', *Journal of Materials in Civil Engineering* 19(4), 358 – 366. Lime-treated expansive soils: Mercury intrusion tests.
- Khosravi, A., Ghayoomi, M., McCartney, J. & Ko, H. (2010), 'Impact of effective stress on the dynamic shear modulus of unsaturated sand', *Advances in Analysis, Modeling & Design. ASCE* 199, 410–419.
- Kim, D.S. (1991), 'Deformational characteristics of soils at small to intermediate strains from cyclic tests', Ph.D. dissertation, The University of Texas at Austin, Austin, Tex.
- Kim T., H. C. (2003), 'Modelling of tensile strength on moist granular earth material at low water content', *Engineering Geology* vol. 69, P. 233–244.
- Kolias, S., Kasselouri-Rigopoulou, V. & Karahalios, A. (2005), 'Stabilisation of clayey soils with high calcium fly ash and cement', *Cement and Concrete Composites* 27(2), 301 – 313. Cement and Concrete Research in Greece.
- Komine, H. and Ogata, N. (1997), 'Prediction for swelling characteristics of compacted bentonite', *Can. Geotech. J.*, 33, 11-22.
- Lade, P. & Overton, D. (1989), 'Cementation effects in frictional materials', *Journal of Geotechnical Engineering* 115(10), 1373–1387.
- Lambe, T. W. & Whitman, R. V. (1969), *Soil mechanics*.
- Lasisi, F. & Ogunjide, A. (1984), 'Effect of grain size on the strength characteristics of cement-stabilized lateritic soils', *Building and Environment* 19(1), 49–54.
- Lasledj, A. (2009), 'Traitement des sols argileux à la chaux: processus physico-chimiques et propriétés géotechniques', PhD thesis, France, 359p, PhD thesis.
- Le Roux, A. (1969), 'Traitement des sols argileux par la chaux', *Bulletin de Liaison des Laboratoires des Ponts et Chaussées*, Paris (40), 59–95.

- Le Runigo, B. (2008), 'Duability of the lime-treated Jossigeny silt under different Hydraulic stresses: assessment of the mechanical, hydraulic microstructural, microstructural behavior', PhD thesis, L'Ecole Centrale de Nantes et l'Universite de Nantes.
- Le Runigo, B., Ferber, V., Y. C.-O. C. D. D. (2011), 'Performance of lime-treated silty soil under long-term hydraulic conditions', *Engineering Geology* 9, 20 – 28.
- Le Runigo, B., Cuisinier, O., Cui, Y., Ferber, V. & Deneele, D. (2009), 'Impact of initial state on the fabric and permeability of a lime-treated silt under long-term leaching', *Canadian Geotechnical Journal* 46(11), 1243–1257.
- Lee, G., Abdelkater, M. & Hamdani, S. (1982), 'Effect of the clay fraction on some mechanical properties of lime-soil mixtures', *Highway Engineer* 29(11).
- Lee, W., Bohra, N., Altschaeffl, A. D., and White, T. D. (1994). Proc. Transportation Research Board 73rd Annual Meeting, Washington, D.C. (n.d.).
- Lee, J.-S. and Santamarina, J. C. (2005), 'Bender Elements: Performance and Signal Interpretation', *Journal of Geotechnical and Geoenvironmental Engineering*, 131, 1063-1070.
- Leong, E., Cahyadi, J. & Rahardjo, H. (2009), 'Measuring shear and compression wave velocities of soil using bender-extender elements', *Canadian Geotechnical Journal* 46(7), 792–812.
- Liang, R., Samer Rabab' ah, S., Khasawneh, M. et al. (2008), 'Predicting moisture-dependent resilient modulus of cohesive soils using soil suction concept', *Journal of Transportation Engineering* 134, 34.
- Liao, C. (2007), 'The wetting effect and shear modulus of unsaturated cohesive subgrade soils'.
- Lim, S., Jeon, W., Lee, J., Lee, K. & Kim, N. (2002), 'Engineering properties of water/wastewater-treatment sludge modified by hydrated lime, fly ash and loess', *Water research* 36(17), 4177–4184.
- Lima, A., Romero Morales, E., Pineda, J., Gens Solé, A. et al. (2011), 'Low-strain shear modulus dependence on water content of a natural stiff clay'.

## Reference

---

- Lin, L. & Benson, C. (2000), 'Effect of wet-dry cycling on swelling and hydraulic conductivity of gcls', *Journal of Geotechnical and Geoenvironmental Engineering* 126, 40.
- Lings, M. & Greening, P. (2001), 'A novel bender/extender element for soil testing', *Geotechnique* 51(8), 713–717.
- Little, D. (1995a), 'Guidelines for mixture design and thickness design for stabilized bases and subgrades', Technical report.
- Little, D. (1995b), 'Handbook for stabilization of pavement subgrades and base courses with lime', Kendall/Hunt Pub. Co.
- Little, D. N., (1995c), 'Stabilization of Pavement Subgrades and Base Courses with Lime', Kendall/Hunt Publishing Company, Dubuque, Iowa.
- Little, D. (1996a), 'Assessment of *in situ* structural properties of lime-stabilized clay subgrades', *Transportation Research Record: Journal of the Transportation Research Board* 1546(-1), 13–23.
- Little, D. N. (1996b), 'Evaluation of resilient and strength properties of lime-stabilized soils from the denver', colorado area, Technical report, Report for the Chemical Lime Company.
- Little, D., Males, E., Prusinski, J. & Stewart, B. (2000), 'Cementitious stabilization', *Transportation in the New Millennium*.
- Little, D. N. (1999), 'Evaluation of structural propertites of lime stabilized soils and aggregates–prepared for the national lime association'.
- Little, D., Nair, S., Program, N. C. H. R. & Board, N. R. C. U. T. R. (2009), 'Recommended Practice for Stabilization of Subgrade Soils and Base Materials', National Cooperative Highway Research Program, Transportation Research Board of the National Academies.
- Liu, S., Zhang, D., Liu, Z., and Deng, Y. (2008), 'Assessment of Unconfined Compressive Strength of Cement Stabilized Marine Clay', *Marine Georesources and Geotechnology*, Vol. 26, pp.19–35.



- Lo Presti, D., Jamiolkowski, M., Pallara, O. & Cavallaro, A. (1996), 'Rate and creep effect on the stiffness of soils', in 'Measuring and Modeling Time Dependent Soil Behavior (GSP 61)', ASCE, pp. 166–180.
- Lo Presti, D., Jamiolkowski, M. & Pepe, M. (2002), 'Geotechnical characterisation of the subsoil of pisa tower', *Characterisation and engineering properties of natural soils* 2, 909.
- Lo Presti, D., Pallara, O., Lancellotta, R., Armandi, M. & Maniscalco, R. (1993), 'Monotonic and cyclic loading behavior of two sands at small strains', *ASTM geotechnical testing journal* 16(4), 409–424.
- Lo Presti, D., Jamiolkowski, M., Pallara, O., Cavallaro, A. & Pedroni, S. (1997), 'Shear modulus and damping of soils', *Geotechnique*, 47(3), 603–617.
- Locat, J., Bérubé, M. & Choquette, M. (1990), 'Laboratory investigations on the lime stabilization of sensitive clays: shear strength development', *Canadian Geotechnical Journal* 27(3), 294–304.
- Locat, J., Tremblay, H. & Leroueil, S. (1996), 'Mechanical and hydraulic behaviour of a soft inorganic clay treated with lime', *Canadian geotechnical journal* 33(4), 654–669.
- Lohani, T., Tatsuoka, F., Tateyama, M., and Shibuya, S., 2006, 'Strengthening of Weakly Cemented Gravelly Soil with Curing Period', *Soil Stress-Strain Behavior: Measurement, Modeling and Analysis, Solid Mechanics and its Applications*, Rome, Springer, The Netherlands, Vol. 146, pp. 455–462.
- Lorenzo, G. & Bergado, D. (2004), 'Fundamental parameters of cement-admixed clay—new approach', *Journal of geotechnical and geoenvironmental engineering* 130, 1042.
- Macedo, A., Vaz, C., Naime, J., Cruvinel, P. & Crestana, S. (1999), 'X-ray microtomography to characterize the physical properties of soil and particulate systems', *Powder technology* 101(2), 178–182.
- Malhotra B.R., B. S. (1983), 'Leaching phenomenon in lime soil mix layers', *Highway Research Bulletin*, New Delhi 22, 15–25.
- Mallela, J., Harold Von Quintus, P., Smith, K. & Consultants, E. (2004), 'Consideration of lime-stabilized layers in mechanistic-empirical pavement design', submitted to National Lime Association .

- Mancuso, C., Vassallo, R. & d'Onofrio, A. (2002), 'Small strain behavior of a silty sand in controlled-suction resonant column-torsional shear tests', *Canadian Geotechnical Journal* 39(1), 22–31.
- Matasovic, N. & Jr., E. K. (1998), 'Cyclic characterization of oil landfill solid waste', *Journal of Geotechnical and Geoenvironmental Engineering*, ASCE 124(4), 197–210.
- Mateos, M. (1964), 'Soil lime research at iowa state university', *Journal of soil mechanics and foundations division*, ASCE 90, No.SM2, 127–153.
- Matesic, L. & Vucetic, M. (2003), 'Strain-rate effect on soil secant shear modulus at small cyclic strains', *Journal of geotechnical and geoenvironmental engineering* 129, 536.
- Mathew, P. & Rao, S. (1997), 'Effect of lime on cation exchange capacity of marine clay', *Journal of geotechnical and geoenvironmental engineering* 123, 183.
- Maubec, N. (2010), 'Approche multi-echelle du traitement des sols a la chaux etudes des interactions avec les argiles', PhD thesis, Universite de nantes.
- Mayne, P. & Rix, G. (1993), ' $G_{max}$ -qc relationships for clays', *ASTM geotechnical testing journal* 16(1), 54–60.
- McCallister, L. (1990), 'Property changes in lime treated expansive clays under continuous leaching', Technical report, DTIC Document.
- McCallister, L. & Petry, T. (1992), 'Leach tests on lime-treated clays', *Geotechnical testing journal* 15(2).
- McNally, G. (1998), 'Soil and rock construction materials', Taylor & Francis.
- McNeal, B.L. (1970), 'Prediction of interlayer swelling of clays in mixed-salt solutions', *Soil Science Society of America Journal*, Vol.34 No.2, p.201-206.
- Meidani, M., Shafiee, A., Habibagahi, G., Jafari, M., Mohri, Y., Ghahramani, A. & Chang, C. (2008), 'Granule shape effect on the shear modulus and damping ratio of mixed gravel and clay', *Iranian Journal of Science & Technology, Transaction B, Engineering* 32(B5), 501–518.
- Merchan, V., Romero, E. & Vaunat, J. (2010), 'Simulation aided testing of hydro-mechanical processes on clay', *EPJ Web of Conferences* 6.

- Millogo, Y., Hajjaji, M., Ouedraogo, R. & Gomina, M. (2008), 'Cement-lateritic gravels mixtures: Microstructure and strength characteristics', *Construction and Building Materials* 22(10), 2078 – 2086.
- Mitchell, J. K., Veng, T. S., and Monismith, C. L., 1974, 'Behavior of Stabilized Soils Under Repeated Loading', *Performance Evaluation of Cement-Stabilized Soil Layers and Its Relationship to Pavement Design*, Department of Civil Engineering, University of California, Berkeley, Berkeley, CA.
- Mitchell, J. (1976), 'The properties of cement-stabilized soils', in 'Proceeding Residential Workshop on Materials and Methods for Low Cost Road, Rail and Reclamation Works, Leura, Australia, September', pp. 6–10.
- Mitchell, J. & Soga, K. (1976), 'Fundamentals of soil behavior', Wiley New York., 422 pages.
- Mleza, Y. & Hajjaji, M. (2011), 'Microstructural characterisation and physical properties of cured thermally activated clay-lime blends', *Construction and Building Materials* .
- Moh, Z. (1962), 'Soil stabilization with cement and sodium additives', *Journal of soil mechanics and foundations division, ASCE* 88, No. 6, 81–105.
- Mooney, M., Toohey, N., Research, C. D. A., Branch, I. & Administration, U. S. F. H. (2010), 'Accelerated curing and strength-modulus correlation for lime-stabilized soils', Technical report.
- Moore, D., Reynolds Jr, R. et al. (1989), 'X-ray Diffraction and the Identification and Analysis of Clay Minerals', Oxford University Press (OUP).
- Muhanna, A., Rahman, M. & Lambe, P. (1998), 'Model for resilient modulus and permanent strain of subgrade soils', *Transportation Research Record: Journal of the Transportation Research Board* 1619(-1), 85–93.
- Muhanna, A., Rahman, M. & Lambe, P. (1999), 'Resilient modulus measurement of fine-grained subgrade soils', *Transportation Research Record: Journal of the Transportation Research Board* 1687(-1), 3–12.
- Muhunthan, B. & Sariosseiri, F. (2008), 'Interpretation of geotechnical properties of cement treated soils', Technical report.

- Muntohar, A. S. (2004), 'Swelling and Compressibility Characteristics of Soil – Bentonite Mixtures', *Dimensi Teknik Sipil*, Vol. 5, No.2, 93-98.
- Muzahim Al-Mukhtar. (2007), 'Remblais expérimentaux – A34 Réutilisation d'argile très plastiques en corps de remblais routiers', In *Terrassements durables-ouvrages en sols traités – TerDOUEST project*.
- Nagaraj TS, Vatasala A, Srinivasa Murthy BR. (1990), Discussion on 'Change in pore size distribution due to consolidation of clays' by F.J. Griffith and R.C. Joshi. *Geotechnique*, 40(2):303–5.
- Nagaraj, T. S., Miura, N., and Yamadera, A. (1998), 'Induced Cementation of Soft Clay', *Proceedings of the International Symposium on Lowland Technology*, Saga University, Japan, Institute of Lowland Technology, Saga, Japan, pp. 267–278.
- Nalbantoglu, Z. & Tuncer, E. (2001), 'Compressibility and hydraulic conductivity of a chemically treated expansive clay', *Canadian geotechnical journal* 38(1), 154–160.
- Narasimha Rao, S., Subba Rao, K. & Rajasekaran, G. (1993), 'Microstructure studies of lime treated marine clays', in 'Proceedings of the international conference on offshore mechanics and arctic engineering', American Society of Mechanical Engineers, pp. 425–425.
- National Lime Association (2004), 'Lime-treated soil construction manual lime stabilization & lime modification', National lime association-the versatile chemical.
- Nazarian, S., Rojas, J., Pezo, R., Yuan, D., Abdallah, I. & Scullion, T. (1998), 'Relating laboratory and field moduli of texas base materials', *Transportation Research Record: Journal of the Transportation Research Board* 1639(-1), 1–11.
- Nazarian, S., Yuan, D. & Tandon, V. (1999), 'Structural field testing of flexible pavement layers with seismic methods for quality control', *Transportation Research Record: Journal of the Transportation Research Board* 1654(-1), 50–60.
- Neville, A. M. (1995), 'Properties of Concrete', Prentice Hall, Harlow, England.
- NF P 94-054. (1991), Standard test for soils investigation and testing- Determination of particle density – Pycnometer method.
- NF P 94-056. (1996), Standard test for soils investigation and testing- Granulometric analysis-Dry sieving method after washing.

- NF P 94-057. (1992), Standard test for soils investigation and testing- Granulometric analysis-Hydrometer method.
- NF P 94-068. (1998), Standard test for soils investigation and testing- Measuring of the methylene blue adsorption capacity of a rocky soil – Determination of the methylene blue of a soil by means of the stain test.
- NF P 94-051. (1998) , Standard test for soils investigation and testing- Determination of Atterberg's limits – Liquid limit test using Casagrande apparatus – Plastic limit test on rolled thread.
- NF P 94-093. (1999), Standard test for soils investigation and testing- Determination of the compaction characteristics of a soil – Standard Proctor test and Modified Proctor test.
- NF P 98 331. (2005), Chaussées et dépendances: Tranchées- ouverture, remblayage, refection.
- NF EN P 11-300. (1992), Standard for classification of materials for use in the construction of embankments and capping layers of road infrastructures.
- NF EN 197-1. (2004), ciment- partie 1 : composition, specifications et critères de conformité des ciments courants.
- NF P15-318. (2006), Liants hydrauliques – Ciments à teneur en sulfures limitée pour béton précontraint.
- Ng, C. & Xu, J. (2012), 'Effects of current suction ratio and recent suction history on small-strain behaviour of an unsaturated soil', *Can. Geotech. J.* 49, 226–243.
- Ng, C., Xu, J. & Yung, S. (2009), 'Effects of wetting/drying and stress ratio on anisotropic stiffness of an unsaturated soil at very small strains', *Canadian Geotechnical Journal* 46(9), 1062–1076.
- Ng, C. & Yung, S. (2008), 'Determination of the anisotropic shear stiffness of an unsaturated decomposed soil', *Géotechnique* 58(1), 23–35.
- Nordlund, R. & Deere, D. (1970), 'Collapse of fargo grain elevator: Journal soil mechanics and foundations division, american society of civil engineers, v. 96, no. sm2', *Proc. Paper 7172*, 585–607.

- Nowamooz, H. & Masrouri, F. (2008), 'Hydromechanical behaviour of an expansive bentonite/silt mixture in cyclic suction-controlled drying and wetting tests', *Engineering Geology* 101(3), 154–164.
- Nowamooz, H. & Masrouri, F. (2010), 'Volumetric strains due to changes in suction or stress of an expansive bentonite/silt mixture treated with lime', *Comptes Rendus Mécanique* 338(4), 230–240.
- Oflaherty, C. & Andrews, D. (1968), 'Frost effects in lime and cement-treated soils', *Highway Research Record*.
- O.G., I. (1970), 'Mechanisms of stabilization with inorganic acid and alkalis', *Australian Journal Research* 8, 81–95.
- Okafor, F. & Okonkwo, U. (2009), 'Effects of rice husk ash on some geotechnical properties of lateritic soil', *Leonardo Electronic Journal of Practices and Technologies* 8(15), 67–74.
- Okyay, U. & Dias, D. (2010), 'Use of lime and cement treated soils as pile supported load transfer platform', *Engineering Geology* 114(1), 34–44.
- Olugbenga, A. (2007), 'Effects of varying curing age and water/cement ratio on the elastic properties of latrized concrete', *Civil Engineering Dimension* 9(2), pp–85.
- Onitsuka, K., Modmoltin, C. & Kouno, M. (2001), 'Investigation on microstructure and strength of lime and cement stabilized ariake clay', *Reports of the Faculty of Science and Engineering, Saga* 30(1), 49–63.
- Ormsby, W. (1973), 'Strength development and reaction products in lime treated montmorillonite water system', *Public Road Research* 37, n°4, 136–148.
- Ortiz, O. F. P. (2004), *Small and large strain monitoring of unsaturated soil behavior by means of multiaxial testing and shear wave propagation*, PhD thesis, Louisiana State University.
- Osinubi, K. (1998), 'Influence of compactive efforts and compaction delays on lime-treated soil', *Journal of transportation engineering* 124(2), 149–155.
- Osinubi, K., Nwaiwu, C. et al. (2006), 'Compaction delay effects on properties of lime-treated soil', *Journal of Materials in Civil Engineering* 18, 250.

- Osula, D. (1996), 'A comparative evaluation of cement and lime modification of laterite', *Engineering geology* 42(1), 71–81.
- Pan, H., Qing, Y. & Pei-yong, L. (2010), 'Direct and indirect measurement of soil suction in the laboratory', *Electronic Journal of Geotechnical Engineering* 15.
- Pardini, G., Guidi, G. V., Pini, R., Regüés, D. & Gallart, F. (1996), 'Structure and porosity of smectitic mudrocks as affected by experimental wetting-drying cycles and freezing-thawing cycles', *CATENA* 27(3-4), 149 – 165.
- Parker, J. (2008), Evaluation of laboratory durability tests for stabilized subgrade soils, Master's thesis, Brigham Young University.
- Parsons, R. & Milburn, J. (2003), 'Engineering behavior of stabilized soils', *Transportation Research Record: Journal of the Transportation Research Board* 1837(-1), 20–29.
- Pathivada, S. (2007), 'Effects of water-cement ratio on deep mixing treated expansive clay characteristics'.
- Pedarla, A. (2009), Durability studies on stabilization effectiveness of soils containing different fractions of montmorillonite, Master's thesis, The University of Texas at Arlington.
- Pedarla, A., Chittoori, S., Puppala, A., Hoyos, L. & Saride, S. (2010), Influence of lime dosage on stabilization effectiveness of montmorillonite dominant clays, ASCE.
- Peng, Y. & He, Y. (2009), 'Structural characteristics of cement-stabilized soil bases with 3d finite element method', *Frontiers of Architecture and Civil Engineering in China* 3(4), 428–434.
- Peron Hervé, Laloui Lyesse. , T. H. L. B. H. (2009), Desiccation cracking of soils, in 'European Journal of Environmental and Civil Engineering', Vol. Volume 13.
- Perret, P. (1979), 'Practical consequences and on-site applications of new experimental data concerning the stabilization of fine soils with lime', *Bulletin de liaison des Laboratoires Ponts et Chaussées* n°99, pp. 110–118.
- Perry, J. (1977), 'Lime treatment of dams constructed with dispersive clay soils', *Transactions of the American Society of Agricultural Engineers* 20(6).
- Peterson, R. W. (1990), 'Influence of soil suction on the shear strength of unsaturated soil', *Miscellaneous Paper GL-90-17*.

- Petry, T. & Lee, T. (1988), Comparison of quicklime and hydrated lime slurries for stabilization of highly active clay soils, number 1190.
- Petry, T. & Little, D. (2002), 'Review of stabilization of clays and expansive soils in pavements and lightly loaded structures- history, practice, and future', *Perspectives in Civil Engineering: Commemorating the 150<sup>th</sup> Anniversary of the American Society of Civil Engineers* 14:6, 307–320.
- Pezo, R. & Hudson, W. (1994), 'Prediction models of resilient modulus for nongranular materials', *ASTM geotechnical testing journal* 17(3), 349–355.
- Phogat, V., Aylmore, L. & Schuller, R. (1991), 'Simultaneous measurement of the spatial distribution of soil water content and bulk density', *Soil Sci. Soc. Am. J* 55(4), 908–915.
- Pires, L., Arthur, R., Correchel, V., Bacchi, O., Reichardt, K. & Brasil, R. (2004), 'The use of gamma ray computed tomography to investigate soil compaction due to core sampling devices', *Brazilian journal of physics* 34(3a), 728–731.
- Pires, L., de Macedo, J., de Souza, M., Bacchi, O. & Reichardt, K. (2003), 'Gamma-ray-computed tomography to investigate compaction on sewage-sludge-treated soil', *Applied radiation and isotopes* 59(1), 17–25.
- Pires, L. F., Bacchi, O. O. & Reichardt, K. (2005), 'Gamma ray computed tomography to evaluate wetting/drying soil structure changes', *Nuclear Instruments and Methods in Physics Research Section B: Beam Interactions with Materials and Atoms* 229(3-4), 443 – 456.
- Piriyakul, K. (2006), Anisotropic stress-strain behaviour of Belgian Boom clay in the small strain region, PhD thesis.
- Plowman, J. M. (1956), 'Maturity and the Strength of Concrete', *Concrete Research*, Vol. 8, No. 22, pp. 13–22.
- Pokhrel, D. (2009), 'Hydro Mechanical Behavior of Unsaturated Soil Subjected to Drying', PhD thesis, The University of Findlay.
- Portland cement association, (1992), 'Soil-Cement Laboratory Handbook'.
- Powell, J. & Butcher, A. (2002), 'Characterisation of a glacial clay till at cowden, humberside', *Characterisation and engineering properties of natural soils* 2, 983.



- Powers, J. (1992), *Construction dewatering: new methods and applications*, Vol. 62, Wiley-Interscience.
- Prusinski, J. & Bhattacharja, S. (1999), 'Effectiveness of portland cement and lime in stabilizing clay soils', *Transportation Research Record: Journal of the Transportation Research Board* 1652(-1), 215–227.
- Puppala, A.J. and Kadam, R. and Madhyannapu, R.S. and Hoyos, L.R. and others (2006), 'Small-strain shear moduli of chemically stabilized sulfate-bearing cohesive soils', *Journal of Geotechnical and Geoenvironmental Engineering* 132(3), 322-336
- Puppala, A., Bhadriraju, V., Madhyannapu, R., Nazarian, S. & Williammee, R. (2005), 'Small strain shear moduli of lime-cement treated expansive clays', *Journal of Geomechanics*, ASCE pp. 58–70.
- Puppala, A., Mohammad, L. & Allen, A. (1999), 'Permanent deformation characterization of subgrade soils from rlt test', *Journal of Materials in Civil Engineering* 11, 274.
- Puppala, A., Ramakrishna, A. & Hoyos, L. (2003), 'Resilient moduli of treated clays from repeated load triaxial test', *Transportation Research Record: Journal of the Transportation Research Board* 1821(-1), 68–74.
- Radhey.S.Sharma & Bukkapatnam, A. T. (2008), An investigation of unsaturated soil stiffness, in 'An investigation of unsaturated soil stiffness. In Proceedings of the 12th International Conference of the International Association for Computer Methods and Advances in Geomechanics (12th IACMAG 2008), Goa, India, 1-6 October 2008. Edited by D.N. Singh. International Association for Computer Methods and Advances in Geomechanics (IACMAG), Ariz.', pp. 2042–2048.
- Rajasekaran, G. & Rao, S. N. (1997), 'The microstructure of lime-stabilized marine clay', *Ocean Engineering* 24(9), 867 – 875.
- Rajeev, P., Chan, D., and Kodikara, J. (2012), 'Ground-atmosphere interaction modelling for long-term prediction of soil moisture and temperature', *Can. Geotech. J.*, 49: 1059-1073.
- Rammah, K.; Val, D. and Puzrin, A. (2004), 'Effects of ageing on small-strain stiffness of overconsolidated clays', *Geotechnique*, 54(5).

- Rao, S. M., Reddy, B. V. V. & Muttharam, M. (2001), 'The impact of cyclic wetting and drying on the swelling behaviour of stabilized expansive soils', *Engineering Geology* 60(1-4), 223 – 233.
- Rao, S. & Rajasekaran, G. (1996), 'Reaction products formed in lime-stabilized marine clays', *Journal of geotechnical engineering* 122(5), 329–336.
- Rasiah, V. & Aylmore, L. (1998), 'Computed tomography data on soil structural and hydraulic parameters assessed for spatial continuity by semivariance geostatistics', *Australian journal of soil research* 36(3), 485–93.
- Rassam, D. & Cook, F. (2002), 'Predicting the shear strength envelope of unsaturated soils', *ASTM geotechnical testing journal* 25(2), 215–220.
- Rattanasak, U. & Kendall, K. (2005), 'Pore structure of cement/pozzolan composites by x-ray microtomography', *Cement and concrete research* 35(4), 637–640.
- Reddy, K. & Saxena, S. (1993), 'Effects of cementation on stress-strain and strength characteristics of sands', *Soil and Foundations* 33(4), 121–134.
- Rios, C.A., Williams, C.D., Fullen M.A. (2009), 'Hydrothermal synthesis of hydrogarnet and tobermorite at 175°C from kaolinite and metakaolinite in the CaO-Al<sub>2</sub>O<sub>3</sub>-SiO<sub>2</sub>-H<sub>2</sub>O system: a comparative study', *Applied Clay Science* 43(2), 228–237.
- Rogers, C., Boardman, D. & Papadimitriou, G. (2006), 'Stress path testing of realistically cured lime and lime/cement stabilized clay', *Journal of Materials in Civil Engineering* 18, 259.
- Rogers, C.D.F. & Glendinning, S. (2000), 'Lime requirement for stabilization', *Transportation Research Record: Journal of the Transportation Research Board* 1721(1), 9–18.
- Rogers, C.D.F. & Glendinning, S. (1996), Modification of clay soils using lime, in 'Proceedings, Seminar on Lime Stabilization', pp. 99–114.
- Rogers, C. & Glendinning, S. (1997), 'Improvement of clay soils in situ using lime piles in the uk', *Engineering geology* 47(3), 243–257.
- Rollings, M. P. & Rollings, R. R. (1996), *Geotechnical materials in construction*.
- Rossi, P., Ildefonse, P., De Nobrega, M. & Chauvel, A. (1983), 'Study of structural and mineralogical transformations caused by compaction with or without lime addition to

- lateritic clays from brazil', *Bulletin of the International Association of Engineering Geology* 28, 153–159.
- Russo, G.; Vecchio, S. & Mascolo, G. Microstructure of a lime stabilised compacted silt  
*Experimental Unsaturated Soil Mechanics*, Springer, 2006, 49-56
- Sabry, M. & Parcher, J. (1979), 'Engineering properties of soil-lime mixes', *Transportation Engineering Journal* 105(1), 59–70.
- Sahaphol, T. & Miura, S. (2005), 'Shear moduli of volcanic soils', *Soil Dynamics and Earthquake Engineering* 25(2), 157–165.
- Sakr, M., Shahin, M. & Metwally, Y. (2009), 'Utilization of lime for stabilizing soft clay soil of high organic content', *Geotechnical and Geological Engineering* 27(1), 105–113.
- Sanchez-Salinerio, I., Roesset, J., Stokoe, I. & Kenneth, H. (1986), Analytical studies of body wave propagation and attenuation, Technical report, DTIC Document.
- Santamarina, C. & Cascante, G. (1998), 'Effect of surface roughness on wave propagation parameters', *Geotechnique* 48(1), 129–36.
- Santamarina, J. & Aloufi, M. (1999), 'Small strain stiffness: A micromechanical experimental study', *Proceedings of Pre-failure Deformation Characteristics of Geomaterials* pp. 451–458.
- Santamarina, J. (2003), 'Soil behavior at the microscale: particle forces', *Geotechnical Special Publication* 119, 25–56.
- Santamarina, J. & Aloufi, M. (1999), 'Small strain stiffness: A micromechanical experimental study', *Proceedings of Pre-failure Deformation Characteristics of Geomaterials* pp. 451–458.
- Santamarina, J. & Cho, G. (2004), Soil behaviour: The role of particle shape, in 'Advances in Geotechnical Engineering: The Skempton Conference', Vol. 1, pp. 604–617.
- Sariosseiri, F. (2008), Critical state framework for interpretation of geotechnical properties of cement treated soils, PhD thesis, Washington State University.
- Sauer, E. & Weimer, N. (1978), 'Deformation of lime modified clay after freeze-thaw', *Journal of Transportation Engineering* 104(2), 201–212.
- Sawangsurriya, A., Biringen, E., Fratta, D., Bosscher, P. & Edil, T. (2006), 'Dimensionless limits for the collection and interpretation of wave propagation data in soils', *ASCE*

- Geotechnical Special Publication (GSP) No.149: 'Site and Geomaterial Characterization', 149, 160–166.
- Sawangsurriya, A., Edil, T. & Bosscher, P. (2008), 'Modulus- suction- moisture relationship for compacted soils', *Canadian Geotechnical Journal* 45(7), 973–983.
- Sawangsurriya, A., Edil, T. & Bosscher, P. (2009), 'Modulus-suction-moisture relationship for compacted soils in postcompaction state', *Journal of Geotechnical and Geoenvironmental Engineering* 135, 1390.
- Schaefer, V., Abramson, L., Drumheller, J. & Sharp, K. (1997), *Ground improvement, ground reinforcement and ground treatment: Developments 1987-1997 (gsp 69)*, ASCE.
- Schnaid, F., Wood, W., Smith, A. & Jubb, P. (1993), An investigation of bearing capacity and settlements of soft clay deposits at shellhaven, in 'Predictive soil mechanics. Proceedings of the worth memorial symposium, 27-29 July 1992, Saint Catherine's College, Oxford'.
- Schneider, J., Hoyos, L., Mayne, P., Macari, E. & Rix, G. (1999), 'Field and laboratory measurements of dynamic shear modulus of piedmont residual soils', *Behavioral Characteristics of Residual Soils, GSP 92*, ASCE, Reston, VA, GSP 92, 12–25.
- Schuettpelez, C. C., D. Fratta, and T. B. Edil. (2009). Evaluation of the Influence of Geogrid Reinforcement on soil Rotation and Stiffness in Compacted Based Course Soil. *Transportation Research Record*. No. 2116, 76 - 84.
- Schuettpelez, C. C., Fratta D., Edil T. B. (2009), 'Mechanistic method for determining the resilient modulus of base course materials based on elastic wave measurements', *Journal of Geotechnical and Geoenvironmental Engineering* Vol. 136, No. 8, 1086 – 1094.
- Schuettpelez, C., Fratta, D., Edil, T. et al. (2010), 'Mechanistic corrections for determining the resilient modulus of base course materials based on elastic wave measurements', *Journal of geotechnical and geoenvironmental engineering* 136, 1086.
- Seed, H., & M., Idriss I. M. (1970), *Soil moduli and damping factors for dynamic response analysis*, Technical Report No. EERC 70-10, University of California, Berkeley, Calif.
- Seed, H., & Chan, C., (1960), *Structure and strength characteristics of compacted clays*, Institute of Transportation and Traffic Engineering, University of California.

- Shea, M. (2011), Hydraulic Conductivity of Cement-Treated Soils and Aggregates after Freezing, PhD thesis, Brigham Young University.
- Sharifipour, M. (2006), 'Caractérisation des sols par propagation d'ondes analyse critique de la technique des bender-extend elements', PhD thèses, L'École Centrale de Nantes et l'Université de Nantes, 192 pages.
- Sherwood, P. (1958), 'Effect of sulphates on cement -stabilized soils', Hwy. Res Board Bull. 198, National Research Council, Washington, D.C.
- Sherwood, P. (1962), Effect of sulphates on cement and lime stabilized soils, Technical report, Hwy.Res. Board Bull, 353, National Research Council, Washington, D.C.
- Sherwood, P. (1993), Soil stabilization with cement and lime.
- Shihata, S. & Baghdadi, Z. (2001), 'Simplified method to assess freeze-thaw durability of soil cement', Journal of materials in civil engineering 13, 243.
- Shirley, D. J. (1978), 'An improved shear wave transducer', J. Acoust. Soc. Am. 63, No. 5, 1643–1645.
- Siavash.Ghabezloo (2008), Comportement thermo-poro-mécanique d'un ciment pétrolier, PhD thesis, École Nationale des Ponts et Chaussées.
- Sirivitmaitrie, C., Puppala, A., Saride, S. & Hoyos, L. (2011), 'Combined lime-cement stabilization for longer life of low-volume roads', Transportation Research Record: Journal of the Transportation Research Board 2204(-1), 140–147.
- Sivapullaiah, P., Sridharan, A. & Ramesh, H. (2006), 'Effect of sulphate on the shear strength of lime-treated kaolinitic soil', Proceedings of the ICE-Ground Improvement 10(1), 23–30.
- Snethen, D. R. (2008), 'Evaluation and field verification of strength and structural improvement of chemically stabilized subgrade soil', Technical report.
- Solanki, P., Khoury, N. & Zaman, M. (2007), 'Engineering behavior and microstructure of soil stabilized with cement kiln dust', Geotechnical Special Publication 172, 1–10.
- Solanki, P., Zaman, M. & Dean, J. (2010), 'Resilient modulus of clay subgrades stabilized with lime, class c fly ash, and cement kiln dust for pavement design', Transportation Research Record: Journal of the Transportation Research Board 2186(-1), 101–110.

- Stavridakis, E. (2006), 'A solution to the problem of predicting the suitability of silty-clayey materials for cement-stabilization', *Geotechnical and Geological Engineering* 24(2), 379–398.
- Stocker, P.T. (1975), 'Diffusion and diffuse cementation in lime and cement stabilized clayey soils-chemical aspects', *Australian Road Research*, 5(9), 6-47.
- Stoltz G., Cuisinier O., Masrouri F. (2010), 'Impact de cycles hydriques sur le comportement hydromécanique d'une argile gonflante traitée à la chaux', *Géotechnique* 6(4).
- Stoltz, G., Cuisinier, O., Masrouri, F. (2012), 'Multi-scale analysis of the swelling and shrinkage of a lime-treated expansive clayey soil', *Applied Clay Science* 61(2012), 44-51.
- Sully, J. & Campanella, R. (1995), 'Evaluation of in situ anisotropy from crosshole and downhole shear wave velocity measurements', *Geotechnique* 45(2), 267–282.
- Sun, D., Sheng, D., Cui, H. & Sloan, S. (2007), 'A density-dependent elastoplastic hydro-mechanical model for unsaturated compacted soils', *International journal for numerical and analytical methods in geomechanics* 31(11), 1257–1279.
- Szczepanski, T. (2008), 'Soil small strain parameters derived from wave velocity measurements', *geologija* Vol. 50, S85–S89.
- Ta, A. M. (2009), 'Etude de l'interaction soil-atmosphère en chambre environnementale', Thèse de l'Ecole Nationale des Ponts et Chaussées, 186 pages.
- Tabatabai, A. M. (1997), *Pavement [Roosazi Rah]*, University's publication center, Tehran, Iran.
- Tang, A.M., Vu, M.N., Cui, Y.J. (2011), 'Effects of the maximum grain size and cyclic wetting/drying on the stiffness of a lime-treated clayey soil', *Géotechnique* 61, 421–429.
- Tang, A.M., Cui, Y.J. (2008), Compression-induced suction change in a compacted expansive clay, in 'Unsaturated Soils. Advances in Geo-Engineering: Proceedings of the 1st European Conference, E-UNSAT 2008, Durham, United Kingdom, 2-4 July 2008', Taylor & Francis Group, p. 369.

- Tang, A.M., Cui, Y.J., Eslami J., Pauline Défossez P. (2009), 'Analysis of the railway heave induced by soil swelling at a site in southern France', *Engineering Geology* 106(1-2), 68 – 77.
- Tascon, A. (2011), Effective depth of soil compaction under a controlled compactive effort at laboratory scale, PhD thesis, University of Wisconsin.
- Tatsuoka, F., Kohata, Y., Uchida, K., and Imai, K., (1996), 'Deformations and Strength Characteristics of Cement-Treated Soils in Trans-Tokyo Bay Highway Project', *Proceedings of Grouting and Deep Mixing, IS-Tokio 96, 2nd Int. Conference on Ground Improvement Geosystems, Balkema, Rotterdam, Vol. 1, pp. 453–459.*
- Tedesco, D. (2006), 'Hydro-mechanical behaviour of lime-stabilised soils', PhD thesis, Università degli Studi di Cassino Facoltà di Ingegneria.
- Texas Department of Transportation (TxDOT), (2005), Guidelines for modification and stabilization of soils and base for use in pavement structures, Technical report, Austin, TX. <ftp://ftp.dot.state.tx.us/pub/txdot-info/cmd/tech/stabilization.pdf>.
- Thagesen, B. (1996), *Highway and traffic engineering in developing countries*, Taylor & Francis.
- Thompson, M. (1966), 'Lime reactivity of Illinois soils', *Journal of soil mechanics and foundations div.*, ASCE 92, No. 5, 67– 92.
- Thompson, M. & Dempsey, B. (1970), 'Quantitative characterization of cyclic freezing and thawing in stabilized pavement materials', *Highway Research Record*.
- Thompson, M. R. & Dempsey, B. J. (1969), Autogeneous healing of lime soil mixture, *Highway Research Record No. 263*.
- Tinjum, J., Benson, C. et al. (1997), 'Soil-water characteristic curves for compacted clays', *Journal of geotechnical and geoenvironmental engineering* 123, 1060.
- Tonož, M., Ulusay, R. & Gokceoglu, C. (2004), 'Effects of lime stabilization on engineering properties of expansive Ankara clay', *Engineering Geology for Infrastructure Planning in Europe* 104, 466–474.
- Townsend, D. & Klym, T. (1966), 'Durability of lime-stabilized soils', *Highway Research Record* 139, 25–41.

- Tremblay, H., Duchesne, J., Locat, J. & Leroueil, S. (2002), 'Influence of the nature of organic compounds on fine soil stabilization with cement', *Canadian Geotechnical Journal* 39(3), 535–546.
- Tripathy S., Subba Rao K. S., Fredlund, D. (2002), 'Water content – void ratio swell–shrink paths of compacted expansive soils', *Can. Geotech* 21(3), 938 – 959. *Issues in Nuclear Waste Isolation Research*.
- Tuncer, E. & Basma, A. (1991), 'Strength and stress-strain characteristics of a lime-treated cohesive soil', *Transportation Research Record* (1295).
- Umesha, T., Dinesh, S. & Sivapullaiah, P. (2009), 'Control of dispersivity of soil using lime and cement', *International Journal of Geology* 3, 8–16.
- Vanapalli, S. & Fredlund, D. (1997), Interpretation of undrained shear strength of unsaturated soils in terms of stress state variables, in '3rd Brazilian Symposium on Unsaturated Soils, April', pp. 21–25.
- Vanapalli, S., Fredlund, D. & Pufahl, D. (1999), 'The influence of soil structure and stress history on the soil-water characteristics of a compacted till', *Geotechnique* 49(2), 143–160.
- Vanapalli, S., Fredlund, D., Pufahl, D. & Clifton, A. (1996), 'Model for the prediction of shear strength with respect to soil suction', *Canadian Geotechnical Journal* 33(3), 379–392.
- Van Impe, W. F., Verástegui Flores, R. D., Mengé, P., and Van den Broeck, M., (2005), "Considerations on Laboratory Test Results of Cement Stabilized Sludge," *Proceedings of the International Conference on Deep Mixing: Best Practice and Recent Advances*, Stockholm, Swedish Geotechnical Institute, Sweden, pp. 163–168.
- Vassallo, R., Mancuso, C. & Vinale, F. (2007), 'Effects of net stress and suction history on the small strain stiffness of a compacted clayey silt', *Canadian geotechnical journal* 44(4), 447–462.
- Vaunat, J., Merchán, V. & Romero Morales, E. (2009), 'The influence of drying on the small strain shear modulus for static compacted boom clay'.
- Viggiani, G. & Atkinson, J. (1995a), 'Stiffness of fine-grained soil at very small strains', *Géotechnique* 45(2), 249–266.



- Viggiani, G., Atkinson, JH. (1995b), 'Interpretation of bender element tests', *Géotechnique*. 45(1), 149-154.
- Vucetic, M. (1994), 'Cyclic threshold shear strains in soils', *Journal of Geotechnical engineering* 120(12), 2208–2228.
- Vucetic, M. & Dobry, R. (1991), 'Effect of soil plasticity on cyclic response', *Journal of Geotechnical Engineering* 117(1), 89–107.
- Walker, P. J. (1995), 'Strength, durability and shrinkage characteristics of cement stabilised soil blocks', *Cement and Concrete Composites* 17(4), 301 – 310.
- Walker, R., Krebs, R. & Esmer, E. (1967), 'Strength loss in lime-stabilized clay soil when moistened and exposed to freezing and thawing', *Highway Research Record* (181).
- Wang, C. (2008), 'The influence of wetting-drying and compaction state on matric suction of subgrade soil' (in Chinese).
- Wang, L. (2002), 'Cementitious stabilization of soils in the presence of sulfate', PhD thesis, Wuhan University of Technology.
- Western Stabilization, (2010), 'Chemical Stabilization-Solving Construction Problems Associated with Expansive Soils'. Source: [www.wstabilization.com](http://www.wstabilization.com).
- Whittig, L., Allardice, W., Klute, A. et al. (1986), 'X-ray diffraction techniques', *Methods of soil analysis. Part 1. Physical and mineralogical methods* pp. 331–362.
- Wichtmann, T. & Triantafyllidis, T. (2009), 'Influence of the grain-size distribution curve of quartz sand on the small strain shear modulus  $G_{max}$ ', *Journal of Geotechnical and Geoenvironmental Engineering* 10(8), 1404–1418.
- Wild, S., Abdi, M., Leng-Ward, G. (1993), 'Sulphate expansion of lime-stabilized kaolinite. ii: Reaction products and expansion', *Clay minerals* 28(4), 569–583.
- XP CEN ISO/TS 17892-1. (2005), *Reconnaissance et essais géotechniques - Essais de laboratoire sur les sols - Partie 1 : détermination de la teneur en eau*.
- XP CEN ISO/TS 17892-2. (2005), *Reconnaissance et essais géotechniques - Essais de laboratoire sur les sols - Partie 2 : détermination de la masse volumique d'un sol fin*.
- XP CEN ISO/TS 17892-4. (2005), *Reconnaissance et essais géotechniques - Essais de laboratoire sur les sols - Partie 4 : détermination de la distribution granulométrique des particules*.

- Yamashita, S., Hori, T. & Suzuki, T. (2003), 'Effects of fabric anisotropy and stress condition on small strain stiffness of sands', *Deformation Characteristics of Geomaterials* **1**, 187–194.
- Yamashita, S., Kawaguchi, T., Nakata, Y., MIKAML, T., Fujiwara, T. & Shibuya, S. (2005), 'Interpretation of international parallel test on the measurement of  $G_{\max}$  using bender elements', *Soils and foundations*, ISSMGE TC-29 Report, 76 pages.
- Yamashita, S., Kawaguchi, T., Nakata, Y., Mikami, T., Fujiwara, T. & Shibuya, S. (2009), 'Interpretation of international parallel test on the measurement of  $G_{\max}$  using bender elements', *Soils Foundation*, 49(4), 631–650.
- Yan, S. & Jin, P. (2004), a study on the correlation relationships between smectite contents and spectral absorption indices of swelling soils, in 'Geoscience and Remote Sensing Symposium, 2004. IGARSS'04. Proceedings. 2004 IEEE International', Vol. 7, IEEE, pp. 4674–4677.
- Yang, S. (2010), 'Discussion of "predicting moisture-dependent resilient modulus of cohesive soils using soil suction concept" by R.Y. Liang, S. Rabab'ah, and M. Khasawneh', *Journal of Transportation Engineering* 136, 691.
- Yin, C., Mahmud, H. & Shaaban, M. (2006), 'Stabilization/solidification of lead-contaminated soil using cement and rice husk ash', *Journal of hazardous materials* 137(3), 1758–1764.
- Yong, R. & Ouhadi, V. (2007), 'Experimental study on instability of bases on natural and lime/cement-stabilized clayey soils', *Applied clay science* 35(3), 238–249.
- Youn, J., Choo, Y. & Kim, D. (2008), 'Measurement of small-strain shear modulus  $G_{\max}$  of dry and saturated sands by bender element, resonant column, and torsional shear tests', *Canadian Geotechnical Journal* 45(10), 1426–1438.
- Yu, X. & Drnevich, V. (2004), 'Time domain reflectometry for compaction control of stabilized soils', *Transportation Research Record: Journal of the Transportation Research Board* 1868(-1), 14–22.
- Yuan, D. & Nazarian, S. (2003), Variation in moduli of base and subgrade with moisture, in 'Transportation Research Board 82nd Annual Meeting, Washington, DC', pp. 12–16.
- Yuan, X., Shudong, L. & Wei, C. (2010), Silt subgrade modification and stabilization with ground granulated blast furnace slag and carbide lime in areas with a recurring high

## Reference

---

groundwater, in 'Mechanic Automation and Control Engineering (MACE), 2010 International Conference on', IEEE, pp. 2063–2067.

Zapata, C., Houston, W., Houston, S. & Walsh, K. (2000), Soil-water characteristic curve variability in 'Advances in Unsaturated Geotechnics: Proceedings of Sessions of Geo-Denver 2000: August 5-8, 2000, Denver, Colorado', Amer Society of Civil Engineers, p. 84.

Zhang, Z. & Tao, M. (2008), 'Durability of cement stabilized low plasticity soils', Journal of geotechnical and geoenvironmental engineering 134, 203.